Analytical and Preparative Separation Methods of Biomacromolecules

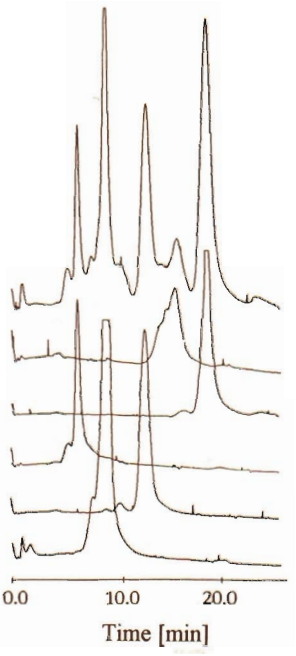

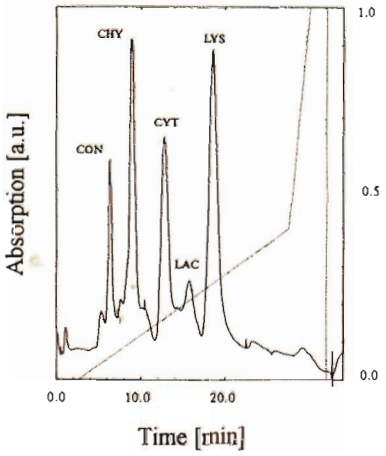

edited by
Hassan Y. Aboul-Enein

Analytical and Preparative Separation Methods of Biomacromolecules

Analytical and Preparative Separation Methods of Biomacromolecules

edited by

Hassan Y. Aboul-Enein
King Faisal Specialist Hospital and Research Centre
Riyadh, Saudi Arabia

MARCEL DEKKER, INC. NEW YORK • BASEL

Library of Congress Cataloging-in-Publication Data

Analytical and preparative separation methods of biomacromolecules / edited by Hassan Y. Aboul-Enein.
p. cm.
ISBN 0-8247-1996-4 (alk. paper)
1. Macromolecules—Separation. 2. Biomolecules—Separation. 3 Chromatographic analysis. 4. Electrophoresis. I. Aboul-Enein, Hassan Y.
QP519.9.S45A53 1999
572.8—dc21 99-26367
CIP

This book is printed on acid-free paper.

Headquarters
Marcel Dekker, Inc.
270 Madison Avenue, New York, NY 10016
tel: 212-696-9000; fax: 212-685-4540

Eastern Hemisphere Distribution
Marcel Dekker AG
Hutgasse 4, Postfach 812, CH-4001 Basel, Switzerland
tel: 41-61-261-8482; fax: 41-61-261-8896

World Wide Web
http://www.dekker.com

The publisher offers discounts on this book when ordered in bulk quantities. For more information, write to Special Sales/Professional Marketing at the headquarters address above.

Current printing (last digit):
10 9 8 7 6 5 4 3 2 1

PRINTED IN THE UNITED STATES OF AMERICA

To my beloved Partent and the most special people in my life,
Nagla, Youssef, Faisal, and Basil

Preface

It is my pleasure to be an editor of this book, which gave me a chance to be exposed to this fascinating field of separation technology of biomacromolecules which represent, medically and biochemically, an important class of compounds.

This book consists of sixteen chapters representing the latest research results and recent developments in the area of high-performance liquid chromatography and capillary electrophoresis. Also, the book includes chapters discussing in detail: biochromatography, displacement chromatography, affinity capillary electrophoresis, and the new technologies of slalom chromatography. The scope of the topics presented are broad and therefore give a comprehensive view of the current status of the established and newly developed separation techniques that are useful for biomacromolecule isolation and purification.

I would like to thank the contributors, internationally renowned experts in their respective research fields, who have made this book possible. Also, my thanks are extended to Marcel Dekker, Inc., and, in particular, Mr. Russell Dekker for his encouragement to publish this book.

As we approach the next millennium and reflect on the rapid developments that have been achieved in the area of biotechnology, I certainly hope that this book will be a useful reference for scientists and researchers dealing with isolation, purification, and analysis of biomolecules.

Hassan Y. Aboul-Enein

Contents

Contributors

Sultan T. Al-Sedairy Research Center Administration, King Faisal Specialist Hospital and Research Center, Riyadh, Saudi Arabia

Olivia Befani Department of Biochemical Sciences and CNR Center of Molecular Biology, Rome University "La Sapienza," Rome, Italy

Rainer Bischoff, Ph.D.* Protein Analytical Group, Transgene S.A., Strasbourg, France

Bernadette Bouchon Protein Analytical Group, Transgene S.A., Strasbourg, France

David R. Brigstock, Ph.D. Associate Professor, Surgery and Medical Biochemistry, Ohio State University and Children's Hospital, Columbus, Ohio

Jean-Pierre Dandeu Unité d'Immuno-Allergie, Institut Pasteur, Paris, France

Marie-Joseé Dumoulin Department of Chemistry and Biochemistry, Université du Québec à Montréal, Québec, Canada

* *Current affiliation:* Senior Research Scientist, Biochemistry and Bioanalytical Chemistry Department, Astra-Draco AB, Lund, Sweden

Thomas H. Fischer, Ph.D. Research Assistant Professor, The School of Medicine, Center for Thrombosis and Hemostasis, University of North Carolina at Chapel Hill, Chapel Hill, North Carolina

Ruth Freitag, Ph.D. Professor, Chemistry Department, ETH Lausanne, Lausanne, Switzerland

Afrozul Haq, Ph.D. Associate Scientist, Biological and Medical Research, King Faisal Specialist Hospital and Research Center, Riyadh, Saudi Arabia

Jun Hirabayashi Department of Biological Chemistry, Faculty of Pharmaceutical Sciences, Teikyo University, Sagamiko, Kanagawa, Japan

Wilfrid Jacques Professor, Department of Chemistry and Biochemistry, Université du Québec à Montréal, Québec, Canada

Ken-ichi Kasai Faculty of Pharmaceutical Sciences, Teikyo University, Sagamiko, Kanagawa, Japan

Václav Kašička, Ph.D. Senior Research Scientist, Department of Biochemistry of Peptides, Institute of Organic Chemistry and Biochemistry, Academy of Sciences of the Czech Republic, Prague, Czech Republic

Young C. Lin, Ph.D., D.V.M. Laboratory of Reproductive and Molecular Endocrinology, Department of Veterinary Biosciences, College of Veterinary Medicine, Ohio State University, Columbus, Ohio

Patricia Martin, Ph.D., D.A.B.T. Senior Research and Development Chemist, Analytical Chemistry Division, R. J. Reynolds Tobacco Company, Winston-Salem, North Carolina

Mircea-Alexandru Mateescu, Ph.D. Professor, Department of Chemistry and Biochemistry, Université du Québec à Montréal, Québec, Canada

Bruno Mondovi, M.D. Professor, Department of Biochemical Sciences and CNR Center of Molecular Biology, Rome University "La Sapienza," Rome, Italy

Nona Remo Rama, B.Sc. Research Technician, Biological and Medical Research, King Faisal Specialist Hospital and Research Center, Riyadh, Saudi Arabia

Sandra M. Scott, B.S. Research Assistant, Research and Development, Environmental and Molecular Toxicology, R. J. Reynolds Tobacco Company, Winston-Salem, North Carolina

Kiyohito Shimura, Ph.D. Associate Professor, Department of Biological Chemistry, Faculty of Pharmaceutical Sciences, Teikyo University, Sagamiko, Kanagawa, Japan

Carr J. Smith, Ph.D., D.A.B.T. Master Scientist, Research and Development, Environmental and Molecular Toxicology, R. J. Reynolds Tobacco Company, Winston-Salem, North Carolina

Ulf-Håkan Stenman, M.D., Ph.D. Laboratory, Helsinki University Central Hospital, Helsinki, Finland

Tatiana Tennikova Professor, Institute of Macromolecular Compounds, Russian Academy of Sciences, St. Petersburg, Russia

Jaroslava Turková, Ph.D., Dr.Sc. Senior Research Scientist, Institute of Organic Chemistry and Biochemistry, Academy of Sciences of the Czech Republic, Prague, and University of Pardubice, Pardubice, Czech Republic

Ursula Turpeinen, Ph.D. Chemist, Laboratory, Helsinki University Central Hospital, Helsinki, Finland

Mehmet Uzumcu, Ph.D., D.V.M. Assistant Scientist, Biological and Medical Research, King Faisal Specialist Hospital and Research Center, Riyadh, Saudi Arabia

Xin-Tao Wang, Ph.D. Department of Chemistry and Biochemistry, Université du Québec à Montréal, Québec, Canada, and Rome University "La Sapienza," Rome, Italy

Philip J. Wyatt, Ph.D. President, Wyatt Technology Corporation, Santa Barbara, California

1

Analysis of HbA_{1C} and Some Hb Variants by HPLC

Ursula Turpeinen and Ulf-Håkan Stenman
Helsinki University Central Hospital, Helsinki, Finland

I. INTRODUCTION

This chapter deals with selected aspects of high-performance liquid chromatography (HPLC) methods for quantitating of glycohemoglobin (HbA_{1C}) and characterizing some Hb variants. Determination of HbA_{1C} by ion exchange HPLC is used for monitoring of glycemic control in diabetic patients. The percentage of HbA_{1C} reflects blood glucose concentrations of the previous 2–3 months. It is therefore considered a valuable indicator of long-term diabetic control [1]. However, the methods currently used for its measurement in clinical chemistry laboratories show large differences between reported values, and comparison of results from different laboratories is difficult [2]. Lack of standardization of glycohemoglobin measurements remains the major source of interlaboratory variation. At present there is no acknowledged reference method or an accepted standard. This fact is well recognized and an IFCC (International Federation of Clinical Chemistry) working group is developing a reference method based on HbA_{1C} as the biochemically well-defined major glycohemoglobin component. Recently, the use of calibration based on a cation exchange HPLC method has been shown to increase the comparability between various analytical methods [3,4].

The classical method for the rapid determination of HbA_{1C} by chromatography on the weak cation exchange resin Bio-Rex 70 was introduced by Trivelli et al. in 1971 [5] based on the method of Allen et al. on Amberlite IRC-50 [6]. Several approaches, including minicolumns [7] and HPLC [8], were used to make ion exchange chromatography acceptable for use in clinical laboratories. Though acceptable resolution can be obtained with Bio-Rex 70, it has lower resolution

and is more time consuming than HPLC methods. Flow rate is limited by the compressibility of the resin and its nonuniform particle size. These drawbacks stimulated development of several methods using ion exchange resins for HPLC, such as Synchropak CM 300 [9], silica-based carboxymethylpolyamide [10], Mono S [8,11], and the Glycopak resin of the Diamat analyzer (Bio-Rad). These methods can usually also be used to measure fetal hemoglobin (HbF). They differ in their sensitivity to interferences such as adducts formed between Hb and urea, aldehydes, or acetylsalicylic acid and other hemoglobin (Hb) variants [12,13].

Glycohemoglobin can also be assayed by affinity chromatography using boronate agarose columns [14]. This method measures HbA_{1C} together with glycohemoglobins, which elute in the HbA_0 fraction in ion exchange chromatography.

In chromatographic methods, abnormal Hb variants may cause erroneous HbA_{1C} results [15,16], but at the same time they permit identification of individuals with such variants. This information is of importance for the interpretation of the HbA_{1C} results. Therefore it is an advantage if an HPLC method used for clinical purposes separates not only HbA_{1C} but also other hemoglobin components to permit identification of abnormal hemoglobins. The good resolution of more than 35 frequently encountered human hemoglobins and HbA_{1C} on PolyCAT A [17] makes it a useful method for preliminary characterization of Hb variants. The Diamat method has been shown to separate seven variants [18], but many overlap partially with the HbA_{1C} peak.

II. CURRENT HPLC METHODS FOR THE DETERMINATION OF HbA_{1C} BY CATION EXCHANGE CHROMATOGRAPHY

A. Mono S

The Mono S system was introduced by Stenman et al. and Jeppsson et al. [8,11]. The Mono S method has been widely used in clinical laboratories. It is precise, accurate, and easily operated [11]. The monodisperse cation resin, Mono S, does not shrink, swell, or leak functional groups with a LiCl gradient in malonate buffers at pH 5.7. The acetaldehyde adduct of Hb in alcoholics may interfere with HbA_{1C} determinations since it coelutes with HbA_{1C}. In uremic patients, carbamylated Hb may increase the HbA_{1C} values by as much as 1%. The separation has been further optimized by using a smaller column load, decreased flow rate, and a steeper LiCl gradient [19]. We have also used Mono S extensively for HbA_{1C} analysis by slightly modifying the original method [8]. Phosphate buffers with 10% acetonitrile and a higher pH of 6.85 were used at 30°C. These changes

improved the separation and the column life increased up to several thousand samples with constant resolution.

B. PolyCAT A

PolyCAT A is a weak cation exchanger with polyaspartic acid linked to silica [20,21]. This resin has been used for the determination of HbA_{1C} [22,23], of several minor molecular forms of hemoglobin [24], and for identification of hemoglobin variants [17]. The separation of HbA_{1C} from other Hb components such as acetylated Hb [13] and HbF depends critically on buffer composition, particularly on the pH and salt gradient. It is often necessary to make minor variations in the steepness of the salt gradient in order to get a good separation. The assay is precise [22] and it depends more on the quality of the chromatographic separation, the level of noise in the spectrophotometer, and the mode of integration than on volumes injected.

PolyCAT A with bis-tris buffers and sodium acetate gradients has been used to separate and quantitate many normal and abnormal Hb components [23,24]. Minor fetal Hb forms can be separated and HbA_{1C} can simultaneously be quantitated. We have compared the performance of PolyCAT A chromatography with a boronate affinity binding assay and the automated Diamat system for the determination of HbA_{1C} [23]. Elution was achieved with a linear gradient consisting of buffers A and B at a flow rate of 1.1 ml/min at room temperature. Buffer A (pH 6.87) contained 10 mmol of bis-tris and 1.0 mmol of KCN per liter. Buffer B (pH 6.57) contained buffer A plus 200 mmol of NaCl per liter. The gradient was: time 0–2 min, 21% B; time 16 min, 47% B; time 22 min, 100% B; time 24 min, 100% B; and time 26 min, 21% B. Integration was performed by the valley-to-valley method.

When we compared the two cation exchange methods, PolyCAT A and Diamat, we obtained an acceptable correlation (Fig. 1). The correlation coefficient was 0.90 but the regression equation (PolyCAT A = 1.06 × Diamat − 3.06) showed that much lower results were obtained by PolyCAT A. This suggests that the HbA_{1C} value measured by the Diamat assay includes a background of 2–3% of the total Hb. This might be due to the fact that the Diamat method also measures carbamylated and acetylated forms of Hb [12] and possibly some other derivatives formed in blood during storage, which can be separated from the HbA_{1C} peak by the use of methods with higher resolution. The PolyCAT A assay has been optimized to separate different Hb variants from HbA_{1C}. However, the difference between the Diamat method and the PolyCAT A assay cannot be explained only by carbamylated and acetylated Hbs, for which levels below 0.4% have been reported [12]. The slope of the regression line, 1.06, shows that the PolyCAT A method reflects differences in glycated Hb in the same way

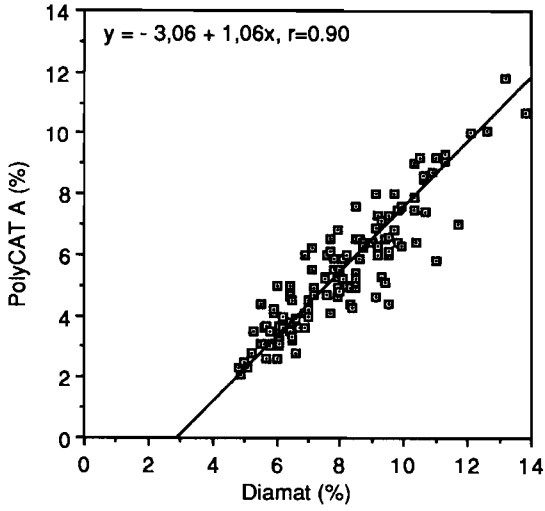

Figure 1 Correlation between the HbA_{1C} values obtained by PolyCAT A (y) and Diamat (x). Corresponding regression equation calculated by the standardized principal component is y = 1.06x −3.06, r = 0.90.

as the Diamat method. The negative bias of about 2–3% of total Hb is present at all levels of HbA_{1C} when PolyCAT A is compared to Diamat.

C. Diamat and Variant Analyzers

The Diamat analyzer of Bio-Rad Laboratories is an automated HPLC instrument using a weak cation exchange column. The support material is silica with carboxymethyl functional groups. The analyzer forms a stepwise gradient of three phosphate buffers of increasing ionic strength to separate the HbA_{1C} from other Hbs. The system has been optimized for the quantitation of HbA_{1C}, and HbA_2 coelutes with HbA_0. Quantitation is based on the absorbance at 415 and 690 nm. Before analysis with the Diamat analyzer 5 µl of the whole-blood sample is diluted with 1.25 ml of hemolysis reagent containing 0.1% (v/v) polyoxyethylene ether in a borate buffer. The tubes are incubated at 37°C for 30 min to remove the labile HbA_{1C} fraction.

The Variant analyzer of Bio-Rad Laboratories offers a broader test selection of methods than the Diamat system. Although the separation principle is the same, with various programs it is possible to separate and quantitate, in addition

to HbA_{1c}, also HbF and HbA_2. The method has been calibrated against the Diamat method. In practice, however, there seems to be a slight difference between these systems, with the Variant giving slightly higher results than the Diamat [25].

III. DETERMINATION OF HbA_{1c} BY AFFINITY CHROMATOGRAPHY

The boronate affinity chromatography method involving minicolumns has gained wide acceptance because it is not affected by Hb variants, slight temperature changes, carbamylated Hb, and the labile glycated fraction [26]. The application of HPLC to affinity methods has the same advantages as the minicolumns. An automatic affinity HPLC system is now available and has been evaluated for the monitoring of glycohemoglobin [27].

A considerable bias has been observed between cation exchange and affinity chromatography. In two studies the correlations between the methods were: affinity chromatography = 1.40 × ion exchange − 2.19 [28] and affinity chromatography = 1.45 × ion exchange + 0.04 [24]. The difference in slope is explained by the fact that affinity methods measure glycated Hbs other than HbA_{1c}. The negative y intercept may be explained by the fact that nonglycated components of HbA_{1c} are measured by the ion exchange chromatography [23]. Methods based on boronate affinity detection of the glycated amino terminus of the β chains of Hb together with glycosylated Hbs eluting in the HbA_0 fraction in ion exchange chromatography may be expected to reflect blood glucose control more accurately than ion exchange chromatography methods, which also measure coeluting nonglycated Hb. However, this has to be determined in a true clinical setting.

IV. REFERENCE VALUES FOR HbA_{1c}

Determination of a method-specific reference range is important in glycohemoglobin analysis, due to differences between methods. We have estimated the reference values of HbA_{1c} which are lower with the PolyCAT A method than with the Diamat method, apparently because of better separation of HbA_{1c} from nonglycated coeluting forms of Hb with PolyCAT A. The reference range for HbA_{1c} is 4.5–5.8% for the Diamat and 2.5–4.4% for the PolyCAT A method [23]. The difference in mean values between the PolyCAT A (3.4%) and Diamat (5.1%) methods was 1.7%.

The reference range with PolyCAT A is lower than that observed with our original HPLC method, 4.2–6.6%, using the Mono S column [8] and that reported by Jeppsson et al., 3.9–5.3%, using the same column but a different gradient [11]. With PolyCAT A and other gradients, reference ranges of 2.8–5.5% [24]

and 3.9–5.7% [22] have been reported. Slightly higher reference ranges of 5.0–7.6% [28] and 4.8–6.4% [29] have been reported for boronate affinity chromatography methods. Of the glycated Hb adsorbed to boronate affinity columns, about 50% elutes in ion exchange chromatography as HbA_{1C}, about 40% in the HbA_0 peak and 10% as HbA_{1a+b} [28]. The values for the PolyCAT A method can be estimated to correspond to about 60–70% of those obtained by boronate affinity chromatography. This suggests that the PolyCAT A method measures the glycated component of the HbA_{1C} peak fairly specifically. A certain change in blood glucose causes a larger change in glycated Hb measured by affinity chromatography than in HbA_{1C}. This is demonstrated by the slope of the correlation, about 1.4–1.5 [24,28] in spite of similar reference values.

V. HPLC CATION EXCHANGE CHROMATOGRAPHY OF Hb VARIANTS

HPLC provides a rapid and sensitive means for the examination of abnormal hemoglobins. Methods with high sensitivity and specificity have been developed for screening and confirmation of hemoglobinopathies in newborns [30,31]. Most methods have used Synchropak CM 300, a silica support with carboxylic acid residues or PolyCAT A. The screening procedures are designed to rapidly detect the major variants. However, the resolution of these methods does not permit differentiation of some commonly encountered hemoglobin variants such as HbE

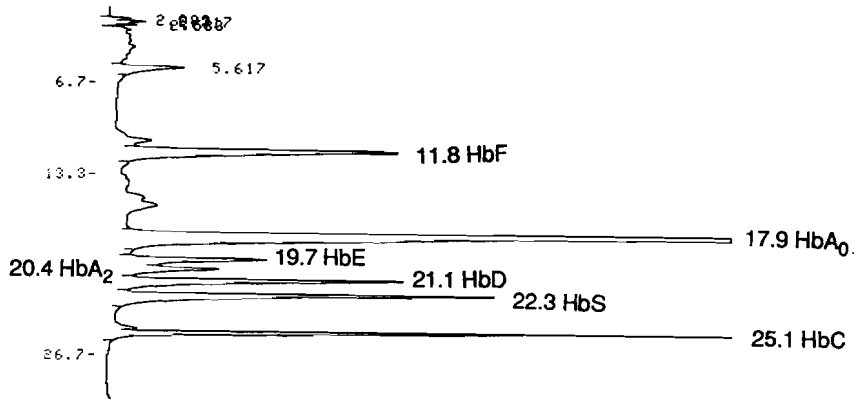

Figure 2 Cation exchange chromatography of HbF, HbA_0, HbE, HbA_2, HbD, HbS, and HbC on PolyCAT A. Time of elution since sample injection is indicated at each peak. Detection at 415 nm.

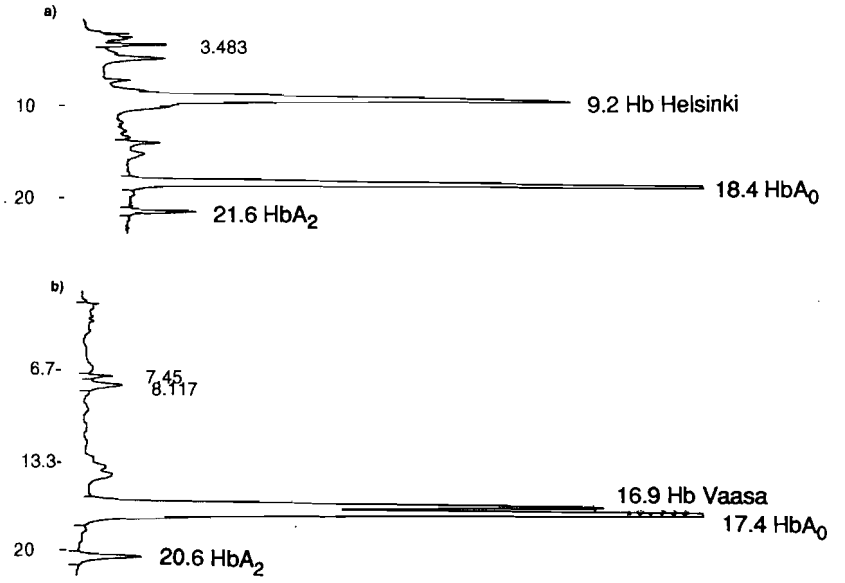

Figure 3 Cation exchange chromatography on PolyCAT A of a red cell hemolyzate with a β-chain variant of (a) Hb-Helsinki and (b) Hb-Vaasa. Time of elution since sample injection is indicated at each peak. Detection at 415 nm.

from HbA_2. The sensitivity to detect hemoglobin variants occurring at low concentrations is also poor.

Recently, Ou and Rognerud [17] described a method for Hb variant analysis on the PolyCAT A column. The good resolution obtained with more than 35 frequently encountered human Hbs also makes it useful for HbA_{1C} determinations and for preliminary identification of Hb variants. Earlier, PolyCAT A was used for screening of cord blood for hemoglobinopathies [32]. The column has the resolution necessary for both screening and confirmatory purposes. We have investigated the use of a 4.6 × 200 mm PolyCAT A column with 5-μm particles for separation of Hb variants. A typical chromatographic separation of an Hb mixture containing A_{1C}, F, A_0, E, A_2, D, S, and C is shown in Fig. 2. We have also separated other Hb variants by using bis-tris buffers and an NaCl gradient (Fig. 3). The baseline resolution permits accurate quantitation of these hemoglobins, which is important for the correct diagnosis of hemoglobinopathies. In addition, HbA_2 can be accurately measured. A slight adjustment of the gradient program may be necessary for optimal separation of all variants.

Recently, a new automatic HPLC system using a Bio-Rad MA7 polymeric cation exchange material has been used to screen newborns for sickle cell anemia

and other hemoglobinopathies [33]. The method is reported to resolve hemoglobins F, A, S, C, E, and D.

The Diamat system is also suitable for hemoglobinopathy screening. Although it was originally designed mainly for determinations of HbA_{1C}, it can be used for detection of some Hb variants. It has been shown to separate seven variants, but many overlap partially with the HbA_{1C} peak [18]. Detection of aberrant peaks with the Diamat method, which interfere with the determination of HbA_{1C}, led us to the detection of two Hb variants, Hb Broussais and Hb Cemenelum [34]. Hb Broussais caused underestimation and Hb Cemenelum overesti-

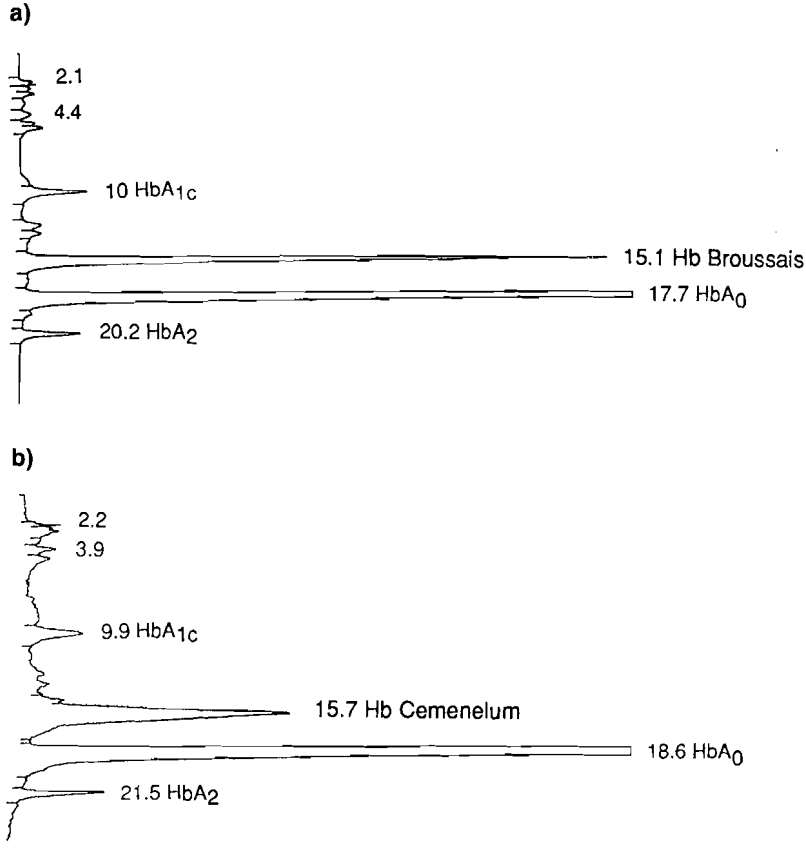

Figure 4 Cation exchange chromatography on PolyCAT A of a red cell hemolyzate with an α-chain variant of (a) Hb-Broussais and (b) Hb-Cemenelum. Time of elution since sample injection is indicated at each peak. Detection at 415 nm.

mation of HbA_{1c} concentration in the Diamat method. With PolyCAT A, both variants were totally separated (Fig. 4). The elution pattern can be used for preliminary identification of these Hb a variants, especially if standards are available.

VI. CONCLUSIONS

HPLC is a widely used technique for the determination of HbA_{1c} although recently developed immunoassays have started competing with HPLC. Since there is no general agreement on standardization of the methods for determination of glycated Hbs, HPLC ion exchange methods measuring HbA_{1c} are used to calibrate both boronate affinity methods and some new immunochemical methods [35]. Because of its good precision, ion exchange HPLC has been recommended as the gold standard for measurement of glycohemoglobin. However, it should be recognized that the presently used reference method is far from ideal because it measures some unglycated other Hb variants but not all of the glycated ones. The ongoing standardization of the HbA_{1c} assay methods initiated by the International Federation of Clinical Chemistry aims at developing a new reference method.

REFERENCES

1. Goldstein DE, Parker KM, England JD, England JE Jr, Wiedmeyer H-M, Rawlings SS, et al. Clinical application of glycosylated hemoglobin measurements. Diabetes 1982;31 (suppl. 3):70–78.
2. John WG. Glycated haemoglobin analyses—assessment of within- and between-laboratory performance in a large UK region. Ann Clin Biochem 1987;24:453–460.
3. Bodor GS, Little RR, Garrett N, Brown W, Goldstein DE, Nahm MH. Standardization of glycohemoglobin determinations in the clinical laboratory: three years of experience. Clin Chem 1992;38:2414–2418.
4. Weykamp CW, Penders TJ, Muskiet FAJ, van der Slik W. Effect of calibration on dispersion of glycohemoglobin values determined by 111 laboratories using 21 methods. Clin Chem 1994;40:138–144.
5. Trivelli LA, Ranney HM, Lai H-T. Hemoglobin components in patients with diabetes mellitus. N Engl J Med 1971;284:353–357.
6. Allen DW, Schroeder WA, Balog J. Observations on the chromatographic heterogeneity of normal adult and fetal human hemoglobin: a study of the effects of crystallization and chromatography on the heterogeneity and isoleucine content. J Am Chem Soc 1958;80:1628–1634.
7. Bissé E, Abraham EC. New less temperature-sensitive microchromatographic method for the separation and quantitation of glycosylated hemoglobins using a non-cyanide buffer system. J Chromatogr 1985;344:81–91.

8. Stenman U-H, Pesonen K, Ylinen K, Huhtala M-L, Teramo K. Rapid chromatographic quantitation of glycosylated haemoglobins. J Chromatogr 1984;297:327–332.
9. Toren EC, Vacik DN, Mockridge PB. Cation-exchange, high-performance liquid chromatographic determination of hemoglobin A_{1C}. J Chromatogr 1983;266:207–212.
10. Gupta SP, Hanash SM. Separation of hemoglobin types by cation-exchange high-performance liquid chromatography. Anal Biochem 1983;134:117–121.
11. Jeppsson J-O, Jerntorp P, Sundkvist G, Englund H, Nylund V. Measurement of hemoglobin A_{1C} by a new liquid-chromatographic assay: methodology, clinical utility, and relation to glucose tolerance evaluated. Clin Chem 1986;32:1867–1872.
12. Weykamp CW, Penders TJ, Siebelder CWM, Muskiet FAJ, van der Slik W. Interference of carbamylated and acetylated hemoglobins in assays of glycohemoglobin by HPLC, electrophoresis, affinity chromatography, and enzyme immunoassay. Clin Chem 1993;39:138–142.
13. Turpeinen U, Stenman U-H, Roine R. Liquid-chromatographic determination of acetylated hemoglobin. Clin Chem 1989;35:33–36.
14. Abraham EC, Perry RE, Stallings M. Application of affinity chromatography for separation and quantitation of glycosylated hemoglobins. J Lab Clin Med 1983;102:187–197.
15. Allen KR, Hamilton AD, Bodansky HJ, Poon P. Prevalence of haemoglobin variants in a diabetic population and their effect on glycated haemoglobin measurement. Ann Clin Biochem 1992;29:426–429.
16. Weykamp CW, Penders TJ, Muskiet FAJ, van der Slik W. Influence of hemoglobin variants and derivatives on glycohemoglobin determinations, as investigated by 102 laboratories using 16 methods. Clin Chem 1993;39:1717–1723.
17. Ou C-N, Rognerud CL. Rapid analysis of hemoglobin variants by cation-exchange HPLC. Clin Chem 1993;39:820–824.
18. Delahunty T. Convenient screening for hemoglobin variants by using the Diamat HPLC system. Clin Chem 1990;36:903–905.
19. Philcox JC, Haywood MR, Rofe AM. Hemoglobin A_{1C} by HPLC with the Pharmacia Mono S HR 5/5 cation-exchange column: influence of sample protein load on optimal chromatographic conditions. Clin Chem 1992;38:1488–1490.
20. Alpert AJ. Cation-exchange high-performance liquid chromatography of proteins on poly(aspartic acid)-silica. J Chromatogr 1983;266:23–37.
21. Ou C-N, Buffone GJ, Reimer GL, Alpert AJ. High-performance liquid chromatography of human hemoglobins on a new cation exchanger. J Chromatogr 1983;266:197–205.
22. Ellis G, Diamandis EP, Giesbrecht EE, Daneman D, Allen LC. An automated "high-pressure" liquid-chromatographic assay for hemoglobin A_{1C}. Clin Chem 1984;30:1746–1752.
23. Turpeinen U, Karjalainen U, Stenman U-H. Three assays for glycohemoglobin compared. Clin Chem 1995;41:190–195.
24. Bisse E, Wieland H. High-performance liquid chromatographic separation of human haemoglobins. Simultaneous quantitation of foetal and glycated haemoglobins. J Chromatogr 1988;434:95–110.
25. Weykamp CW, Penders TJ, Miedema K, Muskiet FAJ, van der Slik W. Standardiza-

tion of glycohemoglobin results and reference values in whole blood studied in 103 laboratories using 20 methods. Clin Chem 1995;41:82–86.
26. Flückiger R and Mortensen HB. Glycated Haemoglobins. J Chromatogr 1988;429: 279–292.
27. Cefalu WT, Wang ZQ, Bell-Farrow A, Kiger FD, Izlar C. Glycohemoglobin measured by automated affinity HPLC correlates with both short-term and long-term antecedent glycemia. Clin Chem 1994;40:1317–1321.
28. Abraham EC, Perry RE, Stallings M. Application of affinity chromatography for separation and quantitation of glycosylated hemoglobins. J Lab Clin Med 1983;102: 187–197.
29. Herold DA, Boyd JC, Bruns DE, Emerson JC, Burns KG, Bray RE, et al. Measurement of glycosylated hemoglobins using boronate affinity chromatography. Ann Clin Lab Sci 1983;13:482–488.
30. Wilson JB, Headlee ME, Huisman THJ. A new high-performance liquid chromatographic procedure for the separation and quantitation of various hemoglobin variants in adults and newborn babies. J Lab Clin Med 1983;102:174–186.
31. Rogers BB, Wessels RA, Ou C-N, Buffone GJ. High-performance liquid chromatography in the diagnosis of hemoglobinopathies and thalassemias. Am J Clin Pathol 1985;84:671–674.
32. van der Dijs FPL, van den Berg GA, Schermer JG, Muskiet FD, Landman H, Muskiet FAJ. Screening cord blood for hemoglobinopathies and thalassemia by HPLC. Clin Chem 1992;38:1864–1869.
33. Eastman JW, Wong R, Liao CL, Morales DR. Automated HPLC screening of newborns for sickle cell anemia and other hemoglobinopathies. Clin Chem 1996;42: 704–710.
34. Turpeinen U, Sipilä I, Anttila P, Karjalainen U, Kuronen B, Kalkkinen N, et al. Two α-chain hemoglobin variants, Hb Broussais and Hb Cemenelum, characterized by cation-exchange HPLC, isoelectric focusing, and peptide sequencing. Clin Chem 1995;41:532–536.
35. Karl J, Burns G, Engel WD, Finke A, Kratzer M, Rollinger W, et al. Development and standardization of a new immunoturbidimetric HbA_{1c} assay. Klin Lab 1993;39: 991–996.

2

Analysis of Posttranslational Modifications in Recombinant Proteins by HPLC and Mass Spectrometry

Rainer Bischoff* and Bernadette Bouchon
Transgene S.A., Strasbourg, France

I. INTRODUCTION

A number of recombinant proteins are being produced as pharmaceuticals with annual sales of U.S. $9 billion in 1994 [1,2]. Therapeutic applications of these biopharmaceuticals include stimulation of cell growth, regulation of the immune system and fibrinolysis, to name a few. These advances of recombinant proteins toward the marketplace was made possible by the development of efficient and reproducible production and purification systems that permit manufacture of these complex molecules in large amounts with consistent quality suitable for human use. Control of the quality of biopharmaceuticals is crucial not only during large-scale manufacturing but also during the research and development phase, as impurities and contaminants have to be characterized and reduced to acceptable levels.

A complete analysis of a recombinant protein necessitates the combined use of separation techniques such as electrophoresis and high-performance liquid chromatography (HPLC) with methods which allow the characterization of the separated molecular species such as protein sequencing and, in particular, mass spectrometry (MS). It is probably fair to say that no instrumental analytical method has had a greater impact on protein analysis in the last 5–10 years than MS [3]. The advent of ionization techniques that allow us to generate gas phase ions of high molecular weight, nonvolatile biomolecules such as electrospray

* *Current affiliation:* Senior Research Scientist, Biochemistry and Bioanalytical Chemistry Department, Astra-Draco AB, Lund, Sweden.

ionization (ESI) [4], and matrix-assisted laser desorption ionization (MALDI) [5] has opened possibilities for obtaining precise molecular mass measurements on proteins, peptides, oligonucleotides, and oligosaccharides. This development has enabled especially the growing biotechnology industry to integrate MS into strategies to characterize recombinant proteins in detail and to assure consistent quality [6–8].

The combination of efficient separation techniques such as HPLC and capillary electrophoresis (CE) with MS is rapidly becoming an indispensable analytical tool in many academic and industrial laboratories [9–14]. The power of analyzing separated components by MS results from the fact that the molecular mass is an inherent property of a given compound. In the case of recombinant proteins, where the amino acid sequence is generally known, it is possible to compare the calculated mass with the measured mass and thus to confirm the expected structure or to detect modifications. More detailed information can be obtained when analyzing defined proteolytic digests of a protein by either off-line (fraction collection) or on-line HPLC-mass spectrometry (LC-MS). Such analyses permit localization of the modified site(s) and collection of precise data about the molecular mass of the modification. Thus it is not surprising that LC-MS studies have focused in many cases on the characterization of posttranslational modifications such as glycosylations and phosphorylations as well as on the identification of modifications that were due to culture, purification, or storage conditions [15–22].

The following studies of two recombinant proteins that are being developed as vaccine candidates against schistosomiasis or Lyme disease illustrate the characterization of posttranslational modifications by combining MS with chromatographic separation techniques. rSmp28, an antigen that was originally isolated from the parasite *Schistosoma mansoni* [23], was expressed to high levels in the cytoplasm of *Saccharomyces cerevisiae*, whereas rOspA, an outer membrane protein of *Borrelia burgdorferi*, the Lyme disease–causing agent, was produced in *Escherichia coli* [24]. Both proteins were shown to be heterogeneous due to posttranslational modifications as determined by isoelectric focusing in the case of rSmp28 [25] or by MS for rOspA [26,27]. In this chapter we describe the analytical strategy that led to the characterization of these modifications, stressing the importance of integrating efficient separation methods such as HPLC with MS.

II. RECOMBINANT *SCHISTOSOMA MANSONI* GLUTATHIONE-*S*-TRANSFERASE rSmp28

Schistosomiasis is a chronic debilitating parasitic disease affecting approximately 200 million people worldwide and causing 500,000 deaths per year. Although

effective chemotherapy exists, reinfection remains a serious problem. It is thus of major interest to develop novel approaches to vaccines based on recombinant proteins such as the recently identified glutathione-*S*-transferase Smp28 [23].

The study on rSmp28, a 210-amino-acid protein expressed intracellularly in *Saccharomyces cerevisiae*, illustrates that highly efficient expression systems in cultures grown to elevated biomass in a bioreactor may lead to unexpected posttranslational modifications. Characterization of such modifications necessitates their detection in samples taken during the cultivation process, isolation of the modified protein, and structural analysis.

A. Modification of rSmp28 During High-Biomass Culturing of *S. cerevisiae* and Isolation of the Major Modified Form rSmp28/2 by Anion Exchange HPLC

rSmp28 was produced as a cytoplasmic protein in *S. cerevisiae*. Overexpression of rSmp28 to more than 6 g/L of culture was accompanied by the appearance of a second form (rSmp28/2) with a measured isoelectric point of 7.9, indicating an increase in net negative surface charge (Fig. 1). Analysis of cellular extracts throughout the process by isoelectric focusing showed that the amount of rSmp28/2 increased with time (Fig. 1: lane 1, preculture; lane 2, after 19.5 h; lane 3, after 51 h). During culture biomass increased from 8.8 g/L cell dry weight at 19.5 h to 78.7 g/L after 51 h and the ethanol concentration in the culture supernatant went through a maximum of 12 g/L at 45 h, indicating some anaerobic glucose metabolism.

Analyses of the protein bands by N-terminal amino acid sequencing using Edman degradation after electroblotting to a polyvinylidene difluoride (PVDF)

Figure 1 Isoelectric focusing of rSmp28 expressed in *S. cerevisiae* at different stages of the culture. Lane 1: preculture used to inoculate the bioreactor. Lane 2: after 19.5 h of culture (biomass: 8.8 g/L cell dry weight). Lane 3: after 51 h of culture (biomass: 78.7 g/L cell dry weight). The pH gradient in the gel as indicated on the right margin was determined with marker proteins of known isoelectric points. (From Ref. 39.)

membrane confirmed that both of them contained the expected N-terminal sequence excluding N-terminal blocking by, for example, formylation or acetylation [25] in contrast to the presence of an *N*-acetylalanine in the natural protein [28]. To further characterize the modification, rSmp28/7 and rSmp28/2 were separated by anion exchange HPLC using a shallow gradient of potassium chloride (KCl) at pH 8.55 (0.5 mM KCl/min) (Fig. 2). Anion exchange HPLC allowed separation of three major forms of the protein (rSmp28/1, 2, and 3). The nature of the modification in rSmp28/3, which appeared only after purification, has not been identified in this case but may be related to the binding of glutathione to the single free cysteine residue (Cys^{139}) as previously shown [13]. rSmp28/1 and rSmp28/2 were baseline-separated and appeared to be homogeneous when analyzed by isoelectric focusing in an immobilized pH gradient (Fig. 2, insert). It is noteworthy that rSmp28/2 was slowly transformed into rSmp28/1 upon incubation at 37°C in water, underscoring the labile nature of the N-terminal modification.

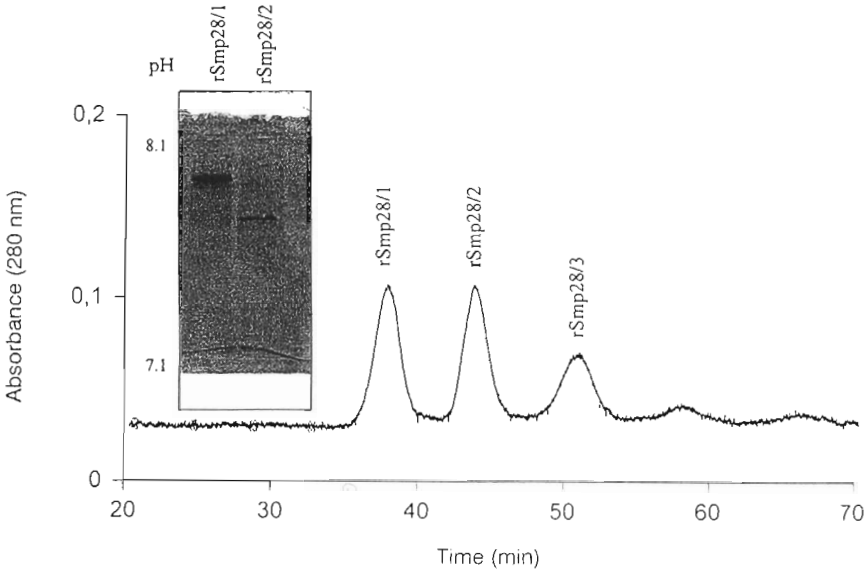

Figure 2 Separation of rSmp28/1 and rSmp28/2 by anion exchange HPLC. A third form (rSmp28/3) with increased affinity for the stationary phase is visible. This form occurred after purification and may correspond to the previously described glutathionylated rSmp28 [13]. Insert: Isoelectric focusing of purified rSmp28/1 and rSmp28/2 in an immobilized pH gradient gel covering the pH range from 7.1 to 8.1. (From Ref. 39.)

B. Peptide Mapping by LC-MS

LC-MS of the tryptic peptide maps of rSmp28/1 and rSmp28/2 resulted in very similar chromatograms (Fig. 3). However, comparison of the traces revealed that the map of rSmp28/2 contained an additional peak at 12.5 min (marked with a circle in Fig. 3B) with a measured mass of 679.8 ± 0.2 Da. Amino acid composition analysis of the corresponding peptide was in good agreement with the expected composition of the N-terminal tryptic fragment AGEHIK, whereas the measured mass deviated by 26.1 Da from the expected value of 653.7 Da. Furthermore, the peptide fragment proved to be inaccessible to automated Edman degradation in contrast to rSmp28/2 from which it was derived. Analysis of the broad peak preceding the modified peptide fragment showed that the peptide map of rSmp28/2 also contained some nonmodified N-terminal peptide (retention time 11.2–11.5 min; labeled with an asterisk in Fig. 3B) with a measured mass of 653.9 ± 0.2 Da. The peptide map of rSmp28/1 contained only the nonmodified N-terminal peptide fragment eluting between 11.2 and 11.5 min (labeled with an asterisk in Fig. 3A; measured mass 653.8 ± 0.4 Da). These results indicated that the labile N-terminal modification of rSmp28/2 had partially rearranged to result in a permanently blocked N-terminal peptide fragment and a smaller amount of the unmodified N-terminal peptide. Complete analysis of the residual peptide map by mass matching and Edman degradation confirmed that all other peptide fragments were unmodified and identical for both rSmp28/1 and rSmp28/2, indicating strongly that the shift in isoelectric point was due to modification of the amino terminal region.

C. Analysis of the Modified N-Terminal Peptide from rSmp28/2 by Reversed-Phase HPLC and Deuterium Exchange Mass Spectrometry

In order to characterize the modification within the N-terminal peptide in more detail, reversed-phase HPLC with a shallow gradient of acetonitrile (0.27%/min) was employed to confirm its homogeneity. Surprisingly, the modified peptide was separated into two components (Fig. 4), which had the same amino acid compositions as well as the same molecular mass of approximately 680 Da. Isomerization of the N-terminal peptide fragment obtained after tryptic digestion of rSmp28/2 can be explained by the fact that the peptide contains a cyclic linkage that formed during digestion. Since this phenomenon was only observed in the case of rSmp28/2, it is likely to be related to the original N-terminal modification that led to the shift in isoelectric point.

To test the hypothesis of a cyclic linkage, both the free and blocked N-terminal peptides were subjected to deuterium exchange followed by MS. In this

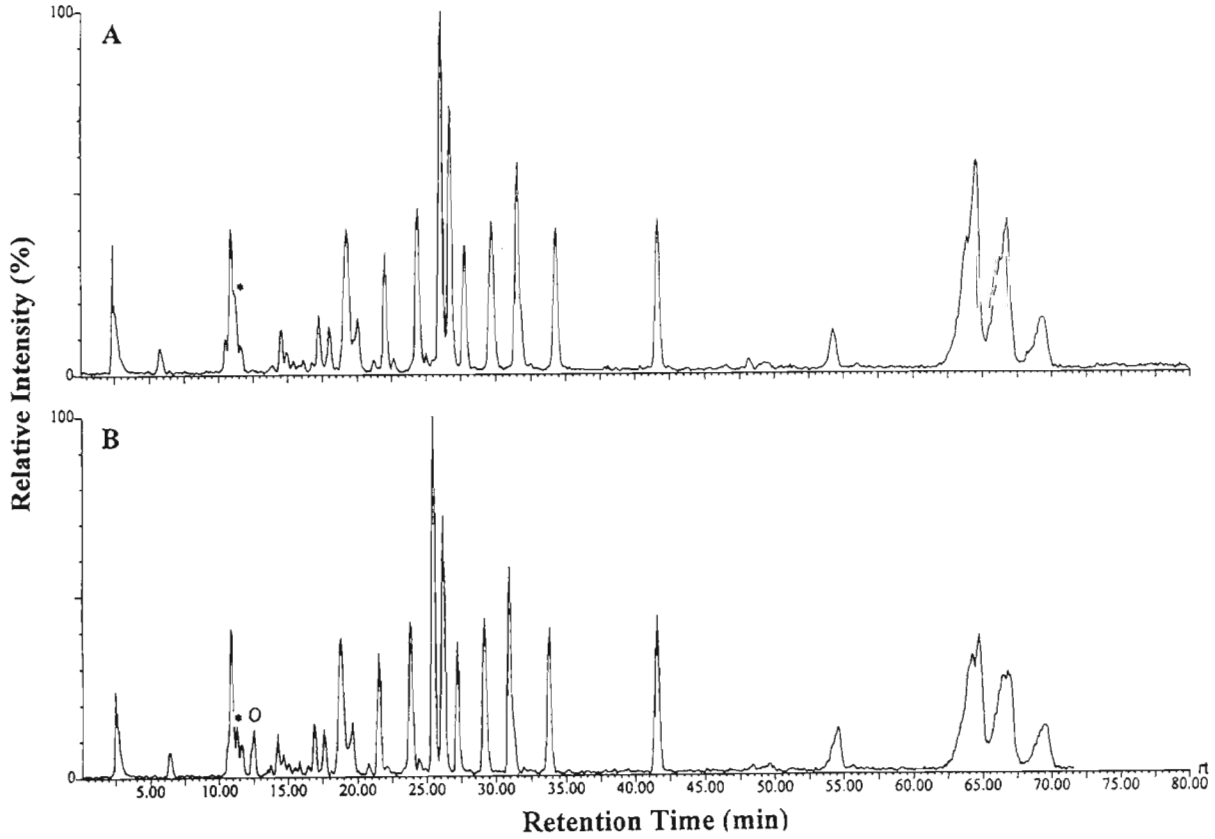

Figure 3 Peptide mapping of rSmp28/1 (A) and rSmp28/2 (B) after tryptic digestion by on-line liquid chromatography electrospray ionization mass spectrometry (LC-MS). Traces show the base-peak intensity corrected total ion current. The modified N-terminal peptide fragment in rSmp28/2 is marked with a circle (B) and the nonmodified N-terminal peptide fragments are labeled with asterisks (A and B). (From Ref. 39.)

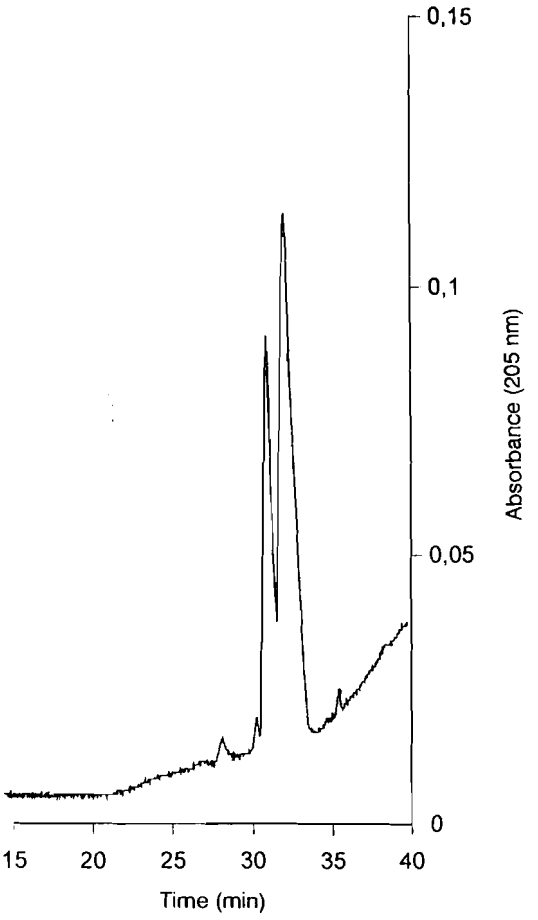

Figure 4 Separation of the modified rSmp28 N-terminal peptide fragment into two isomeric components by reversed-phase HPLC. The separated components proved to have identical amino acid compositions and molecular masses. Both were inaccessible to N-terminal Edman degradation. The ratio between the earlier and later eluting peptides was 1:2 as determined by quantitative amino acid composition analysis. (From Ref. 39.)

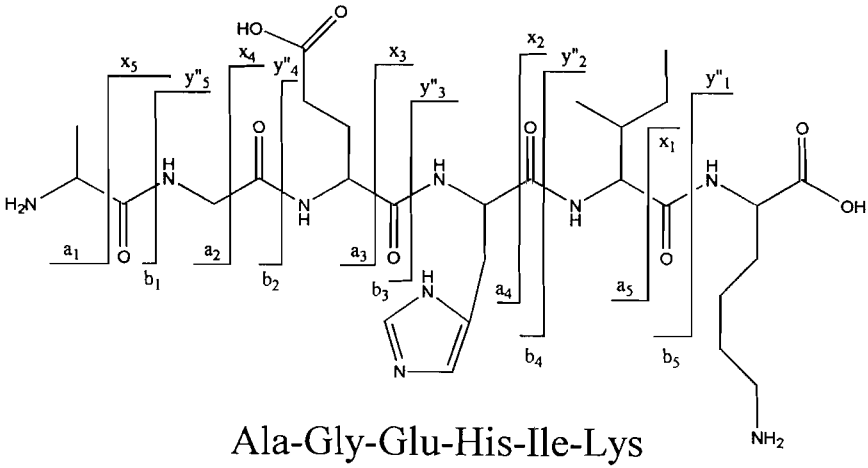

Figure 5 Schematic representation of the structure of the unmodified rSmp28 N-terminal peptide fragment showing the expected number of exchangeable hydrogen atoms and fragmentation sites.

analysis, MS will detect an increase of 1 Da for each exchanged hydrogen atom. Since only acidic hydrogen atoms bound to nitrogen (amines, amides, imidazoles) or to oxygen (carboxylic acids, alcohols) will exchange, one would expect a mass increase of 12 Da for the nonmodified N-terminal peptide (Fig. 5). While the free peptide derived from rSmp28/1 showed the expected mass increase of 12.1 Da (Fig. 6A), its blocked counterpart showed only a mass increase of 10.0 Da, which is consistent with a cyclic modification removing two exchangeable hydrogen atoms (Fig. 6B).

D. Tandem Mass Spectrometry of the Modified N-Terminal Peptide

While the above results indicated that the modification of the N-terminal peptide fragment was due to intramolecular cyclization, it did not allow localization of its position within the peptide or determination of its structure. Tandem MS with collision-induced dissociation (CID) was thus applied to obtain characteristic fragment ions. Due to the limited amount of modified peptide available (approximately 15 pmol), tandem MS was performed using the nanoelectrospray technique, which permits introduction of the sample into the electrospray ion source at a flow rate of approximately 20 nl/min [29]. It was thus possible to extend the measuring time to 2.5 h on a sample volume of 3 µl, which allowed thorough

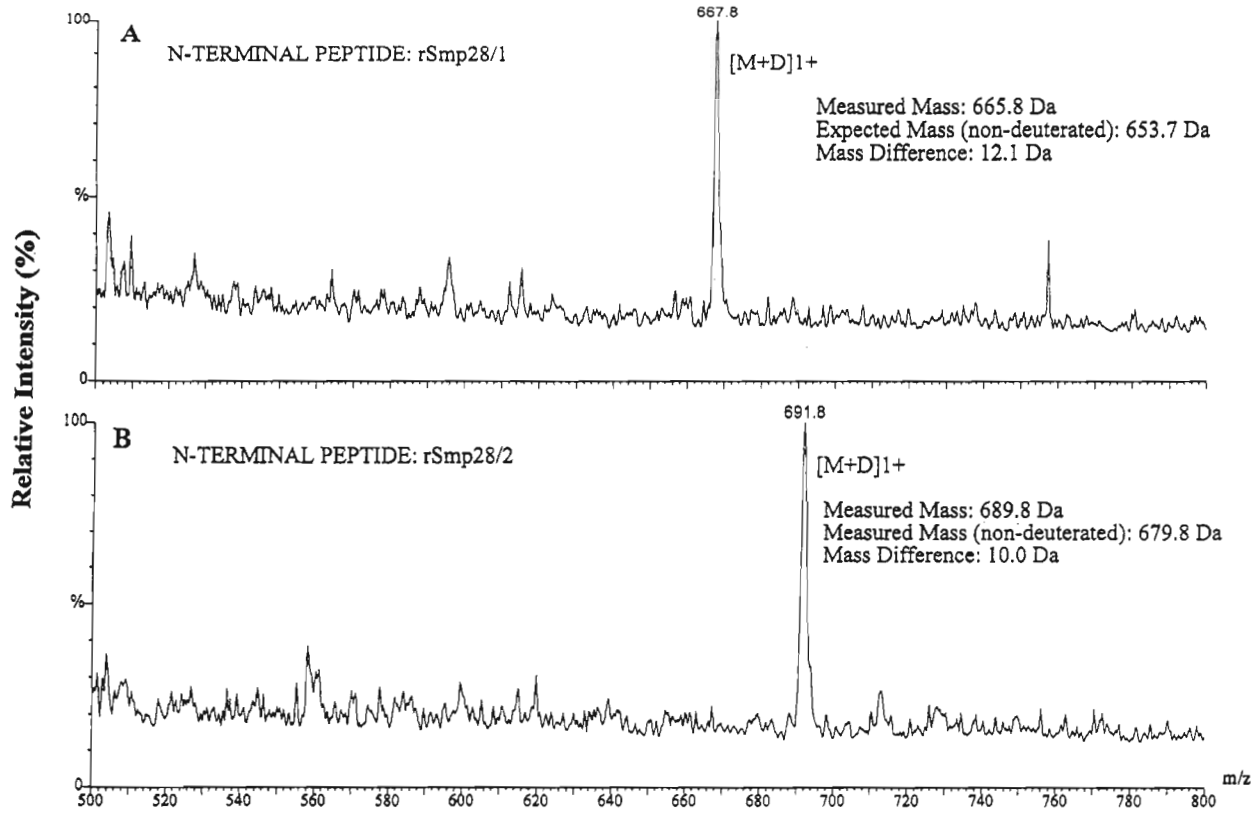

Figure 6 Deuterium-hydrogen exchange of the nonmodified (A) and modified (B) N-terminal peptide fragments of rSmp28 in D_2O (expected number of exchangeable protons in the nonmodified peptide = 12; see Fig. 5). The measured mass of the nonmodified peptide (665.8 Da) differed by 12.1 Da from the expected mass of the nondeuterated form in agreement with its structure, whereas the measured mass of the modified peptide (689.8 Da) differed by only 10.0 Da from the measured mass of its nondeuterated form, indicating the loss of two exchangeable hydrogen atoms. (From Ref. 39.)

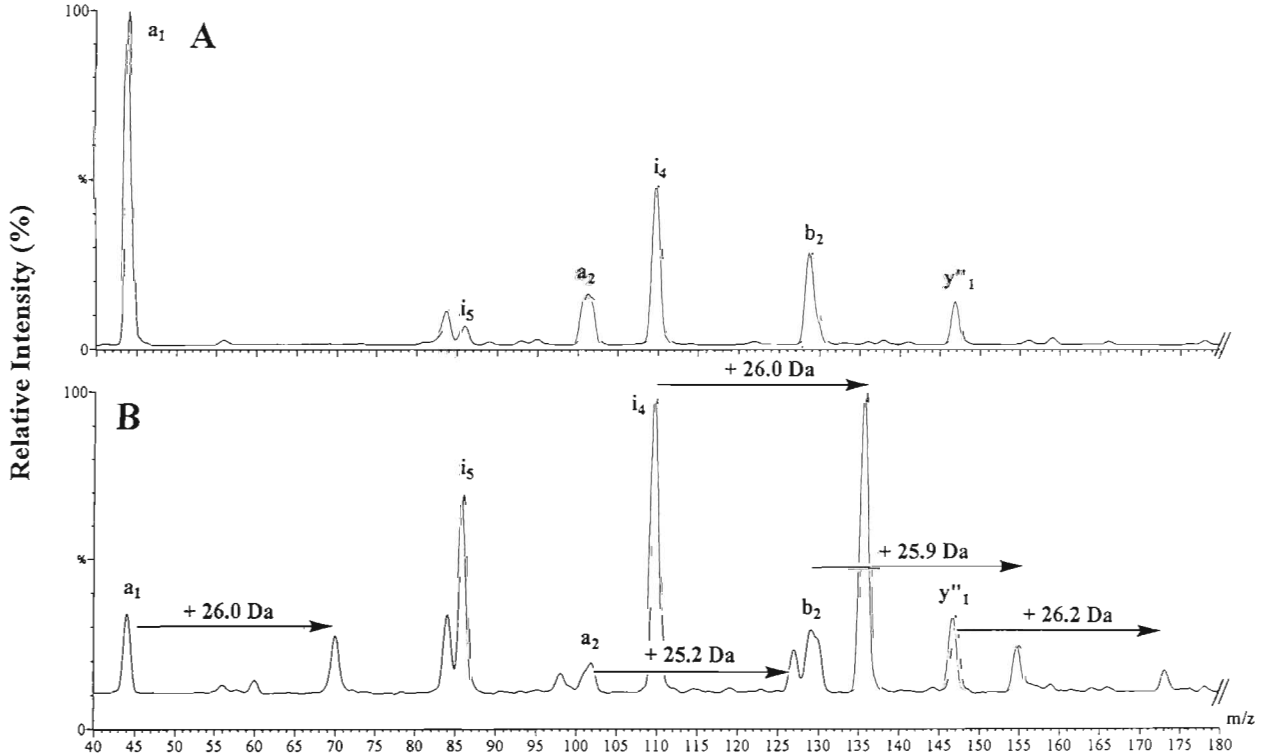

Figure 7 Tandem mass spectrometry of the unmodified (A and C; doubly charged parent ion: 328 amu) and modified N-terminal peptide (B and D; doubly charged parent ion: 341 amu) of rSmp28 using the nanoelectrospray technique [29]. (For exact mass values, see Table 1; the region between 180 and 355 amu is not shown.) Panels A and B show a comparison of the fragments obtained in the range from 40 to 180 Da. It is noteworthy that the a_1 fragment of the modified peptide appeared at the expected mass (m/z = 44.0) as well as at m/z = 70.0 (Δm: +26.0 Da) confirming that Ala^1 was one of the modified amino acid residues. Furthermore, the y''_1 fragment of the modified peptide occurred at the expected mass (m/z = 147.0) as well as at m/z = 173.2 (Δm: +26.2 Da) (Fig. 7B) identifying Lys^6 as another

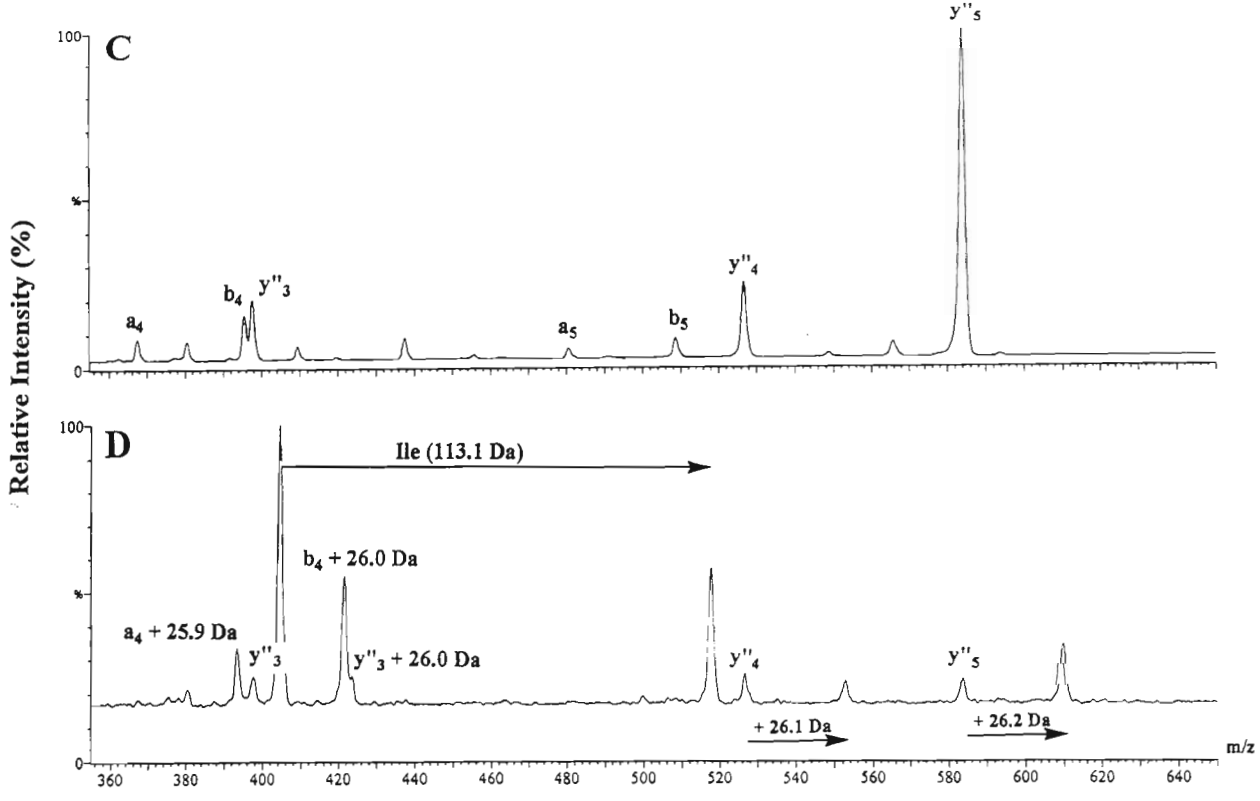

modified site. The abundant immonium ion i_4, which is derived from His[4] [30], occurred at the expected value (m/z = 110.0) and at m/z = 136.0 (Δm: +26.0 Da) in the modified peptide (see Fig. 7B). These results show that cyclization occurred between Ala[1] and Lys[6] as well as with His[4] (see Fig. 8). These results were corroborated by other a, b, and y″ ions in the region between 355 and 650 amu, which showed a +26 Da series in the case of the modified peptide (Fig. 7D) while the unmodified peptide gave the expected fragment ions (Fig. 7C). Fragment ions at 404.5 and 517.6 Da could not be assigned but are related by a Δm of 113.1 Da, which corresponds to Ile. (From Ref. 39.)

Table 1 Comparison of the Measured and Calculated Mass Values for Fragment Ions Obtained by Nanoelectrospray Tandem Mass Spectrometry of rSmp28 N-Terminal Peptides (see Fig. 7).

Fragment ion[a]	Measured mass (Da) Nonmodified peptide	Measured mass (Da) Modified peptide	Expected mass (Da)	Fragment
y''_1	147.0	147.0 and 173.2 (Δm: +26.2)	147.2	Lys
y''_2	260.4	260.2 and 286.4 (Δm: +26.2)	260.4	Ile-Lys
y''_3	397.5	397.6 and 423.6 (Δm: +26.0)	397.5	His-Ile-Lys
y''_4	526.6	526.6 and 552.7 (Δm: +26.1)	526.6	Glu-His-Ile-Lys
y''_5	583.7	583.6 and 609.7 (Δm: +26.1)	583.7	Gly-Glu-His-Ile-Lys
a_1	44.0	44.0 and 70.0 (Δm: +26.0)	44.1	Ala
a_2	101.2	101.8 and 127.0 (Δm: +25.2)	101.1	Ala-Gly
a_3	n.d.[b]	n.d.	230.3	Ala-Gly-Glu
a_4	367.4	393.3 (Δm: +25.9)	367.4	Ala-Gly-Glu-His
a_5	480.6	n.d.	480.6	Ala-Gly-Glu-His-Ile
b_2	129.1	129.2 and 155.1 (Δm: +25.9)	129.1	Ala-Gly
b_4	395.4	421.4 (Δm: +26.0)	395.4	Ala-Gly-Glu-His
b_5	508.6	n.d.	508.6	Ala-Gly-Glu-His-Ile
i_4	110.0	110.0 and 136.0 (Δm: +26.0)	110.1	His-derived immonium ion

[a] According to Ref. 38.
[b] Not detected.

optimization of the fragmentation conditions as well as adjustment of the resolution of the mass analyzers.

Edman degradation had already established that the N termini of the modified peptides were blocked, implicating N-terminal alanine as one of the modified sites. Comparative analyses of fragments generated by CID from the doubly charged molecular ions of both the modified and the unmodified N-terminal peptides (parent ions: m/z = 328 and 341, respectively) confirmed that the N-terminal alanine residue is one of the modified sites, since the a_1 fragment appeared at the expected 44.0 Da in the case of the unmodified peptide whereas a second fragment at 70.0 Da (Δm = 26.0 Da) was generated for the modified peptide (Fig. 7A and B). The fragmentation pattern of the free peptide allowed assignment of the complete y″-ion series and most of the a-ion series (Table 1, Fig. 7A and C), which provided a comparative spectrum to assign the modified sites. Furthermore, three of the five expected b-ions and a histidine-related immonium fragment ion (i_4: m/z = 110.0) were detected [30]. The pattern was in complete agreement with the expected sequence AGEHIK. In comparison, the fragmentation pattern of the modified peptide differed from its nonmodified counterpart with respect to the y″-, b-, and a-ion series as well as the histidine-related immonium ion, which occurred at the expected mass values as well as at mass values that were 26 Da higher (Table 1, Fig. 7B and D). A mass difference of 26 Da was indicative that the respective fragment ion contained the unknown modification. This mass difference was found in all of the five y″-ions and in particular in the y''_1-ion which corresponded to the C-terminal lysine residue (Fig. 7A), indicating that an intramolecular crosslink had formed between Ala^1 and Lys^6. Furthermore, the histidine-related internal immonium fragment ion i_4 (m/z = 110.0) was modified giving rise to a second fragment ion at 136.0 Da. Taken together these results showed that cyclization of the N-terminal peptide derived by tryptic digestion from rSmp28/2 occurred between the N-terminal amino group and the C-terminal lysine residue as well as with His^4 in agreement with the observation that two isomers were formed upon cyclization.

E. rSmp28/2 Is Modified by Acetaldehyde During Culturing of *S. cerevisiae*

The obtained results are consistent with the initial formation of an aldimine at the N terminus of rSmp28 due to the addition of acetaldehyde followed by intramolecular cyclization with either His^4 or Lys^6 during tryptic digestion to produce two cyclic peptide derivatives as shown in Fig. 8. This interpretation is based on the following data. (1) rSmp28/2 is modified in a reversible manner, since rSmp28/1 was regenerated upon incubation for 3 days at 37°C in water. Such chemical instability has also been observed for a peptide that was modified at

its N terminus with acetaldehyde in the case of the hemoglobin β chain [31]. Furthermore, rSmp28/2 is not N-terminally "blocked" when analyzed by Edman degradation excluding modifications such as N-terminal formylation or acetylation and again underlining the labile nature of the modification. (2) Tryptic digestion of rSmp28/2 produced a modified form of the N-terminal hexapeptide AGEHIK that was blocked to Edman degradation. The observed mass difference

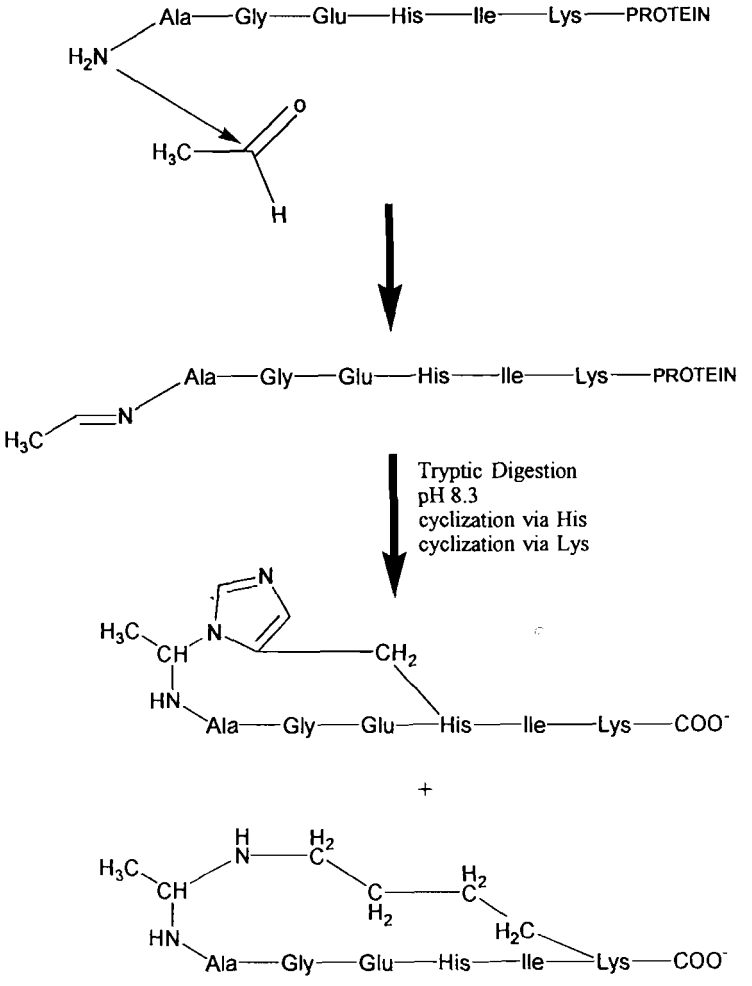

Figure 8 Schematic drawing of the mechanism leading to the generation of two isomeric cyclic peptides after tryptic digestion of the aldimine-modified protein rSmp28/2. (From Ref. 39.)

of 26 Da, measured with a precision of ±0.2 Da, eliminated N-terminal formylation as a possibility and is consistent with the cyclic modification shown in Fig. 8. (3) The isolated peptide was composed of two isomers that lacked two deuterium-exchangeable hydrogen atoms as compared to the nonmodified peptide, which is consistent with the cyclic structures shown in Fig. 8. (4) Fragments obtained by tandem MS localized the 26-Da mass difference to the N-terminal alanine as well as to the C-terminal lysine and the internal histidine residue identifying these amino acids as part of the cycle. This example of an unexpected posttranslational modification shows that its successful identification was due to highly resolving chromatographic methods to purify the modified protein and to obtain the modified peptide after tryptic digestion as well as to detailed mass spectrometric measurements including tandem MS.

III. ANALYSIS OF THE POSTTRANSLATIONAL LIPIDATION OF RECOMBINANT OUTER SURFACE PROTEIN A (rOspA) FROM *BORRELIA BURGDORFERI*

Lyme disease is a tick-borne infection caused by the spirochete *Borrelia burgdorferi*. Infected people develop antibodies in response to several *B. burgdorferi* antigens. The outer surface protein A, OspA, a 257-amino-acid protein, is one of them [32] and is thus considered as a potential vaccine candidate. Cloning of the gene suggested that OspA is likely to be a lipoprotein due to the lipopeptide consensus signal sequence [33]. This was confirmed by incorporation of [^{3}H]palmitate in OspA lipoprotein in vivo [24] and by electrospray mass spectrometry (ESMS) analysis of the purified recombinant protein [26,27].

Bacterial lipoproteins constitute a class of strongly hydrophobic membrane proteins, with an N-terminal cysteine posttranslationally modified to an *S*[2,3-bis(acyloxy)-(2*RS*)-propyl]-*N*-acylcysteine [34] (Fig. 9), according to the model established by Hantke and Braun [35]. Very few structural studies have been performed on such lipoproteins due to their amphipathic nature [26,36] which renders purification of even analytical amounts rather difficult. In order to analyze the lipidation of rOspA produced in *E. coli*, a combination of GC-MS and normal phase HPLC was developed.

A. Fatty Acid Analysis

Analyses of the intact protein indicated that it was posttranslationally modified through lipidation of the N-terminal cysteine [26,27] (see Fig. 9). After detergent removal by acetone precipitation, intact rOspA was submitted to an acidic methanol treatment in order to generate fatty acid methyl esters via transmethylation. Fatty acid methyl esters were extracted into hexane, which permitted their analy-

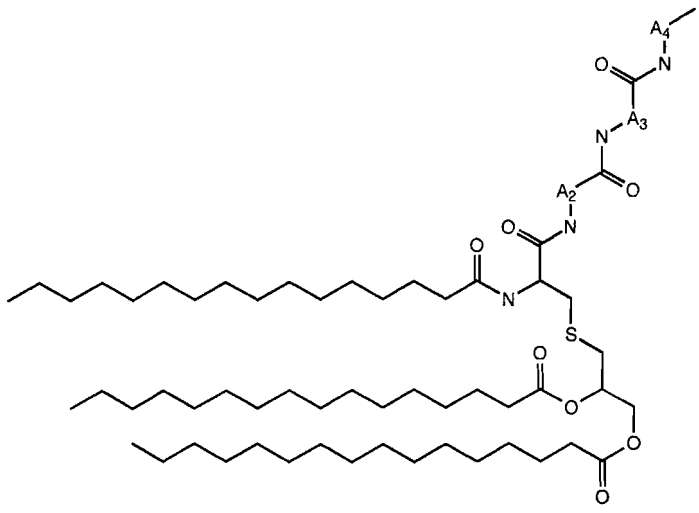

S-[2,3-Bis(palmitoyloxy)-(2RS)-propyl]-N-palmitoyl-(R)-cysteinyl ("Pam3Cys") configuration
(A2, A3, A4, ... : amino acids)

Figure 9 Structure of the lipidated N-terminal tryptic peptide CK of rOspA containing three palmitoyl residues.

sis by GC-MS. The chromatogram (Fig. 10) shows the fatty acid composition of rOspA, with fatty acids ranging from C14 to C18. The individual mass spectra of each of these fatty acids show the molecular ion and the typical fragmentation pattern permitting the identification of saturated fatty acids (C14:0, C16:0; A and C) and monounsaturated fatty acids (C16:1, C18:1; B and D) [37]. C16:0 (65%) and C16:1 (21%) were the major components of the total fatty acid content. To ascertain that the fatty acids were attached to the N terminus as expected, complementary analyses were performed focusing on the lipidated N-terminal tryptic peptide.

B. Purification and Analysis of the N-Terminal Peptide

A tryptic digestion of rOsp A was performed on 1 nmol (25 μg) and the peptides were analyzed by HPLC. While all attempts at using short-chain reversed-phase HPLC supports (C1, C4) failed to give reproducible results, normal phase HPLC on a silica column (Iatrobeads) reproducibly separated the N-terminal lipopeptide from the more hydrophilic peptide fragments. The lipidated peptide eluted first

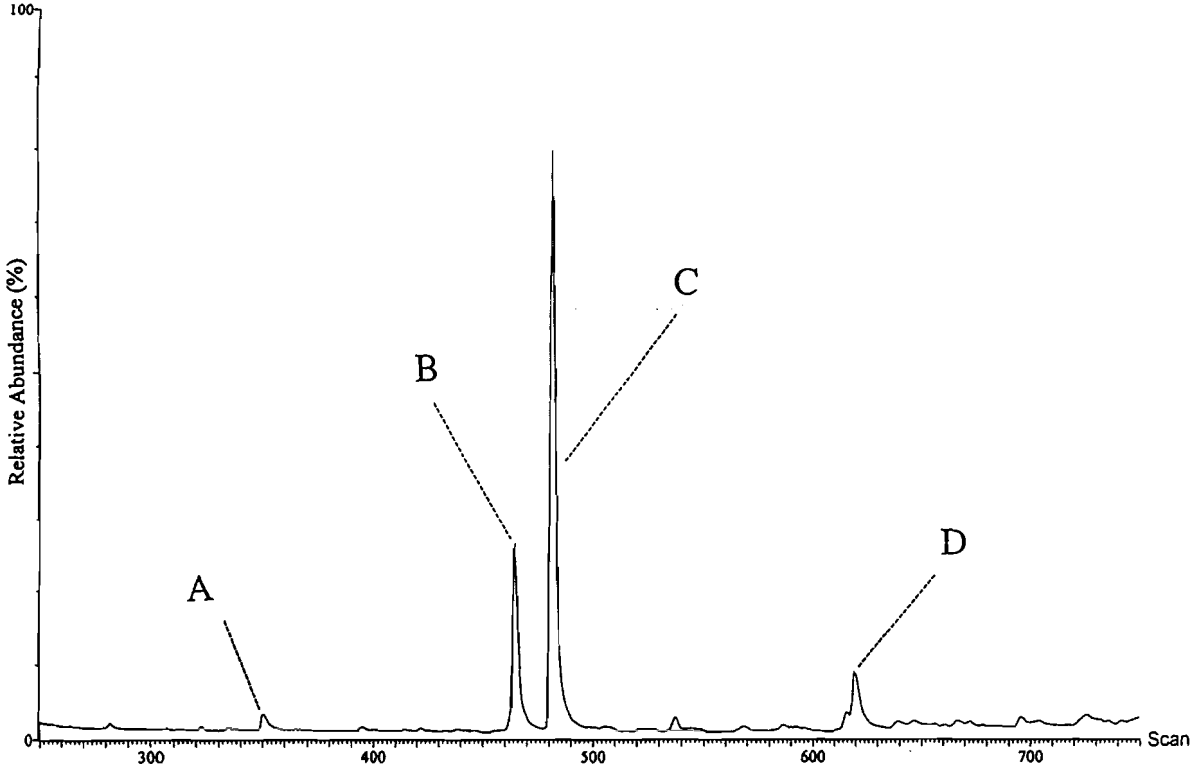

Figure 10 GC-MS analysis of rOspA fatty acids. The trace is the summation of m/z 50–550 ion intensities. Time scale, 1 scan = 1 s. The components labeled A, B, C, and D have been identified by their mass spectrum to be (A) C14:0, myristic acid (expected mass, 242 Da); (B) C16:1 (expected mass, 268 Da); (C) C16:0, palmitic acid (expected mass, 270 Da); (D) C18:1 (expected mass, 296 Da). Due to isomerization that occurs during the acidic treatment, the precise double-bond position could not be assigned in the unsaturated fatty acids. (From Ref. 27.)

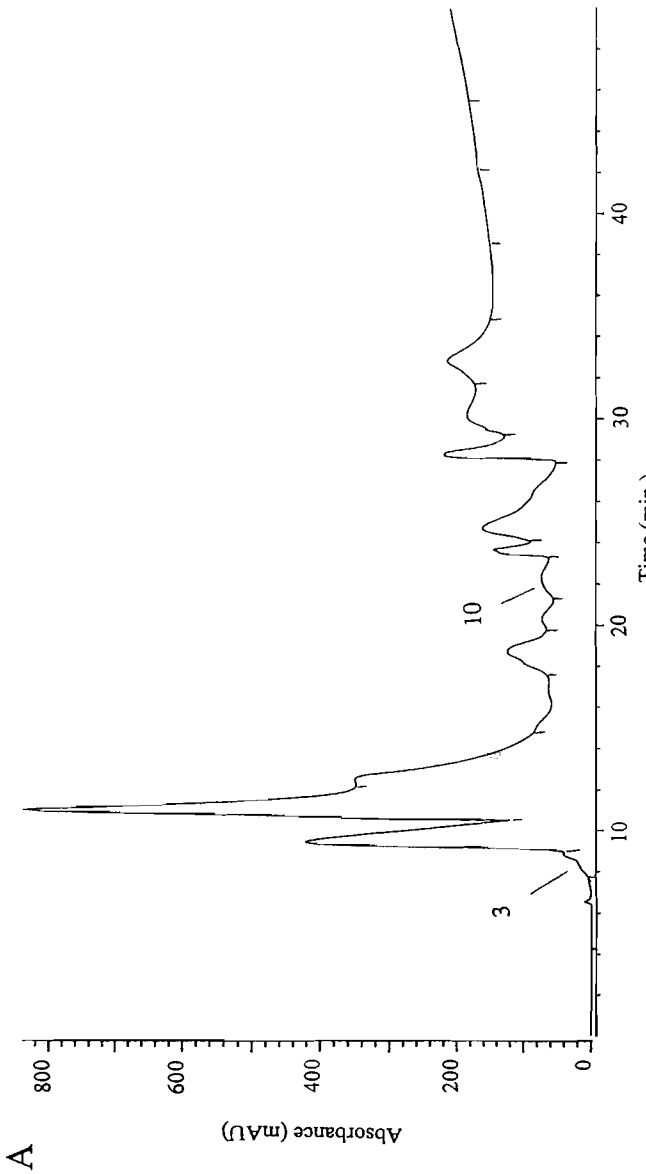

Figure 11 Analysis of the N-terminal peptide of rOspA after tryptic digestion. (A) HPLC of the tryptic digest on a silica column monitored at 205 nm. Tic marks on UV profile indicate fractions collected. Each fraction was analyzed by ESMS; the N-terminal lipidated peptide (T1) was identified in fraction 3.

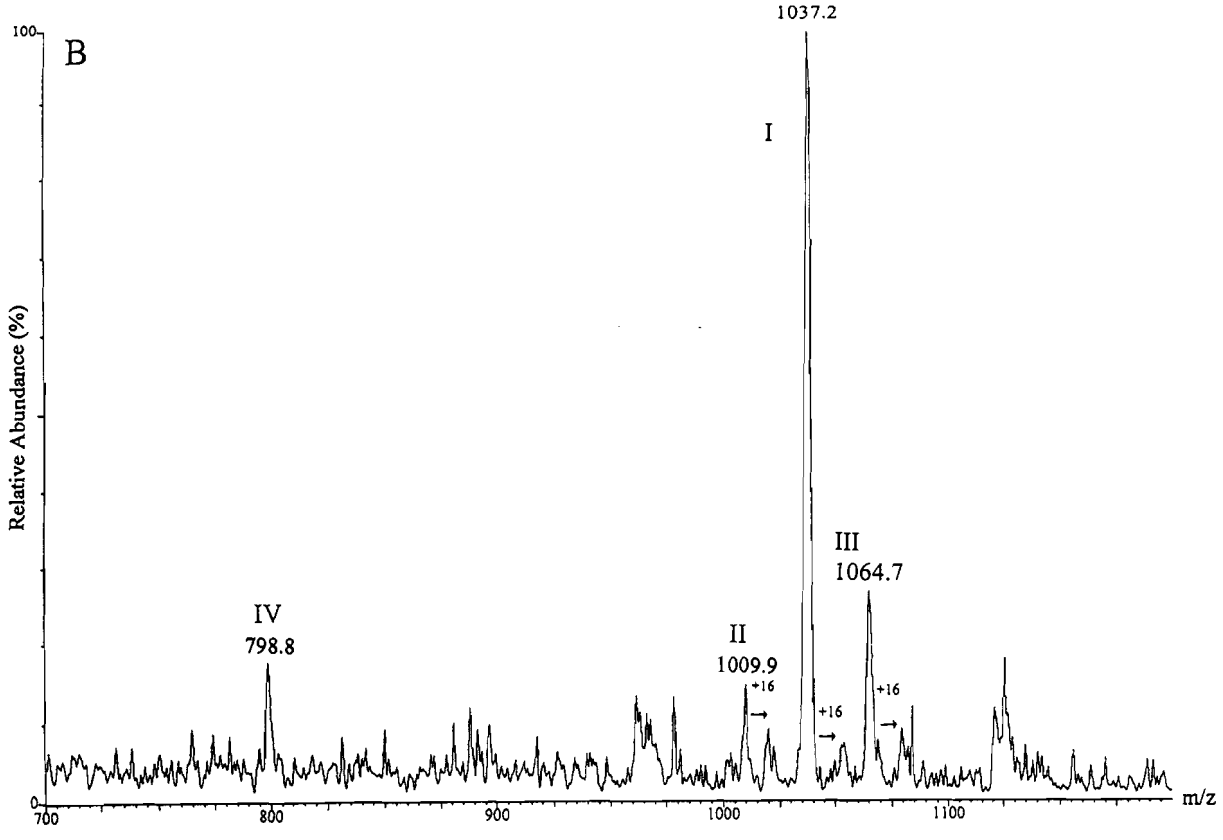

Figure 11 Continued (B) ESMS spectrum of fraction 3 corresponding to rOspA N-terminal peptide (see Table 2). I corresponds to the expected complete form (Pam3CysLys); IV to an incomplete form (Pam2CysLys); II and III to fully lipidated forms but with two palmitates and one myristate or two palmitates and one octadecenoate residue, respectively. Oxidized forms (cysteine sulfoxide) of the different forms were also observed (+16 Da). (From Ref. 27.)

as expected for the most hydrophobic component of the mixture (Fig. 11A). Analysis by ESMS of the collected fraction permitted localization of the N-terminal peptide based on its mass and ionization profile (Fig. 11B). Due to the very short peptidic chain (a single peptide bond, C^1K^2, Fig. 9), absorption at 205 nm was very low, and the peptide appeared as a shoulder on the major chromatographic peak. The purified peptide (<1 μg) was collected for further analysis.

Tryptic peptides are generally characterized during ESMS analysis by the presence of two ionization positions (The N terminus and the basic C-terminal residue, except for the C-terminal peptide of any digest). In the case of rOspA, however, the N-terminal peptide presented only one ionization site due to N-terminal blockage. The most abundant peak in this spectrum (Fig. 11B) corresponded to a molecular mass of 1036.2 Da (expected mass of the N-terminal peptide containing three palmitates: 1038.6 Da; $\Delta m = -2.4$ Da), indicating that one fatty acid was unsaturated. In addition, several minor components were detectable. Peaks corresponding to plus and minus 28Da (II and III in Fig. 11B) were present, indicating different forms of the lipidic moiety, the major one being a peptide with three C16 fatty acids, whereas the minor forms contain two C16s plus one C14 (II in Fig. 11B) and two C16s plus one C18 (III in Fig. 11B) in agreement with the GC-MS data. Another peak corresponded to the loss of one palmitate residue (IV in Fig. 11B, $\Delta m = -238$ Da). This could be attributable to a fragmentation taking place in the source of the mass spectrometer, or most likely to an incomplete lipidation, as previously described on the same molecule [26]. The presence of a population of Pam2Cys-modified rOspA molecules that had been detected in the intact protein was thus confirmed by the analysis of the N-terminal peptide mixture that contained some Pam2CysLys (IV in Fig. 11B; expected mass, 800.2 Da; measured mass, 797.8 Da). The measured mass of the N-terminal tryptic peptide appeared to be 2 Da lower than expected for two C16:0 indicating one unsaturated fatty acid in agreement with the GC-MS data which showed the presence of about 20% of C16:1.

To confirm these results, a fast atom bombardment (FAB) mass spectrum using a magnetic sector mass analyzer was run on approximately 100 ng of the remaining N-terminal peptides. A complex spectrum was obtained (Fig. 12). As the sample had remained in solution for several days prior to FABMS analysis it is likely that the increased complexity was due at least in part to oxidation of the peptide at the cysteine–lipid thioether moiety. Additional peaks (II and III in Fig. 12 and Table 2) corresponding to plus and minus 28 Da on $[M+H]^+$ were present, confirming and extending the ESMS data on the lipidic composition. In particular, the high mass resolution allowed discrimination of two components differing in one unsaturation (Ia and Ib in Fig. 12 and Table 2). Fragmentation (b_1 fragment) data indicated the presence of lysine in agreement with the expected structure of the N-terminal peptide containing one cysteine and one lysine residue. Masses corresponding to the loss of one palmitate residue (IV in Fig. 12,

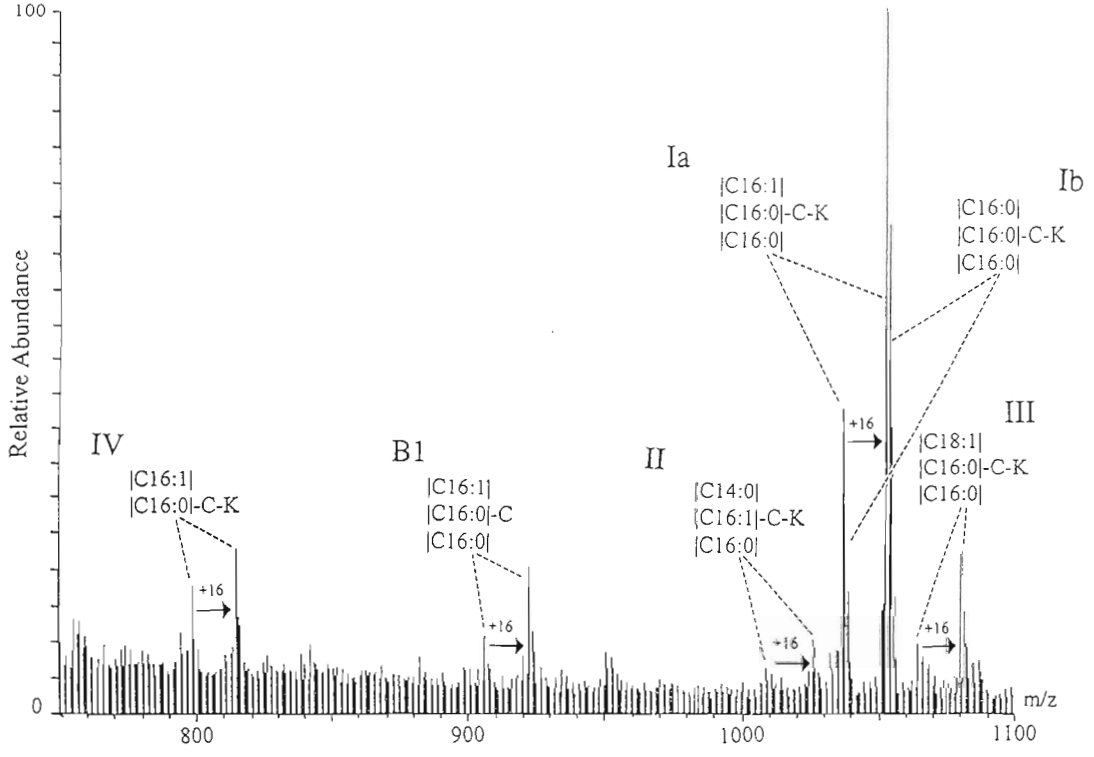

Figure 12 Fast atom bombardment mass spectrometry (FABMS) of rOspA N-terminal peptide (see Table 2). I corresponds to the expected complete form (Pam3CysLys). Series I consists of two components, one with an unsaturation among the three chains (Ia), and one with three saturated chains (Ib). II and III correspond to fully lipidated forms with two palmitate and one myristate or octadecenoate residue, respectively. IV corresponds to an incomplete form (Pam2CysLys). A B1 fragment is obtained due to fragmentation at the lysine residue. Additional masses that are +16Da of the different peptides are also observed and could correspond to their respective oxidation products. (From Ref. 27.)

Table 2 Molecular Species Detected in the ES and FAB Mass Spectra of the Lipidated N-Terminal Tryptic Peptide of rOspA

Theoretical fatty acid composition	Average mass (Da)			Monoisotopic mass (Da)			Proposed structures	Label in Figs. 3 and 4
	Expected[a]	Measured (ESMS)	Δm	Expected[a]	Measured (FABMS)	Δm		
Three C16:0	1038.6	1036.2	−2.4	1037.8	1035.7	−2.1	C16:0-C16:0-C16:1	Ia
					1037.7	−0.1	C16:0-C16:0-C16:0	Ib
Two C16:0 + One C14:0	1010.6	1008.9	−1.7	1009.8	1007.5	−2.3	C16:0-C16:1-C14:0	II
Two C16:0 + One C18:0	1066.7	1063.7	−3.0	1065.9	1063.6	−2.3	C16:0-C16:0-C18:1	III
Two C16:0	800.2	797.8	−2.4	799.6	797.3	−2.3	C16:0-C16:1	IV

[a] Assuming completely saturated structures.

$\Delta m = -238$ Da) confirmed that the major fatty acid residue was C16:0. These results indicated the fatty acid composition of the major components to be C16:0-C16:0-C16:1 and C16:0-C16:0-C16:0 in accordance with results obtained by GC-MS. Of the two minor components, one had a lipidic composition of C14:0-C16:1-C16:0, and the other component had a lipidic composition of C18:1-C16:0-C16:0, according to the GC-MS data.

In conclusion, the use of a combination of GC, normal phase HPLC, and MS allowed a detailed characterization of the lipidation of rOspA. The heterogeneity of the molecule related to its lipidic composition was analyzed using fatty acid analysis by GC-MS. It indicated that C16:0 is the major component as expected [35] but that other fatty acids including C16:1, C14:0, and C18:1 were also present. Purification of the N-terminal peptide and its analysis by ESMS and FABMS indicated that a minor fraction of rOspA molecules contained a Pam2-Cys modification and that the major rOspA form corresponded to a peptide having three C16 residues, two of them being saturated and one being unsaturated. This structure is consistent with the proposed model for bacterial lipoproteins [35] in that the major fatty acid component is palmitate.

IV. DISCUSSION

Posttranslational modifications of proteins are often related to biological function as is strikingly demonstrated by the importance of phosphorylations and dephosphorylations. In this chapter we describe two types of posttranslational modifications: lipidation, which was expected and assures localization of the protein to the outer membrane of *B. burgdorferi*, and addition of acetaldehyde to the amino terminus, which was not expected and results from anaerobic glucose metabolism of *S. cerevisiae* during high-cell-density culturing.

In both cases a combined strategy using efficient separation techniques based on HPLC or GC methods and MS led to a detailed structural understanding of these modifications. A key step to the successful analysis in the case of rOspA was the development of a normal phase chromatographic method that allowed isolation of the amphipathic N-terminal lipopeptide after tryptic digestion of the protein. Final structural proof of the addition of acetaldehyde to the N terminus of rSmp28 was obtained by tandem MS of the modified N-terminal peptide in comparison with its nonmodified counterpart. Methodological advances as described in this chapter will provide a more detailed insight into the structure of recombinant proteins ultimately allowing to define them in physicochemical terms similar to chemically synthesized pharmaceuticals. Such an approach will help to assure the consistent quality of biopharmaceuticals with the goal of producing safe and efficient medicines.

ACKNOWLEDGMENT

The contributions from colleagues in the Yeast and Pilot Development Departments at Transgene and the Laboratoire de Spectrométrie de Masse Bioorganique (Université Louis Pasteur, Strasbourg) are gratefully acknowledged.

REFERENCE

1. Koths K. Curr Biol 1995;6:681–687.
2. Buckel P. Trends Pharm Sci 1996;17:450–456.
3. Andersen JS, Svensson B, Roepstorff P. Nature Biotechnol 1996;14:449–457.
4. Fenn JB, Mann M, Meng CK, Wong SF, Whitehouse CM. Science 1989;246:64–71.
5. Karas M, Hillenkamp F. Anal Chem 1988;60:2299–2301.
6. Carr SA, Hemling ME, Bean MF, Roberts GD. Anal Chem 1991;63:2802–2824.
7. Chait BT, Kent SB. Science 1992;257:1885–1894.
8. Aebersold R, Hess D, Morrison HD, Yungwirth T, Chow DT, Affolter M, Amankwa LN. J Protein Chem 1994;13:465–466.
9. Hopfgartner G, Wachs T, Bean K, Henion J. Anal Chem 1993;65:439–446.
10. Tomer KB, Moseley MA, Deterding LJ, Parker CE. Mass Spectrom Rev 1994;13:431–457.
11. Coulot M, Domon B, Grossenbacher H, Guenat C, Maerki W, Müller DR, Richter WJ. J Mol Struct 1993;292:89–104.
12. Ling V, Guzzetta AW, Canova-Davis E, Stults JT, Hancock WS, Covey TR, Shushan BI. Anal Chem 1991;63:2909–2915.
13. Klarskov K, Roecklin D, Bouchon B, Sabatie J, Van Dorsselaer A, Bischoff R. Anal Biochem 1994;216:127–134.
14. Smith RD, Udseth HR, Wahl JH, Goodlett DR, Hofstadler SA. Meth Enzymol 1996;271 Part B:448–486.
15. Carr SA, Huddleston MJ, Bean MF. Protein Sci 1993;2:183–196.
16. Conboy JJ, Henion JD. J Am Soc Mass Spectrom 1992;3:804–814.
17. Huddleston MJ, Bean MF, Carr SA. Anal Chem 1993;65:877–884.
18. Huddleston MJ, Annan RS, Bean MF, Carr SA. J Am Soc Mass Spectrom 1993;4:710–717.
19. Amankwa LN, Harder K, Jirik F, Aebersold R. Protein Sci 1995;4:113–125.
20. Sutton CW, O'Neill JA, Cottrell JS. Anal Biochem 1994;218:34–46.
21. Huberty MC, Vath JE, Yu W, Martin SA. Anal Chem 1993;65:2791–2800.
22. Bischoff R, Lepage P, Jaquinod M, Cauet G, Acker-Klein M, Clesse D, Laporte M, Bayol A, Van Dorsselaer A, Roitsch C. Biochemistry 1993;32:725–734.
23. Balloul JM, Sondermeyer P, Dreyer D, Capron M, Grzych JM, Pierce RJ, Carvallo D, Lecocq JP, Capron A. Nature 1987;326:149–153.
24. Erdile LF, Brandt MA, Warakomski DJ, Westrack GJ, Sadziene A, Barbour AG, Mays JP. Infect Immun 1993;61:81–90.

25. Bischoff R, Roecklin D, Roitsch C. Electrophoresis 1992;13:214–219.
26. Bouchon B, Van Dorsselaer A, Roitsch C. Biol Mass Spectrom 1993;22:358–360.
27. Bouchon B, Klein M, Bischoff R, Van Dorsselaer A, Roitsch C. Anal Biochem 1997;246:52–61.
28. Bouchon B, Jaquinod M, Klarskov K, Trottein F, Klein M, Van Dorsselaer A, Bischoff R, Roitsch C. J Chromatogr 1994;662:279–290.
29. Wilm M, Mann M. Anal Chem 1996;68:1–8.
30. Falick AM, Hines WM, Medzihradsky KF, Baldwin MA, Gibson BW. J Am Soc Mass Spectrom 1993;4:882–893.
31. Sillanaukee P, Hurme L, Tuominen J, Ranta E, Nikkari S, Seppä K. Eur J Biochem 1996;240:30–36.
32. Barbour AG, Heiland RA, Howe TR. J Infect Dis 1985;152:478–484.
33. Bergstrom S, Bundoc VG, Barbour AG. Mol Microbiol 1989;3:479–486.
34. Hayashi S, Wu HC. J Bioenerg Biomemb 1990;22:451–471.
35. Hantke K, Braun V. Eur J. Biochem 1973;34:248–269.
36. Metzger J, Beck W, Jung G. Angew Chem Int 1992;31:226–228.
37. Murphy RC. Mass Spectrometry of Lipids: Handbook of Lipid Research. Vol. 7. New York: Plenum Publishing, 1993.
38. Roepstorff P, Fohlmann J. Biomed Mass Spectrom 1984;11:601.
39. Roecklin D, Klarskov K, Cavallini B, Sabatie J, Bouchon B, Loew D, Van Dorsselaer A, Bischoff R. Eur J Biochem 1997;245:589–599.

3

Analytical and Preparative Separations of Peptides by Capillary and Free-Flow Zone Electrophoresis

Václav Kašička
Academy of Sciences of the Czech Republic, Prague, Czech Republic

I. INTRODUCTION

Peptides represent a large and complex group of biologically active substances. Their occurrence and function in nature are very variable and of vital importance. Peptides act for example, as hormones, neurotransmitters, immunomodulators, coenzymes or enzyme inhibitors, drugs, toxins, and antibiotics. The demands of chemists, biochemists, and all other specialists dealing with peptide research and applications for the methods that should be able to separate and characterize peptide preparations both qualitatively and quantitatively are continuously increasing. Consequently, the application of capillary and free-flow zone electrophoresis for peptide analysis, preparation, and physicochemical characterization is an area of great importance.

Natural peptides are composed of about 20 amino acid species linked by peptide bonds and sometimes also crosslinked by disulfide bridges. In the synthetic preparations of peptides (analoges, derivatives, and fragments of biopeptides), noncoded amino acid residues and various types of crosslinking might also occur. In practice, an inexhaustible number of variations of amino acid sequences in a polypeptide chain is the cause of an extraordinary diversity of peptides. They differ in their size (depending on the number of the linked amino acid residues, their relative molecular mass can range from few hundreds for

oligopeptides containing 2–10 amino acid residues up to several thousands for polypeptides containing tens of amino acid residues), electric charge, and steric arrangement. Charge and shape of a peptide molecules depend not only on the type and number of amino acid residues but also on their sequence in the peptide chain. All of these differences result in different electrophoretic mobilities of peptides, which allows their separability by electromigration methods. In this chapter some applications of two free-solution (carrierless) electromigration separation methods, high-performance capillary zone electrophoresis (CZE) and free-flow zone electrophoresis (FFZE), to peptide analysis and preparation will be described. Based on the correlation between these two techniques a procedure for conversion of analytical peptide separation into preparative scale will be demonstrated.

II. STRATEGY FOR SELECTION OF SEPARATION CONDITIONS

A. General

Strategy for the rational selection of the experimental conditions of analytical and preparative separations of peptides by CZE and FFZE results from the electromigration properties and other specific characteristics of peptides and from general rules for the development and optimization of CZE and FFZE separation procedures. The basic aspects of this strategy, including detection of peptides in CZE separations, will be described in this section.

B. Electromigration Properties of Peptides

1. Effective Mobility

As electromigration properties of peptides we indicate the properties connected with their electrophoretic mobility, which is the central magnitude of all electromigration separation methods [1–3]. Electrophoretic mobility, m, is defined as a velocity, v, of the movement of a charged component in a liquid medium in the dc electric field of unit intensity:

$$m = v/E \ (m^2 \ V^{-1} \ s^{-1}) \tag{1}$$

where E is the intensity of electric field. The mobility of a peptide, similar to mobility of any other substance, is a complex function of

1. Properties of the peptide itself (charge, size, shape)
2. Properties of a medium (background electrolyte) in which peptide is moving (composition, pH, ionic strength, viscosity, permitivity, and temperature)

3. Interactions of peptide with components of the medium (solvation, dissociation, complex formation)

Depending on so many parameters, peptide mobility has to be referred to given experimental conditions under which it was determined, i.e., it must be related to the given composition, pH, and temperature of the background electrolyte. In this way characterized mobility is called effective mobility and only the effective mobilities of peptides obtained under the same conditions are comparable electromigration characteristics of peptides.

The relationship between effective mobility of peptide P, $m_{P,ef}$, and its effective charge, $z_{P,ef}$, and relative molecular mass, M_P, has been investigated from the beginning of electrophoretic separations of peptides and proteins. First it was quantitatively described by Offord [4] who derived empirically from peptide separations by paper zone electrophoresis the following equation:

$$m_{P,ef} = kz_{P,ef}/(M_P)^{2/3} \tag{2}$$

where k is an empirical constant.

The validity of Offord's relation was confirmed also for free-solution CZE by Rickard et al. [5], whereas Compton [6] prefers the form:

$$m_{P,ef} = Az_{P,ef}/[B(M_P)^{1/3} + C(M_P)^{2/3}] \tag{3}$$

Other forms were suggested by Grossman et al. [7]:

$$m_{P,ef} = A \log (z_{P,ef} + 1)/n^B \tag{4}$$

where *n* is the number of amino acid residues, and by Cifuentes and Poppe [8]:

$$m_{P,ef} = A \log (1 + Bz_{P,ef})/(M_P)^C \tag{5}$$

In all of these equations A, B, and C are empirical constants that are dependent on the electrolyte system used and on the size and structure of peptides investigated. Small peptides may behave as simple organic ions of a compact structure (tightly would coil); longer peptides may occur in the form of random coil or linear chain.

In spite of different forms of the above given relation it can be concluded that the mobility of peptide is directly proportional to its charge and indirectly proportional to its relative molecular mass with exponent in the range 1/3–2/3.

The influence of charge, size, and shape of peptides and proteins on their mobilities is discussed in detail in some special articles, book chapters, and reviews [9–17].

2. Effective Charge

From the physicochemical point of view, peptides are amphoteric (poly)electrolytes or (poly)ampholytes. They contain in their molecules different types of iono-

genic groups, e.g., carboxyl groups of C-terminal amino acids and of side chains of aspartic and glutamic acids, amino groups of N-terminal amino acids and of side chain of lysine, etc. The survey of ionogenic groups present in peptides and the approximate range of their acid dissociation constants excerpted from the literature [18–20] are given in Table 1. The effective (net) charge of peptides (sum of all charges including their signs) is given by the sum of charges of all ionogenic groups present in the polypeptide chain. If amino acid sequence or at least amino acid composition of a peptide is known, then from the present ionogenic groups and from their dissociation constants it is possible to estimate which groups are dissociated at a given pH and how they conribute to the effective charge. Generally, a given group is dissociated to 50% in a solution the pH of which is equal to the pK value of that group. For pH = pK + 1, the group is 90% dissociated and for pH = pK − 1 the group is 10% dissociated.

The amino acid residues of aspartic and glutamic acids are the main contributors of negative charge, whereas arginine, lysine, and partly histidine are carriers of the positive charge in peptide chain.

In addition to this rough estimation, a more precise, computer program–based calculation has been developed that allows one to calculate the effective and specific charges of any peptide whose amino acid sequence is known and for which the pK values of present ionogenic groups are known or can be estimated [21]. The program is based on the mathematical model of the acid–base equilibria of a general ampholyte. It is described in detail elsewhere [22]; here only the main points will be mentioned.

Let us consider a peptide P that can have maximal (positive) charge M and minimal (negative) charge N. M and N express numbers of elementary charges

Table 1 Approximate Range of pK Values of Ionogenic Groups of Amino Acid Residues in Polypeptide Chain

Ionogenic group	Amino acid residue	pK
$-SO_3H$	Cysteic acid	1.3
α-COOH	C terminal of peptide chain	1.8–3.5
β-COOH	Aspartic acid	3.5–4.5
-S-CH2-COOH	S-carboxymethylcysteine	3.4–4.0
γ-COOH	Glutamic acid	4.0–4.5
Imidazolium	Histidine	5.6–6.9
$\alpha\text{-}NH_3^+$	N terminal of peptide chain	7.5–8.6
-SH	Cysteine	9.0–10.5
$\varepsilon\text{-}NH_3^+$	Lysine	9.0–10.8
Phenol	Tyrosine	9.8–11.0
Guanidium	Arginine	10.0–12.5

including sign, i.e., maximum and minimum are meant in the mathematical sense. Let P(J) be an ionic form of peptide P with charge J and K(J) is the apparent dissociation constant of the equilibria between the ionic forms P(J + 1) and P(J):

$$\begin{aligned} &P(J+1) \rightleftharpoons P(J) + H^+ \\ &K(J) = c_{P(J)}\, c_H / c_{P(J+1)} \end{aligned} \tag{6}$$

where $c_{P(J)}$ and $c_{P(J+1)}$ are the equilibrium concentrations of peptide ionic forms P(J) and P(J + 1) and c_H is the equilibrium concentration of hydrogen ions. The molar fraction of component P(J), $D_{P(J)}$, referred to the total concentration, c_P, of peptide P is defined as

$$D_{P(J)} = c_{P(J)} / c_P \tag{7}$$

It was derived that $D_{P(J)}$ can be expressed as a function of c_H with parameters K(J), N, M, i.e.,

$$D_{P(J)} = \frac{\left[\prod_{l=0}^{J-1} K(l)/H^{|J|}\right]^{-1} \cdot (J > 0) + \left[\prod_{l=J}^{-1} K(l)/H^{|J|}\right] \cdot (J < 0)}{1 + \sum_{i=N}^{-1} \prod_{l=i}^{-1} K(l)/H^{|i|} + \sum_{i=1}^{M} \left[\prod_{l=0}^{i-1} K(l)/H^{|i|}\right]^{-1}} \tag{8}$$

where $J \in \langle N, M \rangle$, $J \neq 0$, $H = C_H$. If molar fractions of all ionic forms P(J) are calculated, then the effective charge of peptide P, $z_{P,ef}$, can be determined:

$$z_{P,ef} = \sum JD_{P(J)} \qquad J = N \ldots M \tag{9}$$

From the effective charge, $z_{P,ef}$, the specific charge, $z_{P,sp}$, i.e., the charge referred to unit relative molecular mass, M_P, of peptide P can be calculated:

$$z_{P,sp} = z_{P,ef} / M_P \tag{10}$$

or the ratio of effective charge and relative molecular mass with a general exponent d, called corrected specific charge, $z_{P,sp,cor}$:

$$z_{P,sp,cor} = z_{P,ef} / (M_P)^d \tag{11}$$

From the known molar fractions $D_{P(J)}$ of the individual ionic forms of peptide P and from their known or estimated ionic mobilities, $m_{P(J)}$, the effective mobility of peptide P can be calculated as the weighted sum of ionic mobilities:

$$m_{P,ef} = \sum \text{sign}(J) m_{P(J)} D_{P(J)} \qquad J = N \ldots M \tag{12}$$

where sign(J) = +1 for $J > 0$, sign(J) = −1 for $J < 0$, and sign(J) = 0 for J = 0.

Equation (12) represents a mathematical definition of effective mobility of a general ampholytic electrolyte. Mobilities of cations are positive values, mobilities of anions are negative values.

The calculated dependencies of effective, specific, and corrected specific charges [effective charges divided by relative molecular mass M_r with exponent d = 2/3; see Eq. (11)] of simple peptides of diglycine (N = −1, M = 1, M_r = 132.2, pK(0) = 3.12, pK(−1) = 8.17) and triglycine [N = −1, M = 1, M_r = 189.3, pK(0) = 3.26, pK(−1) = 7.91] on pH are shown in Fig. 1.

It is obvious that from these dependencies the useful information for the selection of pH and composition of background electrolyte (BGE) can be obtained, e.g., the regions of minimal (negative) and maximal (positive) charges, regions of strong or weak dependence of effective and specific charges on pH, and the pH range in which peptide charge is close to zero can be determined.

An important electromigration characteristic of peptides is their isoelectric point (pI), i.e., the pH value of a solution in which the effective charge and consequently the effective mobility is equal to zero. For small oligopeptides containing only few amino acid residues with distant pK values of their ionogenic groups, the pH range in which effective charge is close to zero is relatively broad (see Fig. 1) and instead of isoelectric point we are speaking about isoelectric zone. Isoelectric point differs from the similar characteristic, isoionic point, in that it is related to a given buffer composition in which the measurement of charge (mobility) is performed. This includes electrostatic interactions with all the ions present in the solution whereas the isoionic point takes into account only interactions with protons. The isoelectric and isoionic points are mostly close values, but generally not identical. Peptide moves in a dc electric field as cation at pH < pI and as an anion at pH > pI. The isoionic point can be read from the above given dependence of effective charge on pH (see Fig. 1).

The calculated pH dependence of effective charges and of corrected specific charges, i.e., effective charges divided by relative molecular mass with exponent 2/3, for longer peptides with higher number of ionogenic groups, growth hormone–releasing peptides (GHRPs), insulin and desoctapeptide insulin, are presented in Figs. 2 and 3. Figure 2 shows these dependencies for His^1-GHRP (hexapeptide with the sequence His-D-Trp-Ala-Trp-D-Phe-Lys·NH_2 and with the following parameters of calculation: N = 0, M = 3, M_r = 873.1, pK(2) = 5.8, pK(1) = 7.8, pK(0) = 10.4) and for Tyr^1-GHRP (hexapeptide with the sequence Tyr-D-Trp-D-Ala-Trp-D-Phe-Lys·NH_2 and with the following parameters, N = −1, M = 2, M_r = 899.1, pK(1) = 7.6, pK(0) = 10.0, pK(−1) = 10.4). Figure 3 shows the pH dependencies of effective and specific corrected charge of human insulin (two-chain polypeptide consisting of 51-amino-acid residues, M_r = 5750.0, N = −10, M = 6) and des-B23-30-octapeptide insulin (43-amino-acid residues, M_r = 4837.8, N = −9, M = 5). The accuracy of these calculated

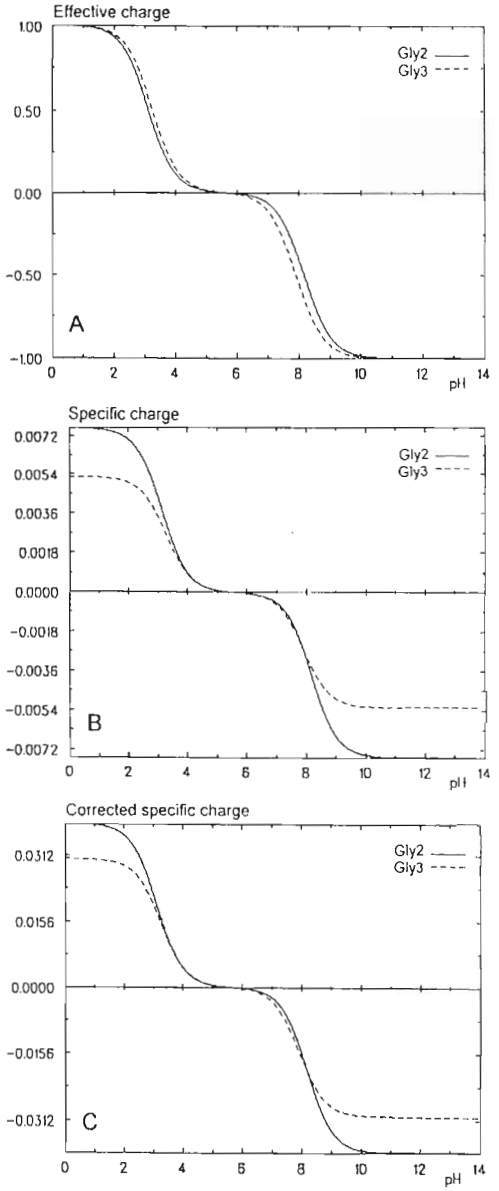

Figure 1 Dependence of (A) effective charge, (B) specific charge (effective charge divided by relative molecular mass), and (C) corrected specific charge (effective charge divided by relative molecular mass with exponent 2/3), of diglycine, curve Gly2, and triglycine, curve Gly3, on pH. Parameters of the calculation, pK values, and relative molecular masses are given in the text.

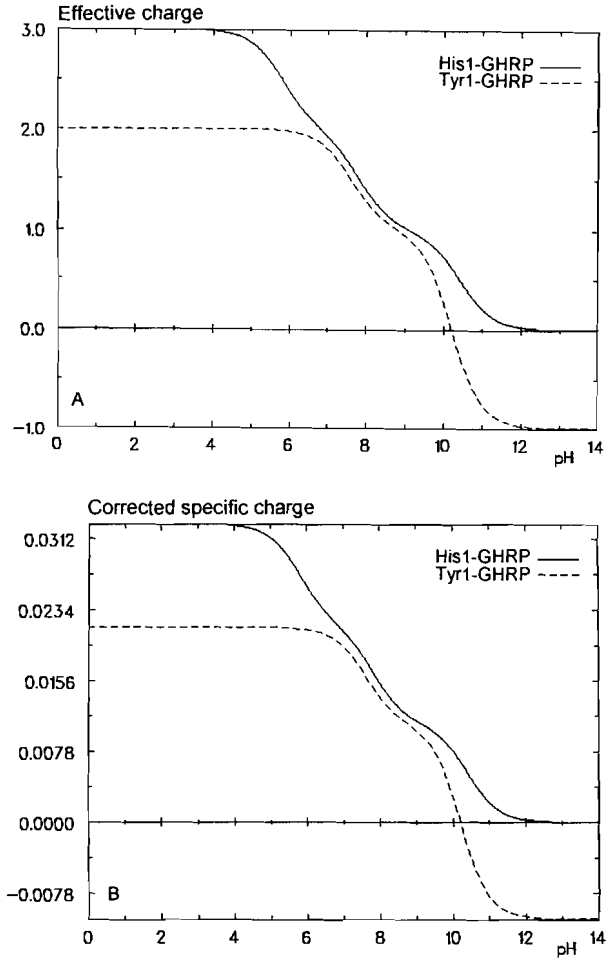

Figure 2 Calculated dependence of (A) effective charge and (B) corrected specific charge (effective charge divided by relative molecular mass with exponent 2/3) of growth hormone–releasing peptides (GHRPs), His^1-GHRP and Tyr^1-GHRP, on pH. Peptide sequences and parameters of the calculation are given in the text.

dependencies is negatively influenced by the fact that the average (estimated) pK values of the present ionogenic groups (see Table 1) were used instead of individual constants of these groups in the given peptides. In reality, pK values depend not only on the amino acid residue itself but on the neighboring amino acid residues and on the steric arrangement of a polypeptide chain. For that reason

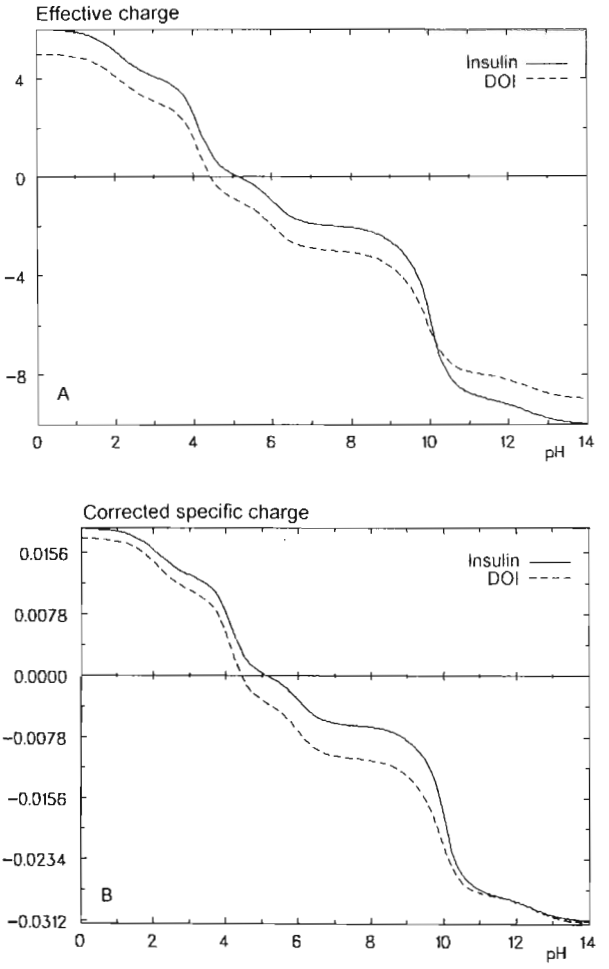

Figure 3 Calculated dependence of (A) effective charge and (B) corrected specific charge (effective charge divided by relative molecular mass with exponent 2/3) of pig insulin and desoctapeptide-B23-B30-insulin (DOI) on pH. Parameters of the calculation are given in the text.

the conclusions derived from the calculated dependencies can be used only as the first approximation for the selection of the suitable pH of BGE, which can be further optimized by experimental tests. Similar strategy for the prediction of peptide charge and mobility from the peptide sequence has been published by Cifuentes and Poppe [8] who try to predict more precise values of individual

pK values of ionogenic groups present in peptide chain taking into account the environment of given ionogenic group.

The pH dependence of the effective charge and/or effective mobility of peptides can also be obtained by other methods, e.g., by acid–base titration curves [23] or electrophoretic titration curves [24,25]. A large set of mobilities of small oligopeptides in the pH range 6–10 was determined by capillary isotachophoresis [26]. Isoelectric point of peptides can be determined by capillary or slab-gel isoelectric focusing [27–29] or by CZE [30], or it can be calculated theoretically on the similar bases as the above-described approach for acid–base equilibria [31,32].

C. Experimental Conditions of Capillary and Free-Flow Zone Electrophoresis

1. General

When selecting the suitable experimental conditions for separation of peptides by CZE and by FFZE, the general rules for the selection of the experimental conditions of CZE [33–37] and FFZE [38] should be followed. In addition, the following specific properties of peptides should be taken into account.

1. Amphoteric character: the effective charge (mobility) of peptide is strongly dependent on pH; peptides can be separated as cations or anions (see Section II.B)
2. Diversity of amino acid composition and sequences resulting in a wide range of solubilities and mobilities, including relatively low mobilities and low solubilities
3. Biological activity, chemical and temperature lability
4. Complexity of peptide mixtures isolated from biological matrices (serum, cerebrospinal fluid, tissue extracts) and interactions of peptides with the components of these matrices
5. Tendency of the long peptides to be adsorbed to the inner walls of the separation compartments

The influence of these factors on the selection of parameters of CZE and FFZE separation is described below.

2. Composition and pH of Background Electrolyte

As follows from the amphoteric character of peptides, for the rational selection of pH of the background electrolyte in which electromigration separation of peptides should be performed it is advantageous to know the dependencies of the effective and specific charges and/or effective mobilities of these peptides on pH, or at least their isoelectric points should be available (see Section II.B).

The pH of BGE should be at least 1–2 units distant from p*I* since close to p*I* both electrophoretic mobility and solubility of peptide are relatively low. The pH of BGE should be taken from the region where the specific charge is greater than about 2×10^{-4} e (e is elementary charge unit), i.e., a polypeptide with relative molecular mass 5000 should possess at least one elementary charge per molecule. With respect to the fact that effective mobility is directly proportional to the effective charge and indirectly proportional to the relative molecular mass [see Eqs. (2)–(5)], it is obvious that the difference of peptide mobilities will be maximal in the same region where the difference of specific charges or corrected specific charges of these peptides is maximal. Consequently, from this region of maximal difference of charges the suitable pH of BGE should be chosen.

For the given example of diglycine and triglycine it is evident that the suitable pH for their separation is either at low acid region (pH < 3) or at alkaline pH (pH > 9), since in these regions the differences of specific and corrected specific charges are maximal. On the basis of these calculations and with respect to other aspects (see below, 0.5 mol/L acetic acid, pH 2.5, was chosen as BGE for the separation of these two peptides, which are often used as test mixture in our laboratory. The record of CZE separation of these two peptides and the electroosmotic flow marker, phenol, is given in Fig. 4.

Similarly, from the course of pH dependence of corrected specific charge of GHRP derivatives (see Fig. 2), it follows that the suitable region for their separation is in the acid pH region and that for pH < 4.5 the difference of cor-

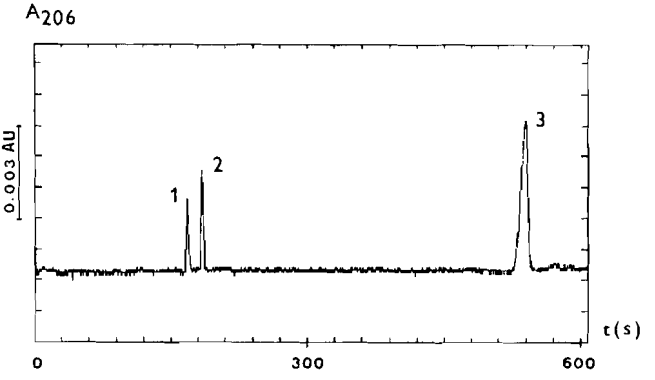

Figure 4 CZE separation of test mixture of diglycine (0.3 mg/ml), peak 1, triglycine (0.3 mg/ml), peak 2, and phenol (0.1 mg/ml), peak 3, using 0.5 mol/L acetic acid, pH 2.5 as BGE in a home-made CZE device described in Section III.B.1. Capillary: i.d. 0.056 mm, total (effective) length 310 (200) mm. Voltage 9.0 kV, current 10.1 μA; A_{206}, absorbance at 206 nm; t, migration time.

rected specific charges (effective mobilities) is independent of pH. Separation at high pH (pH > 11) should be from the point of view of different specific charges also possible but it cannot be recommended because of hydrolysis of amide groups at high pH. As follows from the calculated pH dependence of effective and corrected specific charges of insulin and desoctapeptide insulin (see Fig. 3), the suitable pH of BGE for CZE separation of these two peptides is between 7 and 9 and from this range the pH of the BGE was chosen for monitoring of tryptic conversion of pig insulin to desoctapeptide insulin by CZE (see Fig. 9 in Section III.B.1).

According to the predicted suitable pH for peptide separation the composition of BGE is selected. The main constituent(s) of BGE should possess buffering capacity at a given pH, i.e., their pK should fulfill the conditions $pH_{BGE} = pK \pm 0.5$. The ionic strength of the buffer is typically in the range of 10–200 mM concentrations of the main buffer constituents. At a given pH/ionic strength combination, several buffers can be used in principle. Preference should be given to the amphoteric, so-called Good-type buffers, which are available for the pH region 5.5–11 and which fulfill the condition of sufficient buffering capacity at relatively low electric conductivity [39]. The classical buffers such as phosphate, citrate, and acetate can be used in moderately low pH regions, and borate and phosphate buffers can be used in weakly alkaline pH range. Common buffers utilized for peptide separations by CZE and FFZE are given in Table 2.

Of course, the pH of BGE must be selected not only according to pH dependence of effective and specific charge of peptides to be separated, but also with respect to their solubility, chemical and thermal lability, and biological activity. These aspects are discussed in more details in the following sections.

3. Some Factors Influencing Selection of Background Electrolyte

The optimal pH region and generally the optimal composition of BGE should fulfill the following conditions:

1. There should be sufficient solubility of analyzed peptides (at least about 1 mmol/L).
2. There should be chemical stability of peptides including some their labile groups (amides, disulfides, sugar moieties, etc.).
3. There should be preservation of biological activity (if peptides are used for biological tests after their CZE or FFZE separation).
4. Effective mobilities of peptides and their relative differences should be sufficiently high for their separation (approx. $m_{ef} > 1.10^{-9}$ m^2 V^{-1} s^{-1}, $\Delta m_{ef}/m_{ef} > 0.02$, i.e., the relative difference in mobilities should be higher than around 2%).
5. Adsorption of peptides to capillary wall is suppressed.

Table 2 Suitable Constituents of Background Electrolyte for Capillary and Free-Flow Zone Electrophoresis of Peptides

BGE constituent	p*K*	Mobility
Anions:		
Phosphoric acid	2.1	−35.1
Citric acid	3.1	−28.7
Formic acid	3.8	−56.4
Glutamic acid	4.4	−28.9
Acetic acid	4.8	−42.4
MES[a]	6.1	−26.8
ACES[a]	6.8	−31.3
HEPES[a]	7.5	−21.8
Tricine[a]	8.1	—
Boric acid	9.2	—
Alanine	9.9	−32.7
BALA[a]	10.2	−30.8
CAPS[a]	10.4	—
Cations:		
Gly-Gly	3.1	31.5
BALA[a]	3.5	36.7
EACA[a]	4.4	28.8
Creatinine	4.8	37.2
Histidine	6.0	29.6
Imidazole	7.1	52.0
Tris[a]	8.1	29.5
Ammediol[a]	8.8	29.5
Ethanolamine	9.5	44.3

[a] MES, 2-(*N*-morpholino)ethanesulfonic acid; ACES, *N*-2-acetamido-2-aminoethanesulfonic acid; HEPES, *N*-2-hydroxyethylpiperazine-*N*′-2-ethanesulfonic acid; Tricine, [*N*-(trishydroxymethyl)methyl]glycine; BALA, β-alanine; CAPS, 3-(cyclohexylamino)propanesulfonic acid; EACA, ε-aminocaproic acid; Tris, tris(hydroxymethyl)aminomethane; ammediol, 2-amino-2-methyl-1,3-propanediol.

Some brief rules for the selection of suitable composition and pH of BGE with respect to these demands are given below.

a. Solubility Peptide solubility can be affected by a number of parameters:

1. *pH*. The pH of BGE should be at least 1–2 pH units distant from the isoelectric point since the solubility of peptide is relatively lower at p*I* and its close vicinity.

2. *Ionic strength and the buffer constituents*. The composition of BGE is relatively free, and it is possible to use relatively concentrated solutions of acids and bases (e.g., 0.1 M phosphoric acid, 0.5 M acetic acid, 0.1 M Tris), which is favorable for peptide solubilization. Higher ionic strength can contribute to the better solubility of peptides but overly conductive buffers should be avoided since great Joule heat would be generated in these buffers at high voltages generally applied in CZE and because of problems with Joule heat removal from the flow-through electrophoretic chamber.
3. *Solubilizing additives*. Different types of additives can be added to the BGE to improve the peptide solubilization, i.e., chaotropic agents, such as urea and its derivatives [40], nonionogenic and zwitterionic detergents [41–43], and cyclodextrins and micelle-forming compounds such as anionic detergent sodium dodecyl sulfate, (SDS) or cationic detergent cetyltrimethylammonium bromide (CTAB) [44]. These agents should be added to BGE very carefully because they can also change or reverse the electroosmotic flow, can form complexes or ion pairs with peptides [45], or can change the separation mechanism from charge/size-based separation to hydrophobicity-based separation, e.g., by micellar electrokinetic chromatography (MEKC) [46–48]. This technique is suitable for separation of noncharged peptides or peptides with the same or very similar specific charge, i.e., peptides containing the same charged amino acid residues and similar noncharged amino acid residues. Complete separation of porcine, equine, bovine, and sheep insulins differing in the presence of neutral amino acid residues, threonine, alanine, serine, glycine, valine, and isoleucine in positions 8–10 of A chain of insulins was achieved by capillary MEKC with SDS and CTAB micellar pseudophase with the addition of acetonitrile to the BGE [49]. Capillary MEKC with mixed fluorocarbon-hydrocarbon anionic surfactants (lithium perfluorooctane sulfonate and lithium dodecyl sulfate) allowed separation of nine small tryptophan-containing charged peptides with nearly identical electrophoretic mobility [50]. The above example of insulins separations also demonstrates that, although mostly performed in water buffers, CZE separations of peptides can also be performed in the buffers to which organic solvents such as acetonitrile, methanol, and other alcohols are added [49,51–53]. The organic solvent may not only improve peptide solubility, but due to changed selectivity it can also increase resolution of peptide separations [54,55].

The solubilizing additives also help to reduce the adsorption of separated peptides to the inner capillary wall.

b. Biological Activity, Chemical and Thermal Lability Biological activity (e.g., hormonal or immunochemical function) of peptides is connected with certain conformations of polypeptide molecules which are stable only under the defined conditions. Consequently, if the biological activity of peptide should be preserved, e.g., after preparative separation by FFZE the peptides are used in the tests of biological activity on animals, then this FFZE separation must be performed under conditions whereby irreversible denaturation of peptide does not occur, i.e., composition, pH, solvents, and additives of BGE have to be chosen with respect to this demand. For preserving biological activity and for preventing the losses of separated peptides it is necessary to prevent adsorption of analyzed peptides to the inner walls of the separation compartment by dynamic or covalent inner surface coating [56].

Chemical lability of some groups in the peptide molecule has to be taken into account, e.g., peptides containing amide, disulfide, and sulfhydryl groups should not be analyzed at high pH because of hydrolytic and transsulfidation reactions of these groups at this pH.

In addition, the electric input power should be sufficiently low (lower than 2 W/M of capillary length for capillaries with i.d. 0.05–0.1 mm), and active removal of Joule heat by flowing air or circulating liquid is recommended in order to prevent thermal denaturation of separated polypeptides.

D. Detection

1. Optical Detection

Similar to the other classes of compounds, optical detection is the most frequently used detection mode in CZE separation of peptides. Of the several optical detection modes used in CZE [57], only (spectro)photometric UV absorption and fluorescence detection will be mentioned here in more detail. Descriptions of the other modes, used only rarely for peptide detection, say for refractive index and thermooptical absorbance detection, can be found in the above given review [57].

a. UV Absorption Detection Thanks to the relatively strong absorption of peptide bond CO-NH in the short-wavelength UV region, absorption detection at these wavelengths (200–220 nm) can be used as a universal detection principle. Special UV absorption detectors have been designed utilizing, for example, high-frequency excited iodine discharge lamp with emission at 206 nm [58,59] or Zn or Cd lamps with emission at 214 nm [60], in addition to those utilizing classical deuterium lamp with continuous light emission in the whole UV region [61]. With the fused silica capillaries detection below 200 nm, up to 185 nm, is also possible [62]. Due to the higher molar absorption coefficient of peptides at this region the detection sensitivity is increased, e.g., twofold gain in the signal-to-noise ratio was obtained by changing the detection wavelength from 214 to 200

nm [63], but the choice of BGE is limited to those buffers that do not absorb at this wavelength. Borate and phosphate buffers are useful in this respect, but many biological Good's buffers are inappropriate for use below 215 nm. For polypeptides separated in the presence of low-UV-absorbing BGE constituents and additives, 230-nm wavelength provides a good compromise between detectability and peak–area analysis accuracy on one side and stronger light absorption of the background electrolyte on the other side.

The UV absorption of the peptide zone in the spectral region 200–220 nm characterizes the peptide bond quantity, i.e., a longer peptide provides a higher absorbance signal response at equal molar concentration [64]. Micromolar concentrations of peptides are usually detectable by capillary electrophoresis (CE) with UV absorption detection. Increased sensitivity can be achieved at some special designs, as a Z-shaped cell, a bubble cell, or a sleeve cell [61,65,66].

Peptides containing aromatic amino acid residues can be detected more specifically by UV absorption at 275–280 nm or with a lower sensitivity at 254 nm. The highest absorption coefficient is characteristic for tryptophan residue and also for tyrosine residue, where significant changes of the absorption coefficient influenced by pH occur. Less sensitive is the detection of phenylalanine residue. Although the absorption coefficients and hence the resulting detectability of aromatic residue containing peptides at 280 nm is lower than at 206 nm, more freedom in selection of BGE composition partially compensates for this drawback.

More information about the quality and quantity of peptides separated and confirmation of peak homogeneity and identity can be obtained by multiple-wavelength detection or by full spectrophotometric detection realized by fast scanning spectrophotometric detection or by diode array detection [61]. Spectral analysis and the use of spectral libraries and automated library searches can distinguish closely related peptides, e.g., cyclic and linear forms of synthetic oligopeptides, and allows identification of individual peaks of peptide maps of proteins [67].

b. Fluorescence Detection

Laser-Induced Fluorescence Detection of Native Peptides By its inherent character (measurements are performed with a negligible background signal) fluorescence detection is more sensitive than absorption detection. In the first generation of CE devices the fluorescence detectors with classical light sources (xenon lamps) used in HPLC were adapted for capillary columns [68]. They suffered from the same drawback as the adapted HPLC UV absorption detectors, i.e., the amount of light coupled to the analyte zone in the capillary was rather low.

More successful versions of fluorescence detectors use lasers as sources of excitation light [69–72]. Laser-induced fluorescence (LIF) is the most sensitive detection mode in CZE. With special designs of liquid sheath-flow cuvettes, LIF detection is approaching the absolute limit—detection of a single molecule [73].

The native fluorescence of peptides excited by UV light in the region 200–300 nm is exclusively dependent on the presence of aromatic amino acid residues in the peptide molecule. The optimal excitation wavelength was found at 275 nm [74]. Tryptophan residue obviously plays the dominating role. The quantum yield of the fluorescence of tryptophan residue is positively influenced by a hydrophilic microenvironment. The fluorescence intensity of tyrosine is about two orders of magnitude weaker. Almost negligible is the fluorescence of phenylalanine residue.

In the required UV excitation range 200–300 nm only few lasers can operate. Frequency-doubled Ar laser operating at 257 nm and Kr laser operating at 284 nm were used for detection and spectral differentiation of peptides containing tryptophan and tyrosine [75]. The detection concentration limits related to the above amino acids were 2.10E-10 (Trp) and 2.10E-8 (Tyr). Acquisition of the fluorescence emission spectrum allowed distinction of three classes of peptides, those containing Trp or Tyr or both Trp and Tyr.

Pulsed air–cooled KrF UV laser operating at 248 nm was used for the analysis of tyrosine-and tryptophan-containing dipeptides and proteins [76–78]. The detection limits for these peptides were at least two orders of magnitude lower when compared with UV absorption at 214 nm.

Availability of the above-mentioned deep UV lasers meant a great progress for CE analysis of peptides since it makes possible very efficient excitation of native fluorescence of tryptophan-and tyrosine-containing peptides. This LIF approach greatly simplifies the preseparation sample handling and is useful especially for analysis of peptides occurring in biological fluids and tissue extracts at low concentration levels. High sensitivity and no need for derivatization of peptides and proteins, which is a problem especially at low concentrations of analytes, was utilized for quantitative determination of native peptides and proteins in single cells, as, for example, insulin in single pancreatic cells [79] and hemoglobin in individual human erythrocytes [80].

Laser-Induced Fluorescence Detection of Labelled Peptides A more general and more common way of fluorescence detection of analytes in CE is based on both precolumn and postcolumn labeling of these analytes with a fluorescent marker [81]. Unfortunately, this approach has a number of problems in detection of peptides and proteins. Peptides and proteins usually contain more than one derivatization site, which leads to multiple labeling. More derivatives with different electrophoretic mobilities and consequently multiple peaks are obtained for originally single peptide species. To avoid this problem some special procedures utilizing Edman degradation chemistry [82] or fluorescein isothiocyanate (FITC) labeling at lower than normal derivatization buffer pH [83] have been developed, but some differences in the extent of the precolumn incorporation of the tags causing a rise of multiple peaks after CZE must be taken into account. Often precolumn derivatization reagents reacting with amino group were used as, say,

5-dimethylaminonaphthalene-1-sulfonyl (DANSYL) chloride, naphthalene-2,3-dicarboxaldehyde (NDA), fluorescein isothiocyanate (FITC) and 3-(4-carboxybenzoyl)-2-quinolinocarboxaldehyde (CBQCA) [84]. Subzeptomole detection limits for CZE of FITC derivatives of peptides were reported [72]. CZE peptide mapping of 360 attomole of tryptic human serum albumin (HSA) digest involving selective derivatization of arginine-containing peptides with benzoin was performed by Cobb and Novotny [85]. Selective determination of arginine or tyrosine-containing peptides was achieved by using two different amino acid–selective fluorogenic reagents (benzoin with guanidine moiety for arginine residues and 4-methoxy-1,2-phenylenediamine reacting with formylated tyrosine residues) and utilizing He-Cd laser operating at 325 nm for LIF detection [86]. LIF detection of selectively labeled phosphoserine residue (fluorescein attached to 1,2-ethanedithiol-derivatized phosphoserine) in peptides and proteins allowed direct quantitative evaluation of peptide and protein phosphorylation at the attomole level [87]. Trace levels of peptides (derivatized by fluorescamine) from neuronal and subneuronal samples were analyzed by CE with LIF detection using He-Cd laser at 354 nm [88]. Detection of attomolar concentrations of alkaline phosphatase (corresponding to nine molecules of this enzyme in 1μl sample volume) was achieved by CZE monitoring of the enzymatic conversion of a fluorogenic substrate into the highly fluorescent product using Ar ion laser with excitation wavelength 458 nm [89]. LIF-CZE was used also for the determination of in vivo neuropetide release from the ewe median eminence [90,91] and for monobromobimane-derivatized glutathione and hemoglobin in single erythrocytes [92,93].

Nonfluorescent regents such as fluorescamine and *o*-phthalaldehyde (OPA) may be used both for precolumn and postcolumn derivatization under mild conditions with subsequent chemiluminescent detection [94,95]. Lower resolution of the CZE zones as a result of postcolumn detection usually occurs.

In spite of the above-mentioned problems LIF detection of labeled peptides in general seems to be the most sensitive method for peptide detection in CZE.

2. Mass Spectrometric Detection

Mass spectrometry (MS) represents an ideal detection principle for CZE because of its universality, sensitivity, and selectivity [96–99]. On-line coupling of CZE with MS was made possible thanks to the introduction of two ionization techniques: continuous flow fast-atom bombardment (CF-FAB) [100] and electrospray ionization (ESI) [101], which solved the problem of how to desolvate, ionize, and transfer into gas phase and into vacuum conditions required for MS analysis the analytes separated in liquid phase separation methods such as HPLC and HPCE. Both of these ionization techniques opened the door of MS to the analysis of polar, nonvolatile compounds, including peptides and proteins. The MS detection principle combined with high resolution of CZE is becoming im-

portant for peptide mapping and for separation of peptides, i.e., fragments of proteins originated from specific enzymatic hydrolysis of proteins [20,85]. These peptide maps are frequently used for the confirmation of known protein sequences [102] and for the investigation of posttranslation modification, e.g., phosphorylation of proteins [103]. ESI is the preferred mode of coupling CE apparatus with mass analyzer, namely, because of its capability to generate the ions with multiple charges so that the ion m/z (mass/charge) values for even very large species (such as polypeptides and proteins) may fall within the limited m/z detection range of most mass spectrometers. Equally important is the fact that a population of multiply charged ions having different numbers of charges is created for these larger ions so that the m/z data can be mathematically deconvoluted to give the original molecular masses of the species. CE-ESI-MS is now a widely used technique for separation and identification of closely related peptides, e.g., neurotensin and angiotensin analogs [104], model mixtures of synthetic peptides [105,106], and naturally occurring biologically active peptides, e.g., enkephalins, oxytocin, bradykinin, angiotensin, and bombesin at femtomole to attomole levels [107]. An example of ESI-MS detection of CZE-separated peptide and protein mixtures is shown in Fig. 5. Combination of CZE with tandem MS, CZE-ESI/MS/MS [108–110], allowed determination not only of molecular mass of the whole molecules of proteins and peptides but also of their fragments. From the collision-induced production–ion spectra the amino acid sequences of CZE-separated peptides and proteins were obtained, which allowed their identification by comparison of these sequences with those in a protein database [109,110]. For on-line CZE-MS/MS coupling the best signal-to-noise ratio was obtained when acidic buffers of low ionic strength for CZE peptide separations were applied [108]. Extremely large number of components of complex peptide mixtures originating, for example, from protein hydrolysis (peptide mapping) can be resolved and identified when the MS detector is coupled to an on-line combination of HPLC and CZE, and in such a way a three-dimensional separation, HPLC-CZE-MS, is realized [111].

The newest version of MS, matrix-assisted laser desorption-ionization mass spectrometry with time-of-flight mass analyzer (MALDI-TOF-MS), is combined with CZE separations of peptides and proteins mostly in an off-line mode [112,113]. Its advantage, i.e., soft ionization and generation of predominantly singly charged molecular ions of even polypeptide and protein macromolecules as antibodies [114], is used for exact determination of relative molecular mass with an accuracy of $\pm 0.1\%$ and for identification of peptides and proteins isolated after their CZE separation. In some experimental arrangements the CZE fractions are deposited directly on the MALDI probes so that individual peaks from electropherogram are associated with a single sample spot on the probe [112]. MALDI matrices with high acid concentrations afford enhanced tolerance of CZE buffers to be used for introducing peptides to the mass analyzer. Keough et al. [115]

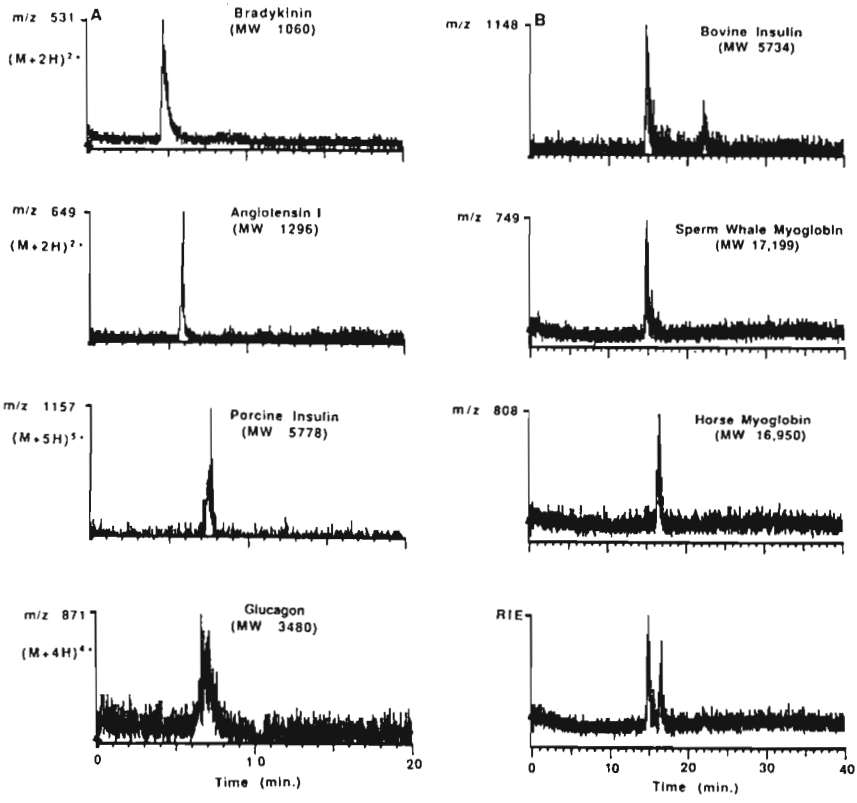

Figure 5 Single-ion electrophoreograms and reconstructed ion electrophoreogram (RIE) for separation of peptide and protein mixture by CZE-ESI-MS. (A) Peptide mixture consisting of approximately 5 pmol/component separated in 0.6 m × 0.1 mm i.d. fused silica capillary at 15 kV using pH 11 sodium phosphate buffer as BGE. (B) Peptide and protein mixture consisting of approximately 2 pmol/component separated in a pH 8.4 Tris-HCl-buffered BGE in an untreated 1.1 m × 0.1 mm i.d. fused silica capillary at 25 kV. (From Ref. 101.)

reported a 250-fmol detection limit for smaller peptides and a 100-fmol off-line detection limit for α-lactalbumin. The MS detection also enables one to detect and characterize absolutely the nonpeptidic part, e.g., the glyco-component, attached to the peptide chain [116].

3. Electrochemical and Conductivity Detection

Electrochemical (EC) methods offer high selectivity and sensitivity for analytes that are easily electrooxidized or electroreduced with the detectability comparable

with that of fluorescence detection methods. The relative simplicity and low cost of EC instrumentation, including the ease with which the small electrodes can be constructed and the associated small currents measured, make the EC methods particularly attractive for CZE applications [117–119]. Most of EC detection in CZE are performed in an amperometric mode. The problem of "decoupling" of small EC potentials (about 1 V) and currents (in the pA range) from the much larger driving CE voltage (10–30 kV) and current (tens of μA) was solved by using porous glass joint or porous membrane covered fracture decoupler or by end-column application of the working electrode [118,120]. The major drawback is the small number of analytically important species that are electroactive at modest potentials at the carbon electrodes conventionally used, e.g., catechols, phenols, aromatic amines, and thiols. This is also the reason why EC techniques have not been applied to the detection of peptides very frequently up to now. Thiol-containing peptides and amino acids, e.g., glutathione, cysteine, and cystine, were determined by amperometric detection at copper microelectrode [121] or at gold/mercury amalgam microelectrode [122]. With the latter the detection limits for glutathione were about 0.5 fmol or 20 nmol/L. Pulsed amperometric detection with gold fiber microelectrode was used for characterization of glycopeptides from recombinant coagulation factor VIIa separated by CZE [123].

An end-column detection cell that can be used for both electrochemical and conductivity detection in CZE was designed by Huang et al. [124] and by Muller et al. [125]. A few other types of conductivity detectors for CZE have been developed [126–128], but mostly they are not used for direct detection of peptides in CZE. However, conductivity detection can be recommended for CZE and CITP determination of small organic and inorganic ions, e.g., anionic counterions (acetates, trifluoroacetates) of basic peptide preparations [21,129,130].

III. ANALYSIS OF PEPTIDE PRODUCTS

A. General

Qualitative and quantitative analysis of synthetic peptides and peptides isolated from natural material is the most common application of CZE in peptide chemistry. In particular, the need for a purity test of synthetic peptides has risen in many areas in the recent years. In biochemistry synthetic peptides are used as substrates and inhibitors of enzymes in the elucidation of the mechanism of their catalytic effect; in the investigation and modeling of the interactions of antigens with antibodies, hormones with receptors, and peptides and proteins with nucleic acids; in the mapping of antigenic determinants (epitopes) of proteins; and in the study of the dependence of secondary and tertiary structure of a peptide chain on amino acid sequence. The use of synthetic peptides in pharmaceutical research and in human and veterinary medicine is also widespread. In the food industry peptides are used as sweeteners and additives.

In a majority of these applications of synthetic, natural, or biotechnologically prepared peptides CZE can be used as a sensitive control method for the determination of their purity, or as a control method of the efficiency of the other, mainly chromatographic separation methods used for their purification. CZE provides rapid and accurate qualitative and quantitative data about the peptide preparations.

Thanks to the high parameters of CZE separations, efficiency achieving hundreds of thousands or millions of theoretical plates, sensitivity in the range of femtomole-attomole of an analyte in the nanoliter-picoliter sample volume, high-speed of analysis with the average time of analysis in the order of few minutes, and its compatibility with different detection modes, CZE is capable of providing not only the data on peptide purity but also on the identity, structural changes, and physicochemical characteristics of the peptides and proteins they constitute. CZE is capable of revealing subtle differences between peptides originating from minimal changes in amino acid sequences of synthetic oligopeptides of the same amino acid composition [131] or in the disulfide bridge position [132]. The latter case can be demonstrated by CZE separation of 70-amino-acid residues containing insulin-like growth factor (IGF-1) (disulfide bridges in positions 6–48 and 47–52) and recombinat IGF-1 byproduct (disulfide bridges in positions 6–47, 48–52) [133]. Reduction of intrachain disulfide bridge in 27-amino-acid residues containing peptide was also monitored by CZE [134]. CZE was capable of separating the deamidation products of human insulin (HI) and human growth hormone (HGH) from their natural molecules, i.e., polypeptides differing in single elementary charge unit per 51-amino-acid residues (HI) or per 191-amino-acid residues (HGH), respectively [135]. CZE was used also for separation of closely related stereoisomers and isoforms of tryptic heptapeptide fragment of HGH [136], for enantiomeric and diastereomeric separations of di-, tri-, and tetrapeptides [137–139] using cyclodextrins as chiral selectors and for resolution of cis and trans isomers of proline-containing peptides [140,141]. In addition to analytical applications, CZE can also be used for the determination of physicochemical characteristics of peptides, as effective mobilities [7, 10,12,142,143], effective charges [16,144], relative molecular masses [16,145], diffusion coefficients [146], and for monitoring of peptide interactions with other biomolecules and for determination of association and/or dissociation constants of peptide complexes with chiral selectors and other ligands [147–149].

B. Evaluation of Peptide Purity

Peptide purity and peptide content in the sample can be quantified by several ways depending on whether the standard of given peptide is available or unavailable. If the standard of a peptide P is available, then the quantity of this peptide in the analyzed sample can be determined absolutely by the calibration curve method

or by the method of internal standard addition, i.e., by comparison of migration times, peak heights, and/or peak areas of standard peptide and of the peptide in the given sample. If the standard is not available, which is the case of peptides synthesized or isolated for the first time, the relative evaluation of peptide purity based on the peak height or peak area ratio has to be used.

1. Relative Degree of Purity

The relative CZE degree of purity of peptide P, $p_{P,CZE,h}$, ($p_{P,CZE,A}$) is defined as the ratio of the peak height (area) of peptide P itself to the sum of heights (areas) of all (n) peaks present on electrophoreogram of the given preparation of peptide P:

$$P_{P,CZE,h} = h_p/\sum h_i \qquad i = 1 \ldots n \tag{13}$$

$$P_{P,CZE,A} = A_p/\sum A_i \qquad i = 1 \ldots n \tag{14}$$

It must be emphasized that both ways of expressing the CZE purity degree can be used only as approximate and relative criteria of peptide purity since the molar absorption coefficients of the individual sample components may be generally different. However, in the case of synthetic peptide preparations most of the admixtures will have the similar structure to that of the main synthetic product and consequently also the similar molar absorption coefficients.

Generally, peak height is less suitable for quantitative analysis than peak area, since peak height is more dependent on the experimental conditions. Stacking or destacking of the sample zone can occur due to concentrating effect of the BGE constituents or the sample matrix components [150]. Differences in mobilities of analytes and BGE constituents cause electromigration dispersion of analyte zones, which also influences their heights.

The peak height–based CZE purity degree is recommended to be used for CZE-grams with great difference in migration times and with similar peak shape and width and when the signal-to-noise ratio is too low for precise integration of peak area. Because of limited linearity between sample amount (concentration) and peak height the difference in the analyte amounts (concentrations) should be within one order.

The advantage of peak area–based quantitative evaluation is that the above-mentioned peak shape distortions do not affect peak area. However, if peak area is used for quantitative evaluation, then a correction for different migration velocities of the analytes has to be taken into account. Due to these differences, analytes with lower migration velocities (mobilities) remain in the detection window for a longer time than those with higher migration velocities (mobilities). Consequently, they exhibit broader peaks with a larger peak area than the faster moving analytes, although the physical length of their zones may be the same as that of

the faster moving analytes. The deviation of peak area caused by this effect can be corrected by dividing the peak area of an analyte by the migration time of this analyte [151].

The migration velocity noncorrected peak area–based CZE purity degree can be used for evaluation of CZE grams where the peaks of some components are broader not because of slow migration through the detector window but due to the adsorption of analytes to the capillary wall or due to electromigration dispersion.

A further few applications of CZE to peptide analysis are demonstrated. All of the presented examples were performed on the home-made CZE device developed in our laboratory [152]. It consists of the untreated fused silica capillary with outer polyimide coating (i.d. 0.056 mm, o.d. 0.200 mm, total length 310 mm, effective length 200 mm), UV photometric detector at 206 nm, and a high-voltage power supply. Peptide samples and electroosmotic flow markers were dissolved in the BGE in the concentration range 0.1–1.5 mg/ml. The sample was introduced into the capillary manually forming a hydrostatic pressure (50 mm of water column) for the time period 5–20 s. High-voltage power supply was utilized in constant voltage mode. Experiments were performed at ambient temperature 22–24°C without active cooling of the separation compartment.

Application of CZE to the determination of peptide purity is demonstrated in Fig. 6. It shows CZE analysis of standard preparation of dalargin, a synthetic hexapeptide with the sequence H-Tyr-D-Ala-Gly-Phe-Leu-Arg-OH, and a derivative of dalargin, a synthetic hexapeptide with the sequence of H-Tyr-D-Ala-Gly-D-Phe-Leu-Arg-NH_2. Whereas no admixtures were found in the standard preparation, i.e., its CZE purity degree approaches 100%, in the case of dalargin derivative in addition to the peak of the main synthetic product two admixtures with lower mobility are present. Peak height–based purity degree of the dalargin derivative preparation is 86.1% and peak area–based purity is 89.6%.

CZE analysis of insect oostatic hormone fragment, a synthetic octapeptide with the sequence H-Tyr-Asp-Pro-Ala-Pro-Pro-Pro-Pro-OH (see Fig. 7), shows the utilization of CZE as a control technique for evaluation of the suitability of other separation technique, namely reversed-phase HPLC (RP-HPLC), for preparative separation (purification) of a given peptide preparation. Comparison of CZE analysis of crude synthetic product of insect oostatic hormone and of the same product purified by RP-HPLC (see Fig. 7) shows that RP-HPLC was a very efficient method in the purification procedure; it was capable of removing completely four admixtures (a1, a2, a4, a5) of the five admixtures (a1–a5) of the crude synthetic product and to decrease substantially the content of the admixture a3, but for the complete purification of the preparation further technique has to be employed or RP-HPLC has to be repetitively used.

The high separation power of CZE is demonstrated by the separation of

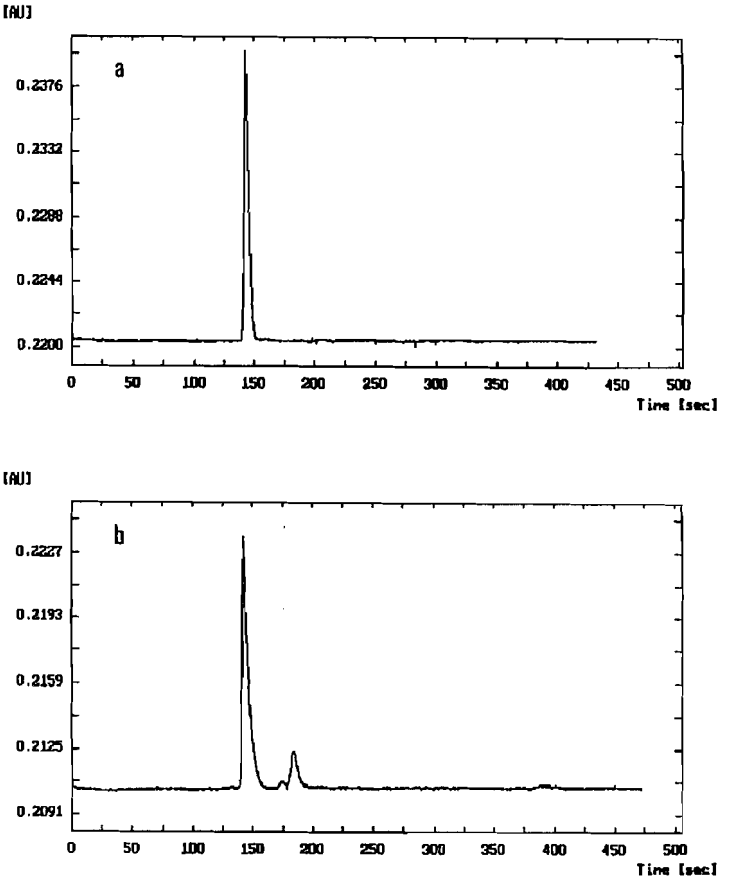

Figure 6 CZE analysis of standard preparation of dalargin, hexapeptide with sequence H-Tyr-D-Ala-Gly-Phe-Leu-Arg-OH (a) and dalargin derivative, hexapeptide with the sequence H-Tyr-D-Ala-Gly-D-Phe-Leu-Arg-NH_2 (b). Sample concentration 0.5 mg/ml. BGE: 0.5 mol/L acetic acid, pH 2.5; capillary: i.d. 0.056 mm, effective length 200 mm, total length 310 mm; voltage 9.0 kV, current 10.1 μA, temperature ambient 23°C; AU, absorbance at 206 nm.

human insulin (HI) and its closely related derivatives and fragments, such as HI with D-phenylalanine in positions 24 and 25 of B chain, HI with *N*-phenylacetyl-protected amino group of lysine in position B29, L-Phe- and D-Phe-B-24,B25-octapeptide-B23-B30-HI (see Fig. 8).

CZE can be used not only for qualitative and quantitative microanalysis of

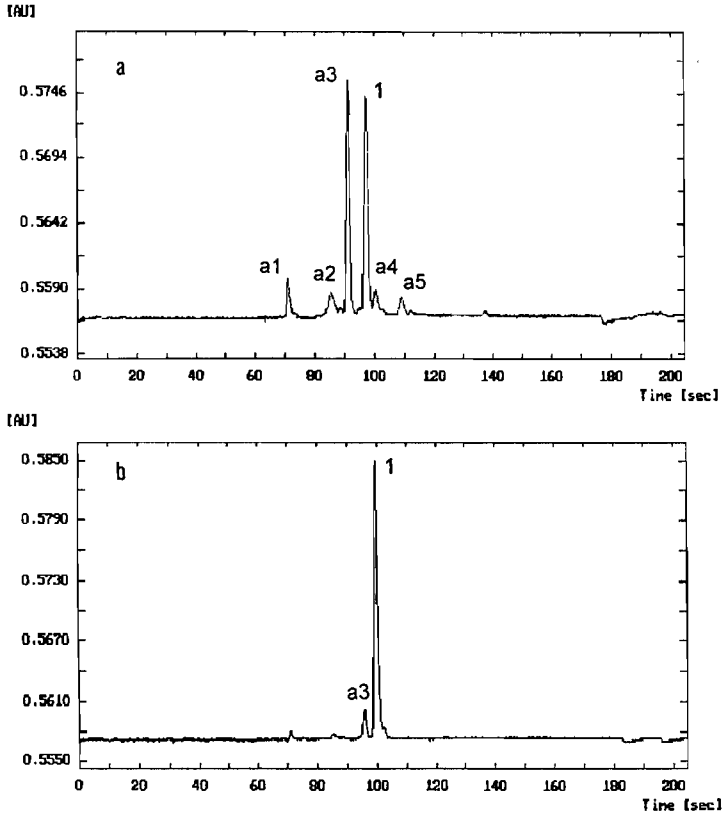

Figure 7 Monitoring of HPLC purification of insect oostatic hormone, synthetic octapeptide with the sequence H-Tyr-Asp-Pro-Ala-Pro-Pro-Pro-Pro-OH by CZE. (a) Crude synthetic product (sample concentration 1.1 mg/ml). (b) Product purified by HPLC (sample concentration 0.6 mg/ml). BGE: 0.04 M Tris, 0.04 M tricine, pH 8.1, constant voltage 10.0 kV, current 14.5 μA. Capillary: same as in Fig. 6. 1, main synthetic product of the insect oosatic hormone; a1–a5, nonidentified admixtures; AU, absorbance at 206 nm.

peptide preparations but also for monitoring of chemical and enzymatic conversions of peptides. Figure 9 shows CZE monitoring of enzymatic cleavage of pig insulin (PI) by trypsin 150 μg of pig insulin was dissolved in 200 μl of the background electrolyte (10 mM tricine, 5.8 mM morpholine, 10 mM tricine, 20 mM NaCl, adjusted by 0.1 M NaOH to pH 8.0) developed earlier for the separation of PI and desoctapeptide insulin. Composition and pH of the BGE was chosen on the basis of the calculated pH dependencies of effective, specific, and

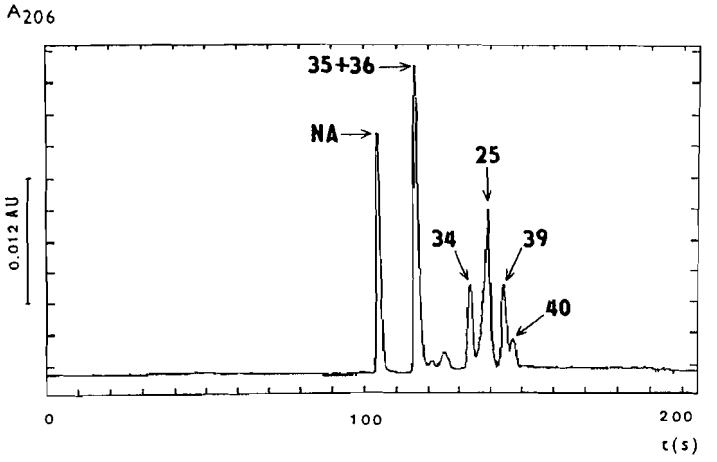

Figure 8 CZE separation of human insulin (HI) and its derivatives and fragments. Sample components dissolved in BGE in concentration range 0.5–1.5 mg/ml. BGE: 10 mM tricine, 5.8 mM morpholine, 20 mM NaCl, pH 8.6 adj. by 0.1 M NaOH, constant current 25 μA, voltage 8.6 kV. Capillary: same as in Fig. 6. 25, Human insulin (HI); 34, [D-Phe]-B24,B25-HI; 39, [D-Phe]-B24,B25-[Lys-N-PhAc]-B29-HI, 40, [Lys-NPhAc]-B29-HI; 35, [D-Phe]-B24,B25-octapeptide-B23-B30-HI; 36, [L-Phe]-B24,B25-octapeptide-B23-B30-HI; NA, nicotinamide (electroosmotic flow marker). A_{206}, absorbance at 206 nm; t, migration time.

corrected specific charges of insulin and desoctapeptide insulin (see Fig 3 in Section II.B). Analysis of uncleaved PI is shown in Fig. 9a. Solution of PI was then mixed with 50 μg of trypsin preparation dissolved in 100 μl of BGE. Nicotinamide (NA) was added to BGE as an electroosmotic flow marker. The reaction mixture was analyzed on-line by CZE in the given time periods; only a few nanoliters of the solution was applied to the capillary without any disturbance of the continuing enzymatic reaction. The reaction was stopped by the addition of benzamidine to the reaction mixture after 60 min. The analyses of the reaction mixture after 7, 20, 40, and 60 min are shown in Fig. 9b–e. The presented electrophoreograms indicate a decreasing concentration (amount) of insulin and an increasing concentration (amount) of desoctapeptide insulin in the reaction mixture in the increasing time. From the CZE analyses of the reaction mixture the kinetics of the tryptic cleavage of PI can be evaluated.

Only illustrative applications of CZE to analysis of peptide products were shown here. More examples can be found in several reviews [11,15,153–157], book chapters [132,158,159], and books [35,160].

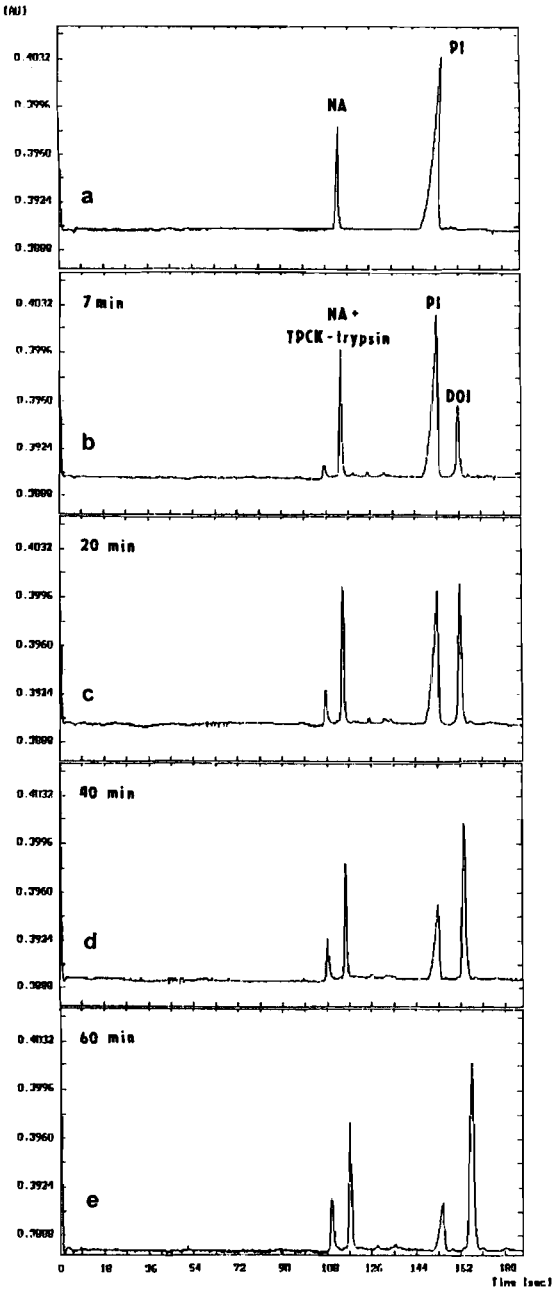
(AU)
PI
NA
a
7 min
NA +
TPCK - trypsin
PI
DOI
b
20 min
c
40 min
d
60 min
e
0
18
36
54
72
90
108
126
144
162
180
Time (sec)

IV. PREPARATIVE SEPARATIONS OF PEPTIDES

A. Micropreparative Peptide Separations by Capillary Zone Electrophoresis

The advantages of CZE in the analysis of peptides were demonstrated in the previous section. In this field CZE is already accepted as a recognized counterpart and/or complement to what have been the most widely spread separation techniques, i.e., different modes of HPLC. However, in the field of preparative peptide separations, the application potential of CZE is much smaller. This is the case for two main reasons:

1. More complicated adaptation of CE systems from analytical to preparative scale due to the fact that both ends of the capillary are dipped into the buffer in the electrode compartments and electric field is applied during the whole time of experiment.
2. Low preparative capacity of capillary systems.

The first problem was overcome by special adaptations of CZE devices and several procedures for fraction collections from the capillary have been developed. One of the first approaches was based on the short interruption of an electric field and during this time the electrode vessel at the outlet end of the capillary was replaced by a microvial with a small volume (few microliters) of (diluted) BGE or water. Then the electric field is switched on again and the zone of interest is let to be eluted by its own electromigration and/or by electroosmotic flow into this microvial [161]. This procedure, called electroelution, was later used in commercial CZE instrumentation, where autosamplers are also used as fraction collectors [162–164]. Sometimes the electroelution is accelerated or completely replaced by hydrodynamic flow introduced at the inlet end of the capillary [165,166]. The disadvantage of this approach is that the eluted sample component is diluted many times in comparison with concentration in the capillary, the electric field has to be interrupted each time the fraction is collected, and it is difficult if not impossible to preserve the spatial resolution of closely neighboring sample zones even when the capillary outlet is moved from one fraction microvial to another using an automated programmable procedure. Nevertheless, after evapo-

---

Figure 9 CZE analysis of pig insulin (a) and monitoring of the cleavage of pig insulin by trypsin after 7, 20, 40, and 60 min (b–e). BGE: 10 mM tricine, 5.8 mM morpholine, 20 mM NaCl, pH 8.0 adj. by 0.1 M NaOH, constant current 20.0 μA, voltage 7.3 kV. Capillary: same as in Fig. 6. For more details, see the text. PI, pig insulin; DOI, desoctapeptide-B23-30-insulin; NA, nicotinamide.

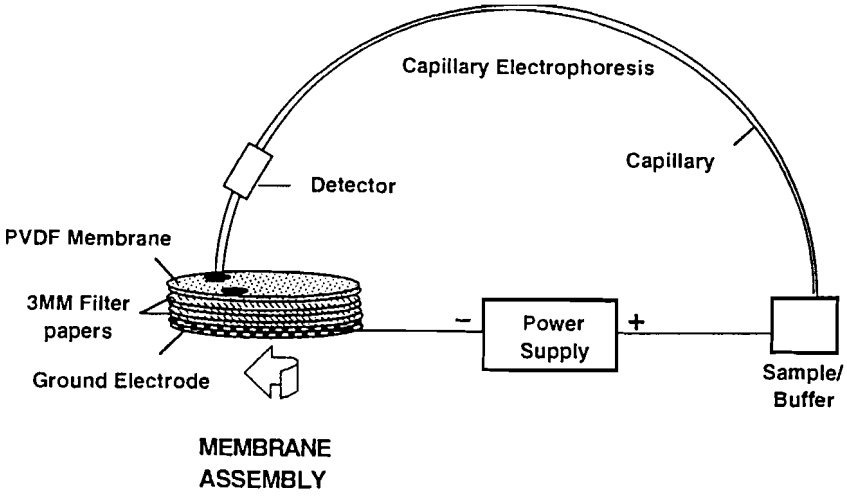

Figure 10 Schematic diagram of the membrane fraction collection for capillary electrophoresis. (From Ref. 174.)

ration of some of the solvent the collected sample component can be reconcentrated to the level detectable by other off-line detection methods. For this post-column off-line detection and/or characterization of the separated peptides, mostly different modes of MS detection or amino acid and sequence analysis are used [167–170].

For the continuous fraction collection in CE it is necessary to use special designs of the separation capillary in which the electrical circuit is completed prior to its outlet. This was achieved by the use of a porous glass joint [171], an on-column frit [172], or on-column microfractures of the capillary [173]. Then the sample components can be collected at an electrically isolated exit, while maintaining the electrical connection between high-potential and grounded electrode.

Another adaptation of the CZE system for micropreparative purposes consists of connection of the outlet end of the capillary with the membrane assembly [174], as indicated in Fig. 10. This membrane assembly, consisting of Immobilon transfer membrane (used for protein blotting) and of two layers of filter paper serving as electrolyte reservoir and stainless steel ground electrode, rotates and the sample components eluted by electromigration and by electroosmotic flow from the outlet end of the capillary are adsorbed to the slowly rotating membrane assembly. Proteins and peptides caught on the Immobilon membrane are then detected by staining, e.g., with Coomassie blue, and can be

subjected to further characterization, e.g., Edman degradation in sequence analyzers.

A special high-precision multicapillary fraction collection for CE has been developed by Muller et al. [175]. They utilize the approach of coaxial sheath liquid interface at the outlet end of the capillary [176]. Through this sheath buffer flow an electric circuit in the separation capillary is completed and simultaneously this sheath buffer flow transports the sample components leaving the exit of the capillary to appropriate collection vials. Up to sixty fractions of microliter or smaller volumes could be automatically collected in capillaries used as collection vials. The collection capillaries were placed on a cylinder and a computer-controlled stepping motor aligned the appropriate capillary with the column exit. Precise collection was achieved by fiberoptic UV detection close to (approx. 1 cm) the end of the capillary.

The second problem of preparative applications of CZE, i.e., limited preparative capacity, is fundamental. Because of small dimensions of capillary separation compartment (typical i.d. is 0.050–0.1 mm), only small amounts of peptides, usually less than 1 μg, can be isolated from capillary systems. These quantities are sufficient only for a limited number of applications, e.g., for further characterization of isolated peptides by the above-mentioned sequence and amino acid analysis, spectroscopic or MS analysis, or for very sensitive enzymatic and immunochemical tests in biochemistry, molecular biology, and medicine [177].

The preparative capacity of capillary systems can be partially enlarged by increasing the inner diameter of the capillary. In the wider bore capillaries (greater than 0.2–0.3 mm) the Joule heat is much worse removed from the separation compartment, which leads to radial temperature gradient and broadening of sample zones, as well as dramatic loss of separation efficiency. Partial increasing of preparative capacity can be achieved in rectangular cross-sectional capillary columns with the dimensions 0.05 × 1 mm [178,179], by microconcentric capillary column [180], or by a relatively higher concentration of peptides to be separated [181], which leads, however, to a lower separation resolution. Higher sample load can be used if an isotachophoretic concentrating effect is employed for the separation of peptides occurring at low concentrations [182]. Sometimes repetitive fraction collection is necessary to get a sufficient amount of peptide needed for further characterization. A procedure for optimization of experimental conditions of preparative CZE was suggested by Cifuentes et al. [183].

B. Preparative Free-Flow Zone Electrophoresis

A principal solution of the problem of enlarging preparative capacity of zone electrophoresis–based separation of peptides is to perform this separation in a free-flow electrophoresis mode, i.e., to realize the zone electrophoretic separation principle in a continuous free-flow arrangement in the flow-through electropho-

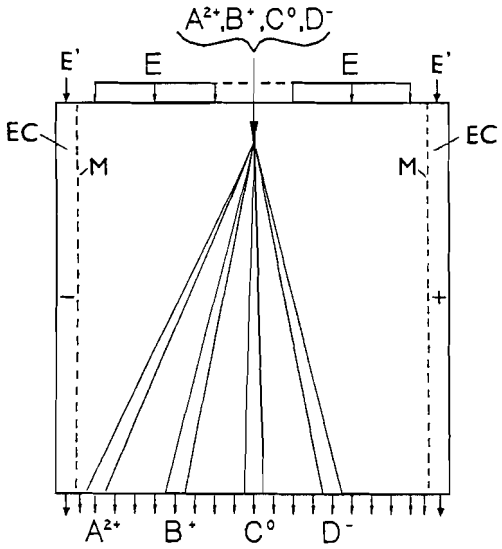

Figure 11 Cross-section of the flow-through electrophoretic chamber and the principle of free-flow zone electrophoresis. A^{2+}, B^{+}, C^{0}, and D^{-} are sample components that are continuously introduced to the injection point of the chamber and collected at the outlet side of the chamber; E, background (carrier) electrolyte laminary continuously flowing through the chamber; E′, background electrolyte circulating in the electrode compartment (EC); M, ion exchange membrane between the separation chamber and the electrode compartment.

retic chamber [184–186]. In this instrumental format the preparative capacity can achieve values up to hundreds of milligrams per hour, which is several order enlargement in comparison with preparative capacity of CZE.

The principle of FFZE [38,187,188] is as follows (see Fig. 11). The separation compartment is formed by two planparallel glass plates. The background electrolyte (carrier buffer) is continuously laminary flowing in the narrow gap (0.5 mm) between these two plates. Sample solution is also continuously introduced into the background electrolyte as a narrow zone. Electrode compartments, separated by semipermeable membranes from the separation part of the chamber, are situated on both sides of the chamber. BGE is turbulently circulating through the electrode compartment. Electric field is applied perpendicularly to the direction of laminar flow of background electrolyte and sample, and causes the different deflection of the sample components movement depending on their effective mobilities. Cations are deflected to cathode, anions to anode, and noncharged components will move in the straight direction if no electroosmotic flow occurs

in the chamber. At the outlet side of the chamber the separated sample components are collected in the fraction collector.

The advantage of FFZE is that it works continuously, in a free solution under mild conditions in which biological activity of separated substances is preserved. FFZE can be applied to preparative separation of a wide range of both low molecular mass and high molecular mass species and also for the separation of cells, organelles, and other bioparticles [187,189–192].

Because of some problems with thermoconvection and sedimentation in FFZE processes on the earth, some attempts to perform FFZE experiments in microgravity conditions inside orbiting space craft have been performed [193–195]. Successful separation of macromolecules (DNA, proteins) and bioparticles was achieved in these experiments, but the improvement of the separation efficiency and capacity was less than originally expected.

Miniaturized FFZE device integrated onto a silicon chip has been developed for continuous microanalysis of biomolecules [196].

C. Correlation of Capillary and Free-Flow Zone Electrophoresis

CZE and FFZE represent two modes of the same separation principle. Both of them are performed in the carrierless medium with the same background electrolyte. Consequently, a direct correlation exists between these two methods, which can be utilized for conversion of capillary microscale separation into preparative ones [152,197]. The bases of this correlation are described below.

The diagram of the electrophoretic, electroosmotic, and hydrodynamic movements in CZE and FFZE and the vector sum of these migration velocities in the capillary and in the flow-through electrophoretic chamber are shown in Fig. 12.

The resulting migration velocity of a charged component in the dc electric field in the capillary, v_r, is given by the sum of electrophoretic velocity, v_{ep}, and electroosmotic flow velocity, v_{eo} (see Fig. 12a):

$$v_r = v_{ep} + v_{eo} \tag{15}$$

The velocities in Eq. (15) can be expressed as the ratio of effective length of the capillary, l_{ef}, and the corresponding migration times, resulting migration time, t_r, electrophoretic migration time, t_{ep}, and electroosmotic migration time, t_{eo}, respectively:

$$\frac{l_{ef}}{t_r} = \frac{l_{ef}}{t_{ep}} + \frac{l_{ef}}{t_{eo}} \tag{16}$$

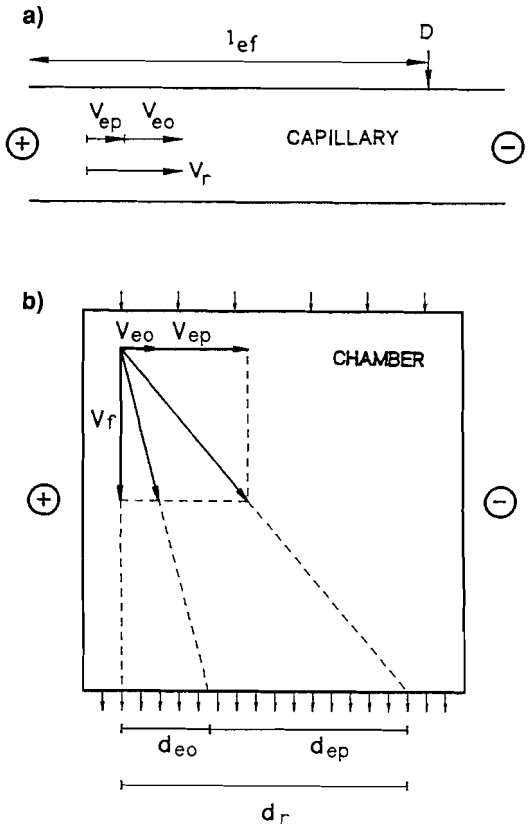

Figure 12 Superposition of the migration velocities in capillary zone electrophoresis (a) and in free-flow zone electrophoresis (b). v_{ep}, Electrophoretic velocity; v_{eo}, electroosmotic velocity; v_r, resulting migration velocity; l_{ef}, effective length of the capillary; D, detection position on the capillary; v_f, hydrodynamic flow velocity; d_{ep}, electrophoretic migration distance; d_{eo}, electroosmotic migration distance; d_r, resulting migration distance. (From Ref. 201.)

From the combination of Eqs. (15) and (16), the following relation can be obtained for the electrophoretic velocity in the capillary:

$$v_{ep,c} = \frac{l_{ef}}{t_{ep}} = \frac{l_{ef}\,(t_{eo} - t_r)}{t_{eo}t_r} \tag{17}$$

Equation (17) allows one to obtain the electrophoretic velocity from the data experimentally available from CZE analysis: t_r is the resulting migration

time of charged analyte, which is moved both by electrophoretic movement and by electroosmotic flow, t_{eo} is the migration time of electroosmotic flow marker (electroneutral compound at given experimental condition), and l_{ef} is the effective length of the capillary (from the injection end to the detector).

The velocity of the electroosmotic flow (EOF) in the capillary, $v_{eo,c}$, can be calculated from the effective length of the capillary, l_{ef}, and the migration time of the EOF marker, t_{eo}:

$$v_{eo,c} = \frac{l_{ef}}{t_{eo}} \tag{18}$$

The resulting migration velocity of the charged component in the flow-through electrophoretic chamber is given similarly as in the capillary by the sum of electrophoretic velocity, v_{ep}, and EOF velocity, v_{eo}, and in addition to it also by the vector sum of these two velocities with the velocity of hydrodynamic flow, v_f, which is perpendicular to the direction of v_{ep} and v_{eo} (see Fig. 12b). The resulting migration distance in FFZE can be expressed as a sum of the electrophoretically migrated distance, d_{ep}, and the electroosmotically moved distance, d_{eo}:

$$d_r = d_{ep} + d_{eo} \tag{19}$$

The electrophoretically migrated distance, d_{ep}, is given by the product of electrophoretic velocity in the flow-through chamber, $v_{ep,f}$, and the mean flow-through time of the BGE in the chamber, t_f.

$$d_{ep} = v_{ep,f}t_f \tag{20}$$

The electroosmotically migrated distance is given by the product of EOF velocity in the flow-through chamber, $v_{eo,f}$, and mean flow-through time of BGE, t_f:

$$d_{eo} = v_{eo,f}t_f \tag{21}$$

From Eqs. (19) and (20) the following relation for electrophoretic velocity in the chamber, $v_{ep,f}$, can be derived:

$$v_{ep,f} = \frac{d_r - d_{eo}}{t_f} \tag{22}$$

Using relation (22) the electrophoretic velocity of the charged analyte in the chamber, $v_{ep,f}$, can be calculated from the experimentally available data, namely, from the resulting migration distance of the charged analyte, d_r, from the migration distance of the EOF marker, d_{eo}, and from the flow-through time of BGE, t_f.

The EOF velocity in the chamber, $v_{eo,f}$, can be calculated from the migration distance of EOF marker, d_{eo}, and from the flow-through time of BGE, t_f.

$$v_{eo,f} = \frac{d_{eo}}{t_f} \tag{23}$$

For the description of the correlation between CZE and FFZE it is advantageous to express the ratio of electrophoretic velocities in the chamber and in the capillary, q_{ep}, and the ratio of EOF velocities in the chamber and in the capillary, q_{eo}.

From Eqs. (17) and (22) the ratio q_{ep} can be expressed as

$$q_{ep} = \frac{v_{ep,f}}{v_{ep,c}} = \frac{t_r t_{eo}\,(d_r - d_{eo})}{l_{ef} t_f \cdot (t_{eo} - t_r)} \tag{24}$$

and from Eqs. (18) and (23) the ratio q_{eo} can be expressed as

$$q_{eo} = \frac{v_{eo,f}}{v_{eo,c}} = \frac{d_{eo} t_{eo}}{l_{ef} t_{ef}} \tag{25}$$

Provided that the adsorption of the sample components to the walls of the separation compartments (both capillary and flow-through chamber) can be neglected it is reasonable to assume that q_{ep} is approximately constant for different charged components separated by CZE and FFZE under the same separation conditions. This is a realistic assumption because it means that if the electrophoretic velocity of component A in FFZE is q times higher than in CZE, then the electrophoretic velocity of component B, analyzed under the same conditions as A, will be also q times higher in FFZE than in CZE. Consequently, as follows from Eq. (24), coefficient q_{ep} (determined for standard component S) can be used to predict the electrophoretic velocities of sample components (A, B, C) in FFZE, if their electrophoretic velocities in CZE were determined under the same conditions as the electrophoretic velocity of standard S. A similar conclusion can be applied for the ratio of EOF velocities in CZE and FFZE, i.e., this ratio can be considered as a constant if the conditions of CZE and FFZE are the same as they were in the experiment when EOF velocity was determined.

Knowing the values of ratios, q_{ep} and q_{eo}, allows us to predict the migration velocities and migration distances of analytes in FFZE from the data obtained by their CZE analysis. This fact alone is the core of the procedure for conversion of analytical CZE separations to preparative FFZE separations.

D. Conversion of Analytical Capillary Electrophoretic Separations into Preparative Free-Flow Electrophoretic Processes

Based on the above given relations and assumptions, a procedure has been developed for the conversion of analytical microscale CZE separations to preparative continuous separation processes realized by FFZE. The procedure consists of the following steps:

(1) Let us have a sample containing charged analyte A (analyte of our interest from both analytical and preparative point of view) and some charged admixtures (A1, A2, . . .) and noncharged component(s) N (EOF marker). First, suitable conditions for CZE analysis of the given sample of analyte A have to be developed under which a good separation of the analyte A from the charged admixtures A1, A2 and noncharged component(s) N is achieved. From this experiment the electrophoretic velocity of the analyte A in the capillary, $v_{ep,c,A}$, is calculated according to Eq. (17), where $t_r = t_{r,A}$ and $t_{eo} = t_N$; $t_{r,A}$ and t_N are the resulting migration times of analyte A and EOF marker N, respectively.

(2) CZE separation of standard component(s) S (S1, S2, . . .) and of EOF marker N is performed under the same condition as CZE analysis of the sample of analyte A and electrophoretic velocity of the standard components S in the capillary, $v_{ep,c,S}$, is calculated according to Eq. (17), where $t_r = t_{r,S}$ and $t_{eo} = t_N$; $t_{r,S}$ and t_N are the resulting migration times of components S and N, respectively. From the migration time of EOF marker N, t_N, the EOF velocity in the capillary, $v_{eo,c}$, is calculated according to Eq. (18), where $t_{eo} = t_N$.

(3) Standard component(s) S (S1, S2, . . .) and EOF marker N are separated in the "standard" (empirically developed) FFZE regimen with the same BGE as that used in CZE. From this experiment the electrophoretic velocity of standard component S in the flow-through chamber, $v_{ep,f,S}$, is obtained according to Eq. (22), where $d_r = d_{r,S}$ and $d_{eo} = d_N$ ($d_{r,S}$ and d_N are resulting migration distances of components S and N, respectively) and EOF velocity in the chamber, $v_{eo,f}$, is calculated according to Eq. (23), where $d_{eo} = d_N$.

(4) From the results obtained in steps 2 and 3, the ratio, q_{ep}, of electrophoretic velocities of standard component S in the flow-through chamber and in the capillary is determined:

$$q_{ep} = \frac{v_{ep,f,S}}{v_{ep,c,S}} \tag{26}$$

Similarly, the ratio of EOF velocities in the chamber and in the capillary, q_{eo}, is obtained:

$$q_{eo} = \frac{v_{eo,f,N}}{v_{eo,c,N}} \tag{27}$$

(5) From the electrophoretic velocity of analyte A (obtained in step 1) and from the coefficients q_{ep} and q_{eo} (obtained in step 4), the electrophoretic velocity of analyte A in FFZE, $v_{ep,f,A}$, and EOF velocity in FFZE chamber, $v_{eo,f}$, are calculated:

$$v_{ep,f,A} = q_{ep} v_{ep,c,A} \tag{28}$$

$$v_{eo,f} = q_{eo} v_{eo,c} \tag{29}$$

Then the predicted resulting migration distance of analyte A in the FFZE chamber, $d_{r,A,pre}$, can be obtained as the sum of electrophoretically moved distance, $d_{ep,A}$, and electroosmotically moved distance, d_{eo}:

$$d_{r,A,pre} = d_{ep,A} + d_{eo} = (v_{ep,f,A} + v_{eo,f})t_f \quad (30)$$

(6) The resulting migration distances can also be calculated for the other components of the sample (admixtures A1, A2, . . . and neutral component(s) N) and their separability in FFZE can be estimated. If the distances of the components of interest at the outlet side of the chamber are sufficient for their separation, then the FFZE separation can be performed under the same conditions as those used for separation of standard components.

If the predicted distances are not sufficient for the separation of sample components of interest, then the separation conditions of FFZE, namely, clamp voltage and/or flow-through time, have to be further optimized. If the predicted distances are too small and the separation of sample components is not achieved, then the voltage and/or flow-through time should be increased. If the predicted distances for the sample components are too long and there is a danger that the fastest component will reach the close vicinity of the ion exchange membrane separating the separation chamber from the electrode compartment (see Fig. 11), where this component can be damaged or lost because of concentration, pH, and conductivity nonhomogeneities occurring in this region, then the clamp voltage and/or flow-through time must be decreased. The migrated distance is approximately directly proportional to the voltage and to the flow-through time, i.e., *p*% prolongation of migration time and *r*% increasing of voltage will result in (p + r)% prolongation of migrated distance. Following this rule suitable separation conditions can be selected.

The above-described procedure allows one to develop suitable separation conditions in the more economical and faster microscale by CZE. Only then can the optimized conditions be converted to the preparative scale realized by continuous FFZE separation.

E. Combined Application of Capillary and Free-Flow Zone Electrophoresis to Peptide Analysis and Preparation

In this section some examples of combined CZE and FFZE applications to analytical and preparative separations of synthetic biopeptides will be demonstrated.

CZE was performed on the experimental device developed in our institute [152], described in more detail in Section III.B above. Acetic acid (0.5 mol/L, pH 2.6) was used as the BGE. Peptide samples and EOF marker (phenol) were dissolved in this BGE in the concentration range 0.1–0.8 mg/ml. The sample was introduced into the capillary manually forming a hydrostatic pressure (50 mm H_2O column) for the time period 5–20 s. Experiments were performed at

ambient temperature 22–24°C without active cooling of the separation compartment.

FFZE experiments were performed in the apparatus developed in our institute [184]. The core of this system is a flow-through electrophoretic chamber consisting of two planparallel glass plates (500 × 500 mm) with a 0.5-mm gap between them. The background electrolyte is introduced through six inlets by a six-piston pump with a flow-through time of 31 min. Sample solution was introduced by a peristaltic pump with a flow rate of 1.5 ml/h. The effective length of the separation trajectory (from the sample inlet to the chamber outlet) was 440 mm. Both sides of the chamber were cooled by the air to −3°C. The separations were performed in the constant voltage regimen (3000 V, 122–125 mA). At the outlet side of the chamber the carrier electrolyte and sample components were collected in 48 fractions and periodically sucked into the fraction collector. The fractions were evaluated by off-line UV absorption measurement at 230 or 280 nm.

The developed procedure for the conversion of analytical CZE separation to preparative FFZE process will be demonstrated by analysis and preparation of [D-Tle^{2,5}]dalargin, synthetic hexapeptide with the sequence H-Tyr-D-Tle-Gly-Phe-D-Tle-Arg-OH. D-Tle indicates amino acid residue of tertiary leucine in the D configuration, the other amino acid residues are in L configuration. [D-Tle^{2,5}]Dalargin is an analog of dalargin, a hexapeptide with the sequence H-Tyr-D-Ala-Gly-Phe-Leu-Arg-OH, an enkephalin-type peptide with opiate activity.

CZE analysis of the crude synthetic product of [D-Tle^{2,5}]dalargin (see Fig. 13) shows that in addition to the main synthetic dalargin product (peak D), there are some other admixtures, apparently side reaction products of the solid phase synthesis. For the better orientation in the CZE-gram some of the admixtures are letter-indicated, the fastest one by F, the slowest charged admixture by S, and the noncharged admixture by N. Since the main dalargin product D is relatively well separated from the other admixtures by CZE, it was decided to use FFZE for preparative purification of the main synthetic product.

However, from the above given theory of the correlation of CZE and FFZE it follows that for conversion of analytical CZE separation into a preparative one realized by FFZE it is necessary to have not only the data from CZE analysis of the given sample, but also the ratios, i.e., q_{ep}, q_{eo} of electrophoretic and electroosmotic velocities in the FFZE chamber and in the capillary, respectively. The values of these coefficients were obtained from the separation of the standard mixture of charged components diglycine and triglycine and a noncharged component phenol by CZE and FFZE using the same background electrolyte, 0.5 mol/L acetic acid, in which a good separation of main dalargin product was achieved by CZE. The record of CZE separation of the standard mixture has already been presented in Fig. 4; the record of FFZE separation of this mixture is given in Fig. 14. FFZE separation of diglycine, triglycine, and phenol was

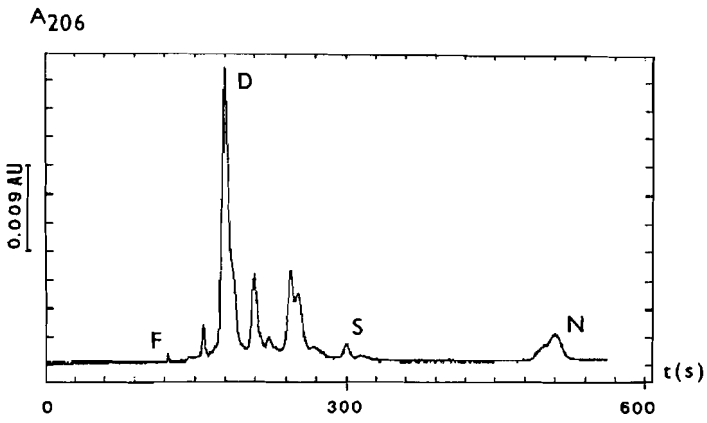

Figure 13 CZE analysis of crude synthetic product of [D-Tle^{2,5}] dalargin. Sample concentration 1.5 mg/ml. BGE: 0.5 mol/L acetic acid. Capillary: i.d. 0.056 mm, effective length 200 mm, total length 310 mm. Voltage 9.0 kV, current 10.1 μA. F, fastest component; D, main synthetic product—[D-Tle^{2,5}]dalargin; S, slow component; N, noncharged component. A_{206}, absorbance at 206 nm; t, time.

evaluated by CZE analysis of FFZE fractions. Although the FFZE separation of diglycine and triglycine was only partial due to the lower separation power of FFZE than that of CZE, it was possible to use the experimental data obtained from this separation (resulting migration distances) for calculation of ratios q_{ep} and q_{eo}. The data of CZE and FFZE separations of the standard mixture and the calculated values of electrophoretic and electroosmotic velocities according to Eqs. (17) and (18) for CZE and according to Eqs. (22) and (23) for FFZE and the values of coefficients q_{ep}, q_{eo} calculated according to Eqs. (24) and (25), respectively, are presented in Table 3. From the migration times of the charged components F, D, S and from the migration time of electroneutral component N (see Fig. 13 and CZE columns in Table 4) the electrophoretic and electroosmotic velocities of these sample components in the capillary, $v_{ep,c}$ and $v_{eo,c}$, were calculated according to Eqs. (17) and (18), respectively (see the CZE columns in Table 4). From these velocities of the sample components in the capillary and using the values of coefficients q_{ep}, q_{eo} (see Table 3), the electrophoretic velocities, $v_{ep,f}$, and the predicted migration distances, $d_{r,pre}$, of the sample components F, D, S, and N in FFZE chamber were calculated (see FFZE columns in Table 4). These predicted migration distances (15–221 mm) and the differences of these distances between individual sample components at the outlet side of the chamber indicated that a sufficient separation will be achieved in the same FFZE regimen that was used for the separation of standard mixture.

For this reason, the conditions of FFZE, under which the standard mixture

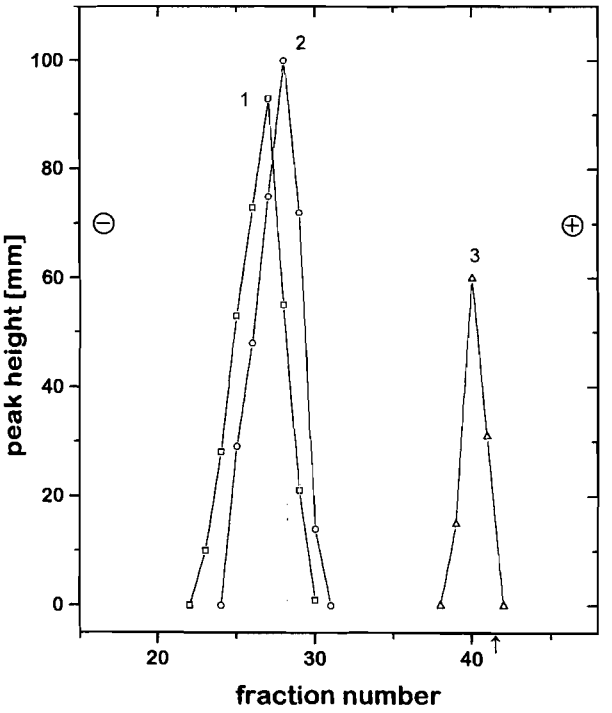

Figure 14 FFZE separation of standard mixture of diglycine (15 mg/ml), peak 1, triglycine (15 mg/ml), peak 2, and phenol (5 mg/ml), peak 3. BGE: 0.5 mol/L acetic acid, flow-through time 31 min, sample flow rate 1.5 ml/h, voltage 3000 V, current 120 mA, temperature −3°C; Peak height = peak height of the analytes obtained by CZE analyses of the aliquots of the FFZE fractions; ↑, sample inlet position.

of diglycine, triglycine, and phenol was separated (clamp voltage 3000 V, flow-through time 31 min), were applied also to the separation of the components of the crude product of [D-Tle^{2,5}]dalargin. The lyophilyzate of the crude synthetic product (190 mg) was dissolved in 5 ml of BGE (0.5 mol/L acetic acid), centrifuged, and applied to FFZE separation. The record of FFZE separation (off-line UV absorption measurement of FFZE fractions) is shown in Fig. 15. Comparing Fig. 13 and 15, the "qualitative" similarity of CZE and FFZE separation profiles can be observed. In addition to the main dalargin product (peak D), the fastest component F, slowest component S, and noncharged component N can be found on both records. The differences in relative peak heights are caused by the different detection wavelengths in CZE (206 nm) and in FFZE (280 nm). Obviously, a better separation of sample components is achieved in CZE than in FFZE. This

Table 3 Migration Times, Migration Distances, Electrophoretic and Electroosmotic Velocities of Standard Components Separated by CZE and FFZE

	CZE			FFZE			FFZE/CZE	
Standard component	t_r (s)	$v_{ep,c}$ (mm/s)	$v_{eo,c}$ (mm/s)	d_r (mm)	$v_{ep,f}$ (mm/s)	$v_{eo,f}$ (mm/s)	q_{ep}	q_{eo}
Diglycine	168	0.805	—	145	0.0699	—	0.087	—
Triglycine	184	0.707	—	135	0.0645	—	0.091	—
Phenol	510[a]	0	0.396	15[a]	0	0.0081	—	0.0205

[a] Resulting migration time, t_r (migration distance, d_r) of phenol is equal to migration time, t_{eo} (migration distance, d_{eo}) of electroneutral EOF marker.

t_r, resulting migration time; $v_{ep,c}$, electrophoretic velocity in CZE; $v_{eo,c}$, electroosmotic velocity in CZE; d_r, resulting migration distance; $v_{ep,f}$, electrophoretic velocity in FFZE; $v_{eo,f}$, electroosmotic velocity in FFZE; q_{ep} (q_{eo}), ratio of electrophoretic (electroosmotic) velocities in FFZE and CZE.

is quite understandable when taking into account the differences in the experimental conditions of these two methods: more efficient anticonvective stabilization and Joule heat transfer in the capillary (i.d. 0.056 mm, wall thickness 0.07 mm) than in the flow-through chamber (rectangular gap 0.5 mm between two glass plates of the thickness 4 mm), about one order lower separation time and sample concentration in CZE than in FFZE, absence of hydrodynamic flow in CZE, and a relatively large width of the collected fraction (10.4 mm) in FFZE.

Table 4 Migration Times, Electrophoretic Velocities, and Predicted and Experimental Migration Distances of Some Components of CZE and FFZE Separation of the Crude Product of [D-Tle[2,5]]dalargin

	CZE			FFZE			
Sample component	t_r (s)	$v_{ep,c}$ (mm/s)	$v_{eo,c}$ (mm/s)	$v_{ep,f}$ (mm/s)	$v_{eo,f}$ (mm/s)	$d_{r,pre}$ (mm)	$d_{r,exp}$ (mm)
F (fast comp.)	123	1.234	—	0.1111	—	221	235
D (dalargin comp.)	175	0.747	—	0.0665	—	139	155
S (slow comp.)	310	0.250	—	0.022	—	56	55
N (noncharged)	510[a]	0	0.396	0	0.0110	15	15

[a] Resulting migration time, t_r, of electroneutral component N is equal to migration time, t_{eo}, of EOF marker.

t_r, resulting migration time; $v_{ep,c}$, electrophoretic velocity in CZE; $v_{eo,c}$, electroosmotic velocity in CZE; $v_{ep,f}$, electrophoretic velocity in FFZE; $v_{eo,f}$, electrophoretic velocity in FFZE; $d_{r,pre}$, predicted migration distance for FFZE; $d_{r,exp}$, experimental migration distance in FFZE.

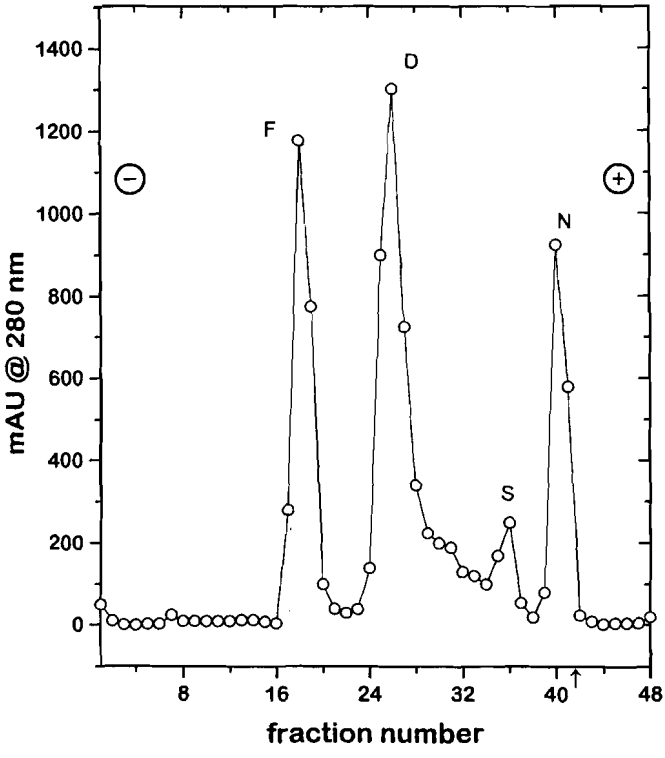

Figure 15 FFZE separation of crude synthetic product of [D-Tle^{2,5}]dalargin. Sample concentration 38 mg/ml. BGE: 0.5 mol/L acetic acid, flow-through time 31 min, sample flow rate 1.5 ml/h, voltage 3000 V, current 120 mA, temperature −3°C. F, fastest component; D, main synthetic product—[D-Tle^{2,5}]dalargin; S, slow component; N, noncharged component; ↑, sample inlet position.

The UV record of FFZE separation in Fig. 15 indicates that a good separation of the main dalargin product, peak D, from the component with higher mobility was achieved, but the separation from the component with lower mobility was not quite complete. CZE analysis of individual fractions of peak D showed that four of these fractions [24–27] contained pure dalargin, as demonstrated by a single peak of CZE analysis of fraction 26 in Fig. 16a. On the other hand, CZE analyses of some other fractions, as, for example, that of fraction 36 (see Fig. 16b), showed that some sample components remained unresolved after FFZE. Due to the lower separation power of FFZE in comparison with CZE, it would be unrealistic to expect the same degree of separation of all sample components,

but it is important that it is possible to develop such conditions of FFZE under which the product of interest is well separated from the admixtures, and it is less important that some byproducts are not completely separated.

The high-purity degree of the main synthetic product was confirmed also by other methods, particularly HPLC and amino acid analysis. The advantage of utilization of acetic acid as BGE is that peptide is obtained in acetate, i.e., a physiologically tolerable form, that can be directly applied to biological tests.

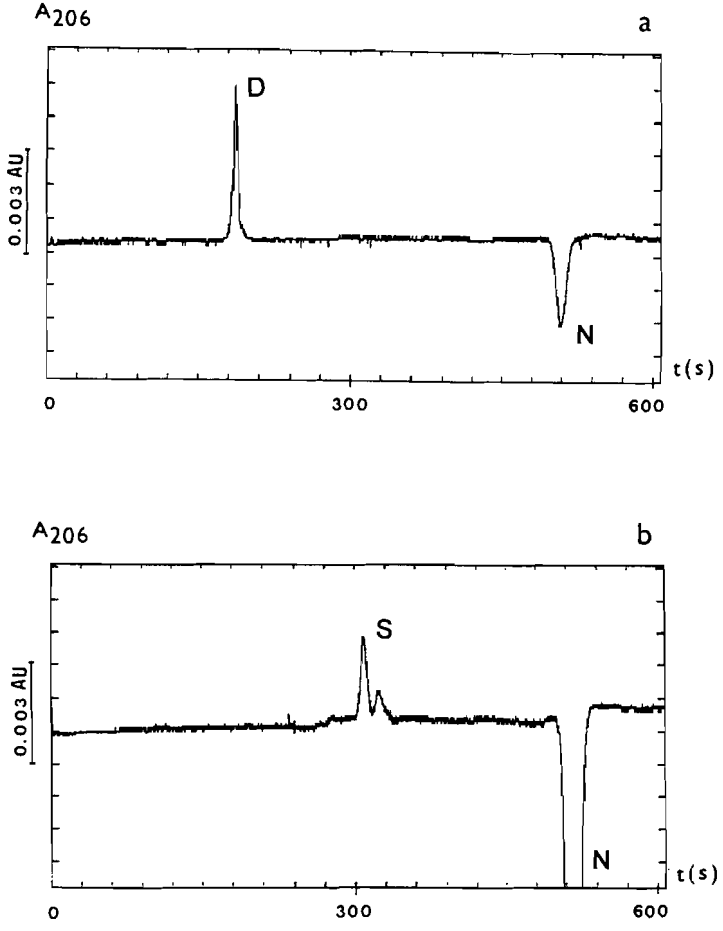

Figure 16 CZE analysis of fraction 26 (a) and 36 (b) of FFZE separation of [D-Tle^{2,5}]dalargin preparation presented in Fig. 15. Aliquot of FFZE fraction was directly applied to CZE analysis. Experimental conditions the same as in Fig. 13. A_{206}, absorption at 206 nm; t, migration time

Comparison of the experimentally determined migration distances of selected components with their predicted migration distances (see Fig. 15 and FFZE columns in Table 4) shows a good predictive power of the theoretical model of the correlation between CZE and FFZE. The relatively small discrepancy between the predicted and experimental distance of the fast sample component F (approx. 6%) confirms quantitative correlation between CZE and FFZE. The relatively larger discrepancy (approx. 10%) between the predicted and experimental migration distance of the main dalargin product is probably caused by the differences in partial adsorption of this sample component to the fused silica capillary wall and to the glass wall of the flow-through electrophoretic chamber and/or by more than one order higher peptide concentration in FFZE than in CZE.

Another example of the application of CZE and FFZE to synthetic peptide analysis and preparation is shown in Fig. 17. Disulfide fragment of human cathepsin D, eicosapeptide with the following structure (indicated as VI),

$$\begin{array}{l} \text{H-Thr-Pro-Pro-Gln-Cys-Phe-Thr-Val-NH}_2 \\ \qquad\qquad\qquad\qquad\qquad\qquad\qquad\qquad\qquad\quad | \\ \text{H-Val-Ser-Val-Pro-Cys-Gln-Ser-Ala-Ser-Ser-Ala-Ser-NH}_2 \end{array} \qquad \text{(VI)}$$

was synthesized by the solid phase method and purified by RP-HPLC [198]. CZE analysis of the HPLC-purified preparation revealed three admixtures of the main synthetic product (see Fig. 17a). The admixture indicated in this figure as I was later on identified as Cys-acetamidomethyl-derivative of octapeptide monomer of the dimer VI. In HPLC this octapeptide derivative was co-eluted with the heterodimer VI but in CZE these two peptide species were well separated. For that reason it was decided to use preparative FFZE for purification of heterodimer VI. The CZE analysis of FFZE-purified preparation of heterodimer VI confirmed the high purity of this preparation (see Fig. 17b) and the suitability of FFZE for separation of the admixtures not removed by HPLC. This is a good example of complementarity of CZE (FFZE) and HPLC for peptide analysis and preparation resulting from different separation principles of these methods.

A combination of CZE and FFZE has been applied to analysis and preparation of some other biopeptides synthesized at our institute, such as growth hormone–releasing peptide (GHRP) and its analogs and fragments [152,199], derivatives of luteinizing hormone–releasing hormone (LHRH) [200], and B23-30-octapeptide fragments of insulin [201].

Combined application of CZE and FFZE represents a new systematic approach to analysis and preparation of synthetic biopeptides. First, CZE is used for analysis of the peptide preparation and suitable conditions for its analysis are developed in a microscale minimizing time and material expenses for the development of the optimized separation conditions. Then, based on the theory of the correlation between CZE and FFZE, the optimized conditions of CZE separation are converted to FFZE separation. FFZE separation of peptide prepara-

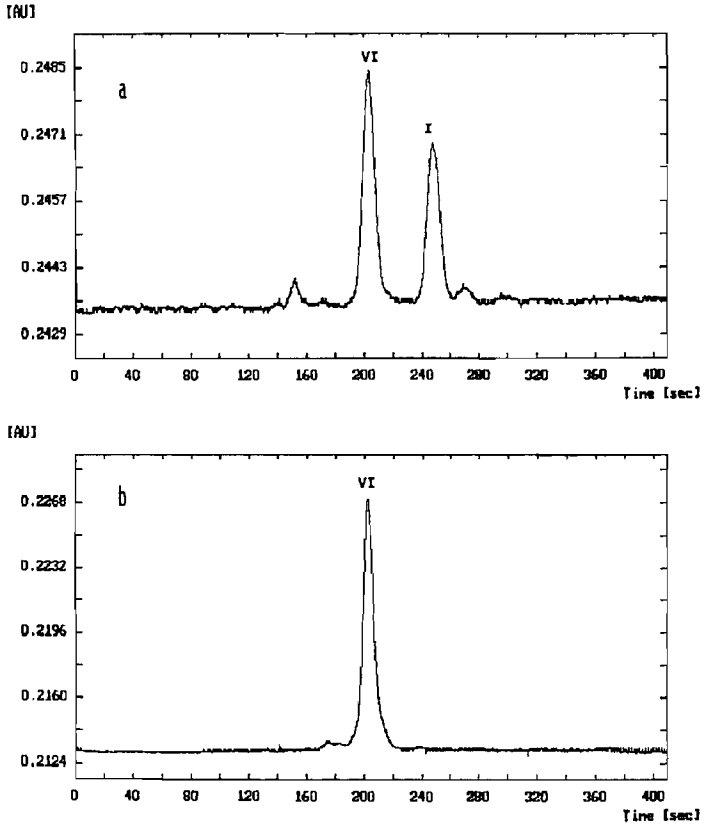

Figure 17 CZE analysis of eicosapeptide disulfide fragment of human cathepsin D preparation purified by HPLC (a) and by FFZE (b). Experimental conditions the same as in Fig. 13. VI, main synthetic product—eicosapeptide disulfide fragment of human cathepsin D. I, octapeptide fragment of eicosapeptide VI. For peptide sequences and other details, see the text.

tion provides an efficient tool for preparative purification of peptide sample with the preparative capacity of tens to hundreds of milligrams per hour. The advantage of this method is that it works continuously, in a carrierless medium, under mild conditions in which the biological activity of separated peptides is retained and the loss of material minimized. The purity of peptide fractions separated by FFZE can then be checked by CZE and/or another method. A combination of more methods based on different separation principles should be preferred because that way more complete information about peptide purity and identity can be obtained.

ACKNOWLEDGMENTS

The results presented in this chapter were obtained with the financial support of the Grant Agency of the Academy of Sciences of the Czech Republic, grant no. 45511, and of the Grant Agency of the Czech Republic, grant nos. 203/93/0718, 203/94/0698, and 203/96/K128, which is greatfully acknowledged. The author thanks his coworkers from the Laboratory of Electromigration Methods of the Institute of Organic Chemistry and Biochemistry—Dr. Z. Prusík, Dr. P. Sázelová, Mrs. V. Lišková, Mr. J. Štěpánek, and Mgr. M. Machová—for their cooperation and assistance in the experimental work and for their help in the preparation of this chapter.

ABBREVIATIONS

BGE background electrolyte
CBQCA 3-(4-carboxybenzoyl)-2-quinolinocarboxaldehyde
CF-FAB continuous flow fast-atom bombardment
CE capillary electrophoresis
CITP capillary isotachophoresis
CTAB cetyltrimethylammonium bromide
CZE capillary zone electrophoresis
DANSYL 5-dimethylaminonaphthalene-1-sulfonyl
EC electrochemical
EOF electroosmotic flow
ESI electrospray ionization
FFZE free-flow zone electrophoresis
FITC fluorescein isothiocyanate
GHRP growth hormone–releasing peptide
HGH human growth hormone
HI human insulin
HPCE high-performance capillary electrophoresis
HPLC high-performance liquid chromatography
HSA human serum albumin
IEF isoelectric focusing
IGF insulin-like growth factor
LHRH luteinizing hormone–releasing hormone
LIF laser-induced fluorescence
MALDI matrix-assisted laser desorption ionozation
MEKC micellar electrokinetic chromatography
MS mass spectrometry
NA nicotinamide
NDA naphthalene-2,3-dicarboxaldehyde

PI pig insulin
RP-HPLC reversed-phase high-performance liquid chromatography
SDS sodium dodecyl sulfate
Tris tris(hydroxymethyl)aminomethane
Tricine *N*-[tris-hydroxymethyl]methylglycine
UV ultraviolet

REFERENCES

1. Vacík J. Theory of electromigration processes. In: Deyl Z, ed. Electrophoresis: A Survey of Techniques and Applications. Pt. A: Techniques. Amsterdam: Elsevier, 1979:1–21.
2. Vacík J. Evaluation of the results of electrophoretic separations. In: Deyl Z, ed. Electrophoresis: A Survey of Techniques and Applications. Pt. A: Techniques. Amsterdam: Elsevier, 1979:39–43.
3. Mosher RA, Saville DA, Thormann W. The Dynamics of Electrophoresis. Weinheim: VCH, 1992.
4. Offord RE. Electrophoretic mobilities of peptides on paper and their use in the determination of amide groups. Nature 1966;211:591–593.
5. Rickard EC, Strohl MM, Nielsen RG. Correlation of electrophoretic mobilities from capillary electrophoresis with physicochemical properties of proteins and peptides. Anal Biochem 1991;197:197–207.
6. Compton BJ. Electrophoretic mobility modeling of proteins in free zone capillary electrophoresis and its application to monoclonal antibody microheterogeneity analysis. J Chromatogr 1991;559:357–366.
7. Grossman PD, Colburn JC, Lauer HH. A semiempirical model for the electrophoretic mobilities of peptides in free-solution capillary electrophoresis. Anal Biochem 1989;179:28–33.
8. Cifuentes A, Poppe H. Simulation and optimization of peptide separation by capillary electrophoresis. J Chromatogr A 1994;680:321–340.
9. Hilser VJ, Worosila GD, Rudnick SE. Protein and peptide mobility in capillary zone electrophoresis. A comparison of existing models and further analysis. J Chromatogr 1993;630:329–336.
10. Basak SK, Ladisch MR. Correlation of electrophoretic mobilities of proteins and peptides with their physicochemical properties. Anal Biochem 1995;226: 51–58.
11. Messana I, Rossetti DV, Cassiano L, Misiti F, Giardina B, Castagnola M. Peptide analysis by capillary (zone) electrophoresis. J Chromatogr B 1997;699: 149–171.
12. Survay MA, Goodall DM, Wren SAC, Rowe RC. Self-consistent framework for standardising mobilities in free solution capillary electrophoresis: applications to oligoglycines and oligoalanines. J Chromatogr A 1996;741:99–113.
13. Micinski S, Gronvald M, Compton BJ. Structure-mobility relationships in free solution zone electrophoresis. Meth Enzymol 1996;270:342–358.

14. Adamson NJ, Reynolds EC. Rules relating electrophoretic mobility, charge and molecular size of peptides and proteins. J Chromatogr B 1997;699:133–147.
15. Cifuentes A, Poppe H. Behavior of peptides in capillary electrophoresis: effect of peptide charge, mass and structure. Electrophoresis 1997;18:2362–2376.
16. Gao JM, Whitesides GM. Using protein charge ladders to estimate the effective charges and molecular weights of proteins in solution. Anal Chem 1997;69:575–580.
17. Chae KS, Lenhoff AM. Computation of the electrophoretic mobility of proteins. Biophys J 1995;68:1120–1127.
18. Stauff J, Jaenicke R. Physikalische chemie der losungen. In: Rauen HM, ed. Biochemisches Taschenbuch. Berlin: Springer-Verlag, 1964:37–121.
19. Prusík Z. Peptides and structural analysis of proteins. In: Deyl Z, ed. Electrophoresis: a survey of techniques and applications. Pt. B: Applications. Amsterdam: Elsevier, 1983:81–107.
20. Rickard EC, Towns JK. Applications of capillary zone electrophoresis to peptide mapping. Meth Enzymol 1996;271:237–264.
21. Kašička V, Prusík Z. Isotachophoretic analysis of peptides. Selection of electrolyte systems and determination of purity. J Chromatogr 1989;470:209–221.
22. Kašička V. Analysis and preparation of peptides and proteins by isotachophoresis. PhD thesis (in Czech). Prague: Czechoslovak Academy of Science, 1985.
23. Mosher RA, Gebauer P, Thormann W. Computer simulation and experimental validation of the electrophoretic behavior of proteins 3. Use of titration data predicted by the protein's amino acid composition. J Chromatogr 1993;638:155–164.
24. Westermeier R. Electrophoresis in Practice: A Guide to Methods and Applications of DNA and Protein Separations. Weinheim: VCH, 1997.
25. Nath S, Schutte H, Hustedt H, Deckwer WD. Correlation of migration behavior in free-flow zone electrophoresis and electrophoretic titration curve. Electrophoresis 1990;11:612–616.
26. Hirokawa T, Kiso Y, Gaš B, Zusková I, Vacík J. Simulated quantitative and qualitative isotachophoretic indices of 73 amino acids and peptides in the pH range 6.4–10. J Chromatogr 1993;628:283–308.
27. Wehr T, Zhu M, Rodriguez-Diaz R. Capillary isoelectric focusing. Meth Enzymol 1996;270:358–374.
28. Righetti PG, Gelfi C, Chiari M. Isoelectric focusing in capillaries. In: Righetti PG, ed. Capillary Electrophoresis in Analytical Biotechnology. Boca Raton: CRC Press, 1996:509–539.
29. Righetti PG, Gelfi C. Isoelectric focusing in capillaries and slab gels: a comparison. J Cap Elec 1994;1:27–35.
30. Yao YJ, Khoo KS, Chung MCM, Li SFY. Determination of isoelectric points of acidic and basic proteins by capillary electrophroesis. Chromatogr A 1994;680:431–435.
31. Sillero A, Ribeiro JM. Isoelectric points of proteins: theoretical determination. Anal Biochem 1989;179:319–325.
32. Henriksson G, Englund AN, Johansson G, Lundahl P. Calculation of the isoelectric points of native proteins with spreading of pKa values. Electrophoresis 1995;16:1377–1380.

33. Grossman PD. Background concepts. In: Grossman PD, Colburn JC, eds. Capillary Electrophoresis. San Diego: Academic Press, 1992:3–43.
34. Boček P. Analytical capillary electrophoresis. In: Churáček J, ed. Advanced Instrumental Methods of Chemical Analysis. Praha: Academia, 1993:97–141.
35. Foret F, Křivánková L, Boček P. Capillary Zone Electrophoresis. Weinheim: Verlag Chemie, 1993.
36. Moring SE. Buffers, electrolytes, and additives for capillary electrophoresis. In: Righetti PG, ed. Capillary Electrophoresis in Analytical Biotechnology. Boca Raton: CRC Press, 1996:37–60.
37. Issaq HJ, Janini GM, Chan KC, Elrassi Z. Approaches for the optimization of experimental parameters in capillary zone electrophoresis. Adv Chromatogr 1995;35: 101–169.
38. Hannig K, Heidrich HK. Free-Flow Electrophoresis. Darmstadt: GIT, 1989.
39. Reijenga JC, Verheggen TPEM, Martens JHPA, Everaerts FM. Buffer capacity, ionic strength and heat dissipation in capillary electrophoresis. J Chromatogr A 1996;744:147–153.
40. Nielsen RG, Rickard EC. Method optimization in CZE analysis of hGH tryptic digest fragments. J Chromatogr 1990;516:99–114.
41. Swedberg SA. Use of non-ionic and zwitterionic surfacants to entrance selectivity in HPCE. J Chromatogr 1990;503:449–452.
42. Greve KF, Nashabeh W, Karger BL. Use of zwitterionic detergents for the separation of closely related peptides by capillary electrophoresis. J Chromatogr A 1994; 680:15–24.
43. Matsubara N, Koezuka K, Terabe S. Separation of eleven angiotensin II analogs by capillary electrophoresis with a nonionic surfactant in acidic media. Electrophoresis 1995;16:580–583.
44. Liu J, Cobb KA, Novotny M. Capillary electrophoretic separations of peptides using micelle-forming compounds and cyclodextrins as additives. J Chromatogr 1990; 519:189–197.
45. Kornfelt T, Vinther A, Okafo GN, Camilleri P. Improved peptide mapping using phytic acid as ion-pairing buffer additive in capillary electrophoresis. J Chromatogr A 1996;726:223–228.
46. Matsubara N, Terabe S. Micellar electrokinetic chromatography. Meth Enzymol 1996;270:319–341.
47. Matsubara N, Terabe S. Micellar electrokinetic chromatography in the analysis of amino acids and peptides. In: Righetti PG, ed. Capillary Electrophoresis in Analytical Biotechnology. Boca Raton: CRC Press, 1996:155–182.
48. Vindevogel J, Sandra P. Introduction to Micellar Electrokinetic Chromatography. Heidelberg: Huthig, 1992.
49. Yashima T, Tsuchiya A, Morita O. Separation of closely related large peptides by micellar electrokinetic chromatography with organic modifiers. Anal Chem 1992; 64:2981–2984.
50. Ye B, Hadjmohammadi M, Khaledi MG. Selectivity control in micellar electrokinetic chromatography of small peptides using mixed fluorocarbon hydrocarbon anionic surfactants. J Chromatogr A 1995;692:291–300.
51. Castagnola M, Cassiano L, Messana I, Paci M, Rossetti DV, Giardina B. Effect

of 2,2,2-trifluoroethanol on capillary zone electrophoretic peptide separations. J Chromatogr A 1996;735:271–281.
52. Oda RP, Madden BJ, Morris JC, Spelsberg TC, Landers JP. Multiple-buffer-additive strategies for enhanced capillary electrophoretic separation of peptides. J Chromatogr A 1994;680:341–351.
53. Johansson IM, Huang EC, Henion JD, Zweigenbaum J. Capillary electrophoresis atmospheric pressure ionization mass spectrometry for the characterization of peptides: instrumental considerations for mass spectrometric detection. J Chromatogr 1991;554:311–327.
54. Hansen SH, Tjornelund J, Bjornsdottir I. Selectivity enhancement in capillary electrophoresis using non-aqueous media. Trends Anal Chem 1996;15:175–180.
55. Sahota RS, Khaledi MG. Nonaqueous capillary electrophoresis. Anal Chem 1994; 66:1141–1146.
56. Chiari M, Nesi M, Righetti PG. Surface modifications of silica walls: a review of different methodologies. In: Righetti PG, ed. Capillary Electrophoresis in Analytical Biotechnology. Boca Raton: CRC Press, 1996:1–36.
57. Yeung ES. Optical detectors for capillary electrophoresis. Adv Chromatogr 1995; 35:1–51.
58. Flint CD, Grochowicz PR, Simpson CF. Design, construction and evaluation of an ultraviolet absorbance detector for dapillary electrophoresis. Anal Proc Anal Comm 1994;31:117–121.
59. Prusík Z, Kašička V, Staněk S, Kuncová G, Hayer M, Vrkoč J. Experimental device for electrokinetic micellar chromatography exploiting some components of capillary isotachophoresis instrumentation. J Chromatogr 1987;390:87–96.
60. Boring CB, Dasgupta PK. An affordable high-performance optical absorbance detector for capillary systems. Anal Chim Acta 1997;342:123–132.
61. Heiger DN, Kaltenbach P, Sievert HJP. Diode array detection in capillary electrophoresis. Electrophoresis 1994;15:1234–1247.
62. Quanta 4000E high performance capillary electrophoresis system. A quantum leap in protein, peptide, and DNA analysis. Technical note, Millipore Corporation, 1993.
63. Heiger D, Grimm R, Herold M. Peptide mapping and analysis using capillary electrophoresis. Hewlett-Packard Application Note, Publication number 1993;12-5091–9062E.
64. Becklin RR, Desiderio DM. The amount of ultraviolet absorbance in a synthetic peptide is directly proportional to its number of peptide bonds. Anal Lett 1995;28: 2175–2190.
65. Heiger DN. High Performance Capillary Electrophoresis: An Introduction. Hewlett-Packard Primer, Publication 12-5091-7913E, 1993.
66. Djordjevic NM, Widder M, Kuhn R. Signal enhancement in capillary electrophoresis by using a sleeve cell arrangement for optical detection. J High Res Chromatogr 1997;20:189–192.
67. Ross G. Applications of the HP-3D Capillary Electrophoresis System. Hewlett-Packard Primer, Publication 12-5963-7140E, 1995.
68. Green JS, Jorgenson IC. Variable wavelength on-column fluorescence detector for open tubular zone electrophoresis. J Chromatogr 1986;352:337–343.

69. Lee TT, Yeung ES. Capillary electrophoresis detectors: Lasers. Meth Enzymol 1996;270:419–449.
70. Nouadje G, Amsellem J, Couderc B, Verdeguer P, Couderc F. Capillary electrophoresis with laser-induced fluorescence detection: optical designs and applications. In: Parvez H, Caudy P, Parvez S, Roland-Gosselin P, eds. Capillary Electrophoresis in Biotechnology and Environmental Analysis. Utrecht: VSP, 1997:49–72.
71. Schwartz HE, Ulfelder KJ, Chen FTA, Pentoney SL. The utility of laser-induced fluorescence detection in applications of capillary electrophoresis. J Cap Elec 1994; 1:36–54.
72. MacTaylor CE, Ewing AG. Critical review of recent developments in fluorescence detection for capillary electrophoresis. Electrophoresis 1997;18:2279–2290.
73. Chen DY, Dovichi NJ. Single-molecule detection in capillary electrophoresis: Molecular shot noise as a fundamental limit to chemical analysis. Anal Chem 1996; 68:690–696.
74. Lee TT, Yeung ES. High-sensitivity laser-induced fluorescence detection of native proteins in capillary electrophoresis. J Chromatogr 1992;595:319–325.
75. Timperman AT, Oldenburg KE, Sweedler JV. Native fluorescence detection and spectral differentiation of peptides containing tryptophan and tyrosine in capillary electrophoresis. Anal Chem 1995;67:3421–3426.
76. Chan KC, Janini GM, Muschik GM, Issaq HJ. Pulsed UV laser-induced fluorescence detection of native peptides and proteins in capillary electrophoresis. J Liq Chromatogr 1993;16:1877–1890.
77. Chan KC, Muschik GM, Issaq HJ. Separation of tryptophan and related indoles by micellar electrokinetic chromatography with KrF laser-induced fluorescence detection. J Chromatogr A 1995;718:203–210.
78. Chang HT, Yeung ES. Determination of catecholamines in single adrenal medullary cells by capillary electrophoresis and laser-induced native fluorescence. Anal Chem 1995;67:1079–1083.
79. Tong W, Yeung ES. Determination of insulin in single pancreatic cells by capillary electrophoresis and laser-induced native fluorescence. J Chromatogr B 1996;685:35–40.
80. Lee TT, Yeung ES. Quantitative determination of native proteins in individual human erythrocytes by capillary zone electrophoresis with laser-induced fluorescence detection. Anal Chem 1992;64:3045–3051.
81. Bardelmeijer HA, Waterval JCM, Lingeman H, Vanthof R, Bult A, Underberg WJM. Pre-, on- and post-column derivatization in capillary electrophoresis. Electrophoresis 1997;18:2214–2227.
82. Zhao JY, Waldron KC, Miller J, Zhang JZ, Harke H, Dovichi NJ. Attachment of a single fluorescent label to peptides for determination by capillary zone electrophoresis. J Chromatogr 1992;608:239–242.
83. Little MJ, Paquette DM, Harvey MD, Banks PR. Single-label fluorescent derivatization of peptides. Anal Chim Acta 1997;339:279–288.
84. Liu JP, Hsieh YZ, Wiesler D, Novotny M. Design of 3-(4-carboxybenzoyl)-2-quinoline-carboxaldehyde as a reagent for ultrasensitive determination of primary amines by capillary electrophoresis using laser fluorescence detection. Anal Chem 1991;63:408–412.
85. Cobb KA, Novotny MV. Peptide mapping of complex proteins at the low-picomole level with capillary electrophoretic separations. Anal Chem 1992;64:879–886.

86. Cobb KA, Novotny MV. Selective determination of arginine-containing and tyrosine-containing peptides using capillary electrophoresis and laser-induced fluorescence detection. Anal Biochem 1992;200:149–155.
87. Fadden P, Haystead TAJ. Quantitative and selective fluorophore labeling of phosphoserine on peptides and proteins: characterization at the attomole level by capillary electrophoresis and laser-induced fluorescence. Anal Biochem 1995;225:81–88.
88. Shippy SA, Jankowski JA, Sweedler JV. Analysis of trace level peptides using capillary electrophoresis with UV laser-induced fluorescence. Anal Chim Acta 1995;307:163–171.
89. Craig DB, Wong JCY, Dovichi NJ. Detection of attomolar concentrations of alkaline phosphatase by capillary electrophoresis using laser-induced fluorescence detection. Anal Chem 1996;68:697–700.
90. Advis JP, Guzman NA. Capillary electrophoresis coupled to fluorescence detection for the determination of in-vivo release of multiple neuropeptides from the ewe median eminence. J Liq Chromatogr 1993;16:2129–2148.
91. Park SS, Hung WL, Schaufelberger DE, Guzman NA, Advis JP. Determination of neuropeptides by capillary electrophoresis. In: Irvine GB, Williams CH, eds. Neuropeptide Protocols. Totowa: Humana Press, 1997:101–111.
92. Hogan BL, Yeung ES. Determination of intracellular species at the level of a single erythrocyte via capillary electrophoresis with direct and indirect fluorescence detection. Anal Chem 1992;64:2841–2845.
93. Wong KS, Yeung ES. Simultaneous monitoring of glutathione and major proteins in single erythrocytes. Mikrochim Acta 1995;120:321–327.
94. Tsukagoshi K, Tanaka A, Nakajima R, Hara T. On-line capillary zone electrophoretic separation-chemiluminescence detection of protein labeled with fluorescamine. Anal Sci 1996;12:525–528.
95. Staller TD, Sepaniak MJ. Chemiluminescence detection in capillary electrophoresis. Electrophoresis 1997;18:2291–2296.
96. Tomer KB, Deterding LJ, Parker CE. Capillary electrophoresis coupled with mass spectrometry. Adv Chromatogr 1995;35:53–99.
97. Smith RD, Udseth HR, Wahl JH, Goodlett DR, Hofstadler SA. Capillary electrophoresis mass spectrometry. Meth Enzymol 1996;271:448–486.
98. Banks JF. Recent advances in capillary electrophoresis electrospray mass spectrometry. Electrophoresis 1997;18:2255–2266.
99. Tomer KB, Parker CE, Deterding LJ. Capillary electrophoresis interfaced with mass spectrometry: electrospray ionization and continuous flow fast atom bombardment. In: Righetti PG, ed. Capillary Electrophoresis in Analytical Biotechnology. Boca Raton: CRC Press, 1996:123–153.
100. Suter MJF, Caprioli RM. An integral probe for capillary zone electrophoresis/continuous-flow fast atom bombardment mass spectrometry. J Am Soc Mass Spectrom 1992;3:198–206.
101. Loo JA, Udseth HR, Smith RD. Peptide and protein analysis by electrospray ionization–mass spectrometry and capillary electrophoresis-mass spectrometry. Anal Biochem 1989;179:404–412.
102. Licklider L, Kuhr WG, Lacey MP, Keough T, Purdon MP, Takigiku R. On-line microreactors capillary electrophoresis mass spectrometry for the analysis of proteins and peptides. Anal Chem 1995;67:4170–4177.

103. Hynek R, Kašička V, Kučerová Z, Káš. J. Fast detection of phosphorylation of human pepsinogen A, human pepsinogen C and swine pepsinogen using a combination of reversed-phase high-performance liquid chromatography and capillary zone electrophoresis for peptide mapping. J Chromatogr B 1997;688:213–220.
104. Koezuka K, Ozaki H, Matsubara N, Terabe S. Separation and detection of closely related peptides by micellar electrokinetic chromatography coupled with electrospray ionization mass spectrometry using the partial filling technique. J Chromatogr B 1997;689:3–11.
105. Banks JF, Dresch T. Detection of fast capillary electrophoresis peptide and protein separations using electrospray ionization with a time-of-flight mass spectrometer. Anal Chem 1996;68:1480–1485.
106. Fang LL, Zhang R, Williams ER, Zare RN. On-line time-of-flight mass spectrometric analysis of peptides separated by capillary electrophoresis. Anal Chem 1994; 66:3696–3701.
107. Major HJ, Ashcroft AE. Analysis of a standard peptide mixture by capillary electrophoresis with mass spectrometry and with tandem mass spectrometry. Rapid Commun Mass Spectrom 1996;10:1421–1426.
108. Moseley MA, Jorgenson JW, Shabanowitz J, Hunt DF, Tomer KB. Optimization of capillary zone electrophoresis/electrospray ionization parameters for the mass spectrometry and tandem mass spectrometry analysis of peptides. J Am Soc Mass Spectrom 1992;3:289–300.
109. Figeys D, Vanoostveen I, Ducret A, Aebersold R. Protein identification by capillary zone electrophoresis/microelectrospray ionization–tandem mass spectrometry at the subfemtomole level. Anal Chem 1996;68:1822–1828.
110. Valaskovic GA, Kelleher NL, Mclafferty FW. Attomole protein characterization by capillary electrophoresis mass spectrometry. Science 1996;273:1199–1202.
111. Lewis KC, Opiteck GJ, Jorgenson JW, Sheeley DM. Comprehensive on-line RPLC-CZE-MS of peptides. J Am Soc Mass Spectrom 1997;8:495–500.
112. Walker KL, Chiu RW, Monnig CA, Wilkins CL. Off-line coupling of capillary electrophoresis and matrix-assisted laser desorption ionization time-of-flight mass spectrometry. Anal Chem 1995;67:4197–4204.
113. Yoo YS, Han YS, Suh MJ, Park J. Analysis of phosphopeptides by capillary electrophoresis and matrix-assisted laser-desorption ionization time-of-flight mass spectrometry. J Chromatogr A 1997;763:285–293.
114. Alexander AJ, Hughes DE. Monitoring of IgG antibody thermal stability by micellar electrokinetic capillary chromatography and matrix-assisted laser desorption/ ionization mass spectrometry. Anal Chem 1995;67:3626–3632.
115. Keough T, Takigiku R, Lacey MP, Purdon M. Matrix-assisted laser desorption mass spectrometry of proteins isolated by capillary zone electrophoresis. Anal Chem 1992;64:1594–1600.
116. Kelly JF, Locke SJ, Ramaley L, Thibault P. Development of electrophoretic conditions for the characterization of protein glycoforms by capillaryelectrophoresis electrospray mass spectrometry. J Chromatogr A 1996;720:409–427.
117. Ewing AG, Mesaros JM, Gavin PF. Electrochemical detection in microcolumn separations. Anal Chem 1994;66:A527–A537.
118. Voegel PD, Baldwin RP. Electrochemical detection in capillary electrophoresis. Electrophoresis 1997;18:2267–2278.

119. Voegel PD, Baldwin RP. Electrochemical detection with copper electrodes in liquid chromatography and capillary electrophoresis. Int Lab 1996;26:16A–16M.
120. O'Shea TJ, Greenhagen RD, Lunte SM, Lunte CE, Smyth MR, Radzik DM, Watanabe N. Capillary electrophoresis with electrochemical detection employing an on-column Nafion joint. J Chromatogr 1992;593:305–312.
121. Ye JN, Baldwin RP. Determination of amino acids and peptides by capillary electrophoresis and electrochemical detection at a copper electrode. Anal Chem 1994; 66:2669–2674.
122. O'Shea TJ, Lunte SM. Selective detection of free thiols by capillary electrophoresis electrochemistry using a gold mercury amalgam microelectrode. Anal Chem 1993; 65:247–250.
123. Weber PL, Kornfelt T, Klausen NK, Lunte SM. Characterization of glycopeptides from recombinant coagulation factor VIIa by high-performance liquid chromatography and capillary zone electrophoresis using ultraviolet and pulsed electrochemical detection. Anal Biochem 1995;225:135–142.
124. Huang XH, Zare RN, Sloss S, Ewing AG. End-column detection for capillary zone electrophoresis. Anal Chem 1991;63:189–192.
125. Muller D, Jelínek I, Opekar F, Štulík K. A conductometric detector for capillary separations. Electroanalysis 1996;8:722–725.
126. Huang X, Pang TKJ, Gordon MJ, Zare RN. On-column conductivity detector for capillary zone electrophoresis. Anal Chem 1987;59:2747–2749.
127. Dasgupta PK, Bao LY. Suppressed conductometric capillary electrophoresis separation systems. Anal Chem 1993;65:1003–1011.
128. Kar S, Dasgupta PK, Liu HH, Hwang H. Computer-interfaced bipolar pulse conductivity detector for capillary systems. Anal Chem 1994;66:2537–2543.
129. Jandik P, Bonn G. Capillary Electrophoresis of Small Molecules and Ions. Cambridge: VCH, 1993.
130. Huang XH, Luckey JA, Gordon MJ, Zare RN. Quantitative analysis of low molecular weight carboxylic acids by capillary zone electrophoresis/conductivity detection. Anal Chem 1989;61:766–770.
131. Grossman PD, Wilson KJ, Petrie G, Lauer HH. Effect of buffer pH and peptide composition on the selectivity of peptide separations by capillary zone electrophoresis. Anal Biochem 1988;173:265–270.
132. Colburn JC. Capillary electrophoresis separations of peptides: practical aspects and applications. In: Grossman PD, Colburn JC, eds. Capillary Electrophoresis: Theory and Practice. San Diego: Academic Press, 1992:237–271.
133. Nashabeh W, Greve KF, Kirby D, Foret F, Karger BL, Reifsnyder DH, Builder SE. Incorporation of hydrophobic selectivity in capillary electrophoresis: analysis of recombinant insulin-like growth factor I variants. Anal Chem 1994;66: 2148–2154.
134. Grossman PD, Colburn JC, Lauer HH, Nielsen RG, Riggin RM, Sittampalam GS, Rickard EC. Application of free-solution capillary electrophoresis to the analytical scale separation of proteins and peptides. Anal Chem 1989;61:1186–1194.
135. Nielsen RG, Sittampalam GS, Rickard EC. Capillary zone electrophoresis of insulin and growth hormone. Anal Biochem 1989;177:20–26.
136. Vinther A, Holm A, Hoegjensen T, Jespersen AM, Klausen NK, Christensen T, Sorensen HH. Synthesis of stereoisomers and isoforms of a tryptic heptapeptide

fragment of human growth hormone and analysis by reverse-phase HPLC and capillary electrophoresis. Eur J Biochem 1996;235:304–309.
137. Wan H, Blomberg LG. Enantiomeric separation by capillary electrophoresis of di- and tripeptides derivatized with 9-fluorenylmethyl chloroformate using vancomycin as chiral selector. J Microcolumn Sep 1996;8:339–344.
138. Wan H, Blomberg LG. Enantiomeric and diastereomeric separation of di- and tripeptides by capillary electrophoresis. J Chromatogr A 1997;758:303–311.
139. Sanger-van de Griend CE, Groningsson K, Arvidsson T. Enantiomeric separation of a tetrapeptide with cyclodextrin: extension of the model for chiral capillary electrophoresis by complex formation of one enantiomer molecule with more than one chiral selector molecules. J Chromatogr A 1997;782:271–279.
140. Moore AW, Jorgenson JW. Resolution of cis and trans isomers of peptides containing proline using capillary zone electrophoresis. Anal Chem 1995;67:3464–3475.
141. Ma S, Kalman F, Kalman A, Thunecke F, Horvath C. Capillary zone electrophoresis at subzero temperatures: separation of the cis and trans conformers of small peptides. J Chromatogr A 1995;716:167–182.
142. Survay MA, Goodall DM, Wren SAC, Rowe RC. Oligoglycines and oligoalanines as tests for modelling mobility of peptides in capillary electrophoresis. J Chromatogr 1993;636:81–86.
143. Kašička V, Prusìk Z, Mudra P, Štěpánek J. Capillary electrophoresis device with double UV detection and its application to the determination of effective mobilities of peptides. J Chromatogr A 1995;709:31–38.
144. Gao JM, Gomez FA, Harter R, Whitesides GM. Determination of the effective charge of a protein in solution by capillary electrophoresis. Proc Natl Acad Sci USA 1994;91:12027–12030.
145. Zhang Y, Lee HK, Li SFY. Separation of myoglobin molecular mass markers using non-gel sieving capillary electrophoresis. J Chromatogr A 1996;744:249–257.
146. Walbroehl Y, Jorgenson JW. Capillary zone electrophoresis for the determination of electrophoretic mobilities and diffusion coefficients of proteins. J Microcolumn Sep 1989;1:41–45.
147. Rao JH, Whitesides GM. Tight binding of a dimeric derivative of vancomycin with dimeric L-Lys-D-Ala-D-Ala. J Am Chem Soc 1997;119:10286–10290.
148. Rao JH, Colton IJ, Whitesides GM. Using capillary electrophoresis to study the electrostatic interactions involved in the association of D-Ala-D-Ala with vancomycin. J Am Chem Soc 1997;119:9336–9340.
149. Letourneau DL, Allen NE. Use of capillary electrophoresis to measure dimerization of glycopeptide antibiotics. Anal Biochem 1997;246:62–66.
150. Křivánková L, Boček P. Synergism of capillary isotachophoresis and capillary zone electrophoresis. J Chromatogr B 1997;689:13–34.
151. Goodall DM, Williams SJ, Lloyd DK. Quantitative aspects of capillary electrophoresis. Trends Anal Chem 1991;10:272–279.
152. Prusík Z, Kašička V, Mudra P, Štěpánek J, Smékal O, Hlaváček J. Correlation of capillary zone electrophoresis with continuous free-flow zone electrophoresis: application to the analysis and purification of synthetic growth hormone releasing peptide. Electrophoresis 1990;11:932–936.
153. Novotny MV, Cobb KA, Liu JP. Recent advances in capillary electrophoresis of proteins, peptides and amino acids. Electrophoresis 1990;11:735–749.

154. Righetti PG, Gelfi C, Perego M, Stoyanov AV, Bossi A. Capillary zone electrophoresis of oligonucleotides and peptides in isoelectric buffers: theory and methodology. Electrophoresis 1997;18:2145–2153.
155. Kuhr WG, Monnig CA. Capillary electrophoresis. Anal Chem 1992;64:R389–R407.
156. Monnig CA, Kennedy RT. Capillary electrophoresis. Anal Chem 1994;66:R280–R314.
157. Stclaire RL. Capillary electrophoresis. Anal Chem 1996;68:R569–R586.
158. Kašička V, Prusík Z. Capillary zone electrophoresis and isotachophoresis of biologically active peptides. In: Parvez H, Caudy P, Parvez S, Roland-Gosselin P, eds. Capillary Electrophoresis in Biotechnology and Environmental Analysis. Utrecht: VSP, 1997:173–197.
159. Castagnola M, Messana I, Rossetti DV. Capillary zone electrophoresis for the analysis of peptides. In: Righetti PG, ed. Capillary Electrophoresis in Analytical Biotechnology. Boca Raton: CRC Press, 1996:239–275.
160. Li SFY. Capillary Electrophoresis. Amsterdam: Elsevier, 1992.
161. Rose DJ, Jorgenson JW. Fraction collector for capillary zone electrophoresis. J Chromatogr 1988;438:23–34.
162. Lee HG, Desiderio DM. Preparative capillary zone electrophoresis of synthetic peptides: conversion of an autosampler into a fraction collector. J Chromatogr A 1994; 686:309–317.
163. Smith AJ. Analytical and micropreparative capillary electrophoresis of peptides. In: Smith BJ, ed. Protein Sequencing Protocols. Totowa: Humana Press, 1997:91–99.
164. Boss HJ, Rohde MF, Rush RS. Multiple peptide fraction collection by capillary electrophoresis with reinjection analysis. Peptide Res 1996;9:203–209.
165. Herold M, Wu SL. Automated peptide fraction collection in CE. LC GC-Mag Separation Sci 1994;12:531–533.
166. Grimm R, Herold M. Micropreparative single run fraction collection of peptides separated by CZE for protein sequencing. J Cap Elec 1994;1:79–82.
167. Lee HG, Tseng JL, Becklin RR, Desiderio DM. Preparative and analytical capillary zone electrophoresis analysis of native endorphins and enkephalins extracted from the bovine pituitary: mass spectrometric confirmation of the molecular mass of leucine enkephalin. Anal Biochem 1995;229:188–197.
168. Boss HJ, Rohde MF, Rush RS. Multiple sequential fraction collection of peptides and glycopeptides by high-performance capillary electrophoresis. Anal Biochem 1995;230:123–129.
169. Bergman AC, Bergman T. Micropreparation of peptides by capillary electrophoresis for matrix assisted laser desorption mass spectrometry. FEBS Lett 1996;397:45–49.
170. Bergman T, Agerberth B, Jornvall H. Direct analysis of peptides and amino acids from capillary electrophoresis. FEBS Lett 1991;283:100–103.
171. Wallingford RA, Ewing AG. Amperometric detection of catechols in capillary zone electrophoresis with normal and micellar solutions. Anal Chem 1988;60:258–263.
172. Huang X, Zare RN. Continuous sample collection in capillary zone electrophoresis by coupling the outlet of a capillary to a moving surface. J Chromatogr 1990;516: 185–189.
173. Fujimoto C, Fujikawa T, Jinno K. Sample collection by a capillary zone electrophoretic system with an on-column fracture. J High Res Chromatogr 1992;15:201–203.
174. Cheng YF, Fuchs M, Andrews D, Carson W. Membrane fraction collection for capillary electrophoresis. J Chromatogr 1992;608:109–116.

175. Muller O, Foret F, Karger BL. Design of a high-precision fraction collector for capillary electrophoresis. Anal Chem 1995;67:2974–2980.
176. Chiu RW, Walker KL, Hagen JJ, Monnig CA, Wilkins CL. Coaxial capillary and conductive capillary interfaces for collection of fractions isolated by capillary electrophoresis. Anal Chem 1995;67:4190–4196.
177. Banke N, Hansen K, Diers I. Detection of enzyme activity in fractions collected from free solution capillary electrophoresis of complex samples. J Chromatogr 1991;559:325–335.
178. Tsuda T, Sweedler JV, Zare RN. Rectangular capillaries for capillary zone electrophoresis. Anal Chem 1990;62:2149–2152.
179. Cifuentes A, Rodriguez MA, Garciamontelongo FJ. Rectangular capillary electrophoresis: study of some dispersive effects. J Chromatogr A 1996;737:243–253.
180. Fujimoto C, Matsui H, Sawada H, Jinno K. The use of a microconcentric column in capillary electrophoresis. J Chromatogr A 1994;680:33–42.
181. Camilleri P, Okafo GN, Southan C, Brown R. Analytical and micropreparative capillary electrophoresis of the peptides from calcitonin. Anal Biochem 1991;198: 36–42.
182. Schwer C, Lottspeich F. Analytical and micropreparative separation of peptides by capillary zone electrophoresis using discontinuous buffer systems. J Chromatogr 1992;623:345–355.
183. Cifuentes A, Xu X, Kok WT, Poppe H. Optimum conditions for preparative operation of capillary zone electrophoresis. J Chromatogr A 1995;716:141–156.
184. Prusík Z. Free-flow electromigration separations. J Chromatogr 1974;91:867–872.
185. Prusík Z. Continuous flow-through electrophoresis. In: Deyl Z, ed. Electrophoresis, Part A: Techniques. Amsterdam: Elsevier, 1979:229–251.
186. Wagner H, Mang V, Kessler R, Speer W. A free-flow system for preparative separations. In: Holloway CJ, ed. Analytical and Preparative Isotachophoresis. Berlin: Walter de Gruyter, 1984:347–356.
187. Wagner H, Heinrich J. Free-flow electrophoresis for the separation and purification of biopolymers. In: Tschesche H, ed. Modern Methods in Protein and Nucleic Acid Research. Berlin: Walter de Gruyter, 1990:69–97.
188. Roman MC, Brown PR. Free-flow electrophoresis. Anal Chem 1994;66:A86–A94.
189. Nath S, Schutte H, Hustedt H, Deckwer WD. Application of continuous zone electrophoresis to preparative separation of proteins. Biotechnol Bioeng 1993;42:829–835.
190. Nath S, Schutte H, Hustedt H, Deckwer WD, Weber G. Separation of enzymes from microorganism crude extracts by free-flow zone electrophoresis. Biotechnol Bioeng 1996;51:15–22.
191. Baier TG, Weber G, Hartmann K, Heinrich U, Schonberg D. Preparative separation of human B and T lymphocytes by free flow electrophoresis. Anal Biochem 1988; 171:91–95.
192. Weber G, Boček P. Optimized continuous flow electrophoresis. Electrophoresis 1996;17:1906–1910.
193. Clifton MJ, Roux-de Balmann H, Sanchez V. Protein separation by continuous-flow electrophoresis in microgravity. AIChE J 1996;42:2069–2079.
194. Kobayashi H, Ishii N, Nagaoka S. Bioprocessing in microgravity: applications of continuous flow electrophoresis to rat anterior pituitary particles—free flow electrophoresis of C-elegans DNA. J Biotechnol 1996;47:367–376.

195. Hymer WC, Salada T, Cenci R, Krishnan K, Seaman GVF, Snyder R, Matsumiya H, Nagaoka S. Bioprocessing in microgravity: applications of continuous flow electrophoresis to rat anterior pituitary particles. J Biotechnol 1996;47:353–365.
196. Raymond DE, Manz A, Widmer HM. Continuous sample pretreatment using a free-flow electrophoresis device integrated onto a silicon chip. Anal Chem 1994;66: 2858–2865.
197. Kašička V, Prusík Z, Pospíšek J. Conversion of capillary zone electrophoresis to free-flow zone electrophoresis using a simple model of their correlation: application to synthetic enkephalin-type peptide analysis and preparation. J Chromatogr 1992; 608:13–22.
198. Ježek J, Velková V, Kašička V, Prusík Z, Ubik K, Bartová K, Mareš M. Side reaction during the deprotection of Cys(Acm)-containing peptides with iodine. Synthesis of disulfide fragments from cathepsin D structure. Collect Czech Chem Commun 1995;60:1042–1049.
199. Kašička V, Prusík Z, Smékal O, Hlaváček J, Barth T, Weber G, Wagner H. Application of capillary and free-flow zone electrophoresis and isotachophoresis to the analysis and preparation of the synthetic tetrapeptide fragment of growth hormone–releasing peptide. J Chromatogr B 1994;656:99–106.
200. Prusík Z, Kašička V, Weber G, Pospíšek J. Correlation of capillary electrophoresis with continuous free-flow electrophoresis systems and their application in peptide separations: analysis and preparation of LHRH derivative. In: Radola BJ, ed. Elektrophorese Forum '91. Technische Universitat Munchen, 1991:201–206.
201. Kašička V, Prusík Z, Sázelová P, Jiráček J, Barth T. Theory of the correlation between capillary and free-flow zone electrophoresis and its use for the conversion of analytical capillary separations to continuous free-flow preparative processes. Application to analysis and preparation of fragments of insulin. J Chromatogr A 1998;796:211–220.

4
Bioaffinity Chromatography

Jaroslava Turková
Academy of Sciences of the Czech Republic, Prague, and University of Pardubice, Pardubice, Czech Republic

I. INTRODUCTION

Macromolecules such as proteins, polysaccharides, and nucleic acids often differ only in their physicochemical properties within the individual groups, and their isolation on the basis of these differences, e.g., by ion exchange chromatography, gel filtration, or electrophoresis, is therefore difficult and time consuming. Consequently, their activity decreases considerably during the isolation procedure owing to denaturation, cleavage, enzymatic hydrolysis, and so forth. One of the most characteristic properties of these biologically active macromolecules is their ability to bind other molecules reversibly. For example, active and regulatory sites of enzymes form complexes with substrates, inhibitors, cofactors, or effectors; antibodies bind antigens against which they were prepared, etc. The formation of these biospecific, dissociable complexes of biological macromolecules serves as a basis for bioaffinity chromatography.

II. THE PRINCIPLE AND USE OF BIOAFFINITY CHROMATOGRAPHY

Bioaffinity chromatography is a form of adsorption chromatography, which is based on the exceptional ability of biologically active substances to bind specifically and reversibly complementary substances. These are generally called ligands, affinity ligands, or affinants. If one of the components of the complex is immobilized, a specific sorbent is formed for the second component of the com-

plex assuming that the conditions necessary for the formation of this complex exist. The binding sites of the immobilized substances must be sterically accessible even after their coupling to the solid support, and they must not be deformed by immobilization.

A solid support with a covalently bound affinant is used as the stationary phase in a chromatographic column. When a crude mixture containing the biologically active products to be isolated is passed through the column of affinity adsorbent, then all of the compounds that under given experimental conditions have no complementary binding site for the immobilized affinity ligand will pass through unretarded. By contrast, products showing affinity for the insoluble affinant are adsorbed onto the column. They can be released by elution with a solution of a soluble affinity ligand or by changing of the solvent composition by so-called deforming buffers (e.g., by a change in pH, ionic strength, temperature, etc.).

Assuming that a single enzyme of the crude proteins has an affinity for the specific adsorbent, the equilibrium between the attached affinity ligand L and the isolated enzyme E is given by the equation:

$$E + L \underset{k_{-1}}{\overset{k_{+1}}{\rightleftharpoons}} EL$$

Affinity constant (= equilibrium or association constant):

$$K_A = \frac{[EL]}{[E][L]} \qquad \text{(e.g., } 10^8 M^{-1})$$

Dissociation constant:

$$K_A = K_L = \frac{[E][L]}{[EL]} \qquad \text{(e.g., } 10^{-8} \text{ M)}$$

Dissociation constants of some affinity pairs were described by Bayer and Wilchek in their review of avidin-biotin technology [1]. The unprecedented interaction between binding proteins' egg-white avidin, or its bacterial counterpart streptavidin, and their target molecule vitamin biotin is based in the exceptionally high affinity constants 10^{15} M^{-1}. Lower affinity constants were described for biospecific complexes: receptors–hormones, toxins, etc. (10^9–10^{12} M^{-1}); antibodies–antigens (10^7–10^{11} M^{-1}); transport proteins–vitamins, sugars, etc. (10^6–10^8 M^{-1}); lectins–carbohydrates (10^3–10^6 M^{-1}); and enzymes–substrates (10^3–10^5 M^{-1}).

Formation of the biologically functioning complexes involves the participation of common molecular forces and interactions systematized under the terms of ionic, hydrogen and hydrophobic bonds, London's dispersion forces, dipole–dipole interactions, charge–transfer interaction, and so on. The simultaneous and

concentrated action of several of these forces in the complementary binding site constitutes the basis of the high specificity and efficiency of the biospecific bond.

The number of noncovalent interactions in complementary binding sites of biospecific complexes can best be shown by x-ray diffraction analysis. The affinity ligand most commonly used in the bioaffinity chromatography of aspartate proteinases is the naturally occurring peptide inhibitor pepstatin. The mode of binding of the first part of the pepstatin molecule (the fragment isovaleryl-valyl-valyl-statine) to the binding site of penicillopepsin was elucidated by James and coworkers [2]. They determined the noncovalent interactions between the pepstatin fragment and penicillopepsin which occur at a distance of 0.4 nm or less. The total number of 87 includes a variety of interactions. The high number of noncovalent interactions between the binding sites of microbial proteinases and pepstatin is why the *Mucor miehei* proteinase cannot be eluted after adsorption to an isovaleryl-pepstatin-Sepharose. However, after Kobayashi and coworkers [3] had replaced immobilized *N*-isovalerylpepstatin by *N*-isobutyryl-, *N*-propionyl-, or *N*-acetylpepstatin they were able to increase the yield of the enzyme eluted from 0 to 12%, 46%, and 90%, respectively. The affinity constants of these complexes were not reported.

The affinity constants of the biospecific complexes of modified pepstatin were determined by Kay and coworkers [4]. The value of the affinity constant of the complex of cathepsin D with isovalerylpepstatin was equal to 10^{10} M^{-1}. After the isovaleryl group had been replaced by the lactoyl group, the affinity constant dropped three orders of magnitude.

This example shows that formation of complexes of lower affinity should be used for biospecific affinity chromatography. However, in connection with the use of biospecific complex formation in bioaffinity chromatography we must always take into consideration the fact that the affinity constant of the biospecific complex is influenced not only by the microenvironment of both solid and liquid phases but by steric accessibility, the conformation and concentration of the affinity ligand, etc. This adsorbent can be useful for the isolation, determination, or removal of biologically active substances. Complexes of higher affinity constants can be used for oriented immobilization, e.g., of enzymes by simple adsorption to their suitable immunosorbent [5].

III. CHOICE OF AFFINITY LIGANDS (AFFINANTS)

A. Highly Specific and Group-Specific Matrices

All of those compounds are suitable as affinity ligands for the isolation of biologically active products that bind such products specifically and reversibly. Hence, given the varied nature of biologically active materials, affinants represent a very

wide range of chemical compounds. Their classification can therefore be based on biochemical function rather than on chemical structure.

Two main criteria determine the selection of an affinity ligand:

1. The affinant to be immobilized must possess a functional group that can be modified for attachment to the solid support without impairing or abolishing its recognition by the complementary molecule. Not all affinants that are suitable for a complementary binding of molecules also have suitable functional groups for their attachment to a solid support. These groups must first be introduced into the affinants, as well as suitably long spacing arms, which are usually indispensable in case of low molecular weight affinity ligands because such arms are necessary to enable a bonding interaction.
2. The affinity ligand should have an adequate affinity for the molecule to be purified. Satisfactory results have usually been obtained with specific complexes having an affinity constant K_A in the region of 10^4–10^8 M^{-1}. However, it is important to mention here that the K_A values under consideration are those determined for the complex of the substance to be isolated with the immobilized affinity ligand and that therefore they need not correspond to the affinity constant values determined in solution. For the determination of K_A the most commonly used method is so-called quantitative affinity chromatography, which is based on the elution of biological macromolecular substances from an affinity matrix with soluble affinant solutions of various concentrations [6].

Many examples of affinants used for the isolation of antibodies, antigens and haptens, cells and cell organelles, cofactors and vitamins, enzymes, enzyme subunits and modified derivatives, glycoproteins and saccharides, hormones, inhibitors, lectins, lipids, nucleic acids, nucleotides and nucleosides, transfer receptors and binding proteins, proteins and peptides containing -SH group, specific peptides, viruses, and other substances by use of low-pressure, high-performance, and large-scale bioaffinity chromatography are shown on pages 372–578 of the book *Bioaffinity Chromatography* [7].

According to the source we can distinguish (1) naturally occurring and (2) synthetic affinity ligands. For the isolation of chymotrypsin and trypsin from a crude pancreatic extract the specific adsorbents were prepared by coupling of two naturally occurring proteinase inhibitors (ovomucoid for trypsin and polyvalent trypsin inhibitor, antilysine, for chymotrypsin) and also synthetic low molecular weight proteinase inhibitors (*N*-benzyloxycarbonylglycyl-D-phenylalanine for chymotrypsin and *p*-aminobenzamidine for trypsin) to a hydroxyalkyl methacrylate copolymer [8]. In Figs. 1 and 2 it is shown that identical results were obtained with specific adsorbents prepared with both high molecular weight and

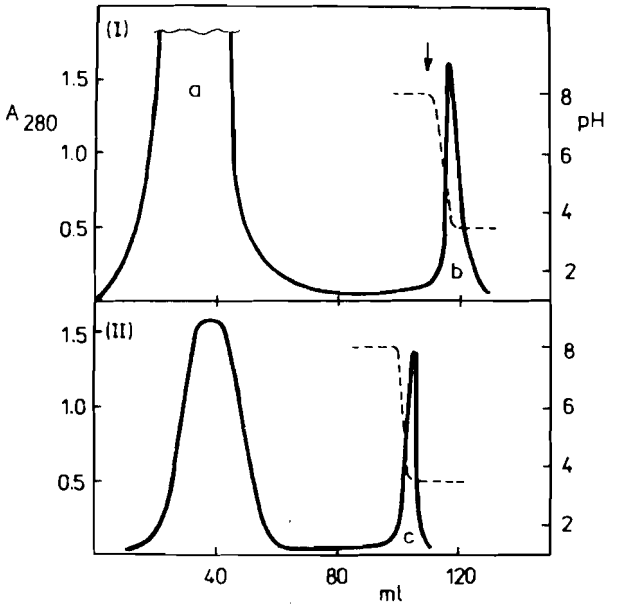

Figure 1 Chromatography of crude pancreatic extract on ovomucoid-Spheron (I) and antilysine-Spheron (II). (I) A sample of active pancreatic extract (100 ml) was placed on a column of ovomucoid-Spheron (10 × 2 cm), which was subsequently eluted with an aqueous solution of ammonium formate (0.05 M formic acid adjusted to pH 9.0 with 5% aqueous ammonia). Fractions (6 ml) were collected at 20-min intervals. The arrow designates the change in pH from 8.0 to 3.5 (0.1 M formic acid adjusted to pH 3.5 with ammonia). (II) The fraction (a) of material not adsorbed (180 ml) was placed directly on the antilysine-Spheron column (10 × 2 cm). The course of the chromatography was analogous to that described for (I). (a) Contaminants and chymotrypsin; (b) trypsin; (c) chymotrypsin; ———, absorbance at 280 nm; ---, pH. (Data from Ref. 8.)

low molecular weight inhibitors. Unlike the naturally occurring inhibitors, which could undergo denaturation because of their protein character, the synthetic low molecular weight inhibitors are completely stable. The capacity of specific adsorbents prepared with these inhibitors can be regenerated virtually without limit, if a stable solid support and stable bonds between the support and the amino groups of peptide inhibitors are used.

According to the specificity we distinguish (1) highly specific and (2) group-specific matrices. The practical utility of specific sorbents increases if, instead of the narrowly specific ligands, a so-called general ligand is used for their preparation. As is implied by the name, a group-specific matrix prepared in this

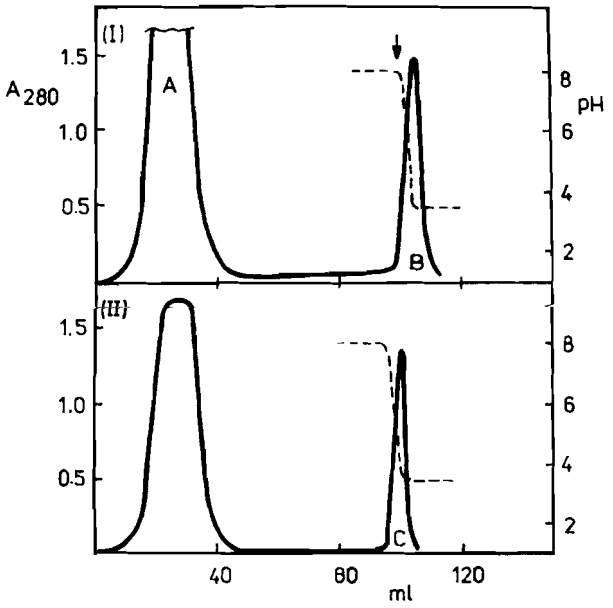

Figure 2 Chromatography of crude pancreatic extract on *N*-benzyloxycarbonylglycyl-D-phenylalanine-NH_2-Spheron (I) and NH_2-benzamidine-NH_2-Spheron (II). (I) A sample of active pancreatic extract (100 ml) was applied to the column of *N*-benzyloxycarbonyl-glycyl-D-phenylalanine-NH_2-Spheron (6.0 × 1.5 cm). The course of the chromatography was identical with that shown in Fig. 1. (II) Fraction (A), filtered through a column of *N*-benzyloxycarbonylglycyl-D-phenylalanine, was placed directly on a column of NH_2-benzamidine-NH_2-Spheron (25 × 1 cm). The course of chromatography is identical with that shown in Fig. 1. (A) Contaminants and trypsin; (B) chymotrypsin; (C) trypsin; ———, absorbance at 280 nm; ---, pH. (Data from Ref. 8.)

manner displays an affinity for a more or less large group of biological macromolecules. For example, the enzymes related to the metabolism of aspartic acid show group-specific adsorption affinity to *N*-(ω-aminohexyl)-L-aspartic acid-Sepharose. Asparaginase, aspartase, aspartate-β-decarboxylase, and asparaginase modified with tetranitromethane [9] could all be sorbed onto this immobilized affinant.

B. Enzymes

The combination of several complementary binding sites on the surface of the enzyme molecule permits the formation of a relatively large number of biospec-

ific complexes to be achieved; these complexes can be utilized for efficient isolation as well as for oriented immobilization. Figure 3 shows the surface of an enzyme molecule covered with several complementary binding sites [10]. Such an enzyme could be, for instance, carboxypeptidase Y (CPY) containing the complementary binding site for glycylglycyl-*p*-aminobenzylsuccinic acid, a specific inhibitor, which after immobilization was used for the isolation of CPY from autolyzates of various kinds of yeast. The active site of the enzyme also contains a free SH- group and therefore can be adsorbed to mercury-Spheron. CPY is a glycoprotein whose carbohydrate moiety specifically interacts with concanavalin A, a lectin. If CPY was adsorbed on immobilized concanavalin A followed by crosslinking with glutaraldehyde, the bound enzyme retained 96% of the native catalytic activity. The antigenic sites of the enzyme can be determined by investigation of the antigenic structures of the peptide chain in experiments with specific antibodies to this enzyme. Enzymes whose coenzymes are nucleotides can form biospecific complexes with nucleotides. Enzymes form complexes with substrates and their analogs, allosteric effectors, metal ions, etc. The type of complex formed determines the mode of their action in chemical processes that take place in the living cell.

The isolation of enzymes by use of immobilized inhibitors is shown in Fig. 1 and 2. The catalytic activity of many enzymes depends on the presence of coenzymes or cofactors. The coenzymes nicotinamide adenine dinucleotide and

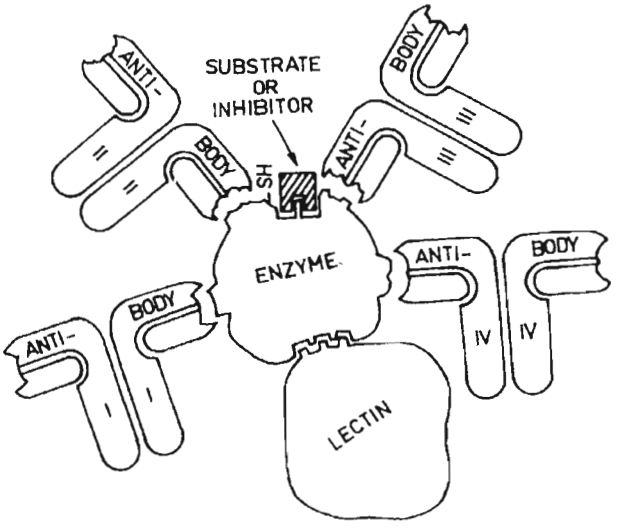

Figure 3 Possible ways in which an enzyme can form biospecific complexes.

other nucleotides of adenine, uridine, guanine, and flavine, coenzymes of pyridoxal, folate and its analogs, biotin, lipoic acid, cobalamines, and porphine derivatives are frequently employed as affinants. The function of immobilized cofactors as bioaffinity ligands depends on the spacer length and on the position of covalent binding. Figure 4 demonstrates four positions on the adenine nucleotide that were derivatized before their attachment to CNBr-activated Sepharose 4B [11]. When comparing the binding of various dehydrogenases and kinases on N^6-(6-aminohexyl)-5′-AMP-Sepharose and P^1-(6-aminohexyl)-P^2-(5′-adenosine)pyrophosphate-Sepharose [12], the strength of the interaction between the enzyme and the immobilized nucleotide was expressed by the so-called binding (β). This term represents the concentration of potassium chloride (mM) in the center of the enzyme peak when the enzymes are eluted with a linear potassium chloride gradient (Fig. 5, Table 1). The results reflect the nature of the enzyme–nucleotide interactions.

The Corey-Pauling-Koltin structural model of NAD and the reactive textile dye Cibacron Blue F3GA (Fig. 6) was published by Thompson et al. [13]. From x-ray studies of the binding of Cibacron Blue F3GA to liver alcohol dehydrogenase performed by Biellman et al. [14] it became evident that the dye binds at the nucleotide binding site of the enzyme with correspondences of the adenine and ribose rings, but not with the nicotinamide. The ever-increasing use of dye-based affinity techniques in many fields of biomedical research and biotechnology is

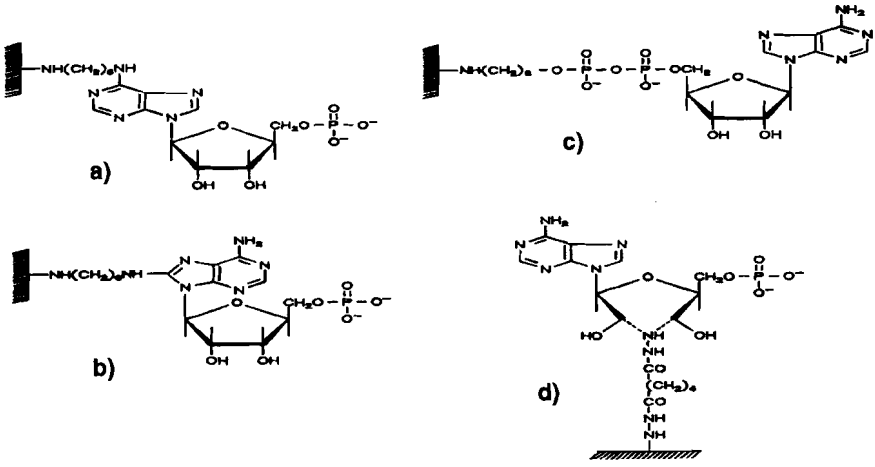

Figure 4 The structures of several immobilized AMP adsorbents. (a) N^6-(6-aminohexyl)-AMP-agarose. (b) 8-(6-Aminohexyl)-AMP-agarose. (c) P^1-(6-Aminohexyl)-P^2-(5′-adenosine)-pyrophosphate-agarose. (d) Ribosyl-linked AMP.

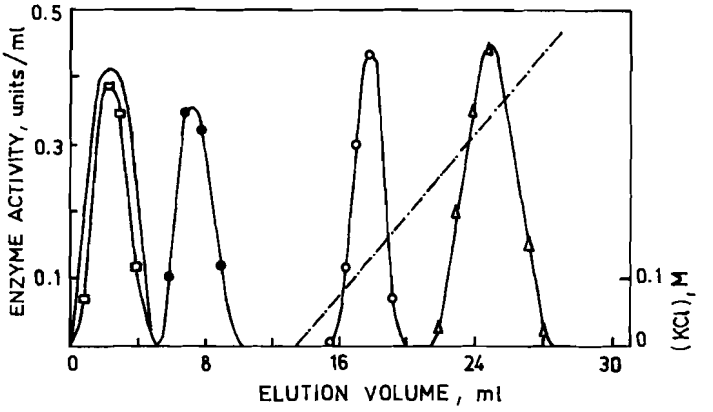

Figure 5 Chromatography of a crude yeast extract on N^6-(6-aminohexyl)-5′-AMP-Sepharose. A sample (100 μl) of a crude yeast extract was applied to a column (50 × 5 mm) containing 0.5 g of N^6-(6-aminohexyl)-5′-AMP-Sepharose equilibrated with 10 mM KH_2PO_4-KOH buffer, pH 7.5. After washing through nonadsorbed proteins, enzymes were eluted with a linear salt gradient (0.1 M KCl; 20 ml total volume) at a flow rate of 8 ml/h. Inert protein (——), glucose 6-phosphate dehydrogenase (□), glutathione reductase (●), malate dehydrogenase (○), and yeast alcohol dehydrogenase (△) were assayed in the effluent (From Ref. 12.)

reflected in many contributions from a worldwide gathering of experts at the International Conference on Modern Aspects of Protein-Dye Interaction: Role in Downstream Processing [15]. Many advantages of using dye ligands, particularly for large-scale applications, were described [15]. Compared to biological ligands, dye ligands are inexpensive materials available in tonnage quantities worldwide. There is a wide range of chromophors available that are dye-based biologically, chemically, and photochemically stable adsorbents, potentially sterilizable in situ, with no degradation of the ligand itself. Because they are reactive materials, they are very easily immobilized to hydroxyl polymers, generally by a single-step process. Such adsorbents have a high capacity, a very broad binding capability in terms of the complementary proteins, and are easily reusable. Several thousand different types of proteins would interact with an immobilized textile dye. Examples are oxidoreductases, phosphokinases, and nearly all coenzyme-dependent enzymes, hydrolases, various transferases, a number of proteins that interact with mono- and polynucleotides, synthetases, hydroxylases, nearly all of the glycolytic enzymes, phosphatases, and a variety of blood proteins and other nonenzyme proteins. A number of studies using classic enzyme kinetics, circular dichroism,

Table 1 Comparison of Binding of Various Enzymes to N^6-(6-Aminohexyl)-5′-AMP-Sepharose (I) and P^1-(6-Aminohexyl)-P^2-(5-adenosine)-pyrophosphate-Sepharose (II).

Enzyme Code number	Name	Binding (β)[a]	
		I	II
EC 1.1.1.27	Lactate dehydrogenase	>1000[b]	>1000[b]
EC 1.1.1.49	Glucose 6-phosphate dehydrogenase	0	170
EC 1.1.1.37	Malate dehydrogenase	65	490
EC 1.1.1.1	Alcohol dehydrogenase	400	0
EC 1.2.1.12	*p*-Glyceraldehyde 3-phosphate dehydrogenase	0	>1000[b]
EC 2.7.2.3	3-Phosphoglycerate kinase	70	260
EC 2.7.1.40	Pyruvate kinase	100	110
EC 2.7.1.1	Hexokinase	0	0
EC 2.7.4.3	Myokinase	0	380
EC 2.7.1.30	Glycerokinase	122	0

[a] Binding (β) is the KCl concentration (mM) at the center of the enzyme peak when the enzyme is eluted with a linear gradient of KCl.

[b] Elution was effected by a 200-μl pulse of 5 mM NADH.

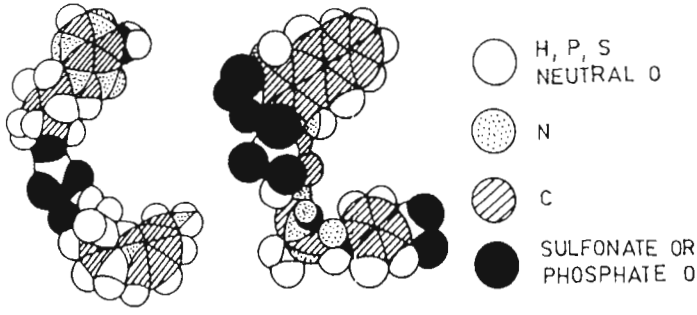

Figure 6 Corey-Pauling-Koltin structural model of NAD and Cibacron Blue F3GA. NAD is shown on the left in the conformation in which it binds to dehydrogenases. The Blue A model is shown on the right in a conformation similar to the NAD. Note the close resemblance in size, orientation of π electrons, and position of negatively charged sulfonate or phosphate groups. (From Ref. 13.)

affinity labeling, x-ray diffraction, and other techniques have been utilized to demonstrate the specificity of dye binding to the active sites of proteins.

C. Antibodies and Antigens

A refinement of the technique has been the development of immunoaffinity chromatography (IAC), which adds the selectivity and specificity of immunological reactions to the separation process. Antigens or antibodies are increasingly used as tools to separate, determine, or isolate complementary immunosubstances.

By binding of antigen to a solid support, a specific immunoadsorbent is formed, which should possess the following properties:

1. It should be capable of adsorbing the complementary antibody from a mixture of components.
2. The liberation of the adsorbed antibody from the specific adsorbent should be quantitative and should be carried out under conditions that are harmless for the specific antibody activity.
3. It should possess a high capacity for the adsorption of the specific antibody.
4. It should retain its biological activity after repeated use and storage.
5. It should possess adequate mechanical properties, permitting centrifugation, filtration, and use in a column.

The fulfillment of these requirements is not dependent on the quality and amount of bound antigen only, but also on the nature of the solid support and the nature of the bond.

Protein A, which is a coat protein extracted from the bacterium *Staphylococcus aureus*, has the unique capacity to bind mammalian immunoglobulins, especially IgG. Protein A-coated glass beads were developed as a universal support medium for HPIAC by Phillips et al. [16]. The preparation and mechanism of IgG antibody binding is demonstrated in Fig. 7. Protein A has the ability to bind to the Fc, or tail, portion of IgG antibodies. Protein A is composed of five subunits, each with its own Fc receptor, but three of these receptors become inactive when the molecule is immobilized. If Protein A is applied as a coating to either solid or controlled pore glass beads, its Fc receptors become points of attachment on which the antibody can be immobilized. The bound antibodies are then covalently immobilized on the Protein A coat by crosslinking them with carbodiimide. In turn this attachment helps to orient the antigen receptors of the antibody toward the mobile phase of the column. In addition, the linear nature of the Protein A molecule becomes a spacer arm for the immobilized antibodies, thus preventing charges, which can rise from the bead surface, inhibiting the formation of the antibody–antigen complex. Lee and Chuang [17] used Protein A immobilized on nonporous silica for the isolation of human immunoglobulin

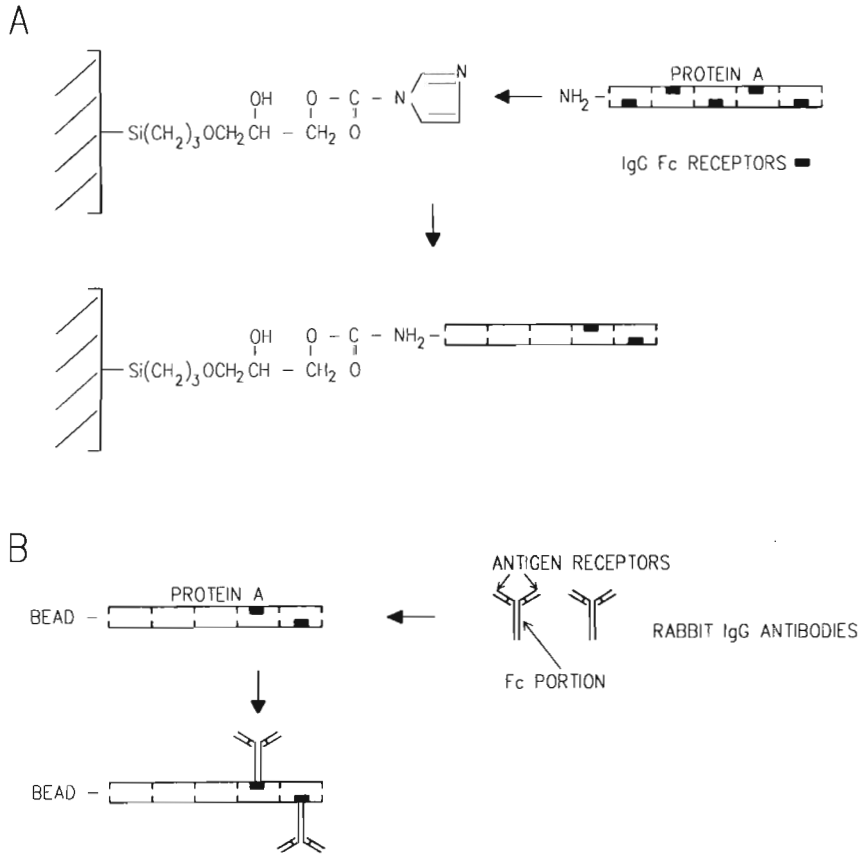

Figure 7 Diagrammatic representation of the process for binding rabbit antibodies to Protein A-coated glass beads. (A) Illustration of the chemistry used to couple Protein A to the carbonyl diimidazole–derivatized glass beads. (B) Mechanism of IgG antibody binding to the Fc receptors on the Protein A-coated glass beads. (From Ref. 16.)

G and for both theoretical and experimental investigation of elution behavior of protein.

D. Lectins, Glycoproteins, and Saccharides

Lectins are proteins or glycoproteins from plants, invertebrates, and bacteria. They form complexes with sugar residues of glucosides, oligo- and polysaccharides, glycoproteins, glycolipids, membrane proteins, enzyme–antibody and glycoprotein conjugates, as well as viruses, cell fragments, and cells. Hydrogen

bonding and electrostatic interactions are fundamentally involved in complex formation. Furthermore, the metal ions Ca^{2+} and Mn^{2+} are essential constituents of the sugar binding sites and are also essential for the tertiary structure. Most known lectins are multimeric, consisting of noncovalently associated subunits, which are either identical (e.g., concanavalin A) or different (e.g., *Ulex europeus* agglutinin). This multimeric structure is the reason for their ability to agglutinate cells or form precipitates with glycoconjugates.

Bioaffinity chromatography for the purification of lectins was reviewed by Lis and Sharon [18]. They described three major types of biospecific adsorbents for the purification of lectins: (1) polysaccharides, either native or modified; (2) matrix-bound glycoproteins and glycopeptides; (3) matrix-bound monosaccharides and disaccharides. Hatakeyama et al. [19] described an assay for lectin activity using microtiter plate with chemically immobilized carbohydrates: lactose, galactose, mannose, glucose, and *N*-acetylglucosamine. After incubation of the lectins (*Ricinus communis* agglutinin, concanavalin A, and wheat germ agglutinin) bound proteins were measured by the protein assay using the colloidal solution.

The isolation of glycoproteins by means of immobilized lectins makes use of their differing affinities for terminal carbohydrate residues characteristic of single glycoproteins. For the elaboration of a suitable procedure for the purification of the given glycoproteins or glycopeptides by means of lectins, Kristiansen [20] recommended the following stages:

1. Identification of the terminal sugar or sugars in the carbohydrate part of the substance under consideration
2. Selection of a lectin with a corresponding specificity
3. Preparation of the selected lectin
4. Immobilization of the lectin by a covalent bond to a solid support
5. Choice of optimum conditions for the adsorption of the isolated substance on the immobilized lectin
6. Choice of conditions for desorption

It is possible to choose either nonspecific elution, consisting mainly in a change in pH or salt concentration; or a specific method can be used, i.e., displacement of the adsorbed glycoprotein by competing carbohydrates. Assuming that the terminal sugar or sugars of glycoproteins have been determined, the choice of a suitable lectin can follow. In most instances lectins are not specific for one sugar only, although great differences exist in the degree of specificity. For example, wheat germ agglutinin has much lower affinity interactions than concanavalin A [19]. Wheat germ agglutinin affinity HPLC (SigmaChrom AF-WGA) was used by Pergami et al. [21] in semipreparative chromatographic method to purify the normal cellular isoform of the prion protein in nondenatured form. It can be the basis for study of the conversion of the cellular isoform in the pathogenesis of

spongiform encephalopathies (prion diseases). Additional ligands in bioaffinity chromatography of glycoproteins can be antibodies against carbohydrate antigens and boronic acid ligands.

E. Nucleotides and Nucleic Acids

The ever-increasing use of genetic engineering is reflected in the rapidly increasing number of publications devoted to the isolation of nucleic acids, genes, oligonucleotides, and nucleic acid fragments, to the purification of special proteins and enzymes, as well as to investigations of protein–nucleic acid interactions. Schott [22] summarized this interesting field in his book *Affinity Chromatography–Template Chromatography of Nucleic Acids and Proteins*. When oligonucleotides of a defined sequence are immobilized on cellulose, base pairing can take place with complementary oligonucleotides having either a homologous sequence or an alternating one according to the Watson-Crick theory. Those nucleotides undergoing such a base pairing are adsorbed onto the cellulose and can thus be separated from any noncomplementary partners present in the mixture. Schott described selective adsorptions of complementary oligonucleotides in the mobile phase on the immobilized template if chromatography takes place under the conditions necessary for base pairing. Desorption was then carried out with a temperature gradient. The application of the principles of molecular biology for the selective separations of nucleotides and peptides was called template chromatography.

The chromatography of peptides on polyvinyl alcohol substituted with oligodeoxythymidylic acid and bound irreversibly on DEAE-cellulose by ionic bonds has been employed for the study of the interactions of peptides with nucleotides. The quantitative measure of the peptide–nucleotide interaction is the increase in the retention of a peptide on oligonucleotide-DEAE-cellulose in comparison with that on unmodified DEAE-cellulose. In order to eliminate possible effects of various column parameters, Schott [22] expressed all elution volumes relative to the elution volume of alanine, which displays no measurable retention on these columns. The relative elution ratio (V_r) is thus obtained as the ratio of the elution volume found for the investigated peptide to that for alanine ($V_r = V_{obs}/V_{Ala}$). The peptide–oligonucleotide interaction is then evaluated on the basis of the difference in the relative elution volumes obtained by chromatography on both columns.

A solid phase triple-helix-mediated affinity capture method was described for the purification of single-stranded M13 DNA for use as template in fluorescence-based DNA sequencing reactions by Johnson et al. [23]. In this method, a biotinylated polypyrimidine oligonucleotide "loop" bound to streptavidin-coated magnetic beads was used to selectively capture single-stranded M13 DNA from high-titer phage supernatant through the formation of a cooperative and a polypurine site previously cloned into the M13 vector.

Eisenberg et al. [24] reviewed the purification of DNA-binding proteins by site-specific DNA affinity chromatography. They described the numerous advantages that they experienced with the purification of DNA-binding protein (OBF1) by use of DNA-cellulose. (1) The DNA affinity matrix has a high protein capacity, which is determined by the number of copies of the protein recognition sequence inserted into the plasmid. It is possible to construct a plasmid in which the protein-binding sequences comprise at least 50% of the total DNA content. Once inserted into the plasmid, followed by DNA amplification in *E. coli*, very large quantities of these sequences could be obtained. Since about 1 mg of DNA can be coupled to 1 g of cellulose powder, it is relatively easy to prepare sufficient quantities of the DNA affinity matrix for a large-scale purification. (2) The protein appears to bind more tightly to the DNA on the column than in solution. They found that in solution the OBF1–DNA complex could not be formed in the presence of NaCl concentrations above 0.2 M, while the binding of OBF1 to the multimeric site-specific DNA-cellulose matrix occured at 0.4 M NaCl. The tight binding to the site-specific DNA-cellulose column ensures effective separation of OBF1 from other DNA-binding proteins by simple salt elutions and, when combined with standard ion exchange chromatography, a highly purified protein may be obtained.

F. Receptors, Binding and Transport Proteins, Hormones, Vitamins, Toxins, Growth Factors, Lipids, and Other Substances

The last decades saw a dramatic increase in the number of analytical problems demanding the determination of trace levels of analytes in complex samples. This can be accomplished by selective sample preparation steps, which eliminates interfering matrix and enriches the analyte to a concentration surpassing the determination limit of the detection method. The introduction of monoclonal antibodies against receptors and their subunits as affinity ligands rather than receptor substrates greatly advanced the application of immunology to membrane biochemistry. A discussion of monoclonal antibodies against acetylcholine, insulin, adrenergic, transferrin, thyrotropin, neurological, viral, and complement receptors was presented by Phillips [25]. Immunoaffinity chromatography of polycyclic aromatic hydrocarbons in columns prepared by sol-gel method was described by Cichna et al. [26]. The paper describes the synthesis of pyrene-selective immunoaffinity columns and their application for the determination of pyrene in water. The immunoaffinity columns prepared had a pyrene breakthrough capacity of 78 ng/g and 38 ng/mg IgG. Corticosteroids dexamethasone and betamethasone were extracted from bovine urine by use of immunoaffinity chromatography by Bagnati et al. [27]. The described extraction and purification

system for the purification of corticosteroids is the combination of immunoaffinity and HPLC columns.

Receptor affinity chromatography based on the specificity and reversibility of the receptor–ligand interaction for the purification of biomolecules by use of matrix-bound receptor was described by Weber and Bailon [28]. As a model system they described the purification of recombinant human interleukin-2 from microbial and mammalian sources using the soluble subunit of the human interleukin-2 receptor attached to silica-based NuGel P-AF polyaldehyde poly-*N*-hydroxysuccinimide. A comparison of receptor and immunoaffinity purification methods showed that the binding capacity of the immobilized receptor is higher than that of the immunosorbent and the receptor affinity–purified interleukin-2 was more homogeneous than the immunoaffinity-purified material.

The primary effect of some hormones is aimed at the plasma membrane of the target cells. The amount of their receptors in the tissues is very small in comparison with other material present. The interaction of such a small amount with the immobilized hormones must be very effective in order to permit a strong binding of large membrane fragments. The isolation of peptide or protein receptors posed a number of difficult problems owing to their scarcity, their location in a complex lipid-rich environment, and the difficulty with which even a starting plasma membrane is prepared. The coupling of peptide hormones to activated Sepharose results in nonspecific attachment that can generate a number of different species with varying affinities for the desired receptor. For these reasons Finn and Hofmann [29] have devoted their efforts to developing biospecific sorbent based on avidin-biotin technology where the hormone can be attached in a targeted fashion. The application of the avidin-biotin systems to the isolation of hormone receptors is shown in Section III.G.

G. Biotin and Avidin or Streptavidin

The binding of water-soluble vitamin biotin to the egg-white protein, avidin, or to its bacterial counterpart, streptavidin, is accompanied by a vast decrease in free energy compared to that observed for other noncovalent interactions. The change of enthalpy, ΔH, for biotin bound to avidin and streptavidin has been determined by Green [30] as being -86 and -98.9 kJ/mol biotin, respectively. Each avidin or streptavidin molecule can bind four molecules of biotin. The change in entropy for this reaction is essentialy zero. The affinity constant for biotin-avidin determined by Green is approximately 10^{15} M^{-1}.

In the past decade the interaction between biotin and avidin or streptavidin has provided the basis for establishing a new avidin-biotin technology. The basic concept is that biotin, coupled to either low or high molecular weight molecules, is recognized by avidin. Methods for the biotinylation of membranes, nucleic acids, antibodies, and other proteins have been developed in many laboratories. Figure 8 shows biotin and various derivatives, suitable for various types of bonds.

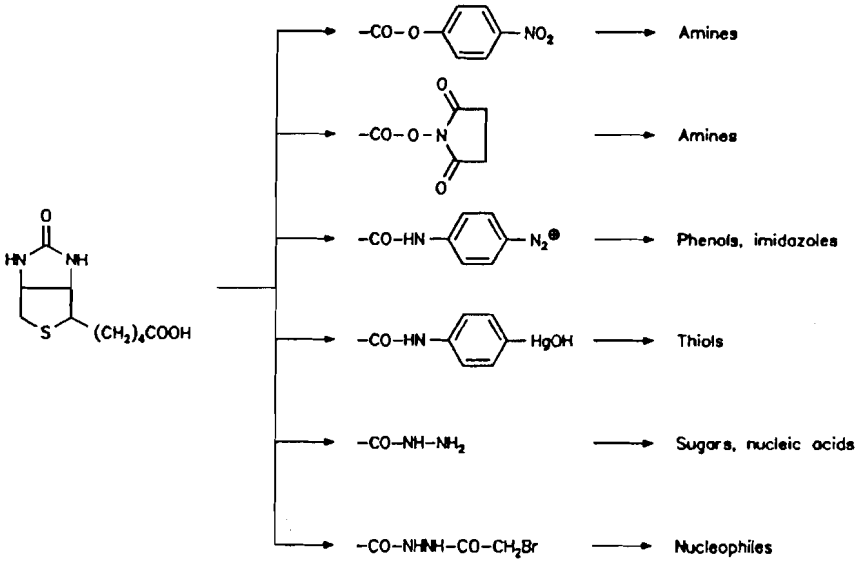

Figure 8 Biotin and derivatives.

However, a spacer arm should be used when proteins are modified by biotin. Detailed information on biotin-binding proteins, the preparation of biotin, avidin, and streptavidin derivatives, assays for avidin and biotin, and applications is given in Volume 184 of Methods in Enzymology titled *Avidin-Biotin Technology*, edited by Wilchek and Bayer [31].

The use of an avidin–biotin complex in bioaffinity chromatography was the isolation of avidin from egg white on a biocytin-Sepharose column [32]. The conditions required for its dissociation were extremely drastic requiring elution by 6 M guanidinium hydrochloride, pH 1.5. In order to decrease the strong affinity of avidin for biotin, Finn and Hofmann [29] used immobilized succinylated avidin for the isolation of hormone receptor. Soluble receptor (R) is percolated through a bioaffinity column to form the complex shown in the center of Fig. 9. The column is then exhaustively washed to remove contaminating materials. Alternatively, the biotinylated hormone ligand (B-H) can be added to a solution of solubilized receptor to form a soluble complex BHR. Applying a solution containing this complex to a column of immobilized succinylated avidin (SA) will result in the formation of the same complex (Fig. 9B). Both of these schemes have been used for the isolation of insulin receptors from human placenta. Removal of active insulin receptor can be achieved by eluting the column with acetate buffer, pH 5 containing either 1 M NaCl or biotin.

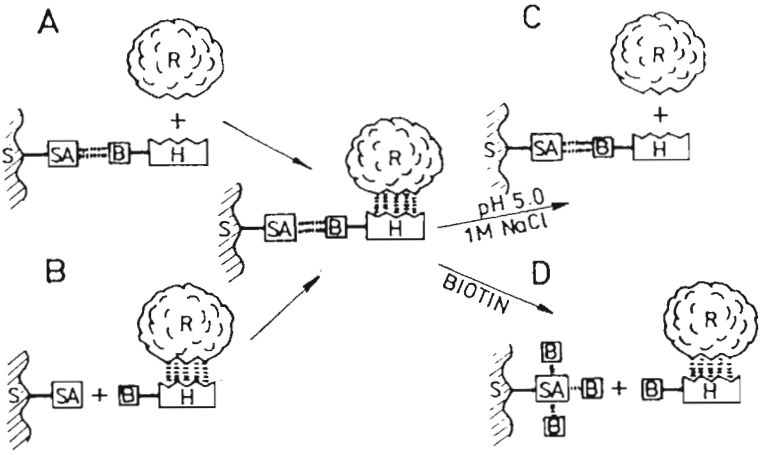

Figure 9 Application of the avidin-biotin system to the isolation of hormone receptors. Dashed lines represent noncovalent bonds. (From Ref. 28.)

Despite the fact that streptavidin is currently about 100 times more expensive than avidin, its use is sometimes justified since immobilized streptavidin exhibits less nonspecific binding. Avidin is highly positively charged at neutral pH, with an isoelectric point above 10. Consequently, it binds negatively charged molecules such as nucleic acids, acid proteins, or phospholipids in a nonspecific manner. This can result in nonspecific staining of, for example, the nucleus and cell membranes. Avidin is also a glycoprotein and therefore interacts with other biological molecules such as lectins or other sugar-binding materials via its carbohydrate moiety. The advantage of using streptavidin lies in the fact that it is a neutral, nonglycosylated protein (pI lower than 7). To decrease its positive charge, the lysines of avidin can be derivatized by succinylation, acetylation, etc. A variety of avidin derivatives with average pI values of 7 or lower are now commercially available. However, the removal of the carbohydrate residue from avidin is much more difficult.

One method that can be generalized to link virtually any DNA substrate by its 3′ or 5′ end to a chromatography matrix via streptavidin-biotin linkage has been described by Fishel et al. [33]. Biotin-streptavidin affinity selection as a valuable tool permitting the analysis of the RNA components of splicing complexes assembled on a wide variety of pre-mRNA substrates has been reviewed by Grabowski [34]. A review of the isolation of cell surface glycoproteins by the use of biotinylated lectin was published by Cook and Buckie [35]. They demonstrated the use of immobilized streptavidin to obviate dissociation of com-

plexes formed between biotinylated concanavalin A and membrane glycoproteins.

The advantage of the biotinylation of antibody carbohydrate moieties using biotin hydrazine for use in immunoaffinity chromatography has been described by Phillips [25]. HPIAC (or HPIC) of specific phosphorylcholine receptors can be employed using biotinylated mouse monoclonal antiidiotypic antibody adsorbed to streptavidin-coated glass beads. Using this technique HPIAC analysis was performed on isolated membranes from primed T cells obtained from mice immunized with phosphorylcholine (PC). These membranes were prepared by hypotonic lysis of the cells, followed by detergent NP40 solubilization of the membrane-rich fraction obtained by ultracentrifugation. The preparation was passed through a Sephadex G25 column to remove excess detergent prior to injection into the HPIAC column. Using monoclonal antiidiotype antibody as the immobilized ligand, a single peak was eluted by sodium thiocyanate gradient at 24 min. Rucklidge et al. [36] used antibody against denatured collagen after adsorption to membrane with attached collagen for biotinylation. Biotinylation in situ may protect the variable region of the IgG compared to antibodies biotinylated in solution, thus increasing their antigen recognition.

H. Cells and Viruses

The bioaffinity chromatography of cells, cell organelles and membranes, phages and viruses was reviewed by Sharma and Mahendroo [37]. Affinity ligands, in their review, are divided into two types: (1) lectins and nonlectin ligands, which contain hormones, neurotransmitters, and related ligands with affinity for cell surface receptors, and (2) further inhibitors of membrane-bound enzymes. A review on the use of immobilized glycoconjugates for cell recognition studies was published by Schnaar [38]. In this review the difference in carbohydrate recognition by chicken and rat hepatocytes was demonstrated. Hepatocytes dissociated from chicken livers bound readily to immobilized *N*-acetylglucosamine, but not to other carbohydrate-derivatized surfaces, whereas rat hepatocytes bound to galactose-derivatized surfaces. The rapid isolation of human erythrocyte plasma membrane was achieved by Kaplan et al. [39] on an affinity matrix consisting of wheat germ agglutinin covalently bound to Sepharose 6MB. After binding the washed cells to the bioaffinity matrix, they were washed extensively and lysed. The resulting ghosts were washed and then eluted from the matrix with *N*-acetyl-β-D-glucosamine.

Bioaffinity chromatographic separation of T cells by the use of monoclonal antibodies was discussed by Braun and Kümel [40] as a valuable tool in studies of the function of T cells and their subsets. According to these authors a broad array of procedures has been developed, of which an indirect use of matrix-bound second antibody appears to be the most practical and advantageous with respect

to purity, functional activity, and viability of separated cells. The most frequently employed affinants for the isolations of viruses are bound antibodies. An example is the isolation of Alleutian disease virus from chronically infected mink [41] by use of Sepharose with coupled IgG. In some cases rather than immobilized lectins, antibodies or Protein A, other specific and reversible cell surface receptor–ligand interactions can be successfully utilized. As an example one may mention the isolation of acetylcholine receptor–bearing neuronal cells from chick embryo sympathetic ganglia by the use of snake venom α-bungarotoxin immobilized on Sepharose 6MB macrobeads [42]. Information on the use of mentioned and many other affinants is given in Ref. 7.

IV. SOLID MATRIX SUPPORTS

A. Required Characteristics

One of the most important factors in the development of bioaffinity chromatography and immobilized enzymes is the development of solid supports. A correct choice of solid support and the covalent coupling between the matrix and the affinity ligand may be essential for the success of the desired bioaffinity chromatographic separation. Solid matrix supports can also have a considerable effect on the stability of the immobilized affinity ligand and the adsorbed material. A solid support may even be an affinity ligand itself, e.g., polysaccharides for some lectins. An increasing number of different types of supports, their activated forms and biospecific matrices prepared from them are now becoming commercially available as ready-to-use adsorbents. In the scope of this chapter only basic solid supports are described and briefly discussed.

An ideal matrix for successful application in bioaffinity chromatography and for the immobilization of enzymes should possess the following properties [43]:

1. Insolubility
2. Sufficient permeability and a large specific area
3. High rigidity and a suitable form of particles
4. Zero adsorption capacity
5. Chemical reactivity permitting the introduction of affinity ligands
6. Chemical stability under the conditions required for the attachment, adsorption, desorption, and regeneration
7. Resistance to microbial and enzymatic attack
8. Hydrophilic character

Complete insolubility is essential not only for the prevention of losses of affinity adsorbent but for prevention of contamination of the substance being isolated by dissolved carrier. However, a universal solid support that fulfills all

of the described requirements does not exist. When a certain affinity ligand is immobilized an individual solid support and method of coupling must be selected with respect to its future use.

Application of bioaffinity chromatography resulting from a changeover from soft gel supports to small rigid particles used in high-performance liquid bioaffinity chromatography (HPLBAC) has been reviewed by Ohlson et al. [44]. A comparison of HPLBAC with soft gel bioaffinity chromatography (BAC) is shown in Fig. 10. Mechanically stable, rigid particles, with small and uniform sizes, provide high flow rates with good mass transfer characteristics, giving overall high operational adsorption capacity. Much more favorable mass transport and adsorption/desorption kinetic behavior with nonporous support has been demonstrated by Anspach et al. [45]. The elution behavior of proteins on a nonporous silica-based adsorbent (with an average diameter of 1.4 μm) was investigated both theoretically and experimentally using human immunoglobulin G and immobilized protein A as the affinity pair by Lee and Chuang [17]. The desorption rate constant and equilibrium association constant under elution conditions were found to decrease elution time and improve the shape of the elution peak. However, the adsorption rate in column chromatography is limited by either slow intraparticle diffusion for large beads or low axial velocities and high-pressure

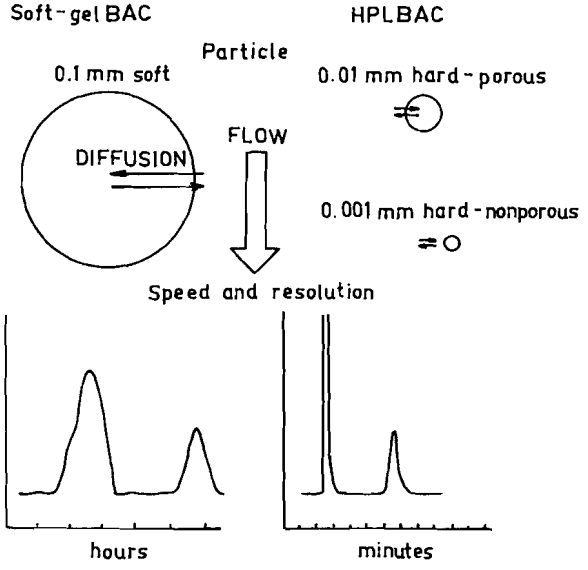

Figure 10 A comparison of bioaffinity chromatographies using soft gel or porous and nonporous small hard particles.

drops for small beads. To overcome these limitations, a membrane-based bioadsorbent has been used for the isolation of human pepsin by Kučerová and Turková [46].

B. Biopolymers

Water molecules are essential for the structure and function of biologically active compounds. BAC is therefore generally performed in the aqueous phase and hydrophilic biopolymers are usually employed as solid supports, chiefly natural polysaccharides, such as agarose, dextran, cellulose, and, to a lesser extent, starch. The modification necessary for the BAC can be carried out in a relatively simply via their OH groups.

1. Agarose and Its Derivatives

Agarose is a linear polysaccharide consisting of alternating 1,3-linked β-D-galactopyranose and 1,4-linked 3,6-anhydro-α-L-galactopyranose residues. Arnott et al. [47] postulated on the basis of x-ray studies that the polysaccharide chains form a double helix, then aggregate via hydrogen bridges and hydrophobic interactions into fibers or bundles with ordered structures. This network phase in a gel that may contain up to 100 times more water than agarose means that the structure contains relatively large voids through which large macromolecules can diffuse. In contradistinction, a gel network comprising a comparable concentration of crosslinked soluble polymer, such as the crosslinked dextrans, would lead to a lattice in which the mean pore size would be considerably smaller. These relationships are shown diagrammatically in Fig. 11 and suggest that agarose has particularly useful special properties as a chromatographic medium. The exclusion limit may be varied within wide ranges because the pore size is inversely proportional to the agarose concentration.

The main producers of agarose are Pharmacia Biotechnology (Uppsala, Sweden), under the trade name Sepharose; Bio-Rad Laboratories (Richmond, CA, USA), under the trade name Bio-Gel A; Reactifs IBF (Villeneuve la Garenne, France), under the trade name Ultrogel A; and agarose gels under the name SAG (Ago-Gel) supplied by Seravac Labs. (Maidenhead, Great Britain) and Mann Labs. (New York).

Supports with large beads are advantageous for the affinity chromatography of cells, so that they can pass through such columns without being physically trapped. For this purpose an agarose gel has been developed with the trade name Sepharose 6MB. The macrobeads have a large diameter (250–350 μm), uniform shape, and low nonspecific adsorption of cells. The stability of an agarose matrix can be considerably increased by crosslinking with epichlorohydrin, 2,3-dibromopropanol, or divinylsulfone. In 1975, Sepharose CL (2B, 4B, 6B) was intro-

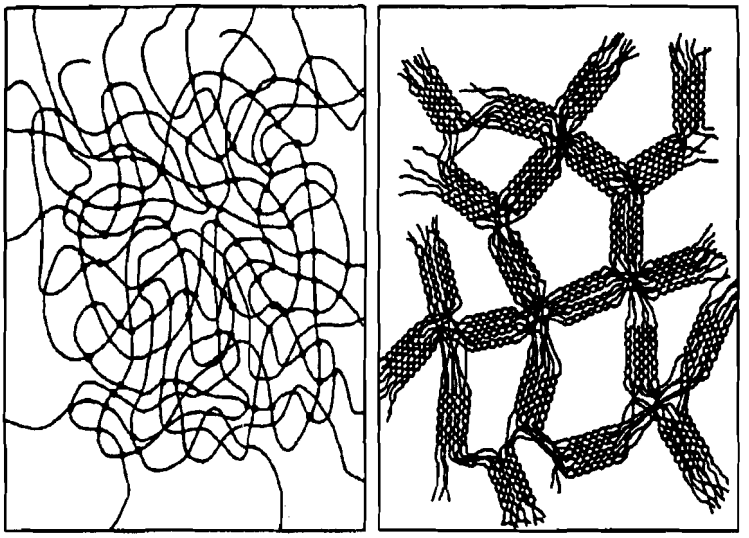

Figure 11 A comparison between an agarose gel (Sepharose) matrix (right) with a crosslinked dextran (Sephadex) matrix (left) at equivalent polymer concentration. The aggregates in agarose gels may contain $10–10^4$ bundles of polysaccharide helices. (From Ref. 47.)

duced, prepared from appropriate types of Sepharoses by crosslinking with 2,3-dibromopropanol in strongly alkaline medium, and further desulfurization by alkaline hydrolysis under reducing conditions. The crosslinking of Sepharose CL does not decrease the effective pore size, thus suggesting that crosslinks take place mainly between chains within a single gel fiber. The structure of agarose makes it inadvisable to dry and reswell the gels. When agarose is not in use it should be stored in the wet or moist state and protected from microbial growth by means of a suitable bacteriostat. The antimicrobial agent that is commonly used is 0.02% sodium azide. In general, when agarose gels are stored for long periods, the temperature should be below 8°C in the presence of a suitable bacteriostat but without freezing. Freezing results in irreversible structural disruption of the gel beads. Freeze-drying can be carried out only after the addition of protective substances, e.g., 15% lactose.

Gustavsson and Larsson [48] described the preparation of superporous agarose, which combines the desirable propertes of traditional agarose supports and a chromatography support for high-performance separations. Pharmacia Biotechnology produces a highly crosslinked agarose matrix, resulting in a very rigid gel, under the trade name Superose 6B. Both the crosslinking and the narrow

particle size (20–40 μm) contribute to its performance as a chromatography support for HPLC separations. The new name for Sepharose high-performance bioaffinity columns are Hi-Trap Column, which have a wide range of life science applications.

Reactifs IBF produces Magnogel A4R, which is a support composed of agarose (4%, w/v) crosslinked with epichlorohydrin. Its magnetic nature results from the incorporation of 7% (w/v) Fe_3O_4 in the interior of the gel beads. It has applications in situations where column operation is not favored, e.g., in viscous solutions or in the presence of insoluble particles such as cell debris.

The polysaccharide backbone of agarose can readily undergo substitution reactions to yield products with a moderately high capacity for further derivatization. Many types of agarose activated for the attachment of biologically active compounds and a variety of affinity sorbents are available from many firms, e.g., Sigma (St. Louis, MO, USA). Derivatives of crosslinked agarose modified for use in bioaffinity chromatography are also produced by Bio-Rad Laboratories under the trade name Affi-Gel.

2. Dextran Gels

Dextran is a branched-chain glucose polysaccharide produced in solutions containing sugar by various strains of *Leuconostoc mesenteroides*. Soluble dextran, prepared by fractional precipitation with ethanol of partially hydrolyzed crude dextran, contains more than 90% of α-1,6-glucosidic linkages with 1,2-, 1,3-, and 1,4-glucoside branching. When crosslinked with 1-chloro-2,3-epoxypropane in alkaline solution, dextran becomes suitable for chromatography.

The most important producer of dextran gels, supplied under the trade name Sephadex, is Pharmacia Biotechnology. The gels are very stable to chemical attack. The glucosidic bond is sensitive to hydrolysis at low pH, although it is stable for 6 months in 0.02 M hydrochloric acid, or for 1–2 h in 0.1 M hydrochloric acid or 88% formic acid. Aldehyde or carboxyl groups are formed under the effect of oxidizing agents. Dextran gels can withstand heating in an autoclave at 110°C (in solution) for 40 min, or at 120°C when dry. Drying and swelling is reversible. The gels swell to some extent even in ethanol, ethylene glycol, formamide, *N,N*-dimethylformamide, and dimethylsulfoxide.

A molecular sieve produced by covalent crosslinking of allyldextran with *N,N'*-methylenebisacrylamide has been developed by Pharmacia under the trade name Sephacryl. The advantage of matrix is the good flow rate that results because the support is exceptionally rigid. Unfortunately, the nonspecific adsorption is increased over that of other dextran gels. The use of dextran gels is partly restricted by their rather low porosity. They are widely used without any modification as specific sorbents for the isolation of a series of lectins. One example is the isolation of concanavalin A from jack bean seeds [49].

3. Cellulose and Its Derivatives

Cellulose is formed by linear polymers of β-1,4-linked D-glucose units with an occasional 1,6 bond. Commercially available celluloses are generally crosslinked with bifunctional reagents, such as 1-chloro-2,3-epoxypropane, and they are very stable to chemical attack. Glycosidic bonds are sensitive to acid hydrolysis, and under extreme conditions an almost quantitative decomposition to pure crystalline D-glucose may take place. On interaction with oxidative reagents, such as sodium periodate, aldehyde, and carboxyl groups are formed. Cellulose can be attacked, e.g., by microbial cellulases.

Macroporous-regenerated cellulose in regular beaded form is produced under the trademark Perloza by Lovochemie A.S. (Lovosice, Czech Republic). Beaded cellulose and its derivatives, in comparison with other biopolymer spherical materials, show good mechanical strength and resistance to shape deformation and therefore provide better through-flow layers in columns. Good mechanical strength is preserved in spite of the high porosity. Due to its chemical composition it is highly hydrophilic and is well tolerated by biosystems. Its insolubility in water and a number of other solvents allows it to be used in aqueous media. Biospecific adsorbents prepared from Perloza was used by Bilková et al. [5]. Medium-pressure Matrex Cellufine gels, composed of spherical beaded cellulose, are supplied by Amicon Co. (Danvers, MA, USA). They offer low nonspecific adsorption, outstanding physical strength, and high-pressure operating capabilities—all at an economic cost. Adsorption of lysozyme on dye affinity sorbent prepared by use of Cellufine was described by Anspach et al. [50]. The use of fibrous cellulose particles as matrices for DNA-bearing supports is shown by Hermanson et al. [51] in their work on immobilized nucleic acids. The isolation of poly-mRNA from tumor cells by use of an oligo(dT)-cellulose slurry in an Eppendorf Event 4160 vacuum filtration unit published was described by Noppen et al. [52]. This method can be used for mRNA determination or purification in diagnostics as well as biological and medical research. Cellulose and its derivatives are produced by a number of firms (e.g., Whatman, Maidstone, Great Britain; Schleicher and Schüll, Zürich, Switzerland; Serva, Heidelberg, Germany; Bio-Rad, Richmond, CA, USA).

C. Synthetic Copolymers

The advantages of HPLBAC, shown in Fig. 10, and the usefulness of the preparation of biologically active compounds on a pilot or industrial scale are the impetus behind the continual development of synthetic polymers. The main appeal of solid supports for these applications is their inherent mechanical stability, which provides good flow characteristics even under high pressures. They can be operated at pressures up to 100 psi and usually tolerate a wide pH range. They are

suitable for affinity ligand immobilization and provide bioaffinity supports with high capacities. They are biologically inert and because of their inert structure are not subject to enzymatic or microbial degradation. The chemical structure of these supports can be characterized by their polyethylene backbone, which creates excellent chemical and physical stability. They also contain modifiable side chains R_1, R_2, R_3, R_4:

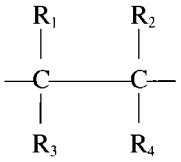

Only a limited number of synthetic polymers will be characterized. However, many synthetic copolymers exist, and their intermediates for bioaffinity chromatography and biospecific sorbents prepared from them are produced by many firms.

1. Acrylamide Derivatives

Polyacrylamide gels are produced by copolymerization of acrylamide with the bifunctional crosslinking agent *N,N'*-methylenebisacrylamide. The monomers used in this synthesis are highly toxic and thus should be handled with care. The main producer of polyacrylamide gels is Bio-Rad under the trade name Bio-Gel P. This gel is produced with a range of pore sizes, from Bio-Gel P-2 with a molecular weight exclusion limit of 1800, to Bio-Gel P-300 with a molecular weight exclusion limit of 400,000. Commercial polyacrylamide beads are purchased in the dry state and are swollen by mixing with water or aqueous solutions for period of 4–48 h depending on the porosity. Bio-Gel P products are stable to most eluants used in biochemical studies, including dilute solutions of salts, detergents, urea, and guanidine hydrochloride, although high concentrations of these reagents may alter the exclusion limits by up to 10%. The use of media with pH values outside the range 2–10 is to be avoided since some hydrolysis of the amide side groups may occur with the consequent appearance of ion exchange groups. Polyacrylamide gels are biologically inert and are not attacked by microorganisms.

Nonionic synthetic supports are obtained by copolymerization of *N*-acryloyl-2-amino-2-hydroxymethyl-1,3-propane diol with hydroxylated acrylic bifunctional monomer. Hydrophilic supports under the trade name Trisacryl GF are manufactured by IBF Reactifs. By strictly controlling the polymerization process, it is possible to synthesize a complete line of products with covering a

wide range of molecular weights from 3000 (Trisacryl GF05) to about 20 million (Trisacryl GF 2000). Trisacryl is characterized by a high degree of hydrophilicity, due both to the presence of primary alcohol groups and also the secondary amide function. It can be used under pressures up to 2–3 bar and is not affected by organic solvents such as alcohols, ketones, dioxane, or chlorinated solvents. It is stable to low (−20°C) and high (121°C) temperatures. Denaturing agents have no effect on the gel because its structure involves no hydrogen bonds. It is also stable to acidic pH, but less stable to high pH because of the slow hydrolysis of the amide linkage. Adsorption of lysozyme on the Trisacryl GF 2000 with attached Cibacron Blue F3GA in comparison with dye affinity sorbents prepared by use of other solid supports was studied by Anspach et al. [50].

2. Methacrylate Supports

The copolymerization of hydroxyalkyl methacrylate with alkylene dimethacrylates gives rise to heavily crosslinked xerogel microparticles which subsequently aggregate and yield macroporous spheroids. Their structure is shown in Fig. 12. These gels have some chemical properties in common with agarose [53]. Hydroxyalkyl methacrylate supports have been marketed under the trade name Separon HEMA and is produced by Tessek S.R.O. (Prague, Czech Republic), or under the trade name Spheron was produced by Lachema (Brno, Czech Republic). These supports have good chemical and mechanical stability and are stable to heating for 8 h in 1 M sodium glycolate at 150°C or boiling in 20% hydrochloric acid for 24 h. They are biologically inert and are not attacked by microorganisms. They can be employed in organic solvents. HPLBAC of porcine pepsin on Separon H1000 modified with ε-aminocaproyl-L-phenylalanyl-D-phenylalanine methyl ester has been described by Turková et al. [54].

Hydroxyethyl methacrylate support is also produced under the trade name Dynospheres by Dyno Particles. Their monodisperse microparticles with a size range of 0.3–5 μm are promising synthetic polymers for HPLBAC application.

The Japanese firm Toyo Soda Manufacturing Co. (Tokyo, Japan) has developed a semirigid gel, a copolymer of oligoethylene glycol, glycidyl methacrylate, and pentaerythrol dimethacrylate under the trade name Toyopearl. The identical copolymer under the name Fractogel TSK HW type is sold by E. Merck (Darm stadt, Germany). Optimal conditions for the activation of free hydroxyl groups on the gel matrix by epichlorohydrin and subsequent immobilization of ligands were investigated by Matsumoto et al. [55]. They successfully prepared affinity adsorbents for bioaffinity chromatography of lectins and trypsin. The advantage of this gel is its pressure stability up to 7 bar. Swelling of dry gels in water is 3–4 ml/g for Fractogel TSK HW-65. Its molecular exclusion limit is 5×10^6 for proteins and 10^6 for polyethylene glycols or dextrans. The negligible change

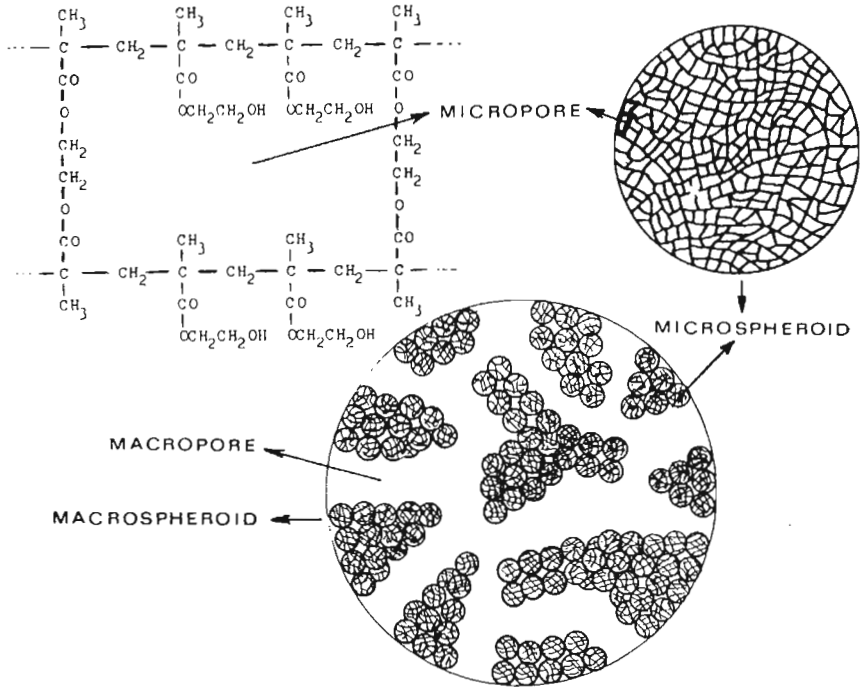

Figure 12 Structure of hydroxyalkyl methacrylate copolymer (Separon HEMA, Spheron).

in swelling volume with changing eluents, results in a very constant gel bed volume. It may be used from pH 1 to 14. The high chemical stability has led to applications at high temperature and therefore it may be autoclaved. Its properties render Fractogel TSK particularly suitable for large-scale industrial application.

Oxirane acrylic beads are obtained by copolymerization of methacrylamide, methylenebismethacrylamide, and allylglycidylether. Due to the nature of monomers the copolymer has neutral and mostly hydrophilic matrix, with a slight hydrophobic component due to the methyl groups along the polymer backbone. The oxirane group content is 1000 μmol/g dry beads. The beads are macroporous and they show a water regain of 2.5 ml/g of dry beads. This water regain is independent of pH (0.5–12.5) and ionic strength. The beads are morphologically and chemically stable under these conditions, even if exposed to them for several weeks. The mechanical stability upon stirring is very good. At present oxirane acrylic beads are produced under the trademark Epergit by Röhm Pharma GMBH

(Darmstadt, Germany). HPIAC using Eupergit C beads was developed and optimized by Fleminger et al. [56].

D. Polystyrene and Its Derivatives

Polymer-coated polystyrene/divinylbenzene beads under the name Poros matrix have been developed by PerSeptive Biosystems (Cambridge, MA, USA). The backbone of the matrix is unique in that it contains a network of large and small pores within each spherical bead [51]. The Poros matrix structure consist of large "through-pores" that allow rapid flow into the interieor of the bead and a network of "diffusive pores" that gives the support good capacity for affinity application. The polymer coating provides active sites for further modification and also blocks the harsh hydrophobic character of the styrene core. Depending on the particular application, PerSeptive has coated beads with crosslinked polyethyleneimine as well as a proprietary polyhydroxylic polymer. Since the base matrix is a stable crosslinked polystyrene, the chemical and physical nature of the support is exceptionally robust. The media is resistant to extremes in pH (1–14) and is compatible with all common buffers and solvents used in HPLC. It can also withstand 0.5 N NaOH and 1.0 N HCl for cleaning and sterilizing purposes. The physical stability of the matrix is reflected by its maximum pressure limit of 3000 psi.

Superparamagnetic polystyrene Dynabeads, consisting of Fe_2O_3-containing core covered with a polymer, are produced by the firm Dynal A.S. (Oslo, Norway). They have a smooth surface that is easily coated with antibodies or other selecting molecules. Combined with a magnet, Dynabeads make a unique tool in positive or negative separation. Monosize magnetic particles in selective cell separation was used by Ugelstad et al. [57] for the successful clinical application of immunomagnetic beads for depletion of tumor cells or T lymphocytes from bone marrow.

E. Combination of Biopolymers with Synthetic Polymers

In order to minimize the reduction of polyacrylamide porosity during activation, copolymers of agarose and polyacrylamide have been produced. This support combines the advantages of each individual polymer, while extending the potential range of derivatization procedures by virtue of the availability of both amide and hydroxyl groups for activation. Polyacrylamide-agarose gels with varying porosities are produced under the name Ultrogels AcA by IBF Reactifs. A schematic representation of the Ultrogel AcA matrix is shown in Fig. 13. Ultrogel AcA is available in four types, each composed of a three-dimensional polyacrylamide lattice enclosing an interstitial agarose gel. The gels are preswollen and calibrated within a narrow size range of 60–140 μm.

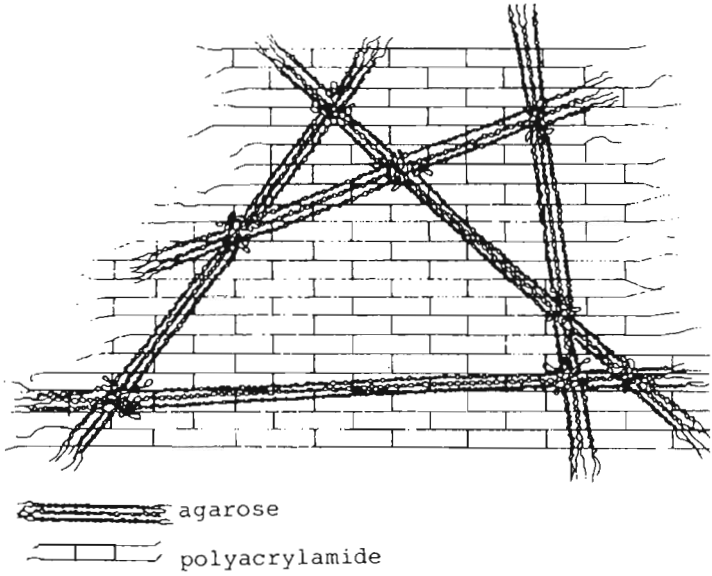

Figure 13 Schematic representation of the Ultrogel AcA matrix.

During chemical reactions involving one of the polymers, certain precautions must be taken in view of the other polymer properties. Thus the gel must not be exposed to strongly alkaline media, since the amide groups will be hydrolyzed to carboxylic acids. The limited heat resistance of the agarose must equally be respected: Ultrogel AcA must not be exposed to temperatures greater than about 40°C. The preparation of polyacrylhydrazidoagarose based on periodate oxidation of Sepharose followed by reaction with polyacrylhydrazide has been described by Miron and Wilchek [58]. These yielded matrices which were colorless and stable after reduction with sodium borohydride. Polyacrylhydrazidoagarose could be used either directly or after further modification with various additional reactive groups.

F. Inorganic Support

Inorganic supports have been reviewed by Weetall and Lee [59]. They classified these supports into a few major categories: metals, metal oxides, ceramics, and glasses. They described the preparations, properties, and applications of porous glass, porous silica, titania, alumina, and zirconia bodies, and iron and nickel oxides. These supports have an inherent advantage in their rigidity. Since inor-

ganic particles are friable materials, one should never use a stirring bar when working with these materials. Particles can be separated for washing or assay by several convenient methods. These include filtration, centrifugation, settling, aspiration, or magnetic separation. Several of these methods can be utilized for sizing inorganic particles, particularly when clumping has occurred or when one wants particles of only a specific size range. Particles may be sized on the basis of settling times, centrifugation speed, or filter porosity. The best method usually determined by considering the size range that is desired and choosing the method most likely to yield the desired particle range.

1. Controlled Pore Glass

Controlled pore glass (CPG) is synthesized by heating certain borosilicate glasses to 500–800°C for prolonged periods of time. These glass mixtures separate on such heat treatment into borate- and silicate-rich phases. The borate phase can be dissolved by treatment with acid, leaving a network of extremely small tunnels with pore diameters of 3–6 nm. Subsequent treatment with mild caustic soda removes silica material from the pore interiors and thus enlarges the pore diameter. Careful control of the various treatments can lead to a porous glass in the range 4.5–2.50 nm. Glass derivatives have outstanding mechanical stability. The rigidity of the beads permits high flow rates and facilitates fast and efficient separations. Glass beads are resistant to microbial attack and may be readily sterilized by disinfectants or autoclaving. The latter is a prime consideration in the purification of pyrogen-free enzymes destined for in vivo or clinical studies. Commercially available porous glass packing materials are produced, among others, by Bio-Rad Labs. (Richmond, CA, USA) under the trade name Bio-Glass, by Corning Glass Works (Corning, NY, USA), Waters Assoc. (Milford, MA, USA), Electro-Nucleonics, Inc. (Fairfield, NY, USA), and Pierce Chemical Company (Rockford, IL, USA) under the name CPG.

Glyceryl-CPG is a controlled pore glass whose surface has been chemically modified to produce a hydrophilic, nonionic coating that shares most of the same operating characteristics as conventional CPG. Glycerolpropyl glass was the weakest adsorber of the protein. Glyceryl-CPG is distributed by Electro-Nucleonics Inc. (Fairfield, NY, USA). Another supplier of glycophase-coated supports under the name glycophase G/CPG is the Pierce Chemical Company (Rockford, IL, USA). This company uses triethoxypropyl glycidosilane as the alkylsilane.

Nonporous glass beads, porous silicas, and soft gels coupled to Cibacron Blue F3GA were employed by Anspach et al. [50] to investigate equilibration times for the adsorption of lysozyme on the different dye affinity sorbents. In the batch mode equilibration times varied from 20 s for nonporous glass beads (20–30 μm) to more than 60 min in the case of a porous sorbent with a particle diameter of 100–300 μm and 60 nm pore size.

2. Porous and Nonporous Silica

The structure of silica is amorphous and its composition can be expressed as $SiO_2 \cdot H_2O$. Its basic unit is tetrahedral (SiO_4) and its porosity depends on the mode of preparation. Silica gel is formed from silicic acid sols by polycondensation of orthosilicic acid. Submicroscopic elemental particles are formed that retain micelles of the starting acid and in the interior. The silica is bound by siloxane Si-O-Si bonds. Every elemental particle touches the surfaces of several neighboring particles and in this way a conglomerate is formed containing pores of various diameters. The density of these inner spaces is very high and after drying they contain large specific inner surface areas of hundreds of m^2/g. The main advantage of silica is its inherent mechanical stability which provides good flow characteristics even under high pressure. The use of silica with pore sizes ranging from 6 to 400 nm, or nonporous silica in small particles 1.5–10 μm, is advisable to provide good mass transfer when performing protein separations. Silica is a commonly used support for high-performance bioaffinity chromatography. Slightly acidic silanol groups on the silica surface act as centers for nonspecific adsorption. Under alkaline working conditions (pH > 8) the surface of silica gel exhibits a high solubility that could be the reason of the contamination of the purified product. The problems of nonspecific adsorption and the solubility of silica have been largely overcome by derivatization of the silanol groups with silanes, yielding silica derivatives coated with a hydrophilic layer. The most common reagent for blocking silanol groups is 3-glycidoxypropyltrimethoxysilane. The resulting epoxide silica can be used for the direct attachment of affinity ligands or can become the starting material for the synthesis of other products. An example is the hydrazide-activated silica supports for HPLBAC developed by Ruhn et al. [60]. They prepared diol-bonded silica from Nucleosil Si-300 or 1000 coated with 3-glycidoxypropyltrimethoxysilane by hydrolysis with sulfuric acid. After periodate oxidation of the diol-silica, an aldehyde silica was produced and used for the optimization of hydrazide-activated silica synthesis by use of oxalic or adipic dihydrazide.

The improvement of affinity chromatographic performance using adsorbents prepared from nonporous monodisperse silicas in contrast to that obtained subjected to porous silica supports with identical activation and immobilization procedures was described by Anspach et al. [50]. The elution of proteins on nonporous silica-based adsorbents was investigated both theoretically and experimentally using human immunoglobulin G and immobilized protein A as the affinity pair by Lee and Chung [17]. Nonporous silica (average diameter 1.4 μm) was silanized with γ-aminopropyltriethoxysilane and activated with glutaraldehyde. A comparison was made between predicted and experimental elution peaks from chromatography of IgG on immobilized protein A. The desorption rate constant and equilibrium association constant under elution conditions were found to have a substantial effect on elution time and peak shape. Many silica gel sup-

ports are available commercially in both irregular or spherical shapes, either uncoated or glycophase-coated. Among them are, for example, silica-based supports under the trademark LiChrospher Si, LiChrospher Diol, etc. (E. Merck, Darmstadt, Germany), Porasil A-F (Waters Associates, Milford, MA, USA), Progel-TSK columns (Supelco, Bellefonte, PA, USA). Ultraaffinity-EP is one of the commercially available epoxide silicas available in prepacked columns (Beckmann Instruments, Berkeley, CA, USA). Immobilization of the ligand onto such a matrix can be performed by passing the material through the column slowly, over a predetermined time period. The use of antichaotropic anions such as phosphates and sulfates is recommended because they stabilize the protein during derivatization and increase their interaction with the activated support. Columns, cartridges, or kits of a silica activated with epoxide functional bonded phases are sold under the name Durasphere AS by Alltech Associates (Deerfield, IL, USA).

3. Iron and Nickel Oxides

Iron oxide can be prepared by several methods. One method involves the use of commercially available iron oxide powders. These can be silanized directly and used for the attachment of affinity ligands [59]. An even dispersion of magnetic material (γ-Fe_2O_3 and Fe_3O_4) throughout the bead is in Dynabeads, which are produced by Dynal A.S. This firm supplies uncoated Dynabeads, activated Dynabeads, and Dynabeads precoated with specific ligands. Their characterization is that they are the only uniform, superparamagnetic, monodisperse polymer particles. Information about them is given in section IV.C. Commercially available particles consisting of an iron oxide core coated with a silane polymer terminating in amine (particle size 1–2 μm), carboxyl (particle size 0.5–1 μm), or sulfydryl (particle size 1–3 μm) functional groups are supplied by Advanced Magnetics Corp. (Cambridge, MA, USA). Latex particles impregnated with iron oxide are also commercially available from Seradyn Inc. (Indianapolis, IN, USA). These materials show paramagnetic properties and have been successfully used in immunoassays. Nickel oxides produced by precipitation or directly supplied by a chemical manufacturer have been used in a manner similar to the iron oxides [59].

G. Membranes and Tubes

Membranes are in many ways similar in structure to synthetic beaded polymer supports. Membrane formation, characterization, and applications are described in a book by Klein [61]. The chemical composition of membranes varies greatly. Sheets can be constructed from any of a number of primary polymers including cellulose, polyamide (nylon), polyacrylonitrile, and many other materials. The most widely used materials for protein purification include cellulose and nylon membranes.

Hydrophilic affinity microporous membranes composed of reactive rein-

forced cellulosic polymers has been introduced by Memtec Corporation [51]. This membrane possesses reactive aldehydes for covalent coupling of amino groups of proteins and other ligands. Reinforced cellulosic polymers are suitable for pleated and specially cut membranes. Similar cellulose membranes produced by Sartorius (Göttingen, Germany) have been used for selective removal of human serum amyloid P component from rat blood by immunoaffinity in an extracorporeal circulation system [62].

Synthetic polyamides, known as nylons, are a family of condensation polymers of dicarboxylic acids and α,ω-diamines. Several types of nylon, differing only in the number of methylene groups in the repeating alkane segments, are available in a variety of physical forms, such as fibers, hollow fibers, foils, membranes, powders, and tubes. The purification of phosphofructokinase from yeast cell homogenate using of the selective adsorption-desorption with Immunodyne nylon membrane has been described by Huse et al. [63]. Immunodyne, Biodyne A, and Loprodyne nylon membranes are supplied by Pall Filtrationstechnik (Dreilich, Germany). Immunodyne membranes are preactivated nylon membranes developed for the covalent fixation of molecules via hydroxyl, carboxyl, or amino groups. The reactive group of Immunodyne membrane has the ability to selectively bind phosphofructokinase and phosphoglycerate kinase from yeast cell extract.

A noninteractive polymer (hydrophilic polyvinylidene difluoride) is the base material of Immobilon AV Affinity Membrane (IAV) produced by Millipore (Bedford, MA, USA). A variety of ligands containing amines or thiols can be covalently immobilized to chemically activated hydrophilic microporous membranes under a range of pH conditions (pH 4–10), ionic strengths (0.01–1.0 M), and temperatures (0–37°C). By varying these parameters, the user can immobilize nanogram to milligram amounts of proteins (150 μg/cm^2 is approximately a protein monolayer). Kučerová and Turková [46] coupled 3,5-diiodo-L-tyrosine to this membrane and used it successfully for the isolation of pepsin from a crude extract of human gastric mucosa. The advantage of membrane-based immobilized ligand was that the time for sorption and desorption of pepsin was very short when batch-wise isolation was used.

The Affinity-15 Membrane Chromatography System is also produced by Sepracor Inc. (Marlborough, MA, USA). Affinity ligands are covalently bound to the membrane using a stable, secondary amine linkage, and therefore ligand leaching is virtually eliminated. Membrane technology for protein purification increases the speed, lowers the costs, and simplifies the protein purification.

H. Commercial Availability of Activated Solid Supports and Biospecific Adsorbents

The rapid evolution of many new unmodified or activated supports, biospecific sorbents in beads, columns, cartridges, etc., is seen in the catalogues of many

companies and in the *International Product Magazine for Biotechnology*. A well-equipped separations laboratory should have a variety of commercially available matrices at hand, as well as a full range of vendor catalogs and technical data sheets on file. Fortunately, a large number of reliable suppliers offers a wide range of practical and efficient matrices. An appendix of the book of Hermanson et al. [51] lists vendors of various useful support materials. Tables 6.4 and 6.5 in the book of Turková [7] also contain examples of commercially available supports with full names and addresses of suppliers. However, many suppliers or their commercially available supports have been rapidly changing and therefore some of the information herein may be out of date.

V. SURVEY OF THE MOST COMMON COUPLING PROCEDURES

When selecting the method of attachment, the primary consideration is which groups of the affinity ligand can be used to form a linkage to a solid support without affecting the binding site. The attachment also should not introduce non-specifically adsorbing groups. From this point of view, it is often best to first couple the spacer to an affinant and, only after it has been modified in this manner, attach it to a solid support. The linkage between the surface of a solid support and an affinant should be stable during adsorption, desorption, and regeneration. When choosing an appropriate method, one should bear in mind the dependence of the stability of the affinant on reaction conditions. It should also be noted that the coupling procedure may be influenced by both the nature of the solid matrix and the substance to be attached. When bifunctional compounds are used for the coupling, complications arising from the crosslinking of both the carrier and the proteins with one another can be expected. Therefore reaction conditions such as pH, temperature, and time should be carefully chosen and monitored during coupling.

When chemically inert solid supports are available, the preparation of bio-specific adsorbents consists of two steps: (1) activation or functionalization of the chemically inert support and (2) coupling of the ligand to this modified matrix. The activation is dictated chiefly by the nature and the stability of the matrix itself. Thus, for example, conditions applicable to the derivatization of glass would totally destroy agarose.

When the attachment of the affinity ligand onto the solid support is completed, it is necessary that any remaining reactive groups be eliminated. The problem of excess reactive groups is encountered in all coupling methods. This problem can be solved by one of two methods: (1) by coupling a highly penetrable substance with no effect on the adsorption-desorption procedure; or (2) by solvolysis, which may be used when the affinants are stable to the conditions needed for the hydrolytic removal of the activated group. The last step in the preparation

of specific sorbents before their use in bioaffinity chromatography consists of thoroughly washing out all substances that are not covalently bound to the surface of the solid matrix.

A. Effect of the Nature of Proteins and Solid Supports

The amount of protein to be coupled as well as the stability and biological properties of immobilized biomolecules can be affected by the choice of solid support and the method of coupling. In order to determine the effect of the nature of the support and the character of the proteins coupled, serum albumin, trypsin, chymotrypsin, papain, and trypsin inhibitor antilysine were attached to glycidyl methacrylate copolymer, oxirane-acrylic beads, epoxy-activated Sepharose, and 2,3-epoxypropoxypropyl derivatives of glass and silica [64]. Figure 14 shows the difference in the coupling of proteins (in mg/g of dry support) to methacrylate copolymer and agarose. It is evident from the figures that the amount of protein attached as a function of pH is affected by both the character of the proteins and the nature of the solid support.

The effect of the solid support was much less pronounced when various proteins were immobilized using benzoquinone. The smaller effect of the solid support was seen when the effect of pH was investigated on the benzoquione-mediated immobilization of trypsin, chymotrypsin, and serum albumin, either to hydroxyalkyl methacrylate copolymer [65] or to agarose [66].

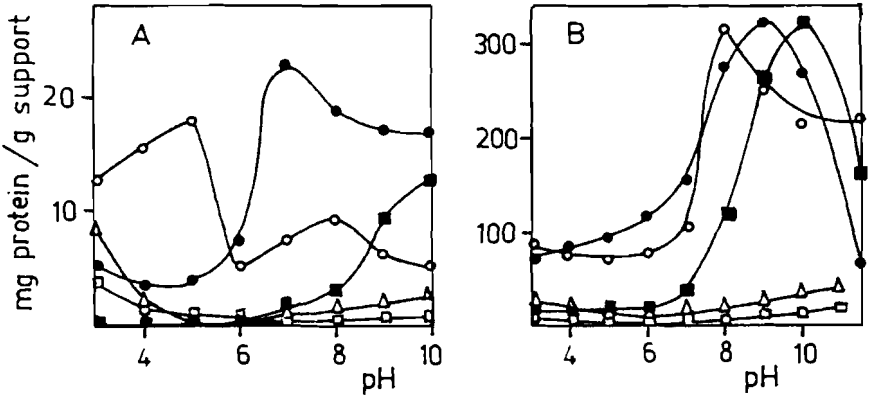

Figure 14 Effect of pH on the coupling of (○)serum albumin, (●)papain, (■)antilysin, (□)trypsin, and (△)chymotrypsin (A) to the glycidylmethacrylate copolymer and (B) to the epoxy-activated Sepharose 6B in dependence on pH. (Data from Ref. 69.)

B. Support Modification and Affinity Ligand Immobilization

1. Epoxide-Containing Supports

Carrier epoxides may react with amino, carboxy, hydroxy, and sulfydryl groups, with some aromatic nuclei, such as indole, imidazole, etc., saccharides polynucleotides, adipic acid dihydrazide, etc. The S-C, N-C, and O-C bonds formed are extremely stable [7]. Smalla et al. [67] used epoxidated hydroxyethyl methacrylate copolymer Separon HEMA for the study of the influence of salts on the coupling of different enzymes. Figure 15 shows the dependence of the activity and protein binding of aminoacylase–Separon HEMA E conjugate on the salt used for the immobilization reaction. Aminoacylase-Separon with the highest activity was achieved using ammonium sulfate. However, as Fig. 16 shows, the optimum concentration of immobilized protein depends on the concentration of this salt. The study of the effect of different concentrations of $(NH_4)_2SO_4$ on the coupling of thermitase, trypsin, chymotrypsin, pepsin, elastase, subtilisin, and carboxypeptidase A showed a varying effect of added salt on the immobilization efficiency. Salt-induced immobilization of DNA oligonucleotides on an epoxide-

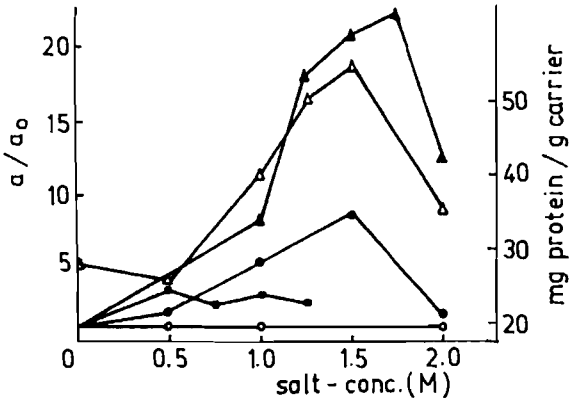

Figure 15 Dependence of the activity and protein binding of aminoacylase-Separon HEMA E conjugate on the salt added during the immobilization reaction. Aminoacylase (5 mg) in 2.5 ml 0.2 M phosphate buffer (pH 8.0); 50 mg Separon HEMA E, 20 h at 5°C. Salts added: (▲) $(NH_4)_2SO_4$, (■) Na_2SO_4, (●) $(NH_4)_2HPO_4$, (○) NaCl. a_o, activity of the enzyme-carrier conjugate in the absence of salts; a, activity of the enzyme-carrier conjugate in the presence of salts as indicated. (△) $(NH_4)_2SO_4$ addition and proteins binding (right axis). Aminoacylase (10 mg) in 2.5 ml phosphate buffer (pH 8.0); 50 mg Separon HEMA E, 30 h at 5°C. (Data from Ref. 67.)

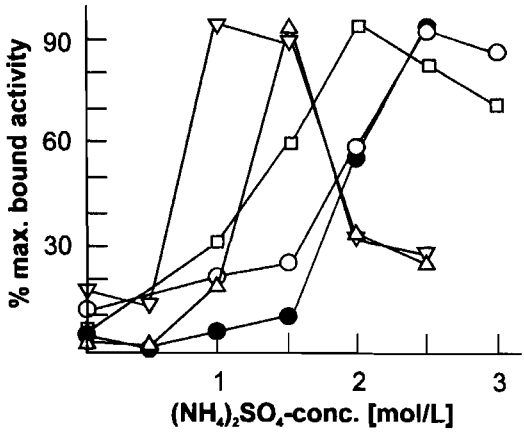

Figure 16 Dependence of the activity of proteinase-Separon HEMA E conjugate on the ammonium sulfate concentration in the medium during immobilization. Maximum bound activity (%) of immobilized proteinases: (▽) pepsin (5 mg) in 2.5 ml 0.1 M acetate buffer (pH 8); (△) elastase (2.5 mg) in 2.5 ml 0.1 M phosphate buffer (pH 8); (□) subtilisin (0.5 mg) in 2.5 ml 0.2 M phosphate buffer (pH 8); (○) chymotrypsin (5 mg) in 2.5 ml 0.1 M phosphate buffer (pH 8); (●) trypsin (5 mg) in 2.5 ml 0.1 M phosphate buffer (pH 8). Conditions: 50 mg Separon HEMA E, 15 h at 20°C for pepsin, chymotrypsin, and trypsin; 20 h at 5°C for subtilisin and elastase. (Data from Ref. 67.)

activated high-performance liquid chromatographic affinity support was studied by Wheatley et al. [68].

Epoxide-containing supports can be obtained directly by copolymerization, e.g., glycidyl methacrylate copolymer (Eupergit C). The disadvantage of biospecific sorbents prepared from glycidyl methacrylate copolymer [69]is the formation of new epoxide groups during prolonged storage, as determined by the coupling of different dipeptides.

Bioxyranes (e.g., 1,4-butanediol diglycidyl ether) can be also used for the introduction of reactive oxirane groups suitable for coupling of sugars via ether linkages with their hydroxyl groups. Proteins and peptides form alkylamine linkages through their primary amino groups. Thioether linkages are formed with substances that contain thiol groups. Coupling of the antibiotic novobiocin via its phenolic hydroxy group to epoxy-activated Sepharose was performed and the product used for the bioaffinity chromatography of DNA gyrase by Staudenbauer and Orr [70]. As a suitable blocker for residual oxirane groups of Eupergit C β-mercaptoethanol was used by Fleminger et al. [56]. Blocking is performed at nearly neutral pH (pH 8.0), and as it does not form charged groups with the matrix (in contrast to ethanolamine), nonspecific ionic adsorption of proteins is

eliminated. Remaining reactive groups can also be eliminated by solvolysis. This method may be used when affinants are stable to the conditions needed for the hydrolytic removal of the activated group. Excess epoxide groups may be hydrolyzed to diols by treatment with 0.1 M perchloric acid or with 10 mM HCl.

2. Hydrazide-Derivatized Solid Supports

A review of hydrazide-derivatized supports in affinity chromatography has been published by O'Shannessy [71]. Under suitably mild conditions, oxidation of glycoproteins with periodate results in the generation of reactive aldehydes that can subsequently be bound with nucleophiles such as primary amines or hydrazides. Both primary amines and hydrazides react with aldehydes only when they are in the unprotonated form. The very low pK of hydrazides, usually around 2.6, in contrast to primary amines, which have pK values in the range of 9–10, allows one to significantly reduce the formation of Schiff bases between protein and oligosaccharide by performing the coupling reaction under mildly acidic conditions at pH 4.5–5.5. Under such conditions the majority of the primary amines of the protein moiety are protonated and unreactive. Also, the product of coupling between an aldehyde and a hydrazide is a hydrazone, which is much more stable than a Schiff base and, according to many authors, does not require reduction. However, van Sommeren et al. [72] observed ligand leakage during both storage and chromatography in immunosorbent prepared by the attachment of antibody to hydrazide-activated agarose. When such a condition of poor stability occurs, the hydrazone produced can be stabilized by performing the reaction in the presence of sodium cyanoborohydride (hydrazine derivative: conjugate-CH_2NHNH support).

Lamed et al. [73] described the coupling of several nucleotide di- and triphosphates after periodate oxidation to adipic acid dihydrazide coupled to CNBr-activated Sepharose. In the case of nucleosides, nucleotides, and RNA, immobilization onto hydrazide-derivatized matrices would appear to be the method of choice. Enzymes with carbohydrate moieties and antibodies contain their active site in the polypeptide part of the molecules. The presence of carbohydrate raises the stability of glycoproteins. The carbohydrate moiety of the protein—after either periodate or enzymatic oxidation—can readily be immobilized to supports containing hydrazide groups, giving conjugates with very good steric accessibility of their active sites and with increased stability [74].

Chemical oxidation of the oligosaccharides may result in the oxidation of some amino acid residues (such as serine, threonine, proline, and methionine), thereby leading to a decrease in enzymatic activity. Therefore, periodate oxidation of sugar residues containing galactose can be replaced by enzymatic oxidation by galactose oxidase [75] and carbohydrate moieties in the Fc portion of immunoglobulin G containing *N*-acetylneuraminic acid and galactose as terminal

sugars by enzymatic oxidation utilizing a mixture of neuraminidase-galactose oxidase. Solomon et al. [76] showed that the coimmobilization of neuraminidase and galactose oxidase on Eupergit C-ADH beads provides an economical, efficient, and selective system for the enzymic oxidation of monoclonal antibodies without impairing their immunological activity. Both enzymes are glycoproteins and therefore immobilization through their carbohydrate moieties after periodate oxidation was used. After coupling of the enzymes to the carrier, the preparations were treated with acetaldehyde to block the residual reactive hydrazide groups. Coimmobilized galactose oxidase and neuraminidase exhibit the well-known advantages of immobilized enzymes, such as repeated use, good recovery of products, and the possibility of continuous use. However, Kelleher et al. [77] suggested the possibility that purified galactose oxidase not only converted the C-6 hydroxymethyl group of galactose to aldehyde but also catalyzed further oxidation to a carboxyl group.

3. Periodate Oxidation

A simple method for the binding of proteins to insoluble polysaccharides after their periodate oxidation has been described by Sanderson and Wilson [78]. The aldehyde formed reacts with the protein. Subsequent reduction with sodium borohydride led to the stabilization of the bonds between the protein and the polysac-

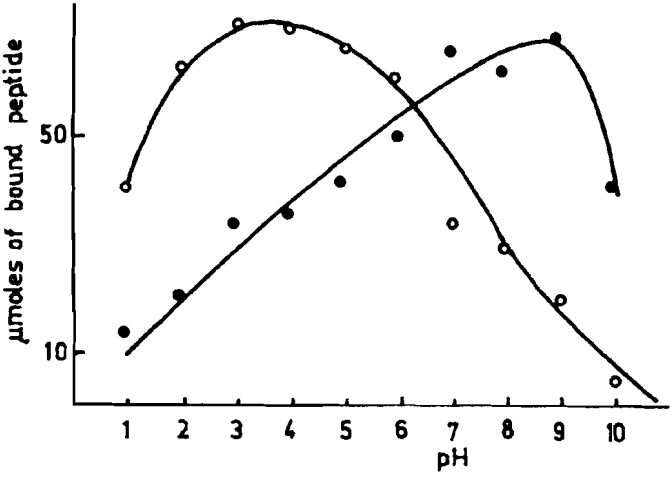

Figure 17 pH dependence of the amount of Gly-D,L-Phe (μmol/g of dry support) bound to Separon H 1000 GLC oxidized by $NaIO_4$ (●) and Separon H 1000 E-NH_2 activated by glutaraldehyde (○). (Data from Ref. 79.)

charide, and to the reduction of the residual aldehyde groups. In order to compare the coupling of ligands to solid supports via presumed aldehyde groups, the amount of Gly-D,L-Phe was coupled to periodate-oxidized glucose-Separon and to Separon with attached hexamethylenediamine and activated by glutaraldehyde in relation to pH [79]. From Fig. 17 it is evident that the two activated matrices are clearly different. Another big difference between these two types of aldehyde groups was also found in the stability of bonds with glycyl-D,L-phenylalanine. Unlike the situation with oxidized glucose residues, in which case the reduction with $NaBH_4$ is necessary, the bond between glutaraldehyde and dipeptide is very stable. There is no difference between reduced and untreated preparation. In both variants no release of nitrogen was found after 11 weeks at pH 7.0 and 24°C.

4. Glutaraldehyde Activation Technique

The glutaraldehyde activation technique can be used with solid supports having carboxamide or primary amine groups. In the latter case, the activated matrix is often colored. Weston and Avrameas [80] developed a method for the direct binding of affinants to polyacrylamide gels using glutaraldehyde which, if present in excess, reacts via one of its two aldehyde groups with the free amide group present in the polyacrylamide gel. The remaining free active group then reacts with the amino group of the affinant added during the subsequent binding reaction. A firm bond is thus formed between the support and the affinant. 6-Aminohexyl-Sepharose 4B was activated with glutaraldehyde by Cambiaso et al. [81] and used for immobilization of immunoglobulins G and A, ferritin, and albumin. A support based on nonporous silicon dioxide of particle size 0.01–0.1 μm, modified by 3-(amino)propyltriethoxysilane and activated by glutaraldehyde, was employed for the immobilization of concanavalin A, immunoglobulins, basic pancreatic trypsin inhibitor, and trypsin by Fusek et al. [82]. Activation of supports by glutaraldehyde for cell immobilization by covalent linkage was used by Jirků and Turková [83].

A number of competing mechanisms have been proposed to describe the reaction between the aldehyde and the amino function of the ligand. The most plausible one is that reported by Monsan et al. [84] who presented evidence showing that glutaraldehyde polymerizes to an unsaturated aldehyde. The latter subsequently reacts with amines to form α,β-unsaturated imines, which undergo resonance stabilization with the neighboring ethylene function. However, not all of the data on the coupling products of glutaraldehyde and polypeptides are fully explained. The products actually formed strongly depend on the pH of the reaction and on the initial ratio and character of the reactants. In addition, competing reaction mechanisms lead to different products. But in all cases the resulting bonds can be expected to be chemically very stable. A number of other bifunctional derivatives are described by Turková [7]. However, when using bifunc-

tional derivatives it should be born in mind that side reactions, such as crosslinking of the support, may occur, and the permeability may decrease drastically.

5. Cyanogen Bromide Activation

One of the first methods introduced to activate agarose, dextran, and, less commonly, cellulose and hydroxyalkyl methacrylate gel was cyanogen bromide activation [85]. The mechanism of activation by CNBr and the subsequent coupling of the affinant was elucidated by Kohn and Wilchek [86]. The coupling of an affinant occurs predominantly via the free amines in the unprotonated state. The following pH values are appropriate for coupling: aliphatic amines, pH ~10; amino acids, pH ~9; aromatic amines, pH 7–8. Ribonucleotides are coupled through their phosphate groups at pH 6. The attachment of amines to cyanogen bromide–activated Sepharose produces an N-substituted isourea that is capable of protonation at neutral and alkaline pH values. This linkage is unstable in the presence of primary amines and ammonia, which is the primary flaw of this method. Discussions of the mechanism for CNBr activation and the difference between a freshly activated and commercially available CNBr-activated Sepharose (which is treated with acid in order to achieve better stabilization of activated resin) have been published by Wilchek and Miron [87]. CNBr-activated Sepharose treated with 1 N hydrochloric acid for 1 h in order to form carbonate can be used to couple amino-containing ligands to the resin, yielding columns that consist of stable and uncharged carbonates. These activated resins will be useful for coupling of low molecular weight ligands such as diaminohexane or aminocaproic acid, as the coupling to the resin has to be performed at high pH (~9.5) because of the low reactivity of the carbonate formed. However, carbonate Sepharose also can be used to couple proteins under mild conditions and in high yields.

6. Coupling with Condensation Agents

One of the most frequent combinations of gel and spacer, used for the binding of low molecular weight affinity ligands, is Sepharose with attached hexamethylenediamine (trade name AH-Sepharose) or ε-aminocaproic acid (trade name CH-Sepharose). In order to couple them to affinants carrying primary aliphatic or aromatic amine or carboxyl groups, condensation via carbodiimide intermediater is used. Dicyclohexylcarbodiimide in pyridine can be used for coupling of nucleotides through their phosphate groups to supports containing hydroxyl groups [22]. The binding reaction between the carboxyl group and the nucleophile can be almost quantitative in the presence of excess of carbodiimide and the nucleophilic reagent such as 1-ethyl-3-(3-dimethylaminopropyl)carbodiimide hydrochloride (EDC) and 1-cyclohexyl-3-(2-morpholinoethyl)carbodiimidemetho-*p*-toluenesulfonate (CMC). Their main advantage is that their corresponding urea derivatives are soluble in water and they can therefore be easily eliminated from the

gel by washing with water. The pH range used for the carbodiimide condensation is 4.7–6.5 and the reaction time is 1.5–72 h at a carbodiimide concentration of 2–100 mg/ml. The disadvantage is that carbodiimides are relatively unstable compounds and must be handled with care because of their toxicity. After the coupling of the affinant, the reaction ought to be continued to block reactive groups by carrying out further carbodiimide reactions with glucosamine or 2-aminoethanol in the case of CH-Sepharose, or with acetic acid as blocking agent for the amino groups of AH-Sepharose.

Boschetti et al. [88] published a comparative study of soluble carbodiimide CMC with a condensation agent, *N*-ethoxycarbonyl-2-ethoxy-1,2-dihydroquinoline (EEDQ). The latter catalyzes the reaction between spacer arm and ligand by forming a mixed anhydride on the carboxyl group of the spacer arm. The mixed anhydride then reacts with the complementary amine to form a stable amide bond. The mixed anhydride can also react with other nucleophilic groups such as sulfhydryl and hydroxyl groups. EEDQ must be used in a water-ethanol mixture, which is an advantage when working with ligands that are only slightly soluble in water. EEDQ is a suitable condensation agent, being stable, nontoxic, and cheap.

7. Active Esters

Cuatrecasas and Parikh [89] described the preparation of *N*-hydroxysuccinimide (NHS) esters of succinylated aminoalkyl agarose derivatives. These active ester derivatives of agarose, when stored in dioxane, are stable for several months. These derivatives very rapidly form stable amide bonds (at 4°C) with nonprotonated forms of primary aliphatic or aromatic amino groups at pH 6–9. Among the functional groups of amino acids tested, only sulfhydryl groups compete effectively with the amino groups during the binding reaction.

Using the esterification of the carboxyl groups of CH-Sepharose 4B with the application of *N*-hydroxysuccinimide, Pharmacia produces activated CH-Sepharose 4B. The pH range suitable for binding on this derivative is indicated by Pharmacia to be 5–10, with an optimum of pH 8. The advantage of lower pH values is in the decreased ester hydrolysis but with a slower reaction rate. Buffers that contain amino acids cannot be used (Tris or glycine buffers) in the coupling reaction. Agarose derivatives containing *N*-hydroxysuccinimide ester have been introduced by Bio-Rad under the names Affi-Gel 10 and Affi-Gel 15. As shown in Fig. 18, Affi-Gel 10 couples proteins best at a pH near or below their isoelectric point, and Affi-Gel 15 couples proteins best near or above their isoelectric point. Therefore, when coupling at neutral pH (6.5–7.5), Affi-Gel 10 is recommended for proteins with isoelectric points of 6.5–11 (neutral or basic proteins) and Affi-Gel 15 is recommended for proteins with isoelectric points below 6.5 (acidic proteins). The difference in coupling efficiency of Affi-Gel 10 and Affi-Gel 15 for acidic and basic proteins can be attributed to interactions

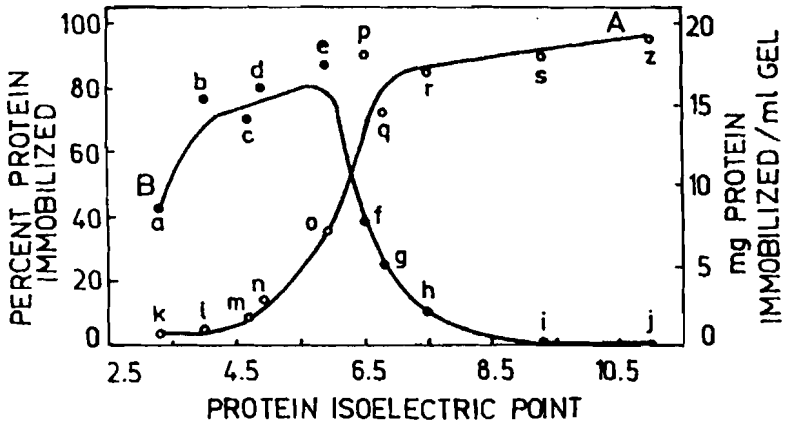

Figure 18 Immobilization of proteins to Affi-Gel 10 and Affi-Gel 15. Protein solutions were gently mixed at 0–4°C with 2 ml Affi-Gel 10 or Affi-Gel 15 for 2 h. The reaction was terminated by addition of ethanolamine, pH 8.0, to a concentration of 0.10 M, and after 30 min transferred to a 1 × 10 cm chromatography column. Unreacted protein was eluted with 7 M urea containing 1 M NaCl. Published values for the isoelectric points used to construct this figure were: fetuin (a,k), pH 3.3; human α-antitrypsin (b,l), pH 4.0; human γ-globulin (f,p), pH 5.8–7.3; human transferrin (e,o), pH 5.9; ovalbumin (c,m), pH 4.7; bovine serum albumin (d,n), pH 4.9; bovine hemoglobin (g,q), pH 6.8; equine myoglobin (h,r), pH 6.8–7.8; cytochrome c (i,s), pH 9.0–9.4; and lysozyme (j,z), pH 11.0. (○) Affi-Gel 10; (●) Affi-Gel 15. (From Frost RG, et al. Biochim Biophys Acta 1981; 670:163–169.)

between the charge on the protein and charge on the gel. Hydrolysis of some of the active esters during aqueous coupling will impart a slight negative charge to Affi-Gel 10. This negative charge will attract positively charged proteins (proteins buffered at a pH below their isoelectric point) and enhance their coupling efficiency. Conversely, the negative charge will repel negatively charged proteins (proteins buffered at a pH above their isoelectric point) and lower their coupling efficiency. Affi-Gel 15, due to the tertiary amine incorporated into its arm, has a slight overall positive charge, and the effects are reversed. Coupling under anhydrous conditions is the preferred method when this is suitable for the ligand. Since there is no hydrolysis of active esters in the absence of water, the only reaction will be that of the ligand with the gel. After the coupling of affinity ligands the unreacted groups can be eliminated by addition of 0.1 M Tris buffer, pH 8.

8. Activation with Carbonylating Reagents

Activation of crosslinked agarose with 1,1′-carbonyldiimidazole (CDI) has been described by Bethell et al. [90]. The activated imidazolylcarbamate supports react

with primary amino groups at pH 8.5–10.0 and are more stable to hydrolysis compared with *N*-hydroxysuccinimide ester–activated supports. CDI-activated agarose has a half-life of more than 14 weeks when stored in dioxane. A further advantage of using CDI-activated agarose is that the resulting *N*-alkylcarbamates are uncharged in normal pH ranges. Optimization of protein immobilization on CDI-activated diol-bonded silica has been described by Crowley et al. [91]. CDI-activated glass matrices are commercially available, e.g., from Pierce Chemical.

9. Triazine Method

The covalent linkage of ligands to hydroxyl-containing supports activated with cyanuric chloride (2,4,6-trichloro-*s*-triazine = TCT) was developed by Kay and Crook [92]. An easily controllable variant for use with macroporous cellulose bead with TCT was developed by Beneš et al. [93]. Bílková et al. [5] used this method of coupling for the immobilization of the natural chymotrypsin inhibitor antilysine. The disadvantage of this method is that the activating reagents are highly toxic.

10. Reversible Covalent Immobilization of Proteins by Thiol-Disulfide Interaction

Carlsson et al. [94] employed epoxide-activated agarose as the basis for the preparation of the mercaptohydroxypropylether of agarose gel, which they used for covalent immobilization of α-amylase and chymotrypsin by thiol–disulfide interchange. This technique consists of two steps: (1) thiolation of enzymes with methyl 3-mercaptopropioimidate; (2) binding of thiolated enzymes to a mixed disulfide derivative of agarose obtained by reaction of the mercaptohydroxypropylether of agarose with 2,2-dipyridyldisulfide. When the preparation had lost its enzymatic activity, the inactive protein was reduced off and the gel used for the binding of a new active thiolated α-amylase.

11. Benzoquinone Activation

The mechanism of the activation of hydroxyl-containing solid supports by means of benzoquinone and coupling of NH_2-containing compounds was described by Brandt et al. [66]. Benzoquinone is a very active reagent and, presumably due to the secondary reaction, the immobilized compounds are usually strongly colored. In Section V. A it was already noted that in contrast to coupling of serum albumin and chymotrypsin to epoxy-activated solid supports, the pH optimum for their coupling to benzoquinone-activated Sepharose 4B and methacrylate copolymer is the same.

12. Diazotization

The first attachment of an affinant to cellulose was carried out by means of diazonium groups by Campbell et al. [95]. The affinants are bound by their aromatic

residues (mainly tyrosine and histidine), but also slowly through their amino groups. Although this method is not frequently used at present, it offers two essential advantages: (1) the bound ligand can easily be split off by reduction with sodium dithionite; (2) this reductive cleavage allows protein-inhibitor conjugates to be isolated intact under mild conditions.

13. Other Methods

A simple method for the activation of supports carrying hydroxyl groups, such as agarose, cellulose, diol-silica, glycophase-glass, or hydroxyalkyl methacrylate copolymer, with 2,2,2-trifluorethanesulfonyl chloride (tresyl chloride), was introduced by Nilsson and Mosbach [96]. The advantage of tresyl chloride is that it is very reactive and therefore allows efficient coupling under very mild conditions, and to a number of different supports, including those used for HPLC. It is suitable for coupling ligands containing $—NH_2$ or —SH.

The use of divinylsulfone in the production of adsorbents was described by Porath and Sundberg [97]. The activation takes place rapidly under fairly mild conditions. The coupling can be performed not only with amino group–containing molecules but with carbohydrates, phenols, and alcohols at a higher pH. As a consequence, divinylsulfone crosslinking considerably improved the flow-through properties of agarose. The product coupled via divinylsulfone is very stable at acidic and neutral pH, but it is labile under alkaline conditions.

The activation of hydroxylic matrices by use of 2-fluoro-1-methylpyridinium toluene-4-sulfone (FMP) has been published by Ngo [98]. FMP-activated gels can be used to couple ligands containing either amine or sulfhydryl groups in slightly alkaline (pH 8–9) aqueous solutions or in organic solvents. The resulting linkages are stable and nonionic. For more detailed information concerning matrix activation and ligand coupling to solid supports, the reader is referred to Hermanson et al. [51] and Turková [7].

C. Molecular Imprinting Technology (MIT)

Molecular imprinting is a way of chemically preparing polymer materials for roles in molecular separation. Through molecular imprinting technology (MIT), it is possible to tailor-make polymers that are selective for different compounds [99]. The principle of molecular imprinting is described in Fig. 19. The first step is prearranging the print molecule and the monomers. After development of complementary interaction between the print molecule (template) and the monomers (a) is the polymerization around the print molecule–monomer complex (b). The last step is the removal of the print molecule from the polymer. Polymerization thus preserves the complementarity to the print molecule and subsequently the polymer selectively adsorbs the print molecule. The print molecule binds

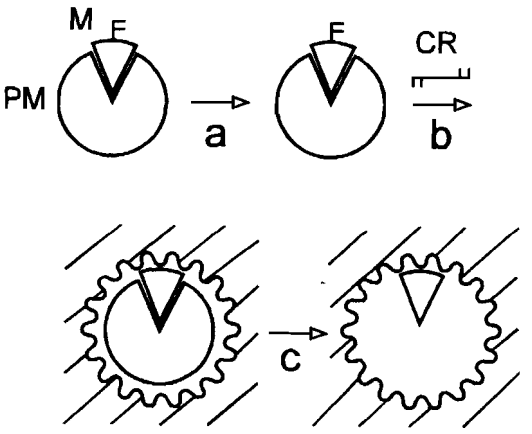

Figure 19 The principle of molecular imprinting. Development of complementary interactions between the print molecule and the monomers (a); polymerization (b); removal of the print molecule from the polymer (c). M, monomers; PM, print molecule; CR, crosslinker.

more favorably to the extracted polymer than do structural analogs. Wulff and Vesper [100] prepared chromatographic sorbents with chiral cavities for racemic resolution. For this purpose, with the aid of a chiral template molecule, functional groups were placed in a highly crosslinked polymer in such a way that they were present in a chiral cavity in a given stereochemistry. For example, 4-nitrophenyl-α-D-mannoside-2,3;4,6-di-*O*-(4-vinylphenylboronate) (A) was copolymerized to a macroporous polymer, from which the template 4-nitrophenyl-α-D-mannopyranoside (B) could be split off. These polymers were used for the chromatographic resolution of the racemate of the template molecule B. Chromatographic resolution of racemic mixtures of amino acid derivatives by use of molecular imprinting of amino acid derivatives in macroporous polymers was described by Sellergren et al. [101].

Synthesis and characterization of polymeric receptors for cholesterol by use of MIT was published by Whitcombe et al. [102]. The polymers obtained by this method were shown to bind cholesterol with a single dissociation constant, thus displaying characteristics similar to the true biological receptor or synthetic host. Mosbach [103] informed of an increasing number of applications of MIT. These include (1) the use of molecularly imprinted polymers as tailor-made separation materials; (2) antibody and receptor binding site mimics in recognition and assay systems; (3) enzyme mimics for catalytic applications; and (4) recognition elements in biosensors. The stability and low cost of molecularly imprinted poly-

mers make them advantageous for use in analysis as well as in industrial scale production and application.

D. General Considerations in the Choice of Sorbents, Coupling and Blocking Procedures

When choosing the carrier and the coupling procedure one should take account not only of the properties associated with the nature of affinity chromatography itself but also of their field of use. Kukongviriyapan et al. [104] described the maximum binding of antibodies against *Naja naja siamensis* toxin 3 (T3) and operational half-life of T3 immobilized at various ligand densities (Table 2). The maximum binding capacity of antibody was obtained on immobilized T3 with the lowest half-life (19 days). The lowest antibody binding capacity was obtained on an adsorbent containing T3 coupled to albumin-Sepharose, where the half-life was 108 days. The investigation described was undertaken to study various parameters in the use of bioaffinity chromatography to purify antibodies against cobra postsynaptic toxin from horse refined globulin for therapeutic purposes.

The choice of coupling procedures and solid supports depends on the use to which the material will be put: analytical, semipreparative, or preparative purposes. It is also necessary to take into consideration whether low or high molecular weight affinity ligands are being used. It should also be borne in mind that the toxicity of such reagents as hydrazine, cyanogen bromide, trichloro-*s*-triazine, and divinylsulfone is high; that of epichlorohydrin, bisepoxiranes, glutaraldehyde, carbonyldiimidazole, benzoquinone, diazonium, and tresyl chloride is moderate; only periodate is nontoxic.

An important factor is a rapid increase in the production of commercially available activated solid supports and many biospecific adsorbents. Hermanson

Table 2 Ligand Density, Maximum Antibody Binding Capacity, and Operational Half-life of Various Adsorbents

Affinity sorbent	Toxin immobilized (mg/ml packed gel)[a]	Maximum binding capacity[b] (mg/mg immobilized toxin)	Half-life (days)
Seph-T3	2.60	4.75	43
Seph-Ae-Suc-T3	2.01	6.00	19
Seph-BSA-T3	1.50[c]	2.60	108
Biogel-Ae-Suc-T3	2.01	5.50	25

[a] Volume of gel was measured in 0.15 N NaCl.

[b] Protein eluted at pH 2.05.

[c] Determined by using ^{125}I-labeled *N. n. siamensis* toxin 3.

Seph, Sepharose 4B; Ae, aminoethyl; Suc, succinyl; T3, *N. n. siamensis* toxin 3.

et al. [51] list 34 suppliers, their addresses, and the products including affinity matrices, activated supports, activation reagents, immobilized ligands, prepacked columns and accessories, and affinity purification kits. Turková [7] lists addresses of 90 companies providing activated supports and biospecific adsorbents, along with examples of their products. However, it was already mentioned that many suppliers or their commercially available supports have been changing rapidly.

VI. GENERAL CONSIDERATION ON AFFINANT–SORBENT BONDING

In order for the immobilized affinity ligands to be readily accessible to the binding sites of biological macromolecules, it is necessary to have more than a solid support with high porosity. The chemical groups of the affinant that participate in the interaction with the macromolecular substance must also be sufficiently remote from the surface of the solid matrix to avoid steric hindrance. The importance of spacing between the low molecular weight ligand and the surface of the matrix in bioaffinity chromatography was illustrated by Cuatrecases et al. [105] in one of the first successful applications of bioaffinity chromatography in the isolation of enzymes. Figure 20 represents the bioaffinity chromatography of α-chymotrypsin, both on Sepharose coupled with ε-aminocaproyl-D-tryptophan methyl ester (A) and on Sepharose coupled with D-tryptophan methyl ester (B), in comparison with chromatography on unsubstituted Sepharose. In the first instance (A), the bound inhibitor has high affinity for α-chymotrypsin and the enzyme can be released from the complex only by decreasing the pH of the eluting buffer. By using 0.1 M acetic acid, pH 3.0, chymotrypsin is eluted in a sharp peak and the volume of the eluted chymotrypsin does not depend on the volume of the sample applied to the column. In the second instance (B), the inhibitor coupled directly on Sepharose has a much lower affinity for the α-chymotrypsin owing to steric hindrance. In this instance a change of buffer is not necessary for enzyme elution and, as can be seen from the graph, the enzyme is eluted in a much larger volume closely after the inactive material. In order to verify that nonspecific adsorption on the carrier did not take place under the given experimental conditions, chromatography of α-chymotrypsin on an unsubstituted carrier was carried out (C).

Studies on the conformation of model peptides in membrane-mimetic environments [106] lead the authors to expect that steric accessibility of the reactive groups of the affinity ligand not only will be determined by their distance from the surface of the solid support but will also depend on the interfacial water region, which does not stabilize the same conformation as does bulk water. The arrangement of the solvent layers on the surface of the solid support will also obviously be one of the main factors affecting the penetration of the bound mole-

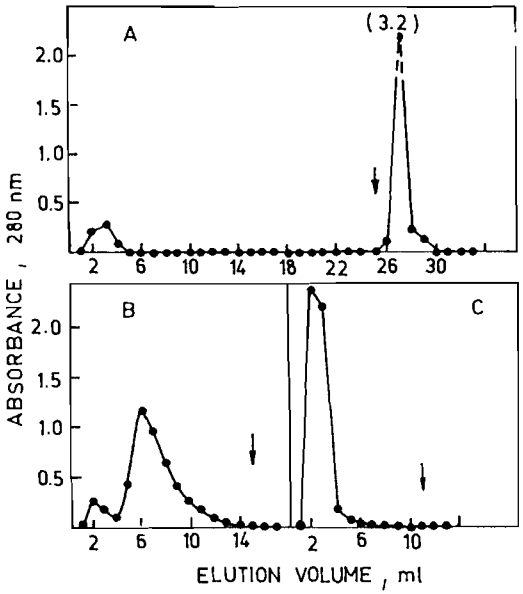

Figure 20 Bioaffinity chromatography of α-chymotrypsin on inhibitor Sepharose columns. The columns (50 × 5 mm) were equilibrated and run with 0.05 M Tris-hydrochloric acid buffer of pH 8.0. Each sample (2.5 mg) was applied in 0.5 ml of the same buffer. Columns were run at room temperature with a flow rate about 40 ml/h and fractions containing 1 ml were collected. The arrows indicate a change of elution buffer (0.1 M acetic acid, pH 3.0). (A) Sepharose coupled with ε-aminocaproyl-D-tryptophan methyl ester. (B) Sepharose coupled with D-tryptophan methyl ester. (C) Unsubstituted Sepharose. The first peaks in A and B were devoid of enzyme activity. (From R Cuatrecasas P, et al. Proc Natl Acad Sci USA 1968; 639–643.)

cules to the surface of the support. As a logical result, the mode of immobilization has a greater effect on the interaction of the substances isolated with immobilized low molecular weight ligands than with high molecular ligands.

Angal and Dean [107] studied the effect of matrix on the binding of human serum albumin to the sulfonated aromatic dye Cibacron Blue 3G-A immobilized on 10 solid supports. The results are summarized in Table 3. A 16-fold range in ligand concentration was observed in the amount of dye immobilized to the various matrices despite the similarity of the reaction conditions used. The adsorption was shown to be selective because rabbit, chicken, and bovine albumin did not bind to the same immobilized dye.

High molecular weight affinity ligands usually offer more possibilities for

Table 3 Comparison of Properties of Different Support Media[a]

Support material	Ligand concn. (μ/ml of gel)	HSA adsorbed (mg/ml of gel)	HSA eluted by desorption (mg/ml of gel)	$10^{-3}\times$ Apparent association constant (M^{-1})
Cellulose	3.2	0.8	0.2	1.1
Sephacryl	1.9	10.7	8.4	25.0
Ultrogel AcA54	0.3	0.2	0.2	3.1
Ultrogel AcA44	0.4	0.3	0.2	4.8
Sepharose 6B	2.3	32.4	20.7	45.3
Sepharose 4B	1.5	15.7	14.1	42.0
Sepharose 2B	0.9	9.1	8.4	35.0
Sepharose CL6B	0.7	5.4	4.2	30.0
Sepharose CL4B	0.4	5.0	4.6	46.8
Sepharose CL2B	0.2	1.7	24.6	24.6

[a] (The value for human serum albumin adsorbed is calculated by difference and after elution with thiocyanate).

HSA, human serum albumin.

the preparation of affinity adsorbents. However, a very important condition in this instance is that the attachment to the solid support should not cause a change in the native conformation of the ligand. To protect the binding site of the lectin, Clemetson et al. [108] coupled the lectins to Sepharose 4B after CNBr activation in the presence of 2% of the appropriate sugar. A solution that may overcome both a low stability and the capacity of biospecific sorbents for some glycoproteins, first of all antibodies and enzymes, may lie in their immobilization through their carbohydrate moieties [74]. The advantage of oriented immobilization by use of biospecific complex formation was shown in Sections III. B and III. G.

In order to minimize the nonspecific sorption of inert compounds to affinity sorbents and for the greatest possible exploitation of the attached affinity ligand it should be used at the lowest possible content in the specific sorbent [7]. The importance of the low concentration of the affinity ligand and the effect of the uneven surface of the gel are illustrated in Fig. 21. This figure illustrates schematically the surface of the macroreticular hydroxyalkyl methacrylate polymer in the form of aggregated beads. After the binding of the affinity ligand via the spacer, well-accessible, less accessible, and sterically inaccessible molecules of the affinity ligand can be recognized. This steric hindrance may in many cases explain the low saturation of molecules of the immobilized ligand with the isolated compound and the heterogeneity in the affinity of immobilized ligands. For the preparation of a homogeneous bioaffinity sorbent it is hence necessary to select conditions for the ligand-carrier binding under which the density of the affinity ligand

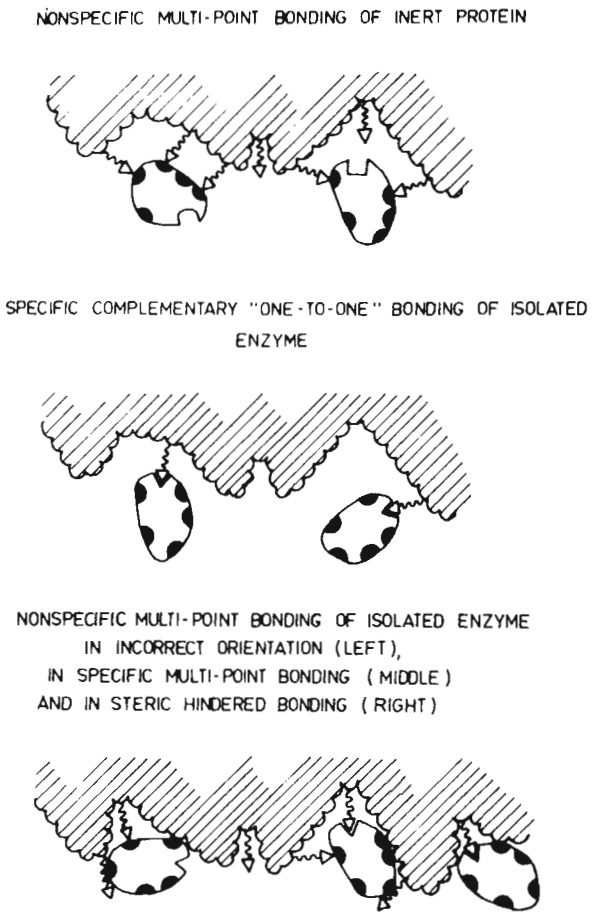

Figure 21 Schematic illustration of the effect of concentration of an immobilized affinity ligand and uneven surface of a solid carrier on specific and nonspecific sorption.

is low and the ligand is preferentially bound only to readily accessible sites (Fig. 21, middle). The low density of the affinity ligand is also required to prevent nonspecific binding. The top part of the figure illustrates the sorption of macromolecules, e.g., enzymes, that do not have a complementary binding site for the immobilized affinity ligand. This binding is caused by the high density of the immobilized affinity ligand, permitting the formation of multiple nonspecific bonds between the macromolecules in solution and the solid phase. These nonspe-

cific bonds allow the compounds present in the mobile phase to bind to the affinity ligand, the spacer, and the surface of the solid matrix. These multiple nonspecific bonds may be stronger than a single complementary bond between the isolated enzyme and immobilized complementary affinity ligand, e.g., an inhibitor. When the nonspecific multiple bonds are involved in addition to the specific complementary bond (bottom part of the figure) they increase the strength of the binding in the specific complex. This results in the elution of an enzyme in several fractions and also gives rise to difficulties in enzyme elution. The multiple nonspecific bonds may then lead to binding of the enzyme to the immobilized ligand in an incorrect orientation (bottom part of the figure left). Thus, affinity chromatography may yield good results only on a sorbent containing a low-affinity ligand concentration (middle part of the figure) where the enzyme can bind only via the complementary bond to the immobilized affinity ligand at a ratio of 1 : 1.

In order to determine experimentally the effect of the concentration of the immobilized inhibitor on the course of affinity chromatography of proteolytic enzymes, specific sorbents for carboxylic proteinases containing different concentrations of ε-aminocaproyl-L-Phe-D-Phe-OMe were prepared by Turková et al. [109]. The inhibitor was coupled to epoxide-containing Separon H 1000; the resulting concentrations of ε-aminocaproyl-L-Phe-D-Phe-OMe in μmol/g of dry gel were 0.85, 1.2, 2.5, 4.5, and 155. Solutions of porcine, chicken, or human pepsin were applied continuously to columns of these affinity sorbents until the effluent showed the same activity as the solution applied (cf. Fig. 22). On columns of affinity sorbents containing the inhibitor attached in the concentration range 0.85–4.5 μmol/g, in all cases one sharp peak of very active pepsin was achieved. The amount of desorbed pepsin was calculated from the adsorbance at 278 nm and proteolytic activity measurement. In contrast, using the affinity sorbent containing the inhibitor at a concentration of 155 μmol/g, several pepsin peaks were seen. This different behavior of the enzyme on affinity sorbents having low and high amounts of immobilized inhibitor may be due to multiple bonding of the enzyme molecule and inert proteins, as illustrated in Fig. 21. The amounts of porcine, chicken, and human pepsins eluted depending on the concentration of ε-aminocaproyl-L-Phe-D-Phe-OMe of the individual affinity sorbents were determined. From the comparison of individual pepsins it was evident that ε-aminocaproyl-L-Phe-D-Phe-OMe-Separon is a very good sorbent only for porcine pepsin. The specific sorbent containing 0.85 μmol of inhibitor per g of dry support sorbed 29.4 mg of porcine pepsin per g of dry sorbent. Using the molecular weight of pepsin (35,000) it can be calculated that 99% of the inhibitor molecules attached were involved in the specific complex. As the amount of the affinity ligand attached increased, the portion of the inhibitor molecules involved in the specific complex with pepsin decreased sharply. With specific sorbents containing 4.5 μmol inhibitor per g only 26% of the total number of inhibitor molecules attached

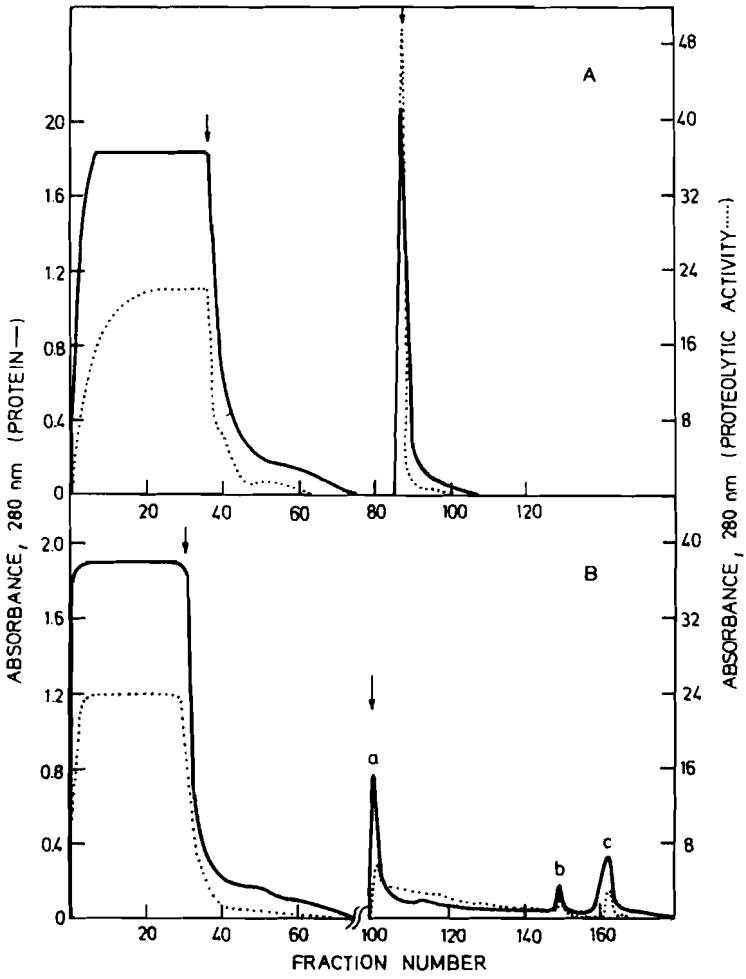

Figure 22 Bioaffinity chromatography of porcine pepsin on ε-aminocaproyl-L-Phe-D-Phe-OCH_3-Sepharon columns with (A) low and (B) high concentrations of the immobilized inhibitor. The solution of crude porcine pepsin was applied continuously onto affinity columns (5 ml) equilibrated with 0.1 M sodium acetate (pH 4.5). At the position marked by the first arrow equilibrated buffer was applied to the columns to remove unbound pepsin and nonspecifically adsorbed proteins. The second arrow indicates the application of 0.1 M sodium acetate containing 1 M sodium chloride (pH 4.5). Fractions (5 ml) were taken at 4-min intervals. The inhibitor concentration of affinity sorbents were (A) 0.85 and (B) 155 μmol/g of dry support. Solid line, protein; broken line, proteolytic activity. a, b, and c, fractions of pepsin of the same specific proteolytic activity. (From Ref. 109.)

take part in the sorption of pepsin. In an affinity sorbent with the lowest concentration of the affinity ligand only, all of the molecules of the affinity ligand are fully available for the formation of the complex with the isolated enzyme.

Liu and Stellwagen [110] used Cibacron Blue F3GA immobilized at several dye densities to study the different adsorptions of monomeric octopine dehydrogenase and tetrameric lactate dehydrogenase. They determined that the half-time for desorption of lactate dehydrogenase from Cibacron Blue F3GA-Sepharose CL-6B was nearly identical (27 s) to the mass transfer half-time of the protein in the matrix. The change in the visible adsorbance of Cibacron F3GA accompanying its complexation with lactate dehydrogenase was used to observe the kinetics of complexation. The results of their experiments indicated that it is chromatographic mass transfer and not the chemistry of complexation that limits zonal chromatography. This is why the effect of immobilized dye concentration on protein complexation is usually studied using zonal chromatography.

VII. APPLICATION OF BIOAFFINITY CHROMATOGRAPHY

A. Isolation, Determination, and Removal of Biologically Active Compounds

Bioaffinity chromatography has increasingly become the method of choice for the isolation, determination, and removal of biologically active substances. The use of biospecific adsorbents is described in an ever greater number of publications. Bibliographic review of the use of bioaffinity chromatography on 200 pages was selected from more than 5000 papers [7]. Examples of classical and high-performance bioaffinity chromatography are shown in preceding sections. The expansion of this method, which has been strongly pursued for potential applications, has been largely due to developments in biotechnology.

The various conditions used in bioaffinity chromatography depend on the nature of the substances to be isolated. Even if in many instances a homogeneous compound could be isolated from the starting material by a single chromatographic step, combinations of affinity chromatography with other purification processes also occur. In high-performance liquid bioaffinity chromatography (HPLBAC) the specificity of bioaffinity chromatography is combined with a high-performance technology based on the use of rigid particles of uniform, small size (1–50 μm in diameter). The difference of affinity chromatography methods using soft gel or porous and nonporous small hard particles has already been shown in Fig. 10. Trends in the application of HPLBAC [44] are concentrated on improvement in analytical and preparative biotechnology. Processes such as the production of monoclonal antibodies or of recombinant DNA-specified proteins and peptides have created a need for the rapid determination of specific

biomolecules in complex mixtures during production. HPLBAC can be used for monitoring biomolecules in complex mixtures, possibly providing on-line analysis in bioreactors and downstream processing. Figure 23 shows the monitoring of Protein A in fermentation broth of *Staphylococus aureus*. The authors used HPLBAC routinely to optimize the culture time and consumption of media in the fermentation. HPLBAC has an important role in the quantitative and qualitative analysis of biologically active molecules, which leads to an assessment of their purity, potency, and safety.

Large-scale affinity chromatography is usually performed in industrial laboratories and most information is thus proprietary. Large-scale protein purification was reviewed by Narayanan [111]. According to him, the requirements of a large-scale purification protocol are largely determined by the nature and quality of the desired final product and its intended use. For example, proteins for therapeutic use need to be extremely pure to minimize the risk of unwanted immunogenic responses. Four factors dictate at what stage affinity chromatography can

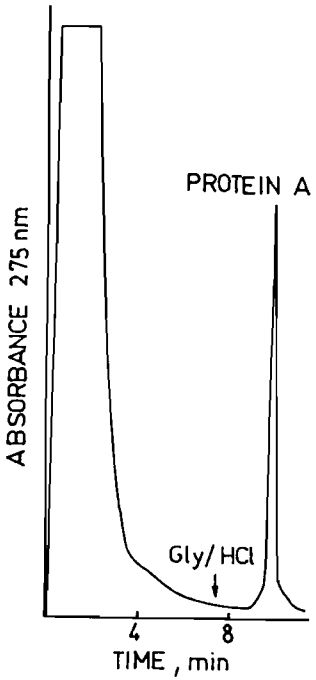

Figure 23 Monitoring of Protein A in a fermentation broth using an IgG-HPLC column (10 μm, 10 × 0.5 cm). Conditions: mobile phase, initially 0.1 M NaH_2PO_4 pH 7.0, 0.15 M NaCl, changed to 0.1 M glycine-HCl, pH 2.2 (at arrow) to elute Protein A. Flow rate, 4 ml/min; sample, 0.96 ml fermentation broth; temperature, 22°C. (From Ref. 44.)

best be exploited: (1) the concentration of the desired product in the starting material; (2) the composition of other components in the starting material, along with its physical and chemical properties; (3) the desired product purity; and (4) the volume of material to be processed. Each stage of an affinity chromatography process—adsorption, washing, elution, and regeneration—needs to be optimized before the process is scaled up. Moreover, each step must be consistent and reproducible. Bioadsorbent stability is an important criterion because the ligands are often labile biological molecules. Affinity media can lose its effectiveness because of unstable ligands, microbial contamination, and column clogging due to the presence of insoluble matter in the sample and in the eluting buffers. Accumulation of denatured protein, lipids, nucleic acids, etc., that are not eluted during the regeneration process can also limit the lifetime of the column. A preparative column is exposed to more protein in three or four preparative cycles than an analytical column is exposed to in two or three hundred cycles. Under these conditions, maintenance of the affinity media becomes very important. Stringent clean-in-place procedures are recommended by the media manufactures to prolong its lifetime. The feasibility of such measures should be taken into consideration before a purification method is scaled up. Suitable affinity ligands for large-scale isolations are polyclonal or monoclonal antibodies because they can be produced against any compound, even if the latter is only partially purified. Furthermore, monoclonal antibodies can be selected with any desired affinity, thereby making the use of biospecific columns, prepared by their immobilization, very attractive. Such antibodies show absolute specifity for only one single epitope: the smallest immunologically submolecular group on an antigen. Monoclonal antibodies can be produced in large quantities by the hybridoma technology developed by Köhler and Milstein [112]. Tarnowski and Liptak [113] used this antibody for the automated immunosorbent purification of interferon. Large-scale purification of monoclonal antibody, which recognized a human melanoma–associated 250-kDa glycoprotein/proteoglycan, was isolated by Lee et al. [114] by use of staphylococcal Protein A-Sepharose. As improvements in the technology of chromatographic support materials are developed, the combination of the unique selectivity of an affinity interaction along with the improved performance of modern supports assures bioaffinity chromatography a commanding position in the future of large-scale purification. At present, affinity chromatography is already being increasingly used in large-scale purification of therapeutic products.

B. Immobilization of Enzymes by Use of Their Suitable Immunosorbent

The high efficiency of most natural processes and their low-energy demands depend on highly active and specific catalysts, i.e., enzymes. In nature, however,

enzymes are produced by organisms for their own use: in regulated metabolic processes their low stability, narrow specificity, and strictly defined requirements are inherently connected with their function. However, it is important to take into account that after completion of their function in living cells, their denaturation and hydrolysis by proteinases occurs. For their stabilization in vivo as well as their function, hydrophobicity plays an important role. However, the contact of nonpolar amino acids with water is enthalpically disadvantageous and results in ice-like water structure. Such contact of water with hydrophobic surface clusters of proteins in vitro decreases protein stability. Hence, reduction of the nonpolar surface area should stabilize proteins. Shami et al. [115] showed the dramatically increased activity of amylase complexed with their antibodies. Sheriff and coworkers [116] used x-ray crystallography to determine the three-dimensional structure of antibody–antigen complex by use of antilysozyme Fab and lysozyme. They demonstrated that more than 80 van der Waals bonds are formed during the antibody–lysozyme interaction. Formation of the complex resulted in exclusion of all molecules of water. The conclusion of cited data was that oriented immobilization of enzymes by use of antigen–antibody interaction can result both in good steric accessibility of the enzyme active site toward high molecular mass substrates and an increased stability. Moreover, biospecific adsorption of an enzyme to a suitable immunosorbent combines the isolation of molecules with their oriented immobilization.

To confirm this hypothesis, polyclonal antibodies suitable for the oriented immobilization of chymotrypsin were prepared by chromatography on a bioaffinity matrix that had the enzyme immobilized through its active site. This was prepared by the attachment of chymotrypsin to pancreatic trypsin inhibitor antilysine, covalently linked to bead cellulose (Fig. 24). After periodate oxidation of their carbohydrate moieties, the isolated antibodies were coupled to a hydrazide derivative of bead cellulose and used for the sorption of chymotrypsin [5]. The failure to detect any chymotryptic activity toward *N*-succinyl-L-phenylalanyl-*p*-nitroanilide showed that the enzyme was immobilized via its active site. No decrease in proteolytic activity resulted from incubation of chymotrypsin with specific antichymotrypsin IgG in a 1:1 molar ratio. These isolated antibodies are thus suited for the preparation of a biospecific affinity matrix bearing immobilized chymotrypsin oriented such that substrate proteins are accessible to its active site. The antigenic affinity of the antichymotrypsin antibodies was essentially unchanged by periodate oxidation of their carbohydrate moieties. Therefore, this procedure was used to covalently attach isolated antichymotrypsin antibodies to a hydrazide derivative of beaded cellulose. The molar ratio of biospecifically adsorbed chymotrypsin molecules to immobilized antibody was 2:1, which is the value predicted for enzyme occupancy of each of the two Fab binding sites in IgG. The immobilized chymotrypsin retained practically 100% of the native catalytic activity determined by use of the high molecular substrate, i.e., denatured hemoglobin. Its proteolytic activity has not changed after more than a year.

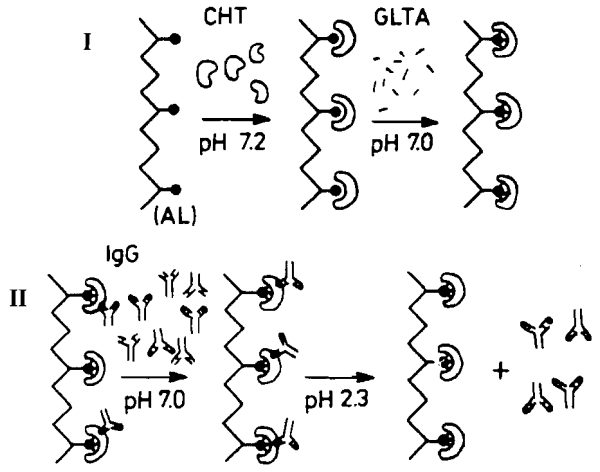

Figure 24 Schematic drawing (I) of oriented immobilization of chymotrypsin (CHT) by use of covalent crosslinking of its active site to immobilized natural polyvalent trypsin inhibitor antilysine (AL) with glutaraldehyde (GLTA) and (II) of use of its column for isolation of immunoglobulin G (IgG) against chymotrypsin (with antigenic sites outside the active site of CHT). Covalent bonds are shown as full lines. (Reproduced from Turková J, et al. Macromol Chem Macromol Symp 1988;17:241–256)

In analogy to nonenzymatic heterogeneous catalysis, in which an important role is played by the rate of diffusion of the reactants to the active surface of the catalyst, the rate of diffusion of the substrates to the binding site of the enzyme significantly affects the kinetic parameters of catalysis by an immobilized enzyme system. Very efficient columns packed with 1-μm nonporous spherical silica particles were described by Venema et al.[117]. In order to eliminate the kinetic limitation of chymotryptic hydrolysis of protein, porous bead cellulose was replaced by 1.2-μm nonporous hydroxyethyl methacrylate beads [118]. Nonporous carrier was prepared by radical dispersion copolymerization of 2-hydroxyethyl methacrylate (HEMA) and ethylene dimethacrylate (EDMA) in the mixture of alcohol-toluene. The polymerization was initiated by dibenzoyl periodate and stabilized by cellulose butyrate. Isolated antichymotrypsin antibodies, attached to nonporous beads containing 1.9 μmol of dihydrazide groups per 1 g of dry product, were used for the coupling of antichymotrypsin antibodies. After the adsorption of chymotrypsin on the prepared immunosorbent, 166.7 μg of chymotrypsin per gram of dry product was obtained (Fig. 25). Immobilized chymotrypsin retained practically 100% of the native proteolytic activity.

Monoclonal antibody (mAB) against horseradish peroxidase does not interfere with its enzyme activity. It also possesses a high affinity toward the enzyme

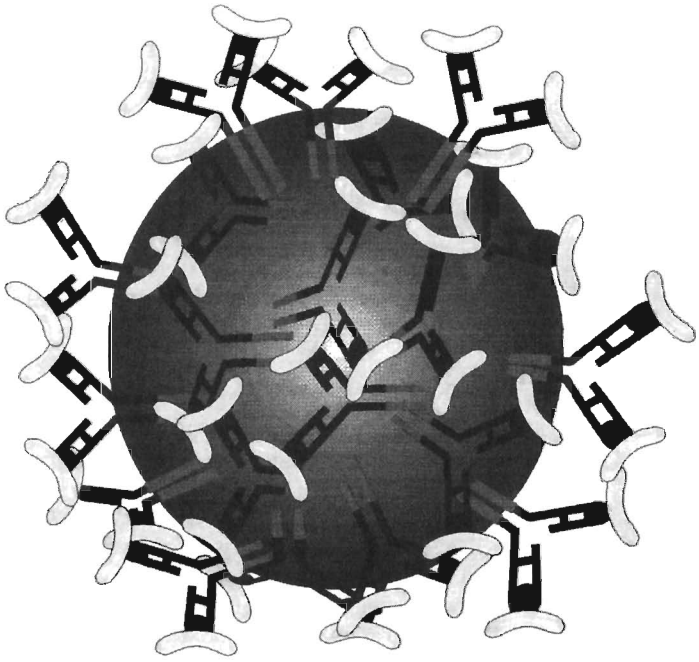

Figure 25 Schematic drawing of chymotrypsin immobilized by use of suitable antibodies coupled through their carbohydrate moieties on bead nonporous poly(HEMA-co-EDMA) beads with adipic acid dihydrazide.

and therefore was used for the preparation of a highly active immobilized enzyme by Solomon et al. [119]. They prepared the complex of peroxidase and mAB in solution and attached this immunocomplex to immobilized anti-Fc antibodies.

REFERENCES

1. Bayer EA, Wilchek M. Application of avidin-biotin technology to affinity-based separations. J Chromatogr 1990;510:3–11.
2. James MNG, Sielecki AR, Moult J. Crystallographic analysis of a pepstatin analogue binding to the aspartyl proteinase penicillopepsin at 1.8 A resolution. In: Hruby VJ, Rich DH, eds. Proceeding of the 8th American Peptide Symposium. Rockford, IL: Pierce Chem 1983:521–530.
3. Kobayashi J, Kusakabe I, Murakami K. Rapid isolation of microbial milk-clotting enzymes by *N*-acetyl (or *N*-isobutyryl)-pepstatin-aminohexylagarose. Anal Biochem 1982;122:308–312.

4. Kay J, Afting EG, Aoyagi T, Dunn M. The effects of lactoyl-pepstatin and the pepsin inhibitor peptide on pig cathepsin D. Biochem J 1982;203:795–797.
5. Bilková Z, Churáček J, Kučerová Z, Turková J. Purification of anti-chymotrypsin antibodies for the preparation of a bioaffinity matrix with oriented chymotrypsin as immobilized ligand. J Chromatogr 1997;689:273–279.
6. Winzor DJ. Review: recent developments in quantitative affinity chromatography. J Chromatogr 1992;597:67–82.
7. Turková J. Bioaffinity Chromatography. 2nd ed. Amsterdam: Elsevier, 1993.
8. Turková J, Seifertová A. Affinity chromatography of proteases on hydroxyalkyl methacrylate gels with covalently attached inhibitors. J Chromatogr 1978;148:293–297.
9. Tosa T, Sato T, Sano R, Yamamoto K, Matuo Y, Chibata I. Characteristics and applications of *N*-(ω-aminohexyl)-L-aspartic acid-Sepharose as an affinity adsorbent. Biochim Biophys Acta 1974;334:1–11.
10. Turková J, Fusek M, Maksimov JJ, Alakhov YuB. Reversible and irreversible immobilization of carboxypeptidase Y using biospecific adsorption. J Chromatogr 1986:315–321.
11. Trayer IP, Trayer HR. Affinity chromatography of nicotinamide nucleotide-dependent dehydrogenases on immobilized nucleotide derivatives. Biochem J 1974;141: 775–787.
12. Craven DB, Harvey MJ, Lowe CR, Dean PDG. Affinity chromatography on immobilized adenosine 5′-monophosphate. Eur J Biochem 1974;41:329–340.
13. Thompson ST, Cass KH, Stellwagen E. Blue dextran-Sepharose: an affinity column for the dinucleotide fold in proteins. Proc Natl Acad Sci USA 1975;72:669–672.
14. Biellmann JF, Samama JP, Bränden CI, Eklund H. X-Ray studies of the binding of Cibacron Blue F3GA to liver alcohol dehydrogenase. Eur J Biochem 1979;102:107–110.
15. Vijayalakshmi MA, Bertrand O, eds. Protein–dye interactions: developments and applications. New York: Elsevier, 1989.
16. Phillips TM, Queen WD, More NS, Thompson AM. Protein A-coated glass beads: a universal support media for high performance immunoaffinity chromatography. J Chromatogr 1985;327:213–219.
17. Lee WC, Chuang CY. Performance of pH elution in high-performance affinity chromatography of proteins using non-porous silica. J Chromatogr A 1996;721:31–39.
18. Lis H, Sharon N. Affinity chromatography for the purification of lectins. J Chromatogr 1981;215:361–372.
19. Hatakeyama T, Murakami K, Miyamoto Y, Yamasaki N. An assay for lectin activity using microtiter plate with chemically immobilized carbohydrates. Anal Biochem 1996;237:188–192.
20. Kristiansen T. Group-specific separation of glycoproteins. Meth Enzymol 1974; 184:629–641.
21. Pergami P, Jaffe H, Safar J. Semipreparative chromatographic method to purify the normal cellular isoform of the prion protein in nondenatured form. Anal Biochem 1996;236:63–73.
22. Schott H. Affinity Chromatography: Template Chromatography of Nucleic Acids and Proteins. Chromatographic Science Series. New York: Marcel Dekker, 1984.
23. Johnson AF, Wang R, Ji H, Chen D, Guilfoyle RA, Smith LM. Purification of single-stranded M13 DNA by cooperative triple-helix-mediated affinity capture. Anal Biochem 1996;234:83–95.

24. Eisenberg S, Francesconi SC, Civalier C, Walker SS. Purification of DNA-binding proteins by site-specific DNA affinity chromatography. Meth Enzymol 1990;182:521–529.
25. Phillips TM. Isolation and recovery of biologically active proteins by high performance immunoaffinity chromatography. In: Kerlavage AR, ed. The Use of HPLC in Receptor Biochemistry. New York: Alan R. Liss, 1989:129–154.
26. Cichna M, Knopp D, Niessner R. Immunoaffinity chromatography of polycyclic aromatic hydrocarbons in columns prepared by the sol-gel method. Anal Chim Acta 1997; 339:241–250.
27. Bagnati R, Ramazza V, Zucchi M, Simonella A, Leone F, Bellini A, Fanelli R. Analysis of dexamethasone and betamethasone in bovine urine by purification with an "on-line" immunoaffinity chromatography–high-performance liquid chromatography system and determination by gas chromatography–mass spectrometry. Anal Biochem 1996;235:119–126.
28. Weber DV, Bailon P. Application of receptor-affinity chromatography to bioaffinity purification. J Chromatogr 1990;510:59–69.
29. Finn FM, Hofmann K. Isolation and characterization of hormone receptors. Meth Enzymol 1990;184:244–274.
30. Green NM. Thermodynamics of the binding of biotin and some analogues by avidin. Biochem J 1966;101:774–780.
31. Wilchek K, Bayer EA. Avidin-biotin technology. Meth Enzymol 1990;184:1–746.
32. Cuatrecasas P, Wilchek M. Single-step purification of avidin from egg white by affinity chromatography on biocytin-Sepharose columns. Biochem Biophys Res Commun 1968;33:235–239.
33. Fishel R, Anziano P, Rich A. Z-DNA affinity chromatography. Meth Enzymol 1990;184:328–340.
34. Grabowski PJ. Isolation and analysis of splicing complexes. Meth Enzymol 1990; 184:319–327.
35. Cook GMW, Buckie JW. Lectin-mediated isolation of cell surface glycoproteins. Meth Enzymol 1990;184:304–314.
36. Rucklidge GJ, Milne G, Chaudhry M, Robins SP. Preparation of biotinylated, affinity-purified antibodies for enzyme-linked immunoassays using blotting membrane as an antigen support. Anal Biochem 1996;243:158–164.
37. Sharma SK, Mahendroo PP. Affinity chromatography of cells and cell membranes. J Chromatogr 1980; 184:471–499.
38. Schnaar RL. Immobilized glycoconjugates for cell recognition studies. Anal Biochem 1984;143:1–13.
39. Kaplan LJ, Barr FG, Daims M, Nelson D, Tanner TB. The use of lectin affinity chromatography for the selective isolation of plasma membranes. Prep Biochem 1984;14:149–161.
40. Braun RW, Kümel G. Separation of T cell subpopulations by monoclonal antibodies and affinity chromatography. Meth Enzymol 1986;121:737–748.
41. Yoon JW, Kenyon AJ, Good RA. Demonstration of Aleutian mink disease virus in cell culture. Nature New Biol 1973;245:205–207.
42. Dvorak DJ, Gipps E, Kidson C. Isolation of specific neurones by affinity methods. Nature 1978;271:564–566.
43. Porath J, Sundberg L. High capacity chemisorbents for protein immobilization. Nature New Biol 1972;238:261–262.

44. Ohlson S, Hansson L, Glad M, Mosbach K, Larson PO. High performance liquid affinity chromatography: a new tool in biotechnology. Trends Biotechnol 1989;7:179–186.
45. Anspach FB, Wirth HJ, Unger KK, Stanton P, Davis JR, Hearn MTW. High-performance liquid affinity chromatography with phenylboronic acid, benzaminidine, tri-L-alanine and concanavalin A immobilized on 3-isothiocyanatopropylethoxysilane-activated nonporous monodisperse silicas. Anal Biochem 1989;179:171–181.
46. Kučerová Z, Turková J. Isolation of human pepsin by use of membrane based bioadsorbent. Internatl J Bio-Chromatogr 1997;2:145–151.
47. Arnott S, Fulmer A, Scott WE, Dea ICM, Moorhouse R, Rees DA. The agarose double helix and its function in agarose gel structure. J Mol Biol 1974;90:269–284.
48. Gustavsson PE, Larsson PO. Superporous agarose, a new material for chromatography. J Chromatogr 1996;734:231–240.
49. Nandedkar UN, Sawhney SY, Bhile SV, Kale NR. Sephacryl S-300—an affinity matrix which distinguished concanavalin A from other D-mannose/D-glucose-specific lectins. J Chromatogr 1987;396:363–368.
50. Anspach FB, Johnston A, Wirth HJ, Unger KK, Hearn MTW. High-performance liquid chromatography of amino acids, peptides and proteins XCV. Thermodynamic and kinetic investigation on rigid and soft affinity gels with varying particle and pore sizes: comparison of thermodynamic parameters and the adsorption behavior of proteins evaluated from bath and frontal analysis experiments. J Chromatogr 1990;499:103–124.
51. Hermanson GT, Mallia AK, Smith PK. Immobilized affinity ligand techniques. San Diego: Academic Press, 1992.
52. Noppen C, Spagnoli GC, Schaefer C. Isolation of Multiple mRNAs from a few eukaryotic cells: a fast method to obtain templates for RT-PCR. Bio techniques 1996;21:394–396.
53. Turková J, Hubálková O, Křiváková M, Čoupek J. Affinity chromatography on hydroxyalkyl methacrylate gels. I. Preparation of immobilized chymotrypsin and its use in the isolation of proteolytic inhibitors. Biochim Biophys Acta 1973;322:1–9.
54. Turková J, Bláha K, Horáček J, Vajčner J, Frydrychová A, Čoupek J. Hydroxyalkyl methacrylate gels derivatized with epichlorohydrin as supports for large-scale and high-performance affinity chromatography. J Chromatogr 1981;215:165–179.
55. Matsumoto I, Ito Y, Seno N. Preparation of affinity adsorbents with Toyopearl gels. J Chromatogr 1982;239:747–754.
56. Fleminger G, Wolf T, Hadas E, Solomon B. Eupergit C as a carrier for high-performance liquid chromatographic-based immunopurification of antigens and antibodies. J Chromatogr 1990;510:311–319.
57. Ugelstad J, Berge A, Ellingsten T, Aune O, Kilaas L, Nilsen TN, Schmid R, Stenstad P, Funderud S, Kvalheim G, Nustad K, Lea T, Vartal, F, Danielsen H. Monosized magnetic particles and their use in selective cell separation. Makromol Chem Macromol Symp 1988;17:177–211.
58. Miron T, Wilchek M. Polyacrylhydrazido-agarose: preparation via periodate oxidation and use for enzyme immobilization and affinity chromatography. J Chromatogr 1981;215:55–63.
59. Weetall HH, Lee MJ. Antibodies immobilized on inorganic supports. Appl Biochem Biotech 1989;22:311–330.

60. Ruhn P, Garver S, Hage DS. Development of dihydrazide-activated silica supports for high-performance affinity chromatography. J Chromatogr 1994;669:9–19.
61. Klein E. Affinity Membranes: Their Chemistry and Performance in Adsorption Separation Processes. New York: John Wiley and Sons, 1991.
62. Adachi T, Mogi M, Harada M, Kojima K. Selective removal of human serum amyloid P component from rat blood by use of an immunoaffinity membrane in an extracorporeal circulation system. J Chromatogr 1996;682:47–54.
63. Huse K, Himmel M, Gärtner G, Kopperschläger G, Hofmann E. Use of an activated nylon membrane (Immunodyne) as an affinity adsorbent for the purification of phosphofructokinase and phosphoglycerate kinase from yeast. J Chromatogr 1990; 502:171–177.
64. Zemanová I, Turková J, Čapka M, Nakhapetyan LA, Švec F, Kálal J. Effect of the nature of proteins on their coupling to different epoxide-containing supports. Enzyme Microb Technol 1981;3:229–232.
65. Stambolieva N, Turková J. Covalent attachment of proteins to Spheron by means of benzoquinone. Collect Czech Chem Commun 1980; 45:1137–1143.
66. Brandt J, Andersson LO, Porath J. Covalent attachment of proteins to polysaccharide carriers by means of benzoquinone. Biochim Biophys Acta 1975;386:196–202.
67. Smalla K, Turková J, Čoupek J, Hermann P. Influence of salts on the covalent immobilization of proteins to modified copolymers of 2-hydroxyethyl methacrylate with ethylene dimethacrylate. Biotechnol Appl Biochem 1988;10:21–31.
68. Wheatley JB, Lyttle MH, Hocker MD, Schmidt DE Jr. Salt-induced immobilization of DNA oligonucleotides on an epoxide-activated high-performance liquid chromatographic affinity support. J Chromatogr A 1996;726:77–90.
69. Turková J, Bláha K, Malaníková M, Vančurová D, Švec F, Kálal J. Methacrylate gels with epoxide groups as supports for immobilization of enzymes in pH range 3–12. Biochim Biophys Acta 1978;524:162–169.
70. Staudenbauer WL, Orr E. DNA gyrase: affinity chromatography on novobiocin-Sepharose and catalyic properties. Nucleic Acid Res 1981;9:3589–3603.
71. O'Shannessy DJ. Hydrazido-derivatized supports in affinity chromatography. J Chromatogr 1990;510:13–21.
72. Van Sommeren APG, Machilsen PAGM, Gribnau TCJ. Comparison of three activated agaroses for use in affinity chromatography: effects on coupling performance and ligand leakage. J Chromatogr 1993;639:23–31.
73. Lamed R, Levin Y, Wilchek M. Covalent coupling of nucleotides to agarose for affinity chromatography. Biochim Biophys Acta 1973;304:231–235.
74. Turková J, Kučerová Z, Vaňková H, Beneš MJ. Stabilization and oriented immobilization of glycoproteins. Internatl J Bio-Chromatogr 1997;3:45–55.
75. Petkov L, Sajdok J, Rae K, Šuchová M, Káš J, Turková J. Activation of galactose-containing glycoprotein and solid supports by galactoe oxidase in presence of catalase for immobilization purposes. Biotechnol Techniques 1990;4:25–30.
76. Solomon B, Koppel R, Schwartz F, Fleminger G. Enzymatic oxidation of monoclonal antibodies by soluble and immobilized bifunctional enzyme complexes. J Chromatogr 1990;510:321–329.
77. Kelleher FM, Dubbs SB, Bhavanandan VP. Purification of galactose oxidase from

Dactylium dendroides by affinity chromatography on melibiose-polyacrylamide. Arch Biochem Biophys 1988;263:349–354.
78. Sanderson CJ, Wilson DV. A simple method for coupling proteins to insoluble polysaccharides. Immunology 1971;20:1061–1065.
79. Koelsch R, Fusek M, Hostomská Z, Lasch J, Turková J. Coupling of ligands to insoluble matrices via aldehyde groups. Biotechnol Lett 1986;8:283–286.
80. Weston PD, Avrameas S. Proteins coupled to polyacrylamide beads using glutaraldehyde. Biochem Biophys Res Commun 1971;45:1574–1580.
81. Cambiaso CL, Goffinet A, Vaerman JP, Heremans JF. Glutaraldehyde-activated aminohexyl-derivative of Sepharose 4B as a new versatile immunosorbent. Immunochemistry 1975;12:273–278.
82. Fusek M, Čapka M, Turková J. Immobilization and nonspecific adsorption of proteins to pyrogeneous highly dispersed silicon dioxide. Biotechnol Lett 1987;9:561–566.
83. Jirků V, Turková J. Cell immobilization by covalent linkage. Meth Enzymol 1987; 135:341–357.
84. Monsan P, Puzo G, Mazarquil H. Étude du mécanisme d'établissement des liaisons glutaraldéhyde-protéines. Biochimie 1975;57:1281–1292.
85. Axén R, Porath J, Ernback S. Chemical coupling of peptides and proteins to polysaccharides by means of cyanogen halides. Nature 1967;214:1302–1304.
86. Kohn J, Wilchek M. Procedures for the analysis of cyanogen bromide-activated Sepharose or Sephadex by quantitative determination of cyanate esters and imidocarbonates. Anal Biochem 1981;115:375–382.
87. Wilchek M, Miron T. Origin of the carbamate functional groups in cyanogen bromide-activated, alkylamine-substituted Sepharose. J Chromatogr 1986;357:315–317.
88. Boschetti E, Corgier M, Garelle R. Immobilization of ligands for affinity chromatography. A comparative study of two condensation agents: 1-cyclohexyl-3-(2-morpholinoethyl)-carbodiimide-metho-*p*-toluene sulfonate (CMC) and *N*-ethoxycarbonyl-1,2-dihydroquinoline (EEDQ). Biochimie 1978;60:425–427.
89. Cuatrecasas P, Parikh I. Adsorbents for affinity chromatography. Use of *N*-Hydroxysuccinimide ester of agarose. Biochemistry 1972;11:2291–2299.
90. Bethell GS, Ayers JS, Hancock WS, Hearn MTW. A novel method of activation of cross-linked agaroses with 1,1′-carbonyldiimidazole which gives a matrix for affinity chromatography devoid of additional charged groups. J Biol Chem 1979; 254:2572–2574.
91. Crowley SC, Chan KC, Walters RR. Optimization of protein immobilization on 1,1′-carbonyldiimidazole-activated diol-bonded silica. J Chromatogr. 1986;359: 359–368.
92. Kay G, Crook EM. Coupling of enzymes to cellulose using chloro-*s*-triazines. Nature 1967;216:514–515.
93. Beneš MJ, Adámková K, Turková J. Activation of beaded cellulose with 2,4,6-trichlortriazine. Bioactiv Compat Polym 1991;6:406–413.
94. Carlsson J, Axén R, Unge T. Reversible, covalent immobilization of enzymes by thiol-disulphide interaction. Eur J Biochem 1975;59:567–572.
95. Campbell DH, Luescher EL, Lerman LS. Immunologic adsorbents I. Isolation of

antibody by means of a cellulose-protein antigen. Proc Natl Acad Sci USA 1951; 37:575–578.
96. Nilsson K, Mosbach K. Immobilization of enzymes and affinity ligands to various hydroxyl group carrying supports using highly reactive sulfonyl chlorides. Biochem Biophys Res Commun 1981;102:449–457.
97. Porath J, Sundberg L. High capacity chemisorbents for protein immobilization. Nature New Biol 1972;238:261–262.
98. Ngo TT. Facile activation of Sepharose hydroxyl groups by 2-fluoro-1 methylpyridinium toluene-4-sulfonate: preparation of affinity and covalent chromatographic matrices. Bio/Technology 1986;4:134–137.
99. Ekberg B, Mosbach K. Molecular imprinting: a technique for producing specific separation materials. Trends Biotechnol 1989;7:92–96.
100. Wulff G, Vesper W. Preparation of chromatographic sorbents with chiral cavities for racemic resolution. J Chromatogr 1978;167:171–186.
101. Sellergren B, Ekberg B, Mosbach K. Demostration of substrate-and enantio-selectivity by chromatographic resolution of racemic mixtures of amino acid derivatives. J Chromatogr 1985;347:1–10.
102. Whitcombe MJ, Rodriguez ME, Villar P, Vulfson EN. A new method for the introduction of recognition site functionality into polymers prepared by molecular imprinting: synthesis and characterization of polymeric receptors for cholesterol. J Am Chem Soc 1995;117:7105–7111.
103. Mosbach K. The emerging technique of molecular imprinting and its future impact on biotechnology. 12th International Symposium on Affinity Interaction, Kalmar, Sweden, June 15–19, 1997, L15.
104. Kukongviriyapan V, Poopyruchpong N, Ratanabanangkoon K. Some parameters of affinity chromatography in the purification of antibody against Naja naja siamensis toxin 3. J Immunol Meth 1982;49:97–104.
105. Cuatrecasas P, Wilchek M. Single-step purification of avidin from egg white by affinity chromatography on biocytin-Sepharose columns. Biochem Biophys Res Commun 1968;33:235–239.
106. Gierasch LM, Lacy JE, Thompson KF, Rockwell AL, Watnick PI. Conformation of model peptides in membrane-mimetic environments. Biophys J 1982;37:275–284.
107. Angal S. Dean PDG. The effect of matrix on the binding of albumin to immobilized Cibacron blue. Biochem J 1977;167:301–303.
108. Clemetson KJ, Pfueller SL, Luscher EF, Jenkins CSP. Isolation of the membrane glycoproteins of human blood platelets by lectin affinity chromatography. Biochim Biophys Acta 1977;464:493–508.
109. Turková J, Bláha K, Adamová K. Effect of concentration of immobilized inhibitor on the biospecific chromatography of pepsins. J Chromatogr 1982;236:375–383.
110. Liu YC, Stellwagen E. Accessibility and multivalency of immobilized Cibacron Blue F3GA. J Biol Chem 1987;262:583–588.
111. Narayanan SR. Preparative affinity chromatography of proteins. J Chromatogr A 1994;658:237–258.
112. Köhler G, Milstein C. Continuous cultures of fused cells secreting antibody of predefined specificity. Nature 1975;256:495–497.

113. Tarnowski SJ, Liptak RA. Automated immunosorbent purification of interferon. In: Mizrahi A, van Wezel AL, eds. Advances in Biotechnical Processes. New York: Alan R. Liss, 1983:271–287.
114. Lee SM, Gustafson ME, Pickle DJ, Flickinger MC, Muschik GM, Morgan AC. Large-scale purification of a murine antimelanoma monoclonal antibody. J Biotechnol 1986;4:189–204.
115. Shami EY, Rothstein A, Ramjeesingh M. Stabilization of biologically active proteins. Trends Biotechnol 1989;7:186–190.
116. Sheriff S, Silverton EA, Padlan EA, Cohen GH, Smith-Gill SJ, Finzel BC, Davis DR. Three-dimensional structure of an antibody–antigen complex. Proc Natl Acad Sci USA 1987;84:8075–8079.
117. Venama E, Kraak JC, Poppe H, Tijssen R. Packed-column hydrodynamic using 1-μm non-porous silica particles. J Chromatogr 1996;740:159–167.
118. Turková J, Bilková Z, Mazurová J, Horák D. Oriented immobilization of chymotrypsin by use of suitable antibodies coupled to porous or non-porous solid support. 12th International Symposium on Affinity Interaction: Fundamentals and Applications of Biomolecular Recognition, Kalmar, Sweden, June 15–17, 1997, PA34.
119. Solomon B, Hadas E, Koppel R, Schwartz F, and Fleminger G. Highly active enzyme preparations immobilized via matrix-conjugated anti-Fc antibodies. J Chromatogr 1991;539:335–341.

5

Characterization and Partial Purification of Steroidogenic Factors from Thymic Epithelial Cell–Conditioned Medium

Mehmet Uzumcu
King Faisal Specialist Hospital and Research Center, Riyadh, Saudi Arabia

David R. Brigstock
Ohio State University and Children's Hospital, Columbus, Ohio

Young C. Lin
Ohio State University, Columbus, Ohio

I. INTRODUCTION

The thymus gland, besides its well-recognized role in the immune system, plays a role in reproductive biology, particularly in regulating ovarian function. Studies using neonatally thymectomized mice or congenitally athymic nude mice (*nu/nu*) have clearly shown that thymus gland influences ovarian function, although the mechanism for this influence is not completely known [1]. In this chapter, we shall summarize the experimental evidence that supports the regulation of the ovaries by the thymus gland and the mechanisms that might be involved. We further describe our characterization and partial purification of two potentially novel thymic factors that directly influence ovarian steroidogenesis in vitro.

II. THYMUS AND OVARIES

A. Influence of the Thymus on the Ovaries

Establishment of a normal reproductive system depends on presence of an intact thymus gland since absence of the thymus causes various reproductive disorders. Neonatal thymectomy in certain strains of mice causes ovarian dysgenesis and sterility in females [2]. Similarly, congenitally athymic nude mice (*nu/nu*) have an accelerated follicular atresia and premature ovarian failure [3]. Both congenitally athymic and neonatally thymectomized mice show delays in vaginal opening and onset of the first estrus [3]. The time of the neonatal thymectomy appears to be critical based on the fact that while thymectomy on day 3 of life causes ovarian dysgenesis, thymectomy on or after day 7 does not cause any apparent ovarian anomaly [2]. Studies have indicated that ovarian histology of neonatally thymectomized mice is similar to that of their littermates at birth. A progressive ovarian dysgenesis starts at day 20 whereby ovary is gradually depleted from follicular structures and invaded by lymphocytes. Ovarian follicles and corpora lutea are then gradually replaced with interstitial tissue and the ovary is atrophied by day 120 [4]. Ovarian dysgenesis following neonatal thymectomy is also observed in other species including rats and primates [5–7]. Endocrine disturbances along with histological disorders are also observed in neonatally thymectomized mice. These disturbances include but are not limited to high levels of androgens [8] and low levels of progesterone and estradiol [9] which are attributed to the destruction of follicular structures and their replacement by interstitial tissue.

B. Proposed Mechanisms for Influence of Thymus on the Ovaries

An explanation suggested for the ovarian dysgenesis in neonatally thymectomized mice is based on the premise that self-reactive CD4+ T cells are continuously produced from thymus and released to the periphery. In euthymic animals, ovarian dysgenesis is not observed because these autoreactive CD4+ T cells were controlled by another CD4+ subset with regulatory or suppressive activity [10]. The suppressive CD4+ cells are also generated from thymus but only after age 3 or 4 days. Thymectomy on day 3 of life causes the shift in the balance between self-reactive and regulatory CD4+ populations to favor the former and explains ovarian dysgenesis as a spontaneously occurring autoimmune disease [10]. Ovarian dysgenesis in thymectomized animal is often associated with other autoimmune disorders such as thyroiditis, gastritis, and parotitis [11–13].

That ovarian dysgenesis is directly due to autoimmunity was shown by transfer experiments by which the disease was transferred by CD4+ T cells from thymectomized animals to young recipients [14]. In addition, the transfer of ovar-

ian dysgenesis was prevented by transfer of CD4+ CD5+ T cells [15]. Furthermore, autoreactive antibodies to the ovary have been shown in neonatally thymectomized mice [16]. However, these antibodies were detected only after the age of 30 days, which fails to explain the initial destruction at the ovary prior to day 30. The possible explanation of this failure is that disturbances of the ovary prior to day 30 are due to the effect of thymectomy at the level of the hypothalamic-pituitary axis. Specifically, the development of the hypothalamus remains incomplete if the thymus is absent or removed at an early age. Therefore, the underdeveloped hypothalamus cannot release sufficient luteinizing hormone–releasing hormone (LHRH), which in turn causes gonadotropin deficiency and ovarian dysgenesis later in the life. Experimental findings using congenitally athymic mice support this hypothesis. This strain of mice exhibits decreased levels of luteinizing hormone (LH) and follicle-stimulating hormone (FSH) in the pituitary gland and in the circulation prior to vaginal opening (i.e., puberty), along with reduced serum estrogen [17]. In addition, a reduced level of LHRH in hypothalami of athymic nude mice was observed while the LH response of these animals to exogenously administered LHRH in vivo was identical to that of their heterozygote (*nu/+*) littermates [18]. Previously, Rebar and coworkers demonstrated that reduced LH and FSH levels in athymic mice could be restored to normal by neonatal thymic implantation [19]. Finally, it has been demonstrated that thymosin fraction–5 (TF-5) and thymosin β4 stimulates LHRH from medial basal hypothalami from normal cycling female rats superfused in vitro [20]. Thus, the evidence from neonatally thymectomized and congenitally athymic mice suggests that the influence of thymus on the reproductive functions is due to at least two mechanisms:

1. *Autoimmune*. Removal of the thymus at an early age causes development of autoimmune antibodies against functional structures at the ovary due to the disturbance of the delicate balance at the immune system.
2. *Endocrine*. Hormonal interactions between the thymus and hypothalamic-pituitary-ovarian axis exist. Since this interaction is disrupted in neonatally thymectomized or athymic mice, ovarian dysgenesis develops later in the life.

In addition to these two separate but interrelated mechanisms, interaction between the thymus and the ovaries may be partly through the direct effect of secretory products of the thymus (i.e. thymic hormones) on the ovary without any involvement of hypothalamus-pituitary axis or immune system. A considerable body of experimental evidence shows that there is a direct influence of various immune products (e.g., interleukins and/or other cytokines) on ovarian function [21].

III. STUDIES WITH THYMIC EPITHELIAL CELL–CONDITIONED MEDIUM

When we initially hypothesized that thymic factor(s) may directly influence ovarian function, there were very few previously published studies in this area [22,23]. Since it was known that thymic epithelial cells are the main source of the thymic hormones [24] and thymic hormones are produced by the epithelial cells in culture [25], we began our investigation in this area by examining the influence of *t*hymic epithelial cell–*c*onditioned *m*edium (TCM) on rat ovarian granulosa cell (RGC) steroidogenesis in vitro [26].

A. Preparation of TCM

TCM was prepared as previously described [27]. Briefly, thymi from 21- to 23-day-old rats were removed and minced into small pieces. The tissue fragments were rinsed and centrifuged (50 *g* for 1 min) 5 times in 40 ml Hank's Calcium-Magnesium Free Balanced Salt Solution (HCMF) to remove most of the lymphocytes. The remaining tissue fragments were digested with a mixture of trypsin (0.125%) and ethylenediaminetetraacetic acid (EDTA) (0.01%) in HCMF at 37°C with stirring for 45 min. The released thymic cells were washed, counted, and plated in 25 cm^2 culture flasks at 2×10^6 cells/ml density. The culture medium used was Minimum Essential Medium D-Valine modification (MEM) supplemented with 10% FBS. After 24 h in culture, the medium was replaced and unattached cells (mostly lymphocytes) were removed. The attached cells were allowed to grow for an additional 3 days and the medium was replaced with fresh medium. The cells were cultured for two additional 5 day periods and the media from these cultures were collected, centrifuged, and stored at −20°C until used for evaluation. *H*eart cell–*c*onditioned *m*edium (HCM) and *m*ock *e*xtract (ME) were used as control media throughout these studies. HCM was prepared from hearts of 21- to 23-day-old rats similar to TCM. To alleviate the potential nonspecific effects of FBS components, ME was prepared in an identical fashion as TCM or HCM, but in cell-free culture dishes.

B. Preparation of RGC

Granulosa cells were prepared from 21- to 23-day-old diethylstilbestrol (DES)–treated Sprague-Dawley female rats as previously described [27]. Briefly, granulosa cells were washed and plated at a density of 4×10^5 viable cells per well in 24-well tissue culture plates containing 1 ml serum-free medium. The cells were first cultured for 24 h at 37°C before TCM treatment.

C. Effect of TCM on Steroidogenesis from RGC

Steroidogenic activity of TCM was tested in time–course and dose–response studies. TCM stimulated both progesterone (P_4) and estradiol (E_2) secretion from

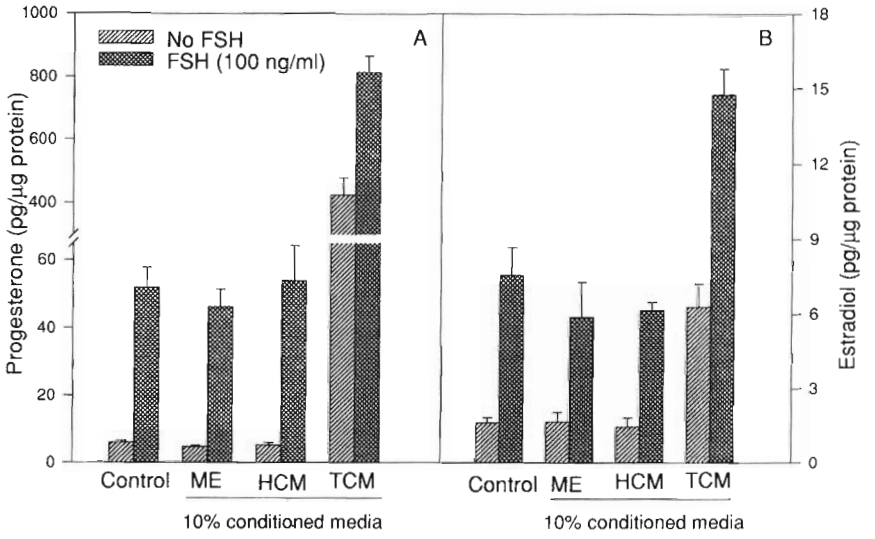

Figure 1 Effect of TCM on basal and FSH-induced P_4 (A) and E_2 (B) secretions from cultured RGC as determined by radioimmunoassay (RIA). Data points are shown as the mean ± SD of picogram quantity of the steroids per microgram of cell protein from quadruplicate-culture wells in a representative experiment that was repeated 3 times with similar results. The control represents the granulosa cells incubated with culture medium containing no conditioned medium. (Modified from Ref. 28.)

RGC in a time- and dose-dependent manner [27]. Later, we observed 80-and 17-fold increases in basal and FSH-induced P_4 secretion from rat granulosa cells treated with 10% TCM for 48 h. (The treatment length was 48 h throughout the entire study.) In addition, TCM stimulated basal and FSH-induced E_2 secretion about four- and threefold, respectively [28] (Fig. 1). Similarly, 10% TCM augmented basal and FSH-induced 20α-hydroxyprogesterone (OH-P_4) approximately 40- and 10-fold. Basal and FSH-stimulated aromatase enzyme activity was also upregulated by TCM. The stimulatory effect of TCM on steroidogenesis from RGC was not due to cellular proliferation or growth since the TCM treatment increased neither total cellular protein content nor [^{3}H]thymidine incorporation to the RGC [28].

D. Physicochemical Characterization of TCM

Boiling at 100°C for 20 min, acidification of pH to 3 by 1 N HCl followed by neutralization, and acetone treatment completely eliminated the P_4 stimulatory

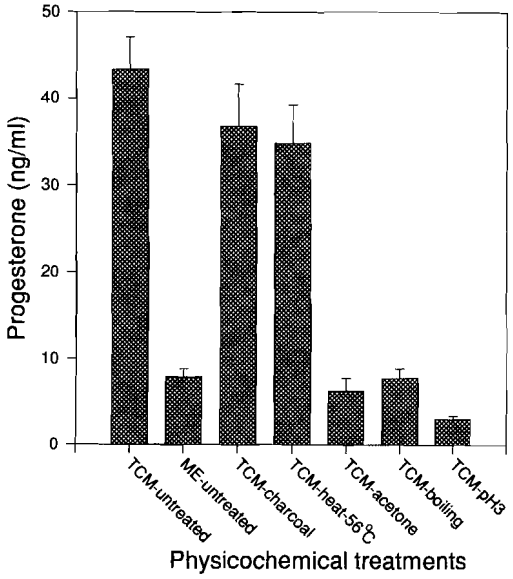

Figure 2 Effect of 25% TCM before or after various physicochemical treatments on P_4 secretion in cultured RGC as determined by RIA. Data points are shown as the mean ± SD of nanogram quantity of P_4 per milliliter of medium from quadruplicate-culture wells (n = 2). The conditions for various physicochemical treatments are as described in Section II.D. (Adapted from Ref. 27.)

action of TCM, while charcoal sedimentation or heating at 56°C for 30 min caused minimal loss of activity [27] (Fig. 2). In addition, HPLC-purified active fractions of TCM lost about 80% of their original activity after one freeze–thaw cycle [29], which is sometimes characteristic of peptide samples. These results showed that stimulatory activity of TCM was heat-and acid-labile and could be destroyed by acetone treatment or freeze–thaw cycles, but could not be sedimented by charcoal. It was tentatively concluded that a peptide or protein factor(s) was responsible for the biological activity in TCM.

IV. STUDIES WITH GEL FILTRATION CHROMATOGRAPHY FRACTIONS OF THE TCM

TCM was fractionated by gel filtration chromatography and the column fractions were tested for their effects on cultured RGC steroidogenesis and morphology [29]. For gel filtration chromatography, TCM was lyophilized using a freeze-dryer (FTS Systems, Inc., Stone Ridge, NY) and reconstituted in 25% of its origi-

nal volume with distilled water. The samples were clarified by centrifugation, filtered using 0.45-μm membrane, and 1 ml of TCM concentrate was applied to TSK-Gel G2000 SW gel filtration column (0.8 × 30 cm; TosoHaas, Philadelphia, PA, USA) equipped with a TSK-GSW guard column (0.8 × 4 cm; TosoHaas). A fast protein liquid chromatography (FPLC; Pharmacia, Piscataway, NJ, USA) system was used to maintain the flow rate at 0.5 ml/min during elution of the proteins with PBS containing 0.5 M NaCl. The column eluate was monitored at 280 nm using an in-line UV detector and 200-μl fractions were collected. Fractions were stored at −70°C prior to assay. The molecular weight of the fractions was calculated by reference to the elution positions of ovalbumin (45 kDa), trypsin inhibitor (20.1 kDa), lactalbumin (14.2 kDa), and epidermal growth factor (6 kDa). Similarly, HCM and ME concentrates were also subjected to the gel filtration FPLC, and the collected fractions were also used as controls. Gel filtration FPLC of TCM resulted in the elution of several major protein peaks as detected at 280 nm [29] (Fig. 3).

A. Effect of TCM Gel Filtration Fractions on Steroidogenesis in RGC

When individual fractions were tested for their ability to stimulate E_2 and P_4 production by RGC, two distinct peaks of activity were observed [29] (Fig. 3). The first peak of activity was eluted in fractions 50–60 that corresponded to $M_r \sim 22{,}000$ (''TCM-22'') and stimulated P_4 production. The peak fraction (no. 53) stimulated P_4 production approximately 10-fold but had no effect on E_2 production. The second peak of steroidogenic activity was eluted in fractions 84–94, which corresponded to $M_r \sim <1000$ (''TCM-1''), and stimulated both the production of P_4 and E_2. The peak fraction of TCM-1 stimulated P_4 and E_2 approximately 15- and 10-fold, respectively. Production of 20α-OH-P_4 from RGC was also stimulated by both TCM-1 and TCM-22. In addition, TCM-1 but not TCM-22 stimulated aromatase enzyme activity in cultured RGC. However, fractions collected from gel filtration FPLC and HCM and ME were shown to be inactive [29].

B. Morphological Changes Caused by TCM-1 in RGC

Phase contrast microscopic examination revealed that TCM-1 but not TCM-22 caused drastic morphological alterations in cultured RGC that resembled morphological alterations observed following FSH treatment of RGC [29] (Fig. 4), or human chorionic gonadotropin (hCG)/cAMP treatment of human granulosa cells [30]. Following their treatment with FSH or TCM-1, RGC became rounded and left finger-like processes attached to the substratum. In contrast, the cells treated with TCM-22 or control medium appeared well spread and polygonal [29] (Fig.

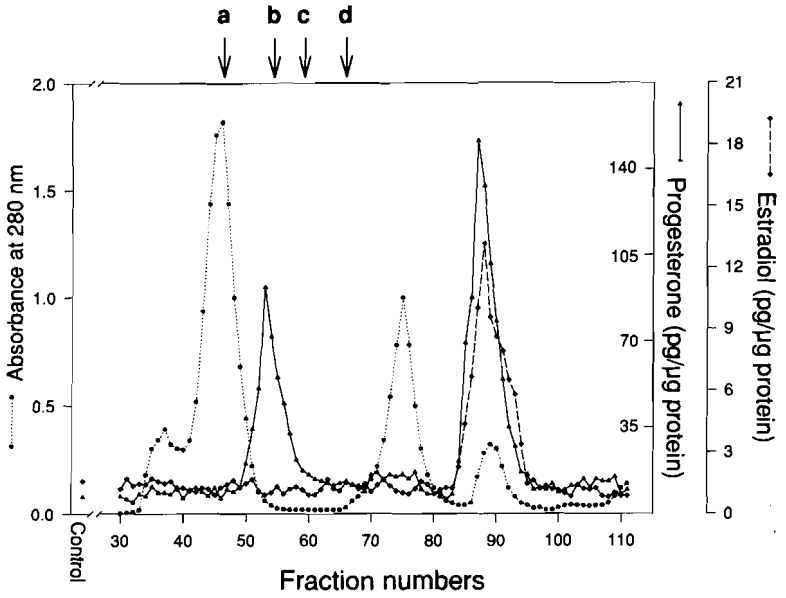

Figure 3 Effect of TCM gel filtration fractions on P_4 (▲) and E_2 (◆) secretion from cultured RGC as determined by RIA. The figure also shows the absorbance of the column eluate at 280 nm (●). In this experiment, control group is the granulosa cells that were treated with culture medium with no gel filtration fraction. The elution positions of molecular weight marker proteins (a) ovalbumin (45 kDa), (b) trypsin inhibitor (20.1 kDa), (c) lactalbumin (14.2), and (d) epidermal growth factor (6 kDa) are indicated at the top (arrows). Data points for the steroids are expressed as picograms per microgram of cell protein from single well. The experiment was repeated for at least 5 times with similar results. (Modified from Ref. 29.)

Figure 4 Morphology of the RGC following a 1-h treatment with FSH (500 ng/ml) (A), TCM-1 (B), and control medium or TCM-22 (C). The cells that were treated with FSH or TCM-1 became rounded (arrows) and left finger-like processes (arrowheads) attaching substratum. The cells that were treated with control medium or TCM-22 were well spread and polygonal in shape. Magnifications of the micrographs are 720×. (Adapted from Ref. 29.)

A

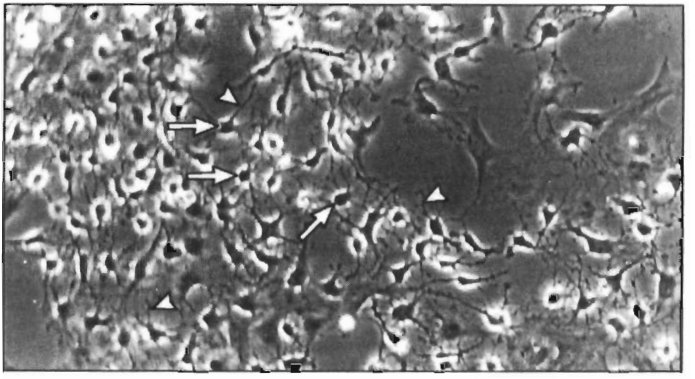

B

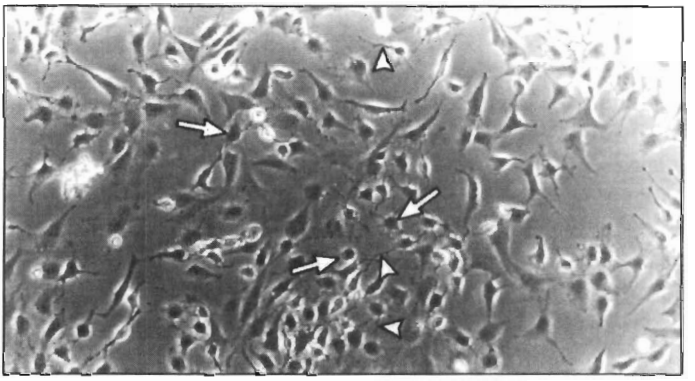

C

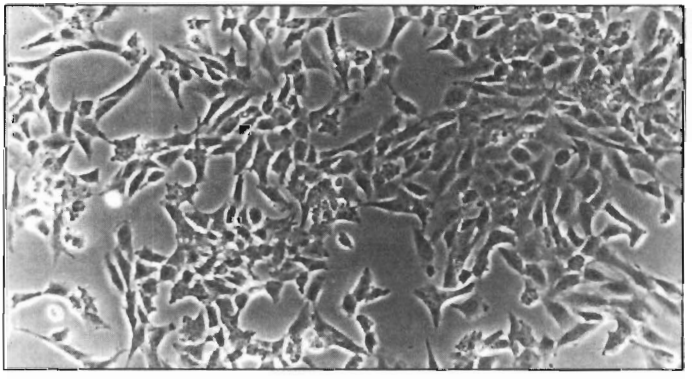

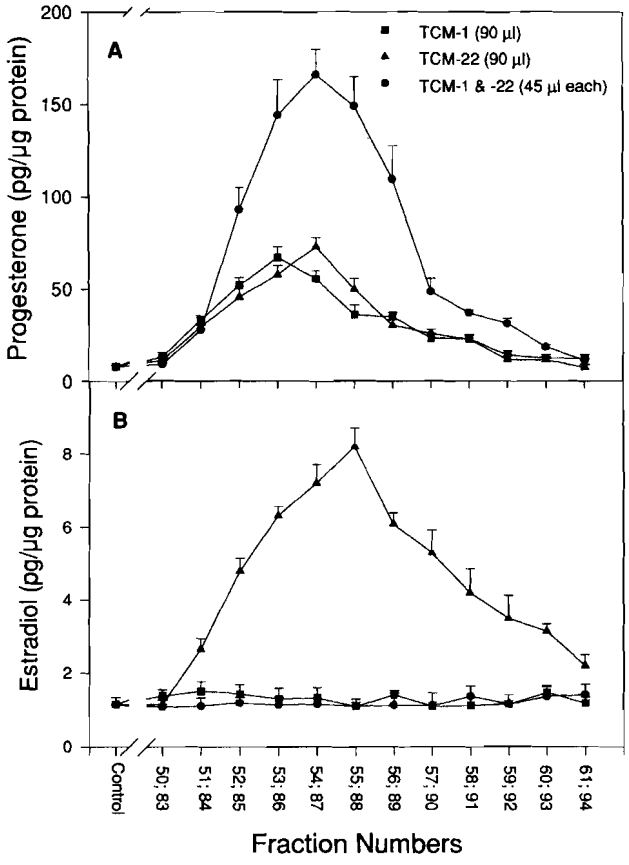

Figure 5 Effect of TCM-1 and TCM-22 alone or in combination on steroidogenesis from RGC. Gel filtration fractions containing 90 µl TCM-1 (fraction 83–94; triangles) and TCM-22 (fraction 50–61; squares) were tested individually or 45 µl of successive fractions from each activity region were combined (i.e., no. 50 with no. 83, no. 51 with no. 84, etc.; circles) and tested for their combined effects on P_4 (A) and E_2 (B) secretion from RGC. In this experiment, control represents the granulosa cell that were treated with culture medium containing PBS/0.5 M NaCl. The steroids were measured by RIA in culture medium and expressed as the mean ± SD of picogram quantity of the steroids per microgram of cell protein in single-culture well (n = 3). (Modified from Ref. 29.)

4). The morphological changes that were induced by either FSH or TCM-1 started approximately 15 min after treatment and were most prominent by 1 h post treatment. The cells started gaining their normal appearance by 12 h and returned to normal by 48 h post treatment.

C. Interaction Among TCM-1, TCM-22, and FSH in Stimulating Steroidogenesis in RGC

To gain a better understanding of the actions of TCM-1 and TCM-22, the combined actions of these two activity regions were tested on P_4 and E_2 production from RGC. In this experiment, granulosa cells were treated with 90 μl of each factor alone or 45 μl of 12 successive TCM-1 fractions (83–94) that were combined with 45 μl of 12 successive TCM-22 fractions (50–61). In combination, TCM-1 and TCM-22 caused significantly more P_4 production than that caused by each factor alone, suggesting a synergistic interaction between the two factors [29] (Fig. 5). However, for E_2 production the stimulatory action of TCM-1 was completely antagonized by TCM-22. Only TCM-1 was stimulatory, whereas TCM-22 alone had no effect on E_2 production. Collectively, these results suggested that these two factors may be unrelated and have a different mechanism of action. In addition, the lack of stimulation by TCM-22 on E_2 production and its antagonistic action on E_2 stimulated by TCM-1 partially explains why unfractionated TCM had relatively minor action on basal E_2 production as compared to its highly significant action on P_4 secretion (4-fold versus 80-fold stimulation) [28].

To assess the interactions between TCM-1 or TCM-22 and FSH, dose–response curves were generated for TCM-1 and TCM-22 in the presence or absence of 100 ng/ml FSH. Both TCM-1 and TCM-22 stimulated basal and FSH-induced P_4 secretion in a dose-dependent manner. While TCM-1 stimulated basal and FSH-induced E_2 secretion, TCM-22 inhibited FSH-induced E_2 secretion and had no effect on basal E_2 [29] (Fig. 6).

V. STUDIES WITH REVERSED-PHASE HPLC–PURIFIED TCM-1 AND TCM-22

To further purify TCM-1 and TCM-22, reversed-phase HPLC was performed on a Hitachi (San Jose, CA, USA) HPLC system using a Microsorb-MV C_8 column (0.46 × 25 cm, 5 μm particle size; Rainin Instrument Co., Inc., Woburn, MA, USA) that was equilibrated with either 0% or 10% (v/v) acetonitrile, both containing 0.1% (v/v) trifluoroacetic acid (TFA) [29]. The eluate from the gel filtration column was divided into two pools comprising fractions 51–59 for TCM-22 or fractions 85–93 for TCM-1. For each HPLC analysis, the samples were

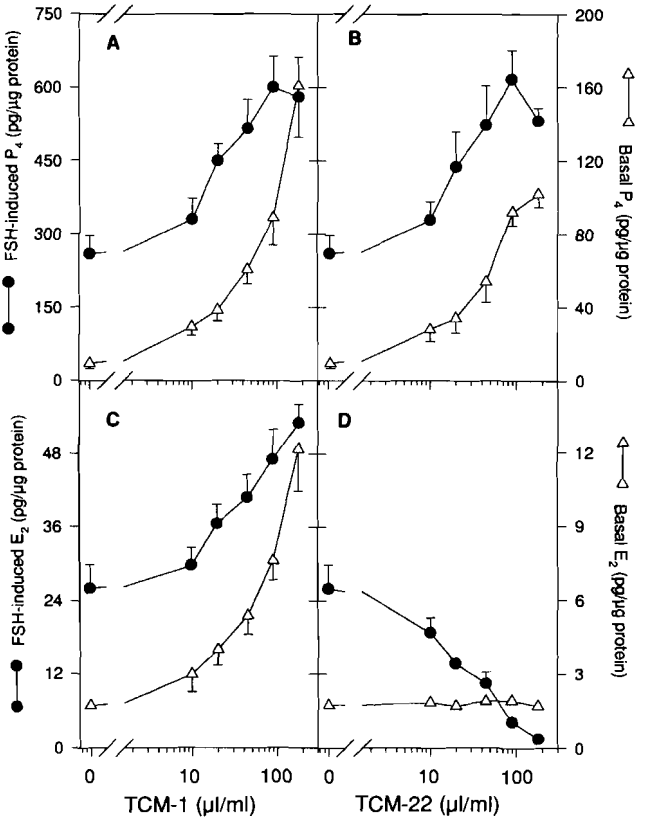

Figure 6 Effect of TCM-1 or TCM-22 on basal and FSH-induced P_4 (upper panels) and E_2 (lower panels) production by RGC. The granulosa cells were cultured with different amounts of TCM-1 (A and C) or TCM-22 (B and D) in the absence (△) or presence (●) of 100 ng/ml FSH. After 48 h of treatment, the steroid concentrations in the medium were determined by RIA. Data points represent mean ± SD of the mean picogram quantity of the steroids per microgram of cell protein from triplicate culture wells (n = 3). (Modified from Ref. 29.)

adjusted so as to contain 0.1% TFA and the same acetonitrile concentration as the equilibration buffer.

For TCM-22, conditions for the elution of column-bound proteins were 10% acetonitrile from 0 to 10 min after sample injection, 10–20% acetonitrile from 10 to 40 min, 20–85% acetonitrile from 40 to 125 min, 85–95% acetonitrile from 125 to 126 min, and 95% acetonitrile from 126 to 135 min. Acetonitrile concentrations for HPLC of TCM-1 were 0% from 0 to 50 min after

sample injection, 0–90% from 50 to 120 min, and 90% from 120 to 130 min. The flow rate was 1 ml/min throughout, and the chromatogram (A_{214}) was archived as previously described [31]. The column eluate was collected into tubes containing 50 µl 0.125/0.25 N NaOH to immediately neutralize the TFA. For TCM-1, fractions of 500 µl were collected 50 min after sample injection and 10-µl aliquots were tested for their stimulation of steroidogenesis or morphological changes in cultured RGC. For TCM-22, fractions of 1 ml were collected immediately after sample injection, and 10 µl was tested for stimulation of P_4 and E_2 secretion from RGC. The remaining portion of the fractions was stored at −80°C until further analyzed for peptide sequence of TCM-1 or re-HPLC of the TCM-22.

A. Effect of Reversed-Phase HPLC–Purified TCM-1 on RGC

TCM-1 activity (i.e., stimulation of P_4, E_2, 20α-OH-P_4, and aromatase activity, and morphological changes) was eluted from the C8 column with a retention time of 92–93 min in fractions 85–87 [29]. The peak HPLC fraction (no. 86) stimulated P_4 and E_2 production about 59- and 31-fold, respectively [29] (Fig. 7). The remaining fractions did not significantly affect steroidogenesis or morphology of the RGC.

B. Effect of Reversed-Phase HPLC–Purified TCM-22 on RGC

TCM-22 activity was eluted from the C8 column as two peaks of activity that had a retention time of 55–56 min (fractions 55–56) and of 58–59 min (fractions 58–59). Peak fractions 55 and 59 stimulated P_4 secretion approximately three- to fourfold over the control and had no effect on E_2 (Fig. 8). The remaining fractions did not significantly stimulate steroidogenesis by RGC. In view of major contaminating proteins in the activity regions, the peak fractions were subjected to a second round of reversed-phase HPLC under identical conditions to those described above. Unfortunately, it was not possible to further to purify the TCM-22 samples and therefore their complete isolation was not possible (data not shown). In the future, alternative chromatographic strategies will be required for further purification and identification of TCM-22.

C. Peptide Sequence Analysis of TCM-1

Since elution of TCM-1 activity from the C8 column was correlated with an A_{214}-absorbing entity the peak fraction was concentrated using a Speed-Vac concentrator (Savant Instruments, Farmingdale, NY) and submitted for N-terminal amino acid sequencing. However, three separate attempts at N-terminal sequenc-

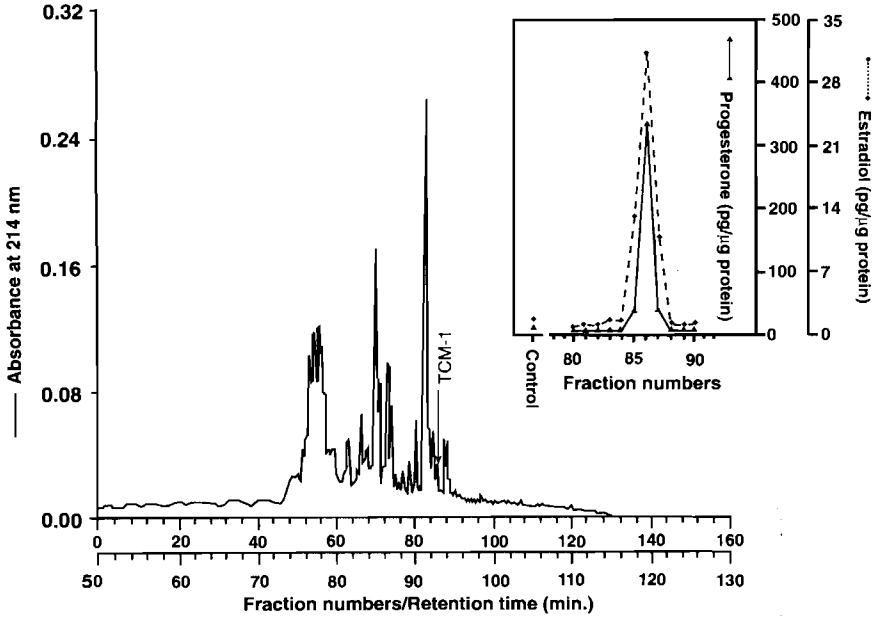

Figure 7 Effect of reversed-phase HPLC-purified TCM-1 on P_4 and E_2 production from RGC. Gel filtration fractions 85–93 from 13 runs were pooled and subjected to C8 reversed-phase HPLC. The eluate was collected into 0.5-ml fractions 50 min after injection of sample. The figure shows the absorbance (214 nm) of the eluate collected between 50 and 115 min after sample injection and the effect of fraction 80–90 on P_4 (▲) and E_2 (◆) production from cultured RGC as determined by RIA (inset). A 10-µl aliquot was tested from fraction 46–133. In this experiment, the control group is the granulosa cells that were treated with culture medium with no addition of HPLC fraction. Data points presented in the steroidogenic activity curves are picogram quantity of the steroids per microgram of cell protein in a single-culture well. The experiment was repeated for three times with similar results. The arrow indicates the peak that contains TCM-1 activity. (Modified from Ref. 29.)

ing of HPLC-purified TCM-1 failed to produce a readable sequence, suggesting either that insufficient peptide was analyzed or that it was N-terminally blocked. In the future, alternative strategies such as enzymatic or chemical cleavage to produce peptide fragments will be required for the successful identification of TCM-1.

VI. CONCLUSIONS

Here we have described the characterization and partial purification of steroidogenic factors in TCM. It has been long recognized that the thymus has an influ-

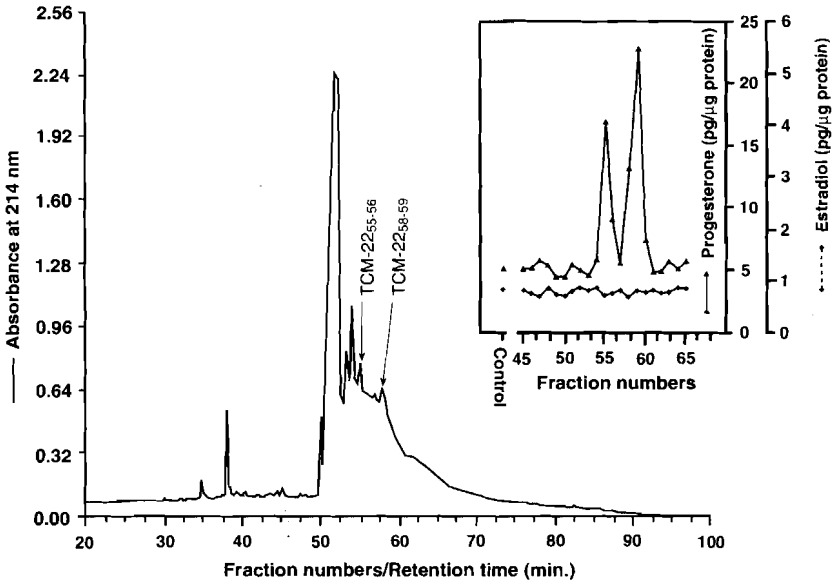

Figure 8 Effect of reversed-phase HPLC-purified TCM-22 on P_4 and E_2 production from RGC. Gel filtration fraction 51–59 from three runs were pooled and subjected to C8 reversed-phase HPLC. The eluate was collected into 1.0-ml fractions starting with the injection of sample. The figure shows the absorbance (214 nm) of the eluate collected between 20 and 100 min after sample injection and the effect of fraction 45–65 on P_4 (▲) and E_2 (◆) production from cultured RGC as determined by RIA (inset). A 10-μl aliquot was tested from fraction 1–90. In this experiment the control group is the granulosa cells that were treated culture medium with no addition of HPLC fractions. Data points presented in the steroidogenic activity curves are picogram quantity of the steroids per microgram of cell protein in duplicate culture wells. The arrows indicate the peaks that contain TCM-22 activity.

ence on the ovaries. When we started our work, the available information suggested that this influence may be through the *autoimmune* and *endocrine mechanisms* described in the Introduction. However, our data and those of others have highlighted the possibility of a direct influence of the thymus on the ovary through thymic factors. Aguilera and Romano [22] reported the presence of a 28-kDa factor in thymic reticuloepithelial cell–or thymus-conditioned media that inhibited hCG-induced P_4 and E_2 production from rat ovarian cell but had no effect on P_4 and E_2 production in the absence of hCG. Interestingly, the same laboratory has recently reported that rat thymus contains a heparin-binding factor that modulates steroidogenesis in the rat testis [32]. Ledwitz-Rigby and Scheid [23,33] reported that thymulin, a nanopeptide produced by the thymus gland,

could enhance gonadotropin-induced P_4 secretion from cultured porcine granulosa cells. It has been shown that thymulin enhanced both FSH- and LH-stimulated P_4 secretion over 2–4 days of incubation, even though basal secretion was not altered and suggested that thymulin could play an important role in granulosa cell maturation. A variety of additional data have also accumulated showing a direct influence of previously characterized thymic factors on ovarian function in mammals. For example: (1) A higher number of germ cells were observed in fetal ovaries cultured in medium supplemented with thymulin or cocultured with fragments of fetal thymus as compared to the control ovaries [34]. A similar effect of thymus fragments and thymulin has recently been observed on fetal rat testes [35,36]. (2) TF-5 was shown to be stimulatory on basal but inhibitory on FSH-induced P_4 and E_2 secretion in RGC [37]. However, it is noteworthy that we failed to show any effect of 5–250 g/ml thymulin and or thymosin α_1 on basal steroidogenesis by RGC in vitro [27]. (3) It was demonstrated that the thymus gland modulates ovarian responsiveness to gonadotropin in vivo [38], and thymulin was shown to be the mediator for the modulatory action [39]. (4) Prothymosin-α mRNA, thymosin-β_4 and β_{10} mRNA, and protein are detected in rat ovaries [40–42]. In addition, gonadotropins and prostaglandin $F_{2\alpha}$ modulated the differential expression of thymosin-β4 and β10 in rat ovary [41,42]. Collectively, these reports support the hypothesis that known "thymic" factors, produced either in the thymus gland itself or locally in the ovary, are capable of affecting ovarian function in mammals. Based on our studies and studies of others mentioned above, we now suggest that thymus directly influences ovarian function through a variety of thymus-derived signaling molecules. Further studies to establish the identity of factors such as TCM-1 and TCM-22 will likely give further impetus to this newly emerging field of reproductive biology.

ACKNOWLEDGMENTS

The studies described from our laboratory in this chapter were supported in part by NIH grant DK 45916, and NATO Scientific Training Program/Scientific and Technical Research Council of Turkey

REFERENCES

1. Chapman JC, Michael SD. Hormonal and immunologic interactions between thymus and ovary. In: Grossman CJ, ed. Endocrinology and Metabolism. Bilateral Communication Between the Endocrine and Immune Systems. New York: Springer-Verlag, 1994:12–35.
2. Nishizuka Y, Sakakura T. Thymus and reproduction: sex-linked dysgenesia of the gonad after neonatal thymectomy in mice. Science 1969;166:753–755.

3. Besedovsky HO, Sorkin E. Thymus involvement in female sexual maturation. Nature 1974;249:357–359.
4. Michael SD, Taguchi O, Nishizuka Y. Effect of neonatal thymectomy on ovarian development and plasma LH, FSH, GH and PRL in the mouse. Biol Reprod 1980; 22:343–350.
5. Lintern-Moore S. Effect of athymia on the initiation of follicular growth in the rat ovary. Biol Reprod 1977; 17:155–161.
6. Hattori M, Brandon MR. Thymus and the endocrine system: ovarian dysgenesis in neonatally thymectomized rats. J Endocrinol 1979;83:101–111.
7. Healy DL, Bacher J, Hodgen GD. Thymic regulation of primate fetal ovarian-adrenal differentiation. Biol Reprod 1985;32:1127–1133.
8. Nishizuka Y, Sakakura T, Tsujimura T, Matsumoto K. Steroid biosynthesis in vitro by dysgenetic ovaries induced by neonatal thymectomy in mice. Endocrinology 1973;93:786–792.
9. Michael SD, Taguchi O, Nishizuka Y, McClure JE, Goldstein AL, Barkley MS. The effect of neonatal thymectomy on early follicular loss and circulating levels of corticosterone, progesterone, estradiol, and thymosin α_1. In: Schwartz NB, Hunzicker-Dunn M, eds. Dynamics of Ovarian Function. New York: Raven Press, 1981: 279–284.
10. Hoek A, Schoemaker J, Drexhage HA. Premature ovarian failure and ovarian autoimmunity. Endocr Rev 1997;18:107–134.
11. Taguchi O, Nishizuka Y, Sakakura T, Kojima A. Autoimmune oophoritis in thymectomized mice: detection of circulating antibodies against oocytes. Clin Exp Immunol 1980;40:450–453.
12. Miyake T, Taguchi O, Ikeda H, Sato Y, Takeuchi S, Nishizuka Y. Acute oocyte loss in experimental autoimmune oophoritis as a possible model of premature ovarian failure. Am J Obstet Gynecol 1988;158:186–192.
13. Tung KS, Smith S, Teuscher C, Cook C, Anderson RE. Murine autoimmune oophoritis, epididymo-orchitis, and gastritis induced by day 3 thymectomy. Am J Pathol 1987;126:293–302.
14. Sakaguchi S, Takahashi T, Nishizuka Y. Study on the cellular events in postthymectomy autoimmune oophoritis in mice. I. Requirement of Lyt-1 effector cells for oocytes damage after adoptive transfer. J Exp Med 1982;156:1565–1576.
15. Sakaguchi S, Takahashi T, Nishizuka Y. Study on the cellular events in postthymectomy autoimmune oophoritis in mice. II. Requirement of Lyt-1 in normal female mice for the prevention of oophoritis. J Exp Med 1982;156:1577–1586.
16. Kosiewicz MM, Michael SD. Neonatal thymectomy affects follicle populations before the onset of autoimmune oophoritis in B6A mice. J Reprod Immunol 1990;88: 427–440.
17. Rebar RW, Morandini IC, Erickson GF, Petze JE. Hormonal basis of reproductive defects in athymic mice: diminished gonadotropin concentrations in prepubertal females. Endocrinology 1981;108:120–126.
18. Rebar RW, Morandini IC, Silva de Sa MF, Erickson GF, Petze JE. The importance of the thymus gland for normal reproductive function in mice. In: Schwartz NB, Hunzicker-Dunn M, eds. Dynamics of Ovarian Function. New York: Raven Press, 1981:285–290.

19. Rebar RW, Morandini IC, Benirschke K, Petze JE. Reduced gonadotropin in athymic mice: prevention by thymic transplantation. Endocrinology 1980;107:2130–2132.
20. Rebar RW, Miyake A, Low TLK, Goldstein AL. Thymosin stimulates secretion of luteinizing hormone–releasing factor. Science 1981;214:669–671.
21. Terranova PF, Rice VM. Review: cytokine involvement in ovarian processes. Am J Reprod Immunol 1997;37:50–63.
22. Aguilera G, Romano MC. Influence of the thymus on steroidogenesis by rat ovarian cells in vitro. J Endocrinol 1989;123:367–373.
23. Ledwitz-Rigby F, Schneid PG. Serum thymic factor enhances porcine granulosa cell responsiveness to gonadotropins in vitro. The Eighth Ovarian Workshop on Regulatory Processes and Gene Expression in the Ovary. Maryville, Tennessee, USA, July 12–14, 1990.
24. Lewis VM, Twomey JJ, Bealmear P, Goldstein G, Good RA. Age, thymic involution, and circulating thymic hormone activity. J Clin Endocrinol Metab 1978;47: 145–150.
25. Dardenne M, Savino W, Gagnerault M-C, Itoh T, Bach J-F. Neuroendocrine control of thymic hormonal production. I. Prolactin stimulates in vivo and in vitro the production of thymulin by human and murine thymic epithelial cells. Endocrinology 1989;125:3–12.
26. Uzumcu M, Lin YC. Factor(s) from thymic cell culture medium conditioned medium (TCM) stimulate(s) progesterone (P) secretion in cultured rat granulosa cells (abstr). Biol Reprod 1990;42 (Suppl 1):163.
27. Uzumcu M, Akira S, Lin YC. Stimulatory effect of thymic factor(s) on steroidogenesis in cultured rat granulosa cells. Life Sci 1992;51:1217–1228.
28. Uzumcu M, Lin YC. Characterization of the stimulatory actions of thymic factor(s) on basal and gonadotropin-induced steroidogenesis in cultured rat granulosa cells. Mol Cell Endocrinol 1994;105:209–216.
29. Uzumcu M, Brigstock DR, Lin YC. Partial purification and characterization of two non-FSH steroid-modulating factors in rat thymic epithelial cell-conditioned medium (TCM). Dom Anim Endocrinol 1998;15:155–168.
30. Soto EA, Kliman HJ, Strauss JF III, Paavola LG. Gonadotropins and cyclic adenosine 3′,5′-monophosphate (cAMP) alter the morphology of cultures human granulosa cells. Biol Reprod 1986;34:559–569.
31. Bray W, Brigstock DR. Raw integrator data storage and retrieval using data acquisition software. Amer Lab 1994;26:38.
32. Porras MG, Reyes J, Romano MC. The rat thymus contains a heparin-binding factor that modulates steridogenesis in the testis. Acta Physiol Pharmacol Ther Latin Am 1996;46:286–293.
33. Ledwitz-Rigby F, Schneid PG. Serum thymic factor enhances porcine granulosa cell responsiveness to gonadotropins in vitro. In: Gibori G, ed. Signaling Mechanisms and Gene Expression in the Ovary. New York: Springer-Verlag, 1991:473–478.
34. Prepin J. Thymus and thymulin increase the proliferation of oogonia in fetal rat ovary in vitro. C R Acad Sci Paris Ser. III 1991;313:407–411.
35. Prepin J. Fetal thymus and thymulin stimulate in vitro gonocytes in fetal testis in rats. C R Acad Sci Paris Ser. III 1993;316:451–454.
36. Prepin J, Le Vigouroux P. Inhibition by TGF-beta 1 of the in vitro thymulin-stimu-

lated proliferation of gonocytes from fetal rat testes. Reprod Fertil Dev 1997;37: 203–206.

37. Gorospe WC, Fong Y-Y, Spangelo BL. Thymosin fraction-5 modulates steroidogenesis and interleukin-6 release by rat granulosa cells in vitro. Endocr J 1993;1:35–39.
38. Rosas P, Hinjosa L, Garcia L. Evidence for the participation of the thymus on the regulation of ovarian development in the prepubertal mouse (abstr). Biol Reprod 1995;52 (Suppl 1):130.
39. Hinojosa L, Rosa P. Effects of the serum thymic factor (FTS) on the gonaodropin-induced ovulation in normal and hypothymic mice (abstr). Biol Reprod 1996;54 (Suppl 1):85.
40. Oikawa M, Dargan C, Ny T, Hsueh AJW. Expression of gonadotropin-releasing hormone and prothymosin-α messenger ribonucleic acid in the ovary. Endocrinology 1990;127:2350–2356.
41. Hall AK, Aten RI, Behrman HR. Differential modulation of thymosin genes in the immature rat ovary by gonadotropins. Mol Cell Endocrinol 1991;79:37–43.
42. Hall AK, Aten RI, Behrman HR. Thymosin gene expression is modulated by pregnant mare's serum gonadotropin, human chorionic gonadotropin, and prostaglandin $F_{2\alpha}$ in the immature rat ovary. Endocrinology 1991;128:951–957.

6

Determination of Affinity Constants of Lectins for Sugars by Affinity Capillary Electrophoresis

Kiyohito Shimura and Ken-ichi Kasai
Teikyo University, Sagamiko, Kanagawa, Japan

I. INTRODUCTION

A variety of life processes are dependent on the specific biological recognition of macromolecules. Modern separation techniques, such as chromatography [1], electrophoresis [2–4], and centrifugation [5], are widely used for the analysis of specific affinities of biological molecules including proteins, nucleic acids, and sugars. These applications are based on the change in the physicochemical properties of interacting molecules as the result of complex formation. The complex may have properties that are different from those of their component molecules with respect to molecular weight, electrical charge, or hydrodynamic properties, thus permitting its separation from the component molecules.

The recently developed microscale separation technique, capillary electrophoresis (CE), has many favorable features that are useful in the analysis of molecular recognition as well as the separation of biological macromolecules [6]. The scale of the separation space in CE is almost one-thousandth of the other separation techniques and the amount of sample required for analysis is quite small: at the nanogram level for proteins with ultraviolet (UV) absorption detection. The temperature of the separation medium can be precisely controlled and molecular interaction can be observed without any insoluble support or gel, which might affect the interaction involved. The application of CE in the analysis of biospecific interactions has been referred to as affinity CE [6–9].

For the estimation of affinity constants, two formats of affinity CE are appli-

cable. Equilibrium mixture analysis, which is suitable for a system that shows slow dissociation kinetics, measures the concentration of the free species in equilibrium mixtures at different concentrations by zone electrophoresis. This allows a binding isotherm to be determined and, thus, an estimation of the affinity constant. Mobility change analysis, which is applicable to a system that shows rapid dissociation kinetics, measures the mobility change of a zone of one component in a solution of the other under a rapid binding equilibrium. The amount of the mobility change can be correlated to the mole fraction of the bound species and also leads to determination of the affinity constant. This latter format of affinity CE is very useful as a microscale technique for the determination of affinity constants for systems with relatively weak affinity, e.g., for systems with a dissociation constant larger than the micromolar level.

The principle of the determination of affinity constants by mobility change analysis has been established through the application of affinity electrophoresis in gel slabs or rods [2,3]. This type of analysis has several advantages. First, it is not necessary to determine precisely the concentration of an interacting component applied as a zone. Considering the difficulty in the determination of precise concentration of small quantities of a protein sample, this feature is particularly valuable. Second, the sample that is applied as a zone need not necessarily be pure, so long as the peak of the component can be traced. This represents a big advantage, especially in cases where the protein is unstable and is prone to denaturation. The simultaneous determination of the affinity constants of a group of molecules sharing the same binding specificities is also possible, provided all components can be separated. Third, the amount of an interacting component applied as a zone can be very small.

In this chapter, we will describe the principle and applications of mobility change analysis with two examples of the analysis of lectin–sugar interactions by affinophoresis and affinity probe capillary electrophoresis (APCE). Before we move to the body of this chapter, it would be useful to briefly review the basics of CE.

II. CAPILLARY ELECTROPHORESIS

CE uses a narrow electrophoresis channel (usually from 10 to 100 μm in inner diameter) that enables the swift dissipation of heat and the application of a high field strength. This shortens the time required for separation, reduces the longitudinal diffusion of analytes, and raises the efficiency of separation. The narrow channel also minimizes convection, allowing electrophoresis in free solution. The quantity of a sample required for analysis becomes significantly smaller as the size of the separation space is reduced. Analytes are detected and quantified by

means of an on-line UV or fluorescence detector. On the other hand, the ratio of the inner surface area to the volume of the inner space where separation takes place is very large and this emphasizes the need for strict control of the adsorption of analytes on the wall.

The basic setup of free solution CE is as follows. Fused silica capillaries coated with polyimide on their outer surface are commonly employed. The coating provides mechanical strength to the capillary that otherwise easily breaks. A small segment of the polyimide coating is removed and the migrating analytes in the capillary are optically detected through the silica wall. The capillary is cooled by a temperature-controlled coolant. The capillary is filled with an electrophoresis buffer and its ends are immersed in the buffer in electrode vessels that are connected to an electrical power supply that can generate an electrical potential up to 30 kV.

The surface of fused silica is negatively charged at neutral pH range due to the ionization of silanol groups. This negatively charged surface is compatible with the separation of neutral and anionic molecules. Separation of cationic molecules, however, might be compromised by ionic adsorption to the surface. The electrophoretic migration of the counterions for these immobile charges on the inner surface produces water flow toward the negative electrode. This flow, called electroosmotic flow (EOF), is characterized by a constant velocity irrespective of the lateral position inside the capillary in contrast to a pressure-driven flow, in which the velocity is highest at the center. EOF can be very large in CE and often larger than the electrophoretic mobility of the analytes. Even small anions can be transferred to the negative end by the overwhelming electroosmosis over their electrophoretic migration. Neutral molecules are transferred to the detection point solely by the influence of EOF and are detected earlier than anionic species migrating toward the positive end (Fig. 1).

An important consequence of the presence of EOF is that the detection time (t) of a particular analyte is a function of its electrophoretic mobility (μ_{ep}), and the electroosmotic mobility (μ_{eo}) of the capillary as well.

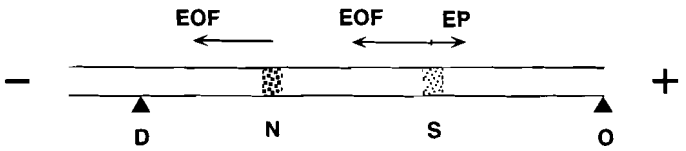

Figure 1 Zonal electrophoresis in a capillary with a negatively charged inner surface. EOF, electroosmotic flow; EP, electrophoretic migration. Negatively charged ions (S) are detected after neutral molecules (N) in the presence of a high electroosmotic flow. D, detector; O, electrophoresis origin.

$$t = \frac{L}{E} \frac{1}{(\mu_{ep} + \mu_{eo})} \tag{1}$$

where L (cm) is the distance between the injection end and the detection point, and E (V cm^{-1}) represents the field strength. The polarity of the mobility is defined as negative for movement toward the positive electrode. Thus, in the case of the negatively charged ion (S) in Fig. 1, μ_{ep} is negative and μ_{eo} is positive. Note that μ_{ep} (cm^2 V^{-1} s^{-1}), a value of fundamental importance in the mobility change analysis, is inversely related to the experimentally measurable value, t. Coelectrophoresis of a neutral marker molecule allows the determination of μ_{eo} in the capillary and, therefore, μ_{ep} of charged substances using Eq. (1). This point will be discussed further in Section III.

The EOF of a bare silica capillary is not very stable and is greatly affected by the adsorption of ions, especially proteins. Experimentally, a sudden decrease in EOF was also experienced for unknown reasons. We used fused silica capillaries coated with succinylpolylysine in experiments described in this chapter. Such capillaries show very stable EOF.

III. EQUATIONS FOR MOBILITY CHANGE ANALYSIS

When a charged particle is placed in an electric field, movement of the particle is induced and reaches a steady state where the electric force is just balanced by the frictional drag, i.e., $qE = kv$, where q is the number of charges on the particle migrating at a steady-state velocity of v under a field of E with a translational frictional constant k. The velocity under unit field is designated as the electrophoretic mobility, μ, with the relation $\mu = q/k$.

When two molecules, A and B, having different electrophoretic mobility (μ_A and μ_B, respectively) form a complex, AB, it could have a mobility (μ_{AB}) different from those of either of the component molecules.

$$\begin{array}{ccc} A + B & \rightleftarrows & AB \\ \mu_A \quad \mu_B & & \mu_{AB} \end{array} \tag{2}$$

The mobility of the complex is usually intermediate between those of its components. In the case of protein–ligand interactions, the charge on the ligand is a major source of the mobility change of the protein.

When electrophoresis of A is carried out in a solution of B, the microscopic electrophoretic mobility of A should discontinuously change between μ_A and μ_{AB} at the moments of dissociation and association with B. As a result, the observed macroscopic mobility of A, μ, should be an average of the two mobilities weighted for the time fractions in which it migrates as the free molecule and as

the complex with B. Using α_{AB} as the time fraction for the complex AB, μ is given by Eq. (3):

$$\mu = (1 - \alpha_{AB})\,\mu_A + \alpha_{AB}\mu_{AB} \tag{3}$$

Equation (3) can be rewritten as $\Delta\mu = \Delta\mu_{max}\alpha_{AB}$, where $\Delta\mu = \mu - \mu_A$ is the macroscopic mobility change of A in the presence of B, and $\Delta\mu_{max} = \mu_{AB} - \mu_A$ is the maximum mobility change of A in the presence of B at infinite concentration or, in other words, the mobility difference between free A and the complex AB. Since α_{AB} is the mole fraction as $\alpha_{AB} = [AB]/([A] + [AB])$, it is related to the equilibrium dissociation constant, $K_d = ([A][B])/[AB]$, by the relation, $\alpha_{AB} = [B]/(K_d + [B])$, and the following equation can be derived [2,3].

$$\Delta\mu = \Delta\mu_{max}\frac{[B]}{K_d + [B]} \tag{4}$$

This relation is identical to Langmuir's adsorption isotherm. The two parameters of affinity electrophoresis, K_d and $\Delta\mu_{max}$, can be determined by using a nonlinear regression analysis by fitting them to measured $\Delta\mu$ values at different concentrations of B. Its analogy to the Henry-Michaelis-Menten equation for enzyme kinetics allows the use of several forms of linearized plots for the determination of the two parameters. The plot of $\Delta\mu$ against $\Delta\mu/[B]$ according to Eq. (5), which is identical to the Woolf-Hofstee plot in enzyme kinetics, should generally be appropriate. The slope of the line gives the negative value of the dissociation constant and the intercept with the $\Delta\mu$ axis gives the $\Delta\mu_{max}$ [10].

$$\Delta\mu = \Delta\mu_{max} - K_d\frac{\Delta\mu}{[B]} \tag{5}$$

Inhibition experiments in the affinity electrophoresis system with neutral ligands allow the determination of the affinity constants for the neutral ligands [2]. Such competition experiments will be the main focus in the examples described below.

In CE, the directly measurable value related to the electrophoretic mobility is the detection time of peaks. Since the electrophoretic mobility is inversely related to detection time [Eq. (1)], the mobility change ($\Delta\mu$) must be calculated by use of the following relation.

$$\Delta\mu = \frac{L}{E}\left[\left(\frac{1}{t} - \frac{1}{t_r}\right) - \left(\frac{1}{t_0} - \frac{1}{t_r'}\right)\right] \tag{6}$$

where t and t_0 are the detection time of component A in the presence and the absence of B, respectively, and t_r and t_r' are the detection time of an electrophoresis marker in the presence and the absence of B, respectively. The prime symbol is attached to show the possible variation of electroosmosis between two runs. The marker should not interact with B and need not necessarily be electrically

neutral. Fluctuations in electroosmosis are canceled out by this equation and the net mobility change of A caused by the interaction with B can be calculated.

IV. ANALYSIS OF PEA LECTIN–SUGAR INTERACTIONS BY AFFINOPHORESIS

When A is a protein and B is a charged ligand, the protein–ligand interaction can be analyzed by mobility change analysis. The ligand, however, might not be

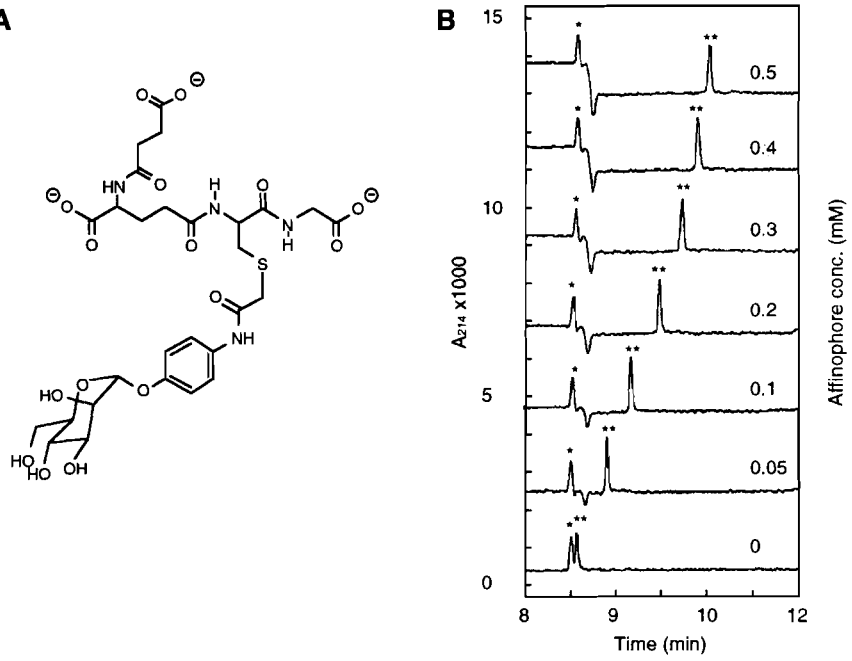

Figure 2 Capillary affinophoresis of pea lectin using a monoliganded affinophore bearing mannoside. (A) The structure of the monoliganded affinophore bearing α-D-mannoside as an affinity ligand on a matrix of succinylated glutathione. (B) Affinophoresis of pea lectin with different concentrations of mannoside affinophore. A sample solution (0.7 nl) containing pea lectin (★★, 0.2 mg/ml) and cytidine (★, 0.2 mM, as an electrophoresis marker) was injected by means of pressure at the positive end of a capillary (25 μm i.d., 375 μm o.d., 57 cm long, internally coated with succinylpolylysine) filled with a solution of the affinophore at the concentrations shown on the right. Electrophoresis was carried out at a field strength of 350 V cm^{-1} (7 μA) at 25°C, with detection in terms of A_{214} at 50 cm from the injection end. Tris-acetate buffer (pH 7.9) was used throughout the system. (From Ref. 10.)

able to produce a sufficient mobility change of the protein for analysis. We have introduced the use of charged soluble polymers, such as succinylpolylysine, as mobile matrices for affinity electrophoresis. We call the charged matrix bearing ligands the "affinophore" and electrophoresis in its presence "affinophoresis" [3,4]. The distinctive feature of affinophores is that the portion responsible for specific binding and that for migration in an electric field are structurally separated, i.e., an affinity ligand and a charged affinophore matrix. Therefore, once a suitable ionic molecule is obtained as an affinophore matrix, the method is applicable to many binding molecules by changing the affinity ligand.

The principle of affinophoresis was successfully applied to the mobility change analysis of lectin–sugar interactions. For the determination of affinity constants of pea lectin, a divalent sugar-binding protein, the use of a monoliganded affinophore is straightforward. The polyliganded affinophores, used in the previous applications, should interact with such a divalent protein in a more complicated manner [11]. N-Succinylated glutathione was used as an anionic matrix for a monoliganded affinophore [10]. The affinity ligand *p*-aminophenyl α-D-mannoside was iodoacetylated at its amino group and coupled to the thiol of the matrix (Fig. 2A). The intermediates and the affinophore were easily purified by using reversed-phase HPLC. The affinophore caused a mobility change of pea lectin in a concentration-dependent manner (Fig. 2B). Pea lectin barely migrated under the present electrophoresis conditions. The interaction with the negatively

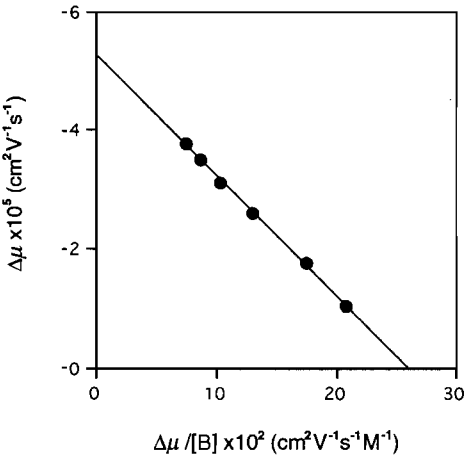

Figure 3 A linear plot for the affinophoresis of pea lectin. The plot was made using the data in Fig. 2B according to Eq. [5]. The slope is the negative value of K_d (0.199 mM) and the intercept with the ordinate gives $\Delta\mu_{max}$ (-5.35×10^{-5} cm^2 V^{-1} s^{-1}). (From Ref. 10.)

charged affinophore increased its mobility toward the positive end, thus lengthening its detection time. The result of the affinophoresis was analyzed according to Eq. (5) based on several assumptions, i.e., equivalency and independency of the two binding sites of the dimeric lectin, and the same mobility change for the successive binding of the two affinophores (Fig. 3). The determination of the two parameters, $K_d = 0.199$ mM and $\Delta\mu_{max} = -5.35 \times 10^{-5}$ cm^2 V^{-1} s^{-1}, for the interaction between the lectin and the affinophore served the basis for the determination of the affinity constants of the lectin to neutral sugars by competition experiments, using affinophoresis. It should be noted that K_d represents the reaction of each binding site, i.e., a microscopic equilibrium constant.

A neutral sugar to be investigated was added only in the positive electrode buffer and the affinophore only in the capillary. Since the neutral sugar does not migrate electrophoretically, it is transferred to the negative end only by EOF faster than the lectin under the affinophoresis conditions, where the lectin migrates electrophoretically toward the positive end. With the affinophore (B) at a

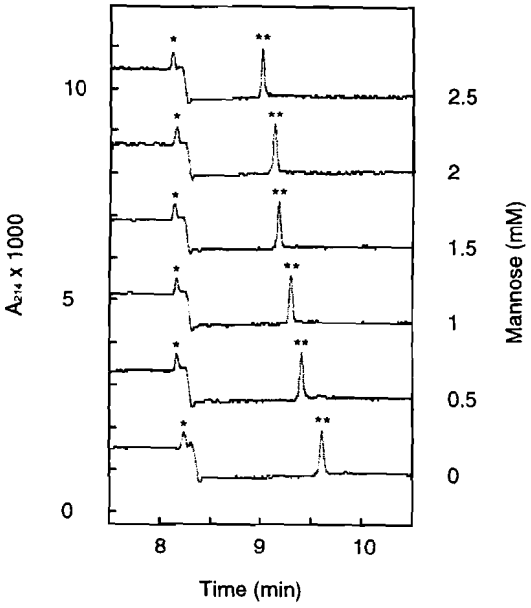

Figure 4 Competition experiment of the affinophoresis by mannose. Affinophoresis of pea lectin was carried out with the affinophore at a concentration of 0.5 mM in the presence of mannose at various concentrations, as shown on the right. Mannose was added only in the positive electrode buffer (100 μl). Other conditions were the same as in the experiments in Fig. 2. ★★, pea lectin; ★, cytidine. (From Ref. 10.)

constant concentration, the macroscopic mobility change ($\Delta\mu_i$) of the lectin became smaller as the concentration of the neutral sugar (I) increased (Fig. 4). The competition analysis is basically the same as that in enzyme kinetics. It can be considered that the K_d value in Eq. (4) increased by a factor of $1 + [I]/K_i$ than that without I in an identical relation to Eq. (4), i.e.,

$$\Delta\mu_i = \Delta\mu_{max} \frac{[B]}{K_{d\,app} + [B]} \tag{7}$$

The $K_{d\,app}$, an apparent dissociation constant, is in a relation with the K_d as $K_{d\,app} = K_d(1 + [I]/K_i)$, where K_i is the dissociation constant of pea lectin for I. Since $\Delta\mu_{max}$ has already been previously obtained, $K_{d\,app}$ can be determined by the measurement of $\Delta\mu_i$ according to Eq. (7). The plot of $K_{d\,app}/K_d$ versus [I] gave lines with a slope of $1/K_i$ (Fig. 5). The K_i values obtained by this method

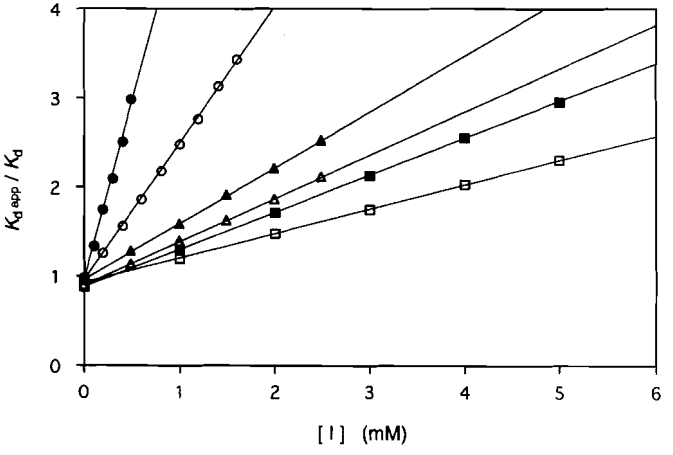

Figure 5 Determination of the dissociation constants of pea lectin for neutral sugars (I) through competition experiments in the affinophoresis. The affinophoresis of the lectin was carried out as described for Fig. 2 except for the addition of various concentrations of neutral sugars to the positive electrode buffer (100 µl). Apparent K_d values ($K_{d\,app}$) were determined from the observed mobility change ($\Delta\mu_i$), the concentration of the affinophore used ([B]), and the $\Delta\mu_{max}$ value using Eq. [7]. The results are plotted according to $K_{d\,app}/K_d = [I]/K_i + 1$.●, p-aminophenyl α-D-mannoside (0.25 mM); ○, methyl α-D-mannoside (0.65 mM); ▲, D-mannose (1.6 mM); △, maltose (2.1 mM); ■, methyl α-D-glucoside (2.4 mM); □, D-glucose (3.6 mM), where the K_i values determined are given in parentheses. (From Ref. 10.)

agreed well with those obtained by calorimetry. For example, K_i for methyl α-D-mannoside was found to be 0.65 mM and was reported to be 0.61 mM by calorimetric measurement. For D-mannose, it was found to be 1.6 mM and was reported to be 1.3 mM, calorimetrically.

V. ANALYSIS OF CONCANAVALIN A–SUGAR INTERACTIONS BY AFFINITY PROBE CAPILLARY ELECTROPHORESIS

In affinophoresis, we directed our attention to the mobility change of a protein. Instead, that of a ligand produced by the interaction with a protein can also be analyzed. A larger mobility change can be expected for a ligand than a protein during their interaction, and this approach should thus be useful when the mobility change of a protein can be barely observed or is negligible. Using a fluorescence-labeled affinity ligand (Fig. 6A), which is called an affinity probe, the affinity constants for concanavalin A (Con A) for monosaccharides were determined by competition experiments [12]. For the preparation of the affinity probe, an identical approach was taken to that for the monoliganded affinophore. The amino group of glutathione was labeled with a fluorescent dye instead of succinylation in the case of the affinophore. Glutathione (oxidized form) was labeled with Lissamine rhodamine B sulfonyl chloride at its amino group and the disulfide was cleaved by dithiothreitol after purification. The affinity ligand, *p*-aminophenyl α-D-mannoside, was iodoacetylated and coupled to the free thiol of the dye-labeled glutathione. The affinity probe having two net negative charges was subjected to electrophoresis along with a hydrolysis product of the reactive dye, a sulfonic acid derivative having one net negative charge, which served as an electrophoresis marker.

The mobility of the affinity probe was originally larger than the marker and was detected later, but its electrophoretic mobility was reduced by interaction with Con A and the order of the two peaks was inverted (Fig. 6B). The analysis using Eq. (5) allowed the determination of the two parameters for the affinity probe–Con A interaction as $K_d = 15.5\ \mu M$ and $\Delta\mu_{max} = 1.20 \times 10^{-4}\ cm^2\ V^{-1}\ s^{-1}$. Once these two parameters are determined, the interaction between Con A and neutral sugars (I) can be analyzed by competitive experiments of APCE. When a neutral sugar having affinity for Con A is added to the Con A solution, the concentration of the free binding site of Con A ([B] in Eq. (4)) will decrease and the suppression of the electrophoresis of the affinity probe is released. Since the values of K_d and $\Delta\mu_{max}$ have already been obtained, [Con A] in the mixture can be calculated by measuring $\Delta\mu$ of the affinity probe. The determination of [Con A] in the mixture allows the calculation of [Con A-I] and [I], since the total concentration of Con A and I is known. The dissociation constant for the

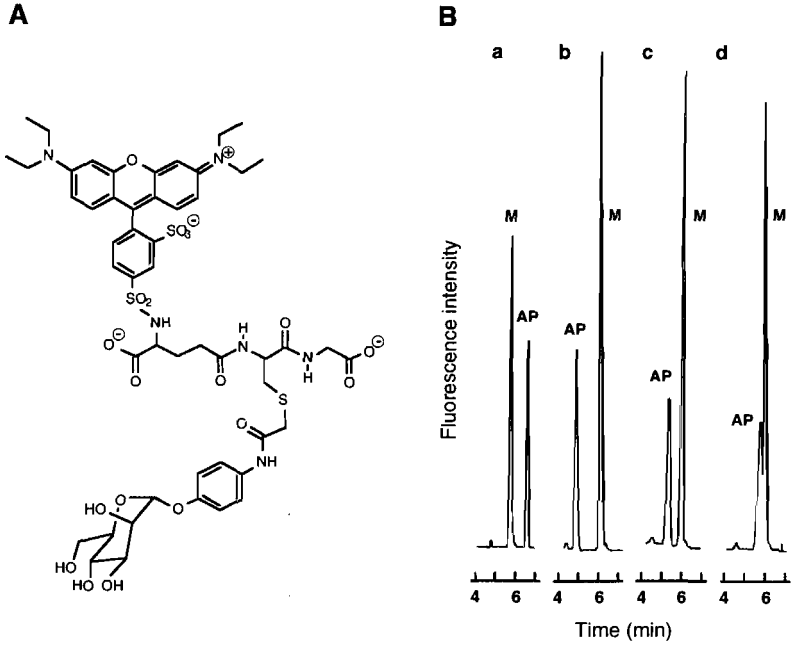

Figure 6 Determination of the dissociation constants of Con A for neutral sugars by affinity probe capillary electrophoresis. (A) The structure of the affinity probe bearing two net negative charges. (B) Affinity probe capillary electrophoresis in the presence of Con A and methyl α-D-mannoside. A mixture (2 nl) of the affinity probe and the electrophoresis marker (10^{-8} M each) was injected at the positive end of the capillary (succinylpolylysine-coated fused silica, 50 μm i.d., 375 μm o.d., 30 cm long) filled with 0.1 M Tris-acetic acid buffer (pH 7.9). Con A and neutral sugars were dissolved in the buffer, introduced into an open-ended polypropylene tube (0.5 mm i.d., 4.7 cm long, 10 μl volume) and placed between the positive end of the capillary and the positive electrode buffer as a bridge. Electrophoresis was carried out at a field strength of 150 V cm^{-1} (10 μA) at 25°C, and the fluorescence (590 nm) was detected 10 cm from the injection end by excitation with a He-Ne laser (543.5 nm, 1 mW). Concentration of Con A: a, 0 μM; b-d, 21 μM. Concentration of methyl mannoside: a and b, 0 μM; c, 120 μM; and d, 300 μM. AP, affinity probe; M, electrophoresis marker. (From Ref. 12.)

Con A–neutral sugar complex, K_i = ([Con A][I])/[Con A-I], can be calculated (Fig. 7). Note the difference in the manner of competition between the two experiments. In the affinophoresis, a neutral sugar binds to molecule A applied as a zone; however, in the case of APCE, it binds to molecule B added in the electrophoresis buffer.

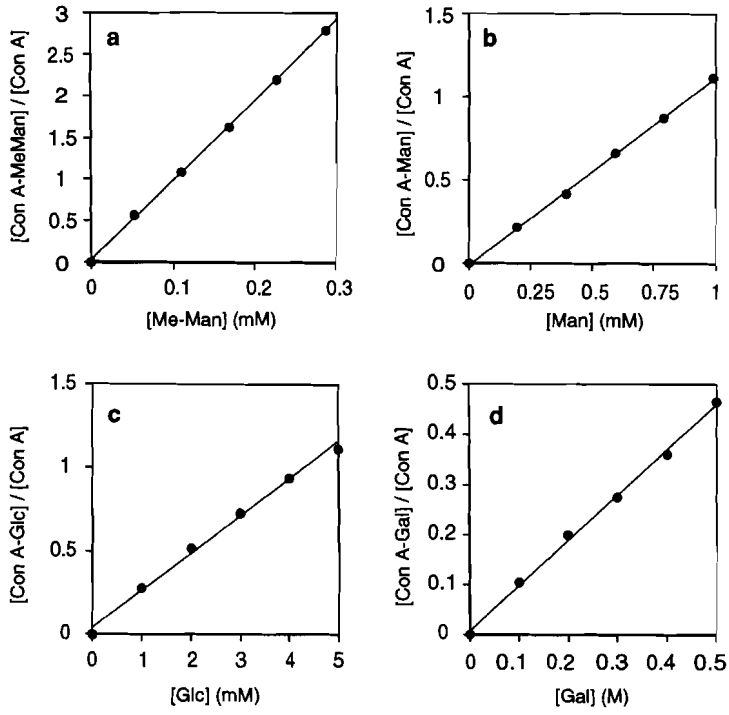

Figure 7 Plots for the determination of the dissociation constants of Con A for neutral sugars (I). Prior to the analysis of neutral sugar-Con A interaction, the affinity probe-Con A interaction was characterized by analysis according to Eq. [5] and K_d and $\Delta\mu_{max}$ were determined to be 15.5 μM and 1.20×10^{-4} cm^2 V^{-1} s^{-1}. When a neutral sugar was added to the Con A solution, the mobility change of the affinity probe was reduced, as the result of the reduction in the number of the free binding sites of Con A available for the interaction with the affinity probe, as shown for methyl mannoside in Fig. 6B. From the reduced mobility change, the equilibrium concentration of free binding site of Con A ([Con A], corresponding to [B] in Eq. [4]) in a mixture with the neutral sugar (I) was calculated according to Eq. [4] using the K_d and $\Delta\mu_{max}$ values determined previously. The determination of [Con A] allowed the calculation of [Con A-I] and [I], since the total concentrations of Con A and I are known. The plot of [Con A-I]/[Con A] vs. [I] gave lines with slopes of $1/K_i$, where $K_i = ([\text{Con A}] \times [\text{I}])/[\text{Con A-I}]$. The plots and the determined values of K_i's are: (a) methyl α-D-mannoside (0.104 mM); (b) D-mannose (0.89 mM); (c) D-glucose (4.5 mM); and (d) D-galactose (1.1 M). (From Ref. 12.)

VI. EXPERIMENTAL SETTINGS

A typical experimental setup for affinophoresis of a protein with a negatively charged affinophore (B) having higher mobility than protein (A) is as follows [10]: Fused silica capillaries coated with succinylpolylysine [12] are filled with a buffer solution containing the affinophore. The same buffer solution is used in the electrode vessels, but without the ligand. A solution of a binding protein is pressure-injected as a small segment at the positive end of the capillary. When an electrical field is applied, the protein is transferred to the negative end by the overwhelming electroosmotic flow of the capillary and the relatively slow electrophoretic migration of the protein. Soon after the initiation of electrophoresis, the protein is surrounded by the affinophore due to its lower electrophoretic mobility toward the positive electrode, as compared to the affinophore. After a transitional period, corresponding to the time required to establish a binding equilibrium in the protein zone, the protein begins to migrate at a higher electrophoretic mobility toward the positive electrode than that observed in the absence of B and its detection time increases. Note that the concentration of the free affinophore in the protein zone has become identical to that in the solution originally used to fill the capillary at this time, since the protein zone is continuously exposed to the unused portion of the affinophore solution due to the mobility differences between the protein zone and the affinophore. The mobility change is calculated from the detection time for the protein and the marker in the presence and absence of the affinophore by Eq. (6), and the results of a set of experiments over a range of concentration of the affinophore can be plotted according to Eq. (5). The plot gives the K_d value and the $\Delta\mu_{max}$.

The range of the concentration of the affinophore should be chosen so that it overlaps with the value of the dissociation constant to be measured and should be sufficiently wide for precise determination of the constant. A protein concentration of 0.1–0.5 μg/μl would be sufficient to measure the detection time of the protein by monitoring the absorption at 214 nm. The volume of the protein sample applied for each run is less than several nanoliters and thus the amount of the protein actually consumed for each run is quite small. The amount of protein injected in the capillary has no effect on the result unless it exceeds that of the affinophore. Since the protein sample does not contain the affinophore, a short time is required before the injected plug of a protein solution is equilibrated with the affinophore and reaches a steady-state velocity as described above. This transitional period will be longer when the affinophore concentration is lower relative to that of the protein solution. This effect is observed as an increasing deviation of $\Delta\mu$ versus $\Delta\mu/[B]$ plot according to Eq. (5) in the lower concentration range of the affinophore and this can be improved by reducing an amount of the protein sample. Regarding the reproducibility of the determination of the K_d values by this technique, the relative standard deviation was about 10% (n = 5)

with a manually operated instrument [12] and 6% (n= 5) with a fully automated instrument [10].

VII. PROSPECTS

Analysis of the interactions of biological macromolecules by electrophoresis has a long history and such applications have been collectively referred to as affinity electrophoresis [2]. Capillary electrophoresis, due to its versatility, shows great promise for a variety of applications of this type. The basic experimental equipment and theory for this technique has been elaborated, thus promising considerable progress for this type of application. In addition, the miniaturized separation space in capillary closely matches the size of cells, i.e., the elementary units of life. The microchannel, constructed in a planar chip [13], will further reinforce the trend of miniaturization of electrophoresis initiated by the use of capillary. The efficiency of the analysis of molecular recognition by affinity electrophoresis suggests that this technique will be of increasing importance in the future.

REFERENCES

1. Kasai K. Trypsin and affinity chromatography. J Chromatogr 1992;597:3–18.
2. Takeo K. Advances in affinity electrophoresis. J Chromatogr 1995;698:89–105.
3. Shimura K. Progress in affinophoresis. J Chromatogr 1990;510:251–270.
4. Shimura K, Kasai K. Affinophoresis: selective electrophoretic separation of proteins by using a specific carrier. In: Karger BL, Hancock WS eds. High Resolution Separation and Analysis of Biological Macromolecules. Part B, Methods Enzymol Vol. 271. New York: Academic Press, 1996:203–218.
5. Shire SJ. Analytical ultracentrifugation and its use in biotechnology. In: Schuster TM, Laue TM eds. Modern Analytical Ultracentrifugation. Boston: Birkhauser, 1994:261–297.
6. Shimura K, Kasai K. Affinity capillary electrophoresis: a sensitive tool for the study of molecular interactions and its use in microscale analyses. Anal Biochem 1997; 251:1–16.
7. Chu Y-H, Avila ZL, Gao J, Whitesides GM. Affinity capillary electrophoresis. Acc Chem Res 1995;28:461–468.
8. Pritchett T, Evangelista RA, Chen F-TA. Capillary electrophoresis-based immunoassays. Bio/technology 1995;13:1449–1450.
9. Heegaard NHH. Characterization of biomolecules by electrophoretic analysis of reversible interactions. Appl Theor Electrophor 1994;4:43–63.
10. Shimura K, Kasai K. Determination of the affinity constants of pea lectin for neutral sugars by capillary affinophoresis with a monoligand affinophore. J Biochem 1996; 120:1146–1152.

11. Shimura K, Kasai K. Capillary affinophoresis of pea lectin with polyliganded affinophores: A model study of divalent-polyvalent interactions. Electrophoresis 1998; 19:397–402.
12. Shimura K, Kasai K. Determination of the affinity constants of concanavalin A for monosaccharides by fluorescence affinity probe capillary electrophoresis. Anal Biochem 1995;227:186–194.
13. Harrison DJ, Fluri K, Seiler K, Fan Z, Effenhauser CS, Manz A. Micromachining a miniaturized capillary electrophoresis-based chemical analysis system on a chip. Science 1993;261:895–897.

7

Displacement Chromatography of Biomolecules

Ruth Freitag
ETH Lausanne, Lausanne, Switzerland

I. INTRODUCTION

Chromatography is based on subtle differences in substance distribution between a fluid, usually mobile, and a solid, usually stationary, phase. Few laboratories in the life sciences do not depend on this extremely versatile, high-resolution separation technique, albeit mostly for analytical purposes. However, the recent growth of the biopharmaceutical and biotechnical industry has also increased the pressure to enrich and isolate a host of compounds from complex mixtures and hence rekindled the interest in chromatography as a preparative rather than an analytical tool. Given the particular needs of the bioindustries, the importance of preparative chromatography is expected to grow in the foreseeable future.

Once before, in the 1940s and 1950s, chromatography was the only available option to separate closely related compounds such as rare earth oxides and hydrocarbons from crude oil on an industrial basis within the technical means of those days. Soon, however, the expensive chromatography was replaced by unit operations such as distillation, extraction, fractionation, etc. A similar development seems unlikely in the case of biopolymers, which are often incompatible with these traditional separation procedures. However, in spite of the obvious advantages, chromatographic operations are still somewhat awkward to implement at the industrial scale. Questions of scalability, continuous operation (rather than the traditional batch approach), and costs obviously need to be addressed. In order to keep up with the growing demands, existent procedures will have to be improved and new and more convenient variants to be developed.

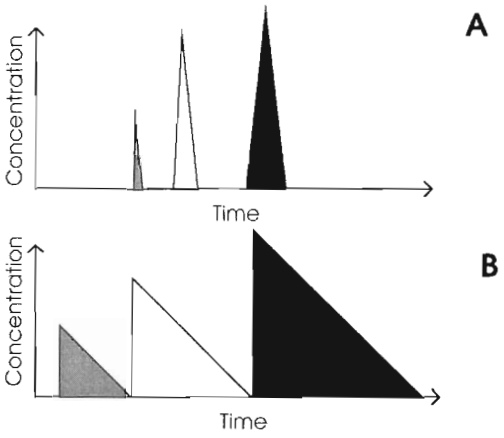

Figure 1 Separation of a multicomponent mixture by linear elution (A) and overloaded elution (B) chromatography.

Preparative chromatographic methods are often directly scaled-up versions of the methods used at the laboratory scale. Thus, the (overloaded) elution mode predominates, and separations as illustrated in Fig. 1 are the goal. The substances are resolved into individual peaks, which are kept apart by substance-free mobile phase volumes. Using this approach, chromatographic units capable of producing tons of material per year have been built. A further increase in scale within a reasonable financial and technical framework seems at present unlikely, hence the growing interest in truly large-scale systems such as simulated moving beds.

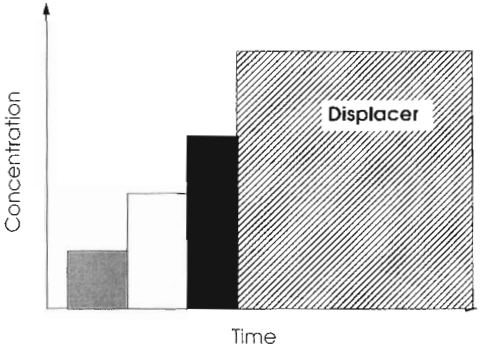

Figure 2 Separation of a multicomponent mixture by displacement chromatography.

In the meantime, the question of what constitutes the most versatile approach to biotechnical downstream processing in the kilogram to ton range awaits its final answer. Especially at larger scale displacement chromatography, a method whereby the components are resolved into consecutive zones of the pure and highly concentrated substances (Fig. 2), may become a serious competitor to overloaded elution chromatography in the establishment of high-resolution, efficient biopolymer isolation schemes.

II. DISPLACEMENT CHROMATOGRAPHY

Displacement chromatography was first recognized as an individual chromatographic mode besides elution and frontal chromatography by Tiselius [1]. To illustrate the basic principle of displacement chromatography it is useful to first imagine a substance A distributed at equilibrium in a two-phase system consisting of a solid adsorbent and a second fluid phase. Under these conditions, a dynamic equilibrium establishes itself and the relative amounts of bound and free A are determined by the corresponding equilibrium isotherm. The equilibrium isotherm can be linear or nonlinear; a nonlinear isotherm can in turn be favorable or unfavorable (Fig. 3). A host of models have been developed to describe the complex isotherm forms encountered for realistic systems. By necessity we will restrict ourselves at this point to the most basic patterns.

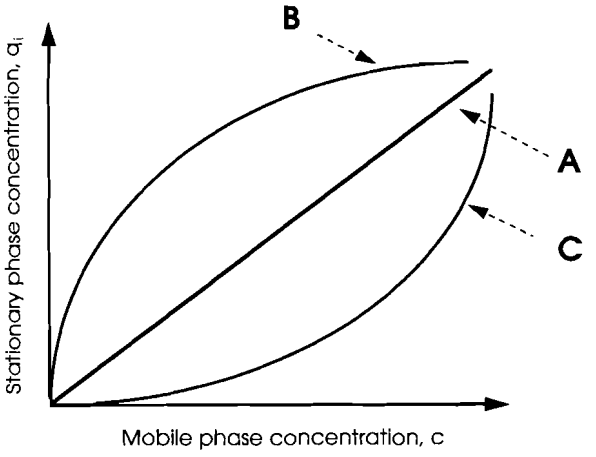

Figure 3 Cases of equilibrium isotherms: (A) linear isotherm, (B) favorable nonlinear isotherm, (C) unfavorable nonlinear isotherm.

When the isotherm is linear, the bound amount is directly proportional to the concentration adjusted for the fluid phase. When the concentration in the fluid phase is increased, the number of adsorbed molecules increases linearly. Should a second substance B be present in the fluid phase, also characterized by a linear equilibrium isotherm, the interaction of the two substances with the solid phase can be considered independently. Not so in case of a nonlinear isotherm. When the isotherm is favorable, the increase in the amount bound decreases with increasing fluid phase concentration, up to a point where it becomes independent of the fluid phase concentration. The adsorbent surface has been saturated and the isotherm runs in parallel with the x axis of the isotherm plot (strongly nonlinear conditions). The opposite behavior is observed in the case of an unfavorable isotherm. However, since displacement chromatography requires favorable isotherms of some kind, we will restrict ourselves to the case of favorable isotherms.

Under nonlinear conditions, the adsorption of a substance A can no longer be considered independently of the concentration of an also present substance B. When both substances are at equilibrium with the two phases, a direct competition for the binding sites ensues and less A will be bound than predicted by the favorable single-component equilibrium isotherm. The equilibrium isotherm of substance A has been suppressed by substance B under nonlinear conditions. In displacement chromatography, the enforced competition for the solid phase binding sites drives the separation. The first step of a conventional, or batch, displacement separation is the adsorption of the substance mixture on the column (Fig. 4). It is sometimes suggested that conditions more favorable to binding in displacement than in elution chromatography be used, although this is not really necessary and may even be disadvantageous. A considerable portion of the stationary phase capacity can and must be exploited during loading, since displacement chromatography is only possible under nonlinear conditions (for definitions, see Appendix). While the feed is introduced, some separation occurs already, due to a frontal chromatographic effect.

In the second phase of the experiment, the actual separation, a solution containing a so-called displacer, is pumped through the column. By definition the displacer should bind more strongly to the solid phase than any of the relevant feed components and therefore be able to compete successfully for the binding sites with all of them. As the displacer front advances, the number of binding sites available to the sample compounds decreases and the more strongly bound substances begin to push the less strongly bound ones ahead. Ideally, all sample components are finally focused into consecutive zones of the pure substances lined up according to increasing adsorption energy. Following the breakthrough of the displacer front, the column needs to be regenerated and conditioned for further use.

The displacement mode was used repeatedly in the early preparative chromatographic separation, and biomolecules, such as amino acids, were among the

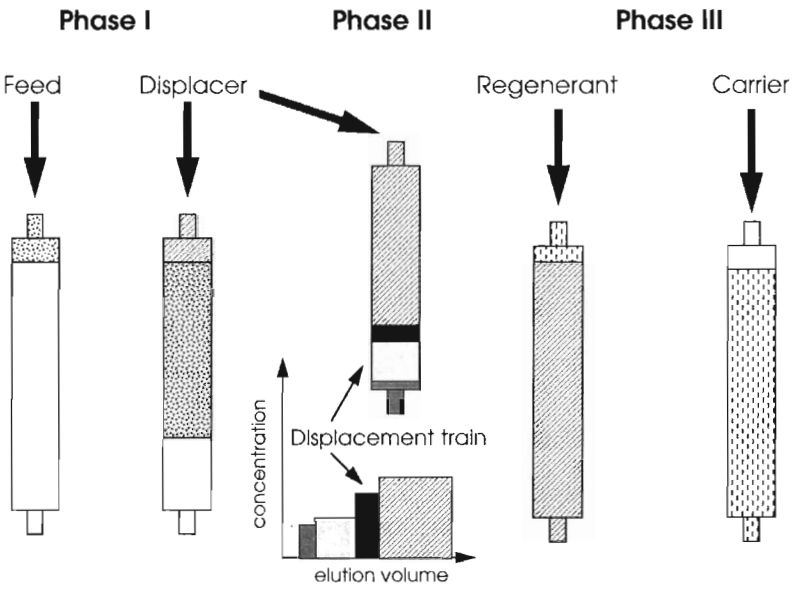

Figure 4 Displacement chromatography.

first applications (for an excellent review of the earlier applications of displacement chromatography, see Ref. 2). The success of the earlier separations was limited, however, since the resolving power in the displacement mode is just as much dependent on column efficiency as in the elution mode. Only in the 1980s, when highly efficient high performance liquid chromatography (HPLC) columns and computers had become ubiquitous and the mathematical tools for dealing with the problems of nonlinear chromatography had been considerably improved, was the displacement mode rediscovered and applied to biomolecules, thanks largely to the dedicated work of Csaba Horvath and his coworkers at Yale.

Mathematically the process can be described by the mass balance together with the appropriate initial and boundary conditions. The mass balance, the initial condition, and the exit boundary condition apply to the chromatographic situation in general.

Mass balance:

$$\partial c_i/\partial t + \phi\partial q_i/\partial t + u_0\partial c_i/\partial z = D\partial^2 c_i/\partial z^2 \qquad i = 1, 2, \ldots, n \tag{1}$$

where c_i is mobile phase concentration: q_i is stationary phase concentration; ϕ is the phase ratio; u_0 is the linear flow velocity; D is the diffusion coefficient: t is time; and z is dimensionless column length.

Initial condition:

$$c_i(0, z) = 0 \qquad 0 \leq z \leq L \qquad i = 1, 2, \ldots, n \tag{2}$$

Exit boundary condition:

$$(\partial c_i/\partial z)_{z=L} = 0 \qquad L = \text{column length} \tag{3}$$

In case of displacement chromatography the inlet boundary condition is given by:

$$c_i(t, 0) = c_{0,i} \qquad 0 < t \leq \tau, \quad i = 1, 2, \ldots, n-1 \quad \text{(Sample)} \tag{4a}$$

and

$$c_n(t, 0) = c_{0,n} \qquad H(t - \tau) \qquad \text{(Displacer)} \tag{4b}$$

where τ is duration of feed introduction and H(t) is step function.

Since in nonlinear chromatography the adsorption behavior of all components is coupled, another equation is needed to create this link. Usually the change of q_i with time is linked to the mobile phase concentration, c_i, of all other compounds by a suitable equation such as the multicomponent Langmuir isotherm equation:

$$q_i = \frac{ac_i}{1 + \sum b_j c_j} \tag{5}$$

with a and b as substance-specific constants that can be calculated from the single-component Langmuir isotherms.

This approach is often a good approximation, since many experimentally recorded isotherms can be fitted to the Langmuir equation. However, the multicomponent Langmuir isotherm model is less useful in biopolymer chromatography for reasons given in Section III.

The effective use of the stationary and mobile phase capacity is among the most obvious advantages of displacement over elution chromatography in preparative separations. Contrary to affinity chromatography, several substances can be purified simultaneously, which is clearly an advantage whenever the feed contains more than one substance of value. Another major advantage of displacement chromatography, especially in the context of large-scale biopolymer chromatography, stems from the fact that the feed, the displacer, and the regenerant are introduced as simple step functions. Displacement chromatography is therefore much easier to operate in a continuous manner than overloaded gradient elution chromatography. For example, de Carli et al. succeeded in operating a continuous annular chromatograph in the displacement mode [3].

III. THEORY OF DISPLACEMENT CHROMATOGRAPHY

During a chromatographic separation various processes take place in and out of the column besides (hopefully) the actual separation (Fig. 5). All of them influence the eventual result to some extent. There may be:

1. Extracolumn band broadening effects (mixing in valves, detector flow cells, laminar/turbulent flow in tubings, etc.)
2. Nonideal flow in the column (axial dispersion)
3. External and internal mass transfer resistance (film and pore diffusion effects)
4. Slow reaction kinetics of the adsorption/desorption reaction
5. Secondary equilibria (chemical reactions in the fluid or solid phase, denaturing, etc.)

The modeling of chromatographic separations is more difficult for nonlinear than for linear conditions, due to the fact that the behavior of the various sample components can no longer be considered independently in this case. The first detailed analysis of nonlinear multicomponent systems was given by Glückauf [4]. Subsequently, more general treatments were offered by Helfferich and Klein [5] as well as Rhee et al. [6]. All of these earlier approaches as well as many current ones assume that chromatography is a predominantly thermodynamically controlled sorption phenomenon, whereas all other (kinetic) effects play a secondary, modifying role. According to this viewpoint, valuable information can be gained from an ideal model. More accurate predictions become possible by considering some of the above-mentioned band broadening effects; however, this is feasible only at the price of increased complexity.

In biopolymer chromatography the kinetics of mass transfer and surface reaction can rarely be neglected completely. These effects can, for example, be incorporated into the model by the introduction of a dispersion coefficient (axial dispersion) and/or pore and overall column efficiency parameters (pore and film diffusion) into the mass balance equation [7,8]. The resulting numerical algorithms have promoted an understanding of nonlinear chromatography to a considerable extent [9,10]. They allow one to take (qualitatively) into account prior to the design of a preparative separation parameters such as column dimensions, particle diameter and porosity, mobile phase flow rate, composition and concentration of the feed (and in our case also of the concentration and heterogeneity of the displacer). Given below is an introduction to the modeling of displacement chromatography with increasing degrees of complexity.

A. The Ideal Model of Displacement Chromatography

The ideal model of chromatography assumes a separation exclusively controlled by the sorption equilibrium thermodynamics. The two phases are constantly at

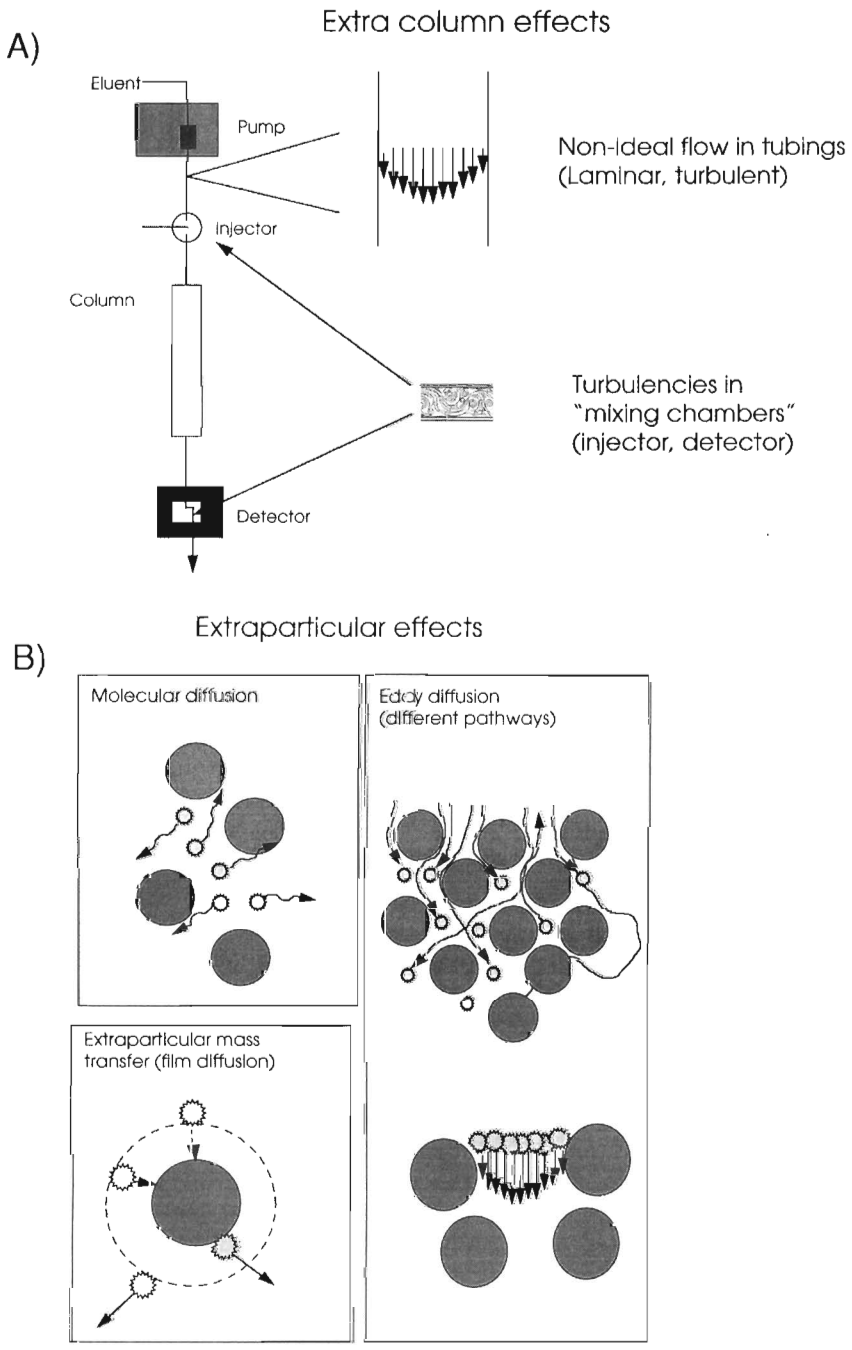

Figure 5 Sources of dispersion in chromatography.

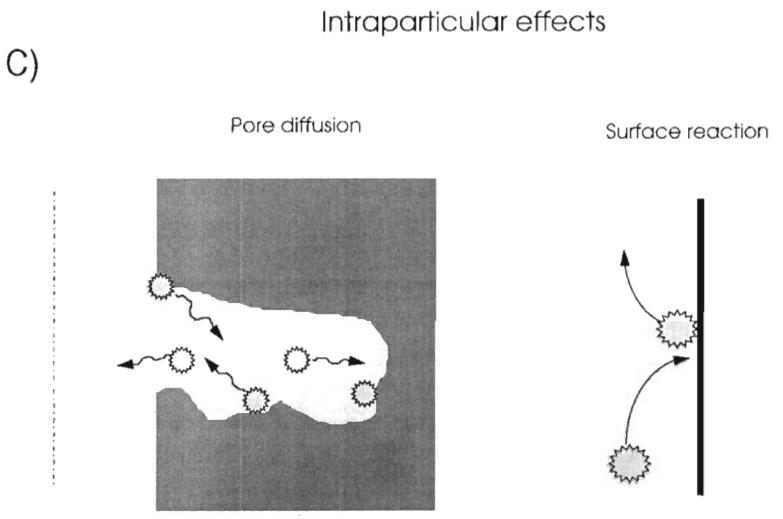

Figure 5 Continued.

equilibrium; there is no axial dispersion; the column efficiency (plate number) is indefinite. As a consequence, the mass balance [Eq. (1)] simplifies to:

$$\partial c_i/\partial t + \phi\partial q_i/\partial t + u_0\partial c_i/\partial z = 0 \qquad i = 1, 2, \ldots, n \qquad (1b)$$

The ideal model has a long tradition going back to Glückauf and Tiselius in the theoretical description of displacement effects. In spite of its acknowledged limitations, it describes correctly the most important aspects of displacement chromatography and the influence of parameters like the sample and displacer concentration on a given separation. This is especially the case under highly nonlinear conditions and for small molecules.

As outlined above, the goal of a displacement experiment is the separation of the feed components into consecutive zones of the pure substances, i.e., establishment of the so-called isotachic state or displacement train. For this to happen it is necessary that the component isotherms be favorable (convex upward). Most authors assume Langmuir-type isotherm shapes with good results. According to the ideal model, under these conditions the displacement train will always evolve after a certain column length.

Under favorable isotherm conditions the front of a substance zone is self-sharpening until, in the absence of modifying dispersive effects, a triangular "peak" is formed, where the concentration jumps suddenly to the maximum value (shock transition) (Fig. 6). This can be observed in overloaded elution chromatography for substances with favorable isotherms. In displacement chromatog-

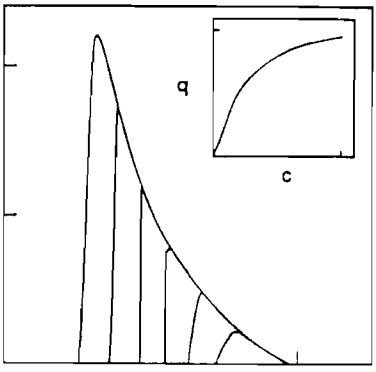

Figure 6 Change in the shape of a given substance's zone under increasingly overloaded conditions in the case of a favorable isotherm.

raphy, the rear boundary of each zone will also be sharpened, since the normally diffuse rear end will be pushed up by the sharp front of the next zone. Every molecule that lags behind will immediately be displaced. The opposite is true for a molecule that for some reason finds itself ahead of its own bulk zone. It will be among molecules with a lesser stationary phase affinity than itself and most likely will be retained until overtaken by its own zone.

Once the displacement train has been established, all substance zones move at the speed of the displacer front, u_D. According to the material balance argument of DeVault [11], the velocity of the latter is given by:

$$u_D = \frac{u_0}{1 + \phi(\Delta q_D/\Delta c_D)} \tag{6a}$$

or

$$u_D = \frac{u_0}{1 + \phi(q_D/c_D)} \tag{6b}$$

Since all zones move at the same speed as the displacer front,

$$u_1 = u_2 = u_3 = \cdots = u_D \tag{7}$$

Equation (6b) applies also to the various compounds, i.e., the ratio q/c for each compound must be equal to q_D/c_D. An operating line with steepness q_D/c_D can be drawn to determine the concentration in the individual zones (Fig. 7).

The exact concentration within a given zone of the displacement train can be calculated by equaling Eq. (6b) for the displacer and the compound and resolving for the compound's concentration. A "water-shed" point can be determined

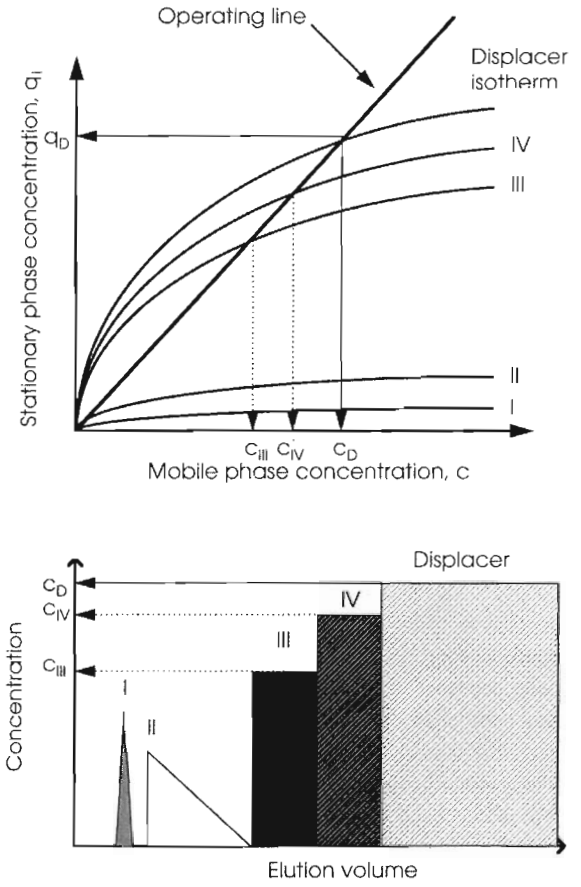

Figure 7 Treatment of displacement chromatography within the hermeneutics of the ideal model. The set of single-component isotherms and their intersection with the operating line defined by q_D/c_D is shown together with the corresponding chromatogram. Substance A elutes ahead of the displacement train, since its isotherm is not intersected by the operating line. The isotherm of substance B just touches the operating line (watershed point), hence the elution of substance B (overloaded conditions) immediately in front of the displacement train. Substances C and D are displaced. Their concentration in the pure zones is defined by the intersection point of their isotherms with the operating line.

where the operating line becomes tangential to the substance isotherm. In this case, the rear end of the eluting peak will just be touched by the front of the displacement train. Substances whose isotherms are not intersected by the operating line elute ahead of the displacement train. The only experimental parameter needed for the treatment of displacement chromatography within the hermeneutics of the ideal model thus are the equilibrium isotherms of the relevant substances and the isotherm of the displacer.

Concentration in the individual zones is determined by the component's isotherm and the displacer concentration. The length of each zone depends on the original amount of the substance in the feed. By changing the displacer concentration, one changes both the speed of the separation [$u_D = f(c_D)$] and the concentration of all substance zones. The concentration in the original feed, on the other hand, is of little importance. According to the ideal model, this is also the case for trace components and highly diluted feeds. In practice, dispersive effects will prevent trace components from reaching their theoretically predicted concentration maximum; however, the application of displacement chromatography to isolate and enrich trace components prior to detailed analysis has been demonstrated in a couple of real-life applications (see Section VI.F below).

Diluted and complex feeds, which are constantly encountered in the case of high-value bioproducts such as recombinant proteins from mammalian cell cultures, are both enriched and concentrated by displacement chromatography. The fact that a concentration plateau rather than a peak is observed can also be advantageous. While concentration is often a major goal in the bioseparations, sometimes unwanted effects such as aggregation, denaturation, or maybe only a troublesome increase in viscosity are observed as a certain critical concentration is surpassed. In the elution mode the peak maximum would have to stay below this critical value. Consequently, the concentration of the pooled fraction would be considerably lower. In displacement chromatography the entire substance zone could be kept just below this value resulting in a much higher average concentration in the pool. In at least two published applications, displacement chromatography was used in the downstream process with the specific aim of keeping the product concentration below the critical level [12,13].

Under the ideal conditions defined above, the displacement train will eventually form. The parameters of this train can easily be calculated given the equilibrium isotherms of the involved substances. Nothing has so far been said about the developing train or the determination of the actual length required for the development. Both can be calculated based on the ideal model provided the system is characterized by Langmuir-type isotherms. Based on these models, Glückauf analyzed displacement phenomena and discussed effects of solute and displacer concentrations as early as 1935. In the late 1960s, Helfferich et al. presented the first algorithm for a mathematical description of displacement chro-

matography based on the theory of interference originally developed for stoichiometric ion exchange systems [14]. Rhee et al. later developed a similar theory based on the theory of systems of quasi-linear partial equations and the methods of characteristics [15].

According to these theories, the system of partial differential mass balance equations for the various compounds coupled via the multicomponent Langmuir isotherms is transformed using the so-called h transformation (Helfferich et al.), or ω transformation (Rhee et al.), into a set of simple (and at that time already solvable) algebraic functions. Although the characteristic parameters cannot be determined explicitly for systems of more than two substances, their calculation by simple numerical methods is possible. The development of the displacement train is usually shown in a normalized distance–time diagram (Fig. 8). The column length necessary for the development of the displacement train can be taken directly from this diagram.

In spite of the simplifications the model of coherence proved to be surprisingly suited for the description of displacement separations of small molecules under highly nonlinear conditions. In 1985 it was extended by Frenz and Horvath

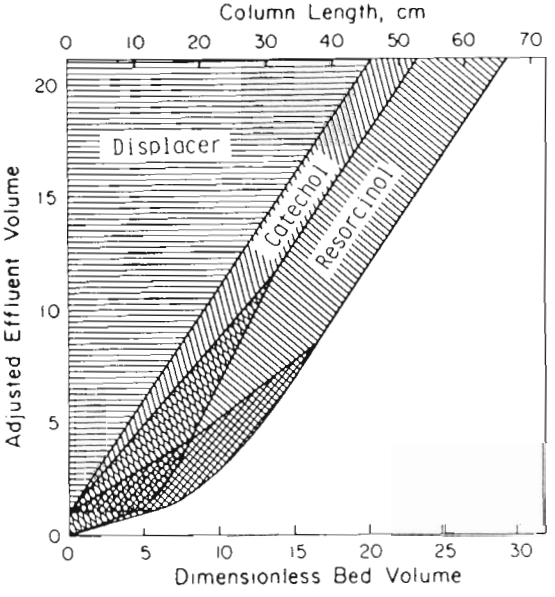

Figure 8 Displacement development graph of a binary mixture. The cross-hatched areas represent mixed regions, the line-shaded areas pure component regions. (From Ref. 16.)

for the separation of proteins by high-performance displacement chromatography (HPDC) [16].

1. The Steric Mass Action Model

The steric mass action (SMA) model of ion exchange displacement chromatography also assumes ideal chromatography conditions [17]. The model has been developed by Brooks and Cramer and describes nonlinear ion exchange chromatography of large molecules (proteins) on the basis of simple mass action. Other than the models proposed by Velayudhan and Horvath [18] or Regnier et al. [19], the SMA model takes into account that large molecules will not only interact with certain adsorptive sites on the stationary phase surface, but will also cover other interaction sites simply due to their bulk (Fig. 9). Most importantly, the model takes into account the fact that a salt gradient is induced in front of the displacer front. This gradient causes changes in the displacement train that are otherwise difficult to account for. Only a few characteristic parameters (the characteristic charge, the steric factor, and the adsorption equilibrium constant) are needed by the model, all of which can easily be determined experimentally.

The model is only able to simulate the fully developed displacement train under ideal conditions. Simulations of the developing displacement train or dispersive effects are beyond its scope. Within its limitations, however, the reported

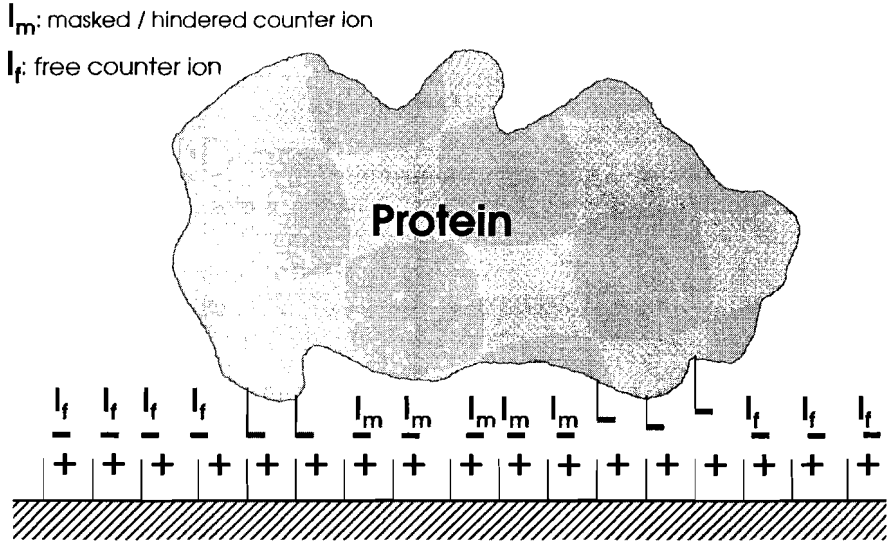

Figure 9 Idealized protein binding to an ion exchanger. (From Ref. 17.)

agreement with the experimental results is good. The model has since been extended to the description of immobilized metal affinity chromatography (IMAC) [20].

B. The Equilibrium-Dispersive Model of Displacement Chromatography

The ideal model of chromatography enjoys continuing popularity in theoretical displacement chromatography. Good qualitative agreement between the theoretical predictions and the experimental results have been reported. This is not surprising considering the conditions of the connected experiments, which employed high-efficiency columns (several thousand plates per meter), strongly nonlinear conditions (high sample concentration, large amounts), and were aimed for the separation of small molecules (fast mass transfer and reaction kinetics). Such experimental conditions approach ideal conditions to a high degree.

However, truly discontinuous concentration changes (shocks) as predicted by the ideal model are never observed during the experiments, no matter how high the column efficiency. Good displacement separations are instead characterized by steep but continuous changes in concentration, since dispersive effects (molecular and eddy diffusion, mass transfer and reaction kinetics, etc.) counteract the equilibrium thermodynamics. The implementation of dispersive effects into the simulations requires a model that somehow takes the limited column efficiency into account. This is more difficult in nonlinear chromatography, where the behavior of each compound depends on that of all others, than in linear chromatography, where the bands of the various compounds can be calculated independently.

The simplest approach to do this is the equilibrium-dispersive or semideal model. This model mirrors the situation of modern chromatography by assuming the dispersive effects to have a modifying but not a fundamental influence on the final band profile. In many cases this model is fully sufficient to predict the influence of the dispersive effects on the separation correctly.

To accommodate for high but not infinite column efficiency, a constant bulk axial dispersion coefficient, D_{bulk}, is introduced into the ideal mass balance equation. Equation (1b) thus becomes:

$$\partial c_i/\partial t + \phi\partial q_i/\partial t + u_0\partial c_i/\partial z = D_{bulk}\,\partial^2 c_i/\partial z^2 \qquad i = 1, 2, \ldots, n \qquad (1c)$$

In most cases the assumption of a constant bulk dispersion coefficient is reasonable at sufficiently high column efficiencies. Large biopolymers (DNA, proteins), however, tend to show a high and concentration-dependent viscosity in their solutions. For such molecules D_{bulk} becomes concentration-dependent and the unmodified equilibrium-dispersive model no longer applies.

An experimental value of the bulk dispersion coefficient can be derived

by applying the plate model of chromatography (tanks in series model). The characteristic parameter of the plate model, the height equivalent of a theoretical plate (HETP), takes axial dispersion and mass transfer kinetics into account [21,22]. For sufficiently high plate numbers (>100/m) the two approaches yield similar results and the dispersion coefficient becomes proportional to the plate height, H, and the plate number, N, of the column:

$$D_{bulk} = Hu_0/2 = Lu_0/2N, \text{ with } N = L/H \quad (8)$$

The plate height can be calculated from the peak width and the retention time of a given tracer under linear conditions as shown in Fig. 10.

In addition to the equilibrium isotherms, the equilibrium-dispersive model requires the experimental determination of the column's plate height as a function of the carrier flow rate (Knox or van Deemter curve). It is assumed that the plate height of a given column is identical under linear and nonlinear conditions.

Currently, there are no closed-form analytical solutions to the equilibrium-dispersive model. The comparative simplicity of the model facilitates the calcula-

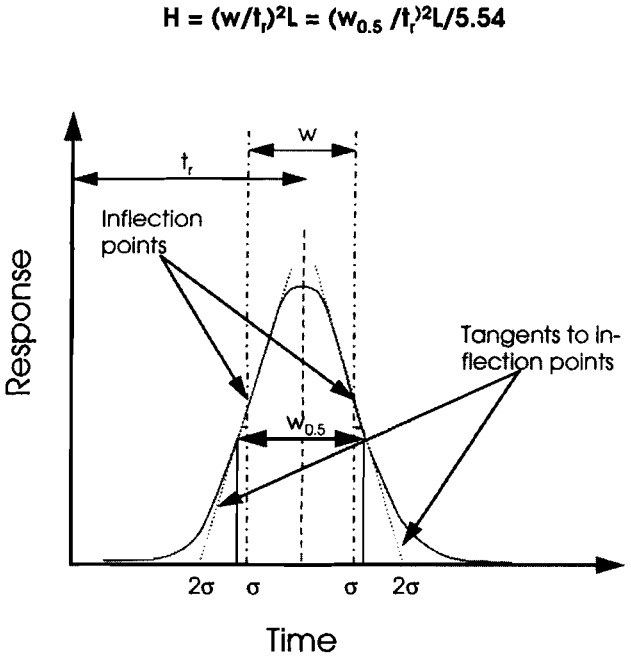

Figure 10 Calculation of the column plate height from experimental results (linear chromatography).

tion of numerical solutions to the relevant equations, using computation methods such as finite differences, finite elements, or collocation. For an excellent introduction to the numerical modeling of displacement chromatography, see Guiochon et al. [23].

Numerical solutions to differential equations always involve the introduction of a truncation error. A very elegant way of turning this into a positive feature is to replace the real axial dispersion by a numerical dispersion artifact, i.e., choosing, e.g., the finite differences in such a way that the numerical error caused by the truncation equals the dispersive term on the right-hand side of Eq. (1c), which is in turn dropped from the equation.

Using numerical calculations, the band profiles can be calculated for any specified parameters and initial conditions. As an example, the development of a displacement train as predicted by the equilibrium-dispersive model is shown in Fig. 11. The predictions show good agreement with the experimental results. The basic features of a displacement train are determined by the equilibrium thermodynamics. The dispersive effects do not introduce new phenomena. Instead their main effect is a smoothing out of the sharp edges predicted by the equilibrium theory. The overall features, such as the length and height of the zones, stay the same. The only difference is that instead of an abrupt change a small overlapping zone containing both substances develops between two consecutive substances in the train. This layer is also called the shock layer. The shock layer has similar properties (velocity, etc.) as the shock: its thickness depends on the dispersive effects.

The equilibrium-dispersive model yields good results as long as the observed band profiles are indeed determined primarily by the nonlinear thermodynamics of equilibrium as described by the ideal model. However, all contributions to the band broadening are considered to be simple additions to the axial dispersion in this model. The fact that the various contributions to the bulk coefficient differ in their dependency on the concentration is ignored. This approximation is no longer valid once the column efficiency becomes low and mass transfer and reaction kinetics begin to determine the band profiles to a similar extent as the equilibrium thermodynamics. In addition, the bulk dispersion coefficient depends on the retention factor, k'. The concentration dependence of k' is also ignored in the model, which assumes k' to equal k'_0, i.e., the value determined for linear conditions. This approximation also generates significant error at low column efficiencies.

C. Kinetic Models for Displacement Chromatography

The equilibrium-dispersive model lumps all dispersive effects into a single coefficient. As we have seen, simulations obtained with this model agree well with the experimental results as long as the assumption holds that the kinetic effects

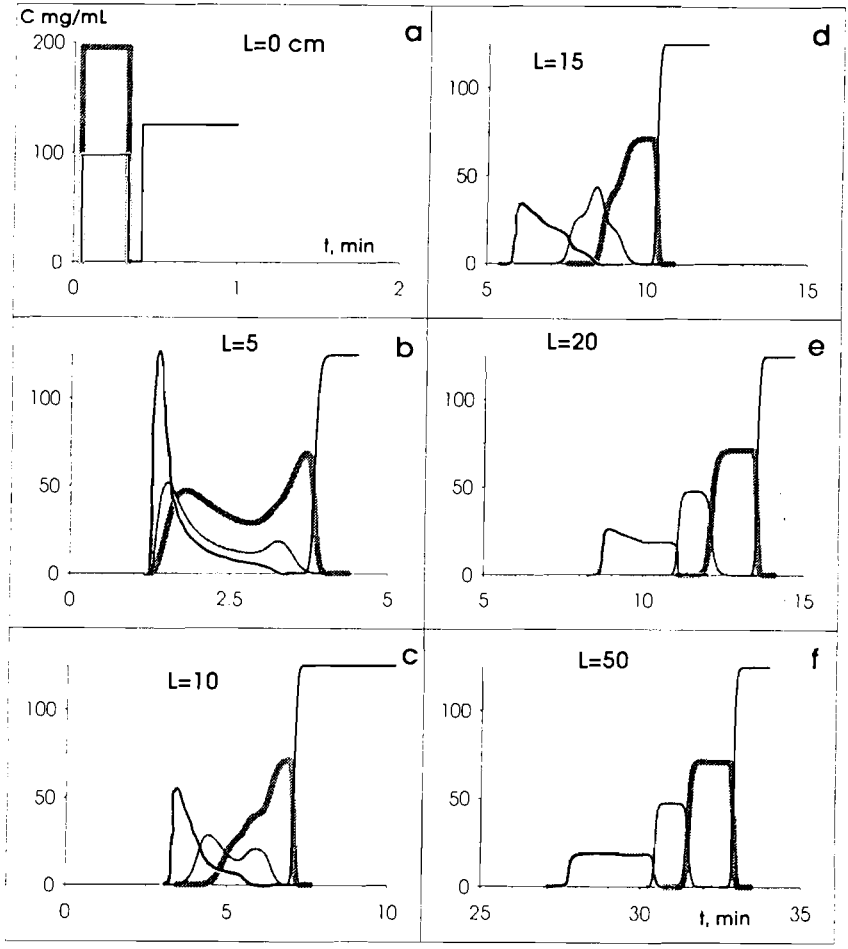

Figure 11 Development of a displacement train as predicted by the equilibrium-dispersive model. (From Ref. 23.)

are merely additions to the dominating axial dispersive effects. As we have also discussed, this assumption is not always allowed for biopolymers, since the mass transfer resistance is often several orders of magnitude higher in the case of these large molecules (small diffusion coefficients). In contrast, certain types of chromatography popular in biopolymer separation are characterized by slow sorption kinetics. Affinity chromatography, for example, quickly becomes surface reaction limited, which may become a problem even in elution chromatography at elevated

flow rates. In cases like this, the equilibrium-dispersive model is not capable of providing helpful simulations. Instead a kinetic model should be used.

In the kinetic models the mass balance equation [Eq. (1)] is combined with a kinetic equation relating the rate of variation of the concentration of each component in the stationary phase to its concentration in both phases and to the equilibrium concentration in the stationary phase. Solutions to the equations of the kinetic models are usually obtained numerically as for the equilibrium-dispersive model. Various models have been proposed, which vary mainly in the choice of the kinetic rate expressions (see table below).

An important decision concerns which degree of complexity is necessary in a given situation. As long as the kinetics are not very slow, the various kinetic models yield similar results, which often resemble the results of the equilibrium-dispersive model [24]. As the influence of the kinetic terms increases, the various models yield results of differing accuracy.

Mass transfer resistance	Ref.
Negligible	Lapidus and Amudson [25]
Langmuir isotherm with quasi-chemical mass transfer rate	Thomas [26], Goldstein [27], Wade et al. [28]
Linear rate equation	
first-order kinetics	Lapidus and Amudson [25]
solid film linear driving force	Glückauf and Coates [29], Hiester and Vermeulen [30], Lin et al. [31], Phillips [8]
liquid film linear driving force	Guiochon et al. [23]
Intraparticle diffusion	Rasmuson and Neretnieks [32]
Intraparticle diffusion/external film diffusion	Rasmuson and Neretnieks [32]
Dual intraparticle diffusion/external film diffusion	Rasmuson [33]

Theoretically, a general rate model that explicitly considers all effects will be the most correct. However, it is also the most complex one and requires the experimental determination of all involved rate constants. In most cases, however, a kinetic model that lumps all kinetic effects into a single expression will suffice.

For increasing mass transfer resistance, such a lumped model predicts a decrease in the length of the zones in the displacement train and a concomitant increase in the shock layer thickness. For very small mass transfer coefficients the plateaus disappear completely and the resolution between successive bands

is poor. An asymptotic solution can be obtained for the concentration profile in the shock layer once the displacement train has been established (Fig. 12). It is usually assumed that both the diffusion coefficients and the rate constants are equal for all compounds; otherwise the actual shock layer thickness lies between the values calculated for the two values.

The shock layer thickness, $\Delta\eta_t$, between two successive zones in the isotachic train according to Guiochon is given by:

$$\Delta\eta_t = \left(\frac{(1 + K_d)^2 D_{ax}}{K_d u_0^2} + \frac{1}{k_f} \right) \frac{1 + \alpha}{1 - \alpha} \ln \left| \frac{1 - \theta}{\theta} \right| \tag{9}$$

with $K_d = k'_d/(1 + b_d c_{d'})$, k_f is the film mass transfer coefficient, and θ is the characteristic parameter (see Fig. 12 for details).

The shock layer thickness thus depends on the axial dispersion coefficient and the mass transfer coefficient of the two components, on their separation factor, and on the concentration and retention factor of the displacer [34]. In a given train the shock layer thickness depends only on the value of α. It does not depend on the retention factor or the feed concentration of the components.

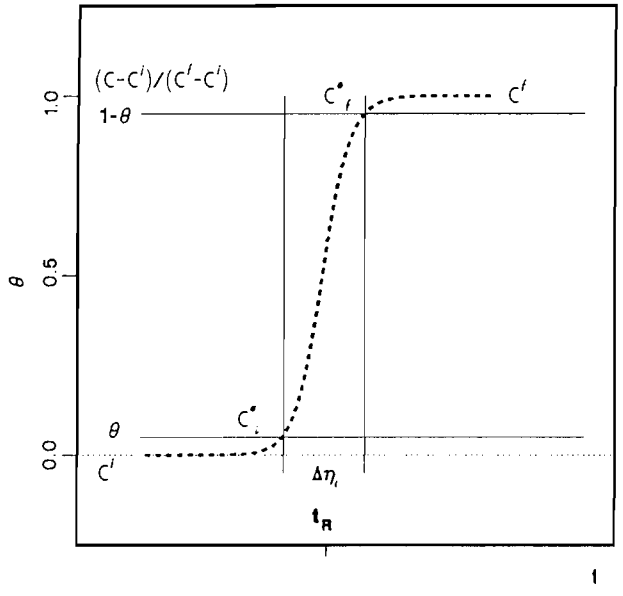

Figure 12 Schematic presentation of the shock layer concept. (From Ref. 23.)

A differentiation Eq. (9) shows that the shock layer thickness would be at minimum for $K_d = 1$, i.e., for

$$k'_d = 1 + b_d c_d \tag{10a}$$

or

$$c_d = (k'_d - 1)/b_d \tag{10b}$$

Consequently, the shock layer is wide whenever $k'_d \ll 1 + b_d c_d$, i.e., at low displacer retention or at high displacer concentration (so-called overdisplacement phenomenon). For $k'_d \gg 1 + b_d c_d$ the shock layer thickness increases linearly with increasing k'_d. As shown by Zhu and Guiochon, there is no optimum displacer retention factor and optimum displacer concentration in displacement chromatography, but a combined optimum given by the above Eqs. (10a) and (10b).

Just as in elution chromatography, however, there is an optimum mobile phase velocity, given by [35]:

$$u_{opt}^{D} = \sqrt{\frac{D_L (1 + K_d)^2 k_f}{K_d}} \tag{11}$$

At low flow velocities, diffusional effects caused by the steep concentration gradients cause a widening of the shock layer. At high flow velocities, the limited mass transfer and reaction kinetics again cause a shock layer broadening. Contrary to the situation in elution chromatography, however, in displacement chromatography the optimum mobile phase velocity depends not only on the axial dispersion and mass transfer resistance, but also on displacer properties such as retention factor and concentration [34]. Differentiation of Eq. (11) shows that an optimal u_{opt} is obtained in the case of $K_d = 1$. In practical terms this means that the optimum flow rate will usually be lower in displacement than in elution chromatography.

Application of the shock layer theory to the displacement situation permits prediction of the influence of parameters such as column length and plate height, particle diameter, carrier flow rate, or sample size and concentration. Briefly, one can state the following rules. These rules apply to the established displacement train, i.e., under conditions whereby a dynamic equilibrium between the band sharpening effects of the thermodynamics and the eroding effects of the finite column efficiency has been fully established (constant pattern behavior). As a consequence, the described limitations correspond to the best achievable conditions for a given experimental setup.

Plate height. The shock layer thickness and concomitantly the intermixing of the substance zones increases with increasing plate height (decreasing column efficiency); consequently, the recovery yield decreases. As a consequence, high-efficiency columns are just as important in nonlinear

(preparative) chromatography as in linear (analytical) chromatography. The fact that displacement chromatography makes better use of the column capacity often allows the use of high-efficiency analytical columns at a semipreparative scale. Parameters influencing the plate height (flow rate, particle diameter) have a direct influence of the shock layer thickness and thus of the chromatographic result.

Displacer concentration. As already seen for the ideal model, an increase in the displacer concentration causes an increase in the substance zone concentration with a concomitant decrease in zone length. While this was not a problem under ideal conditions, the introduction of the shock layer concept shows that concomitant to the narrowing of the substance zone the relative amount found in the shock layer increases. The term "overdisplacement" has been coined for such a situation where bands are so narrow that no concentration plateau of the pure substance is observed while the two shock layers in front and at the end of the zone touch.

Column length/sample size. For a given column diameter, the column length required to achieve the displacement train increases with increasing sample amount. In contrast, the concentration hardly matters. Thus even highly diluted feeds can be processed by displacement chromatography. The loading factor is inversely proportional to the column length and the loading factor for which the isotachic train is formed remains constant.

Separation factor. The separation factor α, as defined as the quotient between the capacity factors, k', of any two compounds, is another important chromatographic parameter, whose influence on the displacement train cannot be fully accounted for by the ideal model. Even with the equilibrium-dispersive model there is no simple equation linking the separation factor to the development of the displacement train. However, it can be shown that the column length required to achieve the displacement train increases rapidly as the separation factor approaches 1. The shock layer thickens in proportion to $(\alpha + 1)/(\alpha - 1)$ and increases dramatically as α decreases toward unity. Displacement chromatography is therefore not superior to elution chromatography in resolving binary mixtures with a very small value of α. The shock layers would encompass the entire displacement train, while the time required to achieve isotachic conditions would result in a very low throughput. The fact that displacement chromatography is equally suited to the separation of closely related substances has been demonstrated by separation of the genetic variants of β-lactoglobulin B [36], or structural and geometric isomers (see Section VI.D).

Trace compounds. According to the ideal model the concentration in a substance zone is independent of the original sample amount. Thus a zone may become infinitesimally narrow in the case of a trace compound. According to the equilibrium-dispersive model, a trace component will be considerably enriched in displacement chromatography, often much more so than in elution chromatography. However, when the zone width reaches the same order of magnitude as the shock layer thickness, no further enrichment takes place. Instead the zone width stabilizes. This behavior is also observed in real-life applications of displacement chromatography.

Displacer Impurities [37]. Any displacer impurity acts as an additional (trace) compound in the displacement train. Impurities with an equilibrium isotherm below that of certain compounds of the separation mixture will contaminate the displacement train. If the separation factors between the bulk displacer and the impurities are close to 1, formation of the fully developed displacement train may be difficult. Therefore homogeneous displacers are preferable.

These predictions are qualitatively correct for any isotherm type provided its shape is convex and no intersection occurs. The latter, however, is quite a common phenomenon in biopolymer chromatography, since the adsorption energy tends to increase with molecular mass, while the saturation capacity decreases in the same direction. A large molecule will therefore be characterized by an isotherm with a steeper initial slope but a lower saturation plateau than a similar but smaller molecule. The result may be an isotherm crossing leading at worst to "elution azeotropes," which no column despite its length will be able to dissolve [38]. Obviously this cannot be accounted for by the competitive Langmuir-isotherm model, which assumes constant separation factors [7].

Other models such as the LeVan and Vermeulen isotherm derived from the theory of the ideal adsorbed solution (IAS) [39] and modified Langmuir models [40] have been suggested to describe the multicomponent adsorption behavior of complex molecules under linear and nonlinear chromatographic conditions. Antia and Horvath have used this theory as a basis for their investigation of the selectivity reversal phenomenon [38]. Langmuir-type single-component isotherms were also assumed in their case. They were able to show that the result of an isotherm crossing is the development of a separation gap in the system (Fig. 13). The position of the gap depends on the saturation capacities of the two compounds. If the operating line crosses the isotherms in this gap, no separation takes place. If it intersects on the right- or the left-hand side of the gap, a separation of the two compounds by displacement is possible. However, the order of the substances in the displacement train is opposite in the two cases. If the initial

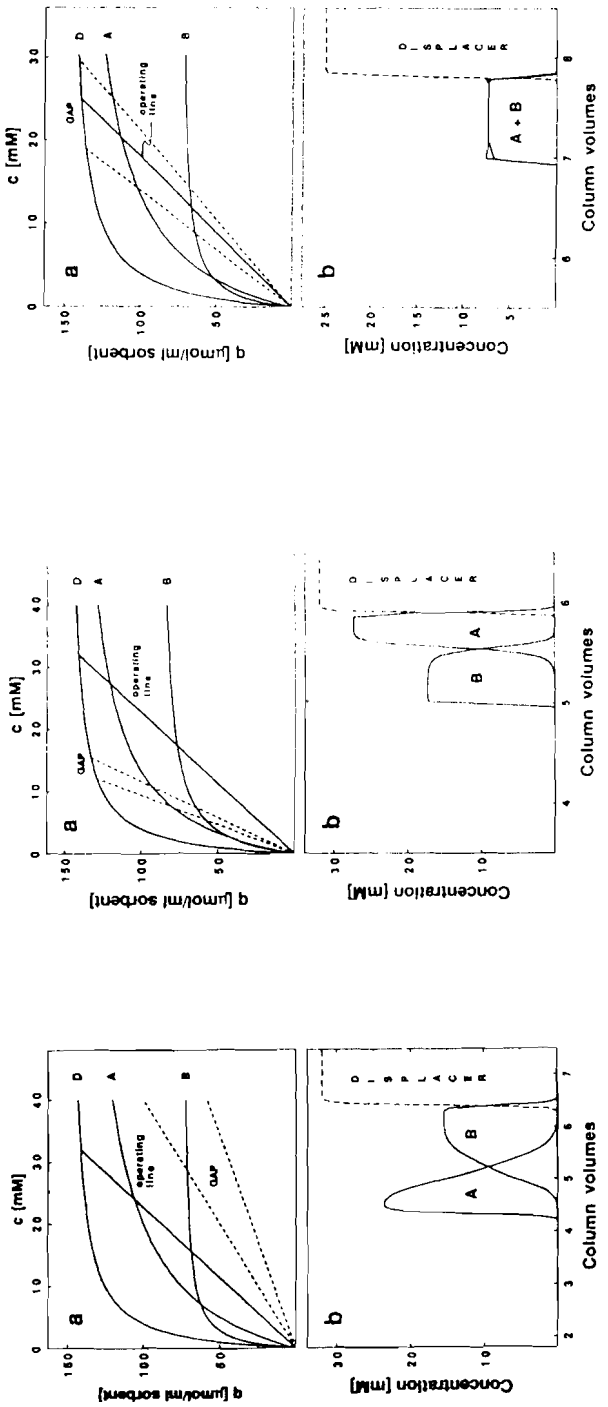

Figure 13 Crossing single-compound isotherms and displacer isotherm with operating line lying (A) left, (B) in, and right of the separation gap. The corresponding displacement chromatograms are also shown. (From Ref. 38.)

slope of the isotherm A is higher than that of substance B, whereas the opposite is true for the saturation capacities, A appears before B in the displacement train if the operating line intersects on the right-hand side of the separation gap and B before A if the points of intersection are placed to the left of the gap. The occurrence of an adsorption azeotrope has been observed experimentally, e.g., by Carta and Dinerman for the separation of α-aminobutyric acid and isoleucin on Dowex 50W-X8 resin [41] and by Kim and Cramer for protein separations in the immobilized metal affinity chromatography (IMAC) mode [42]. A similar reason was proposed by Kasper et al. for their inability to resolve a mixture of antithrombin III and bovine serum albumin (BSA) on hydroxyapatite columns under certain experimental conditions [43].

IV. PRACTICAL METHOD DEVELOPMENT IN DISPLACEMENT CHROMATOGRAPHY OF BIOMOLECULES

The theoretical basis of biomolecule and especially biopolymer displacement chromatography is currently less well developed than that of smaller molecules. Simulations can in most cases aide but not replace the experimental development of the method. Bio(poly)mer displacement chromatography by necessity often takes place under exactly those conditions that were explicitly excluded in the theoretical treatment of the displacement phenomenon, i.e.:

- At comparatively low concentration due to the limited solubility of the biopolymers and to the problems with viscosity observed for highly concentrated DNA and protein solutions
- In the presence of secondary equilibria (denaturation, aggregation, reactions)
- In non-Langmuirian systems characterized by complex, sometimes crossing or unfavorable isotherms
- At comparatively low column efficiency
- Under conditions whereby mass transfer and reaction kinetics are dominant and cannot be treated simply as additions to the axial dispersion
- Under conditions whereby the relevant parameters are noticeably concentration-dependent

The growing number of examples of successful biodisplacement chromatography shows, however, that displacement chromatography is less limited by these circumstances than one would assume from the theoretical considerations.

Development of a biodisplacement chromatography will usually involve the following steps:

Choosing the stationary phase
Optimizing the mobile phase
Adjusting the column length/sample size
Adjusting the flow rate
Finding a displacer and, perhaps,
Adjusting the temperature (an increase in temperature may result in beneficial effects such as a decrease in viscosity or improved mass transfer and reaction kinetics. Many biopolymers are sensitive to elevated temperatures, however, so rarely is this an option in preparative chromatography.)

Since in displacement chromatography the substances are separated into consecutive zones, the monitoring of a displacement separation can be more difficult than in elution chromatography, especially in the semipreparative scale where an unspecific (UV) detector can usually still be used to monitor an elution separation. In displacement chromatography fraction collection is inevitable. The use of on-line analytical HPLC has been suggested to monitor the displacement train and control the fraction collection [44]. Such an approach may become necessary to allow the full automation of the system and to reduce the process time, which up to now is largely increased by the amount of time needed to carry out the off-line fraction analysis.

A. Stationary Phase

Choosing the stationary phase also involves choosing the interaction mode for the separation. The vast majority of the published protein displacement separations has been done on an ion exchange column. Displacement separations of peptides and other smaller biomolecules are mostly carried out in the reversed-phase mode. In these standard cases a host of guiding examples can be found in the pertinent literature; a number of the more recent ones will be discussed below in Section VI. Occasionally other stationary phases have been used, including immobilized metal affinity chromatography (IMAC), antibody exchange (Abx), hydroxyapatite, or hydrophobic interaction chromatography (HIC) phases (see Section VI for details).

Today's high-performance stationary phases are in general not designed for displacement chromatography. If anything, the differences between stationary phase materials and columns from different suppliers is even more pronounced in displacement than in elution chromatography. It is thus highly advisable to investigate a number of columns before coming to a final decision. Some attention should be paid to the availability of the bulk material. The column length is an

important parameter in displacement chromatography (see below) and the length of the available prepacked columns may not be optimal.

The particle diameter of the stationary phase is another important parameter, since mass transfer effects have a substantial effect in biopolymer displacement chromatography. Smaller particles stand for higher efficiencies, i.e., lower theoretical plate heights. However, for a given column length the pressure drop increases considerably with decreasing particle diameter. Most authors advise to use particles of less than 20 μm, although particles of 80 μm and more have occasionally been used with success in displacement chromatography [45]. Theoretically, a minimum in d_p exists, below which a further decrease in the particle diameter will not improve the separation any further since the reaction kinetics become rate limiting [46]. The particle size distribution should be narrow.

Since mass transfer can be even more limiting in displacement than in elution chromatography, the recent arrival of stationary phases for biopolymer chromatography that improve this particular feature may become interesting for displacement chromatography. Examples include the perfusion chromatography beads (PerSeptive Biosystems Inc., Framingham, MA, USA), the HyperD columns (Biosepra Inc., Marlborough, MA, USA), and the continuous bed column (UNO column) recently introduced by Bio-Rad Inc. (Hercules, CA, USA) (Fig. 14).

In perfusion particles the mass transfer is supposedly improved due to the presence of large throughpores in the particles. Convective flow is possible in the throughpores; hence an improvement of the mass transfer. However, the mobile phase flow velocity needs to be quite high—much higher than usual in traditional displacement chromatography—for the perfusion phenomenon to occur. Even then only some 5% of the flow passes through the particle. Perfusion displacement chromatography has been used to separate the genetic variants of β-lactoglobulin at a flow rate of 4 ml/min [47]. Eighteen milligrams was thus prepared within 90 seconds using heparin as displacer. The authors claimed a resolution similar to if not better than that achievable in conventional displacement chromatography at much lower flow rates.

HyperD particles consists of a ceramic support filled with a gel. Mass transfer is highly efficient in such beads, since the intraparticular diffusion of the feed molecules takes place on the surface of the stationary phase (hyperdiffusion).

A continuous bed column is formed by direct radical polymerization of monomers in a tube. The polymer molecules form small nodules (<0.1 μm), which aggregate into a highly porous polymer rod. No extraparticular dispersive effects are possible in a UNO column. Their van Deemter curve usually shows an unusually low optimum, since the nodule size seems to determine the A term. The column efficiencies remains more or less constant even at elevated flow rates in elution chromatography. A 3.5-cm-long anion exchange UNO column (column volume 1 ml) was recently used for displacement chromatography of whey pro-

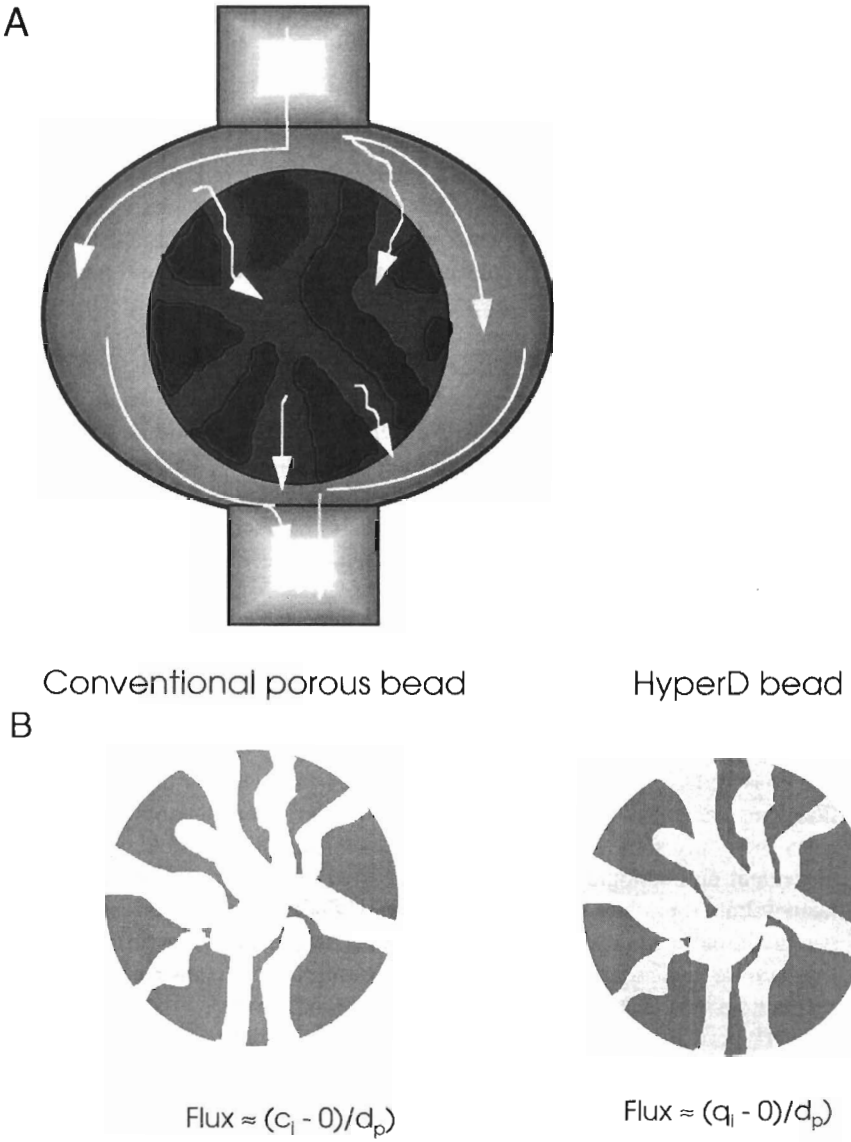

Figure 14 Types of stationary phase materials with supposedly improved mass transfer features: (A) perfusion material (Perfusion chromatography uses a *bead* with 2 types of pores; throughpores: 6000–8000 Å; diffusive-pores; 500–1500 Å; throughpores enable the eluent to pass the beads; diffusive pores are short and allow faster separation times.) (B) hyperdiffusion material, (C) continuous bed column. Continuous Bed matrix uniformity minimizes the band broadening seen in conventional packed beds. The non-porous surface allows extremely fast mass transfer, minimizing band broadening even at high flow-rates. The fimbriated surface structure of the nodules provides a large surface area for good binding capacity.

C

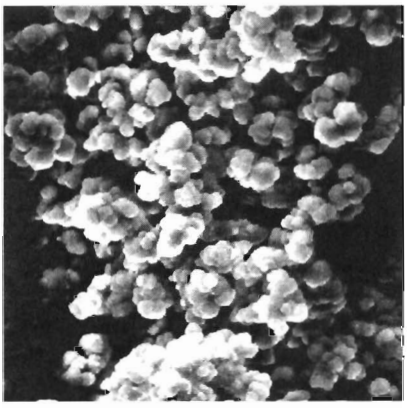

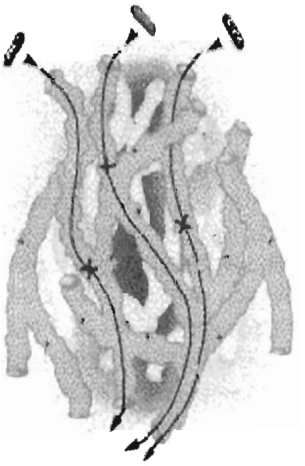

Figure 14 Continued

teins. Compared to similar experiments on traditional beaded supports the shock layer between the two protein zones is small in spite of the shorter column length (3.5 cm for the UNO column versus 5.2 cm for the traditional column). However, the possibility of using elevated flow rates with this column was not investigated.

B. Mobile Phase

In displacement chromatography the mobile phase is often merely considered as an inert carrier. Concomitantly the use of conditions that aid strong binding of the substances and the displacer to the stationary phase are advised. However, this has not been shown to improve the separation. Instead, low retention factors may actually improve displacement separations. The theoretically predicted optimum values lay between 1.2 and 2.0 [46]. The influence of the separation factor, α, on the shock layer thickness between two consecutive substances in the displacement train should be kept in mind. A high value of α helps to achieve good resolution between consecutive zones. Given the tendency of biopolymers to show all-or-nothing binding behavior, the deciding factors in choosing the mobile phase in biodisplacement chromatography are often less chromatographic and more biological in nature, i.e., prevention of denaturation, interaction/aggregation, or solubility.

C. Column Length/Sample Size

The optimization of column length and sample size should be interactive. Some intuition has to be used. The displacement train needs a certain distance to de-

velop and conditions of nonlinearity should prevail during the separation. For any given sample size there is an optimum column length and vice versa. Displacement chromatography of proteins has been shown on columns as short as 5 cm. Extending the column length beyond the optimum will not improve the separation any further. Often it is easier to adjust the sample size to the dimensions of a given column rather than optimize the column length for a given sample. For modern high-performance columns the utilization of up to 80% of the column's capacity should be possible.

Finally the question to be addressed is whether the full development of the displacement train is always necessary. While this does maximize the recovery yield, it does not necessarily correspond to the highest productivity. Throughputs may, for example, be higher when the column is not long enough to allow the full development of the displacement train and instead the mixed zones are recycled. The decision will depend on the position of the target molecule in the displacement train and the stability of the molecule.

D. Flow Rate

The optimum flow rate in displacement chromatography will be up to one order of magnitude lower than in elution chromatography. In almost all cases of biopolymer displacement chromatography, this optimum flow rate will therefore be much too low to be of practical relevance. Most authors use flow rates between 0.1 and 0.5 ml/min in biopolymer displacement chromatography in the semipreparative scale (typical column dimensions cm × mm). At higher flow rates, the quality of the separation tends to decrease rapidly, although flow rates of several milliliters per minute have occasionally been used with success even with analytical scale columns [48].

The lower flow rates in displacement chromatography do not necessarily result in lower throughputs or in an economic disadvantage. In our laboratory, for example, identical columns were used in the displacement and the overloaded elution mode for the separation of whey proteins. The preparation of 1 g of α-lactalbumin of comparable purity took 5 times as long in the elution than in the displacement mode in spite of the one order of magnitude higher flow rate in the elution column (1 ml/min versus 0.1 ml/min). The fact that the sample volume was much smaller in the elution case was largely responsible for this. In addition, the two whey proteins were concentrated by a factor of 3 in the displacement case, whereas dilution was observed for the pooled fractions collected from the elution column. A similar observation was made by Gerstner [49] for the separation of oligonucleotides by displacement and elution chromatography. Although the flow rate was twice as high in the elution than in the displacement mode and the feed per run similar (with 15 L the elution column was 3 times as large as the displacement column), 311 runs were required to produce 5 kg of product in the displacement mode versus 467 runs in case of the elution column. The

number of production days was 26 in the displacement mode compared to 39 days in the elution mode. Due to the higher productivity, the lower consumption of solvent, chemicals, and labor, as well as the much better recovery, the production costs for this amount of product would amount to $3.657 million in the elution case compared to only $2.677 million in the displacement case.

E. Displacer

The preceding subsections dealt with aspects of displacement chromatography, which are not very different from similar considerations in elution chromatography. This is not so in the case of the displacer, which is a unique feature of displacement chromatography. At the same time, the choice of the displacer has consequences not only for the success but for the economic soundness of the final method.

The ideal displacer should have the following features:

It should be nontoxic, stable, detectable, and cheap.
It should combine high solubility in the carrier with a high binding tendency toward the stationary phase.
Regeneration of the column should nevertheless be possible.

In addition, the displacer should be uniform and its removal from the product zone possible. For pharmaceutical applications it might even be necessary to sterilize the material.

Mixtures of small biologicals such as amino acids, peptides, and small proteins (antibiotics, insulin) are usually processed by reversed-phase displacement chromatography. Hydrophobic substances such as 2-(2-butoxyethoxy)ethanol (BEE), decyltrimethylammonium bromide, cetyltrimethylammonium bromide (cetramide), benzyldimethyldodecylammonium bromide, dodecyloctyldimethylammonium chloride, and palmitic acid are standard displacers for these applications [2]. Nucleotide and nucleoside mixtures have been separated using a similar combination between reversed-phase stationary phases and hydrophobic displacers. The separation of oligonucleotides is also possible in the anion exchange mode using dextran sulfate as displacer [49].

Ion exchange chromatography is very popular in preparative protein chromatography because it is known to preserve biological activity to a high degree. To *this day the majority of protein purification schemes contains one or several* ion exchange steps. While hydrophobic interaction chromatography is gaining ground in preparative elution chromatography, the ion exchange mode is still almost exclusively used in protein displacement chromatography. The lack of suitably hydrophobic protein displacers for the hydrophobic interaction mode may be among the reasons for this, since it is easier to find a highly aqueous mobile phase–soluble polyion than similar hydrophobic polymer. For ion exchange applications, a number of (semi)synthetic polyions such as chondroitin

sulfate, dextran sulfate, carboxymethyl starch, alginate, Eudragit, Nacolyte 7105, and polyethyleneimine (PEI) have been suggested as protein displacers [50]. Since 1978, Torres and Peterson have promoted the use of (modified) carboxymethyldextrans (CM-D) for that purpose [51].

In almost any case a protein that is known to bind exceptionally well to a given stationary phase material may be used as a displacer of less well-bound proteins. This approach has also been used repeatedly, last but not least in the few attempts to do hydrophobic interaction displacement chromatography [52]. For example, protamine was suggested as a protein displacer in cation exchange displacement chromatography [53], whereas heparin may act as a nontoxic displacer in anion exchange methods [54]. While proteins as protein displacers yield important data, proteins will hardly become industrial-type biopolymer displacers. Most other substances named above are cheaper and thus more suited to an industrial application. Unfortunately, they are usually highly heterogeneous, difficult to detect, and almost impossible to recycle.

While most applicants clearly prefer to use large-protein displacers, certain low molecular weight substances are also discussed as putative protein displacers in the ion exchange mode, since it was possible to show that even smaller molecules in the range of several hundred to several thousand grams per mole can be effective displacing agents for much larger molecules [55–59]. The removal of any displacer contaminant from the product zone should be much easier in the case of the small displacer molecules, since the large difference in size can be exploited.

Examples of low molecular weight protein displacers include low molecular weight dextran sulfates [58] and pentosan polysulfate (M_w: 3000 g/mol), which were used for the separation of the genetic variants of β-lactogobulin [56]. Polyvinylsulfonic acid (M_w: 2000 g/mol) [59] and pentaerythritol-based dendritic polymers (M_w 480–5100 g/mol) were used as displacers of basic proteins such as α-chymotrypsinogen and cytochrome c on cation exchanger materials [57]. Modified ethylenglycols (M_w: 1000–10,000) and small chelating agents such as EGTA (ethylenglycolbis(β-aminoethylether)-*N,N,N′,N′*-tetraacetic acid, M_w: 380.4 g/mol) and IDA (imminodiacetic acid, M_w: 133.4 g/mol) were suggested as displacers of recombinant proteins and whey proteins from apatite columns [55,60,61].

A comparison of the results obtained with these small displacers to those obtained for similar but larger molecules shows that it is charge density and hence adsorption energy rather than size and absolute number of interaction points that determines the quality of a displacer. It was also seen, however, that the behavior of small displacers depends to a much higher degree on the chromatographic conditions, e.g., the salt content of the mobile phase. As a consequence, the switch from displacer to elution promoter is more likely in the case of these small substances.

Among the host of synthetic and semisynthetic substances that have been used for protein displacement, few if any have been synthesized with that explicit goal in mind. Torres and Peterson were among the first to chemically modify their (high molecular mass CM-D) displacers in order to gain control over the stationary phase affinity [62]. An interesting approach to displacer design was recently suggested by two groups. These synthetic displacer molecules mimic certain features of biopolymers (proteins) such as their solubility behavior in aqueous solutions. The triblock polymethacrylate-based displacers prepared by Patrickios et al. [63] using group transfer polymerization carry a sequence of positively charged groups at one end of the molecule and a sequence of negatively charged ones at the other. In the middle a neutral, hydrophobic block is created to separate the two. The resulting polymers show an isoelectric point much like that of proteins and can be precipitated at the corresponding pH. The authors claim good results with these substances as displacers for anion exchange displacement chromatography.

A similar approach to the problem of displacer recovery, either to rid product zones from contaminating displacer traces or to establish a recycling scheme, was used by Vogt and Freitag [64]. In this case a copolymer was synthesized by radical polymerization that showed a lower critical solution temperature (LCST), a phenomenon that is based on a similar physicochemical basis as the salting-out effect observed for many proteins. Due to a finely tuned balance between hydrophobic and hydrophilic groups, LCST polymers are water-soluble at low temperature, but precipitate rapidly when the temperature is increased and a certain critical temperature, the LCST, is passed. The exact value of the LCST can be adjusted from between 10°C and 90°C, whereas the displacing character of the molecules stays roughly the same. The polymers can be redissolved simply by lowering the temperature again. The cycle can be run through several hundred times; no unspecified protein coprecipitation was observed in the investigated cases. The displacers were used in combination with anion exchange and hydroxyapatite columns.

V. SPECIAL FORMS OF DISPLACEMENT CHROMATOGRAPHY

Most applications of displacement chromatography found in the literature deal with a separation as outline above. The mixture components are focused into consecutive individual zones by means of a displacer. The displacer should ideally be a homogeneous substance. However, two variants of this schema have been developed that use a somewhat different approach. So-called spacer displacement chromatography does not employ a single displacer substance to develop the displacement train but uses a mixture of related compounds as spacer/

displacers [62]. The components of the spacer/displacer mixture vary in their adsorption energy within the range of the feed components. As a result, the more strongly bound molecules of the mixture act as displacer in a manner similar to that of any ordinary displacer, whereas the less strongly bound ones act as spacers between the target molecule zones. Since the spacers are usually chosen to be non-UV-active, the monitoring of the displacement train is facilitated. The spacer displacement chromatography approach is, for example, necessary in thin-layer displacement chromatography (TL-DC), where the analysis of the displacement train would otherwise be difficult. In ordinary column liquid displacement chromatography such an approach has also been used (see Section VI). However, this always entails the contamination of each recovered substance by at least two spacer substances or a loss in yield corresponding to the rejection of the shock layer fraction.

Complex displacement chromatography is related to ordinary displacement chromatography less through its mechanism and more through the chemicals used. A typical application of complex displacement chromatography would be the isolation of a cationic protein (e.g., an mAb) using a cation exchange column and substances such as the carboxymethyldextrans (CM-D) ordinarily used as displacers in anion exchange displacement chromatography [65]. In complex displacement chromatography, the "displacer" forms a complex with the adsorbed target molecules. Once the net charge of the complex becomes sufficiently low, the entire complex desorbs from the surface.

VI. APPLICATION OF DISPLACEMENT CHROMATOGRAPHY

The number of applications of displacement chromatography for bioseparations is still small compared to the elution mode. It is, however, already much too large to be discussed in detail on a case-by-case basis. The following necessarily incomplete list attempts to give an overview of what has already been done. The listed conditions apply to the actual displacement steps. In some cases, different flow rates or temperatures were used during sample loading.

Most authors working in the field of biodisplacement chromatography tend to use standard mixtures to investigate the fundamental parameters and/or to demonstrate the validity of simulations. While these exemplary separations are interesting to anybody intending to develop a biomolecule displacement separation, the results are usually much more straightforward than anything achievable for a "real" sample; they were not included in the following list for obvious reasons. Instead we tried to compile published examples of displacement separations of crude biomolecule mixtures with practical relevance.

A. Protein Separation

Target molecule	Conditions	Comments	Ref.
Crude β-galactosidase (industrial enzyme) from *Aspergillus oryzae*	Method: weak anion IE-DC Column: two TSK DEAE-5PW column in series, 75 × 7.5 mm Flow rate: 0.2 ml/min displacer: chondroitin sulfate	Displacement mode superior in throughput, less waste	[36]
Human serum proteins	Method: anion IE-DC Column: DEAE Bio-Gel A, DEAE Selectagel, 140 × 5.5 mm Displacer: gradient of CM-D with increasingly higher content of carboxyl groups	General method for fractionation of complex protein mixtures Fractions are low in salt and can be directly analyzed by electophoresis Methods for displacer modification are discussed	[66]
Human Gc-2 globulin	Method: two-anion IE-DC at different pH followed by elution chromatography on hydroxyapatite column: DEAE Sephacel, 7 ml Flow rate: 5 ml/h Spacer/displacer: different CM-D	The protein was isolated from the blood of psoriasis patients and only known as one of more than 100 spots in 2D electrophoresis, 6 ml of serum (400 mg protein) gave 0.5 mg pure substance After the second displacement step the protein was only contaminated A-1 lipoprotein By comparison, 4 mg of the protein was recovered from 34 L of serum using 13 elution chromatography and electrophoresis steps	[67]

Target molecule	Conditions	Comments	Ref.
Alkaline phosphatase from *E. coli* periplasm	Column: HPLC DEAE-5PW Displacer: CM-D		[62]
mAb from ascites	Method: complex DC on anion exchanger Complexer/displacer: CM-D	Complex DC was necessary because the mAB was cationic Scale-up from 1 to 450 ml, final purity at largest scale: 79%	[65]
Guinea pig serum	Method: spacer displacement chromatography Column: Fractogel DEAE 650S Flow rate: 10 ml/h Spacer/displacer: heterogeneous mixture of CM-D	Displacement on medium resolution adsorbent	[62]
Mouse liver cytosol proteins	Method: spacer displacement chromatography Column: DEAE cellulose flow rate: 5 ml/h Spacer/displacer: mixture of CM-D	Displacement on low-resolution microgranular cellulose	[62]
Lactate dehydrogenase from beef heart	*Method I*: weak anion IE-DC Column: Tris acyl DEAE, 91 × 10 mm and 250 × 10 mm Displacer: Carboxymethyl starch	Investigation of scale-up parameters (column dimensions, protein load) Comparison to EC	[68]
	Method II: weak anion IE-DC in connection to affinity chromatography (Cibacron Blue) Column: Tris acyl DEAE, 250 × 10 mm Flow rate: 0.5 ml/min Displacers: chondroitin sulfate C, alginate, and Eudragit L and S	Comparison of displacers Eudragits: readily available, cheap, nontoxic	[69]

Target molecule	Conditions	Comments	Ref.
Industrial recombinant human growth hormone	Method: anion IE-DC	Application for final polishing step	[70]
Thrombolytic protein from fermentation broth, containing albumin, insulin, transperrin, aprotinin, methotrexate, and BSA	*Method I*: strong cation IE-DC Column: 88 × 5.0 mm, 8 μm Flow rate: 0.1 ml/min Displacer: DEAE-dextran		[71]
	Method II: ABx-DC Column: 100 × 4.6 and 50 × 4.6 mm, 5 μm Flow rate: 0.1 ml/min Displacer: DEAE-dextran (10 KDa)	ABx phases are multimode antibody exchangers (Bakerbond) combining cation exchange, mild anion exchange, and mild hydrophobic interaction sites on the stationary phase surface The capacity of the ABx phase is higher; better resolution is achieved with the cation exchanger	[72]
Recombinant human antithrombin III from CHO cell culture supernatant	Method: hydroxyapatite-DC Column: 250 × 4 mm, hydroxyapatite, 2 μm, 100 nm Flow rate: 0.1 ml/min Displacer: EGTA	Crossing isotherms Final purity: 90%, recovery: 84% By comparison, a quantitative separation was not possible in the elution mode	[55,60]
Technical dairy whey	Method: strong anion IE-DC Column: BioScale-Q2, 52 × 7 mm, 10 μm Flow rate: 0.1 ml/min Displacer: PAA (M_w 6000 g/mol)	1 ml whey containing all milk proteins save the caseins was processed directly Feed: 3.45 g/L α-lactalbumin, 12.65 g/L β-lactoglobulin, other UV-active compounds Yield: α-lac 78%, β-lg 92% Concentration factor: 3	[61]

B. Amino Acids and Peptides

Modern peptide displacement chromatography started in the early 1980s and is closely connected to the group of Horvath and coworkers. Reversed-phase chromatography dominates that particular area of displacement separations. The separation of the product of a peptide synthesis from its closely related byproducts remains one of the typical applications.

Target molecule	Conditions	Comments	Ref.
Synthetic peptides *N*-Benzoyl-L-arginyl-L-methioninamide *N*-Benzoyl-L-arginyl-L-methionyl-L-leucinamide L-Methionyl-L-leucyl-L-phenylalanineamide *N*-Benzoyl-L-arginyl-L-methionyl-L-leucyl-L-phenylalaninamideamide	Displacer: BEE Decyltrimethylammonium bromide Decyltrimethylammonium bromide Cetryltrimethylammonium bromide Method: direct RP-DC Column: analytical size, various C-18 materials Enzyme reactor: immobilized carboxypeptidase Y	The peptides were both ridded of impurities and concentrated Amino acids eluted ahead of the displacement train In one case 5.2 g was recovered from a 500-ml feed in a single run	[73]
Synthetic peptide fragment corresponding to fragment 163–171 of h-interleucin-β	Method: multidimensional, RP-DC and IE-DC Column, RP-DC: LiChrosorb RP-18, 250 × 4 mm and LiChroprep RP-18, 20, 40, 80 mm Column, IE-DC: Mono-Q 50 × 5 mm, 10 μm and Q Sepharose, 350 × 10 mm Flow rate: 0.5 ml/min (two-column system) Displacer, RP-DC: benzyltributylammonium chloride Displacer, IE-DC: ammonium citrate	Large-scale application from 100 mg to 35 g of Merrifield synthesis-type product (purities >90%) No sample pretreatment necessary	[74]

Target molecule	Conditions	Comments	Ref.
Synthetic peptide containing two epitopes of *Plasmodium falciparum* circumporozoite protein (malaria vaccine)	Method: RP-DC, 23°C Column: Aquapore RP-18 250 × 4.6 mm, 7 μm, 30 nm Flow rate: 0.1 ml/min Displacer: benzyldimethyldodecylammonium bromide	Up to 50 mg was purified in a single experiment (purity >95%)	[74]
Synthetic peptides intended for *Plasmodium vivax* malaria seroepidemiology	Method: RP-DC after lyophilization, gel filtration, and IE-EC Column: Vytac 218TP5 C-18, 250 × 4mm, 5 μm, 30 nm Flow rate: 0.1 ml/min Displacer: BEE	Peptides produced by solid phase synthesis Advantages over elution chromatography demonstrated Up to 107 mg of the crude mixture was processed (final product purity: 85%)	[75]
Mellitin (honeybee venom peptide)/ synthetic variants	Method: RP-DC, 40°C Column: Hy-Tach C-18, 105 × 4.6 mm, 2 μm, nonporous Flow rate: 0.2 ml/min Displacer: benzyldimethylhexydecylammonium chloride	No intraparticular mass transfer possible 5 mg mellitin was isolated in 20 min from a 10-mg mixture	[76]
Crude α- and β-melanocyte-stimulating hormone mixtures	Method: RP-DC, 22°C Column: C-18 based on Hypersil silica, 250 × 4.6 mm, 5 μm Flow rate: 0.1 ml/min Displacer: benzyldimethyldodecylammonium bromide	30 mg was separated in a single experiment	[77]
Insulin (bovine, porcine)	Method: RP-DC Column: Nucleosil C-8, 5 μm Flow rate: 0.1 and 0.2 ml/min Displacer: cetramide	Semipreparative protocol up to 500 mg of raw insulin could be purified (proinsulin level <100 ppm)	[78]

Target molecule	Conditions	Comments	Ref.
Synthetic luteinizing hormone–releasing hormone (LHRH)	Method: RP-DC Column: RP1 DisKit column, 250 × 4.6 mm, 5 μm Flow rate: 0.5 ml/min Displacer: DisKit displacer	A displacement kit containing column, carrier, displacer, and regenerant was employed (BioWest research) Goal was to keep the peptide concentration *below* the critical value to prevent aggregation and precipitation	[12]
N^{α}-9-fluorenoxycarbonyl-*S*-tritylcysteine derivative (Fmoc-Cys-Tert-OH)	Method: normal phase DC Columns: LiChrocart RP-18, 250 × 4 mm, 10 μm (mg scale) compressed 20-,40-,80-mm columns, LiChroprep Si-60 silica, 25–40 μm (g scale) Flow rates: 0.1 ml/min (mg scale) 2 ml/min (g scale) Displacer: benzyltributylammonium chloride	Scale up from 100 mg to 38 g	[79]

C. Antibiotics

Target molecule	Conditions	Comments	Ref.
Commercial polymyxin B sulfate	Method: RP-DC Column: LiChrosorb RP-8 C-8, 250 × 4.6 mm, 5 μm Flow rate: 0.1 ml/min Displacer: dodecyloctyl ammonium chloride	Separation in the constituents Product concentrations between 10 and 20 mg/ml were reached	[80]

Target molecule	Conditions	Comments	Ref.
Oligomyxins A, B, and C	Method: RP-DC Column: Lichrosorb RP-18, 250 × 4.6 mm, 5 μm Flow rate: 0.1 ml/min Displacer: plamitic acid	Highly hydrophobic substances (carrier 75% methanol in water)	[81]
Cephalosporin C from fermentation broth	Method: RP-DC, 35°C Column: Zorbax BP C-18, 350 × 4.6 mm, 5 μm Flow rate: 0.1 ml/min Displacer: BEE	5 ml of culture supernatant was processed in 20 min	[82]

D. Isomers

Displacement chromatography has been repeatedly used by Vigh et al. to separate optical and structural isomers at high throughputs and concentrations [83]. A series of homologous displacers of varied affinity for Cyclobond II columns (α-cyclodextrin silica) was introduced by the same group in 1995 [84].

Target molecule	Conditions	Comments	Ref.
Isobufen	Displacer: 4-*tert*-butylcyclohexanone Flow rate: 0.2 ml/min	Quantitative separation even for α values of 1.08 Purities/yields were similar to elution for the less retained isomer, better for the more retained one	[85]
5,10-Dideazatetrahydrofolic acid	Displacer: cetramide Flow rate: 0.3 ml/min Method: normal phase and RP-DC, 4°C Column: β-cyclodextrin-silica (Cyclobond I), 250 × 2 mm, 2 in series		[86]

Target molecule	Conditions	Comments	Ref.
Enantiomers of 1,2-*O*-dihexadecyl-rac-glycerol-3-*O*-(3,5-dinitrophenyl) carbamate	Method: normal phase DC, 15°C Column: Pirkle-type naphthylalanine silica, 250 × 4 mm, 5 μm Flow rate: 0.5 ml/min Displacer: 3,5-dinitrobenzoyl ester of *n*-heptanol	Separation of a 20-mg sample	[87]
D,L-Methinonine β-naphthylamide	Method: enantioselective DC Column: poly-L-valyl groups as chiral selectors on modified silica, 250 × 4.6 mm Flow rate: 0.2 ml/min Displacer: D,L-mandelic acid		[88]

E. Displacement Chromatography for On-Line Product Removal Schemes

Reversible reactions require the removal of the product for high conversions. At least two cases can be found in the literature whereby displacement chromatography was used for this purpose. One concerns the preparation of a dipeptide from the respective amino acids [89]; the other the synthesis of a nucleotide [90].

Target molecule	Conditions	Comments	Ref.
N-Benzoyl-L-arginyl-L-methionin amide	Method: tandem RP-DC, 50°C, 2 columns were alternated Column: C-18, 250 × 4.6 mm, 10 μm Displacer: BEE Flow rate: 0.1 ml/min Packed bed enzyme reactor (immobilized carboxypeptidase Y) in tandem with displacement column	The enzyme reactor was operated in the recirculation mode (recycling of L-methioninamide) 460 mg of product (purity >99%) in 24 h	[89]

Target molecule	Conditions	Comments	Ref.
Nucleic acid fragments (GpU) Separation from the educt (cyclic GMP) and large excess uridine	Method: RP-frontal chromatography, RP-DC and enzyme reactor in series Column: Zorbax C-18, 250 × 4.6 mm, 5 μm Flow rate: 0.1 ml/min Displacer: *n*-butanol Packed bed enzyme reactor (immobilized ribonuclease T_1)	The enzyme reactor was operated in the recirculation mode 100 mg of GpU (purity 99.7%) in 2.4 h	[90]

F. Displacement Chromatography for Sample Preparation in Analytical Chemistry

Many analytical procedures in biochemistry, molecular biology, and related fields involve the separation of a complex mixture, e.g., a peptide digest, prior to a closer analysis of the individual components of the mixture or at least the resulting less complex mixtures. The displacement process, which will focus even trace components into highly concentrated zones while enriching all mixture components to a high extent, is a prime choice for such a sample pretreatment step. Trace components, which may be difficult to isolate by conventional chromatographic methods, can be obtained in sufficient amounts to allow chemical characterization by established techniques. Frenz et al. used such a hyphenated system to analyze the components of a tryptic digest of a recombinant growth hormone [91,92]. Several of the collected fractions showed a completely different spectrum from those seen in the preceding or following fractions of the major peptides of the digest. Presumably, these fractions represent peptides fragments of incorrectly expressed growth hormone molecules, whose detection would otherwise have been difficult. A microsystem compatible to flow rates in the microliter per minute range has been suggested for direct liquid chromatography–mass spectrometry coupling [93].

Target molecule	Conditions	Comments	Ref.
β-Naphthylamine containing an impurity at the ppm level	Method: RP-DC Column: Adsorbosphere HSC-18, 25 × 4.6 mm Flow rate: 1 ml/min Displacer: diethylphthalate	Due to the focusing effect and the possibility of using a larger sample size, the detection limit for the trace compound could be lowered by three orders of magnitude in DC compared to EC	[94]
Recombinant growth hormone (industrial product, BioWest) containing low-level impurities		Trace components (>0.1%) could be characterized by MS	[70]
Tryptic digest of recombinant growth hormone	Method: RP-DC Column: Nucleosil C-18, 150 × 4.6 mm (2 in series) Flow rate: 1 ml/min Displacer: cetramide	Displacement used in connection to FAB-MS and ESI-MS for the analysis of tryptic digests The exploitable column capacity was up to two orders of magnitude higher in DC than in EC	[91,92]
Genetic variants of β-lactoglobulin	Method: anion IE-DC Column: Protein-Pak Q-8HR, 100 × 5 mm Flow rate: 0.1 ml/min Displacer: 75-kDa dextran sulfate	Displacement used in connection with low-angle laser light scattering photometer for on-line determination of molecular mass of proteins	[95]

G. Thin-Layer Displacement Chromatography

The displacement mode has also been used in thin-layer and forced-flow thin-layer displacement chromatography (TL-DC and FF-TL-DC, respectively) by the group of Kalasz and coworkers [96,97]. The use of spacers is necessary in this case to separate the substance spots.

Target molecule	Conditions	Comments	Ref.
Parent drug and radiolysis products from rat urine	Method: TL-DC Plates: silica gel $60F_{254}$, PSC silica, TLC alumina coated on 200 × 200 mm glass plates	Spacer TL-DC and carrier spacer TL-DC were compared Various spacer/displacer mixtures were used	[98]
Deprenyl and metabolites from rat urine	Method 2D TLC (conventional TLC followed by TL-DC) Displacer: triethanolamine Spacer: Sudan black dye mixture	Analytical application for the identification of metabolites	[99]
Plant ecdysteroids	Method: TL-DC and 2D TLC Plates: silica gel $60GF_{254}$ Displacer: triethanolamine, dimethylaminopropylamine	Pilot system for determining optimum conditions for TL-DC	[100]

H. Miscellaneous

Target molecule	Conditions	Comments	Ref.
Nucleotides	Method: RP-DC Displacer: butanol		[101]
Nucleosides	Method: RP-DC Displacer: benzyltributylammonium chloride		Same
Methyl esters of polyunsaturated fatty acids (EPA, DHA)	Method: RP-DC, 30°C Column: C-18 silica Flow rate: 0.5 ml/min Displacer: oleic acid Carrier 1: acetonitrile/water 80:20 Carrier 2: acetonitrile/water 90:10	Difficult carrier selection: low solubility of polar compounds desired during binding, high solubility for high displacer concentration during separation, solution: two-carrier system Final purities >90%, concentration factors: 4–13	[102]

Target molecule	Conditions	Comments	Ref.
Oligonucleotides	Method: anion IE-DC Column: 10 in. × 10 cm Flow rate: 2.1 L/min (250 cm/h) Displacer: dextran sulfate	Large-scale approach	[49]

VII. CONCLUSIONS

Preparative chromatography remains the method of choice for the separation of many typical complex mixtures encountered in the life sciences. In many situations (trace analysis, diluted feeds, and high-throughputs among them), the displacement approach may in fact be the most practical, most economical, and easiest to realize. The goal of this chapter was to serve as an introduction to the theoretical and practical aspects of displacement chromatography from theory through method development and applications.

VIII. APPENDIX

A. Definitions

Ideal chromatography Ideal chromatography assumes infinite column efficiency, i.e., all possible band broadening effects (mass transfer, reaction kinetics, axial dispersion) are neglected. The two phases are constantly at equilibrium. Models based on ideal chromatography allow, for example, study of the influence of equilibrium thermodynamics alone on a chromatographic separation.

Linear chromatography Linear chromatography is characterized by a linear isotherm, i.e., the equilibrium concentration of a component in the mobile phase and the amount adsorbed onto the stationary phase are directly proportional at all times. The mass transfer processes are also linear. No heat or sorption effects occur. Parameters such as the viscosity of the fluid phase are independent of the composition. The mass flow rate is also constant. The sample concentration has no influence on the peak shape (Gaussian) or the retention time. Both the peak area and the peak height are proportional to the sample concentration. Analytical chromatography usually approximates linear conditions.

Nonideal chromatography Nonideal chromatography allows for band broadening effects, such as axial dispersion, mass transfer and reaction kinetics, molecular and eddy diffusion. Increasingly complex models have been developed that take into account some or all of these effects.

Nonlinear chromatography Nonlinear chromatography takes place in the nonlinear range of the equilibrium isotherm. The ratio of adsorbed to free molecules of a given type thus depends on the mobile phase concentration of the substance itself, but also on that of all other compounds present at the time (coupling of the respective mass balances via the multicomponent equilibrium isotherms). Peak shape and retention time depend on the sample composition.

B. Symbols

a_i substance-specific constant (Langmuir isotherm)
b_i substance-specific constant (Langmuir isotherm)
c_D mobile phase concentration, displacer
c_i mobile phase concentration
D diffusion coefficient
D_{bulk} bulk axial dispersion coefficient (equilibrium-dispersive model)
d_p particle diameter
H height equivalent to a theoretical plate (HETP)
$H(t)$ Step function
K equilibrium constant ($K_D = k'_D/(1 + b_D c_D)$)
k' capacity factor $(t_r - t_0)/t_0$
k_f film mass transfer coefficient
L column length
N apparent plate number of a given column ($N = H/L$)
q_D stationary phase concentration, displacer
q_i stationary phase concentration
u_D velocity of the displacer front (shock layer)
u_0 linear flow velocity (mobile phase)
t time
t_r retention time of a solute (usually approximated as the retention time of the peak maximum)
t_0 retention time of an inert tracer (column holdup time)
z dimensionless column length
$\Delta\eta_t$ shock layer thickness
α separation factor (k'_i/k'_j)
ϕ phase ratio
θ characteristic shock layer parameter (see Fig. 12 for details)
τ duration of feed introduction

C. Abbreviations

Abx antibody exchange
BEE 2-(2-butoxyethoxy)ethanol

BSA	bovine serum albumin
CM-D	carboxymethyldextran
DC	displacement chromatography
EC	elution chromatography
EGTA	ethylenglycolbis(β-aminoethylether)-*N*,*N*,*N*′,*N*′-tetraacetic acid
ESI	electrospray ionization
FAB	fast atom bombardment
HETP	height equivalent to a theoretical plate
HIC	hydrophobic interaction chromatography
HPDC	high-performance displacement chromatography
HPLC	high-performance liquid chromatography
IDA	imminodiacetic acid
IE-DC	ion exchange displacement chromatography
IMAC	immobilized metal affinity chromatography
LCST	lower critical solution temperature
LHRH	luteinizing hormone–releasing hormone
mAb	monoclonal antibody
MS	mass spectrometry
PAA	polyacrylic acid
PEI	polyethyleneimine
RP-DC	reversed-phase displacement chromatography
SMA	steric mass action
TLC	thin-layer chromatography
TL-DC	thin-layer displacement chromatography
2D	two-dimensional
UV	ultraviolet

REFERENCES

1. Antia F, Horvath C. Ber Bunsenges Phys Chem 1989;93:961–968.
2. Cramer SM, Subramanian G. Sep Purif Meth 1990;19(1):31–91.
3. de Carli JP, Carta G, Byers Ch H. AlChE J 1990;36(8):1220–1228.
4. Glückauf E. Proc R Soc London A 1946;186:35.
5. Helfferich F, Klein G. Multicomponent Chromatography. New York: Marcel Dekker, 1970.
6. Rhee H.-K., Aris R, Amudson NR. AlChE J. 1982;28:423.
7. Bellot JC, Condoret JS. J Chromatogr 1993;657:305–326.
8. Phillips MW, Subramanian G, Cramer SM. J Chromatogr 1988;454:1–21.
9. Gu T, Tsai G-J, Tsao GT. Adv Biochem Eng 1993;49:45–71.
10. Katti AM, Guiochon G. J Chromatogr 1988;449:25–40.
11. DeVault D. J Am Chem Soc 1943;65:532.

12. Jakobson J. In: Horvath C, Ettre LS, eds. Chromatography in Biotechnology, ACS Symposium Series, Vol. 529, 1993:77–84.
13. Freitag R, Vogt S. Cytotechnology, accepted for publication.
14. Helfferich F, James DB. J Chromatogr 1970;46:1–28.
15. Rhee H-K, Aris R, Amundson NR. First Order Partial Differential Equations II. Theory and Applications of Hyperbolic Systems of Quasilinear Equations. Englewood Cliffs, NJ: Prentice-Hall, 1989.
16. Frenz J, Horvath C. AIChE J 1985;31(3):400–409.
17. Brooks CA, Cramer SM. AIChE J 1992;38:1969–1978.
18. Velayudhan A, Horvath C. J Chromatogr 1988;443:13–29.
19. Kopaciewicz W, Rounds MA, Fausnaugh J, Regnier FE. J Chromatogr 1983;266:3.
20. Kim YJ. Bioseparation 1995;5:295.
21. van Deemter J, Zuiderweg F, Klinkenberg A. Chem Eng Sci 1956;5:271.
22. Knox H, Saleem M. J Chromatogr Sci 1972;10:80.
23. Guiochon G, Golshan-Shirazi S, Katti A. Fundamentals of Preparative and Nonlinear Chromatography. San Diego: Academic Press, 1994.
24. Golshan-Shirazi S, Guiochon G. J Chromatogr 1992;603:1–11.
25. Lapidus L, Amudson NR. J Phys Chem 1952;56:984.
26. Thomas HC. J Am Chem Soc 1944;66:1664.
27. Goldstein S. Proc R Soc London 1953;A219:151.
28. Wade JL, Bergold AF, Carr PW. Anal Chem 1987;59:1286.
29. Glückauf E, Coates JI. J Hem Soc. 1947;1315.
30. Hiester NK, Vermeulen T. Chem Eng Progr 1952;48:505.
31. Lin B, Golshan-Shirazi S, Gulochon G. J Phys Chem 1989;93:3363.
32. Rasmuson A, Neretnieks I. AIChE J 1980;26:686.
33. Rasmuson A. Chem Eng Sci 1982;37:787.
34. Zhu J, Guiochon G. J Chromatogr 1994;659:15–25.
35. Zhu J, Ma Z, Giochon G. Biotechnol Prog 1993;9:421.
36. Liao A, Horvath C. Ann NY Acad Sci 1988;589:182–191.
37. Zhu J, Katti A, Guiochon G. Anal Chem. 1991;63:2183–2188.
38. Antia FA, Horvath CG. J Chromatogr 1991;556:119–143.
39. Frey DD. J Chromatogr 1987;409:1–13.
40. Lin B, Ma Z, Golshan-Shirazi S, Gulochon G. J Chromatogr 1989;475:1–11.
41. Carta G, Dinerman AA. AIChE J 1994;40(10):1618–1628.
42. Kim YJ, Cramer SM. J Chromatogr 1991;549:89–99.
43. Kasper C, Breier J, Vogt S, Freitag R. Bioseparation 1996;6:247–262.
44. Freitag R, Breier J. In: Pyle DL eds. Separations for Biotechnology, published by the Royal Society of Chemistry, Thomas Graham House, Science Park, Cambridge, UK, 1994:166–172.
45. Subramanian G, Phillips MW, Jayaraman G, Cramer SM. J Chromatogr 1989;484: 225–236.
46. Felinger A, Guiochon G. J Chromatogr. 1992;609:35–47.
47. Gerstner JA, Morris J, Hunt T, Hamilton R, Afeyan NB. J Chromatogr 1995;695: 195–204.
48. Subramanian G, Cramer SM. Biotechnol Prog 1989;5(3):92–97.
49. Gerstner JA. BioPharm 1996;9:30.

50. Freitag R, Horvath C. Adv. Biochem Eng Biotechnol 1995;53:17–59.
51. Peterson EA. Anal Biochem 1978;90:767–784.
52. Antia F, Fellegvari I, Horvath C. Ind Eng Chem Res 1995;34:2796–2804.
53. Gerstner JA, Cramer S. Biotechnol Prog 1992;8:540–545.
54. Gerstner JA, Cramer S. BioPharm 1992;Nov/Dec:42–45.
55. Freitag R, Breler J. J Chromatogr 1995;691:101.
56. Gadam SD, Cramer SM. Chromatographia 1994;39(7/8):409–418.
57. Jayaraman G, Li Y-F, Moore JA, Cramer SM. J Chromatogr 1995;702:143–155.
58. Jen SCD, Pinto NG. J Chromatogr Sci 1991;29:478–484.
59. Jen SCD, Pinto NG. J Chromatogr 1990;519:87–98.
60. Kasper C, Breler J, Vogt S, Freitag R. Bioseparation 1996;6:247–262.
61. Vogt S, Freitag R. J Chromatogr 1997;760:125–137.
62. Torres AR, Peterson EA. J Chromatogr 1992;604:39–46.
63. Patrickios CS, Gadam SD, Cramer SM, Hertler WR, Hatton TA. Biotechnol Prog 1995;11:33–38.
64. Vogt S, Freitag R. (submitted).
65. Tores AR, Peterson EA. J Chromatogr 1990;499:47–54.
66. Peterson EA. Anal Biochem 1978;90:767–784.
67. Torres AR, Krueger GG, Peterson EA. Anal Biochem 1985;144:469–476.
68. Ghose S, Mattiasson B. J Chromatogr 1991;547:145–153.
69. Ghose S, Mattiasson B. Biotechnol Tech 1993;7(8):615–620.
70. Frenz J. LC/GC Int 1992;5(12):18–21.
71. Kim, YJ. Biotechnol Tech 1995;9(6):417–422.
72. Kim, YJ. Biotechnol Tech 1994;8(7):457–462.
73. Cramer SM, Horvath C. Prep Chromatogr 1988;1(1):29–49.
74. Viscome GC, Cardinali C, Longobardi G, Verdini AS. J Chromatogr 1991;549: 175–184.
75. Bianchi E, Del Guidice G, Verdini AS, Pessi A. Int J Peptide Protein Res 1991; 37:7–13.
76. Kalghatgi K, Fellegvari I, Horvath C. J Chromatogr 1992;604:47–53.
77. Viscomi GC, Lande S, Horvat C. J Chromatogr 1988;440:157–164.
78. Vigh G, Varga-Puchony Z, Szepesi G, Gadzag M. J Chromatogr 1987;386:353–362.
79. Cardinalli F, Ziggiotti A, Viscomi GC. J Chromatogr 1990;499:37–45.
80. Kalasz H, Horvath C. J Chromatogr 1981;215:295–302.
81. Valko K, Slegel P, Bati J. J Chromatogr 1987;386:345–351.
82. Subramanian G, Phillips MW, Cramer SM. J Chromatogr 1988;439:341–351.
83. Vigh G, Quintero G, Farkas G. In: Horvath C, Nikelly JG eds. Washington, DC: American Chemical Society (ACS) Symposium Series, Vol. 434, 1990:181–197.
84. Quintero G, Vo M, Farkas G. Vigh G. J Chromatogr 1995;693:1–5.
85. Farkas G, Irgens LH, Quintero G. Beeson M, Al-Saeed A, Vigh G. J Chromatogr 1993;645:67–74.
86. Irgens LH, Farkas G, Vigh G. J Chromatogr 1994;666:603–609.
87. Camacho-Toralba PL, Beeson MD, Vigh G. J Chromatogr 1993;646:259–266.
88. Sinibaldi M, Castellani L, Federici F, Messina A. J Liquid Chromatogr 1993; 16(14):2977–2992.

89. Cramer SM, el Rassi Z, Horvath C. J Chromatogr 1987;394:305–314.
90. El Rassi Z, Horvath C. J Chromatogr 1983;266:319–340.
91. Frenz J, Quan CP, Hancock WS, Bourell J. J Chromatogr 1991;557:289–305.
92. Frenz J, Bourell J, Hancock WS. J Chromatogr 1990;512:299–314.
93. Vigh G, Irgens LH, Farkas G. J Chromatogr 1990;502:11–19.
94. Ramsey R, Katti AM, Guiochon G. Anal Chem 1990;62:2557–2565.
95. Mhatre R, Qian R, Krull IS, Gadam S, Cramer S. Chromatographia 1994;38(5/6): 349–354.
96. Kalasz H, Nagy J, Bathori M. J Planar Chromatogr 1989;2:39–43.
97. Kalasz H, Kerecsen L, Nagy J. J Chromatogr 1984;316:95–104.
98. Kalasz H, Bathori M, Matkovics B. J Chromatogr 1990;520:287–293.
99. Kalasz H. J High Resol Chromatogr & Chromatogr Commun 1983;6:49–50.
100. Kalasz H, Bathori M, Kerecsen L, Toth L. J Planar Chromatogr 1993;6:38–42.
101. Horvath C, Frenz J, el Rassi Z. J Chromatogr 1983;255:273.
102. Huang S-Y, Jin J-D. Bioseparation 1994;4:343–351.

8

High-Performance Membrane Chromatography of Proteins

Tatiana Tennikova
Russian Academy of Sciences, St. Petersburg, Russia

Ruth Freitag
ETH Lausanne, Lausanne, Switzerland

I. INTRODUCTION

According to the International Union of Pure and Applied Chemists (IUPAC) recommendations [1], "chromatography is a physical method of separation in which the components to be separated are distributed between two phases, one of which is stationary (stationary phase) while the other (the mobile phase) moves in a definite direction." Today we also have chromatographic methods whereby the two phases are in countercurrent motion, e.g., the simulated moving bed, the continuous annular chromatography, etc. All chromatographic methods have one thing in common and that is the dynamic separation of a substance mixture in a flow system. Usually the chromatographic separation process takes place in a column packed with the particles of the sorbent (stationary/solid phase). Modern high-performance liquid chromatography (HPLC) uses an extensive arsenal of stationary separative phases that can effectively separate a wide variety of mixtures both of small molecules and of polymeric substances, including most importantly biologicals and biopolymers. According to the modern HPLC theory, the sorbent particles can be regarded as rigid spheres of micrometer size that differ considerably in porosity, i.e., ranging from totally nonporous to flow-through (perfusive) ones.

The adsorptive or interactive forms of HPLC are clearly the most important ones for users in biotechnology and related fields. In these cases an adsorption–desorption respectively a partitioning reaction takes place between the substances to be separated and the sorbent (stationary phase). These interactions can be of an electrostatic, hydrophobic, but also highly specific (biological complementary type) character, as indicated by the respective names, such as ion exchange, reversed-phase, hydrophobic, pseudoaffinity, and affinity chromatography.

As mentioned above, HPLC is a most important tool for the analytical and preparative separations of biomolecules, in particular proteins. The complex and peculiar physicochemical character of these biopolymers has been a constant incentive to the development and deeper understanding of the methods that are used for their analysis and isolation.

II. "ONE-STEP" DESORPTION AND "MULTIPLE-STEP" INTERACTION PROCESS IN CHROMATOGRAPHIC SEPARATIONS

The chromatographic column packed with small particles of porous sorbent is the main locus and thus a most important aspect of the HPLC separation processes under discussion. The molecules of the substances to be separated are dissolved in the mobile phase. In the case of conventional porous particles these molecules are flushed with the mobile phase through the interparticle space of the column and migrate by molecular diffusion through the stagnant fluid layer around each particle to the outer surface of the sorbent bead, followed by penetration into the porous bead by the same mechanism and, finally, adsorption on the inner surface of the pores, where more than 90% of the total surface is found (Fig. 1).

The act of desorption, when molecules adsorbed on the sorbent surface are displaced again by competing molecules from mobile phase (the modifier), is really decisive for the separation, as differences in the desorption reaction rate constants are larger than those of the adsorption reaction rate. It must be well understood that even in a fairly short column the adsorption-desorption process takes place many times and the effect on the separation of the substances is "accumulated" as the substance molecules move from the top to the bottom of the column.

In the interactive types of chromatography the substances can be separated using two modes of elution: *isocratic elution* whereby the modifier (a competitor for the adsorptive sites on the sorbent surface) is added to the eluent at constant concentration, and *gradient elution* whereby the modifier concentration in the mobile phase is increased during the separation either gradually or stepwise. Gra-

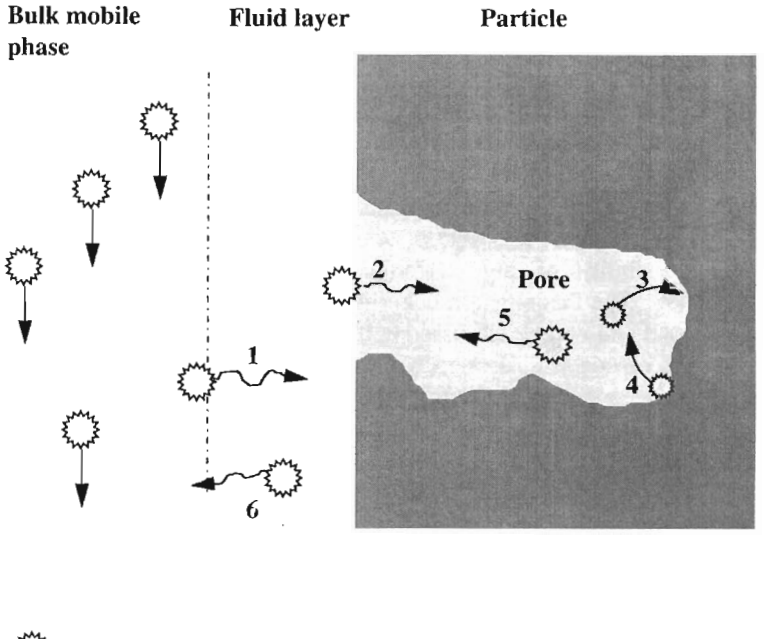

Figure 1 Stages involved in the transfer of an analyte molecule from the bulk of the mobile phase to the sorbent surface, where the adsorption/desorption reaction takes place, and back into the bulk mobile phase. (1) Diffusion from the bulk mobile phase through the stagnant film around the particle to the outer particle surface; (2) molecular diffusion into the pore; (3) adsorption; (4) desorption; (5) molecular diffusion from the inner pore surface through the pore space to the outer surface (pore mouth); (6) diffusion through the stagnant film into the bulk mobile phase.

dient elution is more common in protein chromatography than isocratic elution because proteins tend to vary widely in adsorption energy. Thus it is often impossible to find a single mobile phase composition that will desorb them all.

Since proteins differ widely in adsorption energy due to pronounced differences in the desorption rate constant. Theoretically it is therefore possible to separate different substances in a single desorption step. It is therefore reasonable to suggest that the separation of some definite group of substances (e.g., proteins) is possible without using the whole length of column, i.e., repeated adsorption–desorption events. This theoretical possibility has recently found a practical application in a new chromatographic method, i.e., membrane chromatography. This

type of separation technique employs what is sometimes called a "membrane adsorber" as stationary phase. This term comes from membrane/filtration technology and describes the geometry of the stationary phase in question, an interactive, i.e., adsorptive, "filter" membrane. Various types of filtration operation have been adapted to separation processes simply by using an interactive instead of an inert membrane, including hollow fibers, cross-flow units, and others. These methods have led to some interesting applications, some of which are included in Section VI of this chapter. However, especially in the case of protein chromatography, the possibility of high-performance membrane chromatography (HPMC) also exists. The theoretical model of this exciting new method has by now been developed and will be discussed in the following two sections. HPMC is carried out on a certain well-defined type of separation media, the so-called (convective interactive media) CIM discs, i.e., monolithic macroporous discs with a well-defined and homogeneous pore structure design. Such monolithic layers allow the construction of a rigorous theoretical model of the dynamic interphase distribution of the substances during separation.

Formally, HPMC still falls into the IUPAC definition (see above) of chromatography as a dynamic separation of substances, if we accept the exchange of a flat macroporous adsorptive layer for a complicated and expensive system like a shallow packed column. The interaction mechanism can still be the same, i.e., electrostatic interaction between charged units on the adsorber surface and oppositely charged groups on the protein surface. From the geometrical design of the support one speaks correctly of a "membrane" (or a disc). From a chromatographic point of view, this is still only a sorbent acting in the same way as the packed HPLC column of the conventional systems.

A major difference in the theoretical treatment of disc versus column chromatography remains and that is the small length of the "separation distance," i.e., the thickness of the membrane, which a priori does not make any "multiple" or "repetitive" interaction likely. To gain a very clear picture of what is going on, one should regard the separation as the result of a one-step desorption process. This does not mean that the adsorption step can be neglected in membrane chromatography. On the contrary, since membrane chromatography is a single-step process, the initial adsorption and its energy distribution has much more consequence in membrane than in conventional chromatography, where any distribution will be averaged out over the multitude of repeated adsorption–desorption steps taking place along the column length (along the path of molecular migration). Membrane chromatography represents the unique possibility to see a "momentary" picture of the molecules' distribution after the initial adsorption. It is obvious that the theoretical treatment, as well as the practical applications of this separation process, should take this very important feature into consideration.

III. THEORETICAL MODELS OF INTERACTIVE CHROMATOGRAPHIC SEPARATION

Membrane chromatography is a method based on the *selective separation of adsorbed substances as a consequence of the desorption process* [2]. Taking into account the huge amount of practical and theoretical research concerning models of the interactive types of HPLC, a brief analysis of the major points will be useful to understand the new chromatographic process.

A. Gradient and Isocratic Elution Chromatography

Cited most often are the papers of Snyder et al. [3–5], which can be considered as the most fundamental. These papers are the result of a detailed investigation of the process of gradient and isocratic HPLC of both small and large molecules. Since we are mainly interested in the chromatography of proteins, the most important understanding to be drawn from these papers is that of the role played by the mobile phase modifier during the desorption of the protein molecules during gradient elution. Snyder introduces a definition of the capacity or retention factor k′, which in this case will correspond to a value averaged over the entire column length. Parameter k′ is largely dependent on the act of desorption [5]. The model is based on the idea of a "multiple plate" [6] (or "multiple-step") adsorption–desorption process and applies to both the isocratic and the gradient mode of elution.

From our point of view, the most interesting aspect of this theory is the conclusion that the number of parameters responsible for the effective resolution of a protein mixture does not depend on column length. In the past this has served as a rationale for the development of thin adsorptive porous layers as a stationary phase for protein chromatography.

B. Perfusion Chromatography and Other Modes of Chromatographic Separations with Putatively Improved Mass Transfer

Conventional packed columns require high pressure to drive the mobile phase through the packed bed at a sufficiently high linear flow rate. The high linear flow rates necessary to achieve separations within a practical period of time entail also significant diffusional limitations, particularly when proteins, which have a much lower diffusivity than small molecules, are concerned. Both problems were addressed and partially solved with the development of the so-called perfusion columns [7–9].

Perfusion columns are packed with sorbent particles having bidisperse po-

rous structure. The big pores with a size comparable to the size of the channels formed by the interparticle space allow mass transport into the particle by convection rather than diffusion. The channels "divide" the particle into smaller segments, which is an important factor for the decrease of the distance to be covered by diffusion by a molecule on its way to the adsorptive surface. Thus the mass transfer is much more rapid in perfusion than in conventional porous supports. The second type of pores, which also exists in the perfusion particles, consists of non-flow-through channels of much smaller diameter and was called "diffusion" pores by the inventors. It is implied that the majority of the adsorptive surface is located in the diffusion pores and that the separation takes place there as well, in accordance with the adsorption–desorption mechanism. Thus, the major advantage of perfusion chromatography is the improved mass transfer of the substance from the mobile phase to the stationary one [10–14]. The enhancement is due to the fact that the solubilized molecules are transferred through the stationary phase particle (site of adsorption–desorption) by convection rather than by molecular diffusion.

Membrane chromatography is often linked or compared to perfusion chromatography because some superficial resemblance exists. In membrane chromatography the mobile phase flows through the sorbent layer or, more correctly, through the single "particle," just as in perfusion chromatography. However, these two methods cannot be described with the same mathematical equations. The main difference is that in membrane chromatography the adsorption–desorption process takes place on the walls of flow-through channels under the conditions (pressure, shear stress, etc.) defined by the flow rate of the mobile phase. There are no diffusive pores. Rather than as a column, the membrane can be imagined as a bundle of capillaries of different diameters but of the same extremely small length. In membrane chromatography the step of intraparticle diffusion is absent. So there is no necessity of considering any migration into the particle by molecular diffusion followed by the adsorption on the inner particle surface. From the many equations describing diffusional effects in conventional HPLC, only a single one remains relevant in membrane chromatography. This is the diffusional migration through the boundary layer of liquid close to the walls of pores. Another important difference between the theory of membrane chromatography and that of perfusion chromatography is that the desorption act itself is not considered important in the latter and that perfusion chromatography, just as conventional chromatography, is modeled by assuming repetition (and accordingly, averaging of the parameters) of the adsorption–desorption process as the separation evolves along the column [12–14].

A pronounced improvement of the mass transport kinetics was also observed in another type of HPLC column where totally nonporous particles with bonded adsorptive phase on their surface were used [15,16]. This type of station-

ary phase bears a strong resemblance to chromatographic discs with a controlled porous structure [17–25]. Adsorption occurs at the outer surface of the particles under the direct influence of the mobile phase, which flows through micrometer-sized interparticle channels that the particles form between them. However, in terms of column geometry, the governing principle is again a multistep interaction between the substance and the sorbent surface. Besides that, monosized beads of a certain diameter are necessary to ensure that the size of the flow-through channels is large enough for a practically maintainable pressure–flow curve. This usually means a reduction of the surface area by several orders of magnitude when nonporous rather than porous beds are used. In adsorption and especially so in preparative adsorption chromatography this quickly becomes a handicap.

The monolithic rod columns also show improved mass transfer kinetics [26–38]. Such sorbents are formed by the in situ polymerization of a continuous macroporous polymer network inside a tube. As in the case of the columns packed with nonporous particles (or indeed of chromatographic discs), the various types of diffusional resistance to the mass transport are eliminated in the continuous bed columns. The separation process is characterized by quick kinetics and high resolution of peaks; it again remains a multistep process.

It is interesting to note that while the polymer structure of the monolithic porous rod columns and the monolithic porous discs may be very similar, the process of separation is different in these cases simply as a result of the difference in geometry. The long "rod," just like any other column, allows for a repetition of the adsorption–desorption act. As a result, the chromatographic peaks reflect the average of the various band broadening effects and the peaks will always be narrower than those obtained in an analogous separations using discs. Moreover, the multiple character of the adsorption–desorption event aids high-speed separations of small molecules using the rod columns [32]. In counterdistinction, a separation of the small molecules is much more difficult in disc chromatography, simply because in this case the separation relys mainly on the initial differences in the energy of interaction of the molecules with the surface ligands. For small molecules this difference is normally much smaller.

C. The Stoichiometric Retention Model

In ion exchange protein chromatography it is common to express the experimentally determined parameter k′ (capacity or retention factor) as a function of the charged modifier concentration in the mobile phase. Generally, the relationship can be reduced to an equation of the following form:

$$k' = e^{f(\phi)} \tag{1}$$

where f(ϕ) can be presented as polynom. In the most cases, it is possible to approximate f(ϕ) by a linear relationship that yields an equation like

$$k' = Me^{-S\phi} \tag{2}$$

For practical reasons, the logarithmic form of this equation is normally used:

$$\ln k' = \ln M - S\phi \tag{3}$$

where M and S are constants defined by the nature of the protein and ϕ is a variable value representing the modifier concentration in the eluent.

A very thorough experimental and theoretical investigation of this relation was carried out by Regnier and coworkers [39–41]. In these papers, a theoretical retention model is constructed by applying the law of mass action to describe the various interactions in the system, e.g., competition between protein and modifier, interaction between protein and sorbent or sorbent and modifier. Unfortunately, this model cannot be extended to the nonlinear range of the adsorption isotherm, i.e., the region where most preparative chromatography occurs.

Upon analysis of the various equilibria and writing the corresponding equations, the authors come to the following expression which relates the retention factor to the concentration of the desorbing agent (modifier):

$$k' = N\psi^{-Z} \tag{4}$$

where N is a constant, ψ is the concentration of the modifier [mol/L], and Z is a stoichiometric parameter related to the number of moles of modifier needed for the solvation of the adsorptive sites on the protein, and also to the stationary phase adsorption of the modifier. *The parameter Z is a cornerstone in the theory of the separation of proteins by interactive chromatography*. The value of k′ may change from 0 (at $\psi \rightarrow \infty$) to infinity (at $\psi \rightarrow 0$) in this system.

Equation (4) bears a certain mathematical similarity to Eq. (2). They become identical near the desorbing concentration of the modifier. It may be irritating to realize that the dimensionless factor k′ is expressed as a function of two values, N and ψ (Z is an numerical parameter), which bear dimensions. However, the logarithmic form of (4) has been used successfully in praxis for some time now and an excellent correlation between the experimental results and the predicted values are normally found for both isocratic reversed-phase and ion exchange chromatography of proteins:

$$\ln k' = \ln N - Z \ln \psi \tag{5}$$

D. Retention Model for "Short Separation Layer" Chromatography

A theoretical model of protein retention (and separation) in disc chromatography should without fail take into account equations for the discussed above equilibria.

Since the separation of the substances according to our idea occurs by a one-step act of adsorption–desorption (more exactly, the single step of desorption), the initial distribution of the protein molecules at the adsorptive surface located at the inner walls of the disc pores (channels) is most important. This distribution is governed by the energy of interaction, which in turn is characterized by the Z parameter. The desorbed molecules instantaneously leave their "landing grounds" and are flushed from the disc by the flow of the mobile phase. In this situation the Z parameter is not averaged as in the case of multiple adsorption–desorption acts in a column.

For the chromatography over short distances (discs) it is important to examine the parameter as a function of time and, equivalently, space. The former corresponds to a separation on a very short column with the efficiency of "one theoretical plate" [42], while the latter acknowledges the existing of some definite "length of separation layer" [43,44]—terms that take into account the nonstationary nature of the initial part of the process of gradient elution in a column. It is useful to keep these terms in mind when choosing the gradient shape and comparing it with the real length of separation layer, i.e., the thickness of the actual disc. Unfortunately, it is not possible to give a full summary of the published data, which could be interesting for the theory of HPMC. The interested reader is referred to some of the, in our opinion, most significant papers [45–49].

IV. PRINCIPLES OF PROTEIN SEPARATION IN MEMBRANE CHROMATOGRAPHY

A. Peculiarities of Proteins as Objects of Separation Processes Governed by Mass Transfer Effects

The topic of this chapter is the separation of soluble proteins by HPMC. It is therefore useful to recall some of the main physical parameters governing the behavior of these globular structures [50]. The features to be discussed differ significantly between proteins and smaller molecules when chromatography is concerned. They influence (1) the kinetics of the adsorption process, (2) its thermodynamics, and (3) the character of the interaction between the protein molecules and a surface.

It is first necessary to attribute the diffusional mobility (or diffusivity) of proteins to the kinetic peculiarities. The diffusivity of proteins is two to three orders of magnitude less than that of small molecules (including the solvent and the modifier molecules; in other words, the eluent). This means that the residence time of a protein molecule in the mobile phase between consecutive adsorption–desorption acts is 2–3 times as large as that of a small molecule also present in the eluent, e.g., the modifier.

A thermodynamic peculiarity of proteins, which also differentiates them from small molecules, is the so-called steric factor. It is obvious that a molecule of the size of a protein will experience significant steric limitations when inside the pore channels of a porous particle. In addition, it becomes increasingly difficult to enter the "mouth" of a pore channel. This phenomenon is most important for sorbents with rigid pore structure.

The peculiarity of interaction is also linked with the size of the protein molecule. Protein molecules, which can be seen as large globules, carry at their outer surface the functional groups that provide an adsorptive interaction with the sorbent. The distribution of these interactive groups on the protein surface is not a statistical one; instead, one finds local groups or clusters. This leads to isolated strong interaction sites, which are inhomogeneously distributed over the surface of the protein globule. This distribution, which partially defines the Z parameter, differs widely between molecules. This difference is exploited in their separation by HPMC.

Besides the above-mentioned peculiarities, which influence the chromatographic process, it is useful to remember some others aspects that can also become decisive in the different modes of interaction chromatography. In particular, we should remember the concentration effect, which becomes influential whenever the protein concentration is high enough to make the presence of more than one molecule in a given pore likely. Apart from the concentration effect, proteins will affect the adsorption of each other. This synergistic effect should always be considered together with the concentration effect. Last but not least, it is necessary to acknowledge the effect of "hysteresis," i.e., the fact that for many proteins adsorption and desorption isotherms do not coincide. This phenomenon can be observed because of the multiple-point character of the interaction of the protein with the sorbent surface. The desorption of the protein needs a higher modifier concentration than the one that allows its adsorption.

B. One-Step Desorption Process

Originally, the reason for wanting to model adsorption chromatography on thin layers ("membranes") of sorbent was the observation that often the separation effect of a column seemed to be independent of the column length [5,42–55]. Protein mixtures can often be separated on columns 5–10 cm in length. The models were to aid a better understanding of this phenomenon. A first consequence was a change in the phraseology, e.g., a change from the term "column length" to the concept of "operative thickness (length) of adsorption layer," which corresponds to the minimum distance necessary to achieve a specific separation.

A simple experiment demonstrating this effect can be performed by anybody involved in column chromatography [56]. Inject a sample of a protein mix-

ture into your column, then turn it up-side down and elute in your standard linear gradient. Quite often you will see no difference in the resolution compared to that obtained when the entire "separation length" is used. In this experiment the operative thickness of the separation layer is defined by an amount of protein in the sample.

The traditional understanding of (column) HPLC is that the experimentally observed separation effect is accumulated during multiple acts of adsorption–desorption. Within this theoretical framework, the effect of the initial step is considered as too insignificant to deserve or require an individual evaluation. In this context the theory of HPMC, as outlined below, may well engender a change of mind. Unless indicated otherwise, the model described below interprets separations by disc chromatography as a one-act desorption process even in such cases where the theoretical separation layer thickness does not exactly correlate with the physical thickness of the chromatographic disc.

In our development we propose that expression (4) can indeed be used to describe correctly the experimentally obtained equilibrium adsorption. For convenience's sake we change to a single variable and write the expression for the retention factor in a reduced form:

$$k' = \tau^{-z} \tag{6}$$

which is the result of the following substitution:

$$\tau = \frac{\psi}{\psi_0} \tag{7}$$

where $\psi_0 = N^{1/Z}$ is the value of ψ at $k' = 1$.

By affecting these changes we are no longer troubled by the dimensions or the lack of them for certain of these numbers.

Regnier and coworkers [40] recently published a theoretical model capable of describing the experimental data of the equilibrium separation of proteins according to both the ion exchange and the reversed-phase mechanism for isocratic elution. However, the separation of proteins by adsorption chromatography is usually done by gradient elution, where k' becomes a function of ψ [often given as $\psi = \psi(t)$] in dependence of the gradient shape. Under these circumstances, the adsorption process cannot be considered at equilibrium.

If the adsorption process is to be described in a statistical mode [57,58] the probability of residence of the desorbed protein in the mobile phase at equilibrium (P_b) must be introduced. This probability is defined via the equilibrium retention factor, k':

$$P_b = \frac{1}{1 + k'} = \frac{1}{1 + \tau^{-z}} \tag{8}$$

Note that the probability is normalized because the sum of the probability of residence of the desorbed protein in the mobile phase and the probability of residence of the protein in the stationary phase $P_a = k'/(1 + k')$ needs to be 1. One can correctly estimate the probability of residence of the protein in the mobile phase at equilibrium as the integral over the probability of a transition of the protein from the stationary to the mobile phase under nonequilibrium conditions. The latter, in its turn, is defined as the derivative of P_b over Ψ:

$$\rho = \frac{(k')'_\psi}{(1 + k')^2} = \frac{Z\tau^{-z-1}}{(1 + \tau^{-Z})^2} \tag{9}$$

In other words, ρ is a probability density and the value $\rho(\psi)d\psi$ is the probability of the transition of a protein molecule from the stationary to the mobile phase in a certain mobile phase modifier concentration interval. The value $\psi = \psi_0$ corresponds to the maximum of $\rho(\psi)$.

To make this clearer, one can draw an analogy to the analysis of the pore size distribution in a chromatographic sorbent by mercury porosimetry. In this method, mercury vapor is forced into the pores of the support at different pressures. For each pressure value the corresponding equilibrium amount of mercury in the pores is determined. In our case this is analogous to the determination of the protein amount in a mobile (or stationary) phase as a function of the modifier concentration. In mercury porosimetry, a curve is defined, which links the equilibrium amount of mercury to the pressure drop. This curve represents the integral over the pore size distribution. In the case of a continuous increase of the pressure from zero to a defined value, we obtain the point of the curve corresponding to the adjusted pressure value. Moreover, the measured value will be totally independent of the way the pressure was changed on the way. In the same manner is the distribution of a protein between the mobile and the stationary phase independent of past changes in the eluent composition.

Thus, the concept of a probability density allows to use expression (6) to define the moments of the parameter τ. The first moment describes the average modifier concentration at which the protein is desorbed whereas the second moment defines the dispersion of this desorption process.

C. Peak Parameters in Desorption Chromatography

The experimental values of the Z parameter introduced in Eqs. (4) and (5) fall for all proteins within a narrow interval (10^1–10^2). This is a direct consequence of the peculiarities of protein adsorption discussed above. We will use this fact in the calculations of the moments following below. By combining Eqs. (6), (8), and (9) we obtain the following expression for the first moment:

$$\langle\tau\rangle = \int_0^\infty \tau \cdot \rho(\tau)d\tau = \frac{\pi/Z}{\sin(\pi/Z)} \tag{10}$$

By analogy, for the second moment we find:

$$\langle\tau^2\rangle = \int_0^\infty \tau^2 \cdot \rho(\tau)d\tau = \frac{2\pi/Z}{\sin(2\pi/Z)} \tag{11}$$

Taking into account that $Z \gg 1$, we obtain for the first moment:

$$\langle\tau\rangle \cong \frac{1 + \pi^2}{6Z^2} \tag{12}$$

and for the second moment:

$$\langle\tau^2\rangle \cong \frac{1 + 2\pi^2}{3Z^2} \tag{13}$$

The dispersion is defined by:

$$\sigma^2 = (\langle\tau^2\rangle - \langle\tau\rangle^2) \cong \frac{\pi^2}{3Z^2} \tag{14}$$

From the last equation, an expression for the Z parameter can be derived:

$$Z = \frac{\pi}{\sqrt{3}\sigma} \tag{15}$$

Recently it was shown [57] that expressions (12) and (13) reflect a fundamental property of the process described by Eq. (4).

Combining Eq. (12), for the first moment, with Eq. (7) shows that, given the typical protein values of Z, the average modifier concentration necessary for protein desorption is equal to that for which $k' = 1$. This concentration corresponds to the x axis intercept of a plot of ln k' as a function of ψ (Fig. 2). Whether or not a protein separation according to Eq. (6) is possible depends on the differences in the x axis intercepts of the corresponding plots and thus only on the Z parameters of the proteins [57]. Besides that, it follows that all proteins are separated at the same k' value. This conclusion was reached before [43], but in another context.

Since the dispersion can be calculated from Eq. (14) and the Z parameter from Eq. (15), it follows that the elution peak of a given protein seen after a one-step desorption process is mathematically described by the probability density, ρ, as a function of ψ. To obtain a more accurate expression for Z would necessitate a measurement of the peak shape of the same protein passed through the chromatographic layer in the absence of adsorptive interaction.

It was shown [58] that for processes describable by Eq. (4) or the corre-

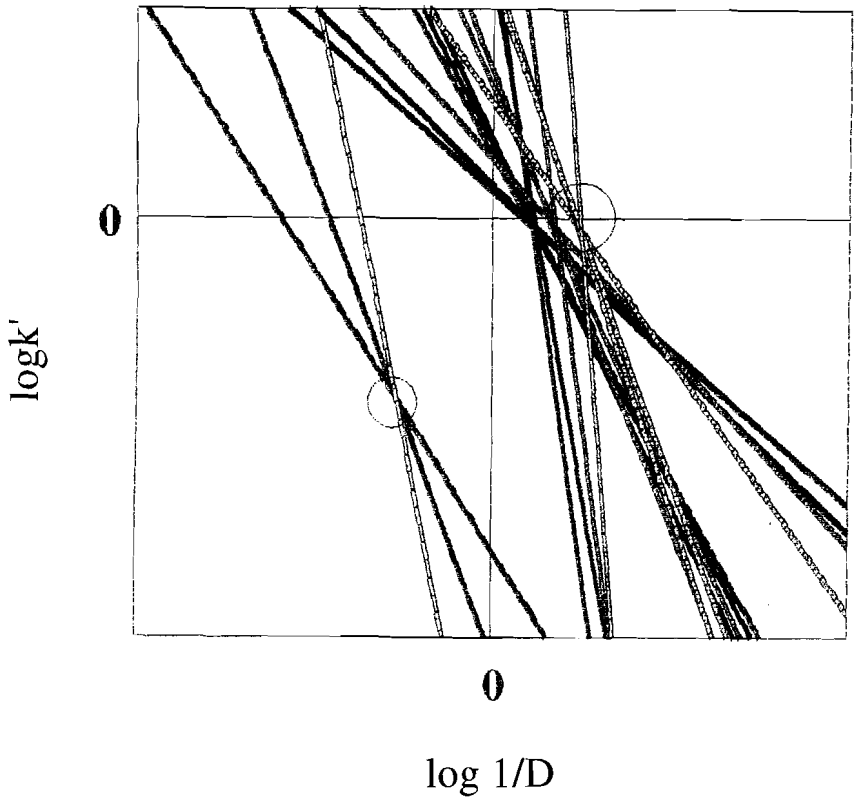

Figure 2 Graphic dependence of the fundamental expression of interactive chromatography of proteins. *The lower "pole" of the crossed straight lines correspond to the membrane separation [59],* whereas *the upper ones reflect the RP-HPLC results using a different kind of displacer [40].*

sponding, linearized Eq. (5), so-called poles can be found, e.g., interceptions between plots of Eq. (5) for different Z values. Without going into detail, we would like to postulate here that similar poles exists for plots of Eq. (14) and that a similar behavior is displayed in all modes of chromatography that described k′ as a function of the molecule and system parameters. In the case of one-step desorption chromatography, experimental proof is shown in Fig. 2, where the

plot of published experimental data (from Refs. 40 and 59) according to Eq. (14) yields straight lines. Figure 2 also shows some basic differences between column and disc protein separations. Obviously, the pole is located at a much lower y value in disc chromatography, while the distance between the x axis intercepts (a measure for the resolution) are wider. The latter fact indicates that HPMC may well be superior in terms of separation power.

D. Resolution and Efficiency in HPMC

It follows from the proposed theoretical model of protein separation by HPMC that the resolving power of this process depends not on the number of theoretical plates (the number of adsorption–desorption acts is one) but on the initial (''momentary'') distribution of the protein molecules according to the distribution of their energy of interaction with the sorbent surface. Obviously, for an increasing Z parameter (sharper logarithmic dependence of k' on the modifier concentration) the distribution of the probability density $[\rho(\psi)]$ of protein transition to the mobile phase will become sharper. In addition, the width of the protein peak depends on the distribution of the Z parameter. The latter becomes broader with increasing Z and exceeds significantly the second moment of the probability density, σ, thus becoming decisive for the peak width actually seen in the chromatogram.

If Eq. (15) is to be used for the determination of Z via the dispersion σ, it is necessary to separate the contribution of Z only to the overall distribution from all other contributions to the peak shape. A possible way of achieving this consists of fractionation of the eluting zone of a protein into small portions using a long-step gradient with very small changes of the modifier concentration in each step (low and long steps). It is then possible to obtain a set of ''components'' with practically identical Z values for a given modifier concentration range [47]. Rechromatographing of the individual fraction of identical Z values will result in peaks of a width that corresponds to the dispersion of the probability density of the protein's residence in the mobile phase.

The resolution obtainable by HPMC will decrease rapidly if the Z values of the substances to be separated are close. Moreover, an existing small difference between the (average values of the) Z parameter can be completely swallowed up by the distribution of the Z values for the individual proteins. As a consequence, proteins having closely similar $\log k'$ versus $\log \psi$ dependencies are most difficult to separate by gradient HPMC.

Since HPMC is interpreted as a one-step desorption process whereby the parameters of the separation are not averaged out during the migration of the substance along the adsorptive layer, the topography of the surface of the channels (pores) significantly influences the width of the eluted peak. The presence of so-called 'connecting drifts' (e.g., stagnant, non-flow-through pores) introduces a

diffusional motive into the otherwise very simple mechanism of HPMC. As a result, the distribution of the adsorption energy will become so wide as to render the probability of separation to practically zero. Not only that, but these pores present a serious kinetic limitation for the leaving of desorbed molecules from the sorbent surface. Wide and asymmetrical peaks with low resolution will be found in the ensuing chromatogram.

The use of very steep modifier gradients allows one to separate components with very close properties by HPMC [20]. It should be noted that in this case small peaks visible in the chromatogram may equally be the result of a momentary energetic inhomogeneity of the adsorptive interaction, which can be caused by an inhomogeneity of the adsorptive surface, or by the presence of impurities in the sample. The latter can be confirmed by repeating the separation. The energetic inhomogeneity has a more or less statistical character; thus peaks caused by this phenomenon will occur at different elution volumes in consecutive chromatograms, whereas peaks due to impurities should be completely reproducible.

E. Fluid Dynamics of Pore Channels

In HPMC the mobile phase streams through pore channels whose walls also form the adsorptive surface. Understanding the related fluid dynamic phenomena is an important first step in the control and optimization of membrane chromatography [59–62].

The overall linear flow velocity U of the mobile phase through the disc can be written as follows:

$$U = FA^{-1}\varepsilon^{-1} \tag{16}$$

where F is the volumetric flow rate, A is the cross-section of the disc, and ε is the porosity.

Equation (16) does not reflect the fact that the flow velocity in the individual pores may not necessarily be equal to the overall velocity U, since it will depend on the size of the pores. From the Hagen-Poiseuille law, we know that the flow through a tube is proportional to the square of its diameter:

$$U = \frac{\Delta P r^2}{8\eta L_t} \tag{17}$$

where ΔP is the pressure drop along the liquid path and η is the dynamic viscosity of the liquid.

Although Eq. (17) applies exactly only to the flow through a straight cylindrical tube of radius r and length L_t, it was recently demonstrated that the flow through a macroporous monolithic layer (disc) can at least be approximated by this law [17].

Rearrangement of Eq. (17) yields:

$$\frac{\Delta P}{U} = \frac{8hL}{r^2} \tag{18}$$

which shows that the pressure drop per unit of linear flow velocity increases exponentially with decreasing tube diameter. In other words, the larger the pore, the lower the flow resistance, and the more liquid flows through this pore at a given pressure.

As a result, the flow through the small pores is very slow and can even approach zero because the overall back pressure within the cartridge, which drives the liquid through the porous matrix, is lower than that required to enforce a flow through the smaller pores. This uneven distribution of flow has the effect of decreasing the surface area available for the adsorption–desorption process. Therefore, membranes with a broad pore size distribution are not desirable because a considerable portion of the pores may not be open to the mobile phase and thus not participate in the separation. The ideal matrix for disc chromatography may thus be assumed to be characterized by large pores and a narrow pore size distribution.

A very simple description of the effect of pores and pore size distributions on chromatographic separations can be based on the residence time of the mobile phase within the membrane t_{res} and the time scale t_{film} of the mass transfer through the film of stagnant liquid to the pore wall (adsorptive surface). In order to achieve a good separation, t_{res} must be larger than t_{film}.

The residence time is a simple function of the thickness of the separation layer L and the flow velocity U:

$$t_{res} \approx \frac{L}{U} \tag{19}$$

while t_{film} increases exponentially with the pore diameter d_p:

$$t_{film} \approx \frac{d_p^2}{4D} \tag{20}$$

where D is the diffusion coefficient of the protein.

The residence time can be controlled through the flow rate and the thickness of the disc, whereas the transport time is controlled by the pore size. Very thin adsorber layers in combination with very large pores are thus not well suited for the separation of proteins. The best separation can be achieved on discs with an optimum size, i.e., pores that are sufficiently small to allow the protein molecule to reach the wall within a reasonable amount of time, while they are also sufficiently large for a fast flow at a reasonable back pressure. The separation will benefit from a narrow distribution of the pore sizes (see above).

Membrane and especially high-performance membrane chromatography has often been met by a certain amount of skepticism from putative applicants. The doubts are often expressed in such questions as "How can the separation of complex protein mixtures be possible with these thin supports?" The presented theoretical considerations hopefully succeeded in removing some of these reservations. Concomitantly we tried to outline some basic differences between the process of column and membrane chromatography, which must be kept in mind if the application of membranes to chromatographic separations is to have the maximal practical impact.

V. APPLICATION OF MEMBRANE CHROMATOGRAPHY FOR PROTEIN SEPARATION

In the first part of this chapter we tried to formulate the theoretical basis of HPMC. Our goal was to define this evolving technique within the general framework of adsorption chromatography, but also to convince the newcomer to the field that it is indeed possible to separate protein mixtures over very short (micrometer to millimeter) separation distances. In the second part of the chapter we will illustrate the advantages of membrane chromatography using examples drawn from the day-to-day laboratory practice. The application of HPMC will be stressed, but other types of membrane chromatography will also be considered.

A. Elevated Flow Rates

Conventional chromatographic columns, especially when used for protein separations, usually show a rapid decrease in column efficiency (plate height) with increasing flow rate. This increase in band broadening is due to mass transfer resistance and should therefore be considerably less pronounced in HPMC. Indeed, as Fig. 3 shows, the "plate height," H, formally calculated using the following formula

$$H = (w_{0.5}/t_r)^2(\delta/5.54) \tag{21}$$

where $w_{0.5}$ is the peak width at half height, t_r is the retention time of the tracer, and δ is the thickness of the membrane, does not increase for flow rates between 0.1 and 30 ml/min. In spite of the fact that the plate height concept does not fully apply to membrane chromatography it must be noted that the peak shapes stay the same in disc chromatography independent of the mobile phase flow rate. Taking into account that short separation layers cause less back pressure than conventional columns, very fast separations should become possible in HPMC. This is indeed the case for ion exchange membrane chromatography as Fig. 4 demonstrates. A mixture of three standard proteins could be resolved equally

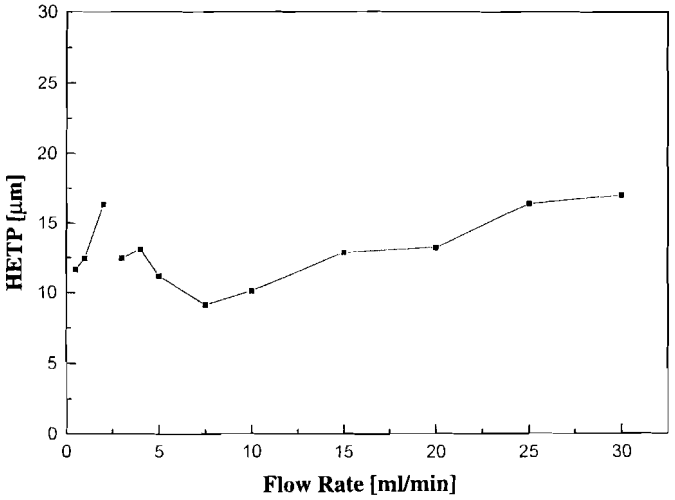

Figure 3 Dependency of the plate height, H, calculated from Eq. (22) as a function of the mobile phase flow rate. Disc, Sartobind Q (Sartorius AG); tracer, lysozyme (1 mg/ml).

well using mobile phase flow rates of 1, 3, 7, and 40 ml/min, whereas the duration of the separation was concomitantly reduced from 30 min to 30 s. (Fig 4a). This is also true for more complex separations such as that of human serum at 1, 5, and 10 ml/min (Fig. 4b) [63] and that of a nucleotide mixture at 1 and 10 ml/min (Fig. 4c). This flow rate independence of the separation is not necessarily found in all varieties of HPMC. While ion exchange chromatography is characterized by very fast surface interaction kinetics, other types, e.g., affinity chromatography, show much slower reaction kinetics. If the flow rate is increased indiscriminately in these cases, a loss in resolution can sometimes be observed [64], simply because the separation becomes reaction-limited.

A second question concerns the effect of the flow rate on the capacity of the disc. Here both the pore size distribution and the construction of the disc cartridge (mainly the inlet where the incoming flow is distributed equally over the entire cross-sectional area) are of major importance. While some discs can be used at flow rates of more than 30 ml/min without significant loss in capacity, others already lose more than 50% of the low flow rate capacity when the flow rate is increased to 10 ml/min [65] (Fig. 5). Affinity discs seem again to be more prone to a loss in capacity than the ion exchange types.

Once the advantage of HPMC over conventional column chromatography in terms of fast and efficient protein separation has been realized, a number of

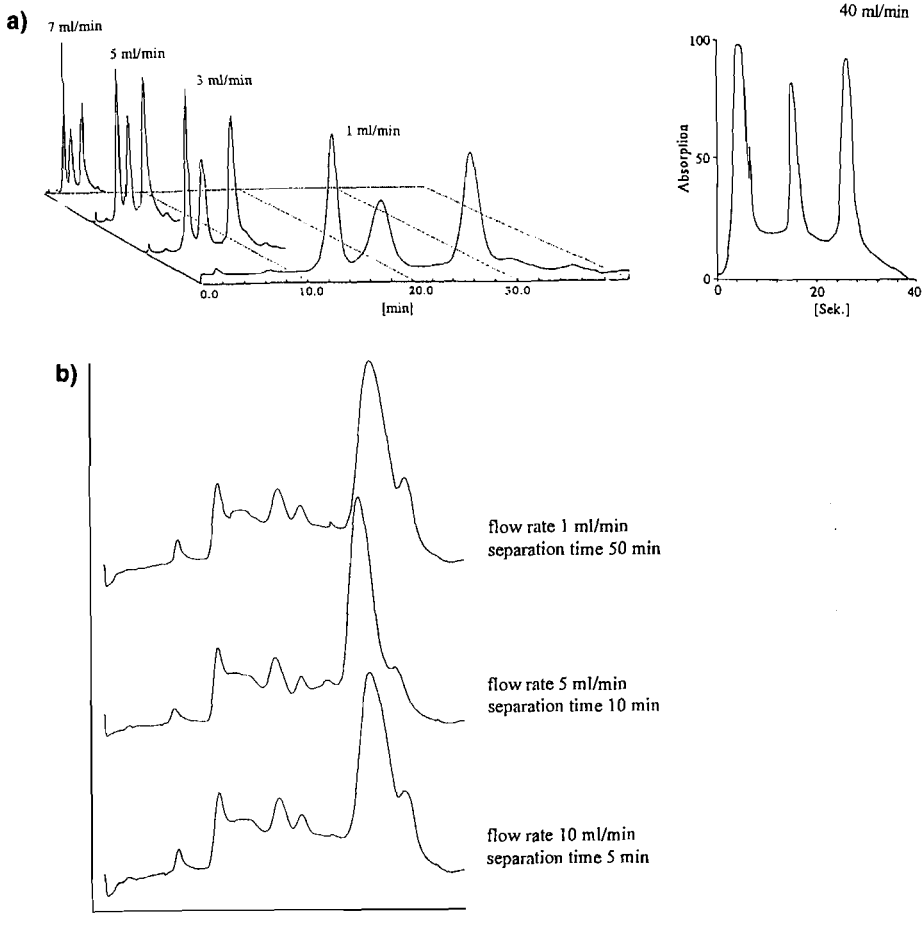

Figure 4 Demonstration of the flow rate dependency of HPMC separations. (a) Separation of a standard protein mixture (cytochrome c, α-chymotrypsinogen, lysozyme, 1 mg/ml each); disc, strong cation exchanger (prototype Sartorius AG). (b) Separation of human serum proteins (total protein 3 mg/ml) on an anion exchange membrane (prototype Sartorius AG). (c) Separation of a nucleotide mixture (NAD/NADH, 50 μg/ml; NADP/NADPH, 150 μg/ml) at 1 ml/min and 10 ml/min on a strong cation exchange membrane (prototype Sartorius AG). (From Ref. 63.)

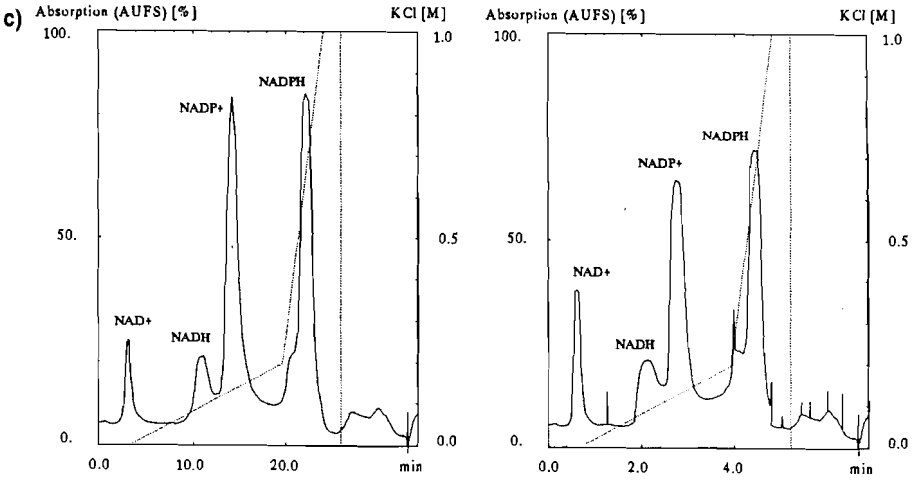

Figure 4 Continued

obvious fields of application appear. Chromatographic discs are real high-performance stationary phases capable of resolving even complex mixtures. In Fig. 6 the example is given of the monitoring of the mounting product concentration in a biotechnological fermentation broth [63]. In this area HPMC could become useful for fast, automatic (given modern chromatography/bioreactor software), and cheap at-line product monitoring. The replacement of the old trouble-prone and low-resolution cartridges used in heterogeneous flow injection analysis (FIA) by the respective discs has recently been proposed by Tennikova et al. [66]. In this context HPMC was shown to improve the detection limit, the resolution, the reliability, and even the standing time of the FI analyzer.

Another important analytical application can be found in the area of hyphenated analytical techniques. Many of these techniques rely on a chromatographic step to resolve a complex sample and then use a second analytical technique (e.g., MS) to gain further information on the individual components. Here again the combination of speed, resolution, and cheapness is intriguing. In Fig. 7, a 1-ml sample of a cell culture supernatant containing a recombinant protein product and 2% fetal calf serum (FCS) is chromatographed using an anion exchange disc (prototype Sartorius AG). The product-containing fraction is automatically injected into a capillary electrophoresis system for quantification [67]. Under optimized conditions, the entire analysis can be carried out in 2 min. Since the product is not only enriched but also concentrated by HPMC, the detection limit of the coupled technique is one order of magnitude lower than that of capillary electrophoresis alone. The reproducibility and standard deviations are similar.

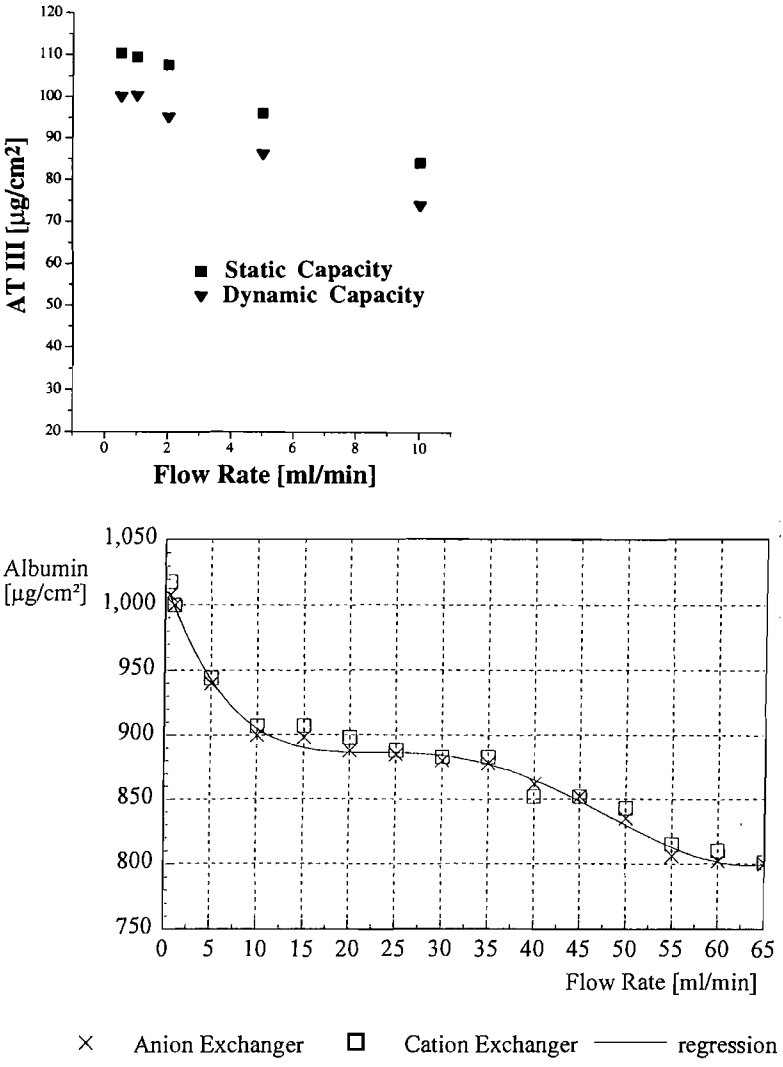

Figure 5 Influence of flow rate on capacity. (top) Static and dynamic antithrombin III binding capacity of a heparin affinity membrane adsorber (prototype Sartorius AG). (From Ref. 65.) (bottom) Static capacity, strong anion/strong cation exchanger (both prototype Sartorius AG). The disc was loaded with human serum albumin until saturation. Afterward the amount retained was eluted and quantified. (From Ref. 67.)

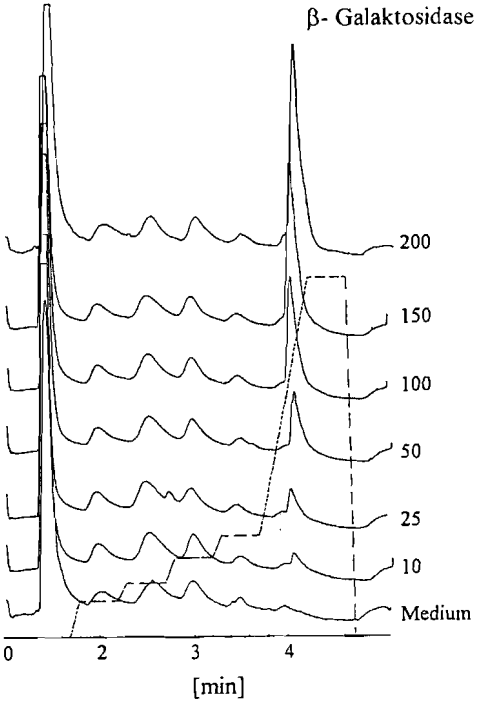

Figure 6 Quantification of β-galactosidase in culture supernatants with an anion exchange membrane adsorber (prototype Sartorius AG). (From Ref. 63.)

B. Preparative HPMC

Given the particular advantages of HPMC, this mode should also be applicable to preparative separations. To date the majority of application protocols is given for small discs (mm × cm range) (see below). Most applicants still tend to use a single-step interaction mode, much in the tradition of affinity filtration, rather than exploiting the full advantages of the new stationary phase geometry in chromatographic terms. Multistage separation processes are therefore still rare, although they do exist [65,68].

Antithrombin III is an anticoagulant with considerable therapeutic value. It has thus become a target substance for biotechnical production and several mammalian cell lines exist, which express human antithrombin III as a recombinant protein. The recovery of the product from the cell culture supernatant is made quite complex by the fact that the product is normally found only in minute amounts (in the case considered here typically 1% of the total protein concentra-

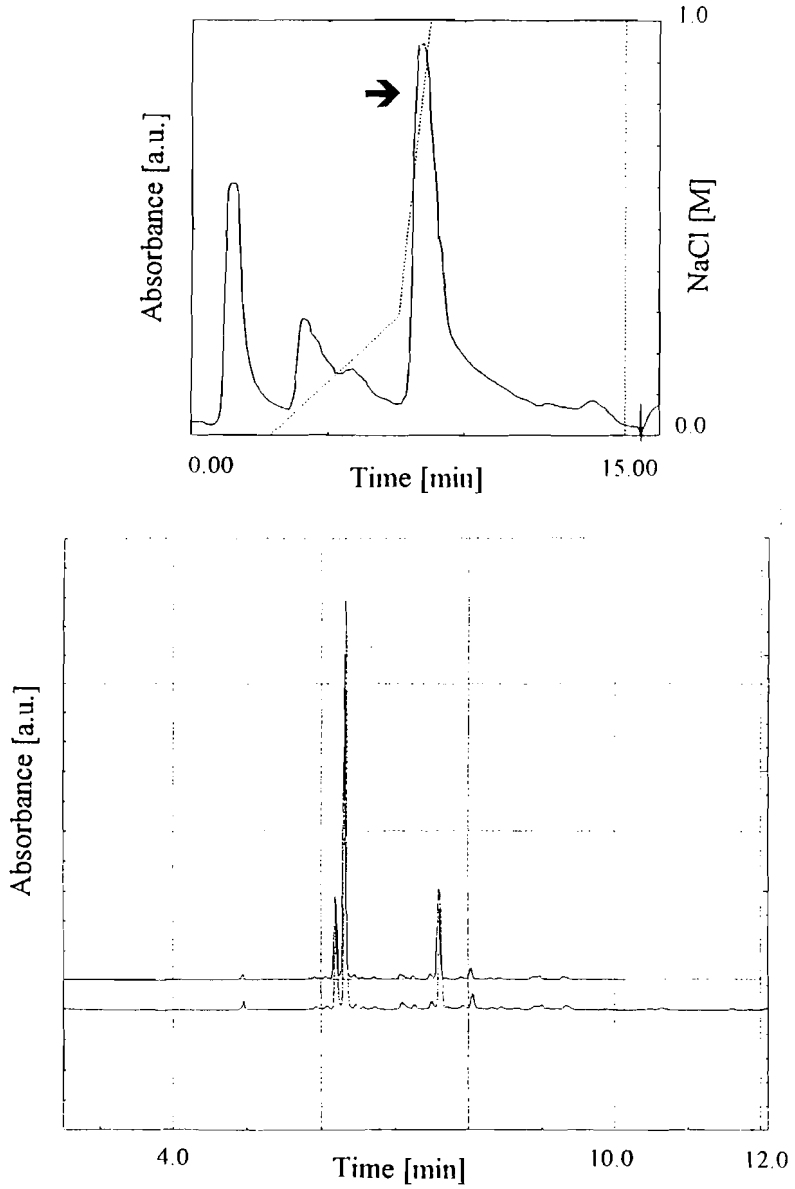

Figure 7 (top) Chromatogram of a cell culture supernatant using a strong anion exchange membrane adsorber (prototype Sartorius AG). The product containing fraction is indicated. (bottom) Electropherogram of the product containing fraction. (From Ref. 67.)

tion) and that large amounts of FCS are normally added to the production environment (here typically 10%). Lowering the serum concentration often yields a product of inferior quality, e.g., low activity, low stability [67]. HPMC was used as a cheap but high-performance preparative approach to process between 0.1 and 10 L of culture supernatant.

In a first attempt, heparin affinity HPMC was used in combination with an ultrafiltration/diafiltration step [65]. While the latter served mainly to concentrate the protein fraction in the culture supernatant, we hoped to isolate pure antithrombin III by the heparin affinity step. Column heparin affinity chromatography is a standard procedure to isolate antithrombin III, since the protein shows a pronounced affinity for its cofactor.

The results of the first attempt are summarized in Table 1. Of the original AT III activity, 81% was recovered by the heparin disc. In addition, the product was concentrated by a factor of 101 during this step. When the protein was analyzed by sodium dodecyl sulfate–polyacrylamide gel electrophoresis and immunodiffusion its purity was established at 64%. Large amounts of both bovine serum albumin and bovine transferrin as well as traces of bovine immunoglobulin G and other unidentified proteins were still present. One hundred sixty minutes was required for the processing of one batch of culture supernatant in this case, corresponding to 0.7 mg/h AT III.

In order to improve the final purity, ion exchange HPMC steps were integrated in the isolation scheme. It was possible to nearly remove the b-IgG by a strong anion exchange disc, as was verified by immunoblotting. The final purity of the antithrombin was 85%, with bovine serum albumin as the major contaminant.

Since none of the procedures was capable of removing the bovine serum albumin totally, a further improvement of the product quality was attempted by

Table 1 Purification of Recombinant Antithrombin III from Cell Culture Supernatants by a Three-Step HPMC Process

	Cell culture supernatant	Ultrafiltration/ diafiltration	Heparin MA
AT III (μg/ml)	7.5	6	608
AT III (μg)	1875	Not determined	1520
Specific activity (U/mg)	700	661.97	571.97
Total protein concentration (mg/ml)	6.1	5.64	0.95
BSA (mg/ml)	3.64	3.36	0.167
β-Transferrin (mg/ml)	0.21	0.187	0.043
β-IgG (mg/ml)	0.77	0.68	0.007

Source: From Ref. 65.

introducing a step for the specific removal of the albumin. Cibacron blue ligands are known to interact with bovine serum albumin but not with antithrombin. It was found that the Cibacron blue disc is best used before both the anion exchange and the heparin disc (Table 2). A cycle required 300 min in this case and yielded approximately 2 mg of product (0.4 mg/h). The final procedure yields a 94% pure product with a recovery of 72%. Purities of >99.9% were reached only when the serum concentration in the culture was lowered to 3%. Then, however, the biological activity of the product suffered [65].

In order to increase productivity, the flow rate over the discs was increased stepwise from the 2 ml/min (0.12 L/h) used during development to 4.8 L/h. The maximum flow rate through the heparin MA had to be restricted to 0.18 L/h during these experiments, since affinity discs show a pronounced flow rate dependency of the dynamic capacity. Nevertheless the cycle time was reduced considerably by this increase of flow rate and the antithrombin throughput concomitantly increased from 0.55 to 13.7 mg/h (Table 3).

The scale-up of HPMC to fully preparative dimensions is also rarely done. The easiest way to increase the scale of a HPMC separation is to increase the number of discs involved, either by inserting several discs into a cartridge (modern disc cartridges can usually incorporate varied numbers of discs) or by short-circuiting several modules. Figure 8 shows such a scale-up by an increase in the number of discs. By increasing that number from 1 to 6, the total amount of trypsin inhibitor, α-chymotrypsinogen, and lysozyme separated could be in-

Table 2 Purification of Recombinant Antithrombin III from Cell Culture Supernatants by a Three-Step HPMC Process

	Cell culture supernatant	Ultrafiltration/ diafiltration	CB-MA	Anion exchange MA	Heparin MA
AT III (μg/ml)	11	10.9	48.1	43.8	657
AT III (μg)	2750	2725	2405	2190	1971
Specific activity (U/mg)	790.9	798.2	684	630.2	577.8
Total protein concentration (mg/ml)	5.7	5.5	8.1	0.36	0.699
BSA (mg/ml)	3.4	3.3	0.22	0.19	0.015
β-Transferrin (mg/ml)	0.16	0.16	0.76	0.021	0.001
β-IgG (mg/ml)	0.79	0.8	3.6	0.003	0

Source: From Ref. 65.

Table 3 Influence of the Mobile Phase Flow Rate on the Separation of Recombinant Antithrombin III by the Three-Step HPMC Process

Flow rate (L/h)	Process time (h)	AT III throughput (mg/h)	AT III (mg)	Yield recovery (%)	Concentration factor	Purity (%)
0.12	2.1	0.55	1.7	69.3	57.7	97
1.2	0.5	5.50	1.7	60.6	50.5	98
2.4	0.35	9.30	1.8	56.7	47.2	94
4.8	0.2	13.70	1.4	52.4	43.7	96

Source: From Ref. 65.

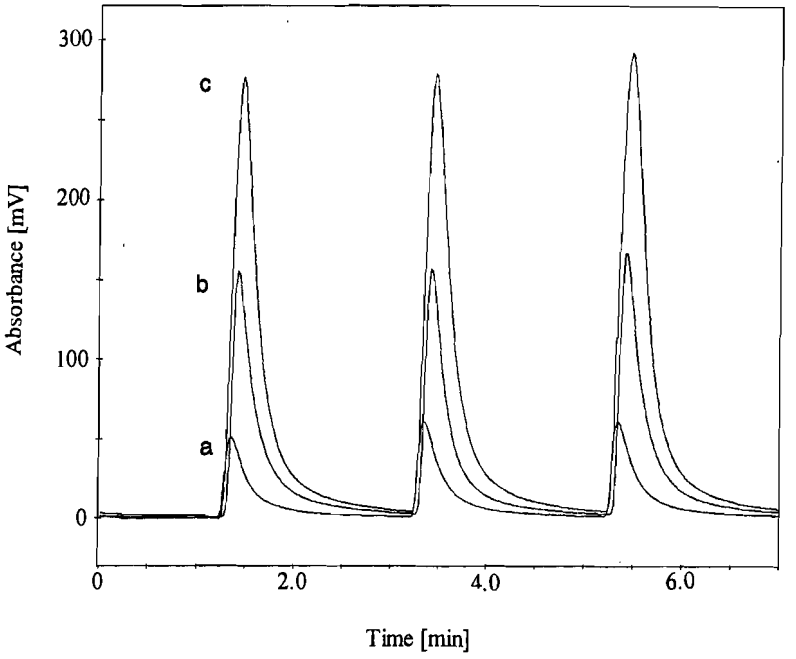

Figure 8 Separation of a standard protein mixture (lysozyme, α-chymotrypsinogen, and trypsin inhibitor) using anion exchange membrane adsorbers (prototype Sartorius AG). (a) One layer, 0.25 mg/ml of each protein. (b) Three layers, 0.6 mg/ml of each protein. (c) Six layers, 1.2 mg/ml of each protein. Flow rate was 12 ml/min throughout. (From Ref. 63.)

creased from 0.25 to 1.2 mg [63]. By keeping the flow rate and the gradient volume constant, the retention times were kept equal. The resolution does suffer slightly, since the protein zones are somewhat broader at higher concentration.

An interesting effect was observed when coupling modules to increase the maximum sample load. When working close to the separation capacity (i.e., the amount of protein that could still be resolved with a resolution of 1 or better) the resolution was found to improve whenever two modules were used in series even though the loading, i.e., the amount of protein per cm^2, was kept constant [69]. In other words, we find a higher separation capacity in the case of two modules than for a single one. No further improvement is observed when more than two modules are stacked. The improvement in separation is not due to the increase in the number of disc layers or simply to an increase in total area, since two consecutive smaller modules [total of six layers (2×3) representing 60 cm^2] resolves a given protein mixture better than a single large one (five layers equal to a total of 100 cm^2).

While such an increase in the number of layers can often suffice to carry a separation from the analytical to the semipreparative scale, a truly large-scale membrane chromatography requires a more significant increase in area. In this context HPMC can profit considerably from filtration theory, to which it bears a certain resemblance. In fact, various forms of filtration have been adapted to membrane chromatography, including cross-flow and hollow fiber modules. Figure 9 shows the scale-up of a separation of three proteins (α-chymotrypsinogen, cytochrome c, lysozyme) from a small module (0.5 cm^2) to a large one (130 cm^2). The flow (ml/cm^2) and the protein load (mg/cm^2) were kept constant, while the volumetric flow rate was increased from 0.2 to 50 ml/min. Given the difficulty of recording a UV trace for the larger modules, the separation stayed much the same.

The largest module (fitted this time with 10 layers, each 130 cm^2) was also used in the processing of technical dairy whey, where throughput is an important point [69]. Five liters of feed solution was passed through this module at a flow rate of 50 ml/min. Using a two-step NaCl gradient (up to 1 M NaCl), 248 mg of protein was eluted within 14 min: 116 mg in step 1 (0.1 M NaCl, mostly α-lactalbumin) and 132 mg in step 2 (0.5 M NaCl, mostly β-lactoglobulin). The recovery was >70% for both proteins.

C. Mixed-Mode HPMC

Save for a few exceptions, such as hydroxyapatite chromatography or the Bakerbond ABX phase (Baker Chemical Co., USA), which were especially developed for antibody purification, mixed-mode interactions are avoided in liquid chromatography. On the other hand, single-stage chromatography is seldomly sufficient for preparative protein separation and multistage procedures, where

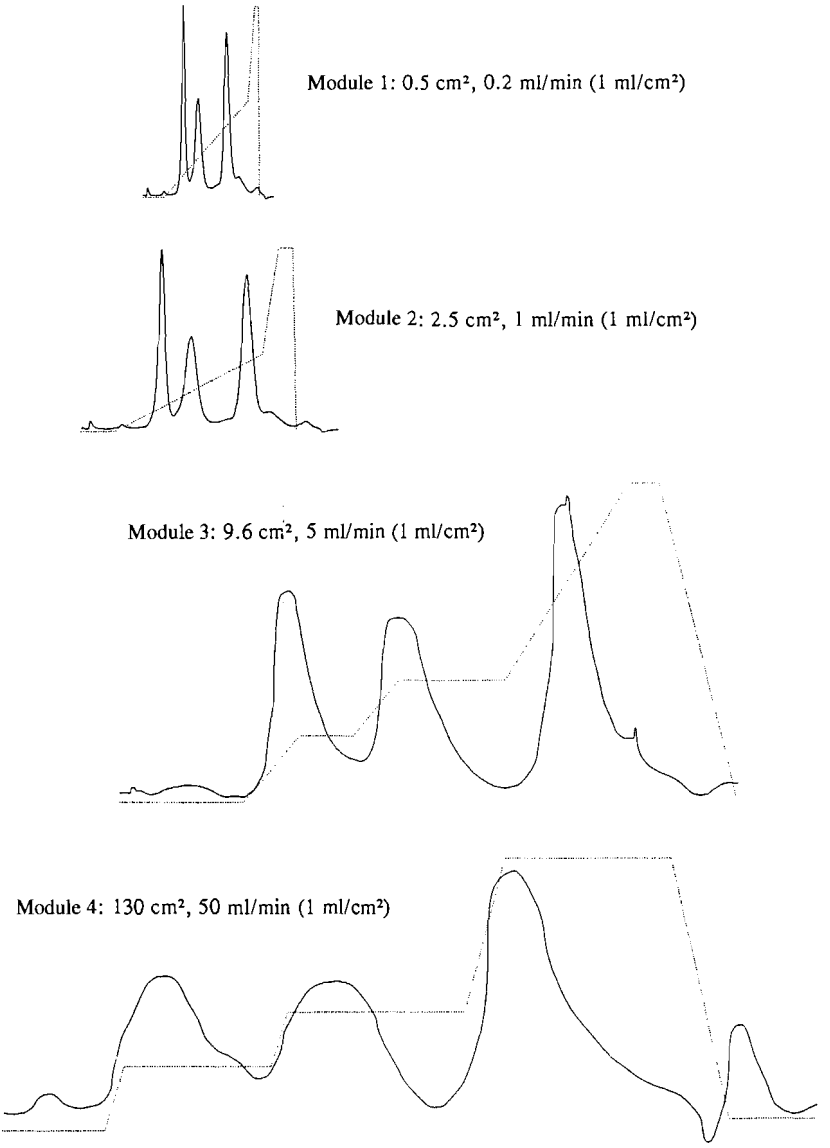

Figure 9 Scale-up of a separation of three standard proteins (α-chymotrypsinogen, cytochrome c, lysozyme, 1 mg/ml each) using cation exchange HPMC (membrane material Sartorius AG). The modules were either self-assembled or standard dead-end filtration modules fitted with the interactive membrane layers.

several types of interaction are exploited in series are the norm. Controllable mixed-mode phases may thus become an interesting tool. However, with conventional porous particle–based stationary phases, mixed-mode supports are difficult to realize in a reproducible, homogeneous, but flexible manner. The number of (usually prepacked) columns to be offered by the suppliers would increase dramatically with the number of possible or desirable combinations. This is radically different in the case of HPMC where the use of stacks of discs has already become routine (see above). In this case even the most complex mixed-mode approach calls only for the insertion of different discs into the cartridge. In fact, an approach using discs with different interactive groups in one housing is currently being promoted by a major HPMC supplier (BIA, Slovenia) under the name of combinatorial liquid chromatography (CLC).

That the separation by one type of disc is not disturbed by any other type can be demonstrated in a simple experiment. Interactive discs, e.g., ion exchange discs, are alternated with inert filtration discs and the chromatograms compared with those obtained for a cartridge filled only with the ion exchange material. In our experience there will hardly ever be a difference unless the putatively inert filter discs are not really inert (in the case of proteins, hydrophobic interactions may be present).

Figure 10 shows the separation of five standard proteins [(β-lactoglobulin (IEP: 5.1), conalbumin (IEP: 6.8), α-chymotrypsinogen (IEP: 9.6), lysozyme (IEP: 10.5), and cytochrome c (IEP: 11.2)] by mixed-mode ion exchange chromatography together with the chromatograms of the single substances on the same stationary phase [70]. Five strong anion exchanger and five strong cation exchanger membrane adsorbers (prototypes Sartorius AG) were alternated in the cartridge. Note that the separation becomes possible at physiological pH with the mixed-mode approach, since it is no longer necessary to go to extreme buffer pH in order to ensure that all proteins carry the same net charge.

Alternating the discs gives a better resolution than using two stacks (Fig. 11) [70]. As always in ion exchange HPMC, the separation seems to be nearly independent of the flow rate. Figure 12 shows again the separation of the standard protein mixture on the alternating discs using flow rates between 2 and 12 ml/min [70]. The gradient volume and shape were kept constant during these experiments. While the separation required 30 min at a flow rate of 1 ml/min it could be performed in 1.6 min with a flow rate of 12 ml/min.

The mixed-mode approach is not restricted to mixed-mode ion exchange HPMC. Mixed mode ion exchange/affinity HPMC is also promising—especially so because it combines the advantages of affinity chromatography, i.e., the ability to be highly selective for the target molecule which is often also considerably concentrated, with that of ion exchange chromatography, e.g., the ability to resolve the entire substance mixture. In mixed-mode ion exchange/affinity HPMC a single-step separation again becomes possible, which would otherwise have

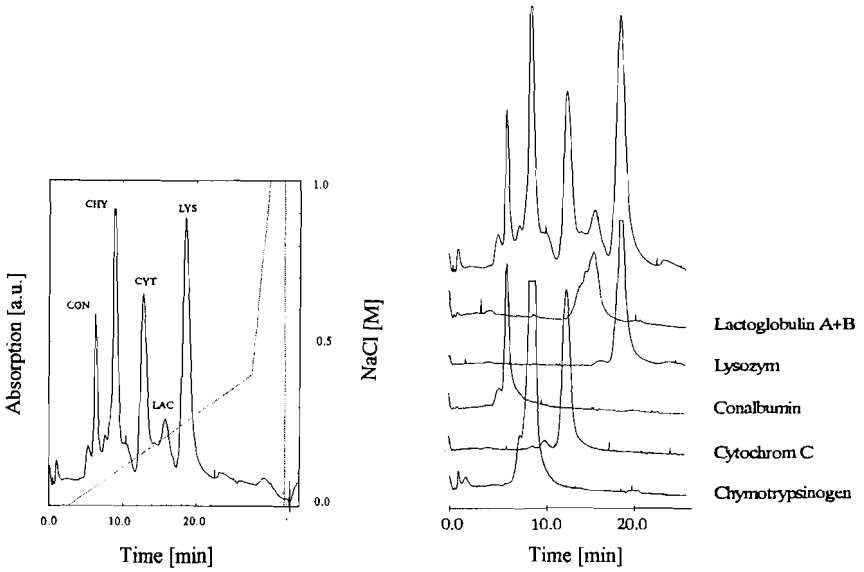

Figure 10 Mixed-mode approach to the separation of a mixture of five standard proteins (left). On the right-hand side the chromatograms of the individual proteins on the mixed-mode phase are given. Five layers of strong anion and strong cation exchange membrane adsorbers (prototype Sartorius AG) were alternated in the cartridge. (From Ref. 70.)

required at least two steps [70]. We have seen above that the isolation of the recombinant anticoagulant antithrombin III from cell culture supernatant requires several chromatographic steps. The removal of bovine serum albumin and bovine transferrin is especially difficult. The separation of the antithrombin III from these two contaminants requires at least two chromatographic steps based on different interaction principles. The albumin can be removed by Cibacron blue affinity chromatography (Fig. 13a), which doesn't help to lower the bovine transferrin concentration. Bovine transferrin, on the other hand, can be removed—due to the difference in IEP—on a strong anion exchange chromatography (Fig. 13b). However, this step does not remove the albumin. Only one possibility has been reported to at least partially resolve the three-protein mixture and that was immobilized metal affinity disc chromatography (IMADC) using Cu^{2+} ions (Fig. 13c). In this case, however, antithrombin activity is found in the breakthrough as well as in one of the later eluting fractions.

By the simple measure of using controlled mixed-mode anion exchange/affinity interaction, on the other hand, the separation of recombinant antithrombin III, bovine serum albumin, and bovine transferrin becomes possible in a single

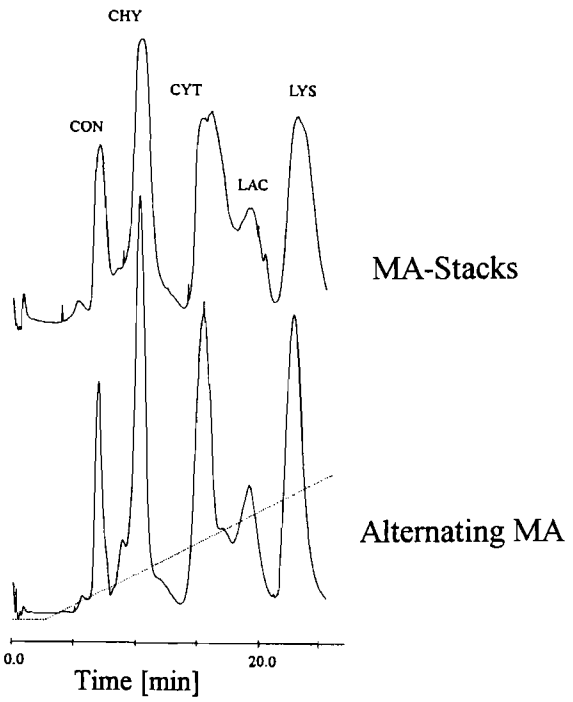

Figure 11 Comparison of the alternating versus the two-stack approach to mixed-mode HPMC of the standard protein mixture. (From Ref. 70.)

mixed-mode HPMC separation at pH 7.0 (Fig. 13d). Since the bovine serum albumin may be expected to interact mainly with the affinity membrane adsorber (i.e., a Cibacron blue disc, prototype Sartorius AG) under these circumstances, it is not surprising that a comparatively high NaCl step gradient (3 M NaCl) is required for elution of that particular protein. The antithrombin III and the bovine transferrin, on the other hand, which should adsorb mainly onto the anion exchanger MA, are eluted in a linear NaCl gradient up to 1 M NaCl.

VI. EXAMPLES

Of the various types of adsorption chromatography, the two most commonly used types of HPMC in preparative protein separations are affinity chromatography ("affinity filtration") and ion exchange chromatography. In spite of the potential

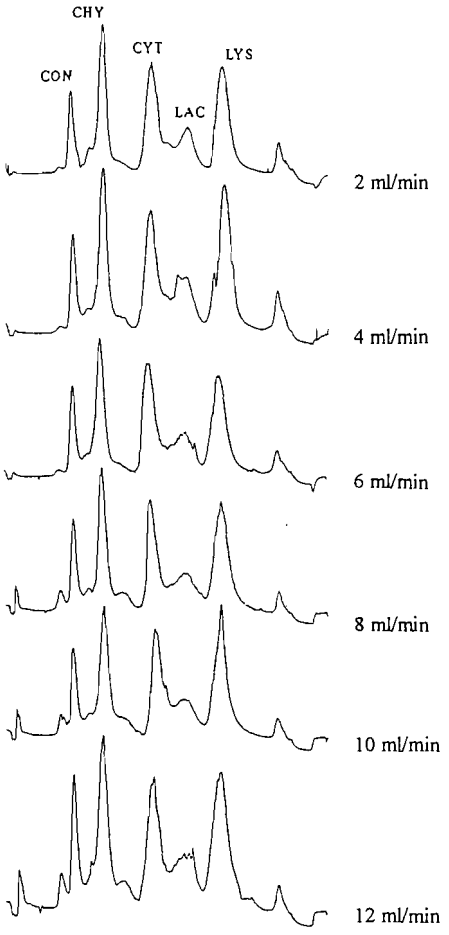

Figure 12 Influence of the mobile phase flow rate on mixed-mode protein HPMC. (From Ref. 70.)

of HPMC in general, only a limited number of applications in biotechnology are known, hardly any of them in a large scale. The following list of examples is not intended to be an all-inclusive summary. However, it is intended as a comprehensive guide to membrane chromatography of proteins and other biopolymers. Some of the papers applied to more than one category but were nevertheless listed only once. The interested reader is also referred to the review by Thömmes and Kula [71].

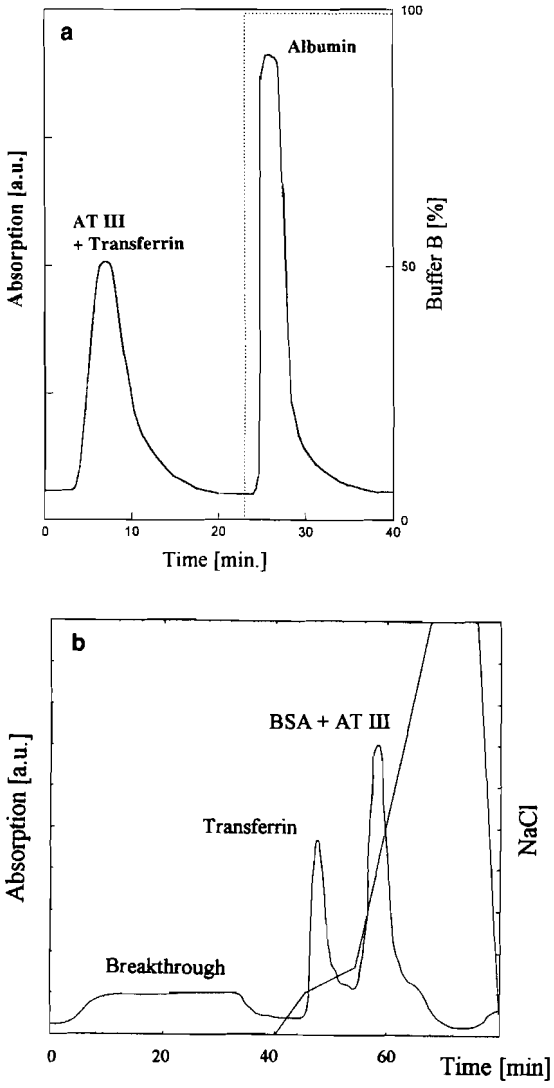

Figure 13 Separation recombinant antithrombin III, bovine serum albumin, and bovine transferrin. (a) Cibacron blue affinity membrane adsorber. (b) Strong anion exchange membrane adsorber. (c) Immobilized metal affinity membrane adsorber (Cu^{2+} ions). (d) Mixed-mode HPMC, using the Cibacron blue membrane adsorber and the strong anion exchange membrane adsorber. (From Ref. 70.)

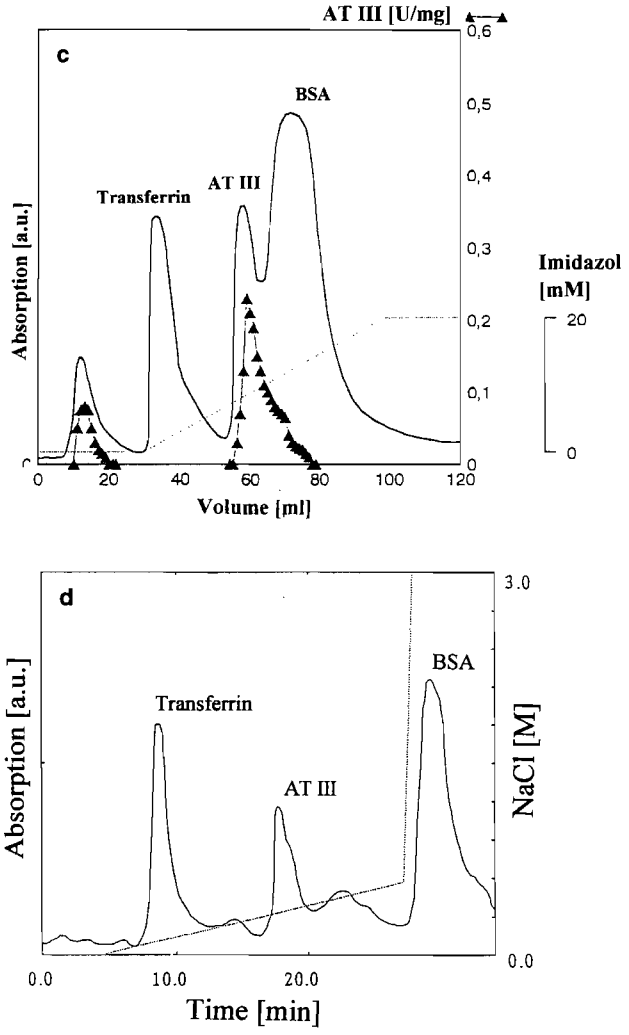

Figure 13 Continued

A. Affinity Filtration

Target molecule	Key phrases	Ref.
Antibodies	Protein A ligands, preactivated discs, discussion of advantages of disc, conference proceedings	Lee et al. 1992 [72]
Human antithrombin III from plasma	High-performance membrane affinity chromatography (HPMAC) is used to monitor the purification by conventional column chromatography	Josic et al. 1993 [73]
Rabbit antibodies, monoclonal antibodies from cell culture	Investigation of epoxy-activated discs, immobilization of Protein A and Protein G, application to antibody purification	Langlotz and Kroner 1992 [74]
Malate dehydrogenase (pig heart, *E. coli*)	Comparison of blue Sepharose (Pharmacia) and Cibacron blue modified discs (Sartorius AG), comparison of dead-end and cross-flow filtration	Krause et al. 1991 [75]
Antithrombin, albumin, various antibodies, recombinant gp 220/350 Epstein-Barr virus surface antigen	Comparison of discs and columns, investigation of different membrane materials, different coupling chemistries for pre-activated discs	Kasper et al. 1997 [76]
Recombinant fusion protein (EcoR V, HIS_6-tag), cytochrom C from various sources varying in the number of surface histidines	Immobilized metal affinity disc chromatography, investigation of the influence of metal ion type, the flow rate, the salt concentration, and the eluting agent, isolation of the fusion protein from cell lysates	Nier et al. 1994 [64]
Carbonic anhydrase from human erythrocytes	Epoxy-activated discs, coupling of *p*-aminomethylbenzolsulfonamide as ligand, coupling of the enzyme itself for kinetic investigations	Abou-Rebyeh et al. 1991 [21]

Target molecule	Key phrases	Ref.
Various	Review article discussing the potential of membrane-based affinity technologies for biotechnology giving some theoretical considerations and examples	Brandt et al. 1988 [78]
Bovine immunoglobulin	Protein G affinity chromatography, investigation of the process parameters (flow rate, feed concentration)	Kochan et al. 1996 [79]

B. Hollow Fiber Systems

The larger part of this chapter has explicitly dealt with chromatographic discs as stationary phase. HPMC can be regarded as a special—and comparatively well understood—form of membrane chromatography in general. Especially in the area of affinity filtration, which operates according to the yes-or-no principle of adsorption, other process modes have been used with much success. Hollow fiber systems are popular because they allow a rapid cross-flow adsorptive filtration of the feed with little danger of pore blockage. A number of examples are listed below.

Target molecule	Key phrases	Ref.
Bovine immunoglobulin G	Hydrophobic amino acids (phenylalanine or tryptophan) as ligands, radiation-induced grafting of glycidyl methacrylate onto a porous polyethylene hollow fiber to allow ligand immobilization	Kim et al. 1991 [80]
Interferon-α2a, interleukin-2, interleukin-2 receptor	Investigation antibody–antigen/receptor-based membrane chromatography	Nachman et al. 1991 [81], 1992 [45]

Target molecule	Key phrases	Ref.
Standard proteins	Immobilized metal affinity chromatography, glass hollow fiber microfiltration system, coupling of imminodiacetic acid (IDA) to the wall, comparison to conventional columns, theoretical treatment of hollow fiber membrane chromatography	Serafica et al. 1994 [82]
Antibodies	Protein A, Protein G, process development, scale-up, various forms of application, conference proceedings	Garg et al. 1992 [83]
β-Galactosidase	Ion exchange hollow fiber system, charged fusion tag	Heng and Glantz 1993 [84]
Bovine serum albumin	Microporous nylon-6 hollow fibers were modified by reaction with lysine, polyclonal antibodies were linked to the surface via their oxidized carbohydrate side chain	Kugel et al. 1992 [85]

C. Therapeutic Proteins

Target molecule	Key phrases	Ref.
Factor VIII from human plasma	Use of ion exchange discs (also for process monitoring) and scale-up via the use of a compact porous tube made from the same material as the discs	Strancar et al. 1997 [86]
Monoclonal antibodies from cell cultures	Cation exchanger, scale-up from disc to hollow fiber system, process up to harvest from 100 L bioreactor, recoveries >96%	Lütkemeyer et al. 1992 [87]

Target molecule	Key phrases	Ref.
Human tumor necrosis factor–α	Recombinant protein produced in *E. coli*, product electrophoretically pure, anion exchange HPMC	Lukas et al. 1994 [24]
Recombinant antithrombin III, monoclonal antibodies from cell cultures	Ion exchange and heparin affinity disc chromatography, scale-up to hollow fiber system (2400 cm^2) in case of ion exchanger, coupling chemistry for heparin	Lütkemeyer et al. 1993 [88]
Serum and plasma proteins	Scale-up from 10- to 50-mm disc (weak anion exchanger), comparison to column chromatography	Josic et al. 1992 [22]
Annexins from liver plasma membranes, monospecific polyclonal antibodies	Anion exchange disc, separation of annexins from each other in 10 min, comparison of disc and cellulose fiber modules, immobilization of annexins to epoxy-activated discs for antibody purification	Josic et al. 1994 [23]
Monoclonal antibodies from cell culture	Thiophilic membranes, membrane stacks and cross-flow module, interpretation of the flux behavior according to filtration theory	Finger et al. 1995 [89]
Kistler and Nitschmann's fraction IV of blood plasma	Weak anion exchanger	Lacoste-Bourgeacq et al. 1991 [90]
Recombinant antithrombin III from cell culture	Multistage disc chromatography process (affinity and ion exchange chromatography), scale-up to 10 L scale	Reif and Freitag 1994 [65]
Whey proteins, permeate components	Comparison to column chromatography, mixed-mode approach, influence of the process parameters (flow rate, pH), scale-up considerations	Splitt et al. 1996 [69]

Target molecule	Key phrases	Ref.
Monoclonal antibodies	Radial streaming ion exchange chromatography, scale-up study (pilot scale), calculation of scale-up factors, comparison with experimental results	Jungbauer et al. 1988 [91]
Human serum albumin (plasma fractionation)	Two-step process yields 98% pure albumin from clarified, microfiltrated, and desalted plasma, comparison to column approach	Gebauer et al. 1997 [92]

D. Endotoxin Removal

The lipopolysaccharides, which are a major component of the cell membrane of gram-negative bacteria, are powerful endotoxins that cause a violent reaction of the immune system of mammals upon entering the bloodstream. Pharmaceuticals and especially injectables need to be endotoxin-free. The removal of endotoxins is not an easy task and chromatographic methods have been suggested. HPMC may present itself as a fast and efficient detoxification (depyrogenation) method.

Target	Comments	Ref.
Depyrogenation of water, buffer, protein solutions	Application note by a membrane manufacturer (Sartorius AG) giving various protocols	Sartorius 1997 [93]
Endotoxin removal from protein mixtures	Strong anion exchange discs, endotoxin removal from bacterial extracts, scale-up to 15 L, reduction from >500,000 to <100 EU/ml	Belanich et al. 1994 [94]

E. Process Monitoring

Target molecule	Comments	Ref.
α_1-Antitrypsin, clotting factor IX	Development of HPMC method explicitly for bioprocess and downstream monitoring, anion exchange, cation exchange, and hydrophobic interaction mode, separation of three standard proteins in less than 1 min	Strancar et al. 1996 [25]

F. Disc/Membrane Systems and General Developments

Target	Comments	Ref.
Investigation of the MemSep system for analytical and preparative applications	30- and 15-mg of protein were purified within 3 min when a cation exchange MemSep 1010 system was operated in the step and linear gradient mode, respectively	Gerstner et al. 1992 [95]
Investigation of kinetics of immunoaffinity membrane chromatography	Theoretical treatment, application of the results to the isolation of biotherapeutics	Nachman 1992 [46]
Model for membrane affinity chromatography	Mathematical model for the simulation and the design of dead-end affinity filtration	Suen and Etzel 1992 [96]
Modeling of disc chromatography	Model and experimental verification for various limiting conditions, application to protein purification and scale-up	Briefs and Kula 1992 [97]
Investigation of mass transfer limitations	Development of a mathematical model to describe various processes during protein separation by HPMC, film mass transfer resistance is found to be the decisive factor	Sarfert and Etzel 1997 [62]

G. Miscellaneous

Target	Comments	Ref.
Membranes exhibiting molecular recognition	Preparation of membranes for affinity separation and immunodiagnostics, optimization of the membrane using biological ligands, introduction of fully synthetic functions (e.g., triazine molecules) that exhibit recognition properties	Bamford and Al-Lamee 1994 [98]
Proteins by affinity adsorption	Affinity ligand is immobilized on nylon belt system, which is passed through the various solutions, continuous purification system	Niven and Scurlock 1993 [99]
Preparation of macroporous discs suitable for chromatography	Synthesis protocol, influence of the synthetic conditions on the chromatographic parameters	Jelinkova and Votavova 1991 [100]
Formed-in-place anion exchange membranes	The membranes are formed by adsorption of polymers (e.g., polyethyleneimine) on formed-in-place microfiltration (titanium dioxide) substrates	Li and Spencer 1992 [101]
Bacterial plasmid DNA	DNA and impurities contained in the cleared bacterial lysates were adsorbed to DEAE cellulose membranes, the impurities were selectively removed and the pure plasmid DNA recovered afterward	Huynh et al. 1993 [102]

VII. CONCLUSIONS

Membrane chromatography of proteins and other biopolymers combines speed, resolution, and capacity in a unique fashion. In the beginning the method was beset with certain problems. But now the theory of HPMC has been developed and the principles underlying the separation have become clear. The decisive factors for designing a true high-performance short-separation-layer phase are known and membrane chromatography may well be on its way to becoming the protein separation technology of the 21st century.

ACKNOWLEDGMENTS

The authors gratefully acknowledge Dr. Michael Tennikov for the fruitful discussion regarding the preparation of this chapter.

REFERENCES

1. Nomenclature for chromatography, IUPAC Recommendations, J Pure Appl Chem 1993;65(4):819.
2. Roper DK, Lightfoot EN. J Chromatogr 1995;702:3.
3. Snyder LR, Stadalius MA, Quarry MA. Anal Chem 1983;55:1412A.
4. Stadalius MA, Quarry MA, Snyder LR. J Chromatogr 1985;327:93.
5. Snyder LR, Stadalius MA. In: Horvath CS, ed., High-Performance Liquid Chromatography—Advances and Perspectives, Vol 4. New York: Academic Press, 1987: 195.
6. Knox JH. J Chromatogr Sci 1977;15:352.
7. Afeyan NB, Fulton SP, Regnier FE. J Chromatogr 1992;544:267.
8. Fulton SP, Afeyan NB, Gordon NF, Regnier FE. J Chromatogr 1992;47:452.
9. McCoy M, Kalghatgi K, Regnier FE, Afeyan NB. J Chromatogr 1996;753:221.
10. Rodrigues AE, Lopez JC, Lu ZP, Loureiro JM, Diaz MM. J Chromatogr 1992;590: 9.
11. Rodrigues AE, Zuping LU, Loureiro JM. Chem Eng Sci 1991;46(11):2765.
12. Liapis AI, Xu Y, Grosser OK, Tongta A. J Chromatogr 1995;702:45.
13. Heeter GA, Liapis AI. J Chromatogr 1996;743:3.
14. Heeter GA, Liapis AI. J Chromatogr 1997;761:35.
15. Unger KK, Jilge G, Kinkel JN, Hearn MTW. J Chromatogr 1986;359:61.
16. Janzen R, Unger KK, Giesche H, Kinkel JN, Hearn MTW. J Chromatogr 1987; 397:91.
17. Tennikova TB, Belenkii BG, Svec F. J Liquid Chromatogr 1990;13:63.
18. Tennikova TB, Bleha M, Svec F, Almazova TV, Belenkii BG. J Chromatogr 1991; 555:99.
19. Svec F, Tennikova TB. J Biocompat Polym 1991;6:393.

20. Tennikova TB, Svec F. J Chromatogr 1993;646:279.
21. Abou-Rebyeh H, Korber F, Schubert-Rehberg K, Reusch J, Josic D. J Chromatogr 1991;566:341.
22. Josic D, Reusch J, Loster K, Baum O, Reutter W. J Chromatogr 1992;590:59.
23. Josic D, Lim Y-P, Strancar A, Reutter W. J Chromatogr B 1994;662:217.
24. Luksa J, Menart V, Molicic S, Kus B, Gaberg-Porekar V, Josic D. J Chromatogr 1994;661:161.
25. Strancar A, Koselj P, Schwinn H, Josic D. Anal Biochem 1996;68:3483.
26. Svec F, Frechet JMJ. Anal Chem 1992;64:820.
27. Wang QC, Svec F, Frechet JMJ. Anal Chem 1993;65:2243.
28. Wang QC, Svec F, Frechet JMJ. J Chromatogr 1994;669:230.
29. Svec F, Frechet JMJ. Chem Mat 1995;7:707.
30. Svec F, Frechet JMJ. J Chromatogr 1995;702:89.
31. Svec F, Frechet JMJ. Science 1996;273:205.
32. Svec F, Frechet JMJ. Macromol Symp 1996;110:203.
33. Hjerten S, Liao, J-L, Zhang R. J Chromatogr 1989;473:273.
34. Hjerten S, Li Y-M, Liao JL, Mohammad J, Nakazato K, Petterson G. Nature 1992; 356:810.
35. Liao J-L, Zhang R, Hjerten S. J Chromatogr 1991;586:21.
36. Hjerten S, Mohammad J, Liao J-L. Biotechnol Appl Biochem 1992:15:247.
37. Hjerten S, Nakazato K, Mohammad J, Eaker D. Chromatographia 1993;37:287.
38. Minakuchi H, Nakanishi K, Soga N, Isizuka N, Tanaka N. Anal Chem 1996;68: 3498.
39. Kopaciewicz W, Rounds MA, Regnier FE. J Chromatogr 1983;266:3.
40. Geng X, Regnier FE. J Chromatogr 1984;296:15.
41. Geng X, Regnier FE. J Chromatogr 1985;332:147.
42. Coffman JL, Roper DK, Lightfoot EN. Bioseparations 1994;4:183.
43. Belenkii BG, Podkladenko AM, Kurenbin OI, Maltsev VG, Nasledov DG, Trushin SA. J Chromatogr 1993;646:1.
44. Dubinina NI, Kurenbin OI, Tennikova TB. J Chromatogr 1996;753:217.
45. Nachman M, Azad ARM, Bailon P. J Chromatogr 1992;597:155.
46. Nachman M. J Chromatogr 1992;597:167.
47. Belenkii BG, Maltsev VG. Bio techniques 1995;18:288.
48. Reif O-W (1994). Ph.D. thesis, University of Hannover, Germany.
49. Roper DK, Lightfoot EN. J Chromatogr 1995;702:69.
50. Tanford C. The Hydrophobic Effect. 2nd ed. New York: Wiley-Interscience, 1980.
51. Pearson JD, Lin NT, Regnier FE. Anal Biochem 1982;124:217.
52. Hearn MTW, Regnier FE, Wehr CT. Proceedings of the First International Symposium on HPLC of Proteins and Peptides. New York: Academic Press, 1983.
53. Blanquet RS, Bui KH, Armstrong DW. J Liq Chromatogr 1986;9:1933.
54. Bulton WC, Nugent KD, Slattery TK, Summers BA, Snyder LR, J Chromatogr 1988;443:363.
55. Yamamoto S, Naganishi K, Matsudo R. Ion-Exchange Chromatography of Proteins. New York: Marcel Dekker, 1988:94.
56. Tennikov MB, Tennikova TB, J Chromatogr (submitted for publication).
57. Tennikov MB, Chem Physics (submitted for publication).

58. Tennikov MB, Tennikova TB. Anal Chem (submitted for publication).
59. Tennikov MB, Gazdina NV, Tennikova TB, Svec F. J Chromatogr (accepted for publication).
60. Weibrenner WF, Etzel MR. J Chromatogr 1994;662:414.
61. Adisaputro IA, Wu Y-J, Etzel MR. J Liquid Chromatogr 1996;19:1437.
62. Sarfert FT, Etzel MR. J Chromatogr 1997;764:3.
63. Reif O-W, Freitag R. J Chromatogr 1993;654:29–40.
64. Reif O-W, Nier V, Bahr U Freitag R, J Chromatogr 1994;664:13–25.
65. Reif O-W, Freitag R. Bioseparation 1994;4:369–381.
66. Kasper C, Hagedorn J, Freitag R, Tennikova T. (submitted for publication).
67. Freitag R, Reif O-W, Weidemann R, Kretzmer G. Cytotechnology 1996;21:205.
68. Champluvier B Kula M-R. Bioseparation 1992;2:343.
69. Splitt H, Mackenstedt I, Freitag R, J Chromatogr 1996;729:87–97.
70. Freitag R, Splitt H, Reif O-W. J Chromatogr 1996;728:129.
71. Thömmes J and Kula M-R. Biotechnol Prog 1995;11(4):357.
72. Lee FH, Murphy K, Lin P, Vasan S, An D, DeMarco S, Forte V, Pietronigro D. Frontiers in Bioprocessing II. Am Chem Soc, Washington, DC, 1992:392.
73. Josic D, Bal F, Schwinn H. J Chromatogr 1993;632:1–10.
74. Langlotz P, Kroner KH. J Chromatogr 1992;591:107–113.
75. Krause S, Kroner KH. Deckwer W-D. Biotechnol Tech 1991;5(3):199–204.
76. Kasper C, Reif O-W, Freitag R. Bioseparation 1997;6:373–382.
77. Abou-Rebyeh H, Körber F, Schubert-Rehberg K, Reusch J, Josic D. J Chromatogr 1991;566:341–350.
78. Brandt S, Goffe RA, Kessler SB, O'Conner JL, Zale SE. Biotechnology 1988;6: 779–782.
79. Kochan JE, Wu Y-J, Etzel MR. Ind Eng Res 1996;35:1150–1155.
80. Kim M, Saito K, Furusaki S, Sato T, Sugo T, Ishigaki I. J Chromatogr 1991;585: 45–51.
81. Nachman M, Azad ARM, Bailon P. Biotech Bioeng 1992;40:564–571.
82. Serafica GC, Pimbley J, Belfort G. Biotech Bioeng 1994;43:21–36.
83. Garg VK, Zale SE, Azad ARM, Holton OD. Frontiers in Bioprocessing II. Am Chem Soc Washington, DC, 1992:321–330.
84. Heng MH, Glatz ChE. Biotech Bioeng 1993;42:333–338.
85. Kugel K, Moseley A, Harding GB, Klein E. J Membr Sci 1992;74:115–129.
86. Strancar A, Barut M, Podgornik A, Koselj P, Schwinn H, Raspor P, Josic D. J Chromatogr 1997;760:117–123.
87. Lütkemeyer D, Siwiora S, and Büntemeyer H. Bioengineering 1992;8(2):34–44.
88. Lütkemeyer D, Bretschneider M, Büntemeyer H, Lehmann J. J Chromatogr 1993; 639:57–66.
89. Finger UB, Thömmes J, Kinzelt D, Kula M-R. J Chromatogr 1995;664:69–78.
90. Lacoste-Bourgearcq JF, Desneux Ch, Allary M. Chromatographia 1991;32(1/2): 27–32.
91. Jungbauer A, Unterluggauer F, Uhl K, Buchacher A, Steindl F. Botech Bioeng 1988;32:326–333.
92. Gebauer KH, Thömmes J, Kula M-R. Biotech Bioeng 1997;54(2):181–188.

93. Clearance of endotoxin from solution by adsorption filtration by Sartobind membrane adsorbers. Sartorius, Focus On: Developing Methods 7.
94. Belanich M, Cummings B, Grob D, Klein J, O'Conner A, Yarosh D, Pharm Technol 1994; March:142–150.
95. Bamford CH, Al-Lamee KG, Adv Ma 1994;6(6):500–502.
96. Niven GW, Scurlock PG, J Biotechnol 1993;31:179–190.
97. Svec F, Jelinkova M, Votavova E, Angew. Makromol Chem 1991;188:167–176.
98. Li Y, Spencer HG. J Biotechnol 1992;26:203–211.
99. van Huynh N, Motte JC, Pilette JF, Decleire M, Colson C. Anal Biochem 1993; 211:61–65.
100. Gerstner JA, Hamilton St. M, Cramer St. M. J Chromatogr 1992;596:173–180.
101. Suen S-Y, Etzel MR. Chem Eng Sci 1992;47(6):1355–1364.
102. Briefs K-G, Kula M-R. Chem Eng Sci 1992;47(1):141–149.

9

HPLC Purification of Recombinant Proteins

Carr J. Smith,[1] Patricia Martin,[1] Sandra M. Scott,[1] and Thomas H. Fischer[2]

[1]*R. J. Reynolds Tobacco Company, Winston-Salem, North Carolina*

[2]*University of North Carolina at Chapel Hill, Chapel Hill, North Carolina*

I. INTRODUCTION

Recombinant proteins are novel proteins produced through DNA technology by the joining of genetic sequences from heterologous sources. Since the first successful DNA cloning experiments in 1973, research has exploded in molecular biology, oligonucleotide synthesis, identification and isolation of enzymes that cleave and join DNA, characterization of bacterial plasmids, and gene expression [31,63]. These areas are now known collectively as the field of biotechnology. In 1976, this research lead to the production of the first recombinant protein, the neurotransmitter human somatostatin [23]. This great achievement was followed shortly by the first commercially successful recombinant protein, human insulin [18].

The scientific, medical, and commercial implications of recombinant proteins were obvious. Very important proteins could now be readily and rapidly produced at a purity previously unavailable. The possibilities for medical diagnostics and pharmaceuticals provided an incredible commercial driving force. Commercially successful recombinant proteins have already been produced for treating cancer, allergies, human immunodeficiency virus (HIV), neurological disease, heart attacks, blood disorders, infections, wounds, and genetic diseases [63]. Commercially successful recombinant proteins include insulin, human growth hormone, interferons, erythropoietin, and tissue plasminogen activator (tPA) [14].

Several steps are involved in producing a recombinant protein. These steps

can be summarized as follows: (1) preparation of the appropriate gene; (2) incorporation of the gene into a vector; (3) transfer of the vector carrying the gene into a recipient (host); (4) selection and cloning of the host cells carrying the gene; (5) expression of the gene; and (6) extraction of the protein [51]. Each recombinant protein has its own distinct chemical, physical, and biochemical properties.

In selecting an expression system for the production of a recombinant protein, the potential use of the protein is a determining factor. The size, complexity, posttranslational modifications, and ease of production and purity of that particular protein are considerations in selection. Research into phenotypical changes occurring in host cells necessitates an expression system closely imitating a protein's natural source [17]. The four major cell types currently employed for protein production include bacterial cells, yeast, insect cells, and mammalian cells. When choosing which expression system to use, conservation of the biological activity (proper folding) of the expressed recombinant protein as well as isolation (purification) of this protein should be considered [17,63].

Escherichia coli and *Bacteroides subtilis* are the two most widely used bacterial cell systems. The advantages of bacterial expression systems are (1) their simplicity and (2) their rapid and large yields at low cost. Bacterial cells can also secrete the recombinant protein into the culture medium facilitating purification. One disadvantage is that the proteins often fail to fold properly, forming insoluble inclusion bodies of biologically inactive proteins. While some small proteins extracted from these inclusion bodies can be successfully refolded, most larger proteins cannot. Bacterial cells also lack necessary enzymes for posttranslational modifications required for proper functioning of the protein [17,63]. *E. coli* was the expression system used to produce the first commercial recombinant protein drug, human insulin [18].

E. coli expression systems offer the option of fusion protein expression [1,32,59]. Fusion proteins are a combination of the gene product of interest (usually eukaryotic) and a second "carrier" gene product (usually prokaryotic) [32,63]. The fusion helps to stabilize the protein in the bacteria. The fusion protein expression strategy allows good translation initiation, overcomes instability, and yields a high degree of expression. The fusion partner also facilitates generic protein purification methods and helps prevent formation of inclusion bodies. The four main gene fusion expression systems in *E. coli* include *Staphylococcus* protein A (SPA), *Schistosoma japonicum* glutathione *S*-transferase (GST), *E. coli* maltose-binding protein (MBP), and *E. coli* thioredoxin [32].

Yeast can be grown as rapidly and economically as bacteria. Yeast can also achieve high cell densities and allow secretion into the culture medium, thereby facilitating purification. An advantage of yeast over bacteria is ability to perform many posttranslational modifications found on human proteins. One potential disadvantage in using yeast cells is the presence of proteases that degrade foreign proteins. Proteolytic degradation can be prevented by constructing

yeast strains in which the genes for these proteases have been deleted [17,63]. A subunit vaccine for hepatitis B virus (HBV) using only a surface protein to initiate the immune response has been successfully produced in yeast [61]. The major advantage is lack of infection risk.

A third, relatively new expression system uses baculovirus to insert foreign proteins into insect cells. Advantages are abundant expression, correct folding, and posttranslational modifications similar to those in mammalian cells. One disadvantage is the higher cost of culturing insect cells over that of bacteria and yeast. Cost is still less than that for culturing mammalian cells [63]. A vaccine for the autoimmune deficiency syndrome (AIDS) virus produced from a recombinant HIV envelope protein by this method has been approved for clinical evaluation [3].

Finally, mammalian cells have been found to be the best place to produce mammalian proteins. Mammalian cell systems are used for both transient and stable expression. Transient expression is used to verify the biological activity of engineered proteins and rapidly evaluate different vectors for the stable expression systems. In contrast, stable mammalian cell expression is more time consuming but is necessary for large-scale production of proteins in mammalian cells. The versatility of protein production possible from mammalian cells is the reward for time and effort spent on the processes of selection, amplification, and growth of stable cell lines. Thus far, there are no examples of proteins that cannot be made in mammalian cells [13,63]. Tissue plasminogen activator (tPA) was the first commercially available drug produced from a stably integrated mammalian cell culture [48]. Factor VIII, a protein required for normal clotting of blood, has also been efficiently produced in a stably integrated mammalian cell culture [45].

If an expression system conserves the biological activity of the recombinant protein, the next consideration is whether this biological activity will be further conserved following purification of the protein [53]. Currently, purification of recombinant proteins generally utilizes the same purification techniques employed for separating other proteins from cell culture media. The large number of proteins produced by the biotechnology revolution have also driven advances in analytical techniques. High-performance liquid chromatography (HPLC) and other analytical scale chromatographic techniques are essential to the achievement of the objectives of this revolution.

The techniques classically used for the purification and characterization of proteins are ultracentrifugation, size exclusion, gel filtration, ion exchange, affinity chromatography, electrophoresis, and radioimmunoassay [6,46]. However, these methods are generally time consuming and difficult to automate. The advent of HPLC brought a new dimension to the purification and analysis of proteins. The major advance was the use of microparticulate packing materials, which permitted the use of high pressure. The cost of moving from traditional liquid chromatography (LC) methods to HPLC was more than offset by improvements in speed, resolution, sensitivity of chromatographic separations, and ease of sample recovery [11]. Ad-

vancements in biotechnology continue to be a major driving force for advances in HPLC for purification and identification of proteins. HPLC can be used alone or in conjunction with classical techniques for protein purification.

Many excellent reviews and monographs have appeared in the literature on the general techniques used in the purification of proteins with many dedicated to HPLC in particular [6,8,9,14,15,46,54,55,65]. Most of the applications for recombinant proteins require high-purity separations (including large scale) and good analytical characterization of the resulting product. Traditionally, proteins and protein pharmaceuticals were extracted from blood and tissue—difficult separations in their own right. Recombinant protein technology has created a new mix from which proteins need to be isolated and purified. The purification of the desired protein from the cell broth requires separation from the host cell proteins and DNA and from other components of the culture medium. Purity is of particular concern for the pharmaceutical proteins because of the possibility of endotoxin contamination from products expressed in *E. coli* or viral products from mammalian cell culture [14,51]. The complexity of the system created by the biological and biochemical processes of recombinant DNA technology demands a robust purification strategy.

HPLC has a prominent role in the purification of recombinant proteins. Final purification is generally achieved via a multistep strategy utilizing various modes of HPLC. Since each recombinant protein has its own distinct chemical, physical, and biochemical properties, the strategy for employing chromatographic modes is unique for each protein. HPLC has great utility in the biotechnology industry because it offers high purity, is generally applicable for laboratory scale purification, and has the potential to be scaled to a preparative level [14,25,46,72].

HPLC is a dynamic tool as new pumps, column packings, and more sensitive detectors continue to be produced [8,9]. The strength of HPLC also comes from its varied physicochemical bases and the interactive way in which techniques can be combined and manipulated to achieve separation and purification. The most frequently used modes of chromatography are ion exchange, reversed-phase (RP) or hydrophobic interaction, size exclusion or affinity chromatography. Biological macromolecules differ physicochemically in size, shape, charge, hydrophobicity, and qualitative and quantitative organization of functional groups within a three-dimensional structure. The various modes of HPLC utilize these different properties as the basis for separation [46,54,55].

Hydrophobic interaction chromatography (HIC) separates on the basis of surface hydrophobicity. Reversed-phase chromatography separates on the basis of general hydrophobicity but generally uses harsher conditions than HIC. Size and shape are the principles underlying size exclusion chromatography. Ion exchange chromatography separates based on charge discrimination. Specific interactions facilitate separation by affinity chromatography. Affinity separations utilize a wide variety of immobilized ligands including metals, enzyme substrate analogs, and monoclonal antibodies for interaction with desired proteins.

Separation on columns by any HPLC mode can be manipulated by adjusting the appropriate mobile phase. Another dimension of the power of HPLC comes from the various methods of detection. Optimized detection methods enhance the sensitivity of HPLC and provide on-line data for component identification. Available detection methods include UV absorbance, scanning and diode array, fluorescence, electrochemical, pulse amperometric detection (PAD), and on-line mass spectrometry [8,9,46,54,55].

The purpose of this chapter is to provide an illustrative overview of HPLC purification of recombinant proteins. An exhaustive summary is not feasible because of the large and ever growing number of recombinant proteins. The reviewed literature is classified by the type of protein purified.

II. PURIFICATION OF FUSION PROTEINS

A large number of different fusion proteins have been isolated using a variety of HPLC columns and solvent systems (Table 1). The following are illustrative as there are many more examples.

A. Extracellular Fusion Proteins

Recombinant human insulin has been isolated by a TSK G3000SW size exclusion column [28]. In a study by Patrick and Lagu, oxidative sulfitolysis and two-dimensional HPLC determined the recombinant human proinsulin fusion protein produced in *E. coli* [47]. An anion exchange TSK DEAE-5PW column, a cation exchange TSK SP-5PW column, and a size exclusion Zorbax GF-250 column were used for the separation.

Several extracellular fusion proteins have been purified on the basis of hydrophobicity. Leukemia inhibitory factor (LIF) was initially expressed as a fusion product with glutathione *S*-transferase and then purified on a glutathione-agarose affinity matrix. After release from the matrix by cleavage with thrombin, LIF was isolated using a 300-Å Brownlee C8 RP column [16]. Monobromobimane has been used to resolve two recombinant proteins by RP-HPLC based on their cysteine content. O'Keefe et al. used a Hy-Tach nonporous C18 column to isolate transforming growth factor α *Pseudomonas aeruginosa* exotoxin A 40 (TGFα-PE40), a recombinant protein synthesized in *E. coli*, and PE40, the C-terminal fragment of TGFα-PE40 [44]. PE40 has a molecular weight (M_r) of approximately 40,000 and copurifies with TGFα-PE40. Finally, isoforms of Bet v 1, the major birch pollen allergen, have been analyzed by HPLC, mass spectrometry (MS), and cDNA cloning. A Waters μBondapak C-18 column was used to separate proteolytic fragments of purified natural Bet v'1 and recombinant nonfusion Bet v 1a [58].

Table 1 Purification of Fusion Proteins

Protein classification	Ref.	Substance purified	Column type	Solvent system
Extracellular	Klyushnichenko VE, Wulfson AN. Recombinant human insulin—II. Size-exclusion HPLC of biotechnological precursors. Factqrs influencing retention and selectivity. Pure Appl Chem 1993;65(10):2265–2272.	Insulin-containing proteins	TSK G3000SW (300 × 7.5 mm)	Reagents used = acetonitrile, methanol, sodium phosphate, phosphoric acid (all esp. pure), water purified on Milli-Q, sodium dodecyl sulfate, guanidine hydrochloride.
	Patrick JS, Lagu AL. Determination of recombinant human proinsulin fusion protein produced in *Escherichia coli* using oxidative sulfitolysis and two-dimensional HPLC. Anal Chem 1992;64(5):507–511.	Human proinsulin fusion protein (ChPI) expressed in recombinant *E. coli*	TSK DEAE-5PW (anion exchange); TSK SP-5PW (cation exchange); Zorbax GF-250 (size exclusion)	*Anion exchange*—"Loading" mobile phase A = 20 mM Tris in 7 M urea (pH 7.0). "Eluting" mobile phase B = 20 mM Tris and 0.5 M sodium sulfate in 7 M urea (pH 7.0). *Cation exchange*—Mobile phase A = 40 mM monobasic potassium phosphate in 7 M urea (pH 3.5). Mobile phase B = 0.5 M in sodium sulfate, 40 mM in monobasic potassium phosphate, and 7 M in urea with pH 3.5. *Size exclusion*—Mobile A phases used in ion exchange: (1) 20 mM Tris in 7 M urea (pH 7.0) & (2) 40 mM monobasic potassium phosphate in 7 M urea (pH 3.5).

	Gearing DP, et al. Production of leukemia inhibitory factor in *Escherichia coli* by a novel procedure and its use in maintaining embryonic stem cells in culture. Biotechnology 1989;7(11):1157–1161.	Leukemia inhibitory factor (LIF) [initially expressed as a fusion product with glutathione *S*-transferase, purified on glutathione-agarose affinity matrix and released from the matrix by cleavage with thrombin]	300-Å Brownlee C8 RP	5 min linear gradient to 40% acetonitrile in 0.1% TFA followed by a 60 min linear gradient to 60% acetonitrile in 0.1% TFA.
	O'Keefe DO, et al. Use of monobromobimane to resolve two recombinant proteins by reversed-phase high-performance liquid chromatography based on their cysteine content. Chromatography 1992;627(1–2): 137–143.	1) transforming growth factor–α *Pseudomonas aeruginosa* exotoxin A 40 (TGFα-PE40), a recombinant protein synthesized in *E. coli* 2) PE40, an $M_r \approx 40{,}000$ C-terminal fragment of TGFα-PE40, which copurifies with TGFα-PE40.	Hy-Tach nonporous C18	Linear gradient of 34–64% acetonitrile in 0.1% TFA
	Swoboda I, et al. Isoforms of Bet v 1, the major birch pollen allergen, analyzed by liquid chromatography, mass spectrometry, and cDNA cloning. J Biol Chem 1995;270(6);2607–2613.	Proteolytic fragments of purified natural Bet v 1 (nBet v1) and Recombinant nonfusion Bet v 1a (rBet v 1a) [Bet v 1 = major allergen of birch pollen]	Waters μBondapak C18	Linear gradient of acetonitrile [solvent A, 0.1% (v/v) TFA in water; solvent B, 0.07% (v/v) TFA in acetonitrile; 0–40% B in 120 min]
Intracellular	Sharma SK, et al. Metal affinity chromatography of recombinant HIV-1 reverse transcriptase containing a human renin cleavable metal binding domain. Biotechnol Appl Biochem 1991;14(1):69–81.	Recombinant HIV-1 reverse transcriptase containing a human renin–cleavable metal binding domain	C4 (Vydac) RP, 300-Å pore size, 4.6 mm × 15 cm	0–70% gradient of 0.1% TFA/H_2O to 0.1% TFA/CAN in 40 min
	Iwakura M, et al. Dihydrofolate reductase as a new "affinity handle." J Biochem (Tokyo) 1992;111(1):37–45.	Chemically synthesized polypeptides of 5–44 amino acids, expressed in *E. coli* as fusion proteins which show dihydrofolate reductase (DHFR) activity.	Inertsil-ODS 5-μm column (RP)	Equilibrated with 0.1% TFA in 15% acetonitrile. Linear gradient of acetonitrile up to 50%.

Table 1 Continued

Protein classification	Ref.	Substance purified	Column type	Solvent system
Surface membrane	Welling GW, et al. Isolation of Sendai virus F protein by anion-exchange high-performance liquid chromatography in the presence of Triton X 100. J Chromatogr 1983;266: 629–632.	Integral membrane protein of Sendai virus (a paramyxovirus of mice): F (fusion protein, M_r = 6500)	Mono Q HR 5/5	24-min gradient from 0.15 M to 1.5 M sodium chloride in 0.02 M sodium phosphate (pH 7.2) containing 0.1% Triton X-100.
	Welling GW, et al. Isolation of detergent-extracted Sendai virus proteins by gel-filtration, ion-exchange and reversed-phase high-performance liquid chromatography and the effect on immunological activity. J Chromatogr 1984;297:101–109.	Integral membrane proteins of Sendai virus (a paramyxovirus of mice): HN (hemagglutinin-neuraminidase, M_r = 68,000) and F (fusion protein, M_r = 6500)	TSK 4000SW (gel filtration); Mono Q HR 5/5 (ion exchange); C1 (reversed-phase)	*TSK 4000 SW*—isocratic elution with 50 mM sodium phosphate, pH 6.5, containing 0.1% SDS. *Mono Q HR 5/5*—24-min gradient from 20 mM Tris-HC1, pH 7.8, containing 0.1% Triton X-100 to 0.5 M sodium chloride in the same buffer. *C1*—25-min gradient of 25% acetonitrile in water with 0.05% TFA to 75% acetonitrile in water with 0.05% TFA.
	Welling GW. Purification strategies for Sendai virus membrane proteins. J Chromatogr 1987;397:165–174.	Integral membrane proteins of Sendai virus (a paramyxovirus of mice): HN (hemagglutinin-neuraminidase, M_r = 68,000) and F (fusion protein, M_r = 6500)	TSK 4000SW (size exclusion); Mono Q HR 5/5 (anion exchange); TSK Chelate-5PW (metal chelate affinity); Phenyl 5PW-RP (reversed-phase)	*TSK 4000SW*—elution with 0.1% SDS in 50 mM sodium phosphate (pH 6.5). *Mono Q HR 5/5*—gradient from 0 to 0.5 M sodium chloride in 20 mM Tris-HCl (pH 7.8), containing 0.1% (w/w) decyl-PEG.

TSK Chelate-5PW—
FIRST PROGRAM: gradient from 0 to 0.1 M glycine in 20 mM Tris-HCl (pH 8.0), containing 0.5 M sodium chloride and 0.1% decyl-PEG (buffer A).
[*Equilibration*—with buffer A. Then loaded with 0.2 M zinc chloride and equilibrated again with buffer A]
SECOND PROGRAM: Gradient from buffer A to buffer B. [Both buffers contained 0.2 M sodium acetate (pH 7.0) and 0.1% (w/w) decyl-PEG. Also, buffer A contained 0.5 M sodium chloride, and buffer B contained 0.5 M ammonium chloride.]
[*Equilibration*—with buffer A. Then loaded with 0.2 M zinc chloride in buffer A and 10 ml of buffer B. Before sample application, column reequilibrated with buffer A].
Phenyl 5PW-RP—24-min gradient from 15% to 75% acetonitrile in water containing 0.05% TFA.

Table 1 Continued

Protein classification	Ref.	Substance purified	Column type	Solvent system
	Welling-Wester S, et al. Effect of detergents on the structure of integral membrane proteins of Sendai virus studied with size-exclusion high-performance liquid chromatography and monoclonal antibodies. J Chromatogr 1988;443:255–266.	Integral membrane proteins of Sendai virus (a paramyxovirus of mice): HN (hemagglutinin-neuraminidase, M_r = 68,000) and F (fusion protein, M_r = 6500)	Two tandem-linked Superose 6HR 10/30 (300 × 10 mm i.d.) size exclusion columns	Following eluents were used: 6 M guanidine hydrochloride in 50 mM sodium phosphate (pH 6.5); 0.25% deoxycholate in 10 mM sodium phosphate (pH 8.1); 0.1% Brij 35 in 50 mM sodium phosphate (pH 6.5); 0.1% triethylamine (pH 3.0) with 0.1% decyl polyethylene glycol–300; 20% acetonitrile in 50 mM sodium phosphate (pH 6.5); 0.1% lauryldimethylamine oxide in 50 mM sodium phosphate (pH 6.5); 0.25% taurocholate in 10 mM sodium phosphate (pH 7.4); 0.03% Tween 20 in 50 mM sodium phosphate (pH 6.5), 0.1% decyl polyethylene glycol–300 in 50 mM sodium phosphate (pH 6.5); 0.1% SDS in 50 mM sodium phosphate (pH 6.5); 0.25% CHAPS in 100 mM sodium phosphate (pH 6.5); 0.1% octylglucoside in 50 mM sodium phosphate (pH 6.5); and 0.05% sarkosyl in 10 mM Tris-HCl (pH 7.5) supplemented with 0.6 M sodium chloride.

Van Ede J, et al. Comparison of non-ionic detergents for extraction and ion-exchange high-performance liquid chromatography of Sendai virus integral membrane proteins. J Chromatogr 1989;476:319–327.	Integral membrane proteins of Sendai virus (a paramyxovirus of mice): HN (hemagglutinin-neuraminidase, M_r = 68,000) and F (fusion protein, M_r = 6500)	Mono Q HR 5/5 (anion exchange); Zorbax Bioseries GF 450 or TSK G4000SW (size exclusion)	*Anion exchange*—gradient from 0 to 0.5 M sodium chloride in 20 mM Tris-HCl (pH 7.8) containing 0.1% (w/w) of detergent. *Size exclusion*—mobile phase was 50 mM sodium phosphate (pH 6.5) containing 0.1% SDS.
Welling-Wester S, et al. Comparison of ion-exchange high-performance liquid chromatography columns for purification of Sendai virus integral membrane proteins. J Chromatogr 1989;1988;476:477–485.	Integral membrane proteins of Sendai virus (a paramyxovirus of mice): HN (hemagglutinin-neuraminidase, M_r = 68,000) and F (fusion protein, M_r = 6500)	*Ion exchange*: Mono Q HR 5/5 (80-nm pores), TSK DEAE-NPR(nonporous); and Zorbax BioSeries SAX (30-nm pores) *Size exclusion*: Two Zorbax GF 450 (250 × 9.4 mm i.d.) in tandem	*Ion exchange*—Linear 12-min gradient from 20 mM Tris-HCl (pH 7.8), containing 0.1% detergent, to 0.5 M sodium chloride in the same buffer. [Preceded by isocratic elution for 5 min] *Size exclusion*—elution with 50 mM sodium phosphate (pH 6.5), containing 0.1% SDS.
Welling GW, et al. Comparison of detergents for extraction and ion-exchange high-performance liquid chromatography of Sendai virus membrane proteins. J Chromatogr 1992; 599(1–2):157–162.	Integral membrane proteins of Sendai virus (a paramyxovirus of mice): HN (hemagglutinin-neuraminidase, M_r = 68,000) and F (fusion protein, M_r = 6500)	*Ion exchange*: MA7Q (nonporous), Zorbax BioSeries SAX (30-nm pores), MonoQ HR 5/5 (80-nm pores), and PL-SAX 4000 Å (400-nm pores) *Size exclusion*: Polyol Si-500 (100 nm × 4.6 mm i.d.)	*Ion exchange*—Linear gradient from 20 mM Tris-HCl (pH 7.8) containing 0.1% $C_{10}E_{5-9}$ (decylPEG-300) to 0.5 M sodium chloride in the same buffer. (Preceded by isocratic elution for 10 min). *Size exclusion*—elution with 50 mM sodium phosphate (pH 6.5) containing 0.1% SDS.

Table 1 Continued

Protein classification	Ref.	Substance purified	Column type	Solvent system
	Welling-Wester S, et al. Effect of different amounts of the non-ionic detergents C10E5 and C12E5 present in eluents for ion-exchange high-performance liquid chromatography of integral membrane proteins of Sendai virus. J. Chromatogr 1993:646(1):37–44.	Hemagglutinin-neuraminidase protein HN (M_r = 68,000) and fusion protein F (M_r = 65,000) [2 integral membrane proteins of Sendai virus]	*Ion exchange*: Mono Q HR 5/5 (''classical system''); Mono Q PC 1.6/5 (Smart system) *Size exclusion*: Superose 6 HR 10/30	*Ion exchange*—Linear gradient from 20 mM Tris-HCl (pH 7.8) containing different detergent concentrations (buffer A) to 0.5 M sodium chloride in the same buffer (buffer B). (Preceded by isocratic elution for 8 min) *Size exclusion*—elution with 50 mM sodium phosphate (pH 6.5) containing 0.1% SDS.
	Folena-Wasserman G. et al. Assay, purification and characterization of a recombinant malaria circumsporozoite fusion protein by high performance liquid chromatography. J Chromatogr 1987;411:345–354.	Recombinant protein R32Leu-Arg [32-tetrapeptide sequence from the immunodominant repeat region of the malaria circumsporozoite protein of *Plasmodium falciparum* (R32) linked to the dipeptide Leu-Arg]	I.D. Brownlee C4 300-Å, 7-µm precolumn coupled to a Vydac C4 300-Å, 5-µm column	Equilibrated with 0.05% aqueous TFA. Linear gradient of 0–40% acetonitrile containing 0.05% TFA over 12 min.
	Mizuochi T, et al. Structural characterization by chromatographic profiling of the oligosaccharides of human immunodeficiency virus (HIV) recombinant envelope glycoprotein gp120 produced in Chinese hamster ovary cells. Biomed Chromatogr 1988;2(6): 260–270.	N-linked oligosaccharides of the HIV recombinant envelope glycoprotein gp120 produced in CHO cells	*Ricinus communis* agglutinin (RCA 120) column (affinity)	Phosphate-buffered saline pH 7.4 (last fraction eluted with 0.05 M lactose).

Nuclear	DuBois GC. Rapid purification of bacterially expressed fusion proteins by high-performance liquid chromatography methods. Gene Anal Tech 1986; 3(1):6–11.	Fusion products of the v-myb oncogene and 13–14 amino acids of the λCII gene (CII-myb fusion protein); fusion proteins from HTLV-1 Px with λCII (CII-HTLV-Px fusion protein)	Waters C18 μBondapack column; Beckman C3 Ultrapore RPSC protein separation; Waters Protein-PAK DEAE 5PW	*Waters C18 μBondapack column* and *Beckman C3 column*—Equilibrated with 0.1% TFA acid in water. Linear gradient of 0–80% acetonitrile, which also contained 0.1% TFA. *Waters Proetin-PAK DEAE 5PW.* Linear gradient of 0–0.3 M sodium acetate in dialysis buffer; Linear gradient of 0–0.5 M NaCl in a dialysis buffer.
Other	Greve KF, et al. Liquid chromatographic and capillary electrophoretic examination of intact and degraded fusion protein CTLA4Ig and kinetics of conformational transition. J Chromatogr A 1996;723(2):273–284.	CTLA4Ig (an immunoglobulin fusion protein)	Tosohaas TSK gel column; Bakerbond Abx "mixed-mode" ion exchange column	*Tosohaas TSK gel column*—Mobile phase was aqueous solution of 0.1 M sodium sulfate, 0.1 M potassium phosphate, monobasic, and 0.05% sodium azide (pH 6.7). *Bakerbond Abx "mixed-mode" ion-exchange column*—Gradient from 0% B [B contained 0.65 M sodium acetate, 20% methanol (pH 7.0)] to 20% B in 0.025 M MES (pH 5.5).

B. Intracellular Fusion Proteins

Metal affinity chromatography has isolated a recombinant HIV-1 reverse transcriptase containing a human renin–cleavable metal-binding domain. The separation used a C4 (Vydac) RP, 300 Å pore size, 4.6 mm × 15 cm column [57]. Chemically synthesized polypeptides of 5–44 amino acids in length were expressed in *E. coli* as fusion proteins that showed dihydrofolate reductase activity. These polypeptides were separated using an Inertsil-ODS 5-μm column [24].

C. Surface Membrane Fusion Proteins

Many surface membrane fusion proteins have been separated by HPLC. Eight publications on the HPLC purification of two different Sendai virus integral membrane proteins [hemagglutinin-neuraminidase (HN) and fusion protein (F)] are reviewed in chronological order to illustrate the progression in the technology over the 10-year period from 1983 to 1993. Sendai virus F protein was isolated by a Mono Q HR 5/5 anion exchange column in the presence of Triton X-100 [67]. Sendai virus is a paramyxovirus in mice. These authors published a second study in which they isolated detergent-extracted Sendai virus proteins by gel filtration, ion exchange, and RP-HPLC [66]. Three years later, this group summarized their findings on purification strategies for Sendai virus membrane proteins [68]. Integral membrane proteins of Sendai virus, HN (M_r = 68,000) and F (M_r = 6500), were separated by a multistep process using the following columns: TSK 4000SW (size exclusion); Mono Q HR 5/5 (anion exchange); TSK Chelate-5PW (metal chelate affinity); and Phenyl 5PW-RP. In 1988, Welling-Wester et al. examined the effect of detergents on the structure of the integral membrane proteins of Sendai virus [70]. Size exclusion HPLC and monoclonal antibodies were used by employing two tandem-linked Superose 6HR 10/30 size exclusion columns. These authors published two more studies in 1989. The first compared the use of nonionic detergents for extraction and ion exchange HPLC of Sendai virus integral membrane proteins [62]. This study initially used anion exchange HPLC on a Mono Q column to isolate the Sendai virus integral membrane proteins. The gradient for this step was from 0 to 0.5 M sodium chloride in 20 mM Tris-HCl (pH 7.8) containing 0.1% (w/w) sodium dodecyl sulfate (SDS). Protein recoveries after the anion exchange HPLC step were determined by size exchange HPLC on either a TSK 400SW or two tandem-linked Zorbax GF 450 columns. The mobile phase for this step was 50 mM sodium phosphate (pH 6.5) containing 0.1% SDS. The second study compared different ion exchange HPLC columns for the purification of Sendai virus integral membrane proteins [69]. In this study, the highest recovery of HN protein was obtained by using either a Mono Q column or a TSK DEAE-NPR column, whereas the highest recovery of F protein was obtained after chromatography on the Mono Q column. In 1992, Welling et al. compared detergents for the extraction and ion exchange HPLC of Sendai

virus integral membrane proteins [64]. Extracted proteins were subjected to ion exchange HPLC using four different columns (MA7Q, Zorbax BioSeries SAX, Mono Q, and PL-SAX). The amount of protein in the extracts and fractions after anion exchange HPLC was determined by size exclusion HPLC on a Polyol Si-500 column, and the relative recoveries of protein were similar for all four anion exchange columns. A final study on the purification of Sendai virus proteins by this group examined the effect of different amounts of the nonionic detergents C10E5 and C12E5 in the eluents from Mono Q HR 5/5 (''classical system'') and Mono Q PC 1.6/5 (Smart system) ion exchange columns [71]. They found that a detergent concentration of less than 0.026–0.05% allows the integral membrane proteins of Sendai virus to remain on the column. The authors used size exclusion HPLC to determine the yield from both classical and Smart anion exchange HPLC systems and found that the Smart system had the advantage that only one-tenth of the sample amount needed for classical HPLC is required to obtain comparable results. A disadvantage of the Smart system was the relatively long time required for equilibrium of the column with different detergents.

A tandem column procedure using an I.D. Brownlee C4 300-Å 7-μm precolumn coupled to a Vydac C4 300-Å 5-μm column isolated a recombinant malaria circumsporozoite fusion protein [13]. Specifically, the isolated recombinant protein R32Leu-Arg was a 32-tetrapeptide sequence from the immunodominant repeat region of the malaria circumsporozoite protein of *Plasmodium falciparum* (R32) linked to the dipeptide Leu-Arg. An affinity column containing *Ricinus cummunis* agglutin (RCA 120) was used to purify N-linked oligosaccharides of the human immunodeficiency virus recombinant envelope glycoprotein gp120 produced in Chinese hamster ovary (CHO) cells [39].

D. Nuclear Fusion and Other Fusion Proteins

Nuclear fusion proteins have also been purified using HPLC. DuBois has reported the rapid purification of bacterially expressed fusion products of the following: v-myb oncogene, 13–14 amino acids of the λCII gene (CII-myb fusion protein), and fusion proteins from HTLV-1 Px with λCII (CII-HTLV-Px fusion protein) [10]. In a recent study by Greve et al., an immunoglobulin fusion protein, CTLA4Ig, was isolated with a Tosohaas TSK gel column and Bakerbond Abx ''mixed-mode'' ion exchange column [19].

III. PURIFICATION OF MALTOSE-BINDING PROTEINS

A variety of maltose-binding proteins (MBPs) have been purified using HPLC techniques (Table 2). Illustrative examples of extracellular, intracellular (cytoplasmic), and surface membrane MBPs purified by HPLC are discussed by protein classification.

Table 2 Purification of Maltose-Binding Proteins

Protein classification	Ref.	Substance purified	Column type	Solvent system
Extracellular	Fassina, Giorgio, et al. High yield expression and purification of human endothelin-1. Protein Expression Purif 1994; 5(6):559–568.	human endothelin (1–21) released from human big endothelin (1–37)	ABI Aquapore 30 × 2.1 mm i.d. RP; ABI Aquapore RP-8 HPLC	Linear acetonitrile gradient (0.1% TFA) from 3% to 60%
	Hiraoka, Osamu, et al. Formation of 1:1 complex of the cytokine receptor homologous region of granulocyte colony-stimulating factor receptor with ligand. Biosci Biotechnol Biochem 1995;59(12):2351–2354.	mCRH-G-CSF complex [a cytokine receptor homologous (CRH) region of the murine granulocyte colony-stimulating factor (G-CSF) receptor expressed by an *E. coli* maltose-binding protein (MBP) fusion system.]	TSK gel G3000SW (gel filtration)	Equilibrated with 20 mM sodium phosphate buffer, pH 7.0, containing 0.2 M NaCl. Eluted with the same solution.
Intracellular	Hoener zu Bentrup, Kerstin, et al. Maltose transport in *Aeromonas hydrophila*: purification, biochemical characterization and partial protein sequence analysis of a periplasmic maltose-binding protein. Microbiology (Reading, U. K.) 1994;140(4):945–951.	Fragments generated by cleaving a periplasmic maltose-binding protein from *Aeromonas hydrophila* with CNBr	Vydac C4	Acetonitrile gradient (0–70%) in 0–1% TFA

	Kim, Do Hyung, et al. Expression and purification of HIV-1 protease utilizing a maltose binding protein. Mol Cells 1994;4(1):79–84.	HIV-1 protease	Mono S HR/5	Equilibrated with the Mono S equilibration buffer (50 mM MES, 1 mM EDTA, 1 mM DTT, 10% glycerol, pH 6.2). NaCl gradient (0–0.1 M for 5 min, and 0.1–0.4 M for 30 min).
	Martinez, Aurora, et al. Expression of recombinant human phenylalanine hydroxylase as fusion protein in *Escherichia coli* circumvents proteolytic degradation by host cell proteases. Isolation and characterization of the wild-type enzyme. Biochem J 1995;306(2): 589–597.	Fusion protein MBP-(Fx_a)-hPAH [a recombinant human phenylalanine hydroxylase (hPAH) fused through the target sequences of the restriction protease factor Xa to the C-terminal end of *E. coli* MBP]	HiLoad Superdex 200 HR (size exclusion)	Mobile phase consisted of 20 mM Na-Hepes and 0.2 M NaCl, pH 7.0
Surface membrane	Quadri, Luis EN, et al. Characterization of the protein conferring immunity to the antimicrobial peptide carnobacteriocin B2 and expression of carnobacteriocins B2 and BM1. J Bacteriol 1995;177(5):1144–1151.	Carnobacteriocin B2 immunity protein (CbiB2)	C8-Vydac (10 × 250 mm, 10-μm particle size, 300-Å pore size)	Gradient from 38.5% to 45.5% of acetonitrile in 0.1% TFA

A. Extracellular Maltose-Binding Proteins

Human endothelin (1–21) has been purified by first employing an ABI Aquapore 30 × 2.1 mm i.d. RP column using a linear acetonitrile gradient [0.1% trifluoroacetyl acid (TFA)] from 3% to 60%. The second step utilized an ABI Aquapore RP-8 column and the same solvent system and gradient [12]. A second extracellular MBP, the mCRH–G-CSF complex, has been isolated [20]. This protein is a cytokine receptor homologous (CRH) region of the murine granulocyte colony-stimulating factor receptor expressed by an *E. coli* MBP fusion system. Gel filtration separation was performed using a TSK gel G3000SW column equilibrated with 20 mM sodium phosphate buffer, pH 7.0, containing 0.2 M NaCl. The same solution was used for elution.

B. Intracellular (Cytoplasmic) Maltose-Binding Proteins

Fragments generated by cleaving a periplasmic MBP from *Aeromonas hydrophila* with CNBr have been separated using a Vydac C4 RP column and an acetonitrile gradient (0–70%) in 0–1% TFA [21]. A Mono S HR/5 column separated HIV-1 protease using an MBP [27]. The column was equilibrated with Mono S equilibration buffer and the protein was eluted with an NaCl gradient. The fusion protein resulting from recombinant human phenylalanine hydroxylase (hPAH) fused to the c-terminal end of *E. coli* MBP was purified using a HiLoad Superdex 200 HR size exclusion column [37]. The mobile phase consisted of 20 mM Na-Hepes and 0.2 M NaCl, pH 7.0.

C. Surface Membrane Proteins

Quadri et al. characterized the protein that confers immunity to the antimicrobial peptide carnobacteriocin B2 and expression of carnobacteriocins B2 and BM1 [50]. In this study, the surface membrane carnobacteriocin B2 immunity protein was eluted from a C8 Vydac column using a gradient from 38.5% to 45.5% of acetonitrile in 0.1% TFA.

IV. PURIFICATION OF OTHER RECOMBINANT PROTEINS

A. Extracellular Proteins

The hyperproduction of polyhedrin insulin-like growth factor 2 (IGF-2) fusion protein has been achieved in silkworm larvae infected with recombinant *Bombyx mori* nuclear polyhedrosis virus [38]. A site for cleavage by CNBr was introduced in the IGF-2 gene, allowing the IGF-2 protein to be released from the polyhedrin fusion protein by CNBr treatment and purified by ion exchange chromatography and HPLC (Table 3). A modified C8 RP-HPLC separation technique was used

Table 3 Purification of Other Recombinant Proteins

Protein classification	Ref.	Substance purified	Column type	Solvent system
Extracellular	Marumoto, Yasumasa, et al. Hyperproduction of polyhedrin-IGF II fusion protein in silkworm larvae infected with recombinant *Bombyx mori* nuclear polyhedrosis virus. J Gen Virol 1987;68(10):2599–2606.	Insulin-like growth factor 2 (IGF-2) (released from polyhedrin-IGF2 fusion protein produced in silkworm larvae infected with recombinant *Bombyx mori* nuclear polyhedrosis virus)	Not given	Acetonitrile gradient in 0.1% TFA
	Hummel, Michael, et al. Gene synthesis, expression in *Escherichia coli* and purification of immunoreactive human insulin-like growth factors I and II. Application of a modified HPLC separation technique for hydrophobic proteins. Eur J Biochem 1989;180(3):555–561.	TrpE/IGF fusion protein (immunoreactive human insulin-like growth factors 1 and 2 fused to the 300 N-terminal amino acids of the *E. coli* trpE gene)	C8 RP	Gradient of 2-propanol in formic acid created within 30 min
	Mueller, Sabine, et al. The formation of diselenide bridges in proteins by incorporation of selenocysteine residues: biosynthesis and characterization of (Se)2-thioredoxin. Biochemistry 1994;33(11):3404–3412.	Purified protein isolate (in which selenocysteine substituted for cysteine residues) expressed from recombinant *E. coli* grown on a medium containing selenocysteine	C4-Dynamax 300 Å; Hytach peptide analytical	Mobile phase was 0.1% TFA in water (A) and 0.75% TFA in acetonitrile (B).

Table 3 Continued

Protein classification	Ref.	Substance purified	Column type	Solvent system
	Vakharia, Vikram N., et al. Synthetic pheromone biosynthesis activating neuropeptide gene expressed in a baculovirus expression system. Insect Biochem Mol Biol 1995;25(5): 583–589.	Pheromone biosynthesis–activating neuropeptide (PBAN) gene product derived from extracellular fraction of 5B1-4 (an insect cell line) infected with vINV-4 (a recombinant baculovirus)	4.6-mm-diam. Aquapore RP-300 column; 2.1-mm diam. Aquapore RP-300 columns	*4.6-mm-diam.*—gradient of acetonitrile rising from 10% at 0.67%/min, in 0.05 M sodium phosphate, pH 6.0; *2.1-mm-diam.* —gradient of isopropanol rising from 10% at 0.5%/min in 0.1% TFA; —gradient of acetonitrile in 0.1% heptafluorobutyric acid; —gradient of acetonitrile in 0.1% TFA.
Intracellular	Xue, Hong, et al. Purification of hyperexpressed Bacillus subtilis tRNATrp cloned in Escherichia coli. J Chromatogr, Biomed Appl 1993;613(2):247–255.	*Bacillus subtilis* $tRNA^{Trp}$ gene product cloned in *E. coli*	Vydac C4-derivatized silica	Eluted with 60 min linear gradient from buffer A (10 mM sodium phosphate, pH 5.5, 1 M sodium formate, 8 mM $MgCl_2$) to buffer B (10 mM sodium phosphate, pH 5.5, 10% methanol), followed by isocratic elution with 100% buffer B for 20 min.
	Yamagata, S., et al. Overexpression of the *Sac-charomyces cerevisiae* MET17/MET25 gene in *Escherichia coli* and comparative characterization of the product with *O*-acetylserine-*O*-acetylhomoserine sulfhydrylase of the yeast. Appl Microbiol Biotechnol 1994;42(1):92–99.	*Saccharomyces cerevisiae* MET17/MET25 gene product *O*-acetylserine-*O*-acetylhomoserine sulfhydrylase (OAS-OAH) expressed in *E. coli*; OAS-OAH from yeast	DEAE-5PW (ion exchange); G3000SW (gel filtration)	Not given

Nuclear	Lillehoj, Erik P., et al. Virion-associated transregulatory protein of human T-cell leukemia virus type I. AIDS Res Hum Retroviruses 1992;8(2):237–244.	Tax (transregulatory) protein of HTLV-1) from HUT-102 cells	C4 RP	Linear gradient of 0–100% aqueous acetonitrile/0.1% TFA
Surface membrane	Bhown, Ajit S., et al. Purification and characterization of the gag gene products of avian-type C retroviruses by high-pressure liquid chromatography. Anal Biochem 1981;112(1):128–134.	Gag gene products of avian type C retroviruses	^{125}I gel permeation columns	Mixture of acetic acid/propanol/highly purified water (20:15:65)
	Kolbe, Hanno V.J., et al. Isolation of recombinant partial gag gene product p18 (HIV-1Bru) from *Escherichia coli*. J Chromatogr 1989;476:99–112.	Recombinant partial gag gene product p18 (HIV-1_{Bru}) [= membrane-associated structural protein of HIV-1]	Sulfoethyl aspartamide; Nucleosil C4; Vydac 218TP54 C18	*Sulfoethyl aspartamide*—Equilibrated with a blank gradient; nonlinear gradient from 0 to 100% Cat Ex-B buffer [40 mM sodium phosphate (pH 7.0)–1 M sodium chloride] in CatEx-A buffer [20 mM sodium phosphate (pH 7.0)–40 mM sodium chloride] followed by return to 100% Cat Ex-A buffer. *Nucleosil C4*—Nonlinear gradient from 90% eluent R1-A (0.1% TFA in Milli-Q water) to 90% eluent RP1-B [0.1% TFA in acetonitrile-Milli-Q water (70:30, v/v)] and then back to 90% RP1-A. *Vydac 218TP54 C18*—Nonlinear gradient from 99% eluent RP1-A to 100% eluent RP1-B and then back to 99% RP1-A.

by Hummel et al. to purify immunoreactive human insulin-like growth factors 1 and 2 fused to 300 N-terminal amino acids of the *E. coli* trpE gene [22]. Using recombinant *E. coli* grown on a medium containing selenocysteine, Mueller et al. biosynthesized and characterized (Se)2-thioredoxin by forming diselenide bridges in proteins that had incorporated selenocysteine residues [40]. Protein isolates in which selenocysteine substituted for cysteine residues were purified with a C4 Dynamax 300-Å column. Vakharia et al. used a baculovirus expression system to express a neuropeptide gene that activates synthetic pheromone biosynthesis [35,60]. Aquapore RP-300 columns were used to isolate the neuropeptide gene product.

B. Intracellular Proteins

Xue et al. hyperexpressed the gene product from *Bacillus subtilis* $tRNA^{Trp}$ cloned in *E. coli* [73]. Vydac C4-derivatized silica was used to isolate the gene product. Overexpression of the *Saccharomyces cerevisiae* MET17/MET25 gene in *E. coli* was conducted by Yamagata et al. [74]. Following overexpression, the gene product was characterized and compared with *O*-acetylserine-*O*-acetylhomoserine sulfhydrylase from yeast. Both ion exchange and gel filtration HPLC were performed on the two proteins to determine behavioral differences. Results implied that no differences in molecular size and electric charge exist. It should be noted that in this case HPLC was used for characterization instead of purification.

C. Surface Membrane Proteins

The gag gene products of avian-type C retroviruses have been purified and characterized using ^{125}I gel permeation columns [4]. A 20:15:65 mixture of acetic acid, propanol, and highly purified water served as the solvent system. A recombinant partial gag gene product p18 that is a membrane-associated structural protein of HIV-1 was isolated from *E. coli* [30]. The complicated separation procedure required the use of sulfoethyl aspartamide, a Nucleosil C4 column, and a Vydac 218TP54 C18 column.

D. Nuclear Proteins

HUT-102 cells were engineered to produce a virion-associated transregulatory protein of human T-cell leukemia virus type 1 [33]. A C4 RP column and a linear gradient of 0–100% aqueous acetonitrile with 0.1% TFA was used to isolate the transregulatory protein.

V. DISCUSSION

Since the advent of recombinant DNA techniques in the 1970s [51], a great number of different proteins have been produced in a variety of expression systems [63]. As biotechnology progresses, molecular biologists are producing an ever greater variety and quantity of recombinant proteins. As the examples in Tables 1–3 illustrate, the purification of recombinant proteins is accomplished using standard protein purification techniques that rely on the ability to separate proteins on the basis of molecular size, electrical charge, hydrophobicity, or affinity for a specific monoclonal antibody. Examination of purification strategies for different protein classifications, i.e., extracellular, intracellular, surface membrane, and nuclear, suggests that there is no overall preferred method for any given protein type. The studies reviewed show that combinations of ion exchange, size exclusion, and RP-HPLC techniques have been used to purify each of these protein categories. Two studies report the use of affinity HPLC to purify surface membrane proteins [39,68]. The affinity method may be particularly suited for surface membrane protein purification. This technique can exploit the unique biological specificity of the protein–ligand interactions [11], which frequently occur at the cell surface in in vivo systems, e.g., the interaction between a carbohydrate moiety and a lectin [39]. The majority of methods for purifying surface membrane proteins required a detergent in the solvent system. Detergents are amphipathic molecules whose hydrophilic head and hydrophobic tail allow them to compete with the phospholipids in the membrane lipid bilayer [36], thereby freeing the membrane protein of interest from the bilayer [65]. Extraction of membrane proteins with nonionic detergents, such as Triton X-100, decylpolyethylene glycol (DecylPEG), and octylglucoside, preserves the biological activity of the protein. Ionic detergents, such as SDS and naturally occurring deoxycholate and taurodeoxycholate bile salts, tend to irreversibly denature proteins. However, transmembrane protein hydrophobic regions have a greater affinity for this type of detergent [65].

In many biological applications, retention of conformational structure and the attendant biological activity is important. For example, because the biological activity of human growth hormone (hGH) is preserved upon production in a bacterial expression system, recombinant techniques can be used to provide this hormone for hGH-deficient children. Previously, the purification method involved painstaking extraction of the hormone from the pituitary of human cadavers. Studies by Nishi et al. and Knudtzon show that the therapeutic effects of pituitary hGH are successfully duplicated by recombinant hGH [29,41].

Retention of the structure–activity relationship in various recombinant cytokines has allowed the large-scale production of these molecules for patient therapy. The biological activity of recombinant interferon-γ (IFNγ) has been shown to supplement the activity of endogenous IFNγ following injection into patients

with malignant tumors [75], and IFNγ has been successfully administered for the treatment of chronic myeloproliferative syndromes and the prevention of chronic granulomatous disease [52]. Also, recombinant granulocyte colony-stimulating factor (G-CSF) and granulocyte-macrophage CSF (GM-CSF) stimulate granulopoiesis after chemotherapy or bone marrow transplantation and mobilize marrow stem cells for peripheral blood stem cell transplantation.

Numerous interleukins retain their biological activity and therapeutic potential when produced as recombinant proteins. Biologically active interleukin-12 (IL-12) has been produced in vitro and in vivo by recombinant techniques [5] and has been shown to provide effective therapy against tumors and infections [7]. Recombinant human (rh) IL-11 has been used clinically to preserve the integrity of gastrointestinal mucosa during cancer treatment regimens [49]. The cytokine synthesis–inhibiting action of IL-10 is duplicated in rhIL-10 and is therapeutic for patients with myelomonocytic leukemia. Likewise, the pleiotropic biological activities of IL-6 on B cells, T cells, and hematopoietic progenitors are preserved in recombinant IL-6 [26] and serve to inhibit advanced renal cell cancer [56]. Lastly, the activity of rhIL-2 provides effective inhibition of growth of breast cancer [34].

Purifying fusion proteins whose synthetic sequences retain their original conformational structures and attendant biological activities is another technical challenge that promises advances in patient therapy. For example, antibody-cytokine fusion proteins combine the unique targeting ability of antibodies with the multifunctional activities of cytokines. Becker et al. produced antibody-IL-2 fusion proteins by fusing a sequence coding for human IL-2 to genes encoding antibodies [2]. Their use of antibodies targeted the IL-2 to the tumor site effectively and eradicated human hepatic and pulmonary melanoma metastases in Severe Combined Immune Deficiency (SCID) mice.

Immunotoxins, fusion proteins made up of a toxin and a monoclonal antibody, also offer an attractive approach to cancer therapy [63]. O'Boyle et al. purified an immunotoxin combining a type 1 ribosome inactivating protein with a murine monoclonal antibody reactive with a polymorphic determinant of class 2 HLA-DR histocompatibility leukocyte antigen (HLA) on human lymphoma cells [42]. Such immunotoxins are advantageous because the antibody delivers the toxin specifically to the target cell.

The use of mammalian cells for protein production has been favored because it is often difficult to retain the desired biological activity when therapeutic proteins are produced in bacteria and yeast. Accordingly, recent efforts have focused on the development of numerous mammalian cell lines to host proteins produced by recombinant techniques [43].

The field of chromatography is vital to recombinant technology. In particular, HPLC has played an important role in the purification of recombinant pro-

teins. Technological advances, e.g., the development of new detergents, will continue to provide new avenues for the use of HPLC.

REFERENCES

1. Balbas P, Bolivar F. Design and construction of expression plasmid vectors in *Escherichia coli*. In Goeddel DV, ed. Methods in Enzymology. Vol 185. Gene Expression Technology. San Diego: Academic Press, 1990.
2. Becker JC, Pancook JD, Gillies SD, Mendelsohn J, Reisfeld RA. Eradication of human hepatic and pulmonary melanoma metastases in SCID mice by antibody-interleukin 2 fusion proteins. Proc Nat Acad Sci USA. 1996;93(7):2702–2707.
3. Berman PW, Gregory TJ, Riddle L, Nakamura GR, Champe MA, Porter JP, Wurm FM, Hershberg RD, Cobb EK, Eichberg JW. Protection of chimpanzees from infection by HIV-1 after vaccination with recombinant glycoprotein gp 120 but not bp 160. Nature 1990;345:622–625.
4. Bhown AS, Bennett JC, Mole JE, Hunter E. Purification and characterization of the gag gene products of avian-type C retroviruses by high-pressure liquid chromatography. Anal Biochem 1981;112(1):128–34.
5. Bramson J, Hitt M, Gallichan WS, Rosenthal KL, Gauldie J, Graham FL. Construction of a double recombinant adenovirus vector expressing a heterodimeric cytokine: in vitro and in vivo production of biologically active interleukin-12. Hum Gene Ther 1996;7(3):333–342.
6. Chicz RM, Regnier FE. High-performance liquid chromatography: effective protein purification by various chromatographic modes. In: Deutscher MP, ed. Methods in Enzymology. Vol 182. Guide to Protein Purification. San Diego: Academic Press, 1990.
7. Chouaib S, Chehimi J. Human interleukin-12: biological role and therapeutic potential. Medicine/Sciences 1996;12(4):451–457.
8. Dorsey JG, Cooper WT, Siles BA, Foley JP, Barth HG. Liquid chromatography: theory and methodology. Anal Chem 1996;68:515R–568R.
9. Dorsey JG, Cooper WT, Wheeler JF, Barth HG, Foley JP. Liquid chromatography: theory and methodology. Anal Chem 1994;66(12):500R–546R.
10. DuBois GC. Rapid purification of bacterially expressed fusion proteins by high-performance liquid chromatography methods. Gene Anal Tech 1986;3(1):6–11.
11. Ettre LS. Evolution of liquid chromatography: a historical overview. In: Horváth C, ed. High-Performance Liquid Chromatography: Advances and Perspectives, Vol 1. New York: Academic Press, 1980.
12. Fassina G, Merli S, Germani S, Ciliberto G, Cassani G. High yield expression and purification of human endothelin-1. Protein Expression Purif 1994;5(6):559–568.
13. Folena-Wasserman G, Inacker R, Rosenbloom J. Assay, purification and characterization of a recombinant malaria circumsporozoite fusion protein by high performance liquid chromatography. J Chromatogr 1987;411:345–354.
14. Frenz J. Chromatographic separations in biotechnology. In: Horvath C, Ettre LS,

eds. Chromatograpy in Biotechnology. Washington, DC: American Chemical Society, 1993.

15. Frenz J, Hancock WS, Henzel WJ, Horvath C. Reversed phase chromatography in analytical biotechnology of proteins. In: Gooding KM, Regnier FE, eds. HPLC of Biological Macromolecules: Methods and Applications. New York: Marcel Dekker, 1990.
16. Gearing DP, Nicola NA, Metcalf D, Foote S, Willson TA, Gough NM, Williams RL. Production of leukemia inhibitory factor in *Escherichia coli* by a novel procedure and its use in maintaining embryonic stem cells in culture. Biotechnology 1989; 7(11):1157–1161.
17. Goeddel DV. Systems for heterologous gene expression. In: Goeddel DV, ed. Methods in Enzymology. Vol 185(1). Gene Expression Technology. San Diego, Academic Press, 1990.
18. Goeddel DV, Kleid DG, Bolivar F, Heyneker HL, Yansura DG, Crea R, Hirose T, Kraszewski A, Itakura K, Riggs AD. Expression of chemically synthesized genes for human insulin. Proc Natl Acad Sci USA 1979;76:106–110.
19. Greve KF, Hughes DE, Richberg P, Kats M, Karger BL. Liquid chromatographic and capillary electrophoretic examination of intact and degraded fusion protein CTLA4Ig and kinetics of conformational transition. J Chromatogr A 1996;723(2):273–284.
20. Hiraoka O, Hiroyuki A, Yoshimi O. Formation of 1:1 complex of the cytokine receptor homologous region of granulocyte colony-stimulating factor receptor with ligand. Biosci Biotechnol Biochem 1995;59(12):2351–2354.
21. Hoener zu Bentrup K, Schmid R, Schneider E. Maltose transport in Aeromonas hydrophila: purification, biochemical characterization and partial protein sequence analysis of a periplasmic maltose-binding protein. Microbiology (Reading, U. K.) 1994;140(4):945–951.
22. Hummel M, Herbst H, Stein H. Gene synthesis, exression in Escherichia coli and purification of immunoreactive human insulin-like growth factors I and II. Application of a modified HPLC separation technique for hydrophobic proteins. Eur J Biochem 1989;180(3):555–561.
23. Itakura K, Hirose T, Crea R, Riggs A, Heyneker HL, Bolivar F, Boyer H. Expression in E. coli of a chemically synthesized gene for the hormone somatostatin. Science 1977;198:1056–1063.
24. Iwakura M, Tsuda K. Dihydrofolate reductase as a new "affinity handle." J Biochem (Tokyo) 1992;111(1):37–45.
25. Jungbauer A. Preparative chromatography of biomolecules. J Chromatogr 1993;639: 3–16.
26. Keever-Taylor CA, Witt PL, Truitt RL, Ramanujam S, Borden EC, Ritch PS. Hematologic and immunologic evaluation of recombinant human interleukin-6 in patients with advanced malignant disease: evidence for monocyte activation. J Immunother 1996;19(3):231–243.
27. Kim DH, Lee J, Sung YC, Choi KY. Expression and purification of HIV-1 protease utilizing a maltose binding protein. Mol Cells 1994;4(1):79–84.
28. Klyushnichenko VE, Wulfson AN. Recombinant human insulin—II. Size-exclusion HPLC of biotechnological precursors. Factors influencing retention and selectivity. Pure Appl Chem 1993;65(10):2265–2272.

29. Knudtzon J. Growth hormone therapy of short stature. Acta Paediatr Scand 1986; 75(3):353–361.
30. Kolbe HVJ, Jaeger F, Lepage P, Roitsch C, Lacaud G, Kieny MP, Sabatie J, Brown SW, Lecocq JP, Girard M. Isolation of recombinant partial gag gene product p18 (HIV-1Bru) from *Escherichia coli*. J Chromatogr 1989;476:99–112.
31. Kornberg A. Why purify enzymes? In: Deutscher MP, ed. Methods in Enzymology. Vol 182. Guide to Protein Purification. San Diego: Academic Press, 1990.
32. LaVallie ER, McCoy JM. Gene fusion expression systems in *Escherichia coli*. Curr Opin Biotech 1995;6:501–506.
33. Lillehoj EP, Alexander SS. Virion-associated trans-regulatory protein of human T-cell leukemia virus type I. AIDS Res Hum Retroviruses 1992;8(2):237–244.
34. Liu DL, Yang MQ, Eberhardt J, Persson B. Repeated immunotherapy using intratumoural injection with recombinant interleukin-2 and tumour-infiltrating lymphocytes inhibits growth of breast cancer and induces apoptosis of tumour cells. Cancer Lett 1996;103(2):131–136.
35. Luckow VA, Summers MD. Trends in the development of baculovirus expression vectors [review]. Bio Technology 1988;6:47–55.
36. Martin DW. Membranes. In: Martin DW, Mayes PA, Rodwell VW and Granner DK, eds. Harper's Review of Biochemistry. 20th ed. Los Altos, California: Lange, 1985.
37. Martinez A, Knappskog PM, Olafsdottir S, Doskeland AP, Eiken HG, Svebak RM, Bozzini M, Apold J, Flatmark T. Expression of recombinant human phenylalanine hydroxylase as fusion protein in *Escherichia coli* circumvents proteolytic degradation by host cell proteases. Isolation and characterization of the wild-type enzyme. Biochem J 1995;306(2):589–597.
38. Marumoto Y, Sato Y, Fujiwara H, Sakano K, Saeki Y, Agata M, Furusaw M, Maeda S. Hyperproduction of polyhedrin-IGF II fusion protein in silkworm larvae infected with recombinant *Bombyx mori* nuclear polyhedrosis virus. J Gen Virol 1987;68(10): 2599–2606.
39. Mizuochi T, Spellman MW, Larkin M, Solomon J, Basa LJ, Feizi T. Structural characterization by chromatographic profiling of the oligosaccarides of human immunodeficiency virus (HIV) recombinant envelope glycoprotein gp120 produced in Chinese hamster ovary cells. Biomed Chromatogr 1988;2(6):260–270.
40. Mueller S, Senn H, Gsell B, Vetter W, Baron C, Boeck A. The formation of diselenide bridges in proteins by incorporation of selenocysteine residues: biosynthesis and characterization of (Se)2-thioredoxin. Biochemistry 1994;33(11):3404–3412.
41. Nishi Y, Masuda H, Nishimura S, Kihara M, Suwa S, Tachibana K, Takeda M, Okada Y, Matsuda I. Isolated human growth hormone deficiency due to the hGH-I gene deletion with (type IA) and without (the Israeli-type) hGH antibody formation during hGH therapy. Acta Endocrinol 1990;122(2):267–271.
42. O'Boyle KP, Colletti D, Mazurek C, Wang Y, Ray SK, Diamond B, Rosenblum MG, Epstein AL, Shochat D, Dutcher JP, Wiernik PH, Klein RS. Potentiation of antiproliferative effects of monoclonal antibody Lym-1 and immunoconjugate Lym-1-gelonin on human Burkitt's lymphoma cells with gamma-interferon and tumor necrosis factor. J Immunother 1995;18(4):221–230.
43. Ogez JR, Builder SE. Downstream processing of proteins from mammalian cells. Bioprocess Technol 1990;10:393–416.

44. O'Keefe DO, Lee AL, Yamazaki S. Use of monobromobimane to resolve two recombinant proteins by reversed-phase high-performance liquid chromatography based on their cysteine content. Chromatography 1992;627(1–2):137–143.
45. Paborsky LR, Fendly BM, Fisher KL, Lawn RM, Marks BJ, McCray G, Tate KM, Vehar GA and Gorman CM. Mammalian cell transient expression of tissue factor for the production of antigen. Protein Eng 1990;3:547–553.
46. Papadoyannis IN, ed. HPLC in Clinical Chemistry. New York: Marcel Dekker, 1990, Chap. 19.
47. Patrick JS, Lagu AL. Determination of recombinant human proinsulin fusion protein produced in *Escherichia coli* using oxidative sulfitolysis and two-dimensional HPLC. Anal Chem 1992;64(5):507–511.
48. Pennica D, Holmes WE, Kohr WJ, Harkins RN, Vehar GA, Ward CA, Bennett WF, Yelverton E, Seeburg PH, Heyneker HL, Goeddel DV, Collen D. Cloning and expression of human tissue-type plasminogen activator cDNA in *E. coli*. Nature 1983; 301:214–221.
49. Peterson RL, Bozza MM, Dorner AJ. Interleukin-11 induces intestinal epithelial cell growth arrest through effects on retinoblastoma protein phosphorylation. Am J Pathol 1996;149(3):895–902.
50. Quadri LEN, Sailer M, Terebiznik MR, Roy KL, Vederas JC, Stiles ME. Characterization of the protein conferring immunity to the antimicrobial peptide carnobacteriocin B2 and expression of carnobacteriocins B2 and BM1. J Bacteriol 1995;177(5): 1144–1151.
51. Richmond S, publisher. Scrip Biotechnology Made Simple, 4th ed. Richmond, Surrey, UK: PJB Publications, 1991.
52. Robak T. Cytokiny w leczeniu chorob krwi (Cytokines in the treatment of blood diseases). Acta Haematol Pol 1995;26(2 Suppl 1):72–78.
53. Sadana A. Inactivation of proteins and other biological macromolecules during chromatographic methods of bioseparation. Bioseparation 1992;3:145–165.
54. Schöneich C, Hühmer AFR, Rabel SR, Stobaugh JF, Bigelow DJ, Williams TD. Separation and analysis of peptides and proteins. Anal Chem 1995;67(12): 155R.
55. Schöneich C, Kivok SK, Wilson GS, Rabel SR, Stobaugh JF, Williams TD, Vandervelde DG. Separation and analysis of peptides and proteins. Anal Chem 1993;65(12): 67R.
56. Schuler M, Peschel C, Schneller F, Fichtner J, Farber L, Huber C, Aulitzky WE. Immunomodulatory and hematopoietic effects of recombinant human interleukin-6 in patients with advanced renal cell cancer. J Interferon Cytokine Res 1996;16(11): 903–910.
57. Sharma SK, Evans DB, Vosters AF, McQuade TJ, Tarpley WG. Metal affinity chromatography of recombinant HIV-1 reverse transcriptase containing a human renin cleavable metal binding domain. Biotechnol Appl Biochem 1991;14(1):69–81.
58. Swoboda I, Jilek A, Ferreira F, Engel E, Hoffmann-Sommergruber K, Scheiner O, Kraft D, Breiteneder H, Pittenauer E. Isoforms of Bet v 1, the major birch pollen allergen, analyzed by liquid chromatography, mass spectrometry, and cDNA cloning. J Biol Chem 1995;270(6):2607–2613.
59. Uhlén M, Moks T. Gene fusions for purpose of expression: an introduction. In:

Goeddel DV, ed. Methods in Enzymology. Vol 185. Gene Expression Technology. San Diego: Academic Press, 1990.
60. Vakharia VN, Raina AK, Kingan TG, Kempe TG. Synthetic pheromone biosynthesis activating neuropeptide gene expressed in a baculovirus expression system. Insect Biochem Mol Biol 1995;25(5):583–589.
61. Valenzuela P, Medina A, Rutter WJ, Ammerer G, Hall BD. Synthesis and assembly of hepatitis B virus surface antigen particles in yeast. Nature 1982;298:347–350.
62. Van Ede J, Nijmeijer JRJ, Welling-Wester S, Oervell C and Welling GW. Comparison of non-ionic detergents for extraction and ion-exchange high-performance liquid chromatography of Sendai virus integral membrane proteins. J Chromatogr 1989; 476:319–327.
63. Watson JD, Gilman M, Witkowski J, Zoller M. Recombinant DNA, 2nd ed. New York: Scientific American Books, W.H. Freeman 1992.
64. Welling GW, Hiemstra Y, Feijlbrief M, Oervell C, Van Ede J, Welling-Wester S. Comparison of detergents for extraction and ion-exchange high-performance liquid chromatography of Sendai virus membrane proteins. J Chromatogr 1992;599(1–2): 157–162.
65. Welling GW, Van der Zee R, Weeling-Wester S. HPLC of membrane proteins. In: Gooding KM, Regnier FE, eds. HPLC of Biological Macromolecules. New York: Marcel Dekker, 1990.
66. Welling GW, Nijmeijer JRJ, Van der Zee R, Groen G, Wilterdink JB, Welling-Wester S. Isolation of detergent-extracted Sendai virus proteins by gel-filtration, ion-exchange and reversed-phase high-performance liquid chromatography and the effect on immunological activity. J Chromatogr 1984;297:101–109.
67. Welling GW, Groen G, Welling-Wester S. Isolation of Sendai virus F protein by anion-exchange high-performance liquid chromatography in the presence of Triton X 100. J Chromatogr 1983;266:629–632.
68. Welling GW, Slopsema K, Welling-Wester S. Purification strategies for Sendai virus membrane proteins. J. Chromatogr 1987;397:165–174.
69. Welling-Wester S, Haring RM, Laurens H, Oervell C, Welling GW. Comparison of ion-exchange high-performance liquid chromatography columns for purification of Sendai virus integral membrane proteins. J Chromatogr 1989;476:477–485.
70. Welling-Wester S, Kazemier B, Oervell C, Welling GW. Effect of detergents on the structure of integral membrane proteins of Sendai virus studied with size-exclusion high-performance liquid chromatography and monoclonal antibodies. J Chromatogr 1988;443:255–266.
71. Welling-Wester S, Feijlbrief M, Koedijk DGAM, Braaksma MA, Douma BRK, Welling GW. Effect of different amounts of the nonionic detergents C10E5 and C12E5 present in eluents for ion-exchange high-performance liquid chromatography of integral membrane proteins of Sendai virus. J Chromatogr 1993;646(1):37–44.
72. Wisniewski R. Principles of the design and operational considerations of large scale high performance liquid chromatography (HPLC) systems for proteins and peptides purification. Bioseparation 1992;3:77–143.
73. Xue H, Shen W, Wong JTF. Purification of hyperexpressed Bacillus subtilis tRNATrp cloned in *Escherichia coli*. J Chromatogr Biomed Appl 1993;613(2):247–255.

74. Yamagata S, Isaji M, Nakamura K, Fujisaki S, Doi K, Bawden S, D'andrea R. Overexpression of the *Saccharomyces cerevisiae* MET17/MET25 gene in *Escherichia coli* and comparative characterization of the product with O-acetylserine.O-acetylhomoserine sulfhydrylase of the yeast. Appl Microbiol Biotechnol 1994;42(1):92–99.
75. Yamasaki T, Kagawa T, Takamura M, Moritake K. Pharmacokinetics of intratumoral interferon-gamma activity following subcutaneous administration of recombinant interferon-gamma in a patient with metastatic brain tumor derived from renal cancer. Neurol Surg 1995;23(2):169–173.

10

Isolation, Purification, and Characterization of Human Seminal Plasma Proteins and Their Immunological Behavior In Vitro

Afrozul Haq, Nona Remo Rama, and Sultan T. Al-Sedairy
King Faisal Specialist Hospital and Research Center, Riyadh, Saudi Arabia

I. INTRODUCTION

Over the last few years, significant data have accumulated concerning components present in the seminal plasma such as hormones, enzymes, peptides, and cytokines [1–4]. This progress has led us to the discovery of other components in seminal plasma, not only in humans but in animals. We have achieved a greater understanding of the functional properties of these components, especially seminal plasma proteins in the male reproductive organs, its role in male fertility, and its immunological effects in vitro. Still, the physiochemical and functional properties of most of these proteins in seminal plasma remain unclear. Therefore, further investigation should be established to determine the complexities of these components present in seminal plasma and whether it has a role in the immunopathogenesis of diseases in the male and female reproductive systems. The protein makeup of seminal plasma appears to be extremely susceptible to variation on account of large number of factors, such as species, age, frequency of semen collection, the nature of ejaculates, the early ejaculates which show a protein profile different from that of the later ejaculates, the hormonal status of the individual, the condition of storage of semen, and possibly other factors such as diet, weather, environmental and emotional factors including stress. Unlike the other

body fluids that are readily accessible for sampling and study, generation of semen, and therefore of seminal plasma, cannot be ordered about. The seminal plasma of all species is rich in proteins but some of the proteins are not indigenous to seminal plasma in that they may originate from serum. The proteins may also leak into the seminal plasma from dead spermatozoa or spermatozoa damaged during centrifugation or handling of the semen. Furthermore, some of the proteins of seminal fluid may be bound to the spermatozoa immediately after ejaculation and thus no longer be available in seminal plasma. The proteins in seminal plasma are contributed from secretions of various male reproductive glands, e.g., epididymis, seminal vesicles, prostate, and Cowper's and coagulating glands. The remaining proteins found in the seminal plasma have been divided into the following groups: proteolytic enzymes; glycolytic enzymes; nucleolytic enzymes; other enzymes; hormones and growth factors; antifertility factors; immunosuppressive factors; androgen-binding proteins; inhibin; immunoglobulins; and other nonenzymatic, nonhormonal proteins.

II. PROTEINS

Proteins are fundamental components of all living cells and include many substances, such as enzymes, hormones, and antibodies, that are necessary for the proper functioning of an organism. Proteins serve as the structural pattern of the protoplasms from enzymes, hormones, chromosomes, and cell components. They constitute about 15% of the protoplasms, are colloidal in nature, and are formed of large molecules of great complexity and variety. These proteins are built up by peptide linkages of amino acids with the peptide bonds between the amino acid group (NH_2) of one amino acid and the acid group (COOH) of the adjacent one. They are made up of 20 amino acids as tripeptide and of several amino acids as polypeptide. The human body produces thousands of different proteins, including those that act as catalysts, those that are localized where they regulate the flow of material in and out of the cell, those that are soluble or membrane-bound, those that can interconvert different types of energy, those that recognize foreign materials and microbes, those that are implicated in the repair of injury, those that respond to biological stress, and those with purely structural roles. Proteins can be structural (intracellular and extracellular proteins); catalytic (enzymes); vectoreal (transport proteins); regulatory (determine the rate at which other proteins are made).

Any deficiencies and excess of these proteins can contribute to human diseases. Significant studies have been done to determine chemical properties that can be derived from the composition and distribution of amino acids. But still, the relationship between the chemical compositiion, structure, and the function of seminal plasma proteins is obscure and intriguing.

A. How Are Proteins Synthesized?

During the development of an organism, cells differentiate to perform specialized functions. It starts with the replication of DNA, when the individual strands separate resulting in two daughter strands of DNA that are identical to the original DNA. Each daughter strand is synthesized in the direction of 5′ to 3′ requiring one strand to be synthesized in a discontinuous fashion. DNA is transcribed into RNA. The structures of DNA and RNA are similar in most respects. The only difference is that in RNA the base uracil (U) replaces T, and U therefore base-pairs with A; the other difference is that the sugar moiety of RNA is ribose instead of deoxyribose. There are three major classes of RNA: messenger RNA (mRNA), transport RNA (tRNA), and ribosomal RNA (rRNA). It is the mRNA that contains sequences that are translated into protein. After the mRNA is formed in the nucleus, it is transported to the cytoplasm where it is translated into protein whose amino acid sequence is determined by the codons of the mRNA according to the genetic code.

III. HUMAN SEMINAL PLASMA

Human seminal plasma (HSP) is a complex fluid mixture of numerous secretions derived from various glands associated with the male reproductive tract, including the testis whose primary exocrine function is the production of sperm and whose secondary function is the production of the secretions that accompany sperm; the epididymis whose main function is the absorption of fluid and the addition of substances to the seminal fluid to nourish the maturing sperms; the prostate, which produces a thin, milky fluid containing citric acid and acid phosphatase added to the seminal fluid at the time of ejaculation; the seminal vesicles, which consist of a coiled tube and produce a secretion that is added to the seminal fluid. Human seminal plasma composes approximately 80–90% of the volume of normal ejaculate. It contains distinct protein components that are important in the survival of the spermatozoa.

The long length of the duct of the epididymis provides storage space for the spermatozoa and allows them to mature. The smooth muscle in the capsule and stroma contract and the secretion from the many glands is squeezed into the prostatic urethra. The prostatic secretion from the many glands is squeezed into the prostatic urethra. The prostatic secretion is alkaline and helps to neutralize the acidity of the vagina. The secretions contain substances that are essential for the nourishment of the spermatozoa. At this point, the sperm are mixed with the fluid from the seminal vesicles, the prostate, and bulbourethral glands and become motile. This combined fluid is called semen, which flows through the remaining urethra during ejaculation. The walls of the seminal vesicles contract

during ejaculation and expel their contents into the ejaculatory ducts, thus washing the spermatozoa from the urethra.

A. Human Seminal Plasma Proteins

Seminal plasma contains different components necessary for the survival of the spermatozoa. Several proteins have been identified in human seminal plasma; some of these proteins are identical, as judged by electrophoretic mobility and immunological methods, to blood plasma proteins such as albumin, globulins, glycoproteins, acrosin inhibitor, and transferrins [5–8]. However, many proteins are specific to seminal plasma, and such proteins are of particular interest since they could be used as markers of seminal stains in forensic medicine. A study of the protein profiles of the seminal plasma of normospermic and vasectomized men would also reveal the origin of the proteins [9]. The proteins of human seminal plasma have been resolved by polyacrylamide gel electrophoresis (PAGE), sodium dodecyl sulfate (SDS)–PAGE, isoelectrocfocusing, and normal gel chromatographic and microdisck-gel electrophoresis methods. Human seminal plasma has been resolved into about 20 protein bands by using SDS-PAGE, with most of the bands lying in the low molecular weight range (10–20 kDa) and a few bands of MW 32, 49, 68, and 75 kDa. No bands were observed above 80 kDa. Human seminal plasma contains membrane cofactor protein (MCP: CD46) of 60,000 MW after gel filtration, which was associated with prostasomes [10]. It has been reported that prostasomes may play a complementary role to other immunosuppressive factors contained in the human semen [11]. These factors may protect the sperm cells from the deleterious effects of phagocytosing cells, prolong their life, and consequently enhance the chance of conception, and at the same time possibly have a permissive effect on sexually transmitted diseases. Prostasomes are trimellar to multimellar vesicles produced by the human prostate and are present in appreciable amounts in normal human semen. These substances may contribute to successful fertilization. A monoclonal antibody (SEM-12) specific for human sperms was isolated [12]. Sperm surface glycoproteins may be involved in sperm-zona pellucida recognition. Some of these proteins are of seminal plasma origin and their expression may change in the process of capacitation and acrosome reaction.

Human seminal plasma was fractionated by affinity chromatography on lentil lectin Sepharose gel chromatography on Ultrogel ACA 34 and immunoaffinity on Mab 456–coupled CNBr-Sepharose 4B [13]. The purified 4E6 antigen consisted of three subunits with molecular weights of 70, 64, and 60 kDa. This antigen is present in high amount in sera of infertile patients and therefore may be involved in the pathogenesis of immunological infertility. Transforming growth factor β (TGFβ) was detected by Nocera and Chu [14] from human seminal plasma protein fractions with molecular weights of 100–440 kDa after gel

filtration. These proteins exhibit immunosuppressive activity and inhibit DNA synthesis. T6Fα was then purified from human seminal plasma on Sephadex G-75 chromatography and high-performance size exclusion liquid chromatography [15]. This growth factor showed mitotic activity. Another component of human seminal plasma was studied as seminal plasma motility inhibitor (SPMI) [16]. This factor has the capacity to inhibit the movement of demembranated and intact spermatozoa. SPMI decreases its biological activity rapidly in semen. Human seminal plasma β-microseminoprotein was purified using DEAE-Sephacel and zinc chelate Sepharose CL-6B column chromatography [17]. β-Microseminoaminoprotein is a nonglycoprotein with a molecular weight of 19 or 17 kDa. An acrosome reaction (AR)-inhibiting glycoprotein (ARIG) from human seminal plasma that was isolated by differential centrifugation, chromatofocusing, and Sephacryl S300 gel filtration was reported [4]. ARIG has a molecular weight of 74 kDa and inhibits sperm exocytosis. Its interaction with spermatozoa may be mediated by carbohydrate-binding proteins on the sperm cell. Moreover, fractionated 59-kDa and 72-kDa proteins in human seminal plasma showed specific immunoreactivity and are documented to be the most frequently involved sperm antigens in the immune response in fertile subjects [18]. After ion exchange and immunoaffinity chromatography of seminal plasma proteins in humans, it has been demonstrated that the presence of kallikrein hK2 and Protein C inhibitor (PCI) regulates its activity in seminal plasma [19]. Several workers documented that seminal plasma TGFβ may have some role to play in sexual transmission of human immune deficiency virus (HIV) [14,20]. The authors' data demonstrated the overexpression of TGFβ in HIV-infected patients, suggesting that TGFβ is an important mediator in HIV infection. The presence of PCI was detected throughout the male reproductive tract in high concentration, about 200 μg/ml, in seminal plasma [21]. Their results suggest that PCI might function as a scavenger of prematurely activated acrosin, thereby protecting intact surrounding cells and seminal plasma proteins from possible proteolytic damage. Receptors for the Fc region of the immunoglobulin G (IgG) (soluble Fc γ RIII) have been recognized as a link between humoral and cellular responses [22]. Its soluble form found in seminal plasma may modulate the immunosuppression of antisperm immune responses in the male and female reproductive tracts.

The suppressive activity of the seminal plasma influences different cells of the immune system. It can be assumed that more than one component of seminal plasma is responsible for its immunosuppressive effect. It may be attributed to the presence of zinc peptide complex in seminal plasma [23]. However, some workers stated that it might be due to uteroglobulin and transglutaminase [24]. Fc receptor–binding protein has a vital role in terms of the immunosuppressive effects of seminal plasma [25]. It may exert specific effects, e.g., receptors Fc fractions of gamma globulin which might bind to inflammatory agents [26]. It has also been reported that prostaglandin E (PGE) in seminal plasma predomi-

nates and raises intracellular cAMP in leukocytes, which may contribute to the immunosuppressive effects of seminal plasma. Immunosuppression may attribute to the presence of a protein similar to pregnancy-associated Protein A [27]. The presence of polyamines like spermin and spermidine has been reported and that could also contribute to immunosuppression of seminal plasma [28]. Immunosuppression might also be due to the seminal nucleases and proteases in seminal plasma [5]. Following is a brief list of important proteins of human seminal plasma that have been studied extensively:

β-Microseminoprotein [29]
Sperm-binding proteins [30,31]
Protein kinase inhibitor [32]
β-Endorphin [33]
Calcium-binding protein (calmodulin) [34]
Zinc-binding proteins [35]
Ion-binding proteins [36]
Placental proteins [37]

B. Seminal Plasma Proteins of Other Species

Several studies have been done on the isolation, purification, and characterization of proteins in human seminal plasma. These studies were not limited to humans but also included animals. Four major proteins of bovine seminal plasma—BSP-A1, BSP-A2, BSP-A3, and BSP–30 kDa (collectively named BSP proteins)—have been purified by affinity chromatography using *p*-aminophenylphosphorylcholine-agarose (PPC-agarose) matrix [38]. These proteins appear to be ubiquitous in mammals and may possibly be involved in the modification of the lipid content of the sperm plasma membrane. Furthermore, BSP–30 kDa protein was studied, and it was found that this protein plays a role in sperm capacitation [39]. These workers also determined its amino acid sequence, disulfide bonds and *O*-glycosylation sites. The mosaic structure of BSP–30 kDa suggests that this glycoprotein might be a factor contributing to the different sperm capacitating effects exerted by heparin in different mammalian species. A phosphodiesterase was purified from bull seminal plasma by column chromatography on DEAE-Sephadex A-50, ConA-agarose, chromatofocusing, and AMP-agarose [40]. This purified enzyme is constituted from a single polypeptide chain of about 125 kDa. Two major proteins from boar seminal plasma designated as PSP-I and PSP-II were purified and characterized [41]. CM-cellulose chromatography, gel filtration on Sephadex G-75, and reversed-phase high-performance liquid chromatography were used for complete purification. Recently, boar and stallion seminal plasma were fractionated using affinity chromatography on heparin-Sepharose [42]. In both species, among other proteins, the heparin-binding (H+) and non-heparin-

binding (H−) fractions each contained glycoforms of either porcine PSP-I or equine HSP-1 and HSP-2. However, porcine H+/PSP-I eluted as a monomeric protein, whereas H−/PSP-I formed a heterodimer with PSP-II, another major seminal plasma protein. On the other hand, stallion proteins H+/HSP-1 and H/HSP-2 eluted together as an aggregate of relative molecular mass (90 kDa), whereas H/HSP-1 and H/HSP-2 eluted as monomers (15 kDa). Altogether these data show that glycosylation has an indirect effect on the heparin binding ability of PSP-I, HSP-I, and HSP-2 through modulation of their aggregation state.

Recently, a fertility-associated protein has been identified in bull seminal plasma as lipocalin-type prostaglandin D synthase. Immunoreactive bands at 26 kDa appeared in western blots of seminal plasma and cauda epididymal fluid (CEF) [43]. A 29-kDa band appeared in blots of rat testis fluid (RTF). Prostaglandin D synthase activity was detected in seminal plasma, cauda epididymal fluid, and RTF. The amino acid sequence was 63–80% identical to that of the enzyme of other mammals.

IV. ISOLATION AND FRACTIONATION PROCESSES

Since proteins are really large molecules, in order to investigate their structure and function, isolation and fractionation processes are required. There is no single or simple way to purify all proteins. Procedures useful in the purification of one protein may result in the denaturation of another (Fig. 1).

We were able to fractionate human seminal plasma using DEAE Sephadex A-50 ion exchange columns [44]. Semen was obtained from healthy donors and seminal plasma was recovered by ultracentrifugation. Seminal plasma was dialyzed against PBS at 4°C overnight and then applied onto a DEAE-Sephadex A-50 ion exchange column using different salt concentrations in phosphate buffer pH 6.0 (Fig. 2). Forty men either fertile or under investigation for infertility donated semen, which was collected by masturbation into sterile plastic containers after 2–3 days of abstinence from ejaculation. The mean age of the test subjects was 34.2 ± 8 (20–45) years. Semen analysis was performed by using Cellsoft Automated Semen Analyzer (Cryo Resources Ltd., New York). All patients (normospermic 20–100 million sperms/ml) included in this study attended the IVF and Infertility Clinics of King Faisal Specialist Hospital and Research Centre, Riyadh (Saudi Arabia). All of the semen samples were centrifuged at 10,000*g* at 4°C for 15 min to remove sperm and the clear supernatant was stored at −70°C until used.

The exchanger chosen was DEAE-Sephadex A-50 because it was reported to provide better results than DEAE-cellulose in the purification of proteins [45]. Two hundred fifty milligrams (25 ml) protein from normospermic human seminal plasma was applied to a XK 50/30 (Pharmacia, Piscataway, NJ, USA) column

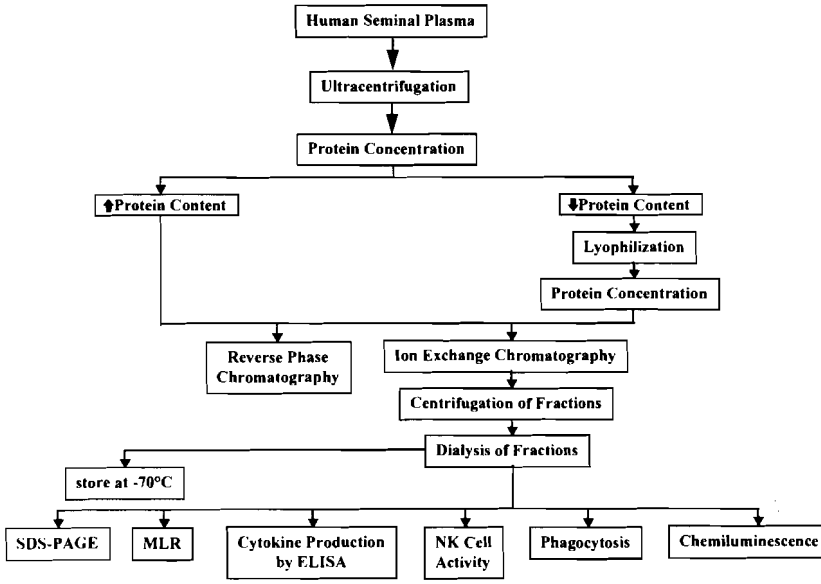

Figure 1 Flow chart for human seminal plasma proteins extraction.

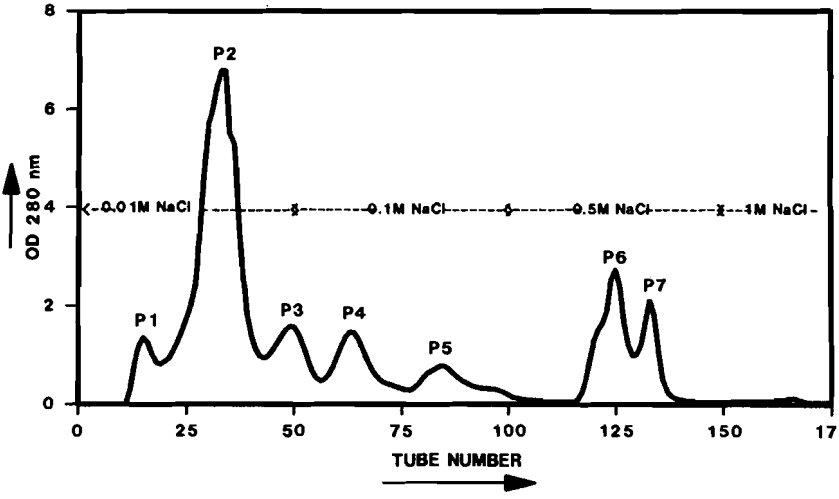

Figure 2 Chromatogram of human seminal plasma proteins on DEAE-Sephadex A-50 column. Experimental conditions: column: XK 50/30 (Pharmacia); sample: 250 mg protein (25 ml in phosphate buffer); eluent: phosphate buffer (PBS; pH 6) with increasing salt concentration (0.01–1 M NaCl) [44].

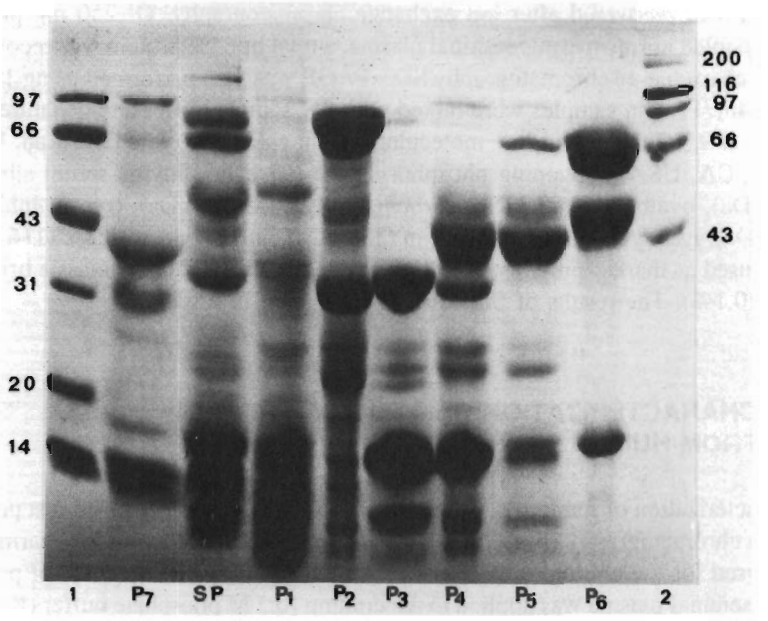

Figure 3 SDS-PAGE of marker proteins and human seminal plasma and its fractions in 12.5% gel. Lane 1, the marker proteins (from top): phosphorylase b (97 kDa), bovine serum albumin (66 kDa), ovalbumin (43 kDa), carbonic anhydrase (31 kDa), trypsin inhibitor (20 kDa), and lysozyme (14 kDa). Lanes P1–P7 represent seminal plasma obtained from DEAE-Sephadex A-50 ion exchange chromatography. Lane 2, the marker proteins (from top): myosin (200 kDa), β-galactosidase (116 kDa), phosphorylase b (97 kDa), bovine serum albumin (66 kDa), and ovalbumin (43 kDa) [44].

(5 × 15 cm) of DEAE-Sephadex A-50. The column was equilibrated with 0.05 M phosphate buffer (pH 6) containing 0.01 M NaCl. Fractions of 10 ml each (40 ml/h) were collected with increasing concentration of NaCl (0.01–1 M NaCl) and read at 280 nm. Concentration of fractionated proteins was carried out by using Centriprep 10 MW cutoff membranes (Amicon, Grace Co., Danvers, MA, USA). All steps of protein purification and concentration were performed at 4°C.

The complete elution profile of human seminal plasma proteins is shown in Fig. 2. Complete separation was achieved in seven peaks. The elution pattern of protein peaks and recovery was reproducible in different sets of experiments. A total protein of 10.4 mg for peak 1, 61.7 mg for peak 2, 17.35 mg for peak 3, 20.6 mg for peak 4, 38.8 mg for peak 5, 12.5 mg for peak 6, and 6.2 mg for

peak 7 was recovered after ion exchange chromatography. Of 250 mg protein from pooled normospermic seminal plasma, a total of 67% protein was recovered after ion exchange chromatography SDS-PAGE was then performed using 12.5% gels [46]. Protein samples were mixed with 2× sample buffer and denatured for 5 min at 95°C. High and low molecular weight calibration kits (Bio-Rad, Richmond, CA, USA) containing phosphorylase b (97 kDa), bovine serum albumin (66 kDa), ovalbumin (43 kDa), carbonic anhydrase (31 kDa), trypsin inhibitor (20 kDa), lysozyme (12 kDa), myosin (200 kDa), and β-galactosidase (116 kDa) were used as marker proteins. Staining was done using R250 Coomassie brilliant blue (0.1%). The results of SDS-PAGE are shown in Fig. 3.

V. CHARACTERIZATION OF A 20-KDA PROTEIN FROM HUMAN SEMINAL PLASMA

Characterization of seminal plasma protein was carried out by using a fast protein liquid chromatography (FPLC) system. Superose HR 10/30 column (Pharmacia) was used for the elution of the protein. A total of 100 μl (0.2 μg/ml) of protein from seminal plasma was applied to the column [0.5 M phosphate buffer ($KHPO_4$ + Na_2HPO_4) with 0.14 M NaCl]. The pH was adjusted to 7.3 by use of orthophosphoric acid. The buffer was degassed, filtered through 0.2-μm disposable filters, and used as mobile phase. The flow rate was 0.2 ml/min and the fraction size fixed at 0.5 ml. Ovalbumin (43 kDa) was used as a reference protein to confirm the performance of the Superose column. These experiments of characterization by FPLC and SDS-PAGE were carried out in the laboratory of Professor J. P. Bouvet in the Institute Pasteur in Paris. The elution profile of a 20-kDa protein as detected by FPLC is shown in Fig. 4. The results of SDS-PAGE are shown in Fig. 5.

VI. IN VIVO IMMUNOLOGICAL EFFECTS OF SEMINAL PLASMA

Proteins of human seminal plasma are known to have immunosuppressive properties. Studies on the immunosuppressive effects of seminal plasma in vivo are scarce. The ability of seminal plasma to exert its immunosuppressive effect was found to be dose-dependent, with smaller doses of antigen being most effective [47]. Mouse seminal plasma also suppressed the in vivo antibody response to bovine serum albumin. Studies have indicated that rectal infusion of prostaglandin E_2 or D_2 into male rats reduces the in vitro response of T lymphocytes to phytohemagglutinin (PHA) [48]. However, the T-cell response of female rats

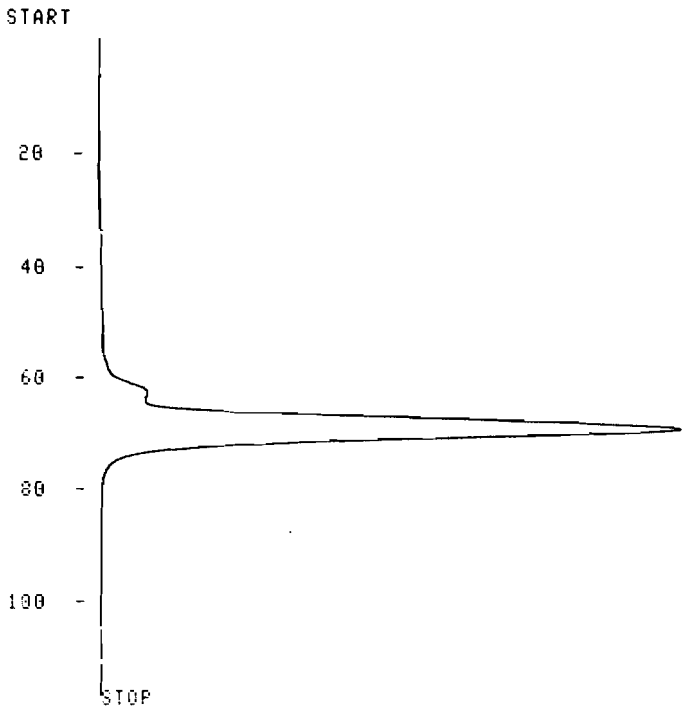

Figure 4 Elution profile of a 20-kDa protein of human seminal plasma by using FPLC (Superose column HR 10/30); 0.5 M phosphate buffer (pH 7.3) with 0.14 M NaCl was used.

treated in the same manner remained unchanged. This is an interesting finding considering that prostaglandins are known to be present in seminal plasma and both prostaglandin E_2 and D_2 suppress immune functions under in vitro conditions.

A. In Vitro Immunological Effects of Seminal Plasma

The immunosuppressive effects of human seminal plasma have been extensively studied employing in vitro tests for immune functions. These studies have clearly indicated that human seminal plasma can, either directly or indirectly, inhibit the activities of most cells that participate in immune responses, such as T cells, B cells, natural killer (NK) cells, macrophages, and polymorphonuclear leukocytes (PMNs) [49]. In addition, human seminal plasma also impairs the activity of

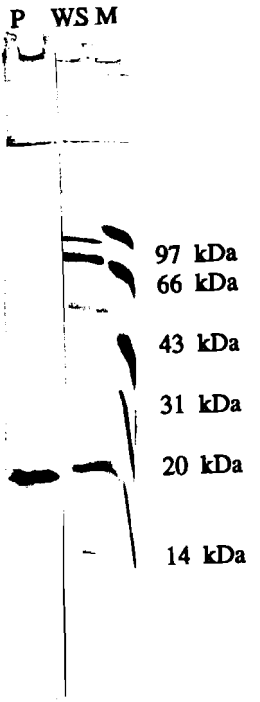

Figure 5 SDS-PAGE (12.5% gel) of marker proteins, whole human seminal plasma, and a 20-kDa protein. Lane M represents protein markers (from top); phosphorylase b (97 kDa), bovine albumin (66 kDa), ovalbumin (43 kDa), carbonic anhydrase (31 kDa), trypsin inhibitor (20 kDa), and lysozyme (14 kDa). Lane WS represents the whole human seminal plasma and lane P represents the 20-kDa protein of human seminal plasma.

the C1 and C3 components of compliment. Recently, we studied the effect of fractionated human seminal plasma on mixed lymphocte reaction (MLR) and found a highly immunosuppressive effect on MLR using various mitogens [44]. This effect was dose-dependent and greatest with 10 mg protein per well. Peak 4 was most potent followed by peaks 7, 3, and 5. Peaks 1, 2, and 6 were found to be stimulatory rather than suppressive. The whole seminal plasma was not suppressive and this effect was more or less the same with 1 μg and 10 μg protein per well. On the other hand, the stimulatory/suppressive effect of seminal plasma on PMA-induced chemiluminescence was noted [50,51], and this could possibly be due to interference with PMA binding to membrane receptors on PMNs. Based on these findings, it is stated that the biological role of seminal plasma might be to protect sperm cells with its antioxidant property from extracellular oxygen radicals in the vagina during intercourse and from side effects of the activation of macrophages and PMNs, namely, during mild infections. In this study, we

found that suppression or stimulation of chemiluminescence by human seminal plasma is dose-dependent and has no correlation with the sperm density. Moreover, seminal plasma stimulated/suppressed chemiluminescence selectively and therefore it may contain molecules of different characteristics [50]. All of these immunomodulatory effects of seminal plasma are important for successful reproduction because they help to reduce the immunogenicity of spermatozoa. Simultaneously, however, the immunosuppressive effects also endanger the host's defense against infection and malignancy [49,52].

Immunosuppressive fraction was isolated from boar seminal vesicle secretion by gel filtration on a Sephadex G-75 column and purified by reversed-phase (RP)–HPLC, and resulted into three major peaks [53]. Immunosuppressive fraction 3 was found to have inhibitory activity, estimated by inhibition of mitogen-lymphocyte proliferation on porcine lymphocytes. There have been numerous studies on the suppressive effect of seminal plasma proteins on T-cell activation and proliferation. Factors that have been identified as contributing to this activity include the prostasomes [54], polyamines [55], prostaglandins of the E series [11,56], and TGFβ [14]. At present, little is known about the role of immunosuppressive factors in male immunological infertility, which accounts for up to 6% of male infertility. It has also been demonstrated that the inability of spermatozoa collected from infertile men to inhibit the lymphocytes of their female partners was associated with the presence of antisperm antibodies in the serum of female partners and a similar link between antibody formation and lymphocyte inhibition in the male has been postulated [49,52,57,58]. In a recent study, an absence of immunosuppressive activity was measured by the inhibition of graft rejection response in vivo in the seminal plasma of men exhibiting immunological infertility. However, it remains to be established whether reduction in immunosuppressive activity measured in seminal plasma is a contributing factor or a consequence of sperm autoimmunity in the male. The polyamine spermine, naturally present at millimolar levels in seminal plasma [59], inhibits proliferation of NK cells and T lymphocytes, directly binds to DNA, and alters cervical cell ploidy, indicating its potential contribution to the etiology of cervical cancer and its possible role in suppression of the destruction of dysplastic and neoplastic cervical epithelial cells by cytotoxic lymphocytes. This study demonstrated that spermine suppresses the sensitivity of cervical carcinoma cells to lymphokine-activated killer (LAK) lymphocytes from more than half of normal individuals. Cervical carcinoma cells are inherently very sensitive to LAK lymphocytes and spermine may be an important immunosuppressive agent in natural immunity against cervical cancer.

B. Luminol-Dependent Chemiluminescence and Phagocytic Activity

Although seminal plasma affects several aspects of the immune system, it is believed that many of the inhibitory properties result from its effects on PMNs,

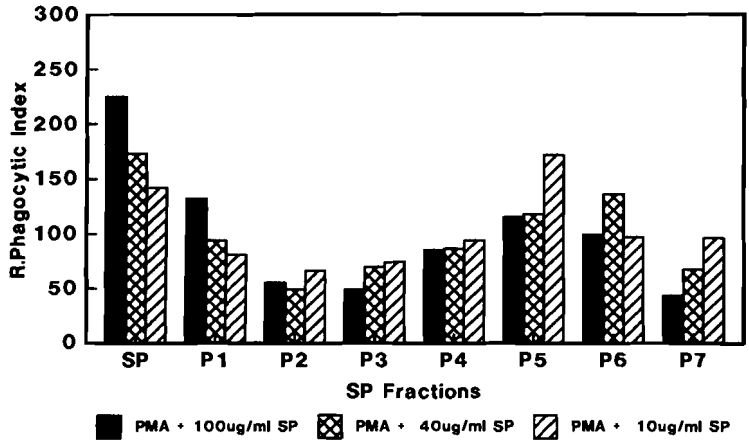

Figure 6 Effect of Seminal plasma (SP) and its fractions (P1 to P7) on phagocytic response to phorbol myristate acetate (PMA). The x axis represents the whole SP and its different fractions (P1–P7), whereas the y axis represents the relative phagocytic index [44].

monocytes, and other accessory cells. The phagocytic system is considered to be the first line of defense against a variety of microorganisms that invade the host. The bactericidal capacity of phagocytes might be impaired if seminal plasma inhibited the production of reactive oxygen species (ROS) [50]. Effects of this kind become more important when the infective microorganisms such as cytomegalovirus and HIV are contained in the ejaculate itself. Ingestion of microorganisms by neutrophils is an active process that requires energy production by the phagocytic cells. Subsequent intracellular events like degranulation and killing depend on the success of ingestion. Phagocytosis denotes the ingestion phase of the process, whereas the phagocytic index refers to the average number of particles ingested, which is considered as the measurement of ingestion rather than phagocytosis. Relative phagocytic index (RPI) was calculated by dividing the counts in the presence of seminal plasma by counts in the absence of seminal plasma and multiplying by 100.

The results of chemiluminescence are expressed in terms of relative phagocytic index using whole blood. When phorbol myristate acetate (PMA) was used, the relative phagocytic index was found to be less than 100% (suppression of chemiluminescence) with peaks 2, 3, 4, and 7, whereas the RPI with peaks 1, 5, 6, and whole seminal plasma was always greater than 100% (stimulation of chemiluminescence). The RPI was 150% with whole seminal plasma when 100 μg/ml protein was used in the presence of opsonized yeast. Peaks 1 and 5 and

Table 1 Effect of Human Seminal Plasma Protein and Its Peaks on Phagocytic Activity of Monocytes and Granulocytes by Flow Cytometry.

	Monocytes			Granulocytes		
		Mean fluorescent channel number			Mean fluorescent channel number	
Sample	% Phagocytosis	Total population	Phagocytic cells	% Phagocytosis	Total population	Phagocytic cells
Control	69	381	548	81	686	836
Whole	69	409	586	69	510	736
Peak 3	59	333	560	53	314	584
Peak 4	60	349	582	60	397	656
Peak 7	67	408	609	56	455	800

whole seminal plasma were stimulatory (RPI > 100%), whereas peaks 2, 3, 4, and 7 were suppressive (RPI < 100%). These results are shown in Fig. 6. The percent phagocytosis effect of peaks 3, 4, and 7 on monocytes and granulocytes was also studied by using flow cytometry (Table 1).

C. Mixed Lymphocyte Reaction

Mixed lymphocyte reaction (MLR) was performed for 5 days in the presence and absence of different concentrations of seminal plasma. Peripheral blood lymphocytes were purified from 15 ml heparinized blood by density gradient centrifugation on Ficoll-Hypaque (Pharmacia). Pooled human stimulating cells were prepared by mixing equal parts of three different lymphocyte suspensions of approximately 1 million cells/ml in RPMI-1640 medium supplemented with penicillin (100 U/ml), streptomycin (100 μg/ml), fungizone (25 μg/ml), and 10% autologous serum from three different normal donors, and were irradiated by 1500 rads (Gamma Cell 1000, Atomic Energy of Canada, Ottawa, Ontario). Cultures were set up in triplicate using 96-well sterile round-bottom microtiter plates (Linbro Chemical Co., New Haven, CT, USA) by mixing 100 μl of responding cell suspension and 100 μl of irradiated pooled cells. Twenty-five microliters of different concentrations (1, 2.5, 5, and 10 μg) of human seminal plasma and its seven fractions were added to each well. Control wells were without seminal plasma and its fractions. Microtiter plates were incubated at 37°C in a humidified atmosphere with 5% CO_2. After 5 days, the culture was pulsed with [^{3}H]thymidine to label nucleic acid in the responder cells. After 16 h, cells were harvested

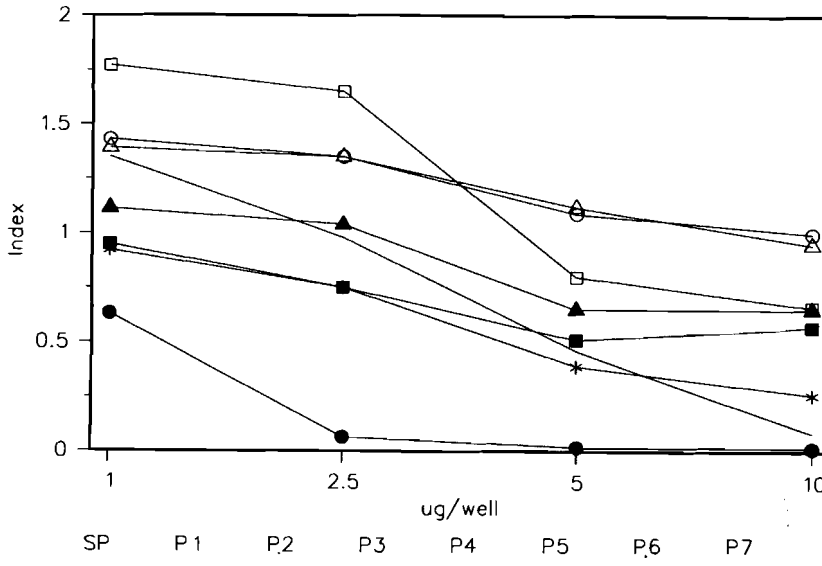

Figure 7 Effect of human seminal plasma (SP) and its fractions on mixed lymphocyte reaction (MLR). SP represents the whole seminal plasma while P1–P7 represent peaks obtained from DEAE-Sephadex A-50 ion exchange chromatography. The x axis represents protein concentration (μg) and the y axis the index [44].

and counted for internalized radioactivity by using a β-scintillation counter. Figure 7 shows the effect of seminal plasma or its fractions on MLR. A highly immunosuppressive effect was observed when fractionated seminal plasma was used. This effect was dose-dependent and found to be maximal with 10 μg protein per well. Peak 4 was most potent followed by peaks 7, 3, and 5. Peaks 1, 2, and 6 were found to confer a stimulatory effect rather than immunosuppression. Whole seminal plasma was not suppressive and the effect was more or less the same at both 1 and 10 μg/well protein concentrations.

VII. CYTOKINES AND HUMAN REPRODUCTION

The relationship between cytokines and human reproduction represents a growing area of interest and investigation because of their involvement in different aspects of reproductive physiology and infertility regulation, including gonadal and sperm functions. Cytokines are powerful mediators capable of regulating the function, growth, and differentiation of the cells of the immune status. There are

studies done by Naz and Kaplan [60] on the detection of tumor necrosis factor–α (TNFα), interleukin-1β (IL-1β), interferon-γ (IFNγ), and interleukin-6 (IL-6) in human seminal plasma. IL-6 was significantly higher in infertile men compared to those of fertile. TNFα and IL-1β were not detected, whereas IFNγ was detected but the difference between the levels of fertile and infertile were not significant. IL-6 could be associated with infertility. Production of IFNγ was determined and showed to be present in higher amounts in the seminal plasma of infertile donors [61]. Recently, the concentrations of various cytokines (IL-1β, IL-2, IL-6, srIL-2, srIL-6) in seminal plasma have been studied [62]. According to these researchers, several lines of evidence indicate that cytokines are involved in male infertility. These cytokines are secreted by different parts of the male genital tract and may exert effects on steroidogenesis, spermatogenesis, and sperm functions.

VIII. POSSIBLE FUNCTIONS OF PROTEINS OF SEMINAL PLASMA

The proteins of seminal plasma are involved in the maintenance of spermatozoa in the female reproductive tract after ejaculation. Some of the proteins, such as the protease inhibitors present in seminal plasma, may prevent damage to spermatozoa/spermatozoal membrane. These proteins may be involved and play a role in capacitation and acrosome reaction; The processes that the spermatozoa of higher species undergo after ejaculation but prior to acquiring ability to fertilize an egg. Proteins with no known enzyme or hormone function include those that appear to be involved in (1) maturation of spermatozoa during passage through the male reproductive tract, (2) agglutination of spermatozoa or coagulation of semen after ejaculation (in some species) and subsequent liquification of semen, (3) maintenance of the viability of spermatozoa, (4) capacitation, (5) acrosome reaction, (6) penetration of spermatozoa through the cervical mucus, and (7) sperm–egg interaction. In addition to these functions, there are certain other classes of proteins present in seminal plasma such as (1) proteins involved in the growth, regulation, and functions of cells, tissues, and organs of the reproductive system (sertoli and prostate), (2) inhibitors of hormones (follicle-stimulating hormone) and enzymes (myosin, ATPase, or proteases) present in seminal fluid that could conceivably inflict damage if their action is not prevented in time, (3) immunosuppressive agents that might prevent and immune response in both males and females to sperm and or male-specific antigens, (4) antimicrobial agents that might prevent infection of the male or female reproductive tract following sexual intercourse, and (5) antifertility agents. Many seminal plasma proteins seem to represent opposite functions, and there are enzymes and their inhibitors, unlike the case in a cell. The balance of these two activities (one promoting fertility and the other promoting antifertility) might provide for a fine control

over a vital function of semen, e.g., fertilization. Chemically and biochemically, spermatozoa may well be the best protected cells in the male. And no one will argue that they deserve to be so well protected. About 15% of a total of 350 proteins thus far shown to be present in seminal plasma and secretions of male reproductive tract are bound to spermatozoa.

IX. CONCLUSION

Proteins of seminal plasma play an important role in protecting the spermatozoa during spermatogenesis (when they express stage-specific antigens) in the male reproductive tract and after coitus in the female reproductive tract. Although these proteins (immunomodulatory factors) also associated with diverse pathological states in both males and females, it could be concluded that they are a necessary evil [9]. Some studies have already stated that fertility is suppressed in couples were antispermatozoal antibodies are present in seminal plasma. The presence of spermatozoal antibodies in the seminal plasma of infertile and vasectomized men is well known. Such a case may represent an immune reaction to spermatozoa due to a lack of immunosuppressive factors. Our results of mixed lymphocte reaction and chemiluminescence further confirmed that seminal plasma contains molecules that are responsible for the suppression of specific and nonspecific responses [44,50,51]. Therefore, identification, purification, and characterization of the various immunomodulating factors, an understanding of the mechanism of action of these factors on various components of the immune system, and the regulation of synthesis of these proteins would ultimately help in understanding the important role of immunosuppression in human reproduction in general and fertilization in particular.

REFERENCES

1. Huang K, Takamura S, Kinochi T, Takayama M, Ishida T, Ueyama H, Nishi K, Ohkubo I. Alanyl aminopeptidase from human seminal plasma: purification, characterization and immunohistochemical localization in the male genital tract. J Biochem 1997;122:779–787.
2. Skidgel RA, Peddesh P, Dars R. Isolation and characterization of a basic carboxypeptidase from human seminal plasma. Arch Biochem Biophys 1988;267:660–667.
3. Comhaire F, Bosmans E, Ombelet W, Punjabim V, Schooonjans F. Cytokines in semen of normal men and of patients with andrological diseases. Am J Reprod Immunol 1993;31:99–103.
4. Drisdel RC, Mack SR, Anderson RA, Zaneveld LJ. Purification and partial characterization of acrosome reaction inhibiting glycoprotein from human seminal plasma. Biol Reprod 1995;63:201–205.

5. Stites DP, Erickson RP. Suppressive effect of seminal plasma on lymphocytes activation. Nature 1975;253:727–729.
6. Caldini AL, Orlando C, Barni T, Messeri G, Pazzegli M, Baldi E, Seris M. Measurement of transferrin in human seminal plasma by chemiluminescent method. Clin Chem 1986;32:153–156.
7. Bryan MKO, Baker HWG, Saunders JR, Kirszbaum L, Walker ID, Hudson P, Liu DY, Glew MD, Apice AFD, Murphy M. Human seminal clusterin (SP-40,40). Isolation and characterization. J Clin Invest 1993;85:1477–1486.
8. Choi NH, Tobe T, Hara K, Yoshida H, Tomita M. Sandwich ELISA assay for quantitative measurement of SP-40,40 in seminal plasma and serum. J Immunol Meth 1990;131:159–163.
9. Shivaji S, Scheit KH, Bhargava PM. Proteins of Seminal Plasma. New York: John Wiley and Sons, 1990.
10. Kitamura M, Namiki M, Matsumiya K, Tanaka K, Matsumoto M, Hara T, Kiyohara H, Okabe M, Okuyama A, Seya T. Membrane cofactor protein (CD46) in seminal plasma is a prostasome-bound with complement regulatory activity and measles virus neutralizing activity. Immunology 1995;84:626–632.
11. Skibinski G, RElly RW, Harrison CM, McMillan LA, James K. Relative immunosuppressive activity of human seminal prostaglandins. J Reprod Immunol 1992;22: 189–195.
12. Iborra A, Morte C, Fuentes P, Garcia-Framis V, Andolz P, Martinez P. Human sperm coating antigen from seminal plasma origin. Am J Reprod Immunol 1996;36:118–125.
13. Dimitrova D, Kehayov I, Kyukechiev S. Purification and characterization of sperm-coating antigen identified by monoclonal antibody. Andrologia 1993;25:271–277.
14. Nocera M, Chu TM. Transforming growth factor beta as an immunosuppressive protein in human seminal plasma. Am J Reprod Immunol 1993;30:1–8.
15. Yie SM, Lobb DK, Clark DA, Younglai EV. Identification of transforming growth factor–alpha like molecule in human seminal plasma. Fertil Steril 1994;6:129–135.
16. Robert M, Gagnon C. Sperm motility inhibitor from human seminal plasma: association with semen coagulum. Human Reprod 1995;10:2192–2197.
17. Ohkubo I, Tada T, Ochiai Y, Ueyama H, Eimoto T, Sasaki M. Human seminal plasma beta-microseminoprotein: its purification, characterization, and immunohistochemical localization. Int J Biochem Cell Biol 1995;27(6):603–611.
18. Paradisi R, Pession A, Bellavia E, Focacci M, Flamigni C. Characterization of human sperm antigens reacting with antisperm antibodies from autologous sera and seminal plasma in a fertile population. J Reprod Immunol 1995;28:61–73.
19. Deperthes D, Chapdelaine P, Tremblay RR, Brunet C, Berton J, Hebert J, Lazure C, Dube JY. Isolation of prostatic kallikrein hK2, also known as hGK-1, in human seminal plasma. Biochim Biophys Acta 1995;1245:311–316.
20. Kekow J, Wachsman W, McCutchan JA, Gross WL, Zacchariah M, Carson DA, Lozt M. Transforming growth factor-β and suppression of humoral immune responses in HIV infection. J Clin Invest 1991;87:1010–1016.
21. Zheng X, Geiger M, Ecke S, Bielek E, Donner P, Eberspacher U, Scheuning WD, Binder BR. Inhibition of acrosin by protein C inhibitor and localization of protein C inhibitor to spermatozoa. Am J Physiol 1994;267:C466–472.

22. Sedor J, Callahan HJ, Perussia B, Laftime EC, Hirsch IH. Soluble Fc gamma RIII (CD16) and immunoglobulin infertility. J Androl 1993;14:187–193.
23. Chvapil M, Stankova L, Bernhard DS, Zukoski CF, Drach GW. Effect of prostatic fluid and its fraction on some function of peritoneal macrophages. Invest Urol 1977; 15:173–179.
24. Mukherjee DC, Agrawal AK, Manjunathn R, Mukherjee AB. Suppression of epididymal sperm antigenicity in the rabbit by uteroglobulin and transglutaminase in vitro. Science 1983;219:989–991.
25. Witkin SS, Richards JM, Bangiovanni AM, Zelikovsky G. An IgG-Fc binding protein in seminal fluid. Am J Reprod Immunol 1983;3:23–27.
26. Kelly RW. Immunosuppressive mechanisms in semen implications for contraception. Human Reprod 1995;10:1686–1693.
27. Bischof P, Marin-Du-Pan R, Lauber K, Girard JP, Herrmann WL, Sizonenko PC. Human seminal plasma contains a protein that shares physiochemical, immunochemical, immunosuppressive properties with pregnancy-associated plasma protein-A. J Clin Endocrinal Metab 1993;56:359–362.
28. Byrd WJ, Jacobs DM, Amoss MS. Synthetic polyamines added to cultures containing bovine sera reversibly inhibit in vitro parameters of immunity. Nature 1977; 267:621–623.
29. Akiyama K, Yoshioka Y, Schimid K, Offner GD, Troxler RF, Tsuda R, Hara M. The amino acid sequence of human beta microseminoprotein. Biochim Biophys Acta 1985;829:288–294.
30. Abrescia P, Lombardi G, De Rosa M, Quagliozzi L, Guardiola J, Metafora S. Identification and preliminary characterization of a sperm-binding protein in normal human semen. J Reprod Fertil 1985;73:71–77.
31. Metafora S, Lombardi G, De Rosa M, Quagliozzi L, Ravagnan G, Peluso G, Abrescia P. A protein family immunorelated to a sperm-binding protein and its regulation in human semen. Gamete Res 1987;16:229–241.
32. Freedman MF, Kopf GS. Characterization of a seminal plasma associated inhibitor of human seminal plasma protein. Biol Reprod 1985;32:322–332.
33. Chan SY, Tang LC. Effect of reserpine on fertilizing capacity of human spermatozoa. Contraception 1984;30:363–369.
34. Marcum J, Dedman MJR, Brinkley BR, Means AR. Control of microtubule assembly–disassembly by calcium-dependent regulatory protein. Proc Natl Acad Sci USA 1978;75:3771–3775.
35. Kavanagh J. Zinc binding properties of human prostatic tissue, prostatic secretion and seminal fluid. J Reprod Fertil 1983;68:359–363.
36. Robert TK, Boettcher B. Identification of human sperm coating antigen. J Reprod Fertil 1969;18:347–350.
37. Sinosich M, Seppala JM, Saunders DM, Grudzinskas G. Pregnancy-associated plasma protein-A and placental protein in human seminal plasma. Ann NY Acad Sci 1985;442:287–292.
38. Leblond E, Desnoyers L, Manjunath P. Phosphorylcholine-binding proteins from the seminal fluids of different specie share antigenic determinants with the major proteins of bovine seminal plasma. Mol Reprod Dev 1993;34:443–449.
39. Calvete JJ, Mann K, Sanz L, Raida M, Topfer-Petersen E. The primary structure of

BSP-30K, a major lipid-, gelatin-, and heparin-binding glycoprotein of bovine seminal plasma. FEBS Lett 1996;399:147–152.
40. Codini M, Fini C, Paolotti P, Floridi A. Bull seminal plasma phosphodiesterase. Purification and general properties. Biochem Int 1992;28(6):989–997.
41. Rutherford KJ, Swiderek KM, Green CB, Chen S, Shively JE, Kwok SC. Purification and characterization of PSP-I and PSP-II, two major proteins from porcine seminal plasma. Arch Biochem Biophs 1992;295:352–359.
42. Calvete JJ, Reinert M, Sanz L, Topfer-Petersen E. Effect of glycosylation on the heparin-binding capability of boar and stallion seminal plasma proteins. J Chromatogr 1995;711:167–173.
43. Gerena RL, Irikura D, Urade Y, Eguchi N, Chapman DA, Killion GJ. Identification of a fertility-associated protein in bull seminal plasma as lipocalin-type prostaglandin D synthase. Biol Reprod 1998;58:826–833.
44. Haq A, Al-Tufail M, Sheth K, Abdullatif M, Hamilton C, Al-Abdul Jabbar F, Al-Sedairy ST. Immunosuppression by human seminal plasma fractionated by DEAE-Sephadex A50 ion exchange chromatography. Andrologia 1992;24:87–94.
45. Heystek J, Brummelhuis HGJ, Krijnen HW. Contributions to the optimal use of human blood II. The large scale preparation of prothrombin. A comparison between two methods using the anion exchanger DEAE-cellulose DE52 and DEAE-Sephadex A50. Vox Sang 1973;25:113–123.
46. Laemli UK. Cleavage of structural proteins during the assembly of the head bacteriophage T4. Nature 1970;227:680–685.
47. Anderson DJ, Tarter TH. Immunosuppressive effect of mouse seminal plasma components in vivo and in vitro. J Immunol 1982;128:535–539.
48. Kuno S, Uneno R, Hayaishi O. Prostaglandin E2 administered via anus causes immunosuppression in male but not in female rats: a possible pathogenesis of acquired immunodeficiency syndrome in homosexual males. Proc Natl Acad Sci USA 1986; 83:2682–2683.
49. Alexander NJ, Anderson DJ. Immunology of semen. Fertil Steril 1987;47:192–205.
50. Haq A, Sheth K, Abdullatif M, Al-Abdul Jabbar F, Hamilton C, Al-Sedairy S. Suppression/stimulation of chemiluminescence by human seminal plasma. Clin Chim Acta 1991;200:67–70.
51. Haq A, Sheth K, Abdullatif M, Al-Tufail M, Al-Abdul Jabbar F, Hamilton C, Al-Sedairy ST. Suppression of luminol-dependent chemiluminescence of phagocytic cells by human seminal plasma. Mol Androl 1992;4:297–307.
52. James K, Hargreave TB. Immunosuppression by seminal plasma and its possible clinical significance. Immunol Today 1984;5:357–363.
53. Dostal J, Veselsky L, Drahorad J, Jonakova V. Immunosuppressive effect induced by intraperitoneal and rectal administration of boar seminal immunosuppressive factor. Biol Reprod 1955;52:1209–1214.
54. Kelly RW, Holland P, Skibinski G. Extracellular organelles (prostasomes) are immunosuppressive components of human semen. Clin Exp Immunol 1991;86:550–556.
55. Curry MC, Hussain JI, Smith CJ, Allen JC. Identification of a macromolecular inhibitor of in vitro lymphocyte proliferation in human seminal plasma as bound spermine. Eur J Cell Biol 1980;21:180–182.

56. Templeton AA, Cooper I, Kelly RW. Prostaglandin concentrations in the semen of fertile men. J Reprod Fertil 1978;52:147–150.
57. Witkins SS. Failure of sperm-induced immunosuppression: association with antisperm antibodies in women. Am J Obstet Gynecol 1989;160:1166–1168.
58. Baker HWG, Clarke GN, Hudson B. Treatment of sperm autoimmunity in men. Clin Reprod Fertil 1983;2:55–71.
59. Evans CH, Lee TS, Flugelman AA. Spermine-directed immunosuppression of cervical carcinoma cell sensitivity to a majority of lymphokine-activated killer lymphocyte cytotoxicity. Nat Immun 1995;14:157–163.
60. Naz RK, Kaplan P. Increased levels of IL-6 in seminal plasma of infertile men. J Androl 1994;15:220–227.
61. Paradisi R, Capelli M, Mandini M, Bellavia E, Flamigni C. Increased levels of interferon-gamma in seminal plasma of infertile men. Andrologia 1996;28:157–161.
62. Dousset B, Hussenet F, Daudin M, Bujan L, Foliguet B, Nobet P. Seminal cytokine concentrations (IL-1beta, IL-2, IL-6, sR IL-6), semen parameters and blood hormonal status in male infertility. Hum Reprod 1997;12:1476–1479.

11

Isolation, Purification, and Structural Study of Allergenic Proteins

Jean-Pierre Dandeu
Institut Pasteur, Paris, France

I. INTRODUCTION

Allergy, from the Greek "allos" (other) and "ergeon" (action), can be defined as a separate behavior in comparison with the classical immune response. It is a modification of the human or animal organism reactivity to a particular immunogen, the "allergen." The molecule responsible for the sensitization was clearly defined at the beginning of the twentieth century by Clemens von Pirquet and then by Paul Portier and Charles Richet in their works on anaphylaxis. Either for sensitization or desensitization an allergen can act at a very low concentration. To become sensitized to an allergen one must be genetically programmed and able to synthesize immunoglobulins of the particular IgE class in response to an antigen. However, an antigen can only be considered as an allergen when it is able not only to induce an IgE response but also to subsequently provoke an anaphylactic or/and inflammatory reaction. Desensitization is a peculiar immunotherapy that leads the patient to synthesize IgG instead of IgE in response to repeated injections of very low doses of allergen that are *practically* unable to induce any anaphylactic reaction. In this case, the best molecule to be used should be one whose structure would have been modified to be nonreactive with the specific IgE present on the mast cells and thus to prevent the cascade of events leading to the inflammation process by inducing an IgG response.

Allergens are biological molecules such as proteins, glycoproteins, or polysaccharides originating from insects, plants, or animals. A biological extract often contains several allergens. The relative molecular mass of these molecules is gener-

ally low and ranges between 10,000 and 50,000. Allergens are frequently qualified by the terms *major* or *minor* allergens. These are referred to their particular frequencies of IgE reactivity in a group of patients clinically allergic to these allergens but are never referred to their concentrations in a biological extract.

Nowadays many allergens have been isolated and purified. The genes of greatest importance have been cloned and the corresponding recombinant proteins synthesized. Both natural allergens and recombinant allergens are rather useful to improve our knowledge on IgE synthesis and regulation but also to advance the field of allergy diagnosis and therapy. We have personally isolated two allergens from cat, one from horse, and one from a house dust mite. In this chapter we would like to point out the usefulness of chromatographic methods in allergen purification. One of the most important techniques generally used to prepare allergenic extracts was first described by Guibert et al. [1], which essentially consists in an aqueous extraction. From this extract the allergenic material was first concentrated by acetone precipitations at 25% and 75%, then by an additional precipitation at 75% of saturation in ammonium sulfate.

We do not pretend to examine all of the work done on so large a topic and we have voluntarily limited this review to a comprehensive summary of our personal results. Mention should be made before any description of chromatographic processes is given that a combination of crossed line immunoelectrophoresis and rocket line immunoelectrophoresis, two techniques previously described by Axelsen et al. [2], are particularly helpful not only for following the degree of purity of a given antigen/allergen but also for demonstrating whether the different antigens are bearing common or different epitopes. In rabbit, the majority of natural proteins are good immunogens and give rise to high IgG antibody titers. Thus, it is easy to identify and follow the purification of a particular antigen using a rabbit antiserum against the crude material from which the allergen of interest will be purified. Each step of the purification process can be followed up by immunoelectrophoresis. The allergenicity of the protein can be determined by testing the ability to bind specific human IgE antibodies present in the sera of sensitized patients. To this end, either crossed radioimmunoelectrophoresis, western blot, or enzyme-linked immunosorbent assay (ELISA) can be performed. If sodium dodecyl sulfate–polyacrylamide gel electrophoreses (SDS-PAGE) remains the most classical tool to define homogeneity of a proteinic fraction or to determine its relative molecular mass, it is sometimes necessary to perform *chromatofocusing or/and capillary electrophoresis* for a better characterization of the molecule of interest.

II. PURIFICATION OF Equ c1, A HORSE MAJOR ALLERGEN [3]

Several authors have demonstrated the presence of allergens in horse hair and dandruff and have isolated several proteins of different molecular weights [4–

7]. The raw material we used to isolate and purify horse allergens was principally obtained during grooming of healthy animals. After an aqueous extraction active material was concentrated by a classical salting-out process using ammonium sulfate followed by an exhaustive dialysis against water not only to eliminate ammonium sulfate but to select molecules of a relative molecular mass above 10,000. For efficient concentration and storage the resulting solution was lyophilized. The most classical way to separate proteins or glycoproteins undoubtedly remains size exclusion chromatography (SEC), which can sometimes lead to almost pure active fractions. This is particularly true when the relative molecular mass of the protein of interest, i.e., Equ c1, is suspected to be around 25,000, as found in the pic SII (Fig. 1). Since ion exchange chromatography, previously used by other authors, was not totally efficient in spite of our several attempts to improve the technique and no more success was obtained with immobilized

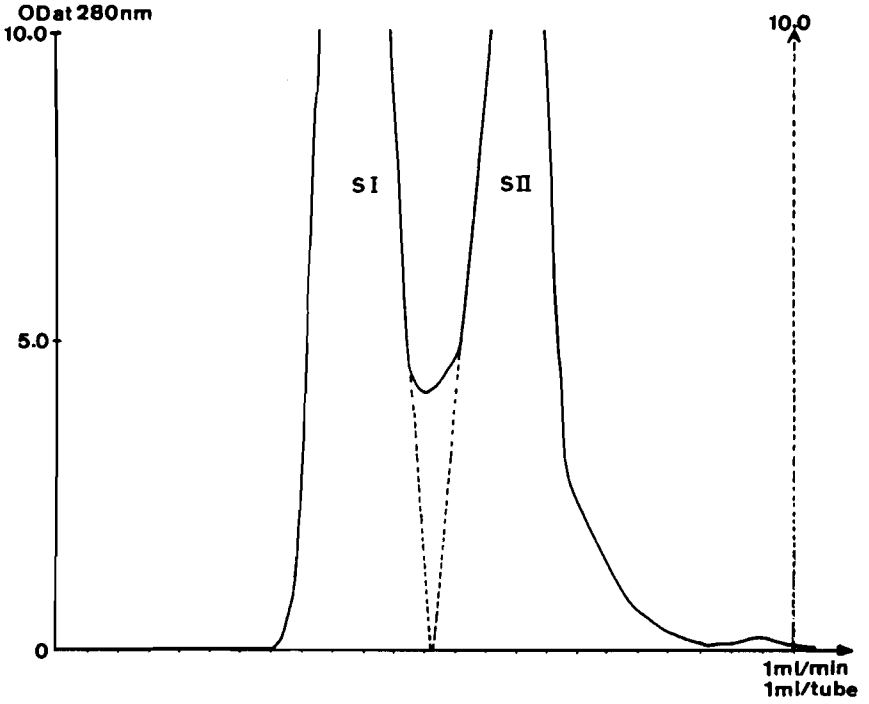

Figure 1 Preparative size exclusion chromatography (SEC) performed on a Superose column HR 16/50. Equilibration and elution were performed with the same buffered salt solution, 1 M NaCl and 0.02 M phosphate buffer (pH 8.00), and 200 mg of horse hair dander extract were loaded onto the column (From Ref. 3.)

metal ions affinity chromatography (IMAC), we successfully tried hydrophobic interaction chromatography (HIC) to prepare a pure allergen from the partially purified fraction defined above.

HIC is a technique whereby proteins are separated according to their selective interaction with hydrophobic groups, such as phenyl groups, bonded to the bed material of a column. Moreover, hydrophobic molecules in an aqueous solvent will self-associate due to these hydrophobic interactions. Antichaotropic salts, e.g., ammonium sulfate, increase the hydrophobic effect [8]. Ammonium sulfate in solution promotes protein aggregation, leading to precipitation, and this property was used to prepare the partially purified horse dander extract. In a solid–liquid phase system, such as HIC, these salts emphasize the interaction with the immobilized hydrophobic groups [9,10]. They have also been shown to promote hydrophobic interactions in contributing to the surface tension of the solution. The salt that increases the surface tension most gives the strongest hydrophobic interaction [11]. The first gels of practicable use for HIC were prepared

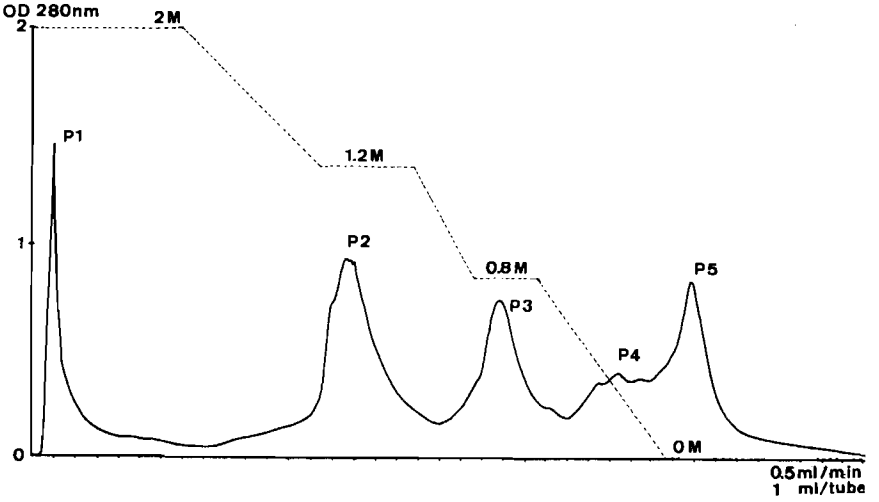

Figure 2 Chromatogram obtained by analytical hydrophobic interaction chromatography (HIC) of fraction SII from SEC, on a phenyl-Superose column HR 5/5 equilibrated with 2 M $(NH_4)_2SO_4$ in 0.02 M phosphate buffer (pH 8.00) (solution A). A 10-mg amount of SII was loaded onto the column. Elution was carried out in four steps. A first isocratic run with 100% solution A was followed by a linear decreasing gradient. Two plateaus were introduced at 40% and 60% of solution B. The last step was performed with 0.02 M phosphate buffer (pH 8.00) (solution B). Flow rate, 0.5 ml/min; UV detection wavelength, 280 nm. (From Ref. 3.)

by Porath et al. [12] and Hjerten et al. [13]. If HIC has been shown useful in purifying enzymes [14,15], hormones [16], and fragments from IgM [17], until now it has never been used to isolate and purify allergenic molecules. Using a column packed with phenyl-Superose (Pharmacia Sweden) an almost 100% purification of the horse major allergen Equ c1 was achieved. Elution of the adsorbed molecules according to the order of increasing hydrophobicity was performed by decreasing the antichaotropic salt concentration, i.e., ammonium sulfate [18]. For analytical purpose this was done in a linear gradient while for preparative ones a stepwise elution was carried out (Fig. 2). Physicochemical, biochemical, and immunochemical analyses stated that Equ c1 prepared in that manner is a pure protein consisting of a single peptide chain with a relative molecular mass of 20,000 and a pI = 3.9. Its partial microsequencing suggested that it could belong to the lipocalin family. This was further confirmed by cDNA cloning and sequencing of the Equ c1 gene [19].

III. PURIFICATION OF Feld 1, A CAT MAJOR ALLERGEN [20]

Several proteins derived from the domestic cat *Felix domesticus* causes allergic disorders. The most important one, previously designated Cat 1, was first described by Ohman [21]. Isolation and purification of this major feline allergen, recently named Fel d1, was achieved by affinity chromatography using polyclonal and monoclonal antibody [21,22]. If this method is somewhat efficient it unfortunately gives a poor yield. Fel d1, which is an acidic protein with a native molecular mass of 35,000, is composed of two chains that are not covalently bound and can be easily dissociated. Each monomer, M_r 17,000, has an equivalent antigenic and allergenic potency. Fel d1 is particularly present in house dust [21,23] from which it can be extracted by water. Since Fel d1 is an acidic protein with pI 3.8, an anion exchanger was used to fractionate the ammonium sulfate–precipitated fraction previously prepared according to the method described above. An analytical chromatography started with an isocratic elution followed by a linear gradient of molarity showed that three fractions can be obtained, each at a very specific concentration of salt. After that result a stepwise elution was defined and an enriched fraction of Fel d1, Q2, was eluted at 1 M NaCl (Fig. 3). This partially purified allergen was then loaded onto a copper chelate column. The chromatogram (Fig. 4) shows that five fractions were obtained following a stepwise elution at different salt concentrations. All fractions were immunologically tested, and the one eluted during the isocratic step appeared as a pure Fel d1 preparation. A second fraction, Q2Cu2, which showed a higher affinity for the copper ions, also appeared to contain Fel d1 but rather contaminated. Thus, we concluded that there were two species of this allergenic protein, which were the monomer and

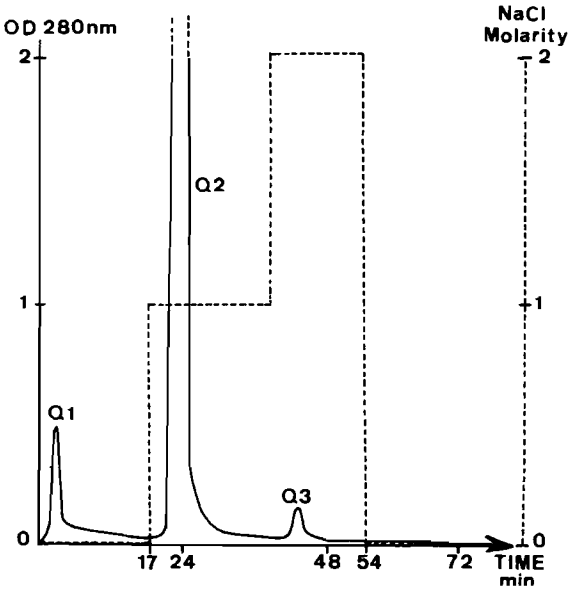

Figure 3 Chromatogram of a partially purified house dust extract on a Mono Q HR 10/10 column equilibrated with 0.125 M NaCl in 0.02 M Tris-HCl buffer (pH 8.6) (solution A). Elution is carried out with 1 M NaCl in 0.02 M Tris-HCl buffer (pH 8.6) (solution B). Flow rate, 1 ml/min; UV detection at 280 nm. (From Ref. 20.)

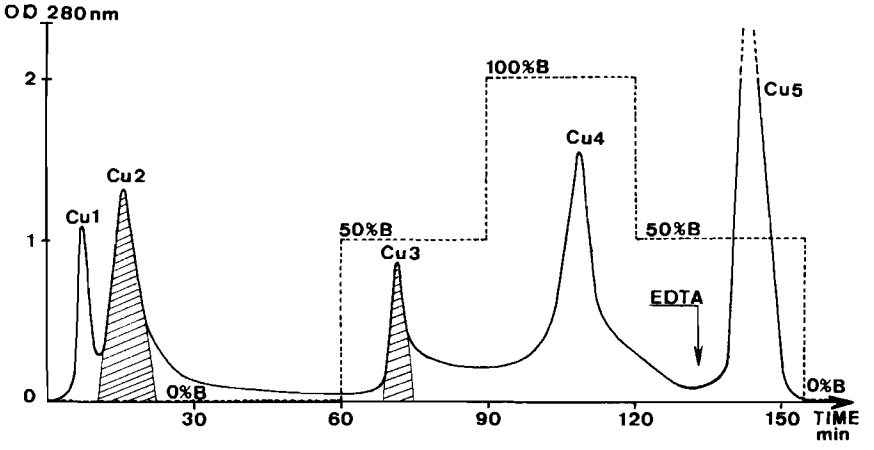

Figure 4 Chromatogram of fraction Q2 from the Mono Q, on a chelating Sepharose fast-flow HR 10/10 column, charged with Cu^{2+} ions equilibrated with 1 M NaCl in 0.02 M sodium phosphate buffer (pH 7.0) (solution A). Elution is carried out with 1 M ammonium chloride in solution A (solution B). Flow rate, 0.5 ml/min; UV detection at 280 nm. (From Ref. 20.)

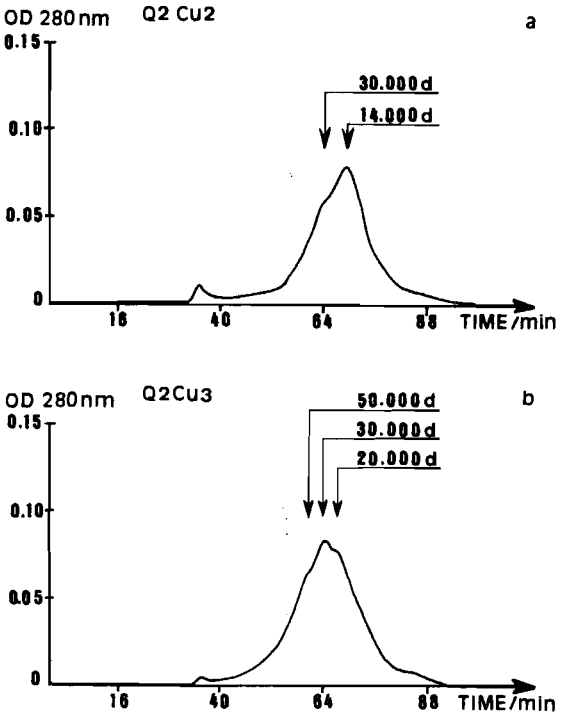

Figure 5 Gel filtration experiments performed on a Superose 12 HR 16/50 column, equilibrated in 1 M NaCl, 0.02 M Tris-HCl buffer (pH 8.6). Flow rate, 1 ml/mn; UV detection at 280 nm. (a) Q2 Cu2 analysis; (b) Q2 Cu3 analysis. d = daltons. (From Ref. 20.)

the dimer, respectively (Fig. 5). These results lead us to assume that the number of exposed metal binding sites on the protein able to bind to the copper ions was greater on the dimer than on the monomer.

This type of experiment underlines the usefulness of affinity chromatography not only to purify allergenic proteins but also to study their structures.

IV. PURIFICATION OF ALBUMIN, A SECOND CAT MAJOR ALLERGEN [24]

Previous studies showed that several allergens can be extracted from cat pelts [25–27]. The major one, Fel d1 [21], was isolated and purified by us [20]. Some

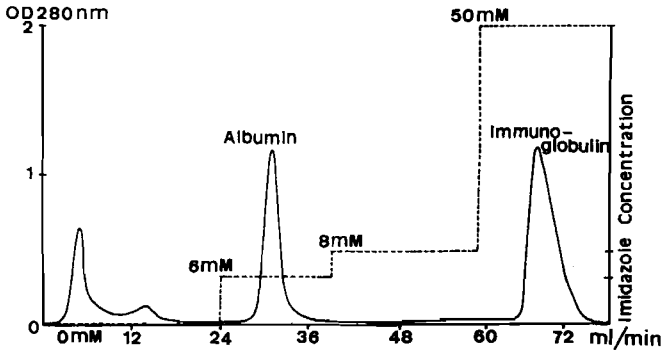

Figure 6 Copper chelate chromatography. Column, HR 10/10 packed with chelating Sepharose fast-flow (Pharmacia), charged with Cu^{2+}, washed with 1 mM imidazole in 1 M NaCl solution buffered with 0.02 M sodium phosphate buffer (pH 7.0), saturated with 10 mM imidazole in the same buffered salt solution. A 1-ml volume of cat serum, previously dialyzed against 1 mM imidazole, was loaded onto the column. Stepwise elution was performed at a flow rate of 1.0 ml/mn. (From Ref. 24.)

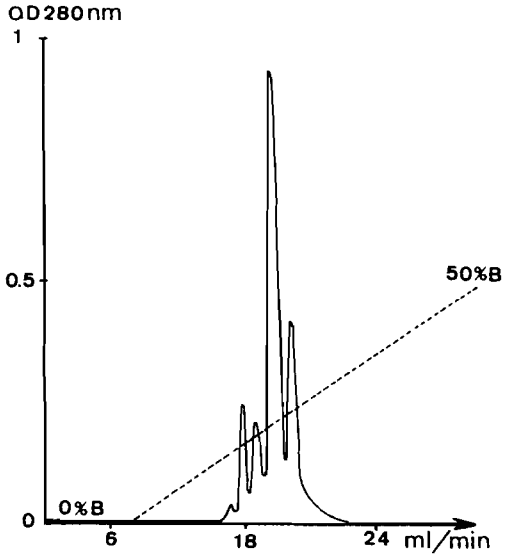

Figure 7 Anion exchange chromatography on Mono Q HR 10/10 column equilibrated with 0.03 M NaCl solution buffered with 0.02 M Tris-HCl (pH 8.0) (solution A). Elution was performed at a flow rate of 1.0 ml/min with a linear concentration gradient of NaCl from 0.03 to 1 M (50% solution B). Solution B consisted of 2 M NaCl solution buffered with 0.02 M Tris-HCl (pH 8.0). A 1-ml volume of cat serum albumin (CSA), from copper chelate chromatography (20 mg), was loaded onto the column. (From Ref. 24.)

other allergens, such as albumin [26–28] and immunoglobulin [28,29], were also described. We focused on cat albumin, which is a potent allergen present in house dust and is responsible for numerous sensitizations and crossed sensitizations with other potent allergens, e.g., dog albumin. A complete study of the cross-reactions between various albumins of animal origin was recently published [30]. To obtain a highly purified cat albumin we defined a simple chromatographic process that eliminates the time-consuming ammonium sulfate precipitation. A slightly diluted cat sera pool was submitted to an IMAC using copper ions as a ligand. During this process immunoglobulins are concomitantly isolated in a relatively pure form (Fig. 6). An anion exchange chromatography (Fig. 7) was then used to obtain a pure cat albumin preparation. After chromato focusing studies (Fig. 8), the fraction appeared to be somewhat homogen eous. To our knowledge, at the time we published this study, copper chel ate chromatography had not been used to isolate and purify cat albumin. This protein was only purified from a Cohn fraction on immobilized nickel [31].

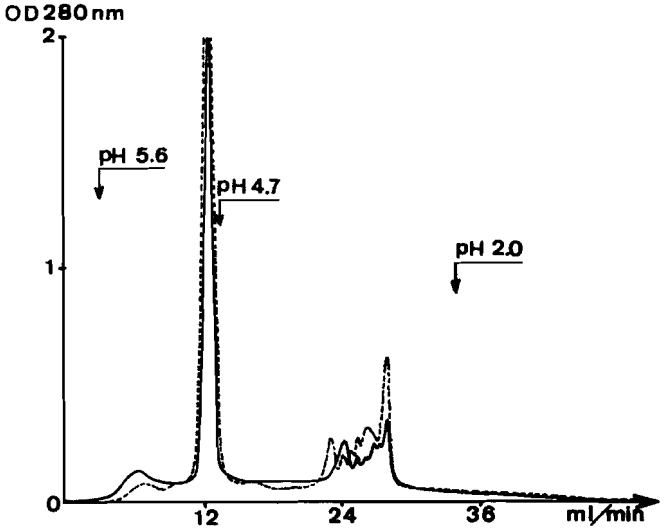

Figure 8 Chromatofocusing with a Mono P HR 5/20 column equilibrated with 0.025 M sodium acetate buffer (pH 5.58). A 200-µl aliquot (4 mg of CSA) was loaded onto the column. Elution was performed at a flow rate of 1.0 ml/min with a Servalyte 2-4 solution (Serva) at 0.2% adjusted to pH 2.05. The pH gradient was recorded using a pH monitor (Pharmacia). Solid curve, CSA from copper chelate chromatography; dashed curve, CSA Cohn fraction V. (From Ref. 24.)

V. PURIFICATION OF Der p1, A HOUSE DUST MITE MAJOR ALLERGEN [32]

The major allergen from *Dermatophagoïdes pteronyssinus* mite was first isolated and purified about 10 years ago [33–35]. It was shown to be a single peptide with some traces of carbohydrates. Its attachment to the cysteine proteases family of enzymes appeared from its mRNA [36,37] and cDNA [38] sequences. A fusion protein produced by a cDNA clone was effectively shown to react with specific rabbit IgG raised against natural Der p1. As the yield of pure protein from bacterial lysate was reported to be very low, we defined in our laboratory a convenient process to prepare Der p1 from a mite culture using a simple chromatographic method. Ion exchange chromatography, already effective with a lot of proteins, was shown to be really efficient to purify Der p1 on a large scale. This process essentially consists of applying an ammonium sulfate fraction obtained from a partially purified mite culture extract to a Mono Q column (Pharmacia, Uppsala, Sweden). The protein of interest was eluted during the first isocratic part of the run, pic Q1 (Fig. 9). All of the controls applied to the so obtained fraction stated that it was a highly purified Der p1 preparation with a real homogeneity in SDS-

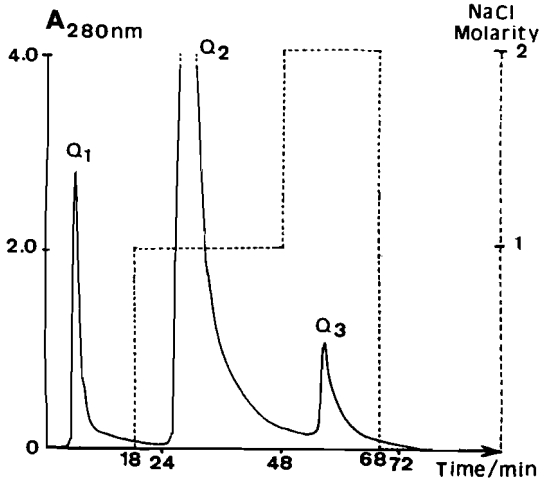

Figure 9 Chromatogram of a partially purified extract from a *Dermatophagoides pteronyssinus* mite culture on a Mono Q HR 10/10 column equilibrated with 0.02 M Tris-HCl buffer (pH 8.6) (solution A). Elution was carried out with 1 M NaCl in 0.02 M Tris-HCl buffer (pH 8.6) (50% solution B), flow rate 1 ml/min, followed by 2 M NaCl in 0.02 M Tris-HCl buffer (pH 8.6) (100% solution B). Flow rate, 3 ml/min; UV detection at 280 nm. (From Ref. 32.)

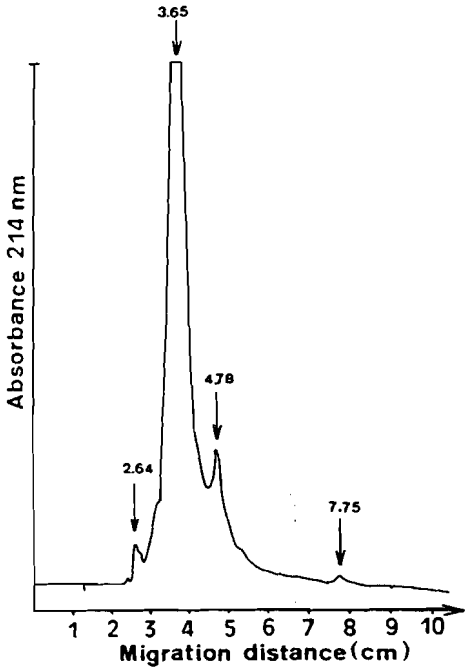

Figure 10 Electropheretogram obtained by capillary electrophoresis. (From Ref. 32.)

PAGE and an M_r of 25,500—a result very close to that reported by other workers [33,37]. Our Der p1 preparation also appeared to be highly homogeneous in capillary electrophoresis (Fig. 10) and in chromatofocusing (Fig. 11), the most critical methods of analysis available at that time. At the level of the 1–25 N-terminal peptide sequence no differences were shown when compared with the same peptide of the cDNA-coded Der p1.

VI. CONCLUDING REMARKS

In this chapter, we have demonstrated that chromatographic techniques, when judiciously combined and completed with convenient methods of detection and analysis, can lead to pure preparations of any protein. This was clearly illustrated above with allergenic proteins. It seems obvious that preliminary analytical experiments are needed to define the most fruitful chromatographic process.

Regarding the study of allergens, there is no doubt that we have not treated the subject extensively, but we tried to illustrate what can be learned from the chromatographic behavior of these particular proteins. Information so obtained

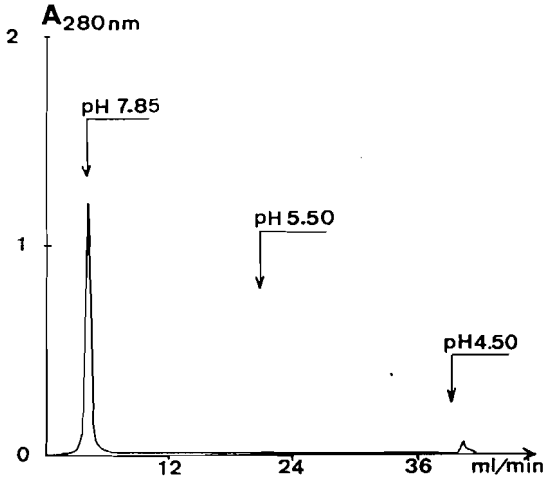

Figure 11 Chromatofocusing with a Mono P HR 5/20 column equilibrated with 0.025 M Tris-HCl buffer (pH 8.0). An 8.5-mg amount of Der p1 (Q1) was loaded onto the column. Elution was performed at a flow rate of 1.0 ml/min with a Servalytes 2-4 solution at 0.2% adjusted to pH 3.0. The pH gradient was recorded using a pH monitor. (From Ref. 32.)

added to the physicochemical characteristic furnished by electrokinetic methods can lead to a better understanding of their structure.

As noted for Equ c*1*, results obtained using chromatographic procedure can be good preliminaries for the molecular approaches leading to expression of a recombinant allergen in a bacterial system. Tryptic fragments of the natural allergen after microsequencing are indeed useful for the design of degenerate primers. Obviously, chromatographic research is still needed for isolation and purification of the recombinant protein.

ACKNOWLEDGMENTS

All figures were reprinted with permission from Elsevier Science NL, Sara Burgerhartstraat 25, 1055 KV Amsterdam, The Netherlands.

REFERENCES

1. Guibert L, Causse-Combes R. Activité allergeènique des fractions obtenues par chromatographie de l'extrait de poussiére de maison. Ann Inst Pasteur 1965;108:579–601.

2. Axelsen NH, Kroll J, Weeke B. A Manual of Quantitative Immuno-electrophoresis, Methods and Applications. Scand J Immunol 1973;2 (Suppl 1):47–56.
3. Dandeu JP, Rabillon J, Divanovic A, Carmi-Leroy A, David B. Hydrophobic interaction chromatography for isolation and purification of *Equ c1*, the horse major allergen. J Chromatogr 1993;621:23–31.
4. Stanworth DR. The isolation and identification of horse-dandruff allergen Biochem J. 1957;65:582–598.
5. Ponterius G, Brandt R, Hulten E, Yman L. Comparative studies on the allergens of horse dandruff and horse serum. Int Arch Allergy Appl Immunol 1973;44:679–691.
6. Löwenstein H, Markussen B, Weeke B. Isolation and partial characterization of three major allergens of horse hair and dandruff. Int Arch Allergy Appl Immunol 1976; 51:48–67.
7. Franke D, Maasch HJ, Wahl R, Schultz-Werninghaus G, Bretting H. Allergens of horse epithelium: I. Physicochemical and immunochemical characterization of five different horse epithelium raw materials used for allergen preparation. Int Arch Allergy Appl Immunol 1990;92:309–317.
8. Porath J. Salt-promoted adsorption: recent development. J Chromatogr 1986;376: 331–341.
9. Tanford C. The hydrophobic effect: Formation of Micelles and biological membranes. New York: Wiley Interscience, 1973.
10. Creighton TE. Proteins, Structure and Molecular Properties. New York: W. H. Freeman, 1984.
11. Melander W, Horvath C. Salt effect on hydrophobic interactions in precipitation and chromatography of proteins: an interpretation of the lyotropic series. Arch Biochem Biophys 1977;183:200–215.
12. Porath J, Sundberg L, Fornstedt N, Olsson NI. Salting-out in amphiphilic gels as a new approach to hydrophobic adsorption. Nature 1973;245(5426):465–466.
13. Hjerten S, Rosengren J, Palhman S. Hydrophobic interaction chromatography: the synthesis and use of some alkyl and Aryl derivatives of agarose. J Chromatogr 1974; 101:281–288.
14. Lau KH, Freeman TK, Baylink DJ. Purification and Characterization of an acid phosphatase that displays phosphotyrosyl-protein phosphatase activity from bovine cortical bone matrix. J Biol Chem 1987;262:1389–1397.
15. Roos P, Nyberg F, Wide L. Isolation of human pituitary prolactin. Biochem Biophys Acta 1979;588:368–379.
16. Prescott M, Peek K, Veitch DP, Daniel RM. J Biochem Biophys Methods. The use of phenyl-Sepharose for the affinity purification of proteinases. J Biochem Biophys Meth 1993;26:51–60.
17. Inouye K, Morimoto K. Single-step purification of F(ab')2 mu fragments of mouse monoclonal antibodies (immunoglobulins M) by hydrophobic interaction high-performance liquid chromatography using TSK gel ether-5PW. J Biochem Biophys Meth 1993;26:27–39.
18. Hjerten S, Yao K, Eriksson KO, Johansson B. Gradient and isocratic high-performance hydrophobic interaction chromatography of proteins on agarose columns. J Chromatogr 1986;359:99–109.
19. Gregoire C, Rosinski-Chupin I, Rabillon J, Alzari PM, David B, Dandeu J-P. cDNA

Cloning and sequencing reveal the major horse allergen Equ cl to be a glycoprotein member of the lipocalin superfamily. J Biol Chem 1996;271:32951–32959.
20. Dandeu J-P, Rabillon J, Beltrand M-J, Lux M, Duval R, David B. Immobilized metal ion affinity chromatography for the purification of Fel d1, a cat major allergen, from a house-dust extract. J Chromatogr 1990;512:177–88.
21. Leitermann K, Ohman JL. Cat allergen I: Biochemical, antigenic and allergenic properties. J Allergy Clin Immunol 1984;74:147–153.
22. Chapman M, Aalberse RC, Brown MJ, Platts-Mills TAE. Monoclonal antibodies to the major feline allergen Fel d1. II. Single step affinity purification of Fel d1, N-terminal sequence analysis, and development of a sensitive two-site immunoassay to assess Fel d1 exposure. J Immunol 1988;140:812–818.
23. Ohman JL, Lorusso JR, Lewis S. Cat allergen content of commercial house dust extract: comparison with dust extracts from cat-containing environment. J Allergy Clin Immunol 1987;79:955–959.
24. Dandeu J-P, Rabillon J, Guillaume J-L, Camoin L, Lux M, David B. Isolation and purification of cat albumin from cat serum by copper ion affinity chromatography: further analysis of its primary structure. J Chromatogr 1991;539:475–484.
25. Ohman JL Jr, Lowell FC, Bloch KJ. Allergens of mammalian origin: characterization of allergen extracted from cat pelts. J Allergy Clin Immunol 1973;52:231–241.
26. Ohman JL Jr, Lowell FC, Bloch KJ. Allergens of mammalian origin: III. Properties of a major feline allergen. J Immunol 1974;113:1668–1677.
27. Andersson MC, Baer H. Allergenically active components of cat allergen extracts. J Immunol 1981;127:972–975.
28. Löwenstern H, Lind P, Weeke B. Identification and clinical significance of allergenic molecules of cat origin. Allergy 1985;40:430–441.
29. Ohman JL, Sundin B. Standardized allergenic extracts derived from mammals. Clin Rev Allergy 1987;5:37–47.
30. Goubran-Botros H, Grégoire C, Rabillon J, David B, Dandeu J-P. Cross-antigenicity of horse serum albumin with dog and cat albumins: study of three short peptides with significant inhibitory activity towards specific human IgE and IgG antibodies. Immunology 1996;88:340–347.
31. Andersson L, Sulkowski E, Porath J. Purification of commercial human albumin on immobilized IDA-Ni^{2+}. J Chromatogr 1987;421:141–146.
32. Dandeu J-P, Rabillon J, Gullaume J-L, Camoin L, Lux M, David B. Isolation of Der pl, the *Dermatophagoides pteronyssinus* major mite allergen, from a crude mite culture extract, purification by ion-chromatography, and comparison between the material obtained and a cDNA-coded Der pl. J Chromatogr 1992;599:105–111.
33. Chapman MD, Platts-Mills TAE. Purification and characterization of the major allergen from *Dermatophagoides pteronyssinus*-antigen P1. J Immunol 1980;125:587–592.
34. Krilis S, Baldo BA, Basten A. Antigens and allergens from the common house dust mite *Dermatophagoides pteronyssinus*. Part II. Identification of the major IgE-binding antigens by crossed radioimmunoelectrophoresis. J Allergy Clin Immunol 1984; 74:142–146.
35. Lind P, Löwenstein H. Identification of allergens in *Dermatophagoides pteronyssi-*

nus mite body extract by crossed radioimmunoelectrophoresis with two different rabbit antibody pools. Scand J Immunol 1983;17:263–273.

36. Stewart GA, Thomas WR. In vitro translation of messenger RNA from the house dust mite *Dermatophagoides pteronyssinus*. Int Arch Allergy Clin Immunol 1987; 83:384–389.
37. Chua KY, Stewart GA, Thomas WR, Simpson RJ, Dilworth RJ, Plozza TM, Turner KJ. Sequence analysis of cDNA coding for a major house dust mite allergen, Der p1. Homology with cysteine proteases. J Exp Med 1988;167:175–182.
38. Stewart GA, Thomson WR, Chua KY, Geysen HM. An allergen and antigenic mapping analysis of a major mite allergen, Der p1. Adv Biosci 1989;74:297–311.

12

Multiangle Light Scattering Combined with HPLC with Examples for Biopolymers

Philip J. Wyatt
Wyatt Technology Corporation, Santa Barbara, California

I. INTRODUCTION

In 1972, Huglin's collection [1] on light scattering from polymer solutions was published. This was a full 2 years before Ouono and Kaye's classic paper [2] reporting the combination of gel permeation chromatography (GPC, often called size exclusion chromatography or SEC) and light scattering (LS). Although Moore [3] had developed the GPC concept a decade earlier and James Waters had launched his company a few years after that, nowhere in Huglin's text are to be found references to the GPC concept. Indeed, Beckman did not introduce its low-angle laser light scattering (LALLS) instrument until 1972, so this powerful technique would remain but a curiosity until Chromatix licensed the concept from Beckman and began their "missionary" work. Nevertheless, even without the ability to fractionate samples before making LS measurements, LS techniques themselves had reached a high degree of sophistication. Perhaps this was best summarized for the field of biopolymers by Burchard and Cowie [4] in their chapter entitled "Selected topics in biopolymeric systems." They stated that "an attempt has been made to present a wide variety of examples which illustrate most effectively the breadth of application of light scattering in this field. The versatility of the technique is probably unique in providing information in depth on biopolymers, and while it is by no means the only method in use, one hopes it will become obvious to the unconverted that to neglect light scattering would be to proceed under a distinct disadvantage." Although the numbers of "uncon-

verted'' are still large not only in the field of biopolymers but in the broad areas of organic polymers as well, the introduction of the DAWN instruments (which implemented the concept of multiangle light scattering, or MALS, combined with GPC) in the mid 1980s has begun to change those numbers. Referring back to the various chapters in Huglin, it is of interest to note that huge areas of application have yet to be examined by the combined GPC/MALS approach. It is the object of this chapter to continue this ''conversion'' process while presenting some important new results for biopolymers.

II. THEORETICAL REVIEW

Despite the increased importance ascribed to LS methods during the past few years, there remains a great deal of uncertainty and misunderstanding about the subject. A few summary remarks are in order. We begin with the basic equation used most frequently to describe the relation between what is measured and what is derived. Equation (1) is the result popularized by Zimm [5] in the development of his now classical technique by which he was able to generate key molecular parameters, i.e., the weight average molar mass, M_w, mean square radius, $\langle r_g^2 \rangle$, and second virial coefficient, A_2, from measurements made on an unfractionated sample comprised generally of an unknown distribution of molar masses and sizes.

$$\frac{K^*c}{R(\theta)} \approx \frac{1}{M_w P(\theta)} + 2A_2c \tag{1}$$

where $K^* = 4\pi^2(dn/dc)n_0^2/(N_A\lambda_0^4)$, N_A is Avogadro's number, dn/dc the refractive index increment, λ_0 the vacuum wavelength, and n_0 the refractive index of the solvent. Most importantly, the excess Rayleigh ratio, $R(\theta)$, and form factor, $P(\theta)$, are defined, respectively, by

$$R(\theta) = f(\theta)_{geom}\,[I(\theta) - I_s(\theta)]/I_0 \tag{2}$$

$$P(\theta) = 1 - \alpha_1 \sin^2 \theta/2 + \alpha_2 \sin^4 \theta/2 - \cdots \tag{3}$$

where

$$\alpha_1 = \left(\frac{4\pi n_0}{\lambda_0}\right)^2 \langle r_g^2 \rangle/3 \tag{4}$$

I_0 is the incident light intensity (ergs/cm^2-s), $f(\theta)_{geom}$ a geometrical calibration constant that is a function of the solvent and scattering cell's refractive index and geometry, $I(\theta)$ and $I_s(\theta)$ the normalized intensities of light scattered into a unit solid angle subtended by the detector at angle θ with respect to the illumi-

nated solution and solvent, respectively. The mean square radius is given by Eq. (5) below, where the distances r_i are measured from the molecule's center of mass to the mass element m_i:

$$\langle r_g^2 \rangle = \frac{\sum_i r_i^2 m_i}{\sum_i m_i} = \frac{1}{M} \int r^2 \, dm \tag{5}$$

Equation (5) applies to a single molecule, but the quantity measured from an unfractionated ensemble is actually a light scattering *average* of the mean square radii present in the sample. See Section IV, below, for further details.

Equation (1) is derived, to order c^2, by Zimm from the more general [5,6] reciprocal form:

$$\frac{R(\theta)}{K^*c} = MP(\theta)\,[1 - 2MP(\theta)A_2c] + M^2P^2(\theta)\,[4A_2^2MP(\theta) + 3A_3Q(\theta)]c^2 \tag{6}$$

In Eq. (6), A_3 is the third virial coefficient and $Q(\theta)$ is a special form factor, of magnitude always less than unity for finite θ, that describes additional light-scattering contributions from the interacting molecules. At $\theta = 0$, both P and $Q = 1$.

Equations (1) and (6) are based on several approximations. First is the assumption that the solvated molecules are well described by the Rayleigh approximation [6], i.e., that the refractive index (RI) of the molecules differs imperceptibly from that of the solvent and that the solvated molecules do not affect the phase of the (plane) wave of (polarized) light incident on the solution. Then there are the assumptions that the concentration of the solute molecules is "vanishingly small" and that the molecules interact with each other at a single point. Although the concentrations of samples after GPC fractionation are generally very small, the assumption that very large molecules may interact only in the single contact point approximation seems somewhat unreasonable. Remarkably, the validity of these assumptions spans a surprisingly broad range of molar masses.

Referring to Eq. (1), we see some other important results of measurements at very low concentrations. When the term $2A_2c$ may be dropped at very low concentrations, the mean square radius may be derived independently of any knowledge of the concentration c or molar mass M. (See also Section IV for a discussion of further limitations.) In this limit, Eq. (1) reduces to

$$\frac{K^*c}{R(\theta)} = \frac{1}{MP(\theta)} = \frac{1}{M}[1 + \alpha_1 \sin^2 \theta/2 - \alpha_2 \sin^4 \theta/2 + \cdots] \tag{7}$$

where α_1 is defined by Eq. (4).

Letting

$$K^*c/R(\theta) = \xi \tag{8}$$

we have the limiting derivative of ξ as $\theta \rightarrow 0$:

$$\frac{d\xi}{d(\sin^2 \theta/2)} = \alpha_1/M \tag{9}$$

Since the intercept at $\xi(0°) = 1/M_w$, the mean square radius is readily calculated from the ratio of the slope to intercept. And *that* ratio is independent of M_w and c! Remember that $1/M_w$ is calculated from the intercept, i.e., using the extrapolated excess Rayleigh ratio, $R(0°)$. So it does not matter what M_w is actually calculated: Set c = any arbitrary constant and one will generate an arbitrary M_w. Both M_w and c drop out of the calculation. The important term is $R(0°)$ and that is obtained by extrapolation using *measured* data.

III. SIGNIFICANCE OF MALS, LIGHT SCATTERING ANOMALIES, AND IMPLICATIONS FOR DATA FITTING: STRAIGHT LINES AND RANDOM COILS

Since the earliest days of on-line light scattering [2] there has been a considerable amount of confusion as to the correct means for extracting the molar mass. At vanishingly small concentrations and in the limit as the scattering angle, at which the measurement is made, approaches zero, the excess Rayleigh ratio divided by the product K*c becomes exactly equal to the weight average molar mass. This is clearly seen from Eq. (7). In this manner, were the scattering angle taken small enough, one could extract the molar mass of each eluting slice without having to extrapolate the measurements following the methods developed by Zimm [5]. The Beckman instrument (eventually developed further and marketed as the Chromatix KMX6) made measurements at angles as low as 3° which, for all intents, could be equated to 0° with only minor error up to molar masses well into the millions.

Measurements at a single angle, of course, are insufficient to generate the corresponding mean square radii, so the LALLS technique can at best generate molar mass with no subsequent details of conformation or branching. The low-angle measurement has other problems as well. In particular, the presence of any dust or debris from column shedding results in additional signals throughout the elution profile that often swamps the molecular signals themselves. Figure 1 shows the strip chart recording by Berkowitz [7] of the familiar broad polystyrene standard NBS 706 illustrating the type of spike noise characteristic of such measurements. (The Berkowitz paper describes various methods to suppress this noise and try to restore the peak.) Figure 2 presents a three-dimensional plot of

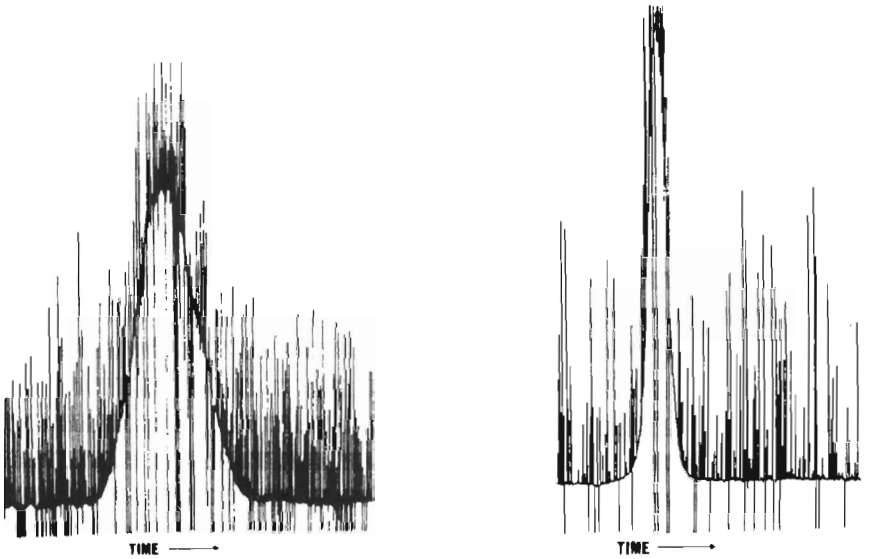

Figure 1 Strip chart recording from raw LALLS data from NBS 706 and NBS 705.

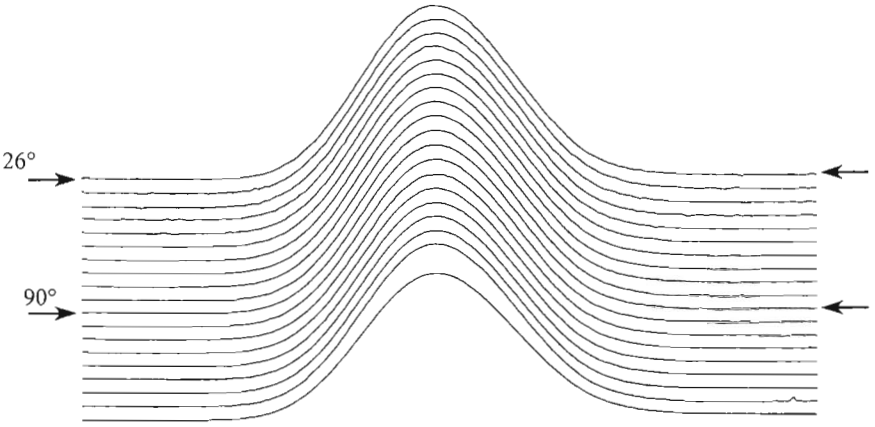

Figure 2 Multiangle chromatograms from NIST SRM 706 polystyrene.

the same standard showing the variation of the noise with scattering angle for a separation in toluene. The data of Fig. 2, however, were obtained with a DAWN-DSP system with a lowest angle collected around 24° in contrast to a 3° collection for the LALLS device. The point to emphasize here is that as the scattering angle decreases, the associated noise generally increases. A scattering angle closer to 0° does not necessarily mean that the extracted molar mass will be any the more accurate. Indeed, there are some unexpectedly erroneous results that can occur by ignoring the significance of the errors associated with the data collected at any angle. Let us examine in more detail the extraction of molar mass (and root mean square, or rms, radii, when attainable) from light scattering measurements.

Figure 3 shows a set of MALS chromatograms at 16 angles (plus the Refractive Index, RI, detector) for an aqueous GPC separation of a nominal 400 kg/mol pullulan "standard." The actual scattering angles accessible (together with their corresponding $\sin^2 \theta/2$ values) with a DAWN K5 glass cell are listed in Table 1. The measurements of Fig. 3 were achieved without detector 1 (3.3°). The chromatography, as indicated by the "noise" at the smaller scattering angles, is of rather poor quality, yet even the smallest scattering angle measured (14.5°) is considerably larger than the 3° data collected from the KMX6. The value of

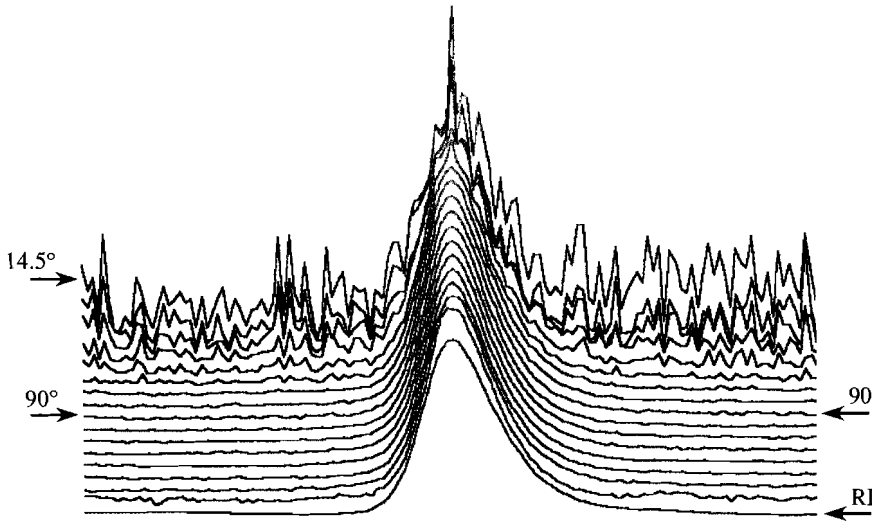

Figure 3 Multiangle chromatograms from a nominal 400 Kg/mol pullulan standard.

Table 1 DAWN Scattering Angles and Values of $\sin^2 \theta/2$ for K5 and Aqueous Solvent

Detector no.	Angle (°)	$\sin^2(\theta/2)$
2	3	0.0007
3	14	0.0149
4	22	0.0364
5	29	0.0627
6	36	0.0955
7	44	0.1403
8	54	0.2061
9	65	0.2887
10	77	0.3875
11	90	0.5000
12	103	0.6125
13	115	0.7113
14	126	0.7939
15	136	0.8597
16	144	0.9045
17	151	0.9373
18	158	0.9636

$\sin^2 \theta/2$, however, is very small relative to the range of angles measured. Figure 4 (top) shows a Zimm plot for the single slice indicated by the vertical line in the overlay plot (bottom) of the RI and 90° LS signals. For chromatographic separations, the concentration at a given slice is assumed to be so small that the second virial coefficient may be set equal to zero with negligible error. Thus the Zimm plot has only a single concentration. The second virial coefficient may be entered manually if required; however, since chromatographic separations are occurring at a single concentration for each slice, the second virial coefficient cannot be derived directly. Note that for rms radii up to about 40 nm, the plot of $K^*c/R(\theta)$ versus $\sin^2 \theta/2$ is *linear*. The weighted fit of the data points to a straight line will then yield the molar mass (intercept at $\sin^2 \theta/2 = 0$) and the mean square radius (slope divided by the intercept times a constant). The questions that now might be asked include: How will these two quantities vary with the lowest angle measured? Will they be more (or less) precise as the position of the lowest angle measured is varied? Indeed, does the low angle even add additional information?

A least-squares fit of a set of data points to a straight line is a straightfor-

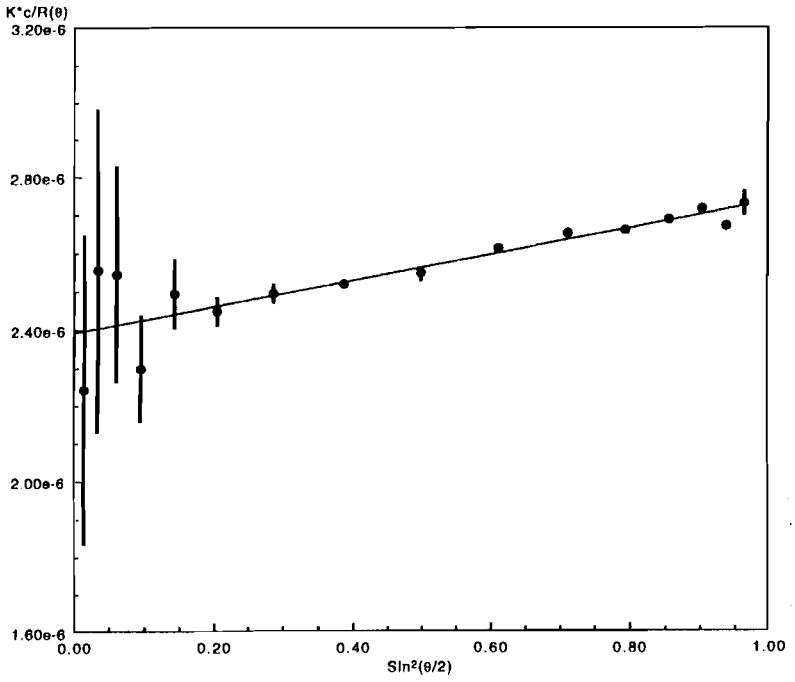

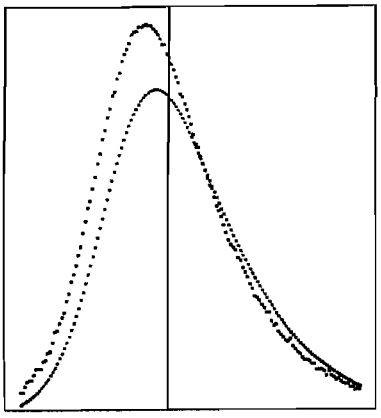

Peak 1, Slice 435, 15.250 mL
Zimm Method, Degree 1
c: (2.140±0.0005) x 10^{-5} g/mL
M: (4.182±0.027) x 10^{5} g/mL
r: 24.8±0.8 nm

Figure 4 Zimm plot for a single collection slice (top) indicated by the vertical indicial mark on the elution curves (RI and 90°LS) on the bottom.

ward process. The minimization of the sum of the squares with respect to the slope a and intercept b (= 1/M) yields the pair of equations:

$$a = \frac{\sum_i^N y_i x_i \omega_i^2 \sum_i^N \omega_i^2 - \sum_i^N y_i \omega_i^2 \sum_i^N x_i \omega_i^2}{\sum_i^N x_i^2 \omega_i^2 \sum_i^N \omega_i^2 - \left(\sum_i^N x_i \omega_i^2\right)^2} \tag{10}$$

and

$$b = \frac{\sum_i^N x_i \omega_i^2 \sum_i^N x_i y_i \omega_i^2 - \sum_i^N x_i^2 \omega_i^2 \sum_i^N y_i \omega_i^2}{\left(\sum_i^N x_i \omega_i^2\right)^2 - \sum_i^N x_i^2 \omega_i^2 \sum_i^N \omega_i^2} \tag{11}$$

where $y = K^*c/R(\sin^2 \theta/2) = ax + b$, $x_i = \sin^2 \theta_i/2$, $y(x_i) = y_i$, and ω_i is the weight or *reciprocal* standard deviation of the measured y_i.

If only a *single* angle is measured (such as with a LALLS system), then the precision of the intercept becomes the same as the precision of the LS signal which, for the noisy chromatography shown in Fig. 3, will show a large standard deviation. Again, the only quantity derived from a LALLS measurement will be the molar mass. If only *two* angles are measured, then Eqs. (10) and (11) take on the simpler forms:

$$a = \frac{y_2 - y_1}{x_2 - x_1} \qquad \text{and} \qquad b = \frac{x_2 y_1 - y_2 x_1}{x_2 - x_1} \tag{12}$$

As expected, these latter results are independent of the standard deviations of the measured data but depend only on the two average values measured. The results shown in Eq. (12) do *not* represent a least-squares fit since there is no redundancy in the measurements; there are as many data as there are variables. The number of degrees of freedom is exactly equal to the number of data. Each angle measured is weighted the same.

Consider a two-angle measurement made at $\sin^2 \theta_1/2$ and $\sin^2 \theta_2/2$ where $\theta_2 > \theta_1$. From Eq. (7), the molar mass determined from measurement of $K^*c/R(\sin^2 \theta/2)$ at the two angles θ_1 and θ_2 (using the straight line fit) is given by $M = 1/b = (x_2 - x_1)/(x_2 y_1 - x_1 y_2)$.

We next evaluate the error in M as we select smaller angles for one of the two angles chosen to fit the straight line.

$$\Delta M = \sqrt{(\partial M/\partial y_1)^2 \Delta y_1^2 + (\partial M/\partial y_2)^2 \Delta y_2^2}$$
$$= \frac{(x_2 - x_1)}{(x_2 y_1 - x_1 y_2)^2} \sqrt{x_2^2 \Delta y_1^2 + x_1^2 \Delta y_2^2} \tag{13}$$
$$= \frac{K^* c (x_2 - x_1)}{R_1^2 R_2^2 (x_2 y_1 - x_1 y_2)^2} \sqrt{x_2^2 R_1^4 \Delta R_1^2 + x_1^2 R_2^4 \Delta R_2^2}$$

In Eq. (13), the standard deviation in Δy is expressed in terms of the standard deviation of the measured excess Rayleigh ratio, ΔR, since $y = K^* c/R$. Thus $\Delta y = -K^* c\, \Delta R/R^2$ and

$$\frac{\Delta M}{M} = \frac{K^* c}{R_1^2 R_2^2 (x_2 y_1 - x_1 y_2)} \sqrt{x_2^2 R_1^4 \Delta R_1^2 + x_1^2 R_2^4 \Delta R_2^2} \tag{14}$$

In the limit as $x_1 = \sin^2 \theta_1/2 \to 0$, Eq. (14) simplifies to

$$\frac{\Delta M}{M} \to \frac{R_1 \Delta R_1}{R_2^2} \tag{15}$$

The choice of a very small angle as one of the two points through which the straight line is to be constructed indicates, from Eqs. (14) and (15), that the error in the derived molar mass, M, will *increase* as the lower angle goes to zero. For noisy chromatography, the fluctuations of $R(\sin^2 \theta_1/2)$ will increase as $\theta \to 0$. Accordingly, if only two angles are chosen for a LS measurement, the selected angles should be as far away from 0° as practical.

For the case of *three* angles, where the lowest angle measured is also expected to have a correspondingly less precise value than either of the other two, replacing only the lowest angle measured with an even smaller angle in no way implies that the final values will be more precise. On the contrary, keeping measurements away from 0° will generally increase the precision of the determination. Furthermore, as should be evident from Eqs. (10) and (11), the fit to the straight line will now be a true least-squares fit and the weighted data will result in the "best" fit being selected.

As might be expected, as the number of angles included in the final calculations is increased, the precision of both molar mass and mean square radius is increased. Table 2 presents the relative precision of these final values for the case of two (very low angle and 90°), three (approximately 40°, 90°, and 140°), and many (see Table 1) angles for the example of Figs. 2 and 3.

One of the possibilities associated with making LS measurements with too few angles lies in the hope of extending the range accessible by assuming a *model* of the molecules measured. For certain types of models, the form factor, $P(\theta)$, is known a priori so there is no need to fit the data to a straight line or higher

Table 2 Precision of Measurements Based on Clean (200 Kg/mol Polystyrene) Chromatography of Fig. 2 and Noisier (400 Kg/mol Pullulan) Chromatography of Fig. 3 as a Function of Number of Detectors Used

Angles	Molar mass (%)	Radius (%)
Clean chromatography		
Many	0.07	0.6
40° + 90° + 130°	0.2	2
15° + 90°	0.6	10
Dirty chromatography		
Many	0.5	3.0
40° + 90° + 130°	1	5
15° + 90°	14	80

order polynomial for the subsequent determination of molar mass and rms radius. Of course, such an assumption flies somewhat in the face of the concept of an "absolute" measurement. Nevertheless, we see frequent use of this assumption either directly or implicit in some software programs. The latter assumption is insidious in that data are processed and results calculated without the possibility of user intervention. If a random coil model is built into the software without the user's knowledge, then there is no basis left for the user to understand why, for example, the results contradict the results of other measurements such as thermal analysis. Let us examine the random coil model and its dual-angle implementation in greater detail.

For a random coil molecule, the form factor $P(\theta)$ takes on the simple closed [5] form:

$$P(\theta) = \frac{2}{u^2}[e^{-u} - 1 + u] \tag{16}$$

where

$$u = \left(\frac{4\pi n_0}{\lambda_0}\sin\frac{\theta}{2}\right)^2 \langle r_g^2\rangle = \mu^2 \langle r_g^2\rangle \tag{17}$$

and $\mu = [4\pi n_0/\lambda_0] \sin \theta/2$. $P(\theta)$ may be expanded in u as

$$P(\theta) = 1 - \frac{u}{3} + \frac{u^2}{12} - \cdots \tag{18}$$

Consider now the case of a two-angle measurement. In this case (and a vanishingly small concentration, whereby we may neglect the term $2A_2c$), Eq. (1) becomes

$$M_wP(\theta) = R(\theta)/(K^*c) \tag{19}$$

where $P(\theta)$ is given by Eq. (16). Equation (19) has two unknowns, M_w and $\langle r_g^2 \rangle$, and thus again like the straight line fit of Eqs. (12), the number of data are equal to the number of degrees of freedom. The average values of $R(\theta)$ measured at θ_1 and θ_2 are the only data available for this fit, i.e., $R(\theta_1)$ and $R(\theta_2)$. The nonlinear Eq. (19) in the two unknowns, M_w and $\langle r_g^2 \rangle$, has (at best) a single solution. Let the two measured excess Rayleigh ratios be $\xi_1 = R(\theta_1)$ and $\xi_2 = R(\theta_2)$. Equation (19) is best solved first by eliminating M_w i.e.:

$$\frac{\xi_1}{\xi_2} = \frac{R(\theta_1)}{R(\theta_2)} = \frac{P(\theta_1)}{P(\theta_2)} = \left(\frac{e^{-u_1} - 1 + u_1}{e^{-u_2} - 1 + u_2} \right) \tag{20}$$

where

$$u_1 = \mu_1^2 \langle r_g^2 \rangle, \; u_2 = \mu_2^2 \langle r_g^2 \rangle, \qquad \text{and} \qquad \mu = (4\pi n_0/\lambda_0) \sin \theta/2 \tag{21}$$

One would generally begin by solving Eq. (20) for $\langle r_g^2 \rangle$ which value is then substituted in Eq. (16) to obtain $P(\theta)$ at the angle for which $R(\theta)$ has the smallest standard deviation. This value and the corresponding $R(\theta)$ are then substituted in Eq. (19) to solve for M_w. The most "accurate" value of M_w derived from Eq. (19) would best be calculated at the angle with the least noise (the largest, θ_2), once $\langle r_g^2 \rangle$ had been calculated from Eq. (20). But note that the nonlinear calculations generating $\langle r_g^2 \rangle$ from Eq. (20) will have a precision that depends on the measured quantities $\xi_1 = R(\theta_1)$ and $\xi_2 = R(\theta_2)$. To maintain the greatest precision in this derivation of $\langle r_g^2 \rangle$, we see again that if only data at two angles are to be collected, the angles should be chosen as far as possible from the small, noisier, forward angles. Once a model is chosen, the smaller angle fits to that model add to the errors of the final results as the experimental uncertainty of those data. The precision of such a determination will depend not only on how small the noise is at the angles selected but on the number of different angles measured as well. Once again, the best way to fit a model such as the random coil model is to extract the key physical constants by fitting weighted data in a least-squares sense. Thus one must use as many angles as possible and certainly at least three.

In closing this section, it is worth remarking that traditional methods for determining functional parameters by comparing with experimentally derived data require that the number of such data exceed substantially the number of

functional parameters or degrees of freedom. Only on this basis can one perform a "chi-squared" goodness-of-fit analysis and thereby establish the quality of the selected model (function) by which the data are governed. Any model must be tested at points throughout its range of application. With only two data points and two angles, the results generated will depend always on the model chosen.

IV. THE "MOMENT" OF THE ROOT MEAN SQUARE RADIUS FROM MALS AND OTHER MOMENTS

One often reads that the rms radius measured by light scattering [8] is actually a z-average radius. (The misnomer "radius of gyration" is frequently found in the literature to describe this same quantity.) It is important to understand just what these so-called moments of the distributions mean since they play an important role for a variety of analyses, not the least of which is the determination of a sample's polydispersity. In addition, concepts such as the measurement and quantitation of branching require that the moments be identical within each suitably fractionated slice of a GPC separation. We begin by considering the MALS measurement of a polydisperse sample. We may rewrite Eq. (7), at vanishingly small concentrations and small angle, to obtain the excess Rayleigh ratio measured from the suspension:

$$\begin{aligned} R(\theta) &= \sum_i R_i(\theta) = K^* \sum_i c_i M_i [1 - \alpha_{i1} \sin^2 \theta/2] \\ &= K^* \sum_i c_i M_i - K^* \sum_i c_i M_i \alpha_{i1} \sin^2 \theta/2 \\ &= K^* c M_w - (4K^*/3) \sum_i c_i M_i \kappa^2 \langle r_g^2 \rangle_i \sin^2 \theta/2 \\ &= K^* c M_w - (4K^*/3) \kappa^2 \sin^2 \theta/2 \sum_i c_i M_i \langle r_g^2 \rangle_i \end{aligned} \tag{22}$$

where M_w is the *weight*-average [see Eq. (25)] molar mass, $c = \sum c_i$, and $\kappa = 2\pi n_0/\lambda_0$, as before. In the limit as $\theta \to 0$, the MALS measurement yields the *weight*-average molar mass, i.e., $R(0°) = K^* M_w c$. Note that the constant K^* has been factored out from the summations over the species present based on the further assumption that the polymer is a homopolymer, or at the very least that the dn/dc value is the same for all species present (including, for example, homogeneous copolymers). In the event that a copolymer or polymer blend has been separated, the mean square radius is not so easily extracted. A more detailed discussion of the modifications to the LS formulation may be found in the paper by Benoit and Froelich [9].

Kratochvil [8] has pointed out that

$$\sum_i c_i M_i \langle r_g^2 \rangle_i = M_w \langle r_g^2 \rangle_z \tag{23}$$

by definition. In other words, the z-average mean square radius has been *defined* by means of a weighting involving both mass and concentration. Let us examine this and related moments more carefully.

The mass moments of a distribution are given traditionally by

$$M_n = \sum_i n_i M_i \Big/ \sum_i n_i = \sum_i c_i \Big/ \sum_i c_i/M_i \tag{24}$$

for the *number*-average molar mass, where n_i is the number of molecules of mass M_i and the summations are over all of the i species present; the concentration c_i of the ith species therefore is equal to $M_i n_i$;

$$M_w = \sum_i c_i M_i \Big/ \sum_i c_i = \sum_i n_i M_i^2 \Big/ \sum_i n_i/M_i \tag{25}$$

for the *weight*-average molar mass; and

$$M_z = \sum_i n_i M_i^3 \Big/ \sum_i n_i M_i^2 = \sum_i c_i M_i^2 \Big/ \sum_i c_i M_i \tag{26}$$

for the z-average molar mass. Of course, Eqs. (24) and (25) have an associated physical meaning in terms of numbers and weights. Each corresponds also to an absolute mass measurement technique. Light scattering is the absolute method of choice to measure the *weight*-average molar mass while osmometry is the absolute technique of choice to measure the *number*-average molar mass of a sample directly. Equation (26) corresponds to the quantity measured by the other absolute measurement technique, sedimentation equilibrium. The subscript "z" has its origin in the German word for centrifuge, *Zentrifuge*. From Eq. (26) it is a simple matter to write expressions for the z + 1, z + 2, etc., moments. Note how these "moments" are related. In particular, each higher moment corresponds to "the next higher weighting" of both numerator and denominator by the factor M_i.

The number- and weight-average values of the mean square radius, $\langle r_g^2 \rangle$, are easily written in terms of their definitions i.e.:

$$\langle r_g^2 \rangle_n = \sum_i n_i \langle r_g^2 \rangle_i \Big/ \sum_i n_i \tag{27}$$

for the *number*-average mean square radius, i.e., the mean square radius of each species is weighted by the *number*, n_i, of such members present. So far so good, but to calculate the weight-average mean square radius we must weight the mean square radius by the *concentration*, c_i, of each species present, i.e.:

$$\langle r_g^2 \rangle_w = \sum_i c_i \langle r_g^2 \rangle_i \Big/ \sum_i c_i \tag{28}$$

In terms of the physical *meaning* of the number and mass weightings, as opposed to the concept of moments [10], Eqs. (27) and (28) indeed represent the correct corresponding weightings for the mean square radius. Defining the z-average mean square radius by Eq. (23) is completely acceptable since this is what MALS actually measures. One might equally well call Eq. (23) the LS average in order to avoid trying to relate the result to a seemingly artificial moment of the distribution of mean square radii present in an ensemble. Indeed, rewriting Eq. (23) as

$$\langle r_g^2 \rangle_z = \sum_i c_i M_i \langle r_g^2 \rangle_i \Big/ \sum_i M_i c_i \tag{29}$$

and Eq. (27) as

$$\langle r_g^2 \rangle_n = \sum_i c_i \langle r_g^2 \rangle_i / M_i \Big/ \sum_i c_i / M_i \tag{30}$$

produces three equations [(30), (28), and (29)] that display the same *type* of moment relationship shown in Eqs. (24), (25), and (26). However, note that once again the formal moments [6] of the mean square radii are with respect to the masses M_i and not the mean square radii. Note that for the special case of a random coil structure at the theta point, $M_i \propto \langle r_g^2 \rangle$. Replacing $\langle r_g^2 \rangle$ by M_i in Eqs. (30), (28), and (29) yields Eqs. (24) through (26), respectively. In order to emphasize that the size moment measured by light scattering is not a true z average,

except for the rare occasion that the molecules being measured are random coils in a theta solvent, the term *LS average* should be used in the future, viz.

$$\langle r_g^2 \rangle_{LS} = \sum_i c_i M_i \langle r_g^2 \rangle_i \Big/ \sum_i M_i c_i \tag{31}$$

V. CONFORMATION AND DIFFERENTIAL WEIGHT FRACTION DISTRIBUTIONS FOR "INCOMPLETE" GPC SEPARATIONS

Sometimes a GPC separation appears to be incomplete, i.e., the mass elution curve ("calibration" curve) is not a monotonically decreasing function of the elution volume. Examples are shown in Figs. 5 and 6. The former corresponds to a polyacrylamide while the latter was obtained from a (polysaccharide) heparin

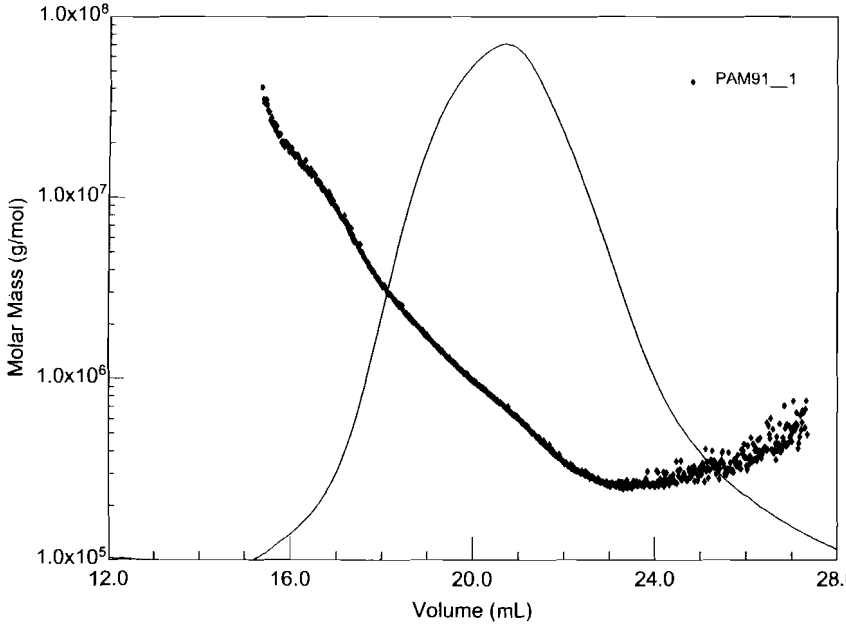

Figure 5 Molar mass versus elution volume of a polyacrylamide sample.

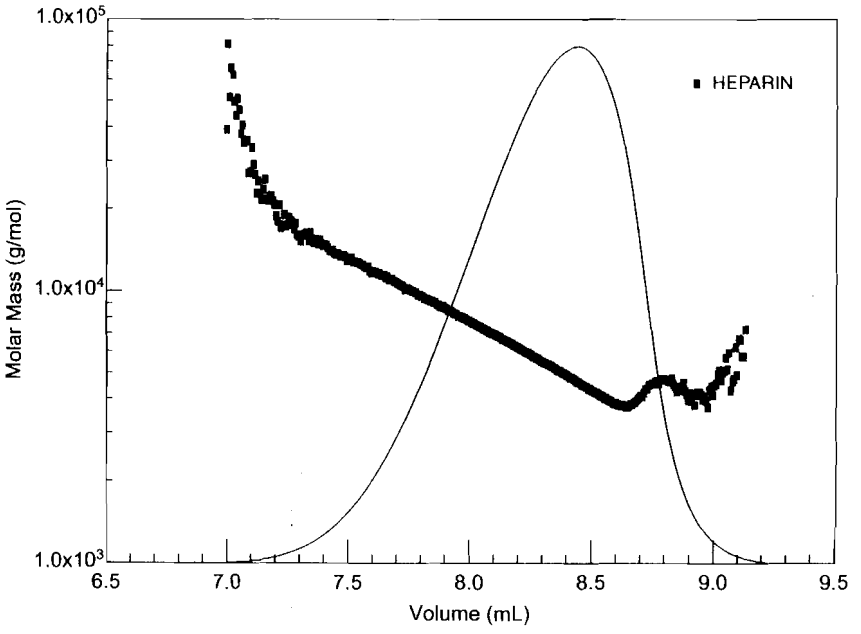

Figure 6 Molar mass versus elution volume of a heparin sample.

sample. Both show the mass elution curves reversing their downward trends and turning upward at larger elution volumes. In both cases the mobile phase was aqueous. Note that these results were obtained via a MALS measurement combined with an RI detector to monitor the concentration. The RI elution curves are shown in the background. The types of mass elution calculated from MALS would not have been calculated from standard GPC plus column calibration. Only an absolute measurement would have disclosed this unusual elution behavior since calibration techniques invariably require a set of standards that produce decreasing molar mass with increasing elution.

A variety of explanations have been presented for the non-GPC effects seen here, though without MALS they are rarely detected. Among them are column interactions and the presence of microgels. The former effects are akin to affinity chromatographic interactions. The latter are based on the fact that highly compact structures with higher molar mass would be expected to elute at later times because their hydrodynamic size, for their greater mass, could be considerably smaller than their noncompact companions. But irrespective of the possible explanation, the mere presence of these fractions requires that they be included in the mass distributions reported as they often represent a considerable fraction of the

sample on column. The most powerful means of presenting the results of a GPC separation is to produce a differential weight fraction distribution. From such a result, the cumulative distribution in addition to the various moments of the distribution may be calculated. The differential weight fraction distribution also represents the most direct means by which samples may be differentiated and column performance evaluated. Let us look at these distributions in greater detail, especially when applied to the results of Figs. 5 and 6.

The differential mass fraction distributions are generally presented as a distribution in $\log_{10} M$ rather than M. This permits the details of distributions spanning several orders of magnitude to be clearly visible. Perhaps most importantly, this type of presentation arose because the calibration curves are generally prepared with standards spanning a few orders of magnitude. An ideal GPC column set will separate linearly with respect to the logarithm of the hydrodynamic size. Since the logarithm of the hydrodynamic radius is proportional to the logarithm of the molar mass for linear molecules, the presentation of distributions in these terms has become an accepted practice. Let us review the definitions of these quantities.

Following Shortt [11], we define W(M) as the cumulative weight fraction of molecules in the selected peak whose mass is less than M. This is the total mass of molecules of mass less than M divided by the total mass of the molecules present. Thus:

$$\int_0^\infty dW(M) = 1 \tag{32}$$

The differential mass fraction, w(M)dM, is the weight fraction of molecules of mass between M and M + dM. Thus, w(M) = dW(M)/dM and again

$$\int_0^\infty w(M)dM = 1 \tag{33}$$

Letting $x(M) = dW(M)/d(\log_{10} M)$, we have

$$x(M) = \frac{M}{\log_{10} e} w(M) = Mw(M) \log_e 10 \tag{34}$$

Referring now to Fig. 5, we must combine the mass elution as a function of elution volume with the corresponding concentration values to generate the differential weight fraction distribution function of Eq. (34). The traditional procedure is to fit the data of Fig. 5 ($\log_{10} M$ as a function of V) by a polynomial (generally linear) and apply the chain rule as follows:

$$x(M) = \frac{M}{\log_{10} e} w(M) = \frac{M}{\log_{10} e} dW(M)/dM$$
$$= \frac{M}{\log_{10} e} dW/dV[dV/dM] \tag{35}$$

However, $dV/dM = [dV/d(\log_{10} M)]\ d(\log_{10} M)/dM = [dV/d(\log_{10} M)]\ [\log_{10} e]/M$. Therefore we have, after canceling the factor $M/\log_{10} e$ in Eq. (35),

$$x(M) = dW/dV[dV/d(\log_{10} M)] = (dW/dV)/[d(\log_{10} M)/dV] \tag{36}$$

For normal separations by the GPC mechanism (size exclusion), the term dW/dV may be replaced by the concentration detector's response. Thus if the concentration detector's baseline subtracted response is h(V), then $dW/dV = -h(V)/\int h(V)dV$, the integral representing the sum over all contributing concentrations. The differential weight fraction has thus been replaced [11] by the normalized concentration fraction. Note the negative sign which corresponds to the

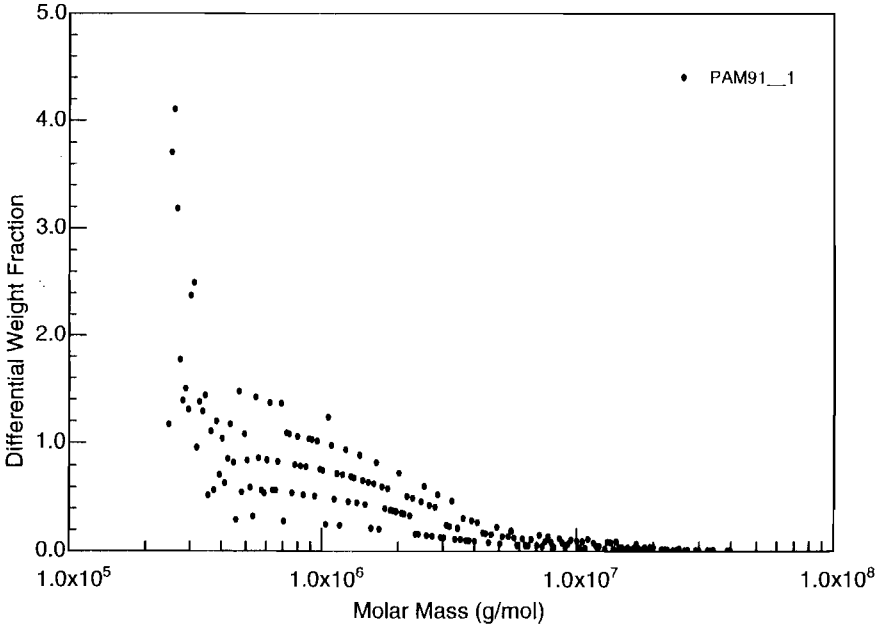

Figure 7 Differential mass fraction distribution for the polyacrylamide sample of Fig. 5 formed by re-sorting the slice collected data into bins in $\log_{10} M$.

fact that the variation of the slope of the "calibration curve," $d(\log_{10} M)/dV$, is negative since larger volumes correspond to smaller molar masses. The differential ("log base 10") mass fraction is then written as

$$x(M) = -[h(V)/\int h(V)dV]/[d(\log_{10} M)/dV] \tag{37}$$

If the term $d(\log_{10} M)/dV$ is linear, then the differential fraction, x(M) is just a rescaled concentration curve. As long as $d(\log_{10} M)/dV$ remains monotonically decreasing, the formalism of Eq. (37) is reasonable. However, when the variation of $d(\log_{10} M)/dV$ becomes zero and even reverses its slope, such as shown in Figs. 5 and 6, the results are both difficult to understand and could be in error. For example, in Fig. 5, a simple fifth-order polynomial does not even fit the data, so that the results based on Eq. (37) may be in considerable error because the larger mass fractions that elute irregularly (non-GPC) are not accorded their proper contributions to the distribution of masses present in the sample. Let us examine these results in more detail.

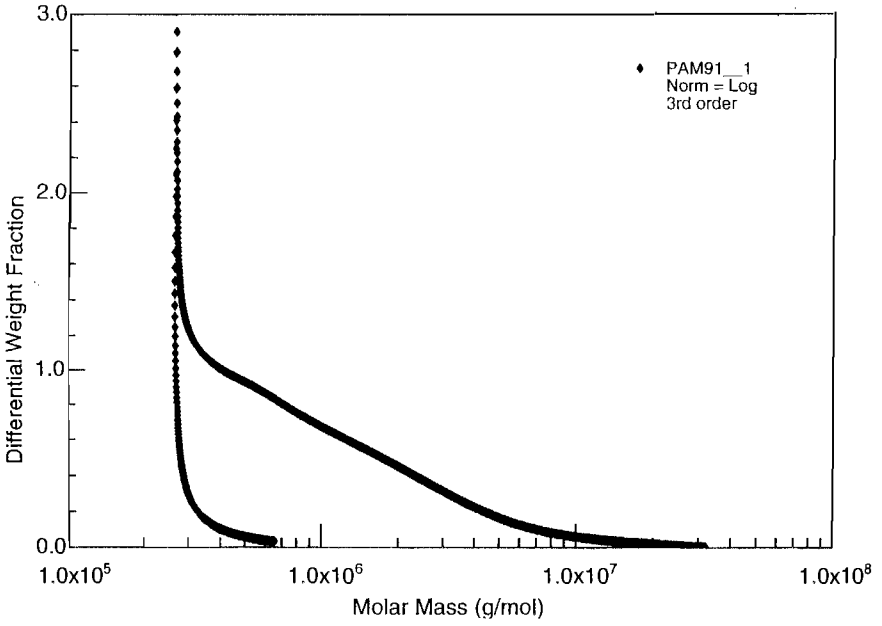

Figure 8 Differential mass fraction distribution for the polyacrylamide sample of Fig. 5 using a third-order fit to the mass elution data. Note the double values about the point of reversal of molar mass versus elution volume, i.e., where $d(\log_{10} M)/dV = 0$.

We begin again with the formalism of Eq. (34). At each elution volume V, there is a corresponding measured value of M as well as a baseline corrected concentration response h(V). The procedure to generate the differential weighted log base 10 mass fraction, x(M), begins weighting the calculated mass M_i by $(\log_e 10)\, h(V_i)/\Sigma[h(V_i)\Delta V_i]$, where the sum is taken over all i slices present in the selected peak being processed. These values are then re-sorted into *mass* bins divided in terms of a $\log_{10} M$ scaling. In this manner, similar mass contributions at different elution volumes would be added together. Applied to the data of Fig. 5, for example, this procedure yields the very discontinuous result of Fig. 7. Because of the uncertainty associated with the calculation of molar mass (the ASTRA program calculates the precision of each measurement reported), one might well consider distributing the mass fraction value into a range of bins rather than into a single mass bin. Thus if the standard deviation of the calculated mass is ΔM, then the mass fraction might be distributed following a Gaussian distribution over a range of bins spanning at least $\pm 2\Delta M$. Even if this procedure were successful, the resulting distributions would still appear strange, and for good

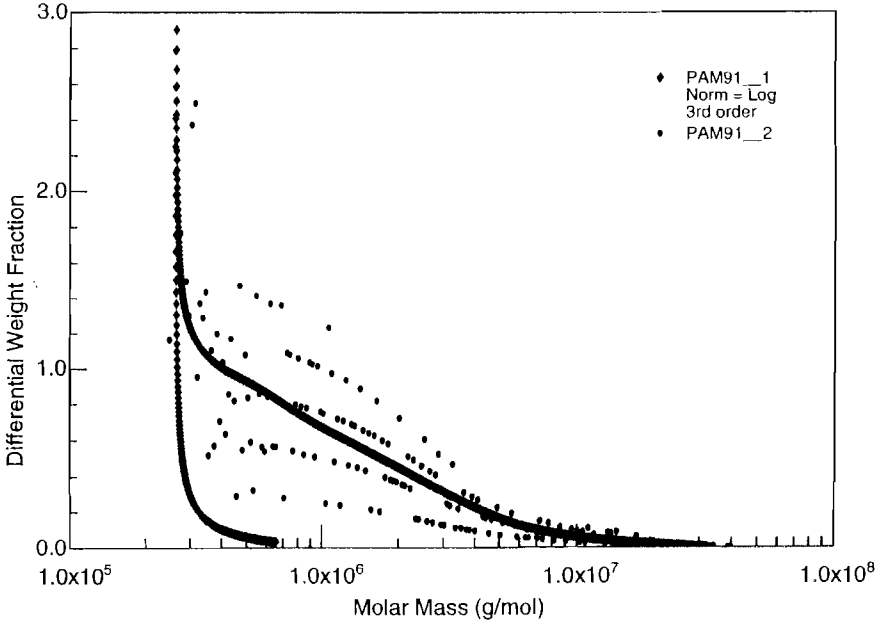

Figure 9 Overlay of the resorted data of Fig. 7 with the analytically fit data of Fig. 8.

reason! Light scattering measurements on occasion show features of the processed sample that are by no means obvious.

Let us return to Fig. 5 and fit the data (smooth) to the simple third-order polynomial indicated by the overlaying curve on Fig. 5. Applying the formalism of Eq. (37) immediately results in the multivalued plot of Fig. 8: a strange, yet expected, differential mass fraction distribution. Overlaying the resorted data of Fig. 7 with the continuous differential mass fraction of Fig. 8 yields Fig. 9. Clearly the two representations are similar, yet Fig. 8 shows more explicitly the two almost distinct distributions of molecules present in the polyacrylamide sample. Even more instructive is an examination of the molecular conformation plot for this non-GPC separation. Figure 10 presents a plot of the rms radii as a function of elution volume. Note that the reversal of the expected decreasing variation of this rms radius occurs at the same elution volume where $d(\log_{10} M)/dV = 0$. Note, however, that the rms radius is *not* the same as the hydrodynamic radius, so that if the separation is still believed to be governed by GPC mechanisms, the drainage properties of the polymer must undergo significant changes beyond

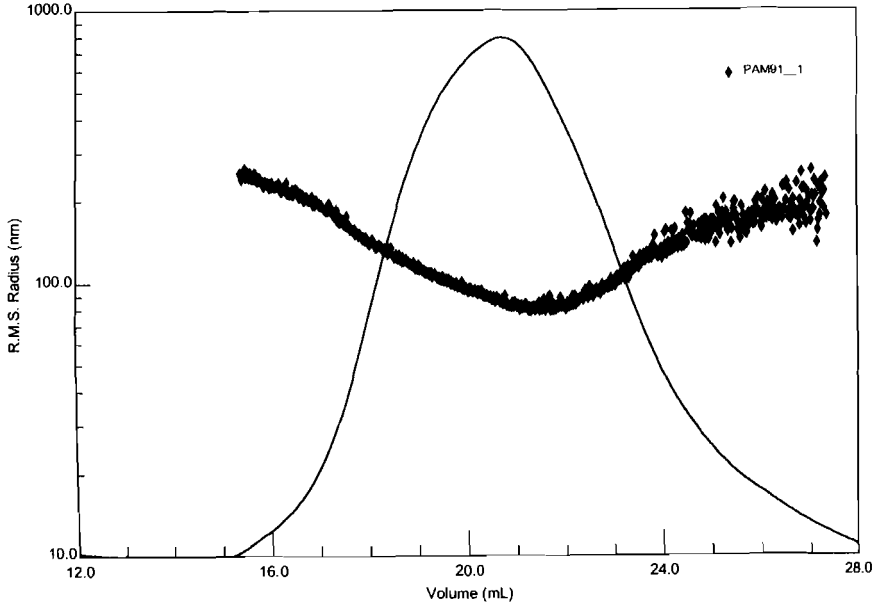

Figure 10 The root mean square radius as a function of elution volume for the sample of Fig. 5.

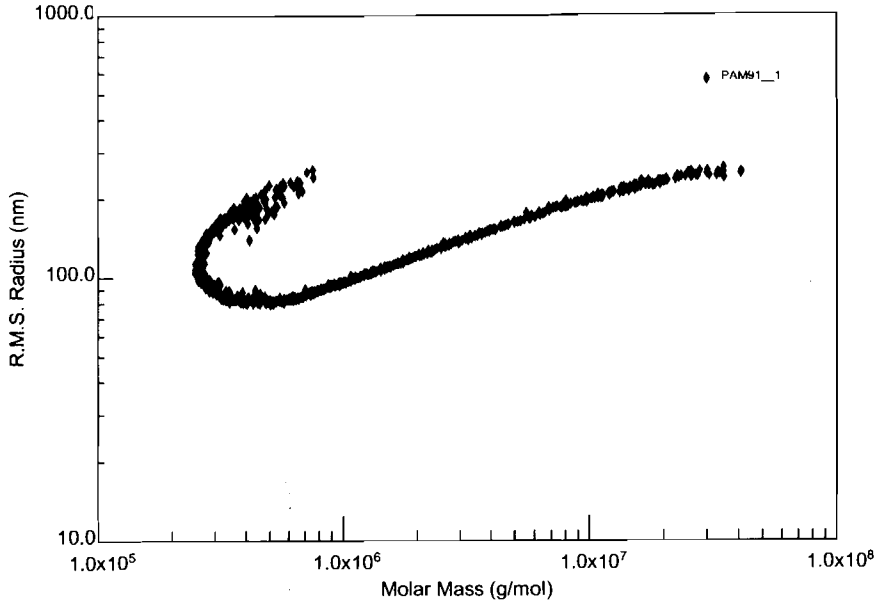

Figure 11 The conformation plot for the polyacrylamide data of Figs. 5 and 10.

the point of the rms radius reversal. Figure 11 presents the conformation plot for this molecular sample, which appears quite normal for molecules eluting before the reversal point, yet which appears very aberrant and distorted for those fractions eluting later in the so-called non-GPC mode. Matsumoto [12] was the first to associate the unusual appearance of the conformation plot with the onset of microgel formation. Whatever the source, the MALS confirms that there is present a fraction of the sample whose conformation is distinctively different than that of a linear or even slightly branched polymer. Conformation plots and differential mass fraction distributions tell much about samples whose elution from GPC columns don't follow the rules.

VI. EXAMPLES OF MALS APPLIED TO OTHER BIOPOLYMERS

Unlike synthetic polymers and most natural polymers such as polysaccharides and complex starches, proteins are produced with polydispersities that are essen-

tially unity. In other words, a protein such as bovine serum albumin is produced at a single molar mass only as determined by the corresponding genetic code. Naturally such proteins can form aggregates whose presence in various biologicals can be immunogenic. Thus the detection of dimers, trimers, and higher order aggregates can become an important task for the quality control of many types of commercially sold biologicals.

Let us consider a few examples of the power of MALS combined with differential refractive index (DRI) detection. In a recent paper by Riggs's group at the University of Texas [13], the use of MALS with a DRI detector produced the values for the broad range of values shown in Table 3. The values calculated from the MALS measurements (DAWN-DSP operating at the He-Ne laser wavelength 632.8 nm) are contrasted to the values calculated based on the expected base pair sequences. A single value of dn/dc (0.19) was used in their measurements using a phosphate buffer saline mobile phase and two Toya Soda GPC columns described in the article.

Light scattering measurements are particularly useful for proteins whenever a DRI detector can be used due to the near-constancy of dn/dc. This is in contrast to reversed-phase chromatography where a UV detector must be used because of the varying refractive index of the mobile phase. This in turn requires the measurement of the corresponding UV extinction coefficient for each protein species. For certain closely related proteins, where a single extinction coefficient may be chosen, the light scattering results for determining molar masses of separated species is equally impressive. Figure 12 shows the UV chromatogram from a set of isolated wheat proteins whose corresponding sequence values are shown in Table 4. These proteins were separated by reversed-chromatography using a gradient of acetyl nitrate in water over the range of 0 to 15%. What is particularly significant about this type of separation is that the elution sequence is not gener-

Table 3 Measured Molar Masses of a Broad Range of Proteins

Protein	Mass from structure (Da)	Light scattering (Da)	Apparent error (%)
Carbonic anhydrase	29,023	29,800	+2.7
Alcohol dehydrogenase	146,980	149,000	+1.4
β-Amylase	224,340	228,000	+1.6
Apoferritin	476,316	484,400	+1.7
Thyroglobulin	669,000	679,000	+1.5
Ornithine decarboxylase	990,684	978,000	−1.3
Octopus hemocyanin	3,440,000	3,450,000	+0.3

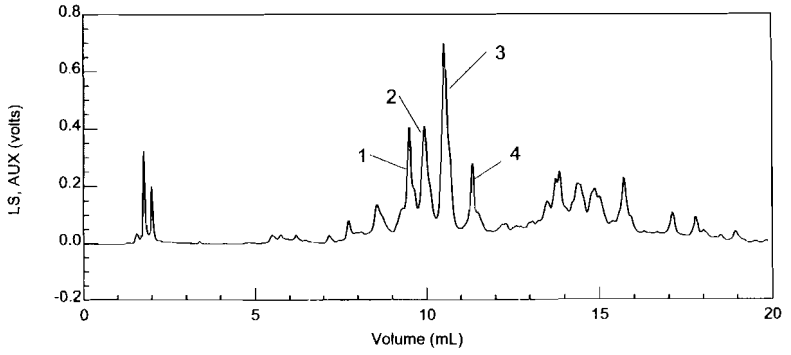

Figure 12 UV chromatogram from a set of isolated wheat proteins whose molar mass and size were calculated from MALS measurements. See Table 4 for details.

ally in any particular order. There is no means to calibrate the columns used for reversed-phase separation as is often the case for GPC separations.

Figure 13 illustrates an important element of MALS combined with a concentration-sensitive detector. Shown here are three differential mass fraction distributions [cf. Eq. (37)] of specially processed recombinant DNA–produced hyaloronic acid. Although all overlap broadly with each other, the direct comparison of their differential mass fractions permits an easy discrimination between them.

Finally, the process of adding polyethylene glycol (PEG) to proteins (so-called pegylation), which has become of considerable importance as a time release drug delivery process, produces a copolymer whose core is a pure, monodisperse protein molecule. By iteratively calculating the copolymer mass at each elution volume (note that each component has a different dn/dc value), staff

Table 4 Calculated Molar Mass and Size for Each of the Four Wheat Protein Peaks Identified in Fig. 12 Contrasted with Their DNA Calculated Values

	Molar mass (kD)		RMS radius (nm)
Proteins	cDNA	DAWN DSP	DAWN DSP
1	68.7	67.6 ± 0.3	11.7 ± 1.5
2	87.2	87.4 ± 0.4	11.4 ± 1.5
3	83.1	79.7 ± 0.4	11.7 ± 1.5
4	N/A	70.6 ± 0.7	13.8 ± 2.6

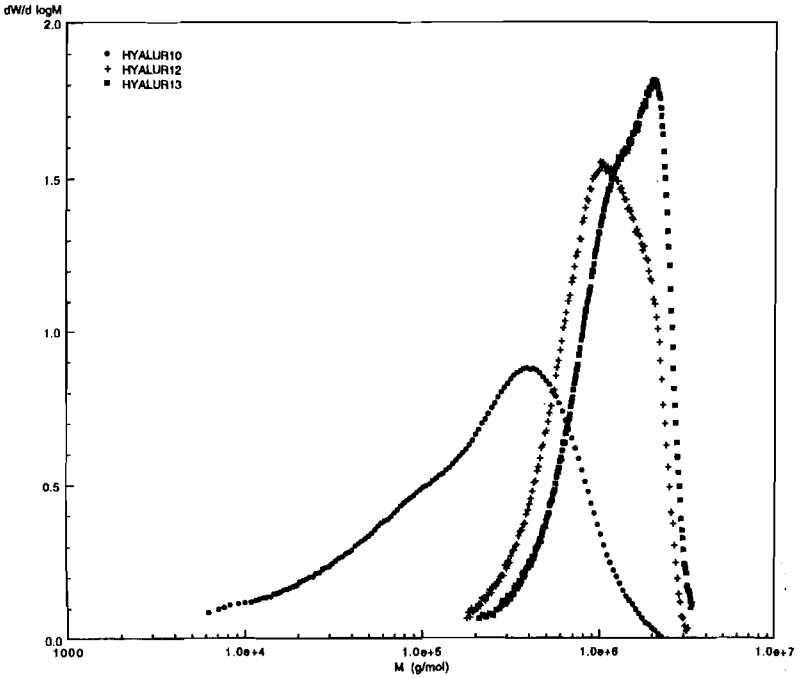

Figure 13 Differential weight fraction distributions for three hyaluronic acid samples.

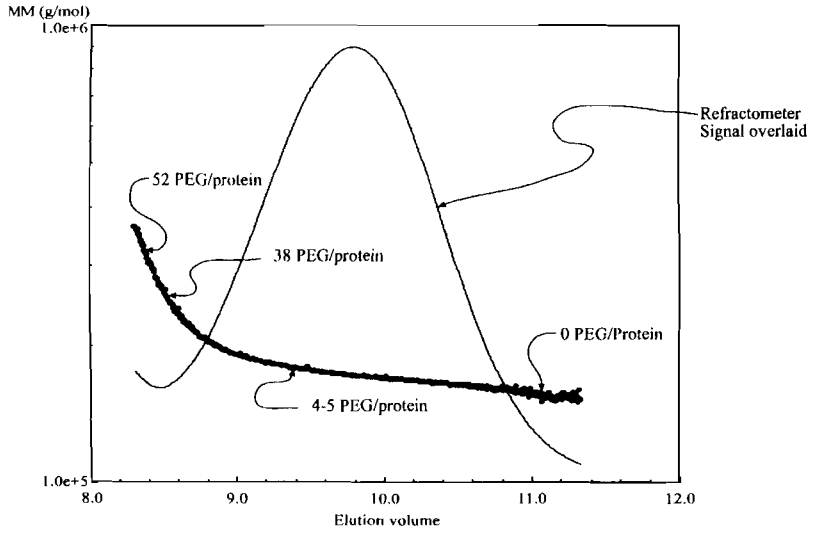

Figure 14 Variation of molar mass with elution volume for a pegylated protein sample. Used a self-consistent iterative method to calculate the number of PEG/protein.

member Robert Paulson in an unpublished Application Note [14] has been able to calculate not only the total molar mass of each eluting fraction but the number of PEG molecules (molar mass about 15,000) attached to each protein molecule (molar mass about 150,000), as illustrated in Fig. 14.

VII. CONCLUDING REMARKS

MALS measurements following fractionation by GPC, reversed-phase, or other techniques represent one of the most powerful means for studying the solution properties of polymers. The distinctions between MALS and single- or dual-angle light scattering measurements have been discussed together with the effects of the latter measurements on the errors of the derived quantities (molar mass, size, conformation, etc.).

Discussion of the various "moments" of the molar mass distributions has shown that for all but random coil molecules in a theta solvent, the light scattering measurement yields an unusual type of moment associated with it. Other mass and size moments derived from measurements of fractionated samples have been explained. For light scattering measurements of homopolymers, MALS determination of rms radii may be made (at the low concentrations characteristic of chromatographically separated samples) without a concentration detector.

The unusual properties of samples whose separation appears in conflict with that expected by normal HPLC means have been studied and shown most vividly through the so-called conformation plot as well as the differential mass fraction distribution. The power of the MALS measurement for understanding complex macromolecular structures has been illustrated by these examples.

ACKNOWLEDGMENTS

This chapter is based on a paper presented at the Waters GPC Symposium, September 1996, San Diego, CA. The exceptional laboratory results, especially the data shown in Figs. 10 through 12, were made under the direction of Dr. Michelle H. Chen. Other individuals who made contributions include Dr. Greg Cauchon, Lena Nilsson, and David Villalpando.

REFERENCES

1. Huglin MB, ed. Light Scattering from Polymer Solutions. London: Academic Press, 1972.
2. Ouano AC, Kaye W. J Polym Sci. A-1 1974;12:1151.

3. Moore JC. J Polym Sci A 1964;2:835.
4. Burchard W, Cowie JMG. In: Huglin MB, ed. Light Scattering from Polymer Solutions. London: Academic Press, 1972.
5. Zimm BH. J Chem Phys 1948;16:1093; ibid., 1099.
6. Wyatt PJ. Anal Chim Acta 1993;272:1–40.
7. Berkowitz SA. Rejection of spike noise from SEC/LALLS experiments. Anal Chem 1986;58:2571.
8. Kratochvil P. In: Huglin MB, ed. Light Scattering from Polymer Solutions. London: Academic Press, 1972.
9. Benoit H, Froelich D. In: Huglin MB, ed. Light Scattering from Polymer Solutions. London: Academic Press, 1972.
10. Billingham NC. Molar Mass Measurements in Polymer Science. New York: John Wiley and Sons, 1977.
11. Shortt DW. J Liquid Chromatogr 1993;16:3371–3391.
12. Matsumoto A. American Chemical Society National Meeting, Sept. 1990, Washington, D.C.
13. Zhu H, Ownby DW, Riggs CK, Nolasco NJ, Stoops JK, Riggs AF. Assembly of the gigantic hemoglobin of the earthworm lumbricus terrestris roles of subunit equilibria, non-globin linker chains, and valence of the heme iron globin. J Biol Chem 1996;271:30007–30021.
14. Cf. the Worldwide Web site *www.wyatt.com*.

13

Purification and Characterization of Connective Tissue Growth Factor Using Heparin Affinity Chromatography

David R. Brigstock
Ohio State University and Children's Hospital, Columbus, Ohio

I. INTRODUCTION

The term *connective tissue growth factor* (CTGF) was first used in 1991 to describe a mitogenic and chemotactic factor for fibroblasts that was produced by human umbilical vein endothelial cells (HUVECs) in vitro [1]. The primary translational products of both human CTGF (hCTGF) and porcine CTGF (pCTGF) are predicted to comprise 349 residues, the first 26 of which are a presumptive signal peptide [1,2]. Mouse CTGF (mCTGF; also termed *fisp*-12 or βIG-M2) is predicted to comprise 348 residues, of which the first 25 are a hydrophobic signal peptide [3,4]. Secreted forms of CTGF from all three species are thus predicted to comprise 323 residues, 38 of which are conserved cysteine residues. Metabolic labeling and immunoprecipitation studies of cell lysates and conditioned medium have shown that CTGF proteins of approximately 38 kDa are produced and secreted in various cell cultures [2,5,6]. CTGF, which is encoded by a transforming growth factor–β (TGFβ)–inducible immediate early gene [3], has been strongly implicated in a variety of fibrotic disorders [7–11], wound healing [12–14], embryonic development [5], and uterine function [2,15]. Although the 38-kDa form of CTGF was initially implicated in many of these processes, low-mass forms of CTGF of M_r 10,000–20,000 have since been discovered in uterine secretory fluids [15] and fibroblast conditioned medium [6].

Partial purification of 38-kDa hCTGF was first achieved using immunoaffinity chromatography with an antiserum to intact platelet-derived growth factor (PDGF) [1]. Since PDGF and CTGF are not structurally related, the reactivity of CTGF with anti-PDGF was serendipitous and attributed to the presence of cross-reactive epitopes on the CTGF and PDGF proteins [1]. More recently, heparin affinity chromatography has been used as an essential step in the isolation of pCTGF from complex body fluids such as uterine secretions [15], as well as for the large-scale purification of recombinant hCTGF produced in a buculovirus expression system [16]. This chapter will demonstrate the use of heparin affinity fast protein liquid chromatography (FPLC) and reversed-phase high-performance liquid chromatography (RP-HPLC) for the isolation and characterization of a 10-kDa form of CTGF in pig uterine fluids.

II. MATERIALS AND METHODS

A. Uterine Secretory Fluids

Uteri were collected at random from pigs that were sacrificed at a local slaughterhouse. After transportation to the laboratory, the lumen of each uterine horn was flushed with 10–50 ml phosphate-buffered saline (PBS). A single collection of uterine luminal flushings (ULF) consisted of approximately 600–1100 ml obtained from 16–26 uteri. ULF were clarified by centrifugation at 13,500*g* for 30 min at 4°C and the supernatant was passed through glass wool to remove floating material. Comparative heparin affinity FPLC was performed on ULF obtained from cycling or pregnant animals (n = 6 per group) that were sacrificed on day 11, the time of onset of blastocyst elongation and peak estrogen production in the pig [17–20].

B. Chromatography

1. Cation Exchange Chromatography

ULF were applied at 3.5 ml/min to a Bio-Rex 70 cation exchange column (5 × 6 cm; Bio-Rad Laboratories, Richmond, CA, USA) which was then washed with 1000 ml of PBS containing 0.2 M NaCl and subsequently developed with a 500-ml gradient of 0.2–2.0 M NaCl in PBS. These procedures were performed at 4°C. Fractions (10-ml) were collected during salt gradient elution of bound proteins and were assayed for their ability to stimulate [^{3}H]thymidine incorporation in Balb/c 3T3 cells. The 0.3–0.7 M NaCl elute was selected for further analysis by heparin affinity FPLC.

2. First-Step Heparin Affinity FPLC

The 0.3–0.7 M NaCl eluate from the Bio-Rex column was diluted threefold with 20 mM Tris-HCl (pH 7.4) containing 0.1% (w/v) 3-[(3-cholamidopropyl)dimethylammonio]-1-propanesulfonate (CHAPS), clarified using a low protein binding 0.45-μm HT Tuffryn Acrodisc filter (Gelman Sciences, Ann Arbor, MI, USA), and applied at room temperature to an EconoPac heparin column (0.7 × 3.6 cm, Bio-Rad) at 2 ml/min using a peristaltic pump. The column was then attached to an FPLC system (Pharmacia LKB Biotech Inc., Piscataway, NJ, USA), washed with 50 ml 20 mM Tris-HCl/0.2 M NaCl/0.1% CHAPS (pH 7.4), and developed at 1 ml/min with a 40-ml 0.2–2.0 M NaCl gradient in 20 mM Tris-HCl/0.1% CHAPS (pH 7.4). Eluted proteins were collected into 1-ml fractions and tested for their mitogenic activity. The absorbance of the column eluate was monitored at 280 nm using an in-line UV monitor.

3. Second-Step Heparin Affinity FPLC

The 0.8 M NaCl eluates from nine individual EconoPac heparin purifications were pooled, diluted threefold with 20 mM Tris-HCl (pH 7.4), clarified by passage through a 0.2-μm HT Tuffryn filter membrane (Gelman Sciences), and applied at room temperature at 1 ml/min to a TSK heparin 5PW column (0.8 × 7.5 cm; TosoHaas, Philadelphia, PA, USA) using a Pharmacia FPLC system. The column was washed and developed as described above for the EconoPac heparin column except that CHAPS was omitted from the buffers to prevent interference in the subsequent HPLC step.

4. First-Step Reversed-Phase HPLC

The 0.8 M NaCl eluate from the TSK heparin column was adjusted to 10% acetonitrile/0.1% trifluoroacetic acid (TFA), clarified using a 0.2-μm HT Tuffryn Acrodisc filter (Gelman Sciences), and applied to a preequilibrated C_8 HPLC column (0.46 × 25 cm, 5 μm; Rainin Instrument Co, Woburn, MA, USA) using a Hitachi HPLC system (Hitachi Instruments Inc., Danbury, CT, USA). After sample application, the column was washed with 10 ml of 10% acetonitrile/0.1% TFA prior to elution of bound proteins with a 10–90% acetonitrile gradient (in water/0.1% TFA) over 136 min. This step was performed at room temperature and the flow rate was 1 ml/min. The absorbance of the column eluate was monitored at 214 nm using an in-line UV monitor. The eluate was collected as 0.5-ml fractions in siliconized tubes containing 50 μl of 125 mM NaOH. Aliquots of selected fractions were dried by evaporation using a SpeedVac concentrator (Savant Instruments, Farmingdale, NY, USA) and reconstituted in 20 mM Tris-HCl (pH 7.4) for SDS-PAGE and for analysis of their mitogenic activity.

5. Second-Step Reversed-Phase HPLC

Bioactive fractions from the first HPLC step were pooled, diluted fivefold with water/0.1% TFA, and applied to a Rainin C_8 HPLC column (0.46 × 25 cm, 5 μm) that was washed and developed with acetonitrile in water/0.1% TFA as described above. Selected fractions were analyzed by SDS-PAGE and mitogenic activity as described above. A single 10-kDa protein that was present exclusively in biologically active fractions was selected for amino acid sequencing.

C. Protein Sequencing

The HPLC-purified 10kDa protein was evaporated to dryness using a SpeedVac concentrator, redissolved in SDS-PAGE sample buffer, subjected to SDS-PAGE, transferred to nitrocellulose, and located by staining the blot with Coomassie R250. The protein was then excised and subjected to N-terminal microsequencing on a model 470A gas phase sequenator (Applied BioSystems, Foster City, CA, USA). Phenylthiohydantoin derivatives in each cycle were separated using C_{18} RP-HPLC. The sequence was assigned using Applied BioSystems sequence analysis software, with independent verification by an experienced operator with no knowledge of the likely identity of the sample.

D. SDS-PAGE and Silver Staining

Samples were electrophoresed on a 18% SDS polyacrylamide gel under reducing conditions at 200 V for 1 h. For analytical work, proteins in the gels were stained with silver as described [21]. For amino acid sequencing, the 10-kDa protein was transferred from the gels to nitrocellulose in 10 mM 3-(cyclohexylamino)propanesulfonic acid (pH 11.0) at 300 mA for 2 h.

E. Bioassay

Column fractions were tested for their stimulation of [^{3}H]thymidine incorporation into the DNA of quiescent Balb/c 3T3 cells. Neutralization studies were performed by coincubation of the 0.8 M NaCl heparin column eluate with 25 μg/ml anti-PDGF IgG (Upstate Biotechnology Inc., Lake Placid, NY, USA) or 10 μl/ml basic fibroblast growth factor (bFGF) antiserum ("77R," kindly donated by Dr. M. Klagsbrun, Children's Hospital, Boston, MA, USA). PDGF and bFGF standards were from R&D Systems (Minneapolis, MN, USA) and Life Technologies (Grand Island, NY).

F. CTGF Peptide Synthesis

A peptide corresponding to residues 247–260 of pCTGF (EENIKKGKKCIRTP) was produced on a Synergy 432A peptide synthesizer (Applied BioSystems) and purified by RP-HPLC using a C18 column as described [15]. One milligram of the peptide in 2 ml of 10 mM Tris-HCl (pH 7.4) was then applied to a TSK heparin column, which was washed and developed as described above. The elution position of the peptide was determined spectrophotometrically at 214 nm.

III. RESULTS

A. Ion Exchange Chromatography and Heparin Affinity FPLC

When ULF were applied to a Bio-Rex 70 column, the flow-through fraction was shown to contain high-mass forms of epidermal growth factor (EGF) that stimulated DNA synthesis in 3T3 cells [22]. However, material which bound to the column and was eluted by 0.3–0.7 M NaCl was also shown to be mitogenic for 3T3 cells (Fig. 1). Affinity chromatography of this eluate using EconoPac heparin

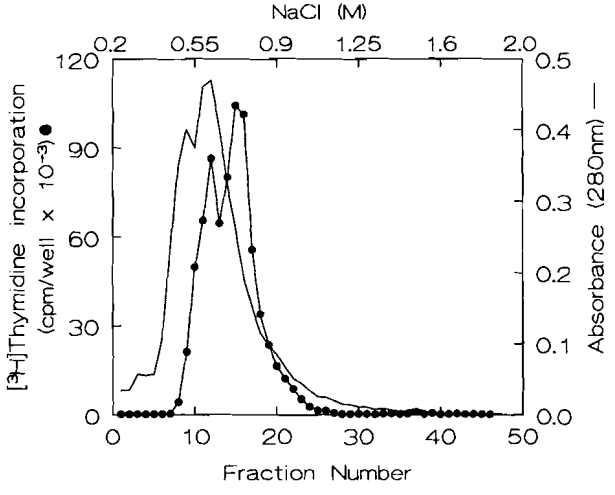

Figure 1 Cation exchange chromatography of pig ULF. Approximately 1100 ml of ULF from 26 animals was applied to a Bio-Rex cation exchange column at 3.5 ml/min. The column was then washed with 1000 ml PBS/0.2 M NaCl and treated with a 500-ml gradient of 0.2–2.0 M NaCl in PBS. Fractions (10 ml) were collected and assayed at 50 µl/ml for their ability to stimulate [^{3}H]thymidine incorporation in Balb/c 3T3 cells.

columns resulted in the elution of four peaks of growth factor activity over a 0.2–2.0 M NaCl gradient (Fig. 2). The first activity peak was eluted by 0.5 M NaCl and shown to contain a PDGF-like factor [23]. The second activity peak was eluted by 0.8 M NaCl and contained a novel factor that was termed HBGF-0.8 prior to its definitive identification as a 10-kDa form of CTGF [15]. The third activity peak was eluted by approximately 1 M NaCl and contained heparin-binding EGF-like growth factor (HB-EGF) and pleiotrophin (PTN) [23,24]. The fourth activity peak was eluted by 1.6 M NaCl and was due to the presence of bFGF [15,23,25].

To further purify 10-kDa CTGF, fractions containing the 0.8 M NaCl eluate from the EconoPac heparin column were pooled, diluted, and subjected to a second step of heparin affinity FPLC using a TSK heparin column. A peak of growth factor activity was subsequently eluted by 0.8 M NaCl (Fig. 3), which in some separations could be resolved into two microheterogeneous forms of 10-kDa CTGF [15]. To show that 10-kDa CTGF was immunologically distinct from

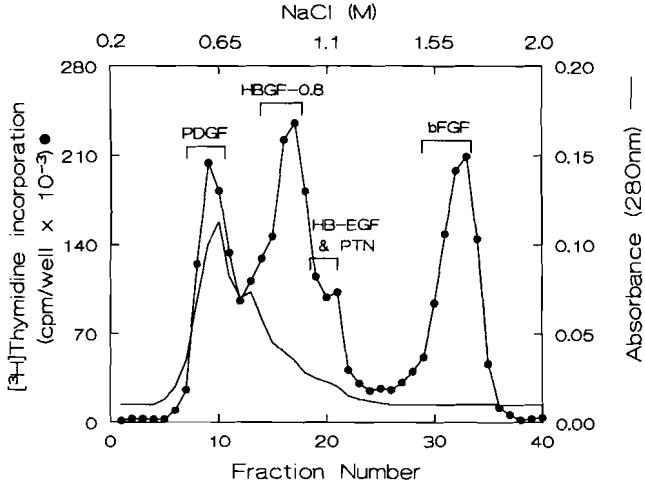

Figure 2 First-step heparin affinity FPLC. Mitogenic fractions from cation exchange chromatography of 900 ml of ULF from 22 animals were pooled, diluted to three-fold, and applied to an EconoPac heparin column, which was then washed with 10 ml 20 mM Tris-HCl/0.2 M NaCl/0.1% CHAPS (pH 7.4) and developed with a 40-ml gradient of 0.2–2.0 M NaCl in 20 mM Tris-HCl/0.1% CHAPS (pH 7.4). Fractions (1-ml) were collected during NaCl gradient elution of the bound proteins and tested at 15 µl/ml for their stimulation of [^{3}H]thymidine incorporation in Balb/c 3T3 cells. The figure shows the identity of various heparin-binding growth factors that were separated from one another.

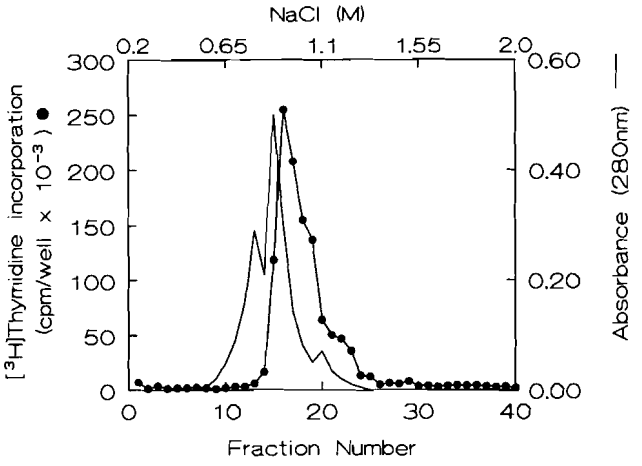

Figure 3 Second-step heparin affinity FPLC. Nine individual samples of ULF (7.15-L total volume from 206 pigs) were individually processed by cation exchange and EconoPac heparin affinity chromatography as shown in Figs. 1 and 2. The 0.8 M NaCl eluates from each heparin affinity purification were pooled, diluted, and applied to a TSK heparin column which was washed with 10 ml of 20 mM Tris-HCl/0.2 M NaCl (pH 7.4) and developed with a 40-ml gradient of 0.2–2.0 M NaCl in 20 mM Tris-HCl (pH 7.4). Fractions (1-ml) were collected during NaCl gradient elution of the bound proteins and tested at 5 µl/ml for their stimulation of [^{3}H]thymidine incorporation in Balb/c 3T3 cells.

bFGF or PDGF and was not contaminated by either of these factors, it was incubated with neutralizing antisera to PDGF or bFGF. As shown in Table 1, CTGF mitogenic activity was unaffected by either of these antisera, which were nonetheless very effective in antagonizing the activity of their respective ligands.

B. Reversed-Phase HPLC

Isolation of 10-kDa CTGF to homogeneity was achieved by performing two steps of C_8 RP-HPLC on heparin-purified samples. Results from the second HPLC step are presented in Fig. 4 that show the elution of a single peak of growth factor activity at 45 min (28% acetonitrile). The elution profile of the mitogenic activity was directly correlated with that of a single peak of protein, which was of M_r, 10,000 as assessed by SDS-PAGE. Based on silver staining of SDS polyacrylamide gels, no proteins other than the 10-kDa polypeptide were present in any of the biologically active fractions (Fig. 4).

Table 1 Lack of Effect of Neutralizing Anti-PDGF or Anti-bFGF on CTGF Mitogenic Activity

Growth factor	[^{3}H]Thymidine incorporation (cpm/well $\times 10^{-3}$) (mean ± SD)	
	Alone	*+anti-PDGF IgG*
No addition	899 ± 99	956 ± 20
PDGF (10 ng/ml)	21,634 ± 6,664	938 ± 20
HBGF-0.8 (15 μl/ml)	47,677 ± 1,316	62,045 ± 6,645
	Alone	*+bFGF antiserum*
No addition	825 ± 143	7,575 ± 369
bFGF (6 ng/ml)	62,365 ± 2,669	7,615 ± 1,519
HBGF-0.8 (15 μl/ml)	85,152 ± 1,330	83,238 ± 2,538

C. Amino Acid Sequencing

Amino acid sequencing of the HPLC-purified protein revealed the N-terminal sequence Glu-Glu-Asn-Ile-Lys-Lys-Gly-Lys-Lys-Xaa-Ile-Arg-Thr-Pro-Lys-Ile (Table 2). This sequence was identical to residues 247–262 of hCTGF or pCTGF, and to residues 246–261 of mCTGF, with the unidentified residue in cycle 10 corresponding to a cysteine residue in the predicted protein sequences from all three species (Table 2). Although CTGF is structurally related to *cyr*61/cef10 and *nov*(26–32), the protein sequence obtained experimentally aligned less well with the corresponding internal sequence of these proteins, demonstrating that the 10-kDa protein was a low-mass form of CTGF that was substantially truncated at its N terminus (Table 2).

D. Biological Activity of 10-kDa CTGF

As well as stimulating DNA synthesis in mouse Balb/c 3T3 cells, submaximal stimulatory doses of 10-kDa CTGF were shown to potentiate the activity of several other 3T3 cell mitogens including EGF, bFGF, PDGF, and insulin-like growth factor–1 (IGF-1) (Table 3). The mitogenic activity of 10-kDa CTGF was highly susceptible to inactivation by exposure to heat or acid (Fig. 5). The 10-kDa CTGF protein was also found to stimulate [^{3}H]thymidine incorporation in primary cultures of pig endometrial stromal cells, suggesting that as a product of uterine tissues CTGF may act via autocrine or paracrine growth stimulatory pathways within the uterus (Fig. 6). Finally, analysis of the amount of 3T3 cell

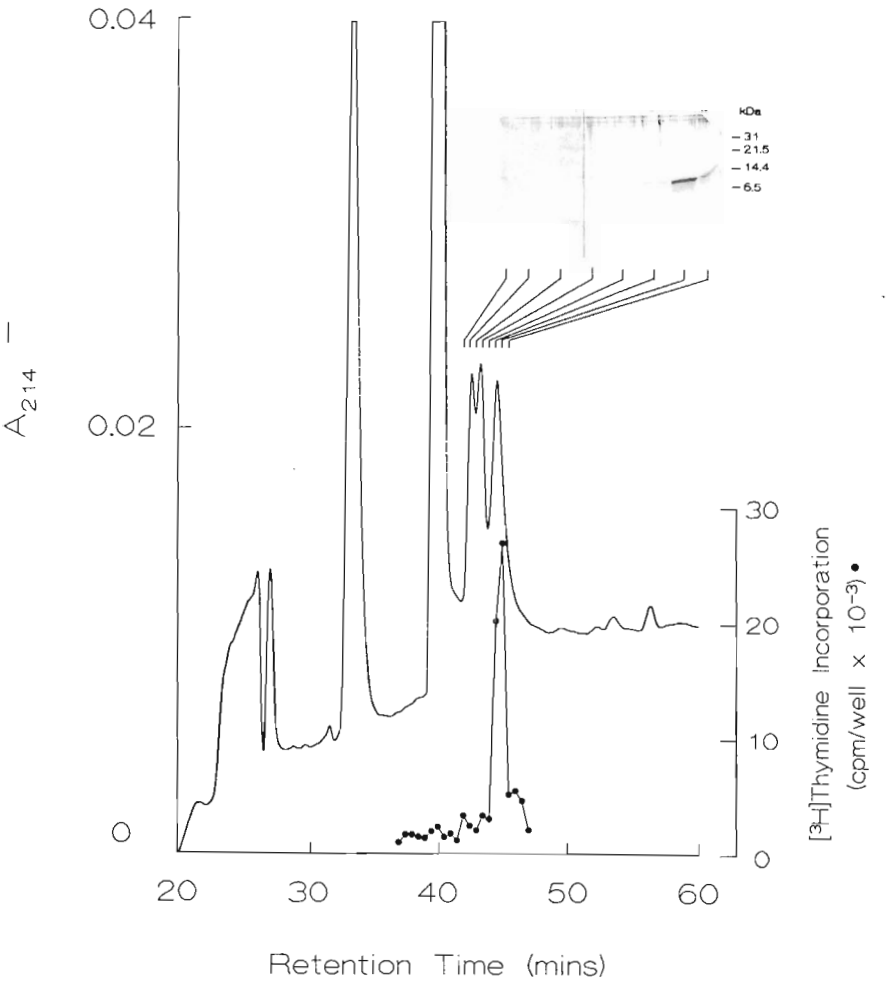

Figure 4 Second-step RP-HPLC. Two peak active fractions from first-step HPLC purification (data not shown) were subjected to second-step HPLC purification as described in "Materials and Methods." The figure shows the elution of protein as measured at 214 nm and the ability of 20 µl of selected fractions to stimulate 3T3 cell DNA synthesis after drying and reconstitution in 10 µl PBS/0.1% BSA. The inset shows a silver-stained SDS polyacrylamide gel of 50-µl aliquots of successive fractions containing the peak of mitogenic activity.

Table 2 N-Terminal Amino Acid Sequences of HBGF-0.8 and Members of the CTGF Family[a]

Protein	Residues	Sequence	Ref.
HBGF-0.8	1–16	E E N I K K G K K X I R T P K I	15
Human CTGF	247–262	– – – – – – – – – C – – – – – –	1
Pig CTGF	247–262	– – – – – – – – – C – – – – – –	2,15
Mouse CTGF	246–261	– – – – – – – – – C – – – – – –	3,4
Mouse cyr61	275–290	Y S S L – – – – – C S K – K – S	3,27
Human cyr61	277–292	Y S S L – – – – – C S K – K – S	28
Chick cef10	272–291	Y A S L – – – – – C T K – K – S	29
Chick nov	249–264	– P S D – – – – – C – Q – K – S	30
Human nov	255–270	Q P T D – – – – – C L – – K – S	31
Xenopus nov	240–255	W H V E – – – – – C V – V R – T	32

[a] Dashes indicate residues that are identical to those of HBGF-0.8.

mitogenic activity in the 0.8 M NaCl eluate after two rounds of heparin affinity FPLC showed that ULFs from pigs on day 11 of pregnancy contained approximately 5 times the level of CTGF-like activity as ULF from pigs on day 11 of the estrous cycle (Fig. 7).

E. Heparin Binding Properties of N Terminus of 10-kDa CTGF

To test the heparin binding properties of the N-terminal region of 10-kDa CTGF, a synthetic peptide corresponding to residues 247–260 of the pCTGF primary

Table 3 Potentiation of Growth Factor Activity by 10-kDa CTGF[a]

	[^{3}H]Thymidine incorporation (cpm/well $\times 10^{-3}$) (mean ± s.d.)	
Treatment	No addition	+10-kDa CTGF
None	293 ± 42	2,843 ± 280
IGF-I (10ng/ml)	621 ± 324	7,699 ± 996
EGF (3ng/ml)	5,418 ± 1,031	49,910 ± 5,457
PDGF (10ng/ml)	36,509 ± 7,407	104,340 ± 23,742
bFGF (0.3ng/ml)	21,095 ± 2,612	46,836 ± 17,091
Calf serum (250μl/ml)	71,731 ± 11,992	—

[a] Heparin-purified 10-kDa CTGF was added at a submaximal dose to triplicate wells of Balb/c 3T3 cells in the presence of the indicated concentrations of other 3T3 cell mitogens.

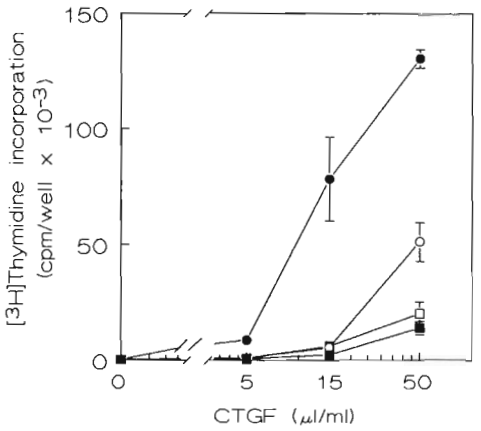

Figure 5 Heat and acid treatment of 10-kDa CTGF. Heparin-purified 10-kDa CTGF was incubated at pH 7.4 for 30 min at room temperature (●), pH 7.4 for 30 min at 56°C (□), pH 7.4 for 5 min at 100°C (■), or pH 1.5 for 3 min at room temperature (○). Samples were assayed for their stimulation of 3T3 cell DNA synthesis at equivalent doses. Values shown are mean ±SD of triplicate determination of [^{3}H]thymidine incorporation.

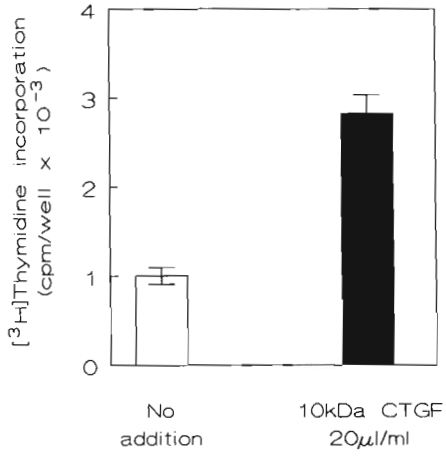

Figure 6 Stimulation of pig endometrial cell DNA synthesis by 10-kDa CTGF. Primary cultures of pig endometrial cells were treated for 18 h with 20 μl/ml heparin-purified 10-kDa CTGF (a concentration that induced maximal stimulation of DNA synthesis in Balb/c 3T3 cells) after which they were incubated with 1 μCi/ml [^{3}H]thymidine for 6 h.

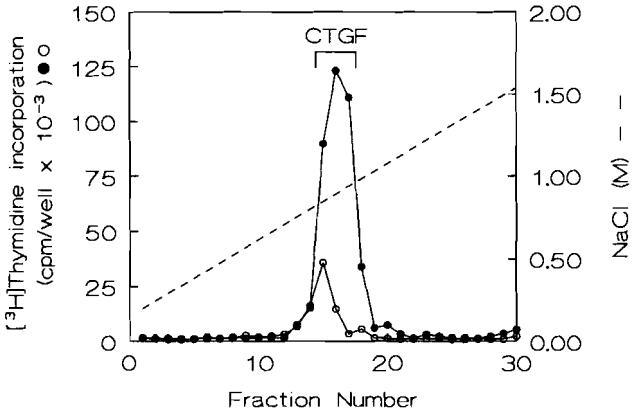

Figure 7 Heparin affinity FPLC of ULF from day 11 pregnant or cycling pigs. ULF from day 11 pregnant (●) or cycling (○) pigs (n = 6 per group) were subjected to two rounds of heparin affinity purification essentially as shown in Figs. 2 and 3 except that no Bio-Rex purification was performed and the first and second heparin affinity steps were performed using heparin-Sepharose and EconoPac heparin columns, respectively. The figure shows the stimulation of 3T3 cell DNA synthesis by selected fractions from the second heparin affinity step when assayed at 2.5 μl/ml on 3T3 cells. The levels of CTGF in ULF were 45.1 units in pregnant animals versus 8.8 units in nonpregnant animals, where one unit is the amount of each growth factor per ml that was required to elicit half the [^{3}H]thymidine incorporation as 20% calf serum.

translational product (i.e., the N terminus of 10-kDa CTGF; see Table 2) was subjected to heparin affinity FPLC. Although the pI of this peptide is the same as that of PDGF (9.6) which is eluted from heparin affinity columns by 0.5 M NaCl [33,34], the CTGF peptide required 0.7 M NaCl for elution from a TSK heparin column (Fig. 8). These results showed that the peptide bound more strongly to heparin than could be explained by its isoelectric point alone and were suggestive of the presence of specific heparin-binding determinants in the peptide.

IV. DISCUSSION

A. Heparin Affinity Purification of CTGF

Over the last 15 years, heparin affinity chromatography has proven a particularly powerful means by which a variety of polypeptide growth factors have been characterized and purified. These include acidic FGF (aFGF), bFGF, HB-EGF,

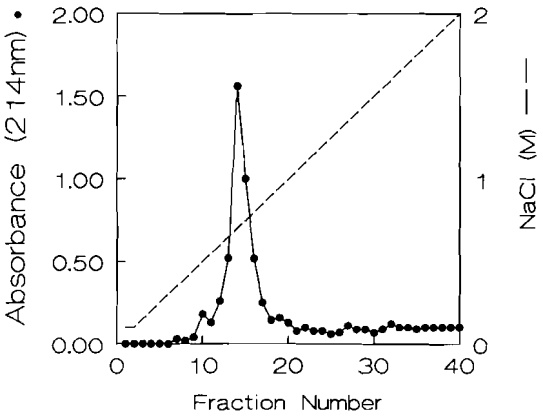

Figure 8 Heparin affinity FPLC of CTGF[247–260]. One milligram of CTGF[247–260] peptide was applied to a TSK heparin column in 20 mM Tris-HCl (pH 7.4) containing 0.2 M NaCl. The column was washed with 10 ml of 20 mM Tris-HCl/0.2 M NaCl (pH 7.4) and bound material was eluted from the column with a 0.2–2 M NaCl gradient in 20 mM Tris-HCl (pH 7.4). Fractions of 1 ml were collected throughout and measured at 214 nm.

PTN, vascular endothelial growth factor, keratinocyte growth factor, and amphiregulin [35–41]. Since many of these factors exhibit different affinities for heparin, the relative binding of these factors to heparin has been a particularly useful criterion for characterizing growth factor of unknown identity, especially when used in conjunction with immunological (e.g., western blot) and biological (e.g., activity, target cell specificity) assays. Indeed, CTGF was first recognized as a fibroblast mitogen in uterine secretory fluids in 1989 as a result of its atypical chromatographic behavior on heparin-agarose [25]. Key features that were subsequently used to distinguish it from other well-characterized growth factors (including FGFs with which it was initially thought to be related [25]) were its (1) elution from heparin by 0.8 M NaCl, (2) molecular mass of 10,000 as determined by nondenaturing gel filtration and SDS-PAGE, (3) target cell specificity (mitogenic for fibroblasts and smooth muscle cells but not endothelial cells), (4) heat and acid lability, (5) potentiation of bFGF-, EGF-, PDGF-, or IGF-induced mitogenic activity, and (6) lack of reactivity with PDGF or bFGF antisera (these results and [15]). However, it was not until the development of this purification protocol that the factor was isolated and definitively identified as a 10-kDa form of CTGF. Heparin affinity chromatography not only played an important role in the initial purification and characterization of 10-kDa CTGF, but also in the separation of two microheterogeneous forms of the protein that differed by the

presence or absence of a single glutamic acid residue (Glu^{247}) at the N terminus (see below and [15]. Using a similar purification strategy, heparin-binding 10- to 12-kDa forms of CTGF have also been isolated from serum-free conditioned medium of mouse or human fibroblasts maintained in vitro [6].

Recently, heparin affinity chromatography was used to substantially purify recombinant human CTGF in a single-step procedure [16]. In those experiments, 38-kDa hCTGF produced by insect cells following infection with recombinant baculovirus was purified by heparin-Sepharose chromatography, yielding a preparation that was >95% pure as assessed by Coomassie staining of SDS-PAGE gels [16]. Metabolically labeled native 38-kDa mCTGF, produced by NIH 3T3 cells, has been shown to be eluted from heparin-agarose beads by 0.4 M NaCl [5]. Recently 1 mg of highly purified recombinant 38-kDa mCTGF was purified from 500 ml of serum-free conditioned medium from recombinant baculovirus-infected insect cells using Sepharose S cation exchange chromatography [5]. Since heparin affinity columns and S ion exchange columns both contain cationic methyl sulfonate groups, it is possible that similar mechanisms are responsible for the binding of CTGF to each type of matrix.

B. Semiquantitative Assessment of CTGF Levels by Heparin Affinity Chromatography

Peaks of growth factor activity that are eluted from heparin columns have been previously used to assess the relative levels of individual HBGFs in various samples. For example, the levels of bioactive aFGF and bFGF, eluting from heparin affinity columns by 1.0 and 1.5 M NaCl, respectively, have been compared in postnatal rat brain on days 10 and 40 [42] and in lysates of cultured smooth muscle cells or endothelial cells [43]. Similarly, levels of PDGF and HB-EGF in, respectively, the 0.5 M NaCl and 1 M NaCl eluates from heparin-Sepharose columns were compared in conditioned medium from mononuclear cells that had been placed in culture for 1–2 days or 7–11 days [34]. For CTGF, this type of semiquantitative approach suggested that there is approximately fivefold more bioactive CTGF in uterine fluids from day 11 pregnant pigs than day 11 nonpregnant pigs. These initial findings suggest either that the embryo contributes to the pool of soluble CTGF in the uterine lumen or that there is greater uterine synthesis and/or release of CTGF during pregnancy.

C. Heparin Affinity Mechanisms of CTGF

While our current knowledge of CTGF–heparin interactions is sparse, we and others have shown that heparin is able to modulate CTGF mitogenic activity [15,16]. Although analysis of the C-terminal 103 residues of CTGF revealed that 10 kDa has a net basic charge (pI 8.3), this property alone is unlikely to account

for the degree of heparin binding observed since 10-kDa CTGF has a lower isoelectric point than PDGF (pI 9.6) yet requires a higher salt concentration than PDGF for elution from heparin (0.8 M NaCl versus 0.5 M NaCl). As we have previously reported, residues 250–255 resemble a heparin-binding consensus sequence and there is a very high proportion (50%) of basic amino acids (K, R) in the 17-residue region CTGF[251–267] [15]. Evidence that the N terminus of 10-kDa CTGF may be involved in heparin binding is illustrated by (1) the requirement for 0.7 M NaCl to elute the peptide CTGF[247–260] from a TSK heparin column, which, by comparison to PDGF, is a higher salt concentration than would be predicted from its pI alone; (2) the observation that CTGF[247–260] binds [^{3}H]heparin more strongly than peptides that flank this sequence [15]; and (3) the finding that a form of 10-kDa CTGF that commences at Glu^{248} exhibits greater heparin binding than the form described here, which commenced at Glu^{247} (and thus differs by the presence of a single acidic residue at its N terminus) [15]. While these data suggest that residues 247–260 are involved in heparin binding, analysis of [^{3}H]heparin binding by a panel of peptides that spanned the C-terminal 103 residues of CTGF suggested that additional domains, including residues 305–328, may also be involved in the interaction between 10-kDa CTGF and heparin [15]. While it has been proposed that residues 206–214 of CTGF resemble a binding motif for sulfated glycoconjugates [26], the involvement, if any, of this domain in mediating interactions between larger forms of CTGF (e.g., the full-length 38-kDa CTGF protein) and heparin has yet to be clarified.

D. Conclusions

Heparin affinity chromatography has played a key step in the isolation of native CTGF from uterine secretions and recombinant CTGF from baculovirus expression systems. While the interaction of CTGF with heparin has been exploited for the purification of 10-kDa and 38-kDa forms of CTGF, this property appears to be the result of the presence of specific heparin binding motifs within the CTGF molecule and may have physiological consequences in that heparin is a regulator of CTGF biological activity. Future studies will undoubtedly focus on additional structural and functional aspects of heparin binding by CTGF, including the possible role that cell surface heparan sulfate proteoglycans play in regulating the bioavailability of CTGF and its binding and activation of cell surface receptors.

ACKNOWLEDGMENTS

I am grateful to Christy Steffen and Greg Kim for excellent technical help, Bill Pope for providing timed cyclic and pregnant pigs, John Lowbridge for protein

sequencing, and Brad Baker for peptide synthesis. This work was supported by NIH Grant HD30334 awarded to D.R.B.

REFERENCES

1. Bradham DM, Igarashi A, Potter RL, Grotendorst GR. Connective tissue growth factor: a cysteine-rich mitogen secreted by human vascular endothelial cells is related to the SRC-induced immediate early gene product CEF-10. J Cell Biol 1991; 114:1285–1294.
2. Harding PA, Surveyor GA, Brigstock DR. Characterization of pig connective tissue growth factor (CTGF) cDNA, mRNA and protein from uterine tissue. DNA Sequence 1998;8:385–390.
3. Brunner A, Chinn J, Neubauer M, Purchio AF. Identification of a gene family regulated by transforming growth factor-β. DNA Cell Biol 1991;10:293–300.
4. Ryseck R-P, Macdonald-Bravo H, Mattei M-G, Bravo R. Structure, mapping and expression of fisp-12, a growth-factor-inducible gene encoding a secreted cysteine-rich protein. Cell Growth Differ 1991;2:225–233.
5. Kireeva ML, Latinic BV, Kolesnikova TV, Chen C-C, Yang GP, Abler AS, Lau LF. Cyr61 and Fisp12 are both ECM-associated signalling molecules: activities, metabolism, and localization during development. Exp Cell Res 1997;233:63–77.
6. Steffen CL, Ball-Mirth DK, Harding PA, Bhattacharyya N, Pillai S, Brigstock DR. Characterization of cell-associated and soluble forms of connective tissue growth factor (CTGF) produced by fibroblast cells in vitro. Growth Factors 1998;15:199–213.
7. Frazier KS, Grotendorst GR. Expression of connective tissue growth factor mRNA in the fibrous stroma of mammary tumors. Int J Biochem Cell Biol 1997;29:153–161.
8. Igarashi A, Nashiro K, Kikuchi K, Sato S, Ihn H, Grotendorst GR, Takehara K. Significant correlation between connective tissue growth factor gene expression and skin sclerosis in tissue sections from patients with systemic sclerosis. J Invest Dermatol 1995;105:280–284.
9. Igarashi A, Nashiro K, Kikuchi K, Sato S, Ihn H, Fujimoto M, Grotendorst GR, Takehara K. Connective tissue growth factor gene expression in tissue sections from localized scleroderma, keloid, and other fibrotic skin disorders. J Invest Dermatol 1996;106:729–733.
10. Oemar BS, Werner A., Garnier J-M, Do, D-D, Godoy N, Nauck M, Marz W, Rupp J, Pech M, Luscher TF. Human connective tissue growth factor is expressed in advanced atherosclerotic lesions. Circulation 1997;95:831–839.
11. Shinozaki M, Kawara S, Hayashi N, Kakinuma T, Igarashi A, Takehara K. Induction of subcutaneous tissue fibrosis in newborn mice by transforming growth factor β—simultaneous application with basic fibroblast growth factor casues persistent fibrosis. Biochem Biophys Res Commun 1997;237:292–296.
12. Igarashi A, Okochi H, Bradham DM, Grotendorst GR. Regulation of connective tissue growth factor gene expression in human skin fibroblasts and during wound repair. Mol Biol Cell 1993;4:637–645.
13. Hammes MS, Lieske JC, Pawar S, Spargo BH, Toback FG. Calcium oxalate mono-

hydrate crystals stimulate gene expression in renal epithelial cells. Kidney Int 1995; 48:501–509.
14. Pawar S, Kartha S, Toback FG. Differential gene expression in migrating renal epithelial cells after wounding. J Cell Physiol 1995;165:556–565.
15. Brigstock DR, Steffen CL, Kim GY, Vegunta RK, Diehl JR, Harding PA. Purification and characterization of novel heparin-binding growth factors in uterine secretory fluids: identification as heparin-regulated 10,000-M_r, forms of connective tissue growth factor. J Biol Chem 1997;272:20275–20282.
16. Frazier K, Williams S, Kothapalli D, Klapper H, Grotendorst GR. Stimulation of fibroblast cell growth, matrix production, and granulation tissue formation by connective tissue growth factor. J Invest Dermatol 1996;107:404–411.
17. Anderson LL. Growth, protein content, and distribution of early pig embryos. Anat Rec 1978;190:143–154.
18. Geisert RD, Brookbank JW, Roberts RM, Bazer FW. Establishment of pregnancy in the pig: II. Cellular remodelling of the porcine blastocyst during elongation on day 12 of pregnancy. Biol Reprod 1982;27:941–955.
19. Perry JS, Heap RB, Burton RD, Gadsby JE. Endocrinology of the blastocyst and its role in the establishment of pregnancy. J Reprod Fert Suppl 1976;25:85–104.
20. Perry JS, Rowlands IW. Early pregnancy in the pig. J Reprod Fertil 1962;4:175–188.
21. Wray W, Boulikas T, Wray V. Hancock R. Silver staining of proteins in polyacrylamide gels. Anal Biochem 1981;118:197–203.
22. Brigstock DR, Kim GY, Steffen CL, Liu A, Vegunta RK, Ismail NH. High molecular weight forms of epidermal growth factor in pig uterine secretions. J Reprod Fertil 1996;108:313–320.
23. Kim GY, Besner GE, Steffen CL, McCarthy DW, Downing MT, Luquette MH, Abad MS, Brigstock DR. Purification of heparin-binding EGF-like growth factor from pig uterine luminal flushings and its production by endometrial tissues. Biol Reprod 1995;52:561–571.
24. Brigstock DR, Kim GY, Steffen CL. Pig uterine fluid contains the developmentally-regulated neurotrophic factor, pleiotrophin. J Endocrinol 1996;148:103–111.
25. Brigstock DR, Heap RB. Brown KD. Polypeptide growth factors in uterine tissues and secretions. J Reprod Fert 1989;85:747–758.
26. Bork P. The modular architecture of a new family of growth regulators related to connective tissue growth factor. FEBS Lett 1993;327:125–130.
27. O'Brien TP, Yang GP, Sanders L, Lau LF. Expression of cyr61, a growth factor-inducible immediate early gene. Mol Cell Biol 1990;10:3569–3577.
28. Jay P, Berge-Lefranc JL, Marsollier C, Mejean C, Taviaux S, Berta P. The human growth factor-inducible immediate early gene, *CYR61*, maps to chromosome 1p. Oncogene 1997;14:1753–1757.
29. Simmons DL, Levy DB, Yannoni Y, Erickson RL. Identification of a phorbol ester-repressive v-src-inducible gene. Proc Natl Acad Sci USA 1989;86:1178–1182.
30. Joliot V, Martinerie C, Dambrine G, Plassiart G, Brisac M, Crochet J, Perbal B. Proviral rearrangements and overexpression of a new cellular gene (nov) in myeloblastosis-associated virus type 1-induced nephroblastomas. Mol Cell Biol 1992;12: 10–21.
31. Martinerie C, Huff V, Joubert I, Badzioch M, Saunders G, Strong L, Perbal B. Struc-

tural analysis of the human nov proto-oncogene and expression in Wilms tumors. Oncogene 1994;9:2279–2732.
32. Ying Z, Ling ML. Isolation and characterization of *xnov*, a *Xenopus laevis* ortholog of the chicken *nov* gene. Gene 1997;171:243–248.
33. Shing Y, Folkman J, Butterfield C, Murray J, Klagsbrun M. Heparin affinity: purification of a tumor-derived capillary endothelial cell growth factor. Science 1984;233: 1296–1299.
34. Besner GE, Higashiyama S, Klagsbrun M. Isolation and characterization of a macrophage-derived heparin-binding growth factor. Cell Regu 1990;1:811–819.
35. Lobb RR, Harper JW, Fett JW. Purification of heparin-binding growth factors. Anal Biochem 1986;154:1–4.
36. Rosenthall RA, Megyesi JF, Henzel WJ, Ferrara N, Folkman J. Conditioned medium from mouse sarcoma 180 cells contains vascular endothelial growth factor. Growth Factors 1990;4:53–59.
37. Cook PW, Mattox PA, Keeble WW, Pittelkow MR, Plowman GD, Shoyab M, Adelman JP, Shipley GD. A heparin sulfate-regulated human keratinocyte autocrine factor is similar or identical to amphiregulin. Mol Cell Biol 1991;11:2547–2557.
38. Shoyab M, Plowman GD. Purification of amphiregulin from serum-free conditioned medium of TPA-treated cell lines. Meth Enzymol 1991;198:213–221.
39. Klagsbrun M. The fibroblast growth factor family: Structural and biological properties. Prog Growth Factor Res 1989;1:207–235.
40. Higashiyama S, Lau K, Besner G, Abraham JA, Klagsbrun M. Structure of heparin-binding EGF-like growth factor: multiple forms, primary structure and glycosylation of the mature protein. J Biol Chem 1992;267:6205–6212.
41. Milner PG, Li Y-S, Hoffman RM, Kodner CM, Siegel NR, Deuel TF. A novel 17 kDa heparin-binding growth factor (HBGF-8) in bovine uterus: Purification and N-terminal amino acid sequence. Biochem Biophys Res Commun 1989;165:1096–1103.
42. Caday CG, Klagsbrun M, Fanning PJ, Mirzabegian A, Finkelstein SP. Fibroblast growth factor (FGF) levels in the developing brain. Dev Brain Res 1990;52:241–246.
43. Weich HA, Iberg N, Klagsbrun M, Folkman J. Expression of acidic and basic fibroblast growth factors in human and bovine vascular smooth muscle cells. Growth Factors 1990;2:313–320.

14

Slalom Chromatography

A New Hydrodynamic-Based Chromatographic Mode Applicable to Size-Dependent Separation and Physicochemical Analysis of Large DNA Molecules

Jun Hirabayashi and Ken-ichi Kasai
Teikyo University, Sagamiko, Kanagawa, Japan

I. INTRODUCTION

Chromatography is one of the best research tools for the biosciences. It makes it possible to analyze biomolecules and to obtain the most valuable and important information on them, such as their chemical, physicochemical, and biochemical properties. At the same time, it affords complete separation of components. Therefore, the more sophisticated the chromatographic mode, the higher the quality of the information obtained. For example, affinity chromatography reveals the nature of the active site of enzymes; gel permeation chromatography discloses the size of biomolecules. Moreover, development of high-performance liquid chromatography (HPLC) has greatly enhanced the utility of chromatography by improving speed, sensitivity, reproducibility, and accuracy.

Use of chromatography as an intelligent tool has not been adequately appreciated in the field of nucleic acid research because of several inherent difficulties [1]. Though size-dependent separation of large polynucleotides such as DNA fragments must be the first step of not only the majority of basic analyses but also

a variety of applications, the chromatographic method has rarely been applied for such a purpose, in contrast to the protein research field where gel permeation chromatography has always been indispensable. This is mainly because gel permeation chromatography is extremely inefficient for the separation of DNA fragments in comparison with agarose gel electrophoresis, which has been much more popular and efficient, as described below.

First, in gel permeation chromatography, separation of component molecules must take place within a relatively small volume, i.e., the elution volume of a salt subtracted by the flow-through volume. This corresponds to the volume of the liquid retained in the stationary phase, in other words, the volume of the liquid retained in the pores of the packing particles. It is difficult to expect high resolution of many components in such a small volume. Second, target macromolecules must diffuse into the pores of packing particles and an equilibrium state must be reached between the moving phase and the stationary phase. The time required to reach an equilibrium state becomes considerably long for large molecules due to their small diffusion constant, and this also reduces the resolution. Third, most DNA fragments are usually too large to be applied to conventional gel permeation media. Even a small DNA fragment has a Stokes radius considerably larger than that of proteins of similar molecular weight. Fourth, the possible risk of cleavage of long DNA molecules due to shear force has also made researchers reluctant to use chromatographic separation. However, in spite of these difficulties, to make full use of chromatography in the field of nucleic acids would seem to be meaningful. Chromatography is often complementary to electrophoresis in terms of both preparative and analytical purposes, and sometimes it can provide unique results. In the field of nucleic acid research, analytical scale chromatography serves both analytical and preparative purposes because if only a trace amount of a DNA or RNA fragment is separated it can be easily multiplied by polymerase chain reaction (PCR) and recombinant DNA techniques.

We recently discovered a new chromatographic mode that enables the separation of DNA fragments according to their size [2,3]. This method, firstly discovered by chance, requires only an ordinary HPLC system and a commercially available column packed with small, rigid, spherical beads, such as those used for high-performance gel permeation. Strikingly, the order of elution was found to be opposite to that expected for gel permeation chromatography, i.e., larger fragments were eluted later than smaller ones. It is not surprising that longer DNA fragments would be retarded more if they interacted with the column packing. The amazing thing, though, is that no evidence could be found of interaction between them. Moreover, separation patterns significantly depended on the flow rate and the size of the packing particles, but not on their pore size or chemical nature. DNA fragments were retarded without any attractive force provided by the column packings. Therefore, it is a quite unusual phenomenon and cannot

be explained by any mechanism based on the equilibrium between moving phase and stationary phase. Therefore, we proposed a possible mechanism based on a hydrodynamic phenomenon.

Here we describe only the essential point of the proposed mechanism (Fig. 1) and its details will be discussed later. When we apply a solution of DNA fragments to a column for HPLC, DNA molecules in the moving phase are stretched by laminar flow and forced to pass through the narrow and tortuous channels created by the gap between tightly packed spherical beads; and thus, they should turn very quickly and frequently. This should be more difficult for longer DNA fragments in comparison with shorter ones. Therefore, the smallest fragment is eluted first, the longest one is eluted last, and the others are eluted in the order of size from smaller to larger. We named this new separation mode "slalom chromatography" because the proposed model reminds us of a person on skis going down a slope and turning quickly around flags [3–5]. Similar observations were made independently by Boyes et al. [6]. In the following sections we

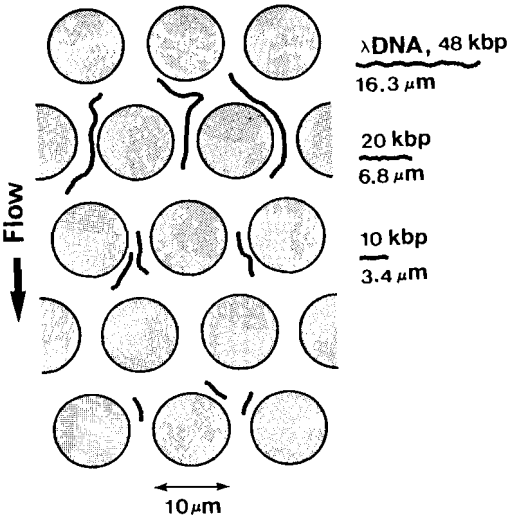

Figure 1 Illustration of DNA separation in slalom chromatography. When applied to a column for HPLC, DNA fragments are stretched due to the occurrence of laminar flow. They should turn rapidly and frequently in passing through the narrow and tortuous openings between closely packed spherical particles. The longer the fragments, the more difficulty for turning around the particles. If the DNA molecules are stretched to the maximum extent, their length will be comparable to the diameter of the packing particles. The distance between particles is exaggerated.

discuss in detail various unusual phenomena that led us to the above hypothetical mechanism.

II. UNIQUE CHARACTERISTICS OF SLALOM CHROMATOGRAPHY

A. Particle Size of Column Packing Has a Great Influence on Separation

Figure 2 shows one of the most important characteristics of slalom chromatography [2,3]. Eight DNA fragments ranging from 10 to 38 kbp could be separated. In these cases, separation media for high-performance gel permeation (Asahipak series, synthetic polymer-based media manufactured by Asahi Chemical Industry,

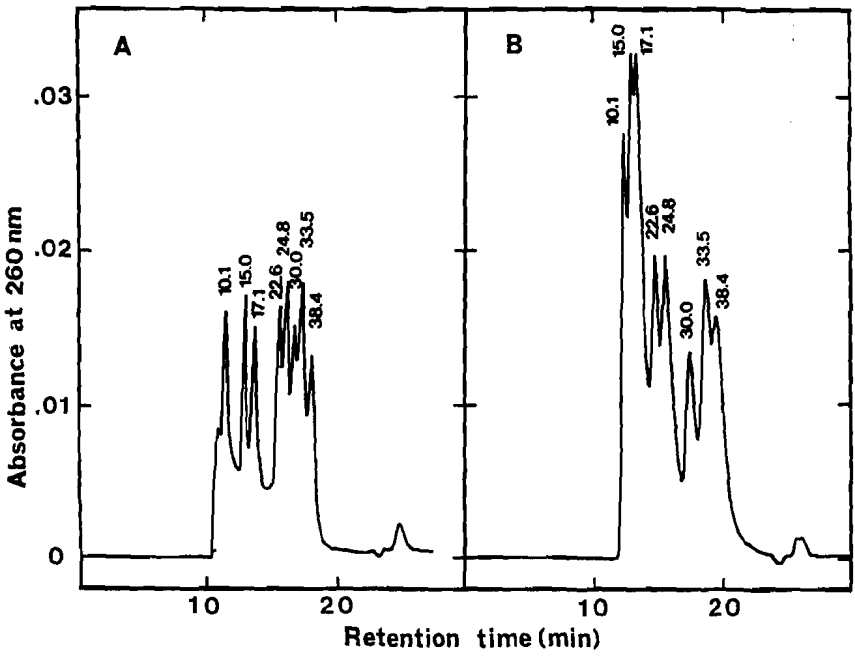

Figure 2 Chromatogram of restriction fragments of λDNA on Asahipak GFT-510 (5-μm particle; A) and GS-510 (9-μm particles; B). Column size were the same (7.6 × 250 μm). A set of DNA fragments was dissolved in 10 mM sodium phosphate buffer, pH 7.0, containing 1 mM EDTA, and applied to the column, and DNA fragments were eluted with the same buffer at room temperature. Flow rate was 0.3 ml/min. Fragment sizes (kbp) are indicated in the figure.

Kawasaki, Japan) were used. Their exclusion limits (for protein, M_r 5×10^5) were the same, but the particle sizes were different. One column was packed with 5-μm particles (Fig. 2a, Asahipak GFT-510) and the other with 9-μm particles (Fig. 2b, Asahipak GS-510). Both columns separated eight fragments in the order of smaller to larger. This order was completely opposite to that expected for gel permeation chromatography. Moreover, though the pore sizes were the same, the column packed with 5-μm particles was superior for the separation of smaller fragments (less then 20 kbp), whereas larger fragments (more than 20 kbp) were better separated by the column packed with 9-μm particles. It is evident that separation occurred by a mechanism other than the gel permeation mode because the order of elution was opposite and the size range depended not on the pore size but on the particle size.

Figure 3 shows the separation pattern of *Hin*dIII–digested λ phage DNA (λ/*Hin*dIII) on columns packed with 5-μm and 9-μm particles. Again, the 5-μm packing gave a better resolution for fragments of less than 10 kbp. Such experiments were carried out more systematically using four columns (average particle diameters of 5.0, 9.0, 13.1, and 19.1 μm, Asahipak GS-310 series), and the results are summarized in Fig. 4 [4]. The relative retention time, defined as the ratio of

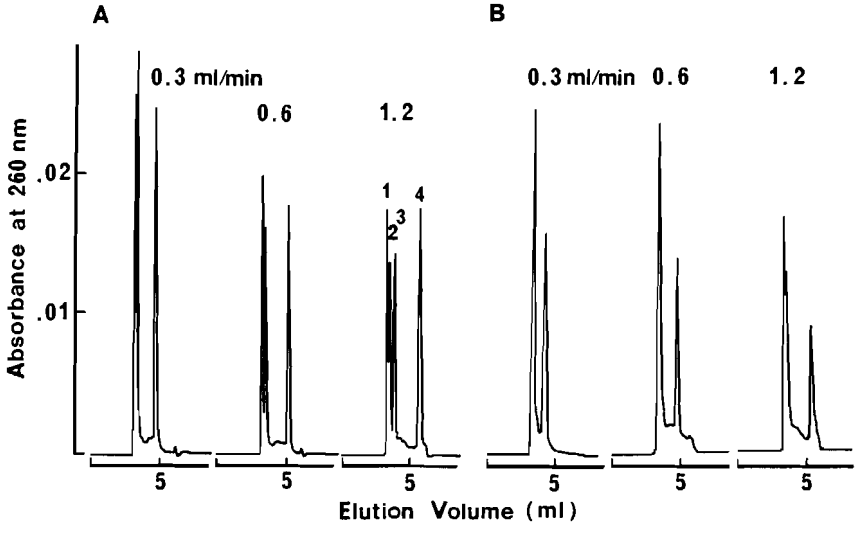

Figure 3 Chromatography of λ/*Hin*dIII digests on Asahipak GS-310 columns packed with 5-μm (A) and 9-μm packings (B). DNA fragments were eluted at a flow rate of 0.3 ml/min. Fragments contained in peak 1 are 0.13, 2.03, and 4.36 kbp. Peak 2, 3, and 4 correspond to 6.56, 9.42, and 23.13 kbp, respectively.

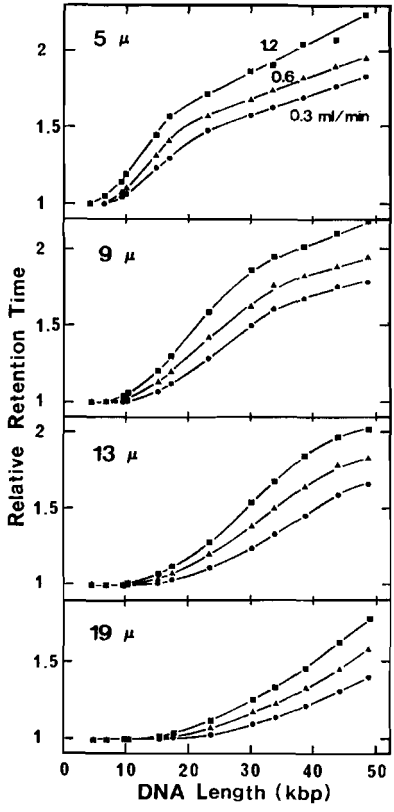

Figure 4 Dependence of relative retention times of DNA fragments on their size. Packings of different particle size (5, 9, 13, and 19 μm) were used, and different flow rates were applied. Relative retention time was plotted as a function of DNA size (kbp). Flow rates were 0.3 (●), 0.6 (▲), and 1.2 ml/min (■).

the retention time of a particular fragment to that corresponding to flow-through fraction, was plotted against the number of base pairs of DNA fragments. Apparently, the four columns have different ranges of resolution. For example, if we pay attention to the curve at a flow rate of 0.6 ml/min (middle curves in Fig. 3a–d), the 5-, 9-, 13-, and 19-μm columns could separate DNA fragments larger than 7, 9, 13, and 17 kbp, respectively, from the fragments that appeared at the flow-through volume (relative retention time = 1.0). In addition, smaller packings showed better resolution for smaller DNA fragments, whereas larger ones were better for larger fragments. High-resolution zones could be assigned as 9–

17, 15–30, 23–40, and 35–50 kbp for the 5-, 9-, 13-, and 19-μm packings, respectively.

B. Higher Flow Rates are More Advantageous for Separation

The results shown in Fig. 4 also revealed that the extent of retardation of DNA fragments was dependent on the flow rate. It is unlikely for gel permeation chromatography that the flow rate would affect the size range of fractionation and that faster flow rates are advantageous for resolution. A lower flow rate is usually preferable to obtain good resolution, as it ensures the equilibrium between the stationary and mobile phases. In slalom chromatography, however, at the lowest flow rate applied (0.03 ml/min, corresponding to a linear flow rate of 0.067 cm/min), all DNA fragments of different sizes were eluted together in the flow-through fraction; no size-dependent separation occurred. When the flow rate was increased, longer DNA fragments began to slow down, and the extent of retardation became greater as the flow rate was increased further. This means that better resolution is attained at higher flow rates and that the range of separable fragment size also increased. Such unusual flow rate dependency also suggested that the mechanism is completely different from an equilibrium phenomenon. At a very low flow rate, all DNA fragments would take a random coil form, which is more compact and would have little difference in the Stokes radius, and therefore they would be eluted together in the flow-through fraction. On the other hand, when a higher flow rate is applied, DNA molecules would be stretched and the slalom effect would thus appear.

C. Pore Size and Chemical Nature of Packings Have Little Influence on Separation

Although the phenomenon of slalom chromatography was first observed with packings for gel permeation, their pore size was found to have no relation to the resolution [2–4]. When columns packed with beads of the same particle size (9 μm) but differing in pore size (e.g., Asahipak GS-220, 310, and 510: exclusion limit for proteins, M_r 3×10^3, 4×10^4, and 3×10^5, respectively) were compared, almost the same relative retention time was obtained for each DNA fragment. This indicates that the DNA fragments did not permeate the pores.

The chemical nature of column packing was also proved to have no influence on separation. Comparative experiments carried out using silica-based particles (TSK G2000SW and TSK G3000SW, 10-μm diameter, manufactured by Toso, Tokyo, Japan) gave essentially the same results as those obtained with synthetic polymer–based particles [3]. Although they have different exclusion

limits (for dextran: G2000SW, M_r 1×10^5; G3000SW, M_r 5×10^5), both separation patterns and flow rate dependency were almost the same, and also very similar to those obtained for the column packed with 9-μm particles.

D. Separation Does Not Depend on Interaction Between DNA Fragments and Packing Particles

In slalom chromatography, size-dependent separation of DNA is not due to electrostatic or hydrophobic interaction with the packing particles. Retention time of DNA fragments was not affected by the addition of NaCl up to 0.5 M or 20% (v/v) acetonitrile [5]. Moreover, separation by the slalom chromatography mode was achieved even with cation exchange columns, which should strongly repel polynucleotides. Two cation exchange columns bearing sulfopropyl groups, TSK SP-5PW and TSK SP-NPR (a nonporous polymer with a particle size as small as 2.5 μm), were examined. SP-5PW gave a chromatogram similar to that obtained with Asahipak of corresponding particle size, i.e., a high-resolution zone was found in the range 15–30 kbp [5]. SP-NPR seemed to resemble GS-310 packed with 5-μm particles to some degree. These results indicate again the absence of interaction between the chromatographic media and DNA fragments, and suggest that the separation was achieved by a hydrodynamic phenomenon.

E. Temperature Affects the Separation

Temperature has a significant effect on the slalom mode separation [5]. The relative retention time of DNA fragments increased significantly when the temperature was lowered. This suggests that the viscosity of the eluent has an important effect, probably because it determines the steepness of the velocity gradient of laminar flow in the narrow channels in the column.

F. Separation Depends on Physical Length of DNA Fragments and Not on Their Molecular Weight

The experimental results described above were obtained for linear DNA molecules. The behavior of circular DNA molecules was also examined. When the circular replicative form (double strand) of M13 phase DNA (7 kbp) and its linearized form were compared, the former was eluted faster than the latter. This showed that even DNA molecules of the same size can be distinguished, if their conformations are different. Longer circular DNAs were also analyzed. Even at the highest flow rate examined, 42-kbp circular DNA was eluted with a similar retention time to that of 20-kbp linear DNA. This result is quite reasonable because the length of circular DNAs in a maximally stretched state will be equal to that of the linear DNA of half size. Therefore, slalom chromatography sepa-

rates DNA fragments according to their physical length and not to their molecular weight.

III. MECHANISM OF SLALOM CHROMATOGRAPHY

A. Characteristics of Slalom Chromatography

From the observations described above, the characteristics of slalom chromatography can be summarized as follows:

1. DNA fragments do not interact with the matrix of the packing material because synthetic polymer–based and silica-based packings gave essentially similar separation patterns, and addition of a salt or organic solvent had little effect. Separation has no relation to the presence of pores in the packing particles. Even nonporous particles and anion exchange particles, which should repel DNA molecules, showed the slalom mode separation.
2. Particle size of packings greatly affects separation. The size range of DNA fragments being separable was found to depend largely on the particle size. Smaller particles could resolve smaller DNA fragments better, whereas larger particles could resolve larger DNA fragments better.
3. Flow rate has a significant effect on the separation range. At a faster flow rate, the relative retention time of DNA fragments increased and resolution became better.
4. Temperature has a significant effect. At lower temperature, DNA fragments were more retarded. This suggests that separation depends on the viscosity of moving phase solvent.

B. A Possible Mechanism of Slalom Chromatography

When a solution of DNA is applied to a column for HPLC, DNA fragments are stretched because of the laminar flow generated by the solvent passing through the narrow channels created by gaps between packing particles. For example, the end-to-end distance of the maximally stretched 23-kbp λ/*Hin*dIII fragment is as long as 7.9 μm, which is comparable to the diameter of the packing particle used (3–10 μm).

Though a small double-stranded DNA molecule (e.g., smaller than 20 bp) has the structure of a rigid rod, large double-stranded DNA fragments (larger than 1 kbp) has a kink at every ~150 bp and consequently forms a random coil, which is entropically the most favorable shape. For example, bacteriophage T4 DNA, 166 kbp (extended length, 50 μm), was found to form a random coil with

a diameter of ~2 μm in its most contracted state. The random coil is very flexible, and its shape changes without a break between the contracted and slightly extended forms by an external force provided by Brownian motion of water molecules. The speed of the intramolecular movement (expansion and contraction) can be as fast as ~15 μm/s, though the migration velocity of the whole molecule (center of gravity) is only 1 μm/s [7]. However, in the presence of laminar flow, the DNA molecule is stretched. As the flow rate increases, its shape changes gradually from an ellipsoid to a solenoid one, then to a thick filament one, and finally to a thin filament one.

DNA molecules are too large to permeate into the pores of packing particles and can only pass through the narrow channels between particles. Since these channels are extremely tortuous, when the moving phase is forced to move, DNA fragments have to turn very frequently. It will be more difficult for longer DNA strands to turn quickly, and this will result in retardation of longer DNA strands. A simple calculation shows that DNA fragments turn about 36,000 times if applied to a column of 300-mm length packed with 10-μm packing particles. Under these conditions, a 23-kbp fragment turns as frequently as 70 times per second, when a flow rate of 0.6 ml/min is applied. If we use smaller packing particles, the channels become narrower and more tortuous; and also, the velocity gradient of laminar flow becomes steeper, which makes shear force stronger. At a flow rate of 1.2 ml/min, in a column of 5-μm particles, the fragment has to turn 72,000 times at a frequency of 280 times per second. On each turn, DNA strands would be exposed to a significant frictional force against the solvent, and this force would increase with the increase in DNA length, so that larger DNA molecules are retarded.

As to the effect of flow rate, at a flow rate of close to zero all DNA fragments are in a random coil state; as none of them are retarded, they are eluted together in the flow-through fraction. Application of a faster flow rate has at least dual effects. First, it increases the frequency of turn. Second, it increases the velocity gradient of the laminar flow. This generates stronger shear force and consequently raises average end-to-end distance of DNA strands, and resulting in stronger frictional force between the DNA strands and the solvent (Fig. 5). These considerations may explain why the use of smaller packing and a higher flow rate is advantageous for the separation of smaller molecules.

This new chromatographic mode is attributed to the combination of several hydrodynamic phenomena, i.e., stretch by laminar flow of DNA fragments that otherwise assume a random coil state because of entropic force; frequent turning of extremely long molecules along the curved surface of packing particles; and an extremely complicated flow pattern due to the channels made between packing particles, which may cause continuous perturbation of the three-dimensional shape of DNA. Although the explanation presented here is undoubtedly oversimplified, it should be a useful model in elucidating the precise mechanism of slalom chromatography.

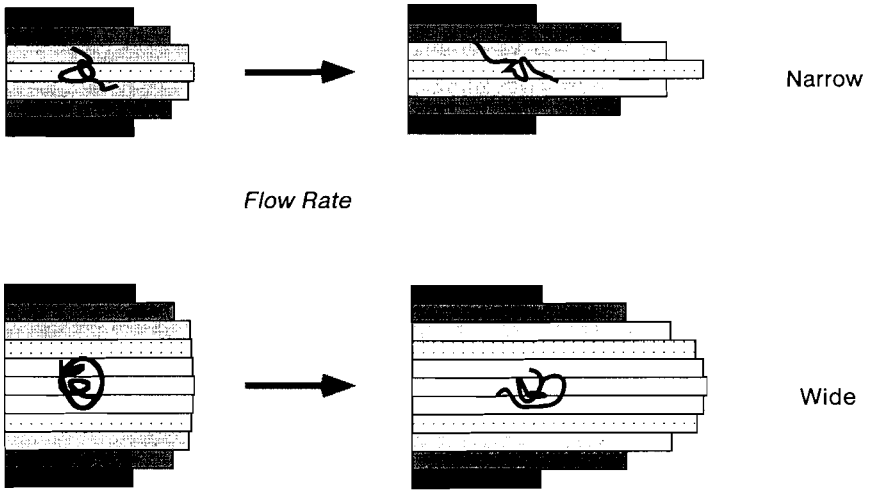

Figure 5 An explanation of the effect of the flow rate and particle size. For simplicity, the channel between closely packed particles is considered as a capillary. As the flow rate is increased, velocity gradient of the moving phase is generated due to laminar flow. In a narrow capillary, the velocity gradient is steep, and then a DNA molecule is subjected to a strong shear force and stretched to a greater extent. As a result, the DNA molecule is retarded greatly due to the slalom effect. On the contrary, in a wide capillary, no significant velocity gradient is generated especially in the central part of the cross-section. Therefore, the DNA molecule is not subjected to a strong shear force, stays as a more compact form, and goes through the capillary without significant retardation.

A mode of size-dependent separation of submicrometer to micrometer order colloid particles, named hydrodynamic chromatography, was reported [8]. It was performed by using a column packed with nonfunctionalized, nonporous particles of around 15–20 μm in diameter. In the column, large colloid particles are excluded from the interface, where the fluid velocity is lowest. The larger the particle, the higher its mean velocity. Consequently, larger particles are eluted faster than smaller ones, as in gel permeation chromatography. Therefore, this mode is different from slalom chromatography.

IV. POTENTIAL APPLICATION TO STUDIES ON PHYSICOCHEMICAL PROPERTIES OF DNA

The utility of this new procedure is not limited to size analysis. This method will undoubtedly provide us valuable information on DNA molecules almost equivalent to those gel filtration has provided on the properties of proteins. Moreover,

this hydrodynamics-based method has potential to analyze not only the sizes of DNA molecules but also physicochemical properties, such as conformation, topology, and rigidity. Preliminary experiments showed that it can distinguish the difference in the topology of circular DNA molecules because different flow rate dependencies were observed for supercoiled, relaxed, and single-stranded DNAs. These results might be attributed to their rigidity or special three-dimensional structure. Therefore, it will be possible to separate and analyze DNA molecules according to their physicochemical properties. If the efficiency of slalom chromatography becomes much higher, isolation of topoisomers of supercoiled DNAs according to the extent of coiling might become possible.

V. MIXED-MODE SLALOM CHROMATOGRAPHY

Although the uniqueness of slalom chromatography is its independency from interaction between solute molecules and packing particles, it might be possible to add weak interaction with the matrix to improve chromatographic performance. This appeared to be the case because column packings having weak hydrophobic nature proved to be effective in improving resolution of DNA fragments smaller than 5 kbp, which had been difficult to separate by pure slalom chromatography [9]. Figure 6 shows separation patterns of λ/*Hin*dIII fragments obtained by use of a column packed with a silica-based media derivatized with

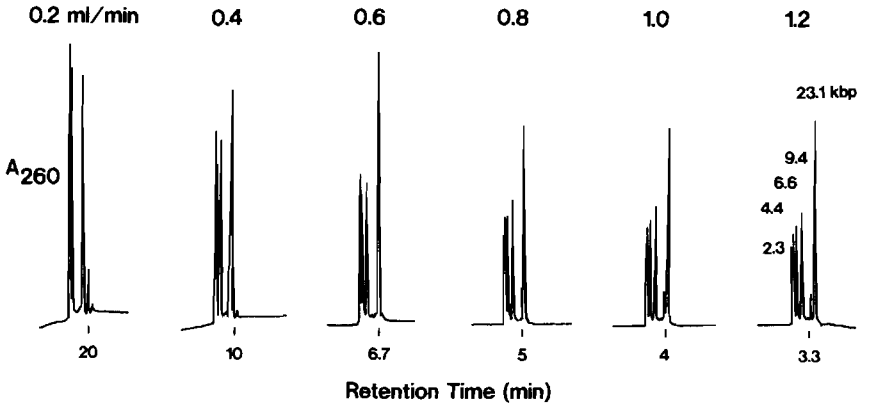

Figure 6 Separation profiles of λ/*Hin*dIII fragments on a Phe-Hypersil-3 column. Flow rates are indicated in the figure. Acetonitrile (20%) was added in the buffer to raise recovery of DNA fragments. At the flow rate of 1.2 ml/min, the best resolution was attained, and a 4.4-kbp fragment was separated from a 2.3-kbp fragment.

phenyl group (Phe-Hypersil-3, 3-μm particles, manufactured by Shandon, Cheshire, UK). A fragment as small as 4.4 kbp was separated from the flow-through fraction at the flow rate of 1.2 ml/min; this had not been achieved previously. It was found that the addition of acetonitrile to the moving phase was necessary to raise the recovery of DNA fragments. It seems necessary to reduce hydrophobic interaction to some extent. If the hydrophobic interaction is too strong, DNA fragments would be adsorbed, and the slalom effect would disappear. In the presence of 20% acetonitrile, the best resolution was obtained. Other weak hydrophobic media (e.g., Capcell-Pak C1, Capcell-Pak Phe, manufactured by Shiseido, Tokyo, Japan) were also found to be effective in separating small fragments, although in the case of Capcell-Pak C1 and Capcell-Pak Phe the addition of NaCl was necessary to attain good resolution. For these media, reinforcement of hydrophobic interaction seems necessary. Although chromatographic conditions have to be appropriately set up for individual packings, several columns developed for reversed-phase chromatography were found to be useful for mixed-mode slalom chromatography. It is advantageous from a practical viewpoint because a number of packing materials have been industrially developed for reversed-phase chromatography, some of which show excellent physicochemical performance.

VI. PRESENT AND FUTURE SLALOM CHROMATOGRAPHY

A. Advantages and Limitations of Slalom Chromatography

At present, slalom chromatography is the only chromatographic method applicable to the size-dependent separation of large DNA molecules. Its uniqueness is the hydrodynamics-based mechanism and length-dependent separation. Column packing particles serve only for the construction of channels. The merits of slalom chromatography are as follows:

1. Both preparative and analytical applications are possible.
2. The experimental procedure is very simple, and results can be obtained rapidly. Only an ordinary HPLC apparatus and easily available HPLC columns are needed.
3. Only an isocratic elution program is needed. Therefore, a process for column washing or reequilibration is not necessary between runs.
4. Separation and recovery of DNA fragments can be completed in a much shorter period than in the case of gel electrophoresis. Recovered DNA fragments are free from undesirable contaminants originating from the agarose gel.
5. DNA can be detected without the use of harmful reagents, such as ethidium bromide.

6. This procedure can be used as an effective tool for physicochemical and hydrodynamic studies of DNA.

There are, of course, limitations that should be overcome in the future:

1. The range of separable size is rather narrow. Commercial columns available can be applicable only to 5–50 kbp DNA fragments.
2. The resolution efficiency is still inferior to that of gel electrophoresis.
3. Chromatography should be performed under relatively high flow rates, which might cause fragmentation of extremely large DNAs. However, DNA fragments of less than 50 kbp proved to be generally very stable under the conditions for most experiments (e.g., flow rate less than 1.2 ml/min), contrary to the expectations of most researchers handling DNA. Therefore, the use of slalom chromatography is strongly encouraged.

B. Comparison with Other Size-Separation Methods for DNA

Pulsed-field gel electrophoresis is widely used as a size separation procedure for extremely large DNAs [10,11]. This technique is based on the difference in the ability of DNA molecules to change direction of migration in response to a frequently changing electric field. Because larger DNA molecules take longer to reorient, size-dependent separation is achieved. This method has features in common with slalom chromatography: both are based on the ability of DNA molecules to adapt to a frequently changing environment (direction of electric field or flow) that depends on size. Although the size range of DNA separable by pulsed-field electrophoresis is much wider than that of slalom chromatography, the latter has a variety of merits (already pointed out), and thus the two methods are complementary. Capillary electrophoresis also seems to be very promising as a procedure for the size-dependent separation of nucleic acids. If the principles of slalom chromatography and capillary electrophoresis can be combined, a much more effective procedure could possibly be realized.

C. How To Make the Best Use of Slalom Chromatography

Slalom chromatography is very efficient and interesting from the viewpoints of both investigation and application. This principle will undoubtedly provide us with a valuable tool for nucleic acid research, just as the invention of gel permeation chromatography has contributed to the biological sciences, especially in the field of protein research. Although only applications to DNA have been reported so far, it should also be useful for RNA and other fibrous macromolecules such as proteoglycans. Possible applications include the following:

1. Size-dependent separation of DNA
2. Estimation of size of nucleic acids
3. Monitoring and analysis of size changes of nucleic acids
4. Separation of nucleic acids based on conformation or topology
5. Analysis of interaction of nucleic acids with other molecules, such as nucleic acid–binding proteins
6. Distinction of types of circular DNA, e.g., supercoiled, relaxed, and single-stranded
7. Studies of the physicochemical properties of nucleic acids, e.g., rigidity, elasticity, bendability, etc.
8. Hydrodynamic studies of nucleic acids

The combination of hard, spherical packings and the application of high flow rates led to the discovery of this hydrodynamics-based chromatography. It is very unlikely that slalom chromatography is the only technique that can be based on hydrodynamic principles. Likewise, other interesting and effective chromatographic modes applicable to a variety of macromolecules will probably be discovered if extensive studies are done by researchers in a variety of fields. Such research will contribute greatly not only to expanding the horizon of chromatographic science but to developing a number of effective and intelligent research procedures.

REFERENCES

1. Kasai K. Size-dependent chromatographic separation of nucleic acids. J Chromatogr 1993;618:203–221.
2. Hirabayashi J, Kasai K. Slalom chromatography. A new size-dependent separation method for DNA. Nucleic Acid Symp Ser 1988;20:67–68.
3. Hirabayashi J, Kasai K. Size-dependent, chromatographic separation of double-stranded DNA which is not based on gel permeation mode. Anal Biochem 1989; 178:336–341.
4. Hirabayashi J, Itoh N, Noguchi K, Kasai K. Slalom chromatography: size-dependent separation of DNA molecules by a hydrodynamic phenomenon. Biochemistry 1990; 29:9515–9521.
5. Hirabayashi J, Kasai K. Slalom chromatography. A size-dependent separation method for DNA molecule based on a hydrodynamic principle. In: Ngo TT, ed. Molecular Interactions in Bioseparations. New York: Plenum Press, 1993:69–87.
6. Boyes BE, Walker DG, McGeer PL. Separation of large DNA restriction fragments on a size-exclusion column by a nonideal mechanism. Anal Biochem 1988;170:127–134.
7. Yanagida M, Hiraoka Y, Katsura I. Dynamic behavior of DNA molecules in solution studied by fluorescence microscopy. Cold Spring Harbour Symp Quant Biol 1982; 47:177–187.

8. Small HJ. Hydrodynamic chromatography. Technique for size analysis of colloidal particles. Colloid Interface Sci 1974;48:147–161.
9. Hirabayashi J, Kasai K. Applied slalom chromatography. Improved DNA separation by the use of columns developed for reversed-phase chromatography. J Chromatogr 1996;722:135–142.
10. Schwarz DC, Cantor CR. Separation of yeast chromosome-sized DNA by pulse field gradient gel electrophoresis. Cell 1984;37:67–75.
11. Carle GF, Olson MVG. Separation of chromosomal DNA molecules from yeast by orthogonal-field-alteration gel electrophoresis. Nucleic Acids Res 1984;12:5647–5664.

15

Simultaneous Chromatographic Separation of Ceruloplasmin and Serum Amine Oxidase

Mircea-Alexandru Mateescu,[1] Xin-Tao Wang,[1,2] Olivia Befani,[2] Marie-Joseé Dumoulin,[1] and Bruno Mondovi[2]
[1] *Université du Québec à Montréal, Québec, Canada*
[2] *Rome University "La Sapienza," Rome, Italy*

I. INTRODUCTION

Ceruloplasmin (CP) is the multifunctional blue [1] copper–containing plasma protein (α_2-globulin), with an important role in copper transport [2]. Acting as an oxidase, ceruloplasmin (EC 1.16.3.1) is involved in the regulation of the level of several phenols and aromatic amines. Also known as ferroxidase I, CP promotes the oxidation of ferrous ions ($Fe^{2+} \rightarrow Fe^{3+}$), thus preventing the accumulation of highly toxic Fe^{2+} ion [3]. Ceruloplasmin is also a powerful plasma antioxidant and oxygen free radical (OFR) scavenger [4–7]; furthermore, ceruloplasmin is an antiinflammatory protein that acts as an acute phase serum reactant against the oxygen metabolites released by the macrophages [8].

In recent years it has also been shown that CP acts as a neuromodulator (depolarizes neuronal cell membrane by inhibiting K^+ channels [9]) and cardioprotector (with an antifibrillatory action on isolated hearts subjected to ischemia-reperfusion) [10]. The antiarrhythmic effects of CP appeared closely related to its molecular and conformational integrity [10].

Recently, CP was shown to be involved in angiogenesis, in relation to its

This chapter was adapted from X. T. Wang et al., Prep Biochem 1994; 24: 237–250.

function as copper carrier. There is a recently growing interest for genetic diseases characterized by a CP deficiency or by a defective loading of copper into CP. Wilson's, Menkes', Parkinson's, Alzheimer's, and, as recently found, hemosiderosis are diseases related to CP deficiency.

Despite the abundant literature linking CP to several pathological conditions, little research has been done on its possible therapeutic applications, probably because of its high susceptibility to proteolysis and instability, even during the purification steps. In fact, structural aspects of CP, mainly related to the molecular characteristics and the copper content, have been controversy (mostly due from its high susceptibility at proteolysis). Also controversial was its complex physiological role (antioxidant/prooxidant) related to the molecular integrity of the molecule, as recently reported [11].

The "blue copper" center of CP has a characteristic absorption band at 610 nm and is electronic paramagnetic resonance (EPR)–detectable. It is now accepted that CP contains six copper atoms per molecule and that CP structure consists of six domains [12]—surprisingly, in a configuration closed to that of clotting Factor VIII. Three copper atoms are aggregated in a cluster which is the blue copper center of ceruloplasmin. Two others form a diamagnetic pair. The last one is paramagnetic (EPR-detectable). An absorbancy ratio $A_{610\,nm}/A_{280\,nm} = 0.040$ was considered in the literature as characteristic for the homogeneous standard pure enzyme.

Previously reported was a new single-step chromatographic method for the fast ceruloplasmin purification [13], starting directly from plasma, which leads to a purified, electrophoretically homogeneous CP. The procedure is based on the highly selective retention of CP on the aminoethyl (AE)–agarose, a new chromatographic material (not commercially available), realized in our laboratories [13–15]. This single-step purification procedure described by Calabrese et al. [14] is very fast, requiring only plasma dilution (about 20 times), followed by AE-agarose chromatography and a final concentration of the purified CP. Despite the speed at the laboratory scale, for scaling-up purposes, handling of large volumes (dozens of liters) of diluted plasma is somewhat cumbersome. Furthermore, when large plasma volumes are used, some clotting phenomena can occur during the chromatographic step, producing a decrease in flow rate, difficulties in regeneration, and partial loss of the chromatographic material. At the same time, handling of large protein volumes for the final concentration is also cumbersome. These limitations can be completely overcome by the recently reported purification procedure [16], here described.

Bovine serum amine oxidase (SAO), also known as benzylamine oxidase belongs to the semicarbazide-sensitive amine oxidase (SSAO), is a copper enzyme (EC 1.4.3.6) catalyzing the oxidative deamination of various biogenic primary amines, with release of aldehydes, ammonia, and hydrogen peroxide. Considering the toxicity of aldehyde and H_2O_2, SAO was suggested as an antitumoral agent [17] with an important cytotoxicity-inducing activity [18]. Recent data

showed that SAO has a multifunctional role as regulator of polyamine level [19], as cardioprotective agent [20,21], and as modulator of ionic channel [22]. It was also shown that SAO substrate specificity is not limited only to small molecular biogenic amines such as spermine and spermidine, but is extended to polylysine and some peptides or proteins [23]. This suggested the hypothesis that SAO can be involved in the process of protein posttranslational modification [23]. The enzyme was first isolated in crystalline form by Yamada and Yasunobu [24]. Presently, several purification procedures are available. An affinity separation of SAO on AH-Sepharose was described by Svenson and Hynning [25] and a two-step procedure (ammonium sulfate and affinity chromatography on AH-Sepharose followed by elution with aniline SAO inhibitor) was reported by Vianello et al. [26]. The method described by Mondovi et al. [27] (ammonium sulfate precipitation followed by chromatography on AH-Sepharose and Con A-Sepharose) leads to high SAO-specific activities (0.33 EU/mg). Since the AH-Sepharose is no longer commercially available, it has been substituted with Q-Sepharose [28]. The procedure usually leads to a purified SAO [27] with a slightly lower specific activity (0.28 EU/mg). In some chromatographic runs on Q-Sepharose, the peaks of ceruloplasmin and bovine serum amine oxidase were partly overlapped, thus lowering the purification yield and the specific SAO activity. This can be satisfactorily improved by elimination of CP from the plasma protein preparation before passing it through a Q-Sepharose column, leading to higher specific activities and yields.

SAO and ceruloplasmin exhibit several common features. Both are serum copper proteins of a relative high molecular mass: 180,000 Da (two monomers of 90 kDa) for SAO and 132,000 Da for CP. Both enzymes are involved in oxidative processes and both are glycoproteins (6–12% carbohydrate). Both proteins have antioxidant properties and act as cardioprotective [20,29] and neuromodulatory agents [9,22]. Furthermore, the two proteins exhibit, to a certain extent, a similar behavior toward some chromatographic materials (e.g., Q-Sepharose and AH-Sepharose), often leading to interference during the purification procedures. A joint purification procedure leading to higher purity parameters or yields should therefore be of interest to laboratories working in the field of copper proteins.

In this study, a joint chromatographic purification procedure of CP and SAO is described and the results are compared with independent CP [14] and SAO [27] purification procedures.

II. EXPERIMENTAL

A. Chromatographic Material

Aminoethyl agarose is a chromatographic material (not commercially available) obtained in laboratory by the treatment of agarose beads (i.e., Superose 6B, Phar-

macia, Uppsala, Sweden) with 1-chloro-2-ethylamine (chlorohydrate) (Aldrich, Milwaukee, WI), under conditions previously described [13–15]. Practically, 300 mL of Superose 6B was suspended to about 500 mL and heated to 70°C. Then 130 g of 2-chloroethylamine hydrochloride was added to the suspension with stirring. A volume of about 25 mL of 10 N NaOH was added to the suspension to adjust the pH to 10. The reaction mixture was incubated for 2 h with continuous stirring. During the first 20 min of the incubation, small volumes (few milliliters) of 10 N NaOH were added from time to time in order to maintain the pH at 9–10. After the reaction, the gel was washed by filtration on a Büchner funnel until pH $\approx$ 7 in washing solution. The resulting chromatographic material contains aminoethyl functional groups and will be named here as AE-agarose.

Ceruloplasmin enzyme activity was determined, with p-phenylenediamine as substrate, following the Osaki et al. method [30]. One enzyme unit is considered the amount of enzyme that would generate an increase of one absorbancy unit/min at λ = 540 nm.

SAO enzymatic activity was assayed spectrophotometrically, with benzylamine as substrate, according to Tabor et al. [31]. One enzyme unit (EU) was defined as the amount of enzyme able to catalyze the formation of 1 μmole of benzaldehyde/min under the reaction conditions.

The protein concentrations were determined by the Bradford method [32].

B. Joint Purification Procedure of Ceruloplasmin and SAO

The joint purification flow of CP and SAO as well as the reference methods for the single-step purification of CP [14] and for the SAO [27] are schematically presented in Fig. 1. If CP purification is required, especially when large amounts are required, channel c should be followed and the procedure is ended with the AE-agarose chromatographic step. In detail, the purification of CP and/or of SAO can be carried out following the procedure here presented.

1. Collection of Plasma

A volume of 10 L of bovine blood was collected at the slaughterhouse, mixed with 1 L of 2.5% sodium citrate solution and centrifuged at 3000*g* for 20 min, retaining the plasma. The crude CP-specific activity is usually about 8.14×10^{-4} EU/mg and SAO specific activity of about 2.4×10^{-4} to 7.0×10^{-4} EU/mg.

2. Ammonium Sulfate Fractionated Precipitation

Ammonium sulfate was added to 4 L of plasma to 35% of saturation, stirred for 2 h at 4°C and centrifuged at 10,000 g for 20 min, retaining the supernatant to which ammonium sulfate has been added up to 55% saturation, maintaining the stirring for 30 min at 4°C and then centrifuging at 10,000*g* for 20 min. The

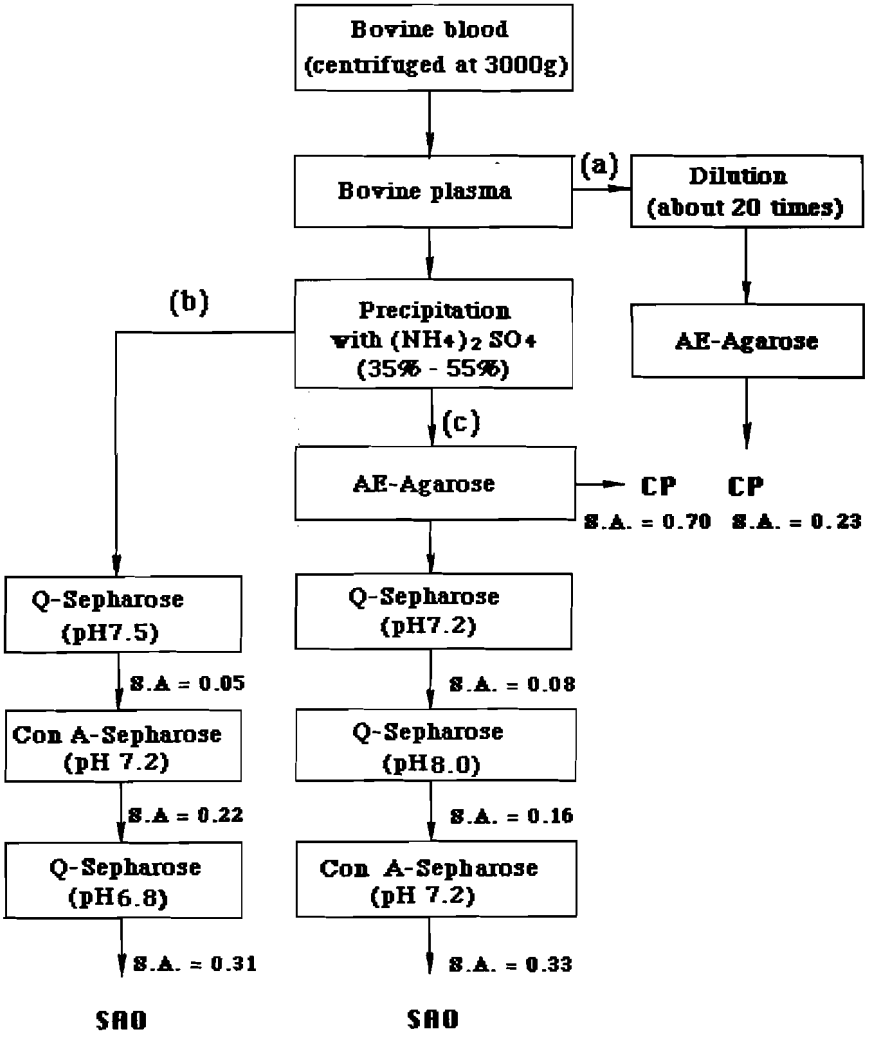

Figure 1 Separation flow of CP and SAO. Channel a: "Single-step" CP purification [14]. Channel b: current method of SAO purification [27]. Channel c: joint SAO and CP purification. (From Ref. 16.)

precipitate was retained and dissolved in 200 mL of 0.1 M potassium phosphate buffer, pH 7.2. The solution was dialyzed for 20 h against 20 L of a 10 mM potassium phosphate buffer, pH 7.2 with two changes of buffer. The dialyzed plasma proteins solution was centrifuged at 10,000*g* for 20 min and the precipitate discarded.

3. AE-Agarose Chromatography and CP Purification

The AE-agarose column (30 × 2.5 cm) was equilibrated with a 10 mM potassium phosphate buffer, pH 7.2, which was also used as first eluent. Half of the dialyzed plasma protein solution (Fig. 1) was applied onto the AE-agarose column, at a flow rate of 120 mL/h. The nonretained fraction was collected for further SAO purification. The AE-agarose column was then washed with: 500 ml of starting 10 mM phosphate buffer, then with 200 mL of 20 mM buffer solution, and finally with 100 mL of 30 mM phosphate buffer, all at pH 7.2. The retained CP was eluted with 100 mL of a 0.2 M phosphate buffer, collecting (Frac-200, Pharmacia, LKB) fractions of 2 mL each. The fractions with the ratio A_{610}/A_{280} higher than 0.045 were collected in a pool with a CP concentration of 8 mg/mL. Purified CP was stored at −20°C.

Ultrafiltration. If CP concentrations higher than those obtained directly from the column are required, a further ultrafiltration step (Amicon 8200, membrane YM 100) will lead to a final purified CP at a concentration of about 20 mg/mL.

4. Q-Sepharose Chromatography (pH 7.2) and SAO Purification

A Q-Sepharose column (40 × 2.5 cm) was equilibrated with 10 mM potassium phosphate buffer at pH 7.2. The SAO-containing fraction not retained by the AE-agarose was applied onto the Q-Sepharose column at a flow rate of 150 mL/h. The column was first washed with 500 mL of starting 10 mM phosphate buffer and then eluted with a linear concentration gradient from 0.05 M to 0.35 M NaCl in 10 mM starting buffer. The gradient was generated by a double-chamber (300 mL each) device. The elution rate was 100 mL/h, collecting fractions of 8 mL each. The fractions with SAO-specific activity higher than 0.05 EU/mg were retained and pooled.

5. Q-Sepharose Chromatography (pH 8.0)

The Q-Sepharose column was regenerated and equilibrated with a 20 mM potassium phosphate buffer at pH 8.0. The protein solution (step 4) was diluted (1:1) with the starting buffer and carried onto the column, washed with 300 mL starting buffer, and eluted with a continuous gradient from 0.05 M to 0.35 M

NaCl in 20 mM buffer, as described above. The fractions with SAO-specific activity higher than 0.14 EU/mg were collected.

6. Con A-Sepharose Chromatography

A Con A-Sepharose column (30 × 2.0 cm) was equilibrated with 0.1 M potassium phosphate buffer at pH 7.2. The SAO-containing solution (step 5) was diluted (1:1) with starting buffer and applied onto the column and washed first with 500 mL of starting 0.1 M phosphate buffer and then with 300 mL of 0.02 M methyl-α-D-glucopyranoside in 0.1 M phosphate buffer at pH 7.2. The SAO was then eluted with 200 mL of 0.5 M methyl-α-D-mannopyranoside in 0.1 M phosphate buffer, at pH 7.2, collecting fractions of 6 mL. The samples with SAO-specific activity higher than 0.30 U/mg were pooled and dialyzed against 0.1 M potassium phosphate buffer at pH 7.2, for 6 h, concentrated by ultrafiltration and stored in fractions of 1 mL, in Eppendorf tubes at −20°C.

C. Single-Step CP Purification by AE-Agarose Chromatography

The modified CP purification method here described was compared to the initial CP purification done under the conditions described by Calabrese et al. [14], as a fast single-step chromatographic method based on the specific CP retention on AE-agarose from a whole plasma preparation, without previous ammonium sulfate precipitation. This method, easily applicable to small and medium laboratory scale CP preparations, has been carried out in parallel with the joint purification here described (Fig. 1) starting from the same bovine plasma prepared as described above. Practically, a volume of 200 mL plasma was diluted with 3 mM potassium phosphate pH 7.2 buffer about 20 times, such as to reach a conductivity of 1.4 millimho, a value similar to that of 10 mM phosphate buffer. The diluted plasma was loaded to AE-agarose column (30 × 2.0 cm), previously equilibrated in 3 mM potassium phosphate buffer, pH 7.2. The column was washed first with 200 mL of 10 mM phosphate starting buffer, then with 100 mL 20 mM phosphate buffer, and finally with 50 mL of 40 mM phosphate buffer, pH 7.2. Ceruloplasmin was retained while the other proteins were eluted from the column. Ceruloplasmin was then eluted with 100 mL of 0.1 M potassium phosphate buffer. With the increase in ionic strength, the CP first concentrates at the bottom of the column and then elutes, the blue fractions being collected.

The purified CP (specific activity of 0.23 EU/mg) was electrophoretically homogeneous and with the absorbancy ratio A_{610}/A_{280} of 0.045 (value corresponding to the standard criteria for the purified enzyme [4–8]); UV-VS absorption spectra were recorded on a Beckman DU-6 spectrophotometer.

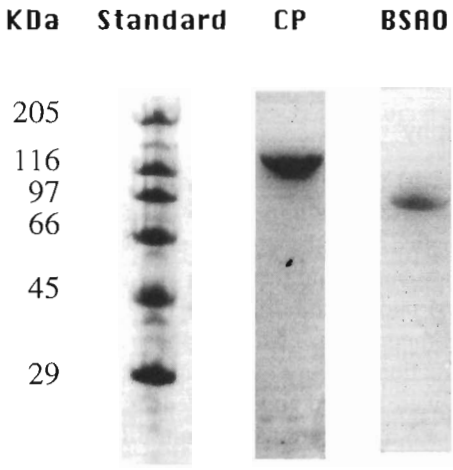

Figure 2 PAGE electrophoretic patterns of the purified CP and SAO. Electrophoresis was carried out by Pharmacia-LKB Phast System, in the presence of 5% β-mercaptoethanol. (From Ref. 16.)

D. SAO Purification

The SAO separation method according to Mondovi et al. [27], slightly modified [B. Mondovi and O. Befani, unpublished data, 1992] as is now currently applied (without the AE-agarose column), was carried out in parallel with the joint purification here described (Fig. 1), starting from the same bovine plasma prepared as described above.

Electrophoresis

The degree of homogeneity as well as the molecular integrity and characteristics of purified CP and SAO were evaluated by SDS-PAGE fast electrophoresis (Phast System, Pharmacia-LKB), in the presence of 5% β-mercaptoethanol (Fig. 2).

III. RESULTS AND DISCUSSION

The characteristics of CP purification by the modified procedure here described, and by the single-step procedure [14], are summarized in Table 1. It was found that the modified method (including ammonium sulfate precipitation) yields larger amounts of purified CP protein (123 mg versus 50.6 mg) for a separation run and many more enzyme units (85.5 EU versus 11.5 EU) than the "single-

Table 1 Comparison of CP Purification by the "Single-Step" Method [14] and by the Modified Procedure

Purification characteristics	"Single-step" method [14]	Modified method
Starting material volume (mL plasma)	200[b]	2000
Total CP activity (EU) in plasma	12.37	132.7
Total protein amount (mg) in plasma	15,200	152,000
Specific CP activity in plasma (EU/mg protein)	8.14×10^{-4}	8.14×10^{-4}
Specific activity (EU/mg) of purified CP	0.23	0.70
Purification factor[a]	282	860
Purity (A_{610}/A_{280})	0.045	0.057
Total recovered activity (EU) of purified CP	11.5	85.5
Total purified CP protein (mg)	50.6	123.0
Yield (recovered EU) (%)	93	69

[a]Defined as the ratio: specific activity of purified enzyme/specific activity in the starting material.
[b]Lower starting volume than for the combined method, since the required 1:20 dilution leads to 4 L (difficult to handle in the chromatographic run).
Source: From Ref. 16.

step" method [14]. However, the recovery appears higher for the initial single-step procedure (50.6 mg CP yielded from 200 mL plasma versus 123 mg CP from 2000 mL plasma). Considering the amount of CP in plasma (200–300 mg/L), the CP recovery by the single-step procedure [14] is very high (250 mg/L). On the other hand, the modified method, despite a lower recovery (60–65 mg CP/L), seems more advantageous because dealing with smaller volumes yields a higher CP amount (120–125 mg) per separation run.

The characteristics of CP purified by the modified method (including ammonium sulfate precipitation) are better than those obtained by the single-step procedure. For instance, the specific activity is three times higher (0.70 versus 0.23 EU/mg) while the purity expressed by the spectral parameters (A_{610}/A_{280}) are improved by more than 25% (higher than 0.057 versus 0.045). The improvement in CP purification can be related to the partial elimination of contaminants as well as of clottable proteins (in fact, no clotting phenomena were observed during the AE-agarose chromatographic run). Minimizing the sample story, the risk of protein degradation is limited. In fact we suppose, following a reexamination of CP spectral properties (EPR [14]), that CP purified by chromatography on AE-agarose is closer to its real native structure than commercial CP obtained by other methods.

This method can also allow the CP immobilization directly on this specific chromatographic support during its purification [33]. The conjugation of CP with

biocompatible polymers is important because the immobilized enzyme conjugates show sought-after advantages such as higher stability, lower antigenicity, and the possibility of continuous use in various devices.

The characteristics of the SAO purification following the previous method [27] and by the combined purification here described are presented in Table 2.

As shown in Table 2, the combined purification, when compared to the current method, leads to a 16% increase in purified enzyme (42.0 versus 36.2 mg) and a 24% increase in total SAO enzyme units (13.9 versus 11.2 EU) as well as to a slightly higher SAO specific activity (0.33 versus 0.31 EU/mg). The increase in purification yield obtained by the combined procedure is about 25%.

The electrophoretic sodium dodecyl sulfate–polyacrylamide gel electrophoresis (SDS-PAGE) patterns of the purified CP and SAO are shown in Fig. 2. The combined purification method leads, in the case of both CP and SAO, to electrophoretic homogeneity, with preservation of their molecular integrity. The CP appears homogeneous with an unique band corresponding to the molecular mass of 132 kDa. The SAO monomers also appear homogeneous (a band at 90 kDa).

Although an additional AE-agarose step is required, the depletion of CP and other contaminants (eluted with 20 and 30 mM phosphate buffer) appears to be an advantage, since these proteins can interfere with SAO. In the first Q-Sepharose chromatographic step following the current SAO purification method

Table 2 Comparison of Characteristics of SAO Obtained by the Current Method of Mondovi et al. [27] including a Q-Sepharose Step and by the Combined CP-SAO Purification Method Here Described, with the Additional Step of AE-Agarose Chromatography

Purification characteristics	Current method	Combined method
Starting material volume (mL plasma)	2000	2000
Total SAO activity (EU) of starting plasma	57.8	57.8
Total protein amount (mg) in plasma	152,000	152,000
Specific SAO activity in plasma (EU/mg protein)	3.8×10^{-4}	3.8×10^{-4}
Specific activity (EU/mg) of purified SAO	0.31	0.33
Purification factor[a]	789	868
Purity (A_{480}/A_{280})	0.012	0.013
Total purified SAO protein (mg)	36.2	42.0
Total activity (enzyme units) of purified SAO	11.2	13.9
Yield (recovered EU) (%)	19.4	24.0

[a]Defined as the ratio: specific activity of purified enzyme/specific activity in the starting material.
Source: From Ref. 16.

[27], the elution profile (Fig. 3a) shows a slight overlap between the CP and SAO peaks. As a result of the additional AE-agarose step provided by the combined CP-SAO separation procedure, the chromatographic interference by CP is avoided (Fig. 3b). With a previous AE-agarose column, the SAO specific activity after the first Q-Sepharose purification step was increased by about 35% (the result of four different separation runs) when compared with the current method (without the AE-agarose step).

As shown in Fig. 1, differently from the previous separation procedure, the Con A-Sepharose step was carried out after the second Q-Sepharose column. The advantage of this inversion is that the use of a second Q-Sepharose column leads to a major increase in specific activity, with a simultaneous decrease in the volume to be handled in the last Con A-Sepharose step.

We are not considering the joint CP and SAO purification method presented here as a new method for either CP or SAO purification. However, it is worth mentioning that the mutually improving effect generated by associating the two methods of the independent CP and SAO purification procedures into a joint method for CP and SAO purification leads to better characteristics for each purified protein. The improvement is more important for the CP purification, as it leads to several fold increases in different characteristics (specific activity and the total activity units obtained by a separation run) and to a better molecular integrity as reflected by the A_{610}/A_{280} ratio. The increased yield of SAO of more than 25% by the joint purification technique is also useful.

The current procedures for the SAO purification [27] require dialysis and concentrations between each chromatographic step. In the modified method, dialysis and concentration between the chromatographic columns can be eliminated and replaced by simple dilution (1:1) of the enzyme solution with one volume of the buffer used to equilibrate the subsequent column. This improvement allows a faster purification run, leading to higher yields, increased specific activities, and ameliorated spectral characteristics. For instance, with these modifications, the yield is increased (100 to 115 mg SAO from 10 L of blood). The specific enzymatic activity is 0.32 to 0.35 EU/mg and the absorbancy ratio $A_{480\,nm}/A_{280\,nm}$ = 0.013 (denoting a high quality of the enzyme). At the same time, the eluent volumes were reduced. For example, the eluent volume of the first Q-Sepharose column was reduced from 1800 mL to 600 mL (while maintaining the initial and final gradient concentrations) and thus the method is faster and easier to apply. The modified method is therefore time saving (only 3 days for the whole separation instead of 4–5 days for the current procedure) and leads to improved yields and quality of SAO. Apart from the mutual improvement effects, better yields, and molecular characteristics, the combined purification procedure may be of interest for large-scale or industrial preparations, since the same inexpensive bovine plasma source and preliminary precipitation as well as the AE-agarose steps are common steps for both CP and SAO purification.

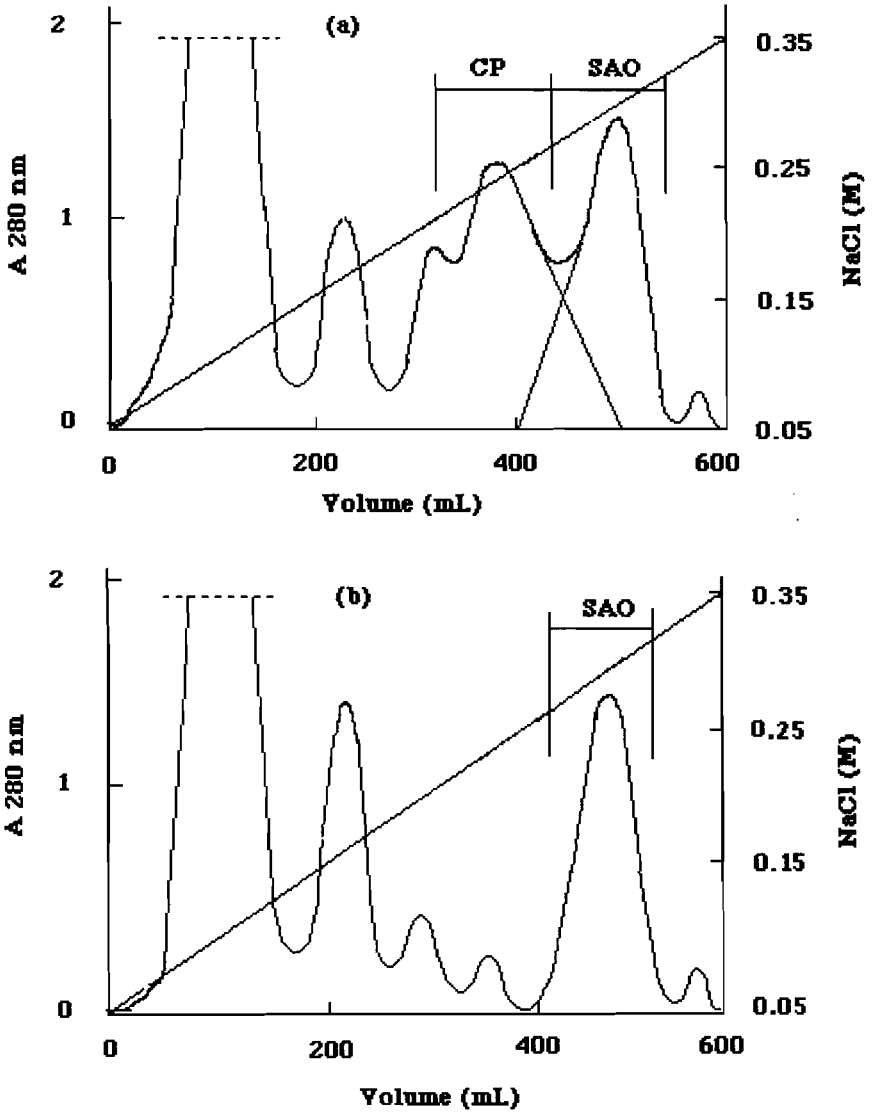

Figure 3 Typical elution profiles of plasma proteins fractions on Q-Sepharose column without (a) and with (b) a previous chromatographic step on AE-agarose column. (From Ref. 16.)

ACKNOWLEDGMENTS

The financial supports provided by MRC (Canada)–CNR (Italy) international collaboration, by MURST and by CNR grant-Biotechnology and Molecular Biology, contract No. 97.04376.CT17, as well as a postdoctoral fellowship from "Fondation UQAM" offered to X. T. Wang, are gratefully acknowledged.

REFERENCES

1. Gutteridge GM, Stocks J. Ceruloplasmin: physiological and pathological perspectives. Crit Rev Clin Lab Sci 1981;14:257–329.
2. Paulik MD, Weiss ML. In: Putnam FW, ed. The plasma proteins, Vol. 2. New York: Acad Press, 1975;51–108.
3. Gutteridge JMC, Richmond R, Halliwell B. Oxygen free radicals and lipid peroxidation: inhibition by the protein ceruloplasmin. FEBS Lett 1980;122:269–274.
4. Lovstad RA. The protective action of ceruloplasmin on Fe^{2+} stimulated lysin on rat erythrocytes. Int J Biochem 1981;13:221–228.
5. Al-Timimi DJ, Dormandy TL. The inhibition of lipid auto-oxidation by human ceruloplasmin. Biochem J 1977;168:283–291.
6. Mateescu MA, Chahine R, Roger S, Atanasiu R, Yamaguchi N, Lalumiere G, Nadeau R. Protection of myocardial tissue against deleterious effects of oxygen free radicals by ceruloplasmin. Arzneim Forsch 1995;45:476–480.
7. Dumoulin MJ, Chahine R, Atanasiu R, Nadeau R, Mateescu MA. Comparative antioxidant and cardioprotective effects of ceruloplasmin, superoxide dismutase and albumin. Arzneim Forsch 1996;46:855–861.
8. Goldstein IM, Kaplan HB, Edelson SH, Weissman G. Ceruloplasmin. A scavenger of superoxide anion radicals. J Biol Chem 1979;254:4040–4052.
9. Wang R, Zhang L, Mateescu MA, Nadeau R. Ceruloplasmin: an endogenous depolarizing factor in neurons? Biochem Biophys Res Commun 1995;207:599–605.
10. Atanasiu R, Dumoulin MJ, Chahine R, Mateescu MA, Nadeau R. Antiarrhythmic effects of ceruloplasmin during reperfusion in the ischemic isolated rat heart. Can J Physiol Pharmacol 1995;73:1253–1261.
11. Fox PL, Mukhopadhyay C, Ehrenwald E. Structure, oxidant activity, and cardiovascular mechanisms of human ceruloplasmin. Life Sci 1995;56:1749–1758.
12. Pemberton S, Lindley P, Zaitsev V, Card G, Tuddenham EG, Kemball-Cook G. A molecular model for the triplicated A domains of human factor VIII based on the crystal structure of human ceruloplasmin. Blood 1997;89:2413–2421.
13. Dimonie M, Schell HD, Hubca G, Mateescu MA, Todireanu S, Languri J, Maior O, Iosif M. Polyvinyalcohol synthesis by suspension methanolysis of polyvinylacetate. Derivatization and some applications. J Macromol Sci 1985;22A:729–754.
14. Calabrese L, Mateescu MA, Carbonaro M, Mondovi B. Reexamination of spectroscopic properties of ceruloplasmin freshly isolated with a novel, very rapid single-step procedure. Biochem Int 1988;16:199–208.

15. Calabrese L, Mateescu MA, Riccio P-L, Carbonaro M, Natoli G, Mondovi B. Single step chromatographic purification of plasma ceruloplasmin. Italian Patent 47914A86 (1986).
16. Wang XT, Dumoulin MJ, Befani O, Mondovi B, Mateescu MA. Joint chromatographic purification of bovine serum ceruloplasmin and amineoxidase. Prep Biochem 1994;24:237–250.
17. Mondovi B, Gerosa P, Cavaliere R. Studies on the effect of polyamines and their products on Ehrlich ascites tumours. Agents Actions 1982;1:450–451.
18. Agostinelli E, Bates DA, Przybytkowski E, Mateescu MA, Mondovi B. Cytotoxicity of polyamines in Chinese hamster ovarian (CHO) cells in the presence of serum amine oxidase. Life Chemistry Reports 1991;9:193–204.
19. Mondovi B, Riccio P, Agostinelli E. The biological functions of amine oxidases and their reaction products: an overview. Adv Exp Med Biol 1988;250:147–161.
20. Mateescu MA, Dumoulin MJ, Wang XT, Nadeau R, Mondovi B. A new physiological role of copper amine oxidases: cardioprotection against reactive oxygen intermediates. J Physiol Pharmacol 1997;48 Suppl 2:110–121.
21. Mondovi B, Wang XT, Pietrangeli P, Wang R, Nadeau R, Mateescu MA. New aspects on the physiological role of copper amineoxidases. Curr Top Med Chem 1997; 2:31–43.
22. Wu L, Mateescu MA, Wang XT, Mondovi B, Wang R. Modulation of K^+ channel currents by serum amineoxidase in neurons. Biochem Biophys Res Commun 1996; 220:47–52.
23. Wang XT, Pietrangeli P, Mateescu MA, Mondovi B. Extended substrate specificity of serum amine oxidase: possible involvement in protein posttranslational modification. Biochem Biophys Res Commun 1996;223:91–97.
24. Yamada H, Yasunobu KT. Purification, crystallization and properties of plasma monoamine oxidase. J Biol Chem 1962;237:1511–1516.
25. Svenson A, Hynning PA. Preparation of amine oxidase from bovine serum by affinity chromatography on aminoheyxyl-Sepharose. Prep Biochem 1981;11:99–108.
26. Vianello F, Di Paolo ML, Zennaro L, Stevanato R, Rigo A. Isolation of amine oxidase from bovine plasma by a two-step procedure. Protein Expression Puri 1992;3: 362–367.
27. Mondovi B, Turini P, Befani O, Sabatini S. Purification of bovine plasma amine oxidase. Meth Enzymol 1983;94:314–318.
28. Susan-Janes M, David MV, Wemmer D, Smith AJ, Kaur S, Maltby D, Burlingam AL, Klinman JP. A new redox cofactor in eukaryotic enzymes: 6-hydroxydopa at the active site of bovine serum amine oxidase. Science 1990;248:981–987.
29. Atanasiu R, Gouin L, Mateescu MA, Cardinal R, Nadeau R. Class III antiarrhythmic effects of ceruloplasmin on rat heart. Can J Physiol Pharmacol 1996;74:652–656.
30. Osaki S, Johnson DA, Frieden E. The possible significance of the ferrous oxidase activity of ceruloplasmin in normal human serum. J Biol Chem 1966;241:2746–2751.
31. Tabor CA, Tabor H, Rosenthal SM. Purification of amine oxidase from beef plasma. J Biol Chem 1954;208:645–665.
32. Bradford M. A rapid and sensitive method for the quantitation of microgram of protein utilizing the principle of protein-dye binding. Anal Biochem 1976;72:248–254.
33. Mateescu MA, Fortier G, Neidhart S, Roger S. Selective immobilization of ceruloplasmin on the chromatographic material used for its purification. Chromatographia 1988;26:110–121.

16

Fast, Single-Step Affinity Chromatography Purification of Hemoglobin

Mircea-Alexandru Mateescu and Wilfrid Jacques
Université du Québec à Montréal, Québec, Canada

I. INTRODUCTION

Hemoglobin (Hb), the main oxygen carrier, is a tetramer in which each monomer (α_1, α_2, β_1; and β_2) contains a porphyrin prosthetic group. Initiated in 1937, the long path to understanding Hb biochemistry led to high-resolution X-ray Hb analysis (Perutz, 1968), which was a landmark achievement for the formulation of the "Perutz mechanism" based on the stereochemistry of the cooperative effects in Hb oxygenation [1]. One of the most complex proteins, Hb is also the most studied over the last 30 years. Since oxygen exchange is controlled by the reversible steric configuration of the protein, Hb has been nominated as an "honorary enzyme" (Voet and Voet [2]).

Hemoglobin is not a glycoprotein, but it can be easily glycosylated with free glucose, by a nonenzymatic mechanism. About 6% of the erythrocytary Hb is glycosylated in normal subjects. In diabetes the glucose level can be three times higher [3,4], leading, with different rates, to glycated forms HbA_{1a}, HbA_{1b}, and HbA_{1c}. More knowledge of interactions of Hb with sugars is of interest since the oxygenation–deoxygenation capacity of the glycated Hb is reduced by 20–25%. Furthermore, the effects of the alteration of oxygen transport function are enhanced by the relatively high half-life of Hb, up to 120 days. It was also

---

Part of this work was adapted from W. Jacques and M. A. Mateescu, *Anal. Lett.* 1993;26:875–886.

reported [5] that, unexpectedly, the velocity of glycosylation of the amine terminal group of the β subunit located on the allosteric center of Hb is three times higher than the glycosylation rate of other amine groups on the Hb surface. Since the mechanism is nonenzymatic, the kinetics is in disagreement with the statistical distribution of amine groups susceptible to glycosylation.

On the basis of the peculiar kinetics of glycosylation, we have advanced the hypothesis of a selective recognition center for sugars. Previously [6,7], we have described specific interactions of Hb with some polysaccharides as CL-amylose (CLA) and CL-agarose, while practically no interaction has been observed with CL-dextran (Sephadex). All of these chromatographic materials are obtained by the polysaccharide chain treatment with epichlorohydrin [8,9], leading to swellable three-dimensional polymeric structures. The fact that Hb is retained by CL-amylose (main chains based on glucose units linked by α-1,4-glycosidic bonds) and not by Sephadex (main chains based on glucose units linked by α-1,6-glycosidic bonds) suggests that Hb can selectively recognize and differentiate between the two types of linkages characteristic for each polymer. At the same time it was shown that Hb can recognize the CL-agarose (main chains based on galactose and 3,6-anhydro-L-galactose), indicating that both the type of linkage and the saccharidic units forming the carbohydrate polymer are important [7]. Furthermore, the study described specific interactions of Hb with mono- and disaccharides. The competitive elution of Hb retained by affinity on CL-amylose and on CL-agarose (Sepharose CL-4B) chromatographic materials, with different sugars as competitive "affinants," showed that glucose, fructose, and cellobiose are poor eluants, whereas lactose is a good competitive eluant, suggesting that it better interacts with Hb and, more important, that the interaction is selective [7].

Another related study reported Hb separation by specific affinity chromatography retention on CL-amylose, with a capacity of 4.5–10 mg Hb/ml gel bed, followed by desorption with deforming eluants, as NaCl [6]. The CL-amylose material was previously used in exclusion chromatography [9] and in affinity chromatography for α-amylase separation [10].

This new aspect on the Hb properites can offer a better understanding of Hb–carbohydrate and Hb–glycoprotein interactions and, at the same time, a possibiltiy to purify Hb directly from erythrocytary lysate, by a single-step chromatographic procedure on crosslinked amylose columns [6]. These Hb separation experiments were carried out using commercial bovine Hb (Sigma Chemical Co.) solutions.

Hemoglobin and its derivatives are currently isolated by various ion exchange chromatographic techniques. However, several difficulties have been reported, mainly related to the Hb contamination with various compounds, and often a rechromatography is required. Thus, alternative procedures have been elaborated based on the Hb elution from the starch gel after the electrophoretic

Hb separation [11]. Several separation procedures were described for the Hb purification by affinity chromatography on ATP-agarose columns [12,13]. This method is efficient for separation of Hb from red cells derived from unconventional sources (blood from surgery, placenta, etc.) [12], but is long enough, since ultracentrifugation and dialysis steps are required after hemolysis and prior to ATP-agarose column. The procedures that allow the preservation of Hb capacity to retain and to exchange oxygen as oxyhemoglobin (i.e., the crosslinked Hb or the ATP–Hb complex [13]) are of great interest for the transfusional medicine. Fast methods, minimizing the sample story (preventing the accumulation of methemoglobin) and large-scale procedures, are of great interest for laboratories involved in Hb purification.

We are now presenting a fast, single-step, easy-to-apply method for the Hb purification directly form erythrocytes, by affinity chromatography on polysaccharidic chromatographic materials such as CL-agarose i.e., Superose 12 and Sepharose CL.

II. EXPERIMENTAL

A. Materials and Reagents

Agarose-based chromatographic materials (Sepharose CL-4B, Sepharose CL-6B, Superose 12 Prep. Grade, Sephadex G-25, and Sephadex G-100) were from Pharmacia LKB (Uppsala, Sweden). Commercial bovine hemoglobin (lyophilized powder), bovine serum albumin (BSA), and Coomassie brillant blue R-250 were from Sigma Chem. Co (St. Louis, Missouri). CL-amylose (CLA) is a semisynthetic polyglucose chromatographic material realized by amylose crosslinking with epichlorohydrin [6,7,9]. As the Sephadex gel, CLA was here used almost for comparison in terms of Hb interactions with agarose-based materials. Human blood was obtained from the Hôpital Charles-Lemoyne, Longueuil (Québec), Canada.

B. Separation of Erythrocytary Hemoglobin by Single-Step Affinity Chromatography on Agarose-Based Column

1. Bovine Erythrocytary Lysate

The crude bovine erythrocytary extract was prepared from fresh red blood cells separated from plasma by centrifugation at 1000*g* for 30 min at 4°C. The supernatant was discarded and the erythrocytes were washed with an equal volume of isotonic (0.9%) NaCl solution, followed by centrifugation under the same conditions as before. The washings were repeated three times. Then 1 volume of erythrocyte sediment was suspended in 10 volumes of bidistilled water for hemolysis

and the suspension was centrifuged at 12,000*g* for 20 min at 4°C, retaining the supernatant.

2. Human Erythrocytary Preparation

Human blood was subjected to the same procedures as bovine blood. Human Hb extract (supernatant) was stored at −20°C. Since the Hb interaction with polysaccharides is highly sensitive to ionic strength, the Hb extract conductivity has been determined and adjusted to values less than 15 mmho, by dilution or dialysis.

This chapter describes the fast Hb purification at a laboratory scale. The recommended chromatographic material is Superose 12 Prep. Grade, which has the best retention capacity. Alternatively, other crossliked materials, selected from Sepharose CL-4B, Sepharose CL-6B, or CL-amylose, can be used leading to Hb with comparable homogeneity but with moderately lower yields.

3. Affinity Chromatography Hemoglobin Separation on Agarose-Based Column

For separation, a volume of about 2–3 ml (or more) of sample (5–10 mg/ml) of commercial Hb dissolved in bidistilled water or erythrocytary extract was applied to the Superose 12 column (10 × 2.5 cm, 40-ml gel bed). The column was first washed with bidistilled water for the elution of nonretained contaminants and then eluted isocratically with 0.9% NaCl or with an increasing continuous gradient up to 5% NaCl solution, with an elution flow of 25 ml/h. The gradient elution was realized with a gradient mixer system (Pharmacia), over a volume of 60 ml. The entire operation has been carried out at 20 ml/h (with a Marlow peristaltic pump), collecting fractions of 2 ml (Gilson fraction collector). Since Hb is eluted with a relatively low concentration (0.1–1%) NaCl, for further separation runs a 0.9% NaCl concentration was used for the Hb elution step.

The column hemoglobin retention capacities (expressed in mg Hb/ml gel bed) of various chromatographic materials were determined under the same conditions: microcolumns (5 × 0.6 cm) with a 3-ml gel bed, equilibrated in demineralized water and a flow rate of 20 ml/h). The columns were overloaded with commercial Hb samples and washed to eliminate nonretained Hb. The capacity was established by the integration of the Hb amounts determined in each collected fraction (following elution with 0.9% NaCl solution), as previously described [6]. Retention capacities for the types of chromatographic material used (Superose 12, Sepharose CL-4B, Sepharose CL-6B, CL-amylose-40) were evaluated and compared with those of Sephadex G-25 and Sephadex G-100 [14]. Retention capacities were also evaluated for related hemoglobin proteins as globin (heme-free hemoglobin monomer) and for horse heart myoglobin.

Hemoglobin concentration has been determined spectrophotometrically at

λ = 406 nm (characteristic for the heme prosthetic group) and at λ = 280 nm (characteristic for the proteic part, the globin). Calibration curves have been obtained from commercial Hb samples in concentration up to 250 μg/ml, as standard.

The Hb purity degree was determined from the A_{406nm}/A_{280nm} ratio, and also checked by sodium dodecyl sulfate–polyacrylamide gel electrophoresis (SDS-PAGE) (10% polyacrylamide) as described by Laemmli [15] and staining with Coomassie brilliant blue R-250. The molecular integrity of the Hb tetramer purified on Superose 12 column was confirmed by exclusion chromatography on Sephadex G-100 (1 × 70 cm) column equilibrated in 0.045 M sodium phosphate buffer, pH 7.2. The column parameters were evaluated with 0.5 ml calibrating mixture consisting of blue dextran T-2000 (for the void volume, V_0), BSA, and cytochrome *c*, in concentrations of 2 mg/ml each.

III. RESULTS AND DISCUSSION

The chromatographic profile of Hb purification by affinity retention on Superose 12 column and deforming elution with 0.9% NaCl (0.15 M) solution is presented in Fig. 1A. Since hemoglobin is sensitive to ionic strength, the deforming saline solution produces a fast and total Hb desorption in a sharp peak. Similar results were obtained with methemoglobin and this, irrespective of the oxy- or deoxy-Hb form (data not shown).

Since it was previously reported [7] that among monosaccharides only galactose was able to generate a desorption (with a diffuse peak) and among disaccharides only lactose (glucose linked to galactose) generated a sharper elution of Hb from the CL-amylose, the conclusion was that Hb preferentially interacts with galactose-containing sugars. Thus, Hb retention capacities on crosslinked agarose (containing galactose and 3,6-anhydro-L-galactose units), chromatographic materials (Sepharose CL-4B, Sepharose CL-6B, and Superose 12), and on CL-amylose (a material exhibiting long chains of glucose repetitive units linked by α-1,4-glucosidic bonds that can be selectively and reversibly recognized by Hb [6]), were determined (Table 1). Sepharose CL-4B has a retention capacity (8.4 mg Hb/ml gel bed) comparable to that observed for the CL-amylose (8.0 mg Hb/ml gel bed). The Hb retention capacities of various agarose chromatographic materials (Table 1) depend directly on the concentration of agarose in the gel bed.

Since the best retention capacity (23 mg/ml) was obtained with Superose 12 (Prep. Grade), the experimental details of the procedure for Hb purification are based on this chromatographic material.

Commercial Hb in aqueous solution can be retained on crosslinked agarose or amylose columns and recovered by elution with physiological (0.9%) NaCl

Table 1 Available Hemoglobin Retention Capacity of Different Carbohydrate Chromatographic Materials

Chromatographic material	Hb retention capacity (mg Hb/ml gel bed)	Carbohydrate matrix
CL-Amylose (CLA-40)[a]	8.0 ± 0.6	Crosslinked amylose
Sepharose CL-4B[b]	8.4 ± 0.8	Crosslinked agarose
Sepharose CL-6B	16.5 ± 0.9	Crosslinked agarose
Superose 12 Prep grade	22.9 ± 1.1	Highly crosslinked agarose

[a] CLA-40: Crosslinked (CL)-amylose; The number indicates the crosslinking degree expressed as the amount in grams of epichlorohydrin used to crosslink 100 grams of amylose.

[b] For agarose chromatographic materials, the number indicates the approximate percentage of carbohydrate in the gel; B stands for bead form.

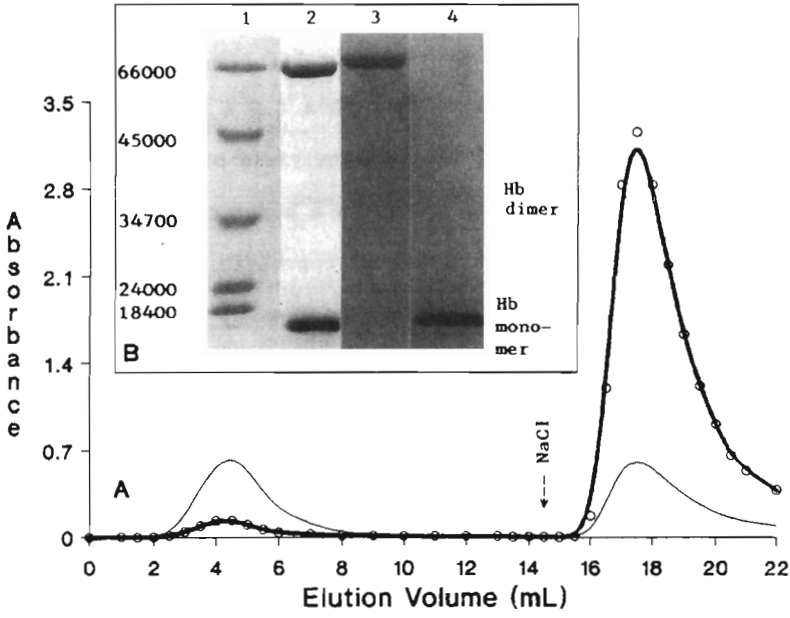

Figure 1 Typical chromatographic (A) and electrophoretic (B) separation profiles of a mixture of bovine serum albumin (BSA) (1 mg/ml) and commercial hemoglobin (Hb)(1 mg/ml) on a Superose 12 column (4 ml gel bed). The absorbances A_{406nm} (-o-) and A_{280nm} (—) yielded for the first peak a ratio value $A_{406nm}/A_{280nm} = 0.21$ and for the retained Hb $A_{406nm}/A_{280nm} = 5.2$. The sample volume was 2 ml. SDS-PAGE was run for standard molecular weight (lane 1), Hb and BSA mixture before separation (lane 2), nonretained (ascribed to BSA) fraction (lane 3), and retained Hb eluted from the CLA column (lane 4).

solution. In the case of Hb associated with other proteins, e.g., with BSA in equal concentrations in aqueous samples, a selective retention of Hb on the Superose 12 column was observed, while a total elution of the nonretained BSA was found in the first peak (Figure 1).

No Hb retention was observed in identical chromatographic conditions on Sephadex G-25 or Sephadex G-100 (crosslinked dextran based on α-1,6-glucosidic bonds). These data clearly indicated that Hb can specifically recognize and be retained at the level of galactose and 3,6-anhydro-L-galactose sequences of the Superose 12 chromatographic material. The Hb was eluted in a single step, with a 0.9% NaCl solution (Figure 1A). It is worth noting that, being sensitive to ionic strength, Hb can be desorbed at even lower NaCl concentrations. The yield of Hb recovery was higher than 85%.

The BSA was chosen as a model contaminant because this protein, like Hb, is not a glycoprotein, and presents a molecular weight of 68 kDa, close to that of Hb (64 kDa). The presence of small amounts of Hb in the first peak of BSA or other contaminant proteins, even if the column is not overloaded, can be ascribed to the presence of some modified forms in the commercial Hb (beyond the methemoglobin and the dimers, which can be associated with Hb in commercial preparations). In fact, the presence of dimers (32 kDa) was confirmed as a minor peak in the commercial Hb, by exclusion chromatoraphy of Sephadex G-100, eluted after the major tetrameric Hb peak (64 kDa).

The SDS-PAGE runs (Fig. 1B) clearly indicated the specific retention of Hb on Superose 12, whereas BSA is not retained at all. In fact, only Hb recovered from the column was visualized on lane 4 as a single band corresponding to the Hb monomer (16 kDa) and another minor one for the dimer (32 kDa).

On the basis of this specific Hb retention onto the Superose 12 column, the proposed affinity chromatography method allows the single-step purification of Hb, directly from erythrocytary lysate. A selective chromatographic retention of erythrocytary Hb (Figure 2) from a crude heterogeneous extract obtained by red cell hemolysis in water (1:11 v/v), was found. As in the case of commercial Hb, recovery of the erythrocytary Hb can be easily realized by direct elution with physiological 0.9% NaCl solution (Figure 2A).

The absorbancy ratio A_{406nm}/A_{280nm} was considered (beyond SDS-PAGE) a criterion to assess the purity of Hb eluted from the column. The purification parameters are presented in Table 2. For all of the purified Hb recovered peaks, the A_{406nm}/A_{280nm} ratio values were 4.3 (as for the standard commercial Hb) or even higher, up to 5.3, indicating an improvement of the degree of purity of the commercial Hb. The first nonretained peaks (contaminants and eventually overloaded Hb) present lower ratio values, due to various contaminants absorbing at 280 nm. The retention capacity and the elution profiles were obtained with small columns (1 × 5 cm), but the scaling-up process with bigger columns (50- to 100-ml gel bed or more) allows the large-scale purification of Hb from blood

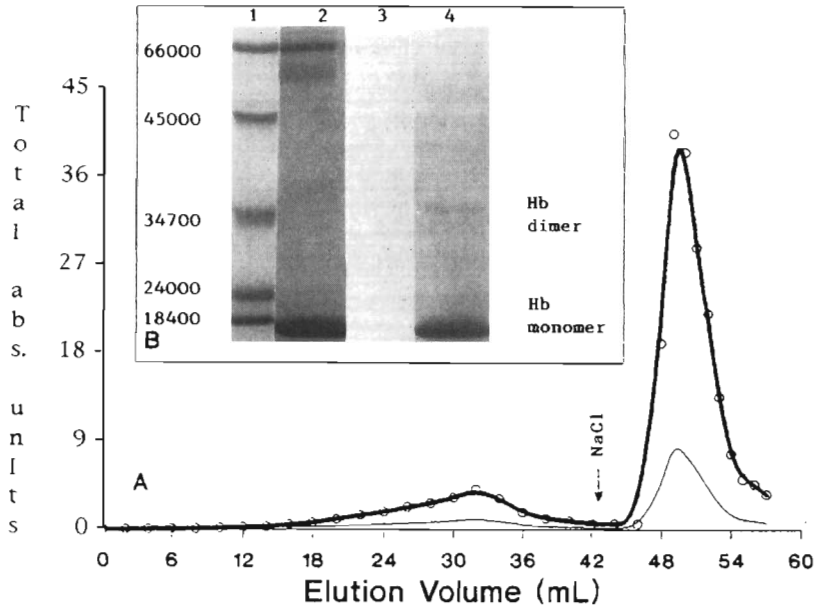

Figure 2 Typical chromatographic (A) and electrophoretic (B) profiles of the erythrocytary separation on a Superose 12 column (3-ml gel bed). The absorbances A_{406nm} (-o-) and A_{280nm} (—) yielded for the erythrocyte lysate a ratio value $A_{406nm}/A_{280nm} = 3.7$ and for the retained Hb $A_{406nm}/A_{280nm} = 4.5$. SDS-PAGE was run for standard molecular weight (lane 1), heterogeneous erythrocytary hemolysate before separation (lane 2), nonretained fraction (lane 3), and retained Hb eluted from the Superose 12 column (lane 4). The separation conditions are presented in the "Materials and Methods" section.

Table 2 Hemoglobin Purification by Affinity Chromatography on Superose 12 Column

Purified Hb (sources)	A_{406nm}/A_{280nm}	Retention capacity (mg Hb/ml gel bed)	Observations
Commercial Hb[a]	5.2 ± 0.2	22.9 ± 1.1	A unique electrophoretic band (64 kDa) was confirmed by exclusion chromatography on Sephadex G-100.
Hb from erythrocytarylysate	4.9 ± 0.3	23.5 ± 1.8	

[a] For the commercial Hb (Sigma Chemical Co.) before the column, the A_{406}/A_{280} ratio was 4.3. The data represent a mean of four experimental values.

sources. The Superose 12 columns were repeatedly used for tens of cycles without significant alteration of the retention capacity. A condition for the column to work is that it be thoroughly washed first with 0.1 M NaOH and then with H_2O, from one cycle to another (until conductivity in washing eluate decreases at less than 15–30 mmho). However, after more than 50 cycles, and under certain conditions, the mechanical properties could be partially affected by alkaline (0.1 M NaOH) washings between the affinity cycles.

The erythrocytary Hb recovered from CLA-40 column (Figure 2B) was electrophoretically (SDS-PAGE) homogeneous, obtaining a strong band characteristic for Hb monomer (16 kDa) and another minor band for the Hb dimer (32 kDa) only, as for the purified commercial Hb (Figure 1B, lanes 2 and 4). Dissociation into monomers is due to the presence of SDS in the electrophoretical gel and has been reported by other groups [16].

The molecular integrity of purified Hb (64 kDa) was confirmed by exclusion chromatography on Sephadex G-100, where a unique peak was observed at the same elution volume (V_e) generating a $K_a = 0.17$, close to that found for BSA (68 kDa).

The specific affinity interaction of bovine Hb with CL-agarose (Superose 12) and with CL-amylose was comparable with that found for human Hb; the elution profiles (data not shown) were similar to those of bovine Hb. Furthermore, the affinity retention on Superose 12 and on CL-amylose seems to be specific for Hb and also for some related proteins. Globin, the heme-free hemoglobin monomer, was shown to interact moderately with the CL-amylose, but to a lesser extent than Hb [14], whereas heme is not retained at all. The similarities between the affinity behavior of human and bovine Hb on agarose chromatographic materials, here mentioned, as well as previous data [14] showing affinity interaction of horse heart myoglobin with the CL-agarose, suggest that the interaction with these polysaccharides can be a general property of hemoglobins and related proteins of various species. The selective sugar recognition of hemoglobins and related proteins appears to be irrespective of the origin (human or bovine hemoglobin and horse heart myoglobin). The retention capacities of CL-amylose for myoglobin (18.8 kDa) was of 20 mg/g dry support [14], a value of about 25% of the retention capacity of 86 mg/g dry support for the tetrameric bovine Hb (64 kDa). Since myoglobin's structure is very close to the Hb monomers (16 kDa), it is possible to suppose a unique type of sugar recognition center on the Hb molecule. This supposition fits with the data of Haney and Bunn [5], on the higher rate and yield of nonenzymatic glycosylation of one β subunit, leading to an excess of HbA_{1c} glycosylated form when compared to the forms HbA_{1a}, and HbA_{1b}.

The advantage of the method described here is that no other plasma or erythrocytary proteins interact, under the experimental conditions presented, with these CL-amylose and CL-agarose chromatographic materials that are not

derivatized with functional ionic exchange groups. In fact, affinity chromatography on Superose 12 allows the single-step separation of Hb, electrophoretically homogeneous, from the erythrocytary extracts. This is possible due to Hb specific affinity for nonsubstituted agarose or amylose materials.

As previously mentioned, the elution of Hb retained by Superose 12 is very sensitive to ionic strength; NaCl concentrations as low as 0.01 N can produce a total Hb desorption by deforming elution [6]. It was also previously shown that, as an alternative, Hb can be desorbed by competitive elution with a continuous gradient of lactose [7]. Hemoglobin elution started at 0.05 M lactose, whereas the other sugars such as glucose, fructose, and saccharose, even at a concentration of 0.5 M, were unable to desorb Hb [7]. These elution data suggest that the Hb interaction with (poly)saccharides is specific and highly related to the folding arrangement of the protein. Further works are in course for the quantification of different Hb–sugar interactions, and for the localization and characterization of the saccharide recognition center for normal and pathological hemoglobins from different origins. Aspects of the Hb–sugar interactions will be dealt with in further reports.

Since agarose chromatographic materials (Superose) resist at high compression effort, the fast, single-step method reported here can be extended for large-scale Hb affinity purification in batch, continuous recycling, and fast protein liquid chromatography (FPLC). The method is easy to apply, allowing purification of electrophoretically homogeneous Hb within a few hours.

ACKNOWLEDGMENTS

A FCAR fellowship awarded to W.J. for graduate studies at UQAM is gratefully acknowledged.

REFERENCES

1. Perutz MF. Stereochemistry of cooperative effects in haemoglobin. Nature 1970; 228:726–734.
2. Voet D, Voet JG. Biochemistry. New York: John Wiley and Sons, 1990:211–243.
3. Kokiloo N, Siddiqui M. Interrelationship between blood glucose level, plasma proteins and hemoglobin glycosylation. Ind J Clin Biochem 1987;2:34–38.
4. Kennedy L, Lyons TJ. Non-enzymatic glycosylation. Br Med Bull 1989;45:174–190.
5. Haney DN, Bunn F. Glycosylation of hemoglobin in vitro: affinity labeling of hemoglobin by glucose-6-phosphate. Proc Natl Acad Sci USA 1979;73:3534–3538.

6. Jacques W, Mateescu MA. Affinity chromatography of hemoglobin on cross-linked amylose. Anal Lett 1993;26:875–886.
7. Jacques W, Mateescu MA. Specific hemoglobin (poly)saccharide recognition. J Mol Recogn 1995;8:106–110.
8. Porath J, Flodin P. Gel filtration: a method for desalting and group separation. Nature 1959;183:1657–1659.
9. Serban M, Schell HD, Mateescu MA. Preparation and properties of new amylose based chromatographic materials with application in exclusion chromatography (in German). Rev Roum Biochim 1975;12:187–191.
10. Schell HD, Mateescu MA, Bentia T, Jifcu A. Alpha-amylase purification and separation from glucoamylase by affinity chromatography on cross-linked amylose. Anal Lett (NY) 1981;14(B):1501–1514.
11. Luan Eng LI. Simple method for the isolation and purification of hemoglobin components. J Chromatogr 1976;117:53–58.
12. Carleton JCH, Er SS. Purification of stroma-free haemoglobin by ATP-agarose affinity chromatography. J Chromatogr 1986;374:143–148.
13. Carleton JCH, Er SS, Hronowski LJ, Persaud K, Ansari MR. ATP-hemoglobin purification by ATP-agarose affinity chromatography. J Chromatogr 1986;381:153–157.
14. Jacques W, Mateescu MA. Selective hemoglobin–polysaccharide interactions. 4th Meeting on Biochromatography and Molecular Biology. La Grande Motte, France, May 12–14, 1992.
15. Laemmli EK. Cleavage of structural proteins during the assembly of the head of bacteriophage T4. Nature 1970;227:680–685.
16. Fantl WJ, Manning LR, Ueno H, Di Donato A, Manning JM. Properties of carboxymethylated cross-linked hemoglobin A. Biochemistry 1987;26:5755–5761.

Index